Alma Mater Studiorum – Università di Bologna

Dipartimento di Farmacia e Biotecnologie

Dottorato in Chimica
Ciclo XXVI

SC: 03/D1 SSD: CHIM/08

Chiroptical properties of bioactive molecules: sensitivity to conformation and solvation

Tesi presentata da:
Daniele Tedesco

Coordinatore dottorato:
Prof. Aldo Roda

Relatore:
Prof. Carlo Bertucci

Esame finale anno 2014

This Ph.D. thesis was awarded the G.P. Spada Medal for the Best Ph.D. Project of the Year in Organic and Medicinal Chemistry by the Alma Mater Studiorum – University of Bologna.

Bologna, 12 February 2014

Index

Abstract

Chiroptical spectroscopies play a fundamental role in pharmaceutical analysis for the stereochemical characterisation of bioactive molecules, due to the close relationship between chirality and optical activity and the increasing evidence of stereoselectivity in the pharmacological and toxicological profiles of chiral drugs. The correlation between chiroptical properties and absolute stereochemistry, however, requires the development of accurate and reliable theoretical models. The present thesis will report the application of theoretical chiroptical spectroscopies in the field of drug analysis, with particular emphasis on the huge influence of conformational flexibility and solvation on chiroptical properties and on the main computational strategies available to describe their effects by means of electronic circular dichroism (ECD) spectroscopy and time-dependent density functional theory (TD-DFT) calculations.

The combination of experimental chiroptical spectroscopies with state-of-the-art computational methods proved to be very efficient at predicting the absolute configuration of a wide range of bioactive molecules (fluorinated 2-arylpropionic acids, β-lactam derivatives, difenoconazole, fenoterol, mycoleptones, austdiol). The results obtained for the investigated systems showed that great care must be taken in describing the molecular system in the most accurate fashion, since chiroptical properties are very sensitive to small electronic and conformational perturbations. In the future, the improvement of theoretical models and methods, such as *ab initio* molecular dynamics, will benefit pharmaceutical analysis in the investigation of non-trivial effects on the chiroptical properties of solvated systems and in the characterisation of the stereochemistry of complex chiral drugs.

Part I

Introduction

Nature is a language
Can't you read?

— The Smiths, *Ask*

Chapter 1

Overview

1.1 Aim of the thesis

The intrinsic limitations of standard analytical techniques, which fail to discriminate the enantiomers of chiral molecules, prompted the development of specific enantioselective methods, all based on the interaction between chiral analytes and an anisotropic medium. In separation sciences, the employment of chiral selectors of known stereochemistry has become a standard and widespread method, which is also routinely employed in drug analysis.

In spectroscopy, the direct relationship between the chirality of chemical systems and their differential interaction with polarised radiation is the physical reason for which spectroscopic techniques based on chiroptical properties, such as optical rotatory dispersion (ORD) and circular dichroism (CD), have established themselves among the main tools for the investigation on the stereochemistry of chiral drugs: stereochemical characterisation is indeed fundamental in pharmaceutical research, due to the increasing evidence of stereoselectivity in the pharmacological and toxicological properties of drugs.[1–4] The field of application of chiroptical spectroscopies is wide and ranges from the determination of the absolute configuration (AC) of organic molecules to the assessment of the conformational and supramolecular organisation of large biomolecules.

The correlation between chiroptical properties and the dissymmetric disposition of atoms at the molecular level, however, is not a trivial task and requires the development of accurate and reliable theoretical models. For this purpose, the impressive improvement in the accuracy of quantum mechanical (QM) methods

and the availability of increasingly powerful computational resources have laid the path to a renewed interest in the stereochemical characterisation of chemical systems by theoretical determination of their chiroptical properties.[5]

The present thesis deals with the application of theoretical chiroptical spectroscopies in the field of drug analysis, with particular emphasis on the huge influence of conformational flexibility and solvation on chiroptical properties and on the main computational strategies available to describe their effects. Six examples of stereochemical characterisation of chiral bioactive molecules will be reported, which were achieved by means of a combined approach involving experimental analytical techniques, in particular electronic circular dichroism (ECD) spectroscopy, and computational techniques, mainly based on time-dependent density functional theory (TD-DFT).

1.2 Outline of the thesis

The thesis is divided in six parts:

1. a brief introduction covering the theoretical concepts at the basis of spectroscopy and reviewing the main methods used in stereochemical analysis to correlate chiroptical properties and absolute stereochemistry.[6]
2. a part covering the projects mainly concerned with the stereochemical characterisation of chiral bioactive molecules of unknown stereochemistry (fluorinated 2-arylpropionic acids,[7] difenoconazole[8] and mycoleptones[9]);
3. a part covering the projects mainly concerned with the strong effect of conformational flexibility on the chiroptical properties of chiral molecules (β-lactam derivatives[10] and fenoterol[11]);
4. a part covering the project mainly concerned with the investigation of solvation effects on the definition of chiroptical properties (austdiol);
5. a conclusion, where all the projects are summarised and critically discussed;
6. an appendix, where the tools used in the processing of computational data are explained.

The methods and results of each project are discussed in separate chapters, which are based on the corresponding peer-reviewed publication (except austdiol).

1.3 Acknowledgements

Most of the experimental work discussed in this thesis was carried out using the facilities in the Pharmaceutical Analysis Section at the Department of Pharmacy and Biotechnology of the University of Bologna, while most of the computational work was performed on the computing cluster of Prof. Riccardo Zanasi's research group at the University of Salerno. Particular acknowledgements are also reported in each chapter.

I owe eternal gratitude to the supervisors of the projects I carried out during the last 5 years, first as an undergraduate student then as a Ph.D. student: Prof. Carlo Bertucci, Prof. Riccardo Zanasi, Prof. Dr. Barbara Kirchner and Dr. Alex F. Drake. Each of them gave me the opportunity to test my skills in research in full autonomy, supported me to follow my aspirations and taught me more that I could ever imagine to learn.

I will always be grateful to my family for the patience they had during these challenging years, for the pride they showed for me in good times and the love they gave me in bad times: I love you for all you did for me.

Thanks to all my colleagues in Bologna and Leipzig, in particular to Marco Pistolozzi, Manuela Bartolini, Angela De Simone, Cecilia Fortugno, Cláudia Seidl and Eva Perlt: you are not colleagues, you are friends.

Thanks to all the friends who have always been on my side: Aurélie Bruno, Matteo Staderini, Silvia Immediato, Andrea Felicetti, Giosuè Brulla, and everybody else I didn't mention. You helped me a lot through tough times, and I'll never forget that.

This thesis is dedicated to my best friend Rocco Truncellito: it doesn't matter where you are now, you're always here with me.

Chapter 2

Spectroscopy

2.1 Molecular absorption

In chemical systems, the total energy of a molecule is the result of several contributions, such as interactions between electrons and nuclei, electronic and nuclear spin orientations, vibrations, rotations and translations. According to quantum theory, these contributions generate a set of quantised (discrete) energy states available for each molecule.

Transitions from a state of lower energy to a state of higher energy require the exact amount of energy corresponding to the difference between two energy levels to be supplied to the atom or molecule by an external source, i.e. electromagnetic radiation. The frequency (ν) of an electromagnetic radiation capable of promoting the transition between two different energy states is defined by Planck's equation:

$$\Delta E = h\nu \ , \tag{2.1}$$

where ν is in s^{-1}, ΔE is the energy difference between the two levels and h = 6.62606957·10^{-27} erg s [a] is the Planck constant.[12] As a result, radiation is absorbed by the molecule; the intensity of absorption at a given frequency is related to the absorption cross section of a molecule (W) by the following relation:

$$\ln \frac{I_0}{I_t} = WNl \ , \tag{2.2}$$

[a] The erg is the physical unit for energy in the cgs system. 1 erg = 1 g cm^2 s^{-2}. Throughout the chapter, the cgs system of physical units will be used, due to its widespread use in the theoretical treatment of absorption in literature.

where I_t and I_0 are respectively the intensities of the transmitted and incident radiation, l is the pathlength of the sample in cm and N is the number density of the molecule in the sample in cm^{-3}; W is then expressed in cm^2.

This equation is very similar to the usual formulation of Lambert-Beer law:

$$A = \log \frac{I_0}{I_t} = \varepsilon C l \ , \tag{2.3}$$

where A is the absorbance of the sample, C the molar concentration in mol L^{-1} and ε is the molar absorption coefficient in the usual units of M^{-1} cm^{-1}. Equations 2.2 and 2.3 can be combined to give:

$$W = \frac{\ln 10 C}{N} \varepsilon = \frac{10^3 \ln 10}{N_A} \varepsilon \ , \tag{2.4}$$

where N_A = 6.02214129·10^{23} mol^{-1} is Avogadro's number[12] and C has been converted to N ($C = 10^3 N / N_A$); the conversion factor 10^3 accounts for the change in units.

The intensity and frequency of ultraviolet absorption bands, however, are usually reported and discussed in terms of molar absorption coefficients (ε_{max}) and wavelengths (λ_{max}), since these values are easily obtained by experimental analysis; these quantities are not useful when a theoretical approach is necessary. A rigorous evaluation of the intensity of absorption requires the isolation of each absorption band and the measurement of the area under the absorption curve; in the frequency domain, then, equation 2.4 becomes:

$$W = \frac{10^3 \ln 10}{N_A} \int \varepsilon(\nu) \, d\nu \ ; \tag{2.5}$$

in cgs units, the integrated intensity of absorption is expressed in cm mol^{-1}; if ε is expressed in M^{-1} cm^{-1}, the integrated intensity may be expressed in M^{-1} cm^{-2} = 10^3 cm mol^{-1}. However, intensity values are often reported in km mol^{-1} = 10^2 M^{-1} cm^{-2} = 10^5 cm mol^{-1}.

The isolation of bands is often difficult to obtain from experimental spectra, so ε_{max} is usually preferred as a convenient method of reporting spectroscopic data. The absolute intensity of absorption, however, may be calculated theoretically for each transition.[13,14]

As light is absorbed or emitted by the molecule, an electric transition dipole moment (μ_j) is generated by the charge displacement due to the transition between the ground state and an excited state j. The electric dipole moment of a

molecule (μ) is defined by the distance $\mathbf{r}$ between the centres of gravity of the positive (nuclei) and negative (electrons) charges multiplied by the magnitude of the charges (e). The quantum mechanical expression of the electric dipole moment vector ($\boldsymbol{\mu}$) is given by:

$$\boldsymbol{\mu} = \langle \Xi_0 | \hat{\boldsymbol{\mu}} | \Xi_0 \rangle \ , \tag{2.6}$$

where the operator $\hat{\boldsymbol{\mu}}$ extends over all nuclei and electrons, $e = 4.80320425 \cdot 10^{-10}$ statC [b] is the elementary charge,[12] and Ξ_0 is the total (electronic, vibrational and rotational) wave function of the molecule in the ground state.

Similarly, the electric transition dipole moment vector $\boldsymbol{\mu}_j$ is given by:

$$\boldsymbol{\mu}_j = \langle \Xi_0 | \hat{\boldsymbol{\mu}} | \Xi_j \rangle \ . \tag{2.7}$$

Assuming that the vibrational and rotational contributions to the total wave functions can be factored out according to the Born-Oppenheimer approximation,[15] equation 2.7 reduces to the electronic wave functions (Ψ):

$$\boldsymbol{\mu}_j = \langle \Psi_0 | \hat{\boldsymbol{\mu}} | \Psi_j \rangle \ ; \tag{2.8}$$

the dipole strength of the transition, D_j, is then defined as: [c]

$$D_j = \| \boldsymbol{\mu}_j \|^2 \ . \tag{2.9}$$

Similarly, the quantum mechanical expression of the magnetic transition dipole moment vector ($\mathbf{m}_j$) can be defined as:

$$\mathbf{m}_j = \langle \Psi_0 | \hat{\mathbf{m}} | \Psi_j \rangle \ , \tag{2.10}$$

where the operator $\hat{\mathbf{m}} = -\frac{e}{2m_e c} \sum \mathbf{r} \times \hat{\mathbf{p}}$ extends over all electrons, $m_e = 9.10938291 \cdot 10^{-28}$ g is the electron mass,[12] $c = 2.99792458 \cdot 10^{10}$ cm s^{-1} is the velocity of light,[12] $\hat{\mathbf{p}} = -\mathrm{i}\hbar\boldsymbol{\nabla}$ is the momentum operator, $\hbar = h/2\pi$ is the reduced Planck constant, and $\boldsymbol{\nabla} = \left(\frac{\partial}{\partial x}\mathbf{i} + \frac{\partial}{\partial y}\mathbf{j} + \frac{\partial}{\partial z}\mathbf{k} \right)$ is the Laplace operator, which describes the motion of a microscopic particle. [d]

[b] The electrostatic unit of charge (esu) or statcoulomb (statC) is the physical unit for electrical charge in the cgs system. 1 esu = 1 g$^{1/2}$ cm$^{3/2}$ s^{-1}.

[c] The physical unit of μ_j in the cgs system is the debye (D); 1 D = 1 statC cm = 1 g$^{1/2}$ cm$^{5/2}$ s^{-1}.

[d] $\mathbf{i}$, $\mathbf{j}$ and $\mathbf{k}$ are the unit versors of the Cartesian coordinate system along the x-, y- and z-directions, respectively.

Einstein introduced two types of coefficients: A to describe the probability of spontaneous emission, and B to describe the probability of induced absorption and emission.[16–18] The Einstein coefficient for induced absorption from the ground state (B_{0j}) is related to the dipole strength and to the absorption cross section by the following relations:

$$B_{0j} = \frac{8\pi^3}{3h^2c} D_j G_j \ ; \tag{2.11}$$

$$W = B_{0j} h\nu \ , \tag{2.12}$$

where G_j is the degeneracy factor of state j (i.e. the number of degenerate wave functions to which absorption can lead; usually, $G_j = 1$). In this formulation, B_{0j} is expressed in cm^2 erg^{-1} s^{-1} = s g^{-1}.

In quantum mechanics, the intensity of a transition is espressed by means of a dimensionless quantity, called oscillator strength, f_j, which is directly related to the absorption cross section W by:

$$f_j = \frac{m_e c}{\pi e^2} W \ ; \tag{2.13}$$

the combination of equations 2.11, 2.12 and 2.13 gives the relation of f_j with the dipole strength D_j:

$$f_j = \frac{m_e c h}{\pi e^2} B_{0j} \nu = \frac{8\pi^2 m_e}{3he^2} D_j G_j \nu \ . \tag{2.14}$$

At this point, the frequency can be substituted with the wavenumber ($\sigma = \nu / c$, expressed in cm^{-1}); consequently, equation 2.14 becomes:

$$f_j = \frac{8\pi^2 m_e c}{3he^2} D_j G_j \sigma \ . \tag{2.15}$$

Finally, the combination of equations 2.4 and 2.13 yields the expression relating the oscillator strength (f_j) to the molar absorption coefficient (ε):

$$\begin{aligned} f_j &= \left(10^3 \ln 10\right) \frac{m_e c}{\pi N_A e^2} \int \varepsilon(\nu) \, \mathrm{d}\nu \\ &= 1.44066 \cdot 10^{-19} \int \varepsilon(\nu) \, \mathrm{d}\nu \ , \end{aligned} \tag{2.16}$$

which, in the wavenumber domain, becomes:

$$f_j = \left(10^3 \ln 10\right) \frac{m_e c^2}{\pi N_A e^2} \int \varepsilon(\sigma)\, \mathrm{d}\sigma$$
$$= 4.31899 \cdot 10^{-9} \int \varepsilon(\sigma)\, \mathrm{d}\sigma\ . \tag{2.17}$$

2.2 Molecular optical activity

Optical activity is the physical phenomenon arising from the differential interaction of chiral molecules with the left and right circular polarisations of radiation. A detailed treatment on the historical and theoretical backgrounds of optical activity is beyond the aims of this chapter, and only a brief overview will be provided: the interested reader is referred to a selected list of excellent contributions on this subject.[19–30]

From the point of view of classical electrodynamics, the electric displacement field (**D**) and the magnetic field (**B**) for an electromagnetic wave travelling through a medium are desbribed by the following equations:

$$\mathbf{D} = \epsilon \mathbf{E} - g \frac{\partial \mathbf{H}}{\partial t}\ ; \tag{2.18}$$

$$\mathbf{B} = \mu \mathbf{H} + g \frac{\partial \mathbf{E}}{\partial t}\ , \tag{2.19}$$

where **E** and **H** are respectively the electric field and the magnetic field strength, ϵ and μ are respectively the electric permittivity and magnetic permeability of the medium. The g factor describes the dependence of the induced electric field **D** upon the time evolution of the magnetic field **H** and the dependence of the induced magnetic field **B** upon the time evolution of the electric field **H**.

At the molecular level, a similar dependence can be recognised for the electric ($\boldsymbol{\mu}_j$) and magnetic ($\mathbf{m}_j$) transition dipole moments:

$$\boldsymbol{\mu}_j = \alpha \mathbf{E}' - \frac{\beta}{c} \frac{\partial \mathbf{H}}{\partial t} = \alpha \left(\mathbf{E} + \frac{4\pi}{3} \mathbf{P} \right) - \frac{\beta}{c} \frac{\partial \mathbf{H}}{\partial t}\ ; \tag{2.20}$$

$$\mathbf{m}_j = \chi \mathbf{H} + \frac{\beta}{c} \frac{\partial \mathbf{E}'}{\partial t} = \chi \mathbf{H} + \frac{\beta}{c} \left(\frac{\partial \mathbf{E}}{\partial t} + \frac{4\pi}{3} \frac{\partial \mathbf{P}}{\partial t} \right)\ , \tag{2.21}$$

where $\mathbf{E}' = \mathbf{E} + \frac{4\pi}{3}\mathbf{P}$ is the effective electric field, **P** is the polarisation field of the medium, and the scalar parameters α and χ are respectively the polarisability

and the magnetisability of the molecule. The **P** field and the analogous magnetisation field (**M**) are connected to the transition dipole moments by the following relations:

$$\mathbf{P} = N\boldsymbol{\mu}_j \ ; \tag{2.22}$$

$$\mathbf{M} = N\mathbf{m}_j \ , \tag{2.23}$$

where N is the number density of the molecule in the sample in cm^{-3}.

In equations 2.20–2.21, the β/c factor plays the same role as the g factor in equations 2.18–2.19; both factors describe an anisotropic perturbation related to the interaction with circularly polarised radiation. The relationship between the two factors can be derived by the combination of equations 2.20–2.22, yielding:

$$g = 4\pi N \frac{\beta}{c} \frac{\epsilon + 2}{3} = 4\pi \frac{\beta}{c} \gamma_s \ , \tag{2.24}$$

where $\gamma_s = \dfrac{\epsilon + 2}{3}$ is the Lorentz factor. The β parameter is the averaged trace of a rank-2 tensor, $\boldsymbol{\beta}$, called Rosenfeld or optical rotation tensor:

$$\beta = \frac{1}{3} \mathrm{Tr}\, \boldsymbol{\beta} \ , \tag{2.25}$$

which, in turn, is related to the mixed electric dipole-magnetic dipole polarisability of the molecule, $\mathbf{G'}$:

$$\boldsymbol{\beta} = -\frac{1}{2\pi\nu} \mathbf{G'} \ , \tag{2.26}$$

and to the rotational strengths (R_j), the quantum mechanical quantities describing the response of molecules upon the interaction with left and right circularly polarised radiation. In the frequency domain, the relationship between the β parameter and the rotational strengths of the molecules is expressed by the following equation:

$$\beta(\nu) = \frac{c}{3\pi h} \sum_{j \neq 0} \frac{R_j}{\nu_j^2 - \nu^2} \ , \tag{2.27}$$

where the sum extends over all excited states.

Rosenfeld defined R_j as the imaginary part of the scalar product of the electric ($\boldsymbol{\mu}_j$) and magnetic ($\mathbf{m}_j$) transition dipole moment vectors:[31]

$$R_j = \Im \left(\boldsymbol{\mu}_j \cdot \mathbf{m}_j^* \right) = \Im \left(\langle \Psi_0 | \hat{\boldsymbol{\mu}} | \Psi_j \rangle \langle \Psi_j | \hat{\mathbf{m}} | \Psi_0 \rangle \right) \ ; \tag{2.28}$$

a simpler formulation of R_j is given by:

$$R_j = \|\boldsymbol{\mu}_j\| \cdot \|\mathbf{m}_j\| \cdot \cos\eta \ , \tag{2.29}$$

where the norm brackets denote the vector magnitudes and η is the angle between $\boldsymbol{\mu}_j$ and $\mathbf{m}_j$. For a transition, $R_j = 0$ when either $\|\boldsymbol{\mu}_j\| = 0$, $\|\mathbf{m}_j\| = 0$, or when the vectors are perpendicular to each other ($\eta = \pi/2$; $\cos\eta = 0$). One of these conditions holds for every transition in non-chiral molecules, which accordingly do not exhibit optical activity, and should also hold for inherently non-chiral chromophores, such as phenyl and carbonyl groups. However, a chiral environment, i.e. the asymmetric disposition of substituents around the chromophore in a chiral molecule, induces perturbations in the charge displacement of the transition, thus giving rise to a helical path: the rotational strength for the transition is non-zero and the molecule exhibits optical activity. At the macroscopic level, optical activity gives rises to two phenomena: optical rotation and circular dichroism.

2.3 Optical rotation and circular dichroism

Optical rotation (OR) is a consequence of circular birefringence, which consists in the different velocity of propagation, i.e. refractive index (n), for the two circular polarisations ($n_{\mathrm{LCP}} \neq n_{\mathrm{RCP}}$). Since a linearly polarised radiation may be considered as the combination of coherent LCP and RCP components of equal amplitude, circular birefringence induces a change in the phase difference of the LCP and RCP components. As a result, the plane of polarisation of a linearly polarised radiation, passing through an optically active medium, is rotated by an angle α, which is dependent upon temperature (t) and wavelength of the radiation (λ). The resulting OR is either measured at a single wavelength or as a function of wavelength (optical rotatory dispersion, ORD).

The circular birefringence is related to the g parameter by the equation:

$$n_{\mathrm{LCP}} - n_{\mathrm{RCP}} = 4\pi\nu g \ , \tag{2.30}$$

while the corresponding optical rotation φ of a chiral molecule at frequency ν is given by:

$$\varphi(\nu) = \frac{\pi\nu}{c}\left(n_{\mathrm{LCP}} - n_{\mathrm{RCP}}\right) \ ; \tag{2.31}$$

consequently, the combination of equations 2.24, 2.30 and 2.31 yields:

$$\varphi(\nu) = \frac{16\pi^3 N \nu^2}{c^2}\beta(\nu) = \frac{16\pi^3 N_A C' \nu^2}{c^2 M}\beta(\nu) \ , \tag{2.32}$$

where φ is in rad cm^{-1}, C' is the concentration in g cm^{-3} and M is the molecular weight in g mol^{-1}; from now on, the Lorentz factor ($\gamma_s \sim 1$) will be omitted.

The experimental OR values are reported as specific rotatory powers, $[\alpha]^t_\nu$, expressed in deg cm^3 g^{-1} dm^{-1}:

$$[\alpha]^t_\nu = \frac{\alpha(\nu)}{C'l} \ , \tag{2.33}$$

where t is in Celsius scale, α is in deg and the pathlength l is in dm. Usually, the specific rotatory power is measured at the D spectral line of sodium (589.3 nm; $[\alpha]^t_D$).

Taking into account the conversion from φ (rad cm^{-1}) to α (deg) :

$$\frac{\alpha(\nu)}{10l} = \frac{180\varphi(\nu)}{\pi} \ , \tag{2.34}$$

equations 2.32, 2.27 and 2.33 can be combined to yield:

$$\begin{aligned}[\alpha]^t_\nu &= \frac{1800}{\pi C'} \cdot \frac{16\pi^3 N_A C \nu^2}{c^2 M} \cdot \frac{c}{3\pi h} \sum_{j\neq 0} \frac{R_j}{\nu_j^2 - \nu^2} \\ &= 9600 \frac{\pi N_A \nu^2}{hcM} \sum_{j\neq 0} \frac{R_j}{\nu_j^2 - \nu^2} \ .\end{aligned} \tag{2.35}$$

On the other hand, circular dichroism (CD) is the differential absorption of LCP and RCP radiation, i.e. the molar absorption coefficients (ε) for the two polarisations are different ($\varepsilon_{LCP} \neq \varepsilon_{RCP}$). This differential absorption ($\Delta\varepsilon = \varepsilon_{LCP} - \varepsilon_{RCP}$), also called Cotton effect (CE), occurs for each electronic and vibrational transition of a chiral molecule. Electronic circular dichroism (ECD) and vibrational circular dichroism (VCD) spectra arise from the same physical phenomenon and are simply measured in different ranges of the electromagnetic spectrum. The insurgence of CD is related to the charge displacement occurring during the transition from ground to excited state. In chiral molecules, the charge displacement occurs along a helical path: one of the two circular polarisations interacts more effectively, and is more absorbed, than the other.

The intensity of differential absorption for each transition is related to the correspoinding rotational strength (R_j) through the following equation:

$$R_j = \left(10^3 \ln 10\right) \frac{3hc}{32\pi^3 N_A} \int \frac{\Delta\varepsilon\,(\sigma)}{\sigma}\, \mathrm{d}\sigma \tag{2.36}$$

$$= 2.29648 \cdot 10^{-39} \int \frac{\Delta\varepsilon\,(\sigma)}{\sigma}\, \mathrm{d}\sigma\ ; \tag{2.37}$$

all the quantities are expressed in cgs units except $\Delta\varepsilon$, which is expressed in $M^{-1}\ cm^{-1}$; R_j is then expressed in erg cm^3 or other equivalent units, e.g. erg esu cm G^{-1} [e] and $esu^2\ cm^2$. All these units reduce to g $cm^5\ s^{-2}$.

[e] The gauss (G) is the physical unit for magnetic flux density in the cgs system. 1 G = 1 $g^{1/2}\ cm^{-1/2}\ s^{-1}$.

Chapter 3

Stereochemical analysis

This chapter is based on a peer-reviewed publication:
Carlo Bertucci, Daniele Tedesco (**2012**). Advantages of electronic circular dichroism detection for the stereochemical analysis and characterization of drugs and natural products by liquid chromatography. *Journal of Chromatography A 1269*, 69–81.

Abstract: The need for analytical methods for the determination of the enantiomeric excess of chiral compounds increased significantly in the last decades, and enantioselective separation techniques resulted particularly efficient to this purpose. Moreover, when detection systems based on chiroptical properties (optical rotation or circular dichroism) are employed in high-performance liquid chromatography (HPLC), the stereochemistry of a chiral analyte can be fully determined. Indeed, the coupling of HPLC with chiroptical detection systems allows the simultaneous assessment of the absolute configuration of stereoisomers and the evaluation of the enantiomeric/diastereomeric excess of samples. These features are particularly important in the study of drugs and natural products provided with biological activity, because the assignment of their absolute stereochemistry is essential to establish reliable structure–activity relationships. The following review aims to discuss the analytical advantages arising from the employment of electronic circular dichroism (ECD) detection systems in stereochemical analysis by HPLC upon chiral and non-chiral stationary phases and their use for the stereochemical characterization of chiral drugs and natural compounds. The different methods for the correlation between absolute stereochemistry and chiroptical properties are critically discussed. Relevant HPLC applications of ECD detection systems are then reported, and their analytical advantages are highlighted. For instance, the importance of the concentration-independent anisotropy factor (g-factor; $g = \Delta\varepsilon/\varepsilon$) for the determination of the stereoisomeric composition of samples upon non-chiral stationary phases is underlined, since its sensitivity makes ECD detection very well suited for the enantioselective analysis of large libraries of chiral compounds in relatively short times.

Since the perturbations induced on the transition moments are dependent upon the arrangement of atoms around the chromophore, chiroptical properties are a powerful and sensitive tool to investigate both the absolute configuration (AC) and equilibrium conformation of molecules.[30,32] In particular, the conformational sensitivity of circular dichroism (CD) is widely employed in supramolecular chemistry[33] and in the study of biological macromolecules and biomolecular interactions, such as conformational studies on proteins[34–36] and DNA,[37] binding studies on protein–ligand complexes[38,39] and protein–protein biorecognition processes.[40]

The rotational strengths of a transition have equal magnitude and opposite sign for enantiomers, due to the mirror-image relationship of their chemical structure, and therefore their CD profiles are opposite. Moreover, the CD profiles are qualitatively different for diastereomers. The structural information given by CD spectroscopy may therefore be directly used to assign the absolute stereochemistry of chiral molecules.

For this purpose, several methods were developed over the years in order to correlate the experimental chiroptical properties with the chemical structure of analytes and achieve a reliable and accurate stereochemical characterisation. These methods may be roughly classified into three main categories, according to their degree of generalisation:

a. *empirical methods*;

b. *semi-empirical methods* (helicity rules, sector rules);

c. *non-empirical methods* (independent systems theory, QM calculations).

The basic principles of each method, along with some representative applications, will be reported in the next sections. Particular attention will be focused on QM calculations of chiroptical properties, which are becoming the method of choice due to the impressive advancements in theoretical models and computing power over the last decades. Before continuing, however, a clarification about terminology seems necessary in order to avoid further confusion. In stereochemical analysis, *semi-empirical methods* stand for a class of simplified theoretical models (*rules*) which attempt to generalise the chiroptical properties of specific chromophores on the basis of empirical observations: no theoretical calculations are needed for the application of such methods, even though a more rigorous theoretical foundation has been provided for some of them. These methods are not related by any means to *semi-empirical methods* in computational chemistry, which are approximations of the Hartree–Fock QM methods; incidentally, semi-

empirical QM methods fall into the category of non-empirical methods, according to the classification made in stereochemical analysis.

3.1 Empirical methods

In empirical methods, absolute configuration (AC) assignments are made by simple comparison between the electronic circular dichroism (ECD) spectra of compounds of unknown stereochemistry and the ECD spectra of reference compounds of known AC, having the same chromophoric system and closely similar chemical structures. Despite being relatively fast and straightforward, AC assignments by empirical methods are limited to well-defined, specific applications must be performed with extreme caution, since the applicability of this approach implies that the structural changes among a class of analogous compounds do not affect the electronic configuration of the chromophores to a significant extent. On the other hand, molecules having similar structures but bearing different chromophores cannot be correlated by these methods.

An example of application of empirical methods is the AC assignment of a series of racemic 1,4-benzodiazepin-2-ones, which were resolved by an enantioselective HPLC-CD method[41] (Figure 3.1). The reference compound, (3*S*)-7-chloro-1,3-dihydro-3-(prop-2-yl)-5-phenyl-2*H*-1,4-benzodiazepin-2-one (**2**), shows a negative Cotton effect (CE) in the 350–300 nm range and a positive CE in the 300–250 nm range. The examined compounds present the same chromophore, and the ECD spectra of the first eluted enantiomers are in a mirror-image relationship with the reference compound: therefore, a (*R*) stereochemistry can be assigned to these enantiomeric fractions.

Empirical methods were also employed for the stereochemical characterisation of a series of 4-aryl-substituted 3,4-dihydropyrimidin-2(1*H*)-ones (DHPMs), which display important antihypertensive properties, by enantioselective HPLC followed by ECD analysis.[42] The ECD spectrum of (4*S*)-4-(2-naphthyl)-1,3,6-trimethyl-5-methoxy-carbonyl-DHPM shows a positive CE centred at around 300 nm, due to the enamide chromophore, followed by a negative CE centred at around 220 nm. On this basis, the same AC can be successfully assigned to the first enantiomeric fractions on a Chiralcel OD-H column for other DHPM derivatives, which present variously substituted phenyl groups at C4 and show similar ECD profiles with CEs of the same sign.

Figure 3.1. AC assignment of benzodiazepinone derivatives by empirical methods, with **2** acting as the reference compound.[41]

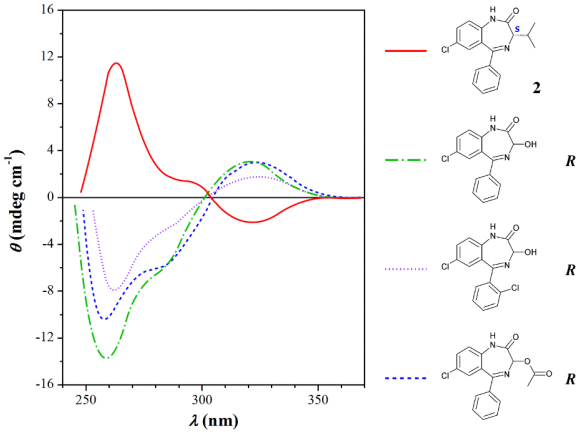

A recent application of empirical methods involved the stereochemical characterisation of a series of aryl-substituted 1-(4-(hydroxymethyl)phenyl)-imidazole ethers, which are potential non-peptidic β-secretase inhibitors.[43] The AC for the enantiomers of the 4-methylphenyl derivative was initially assessed by chemical correlation with the synthetic precursor. After the semi-preparative enantioresolution on a Chiralpak IA column, ECD analysis showed a positive CE in the 270–230 nm range and a negative CE centred at around 220 nm for the (+)-(*R*)-enantiomer, and opposite CEs for the (−)-(*S*)-enantiomer. Finally, the AC and elution orders for the enantiomers of other derivatives were assessed by comparison of their ECD profiles with the ECD spectra of the enantiomers of the 4-methylphenyl derivative, acting as the reference compound.

3.2 Semi-empirical methods

Semi-empirical methods were previously defined as simplified theoretical models, developed to generalise the chiroptical properties of specific chromophores on the basis of empirical observations. These methods may be classified as follows (Figure 3.2):

a. *helicity rules*, applied to inherently chiral chromophores whose intrinsic chirality directly affects the chiroptical properties;

b. *sector rules*, applied to inherently non-chiral chromophores whose chiroptical properties are influenced by the chiral perturbation of substituents.

Figure 3.2. Graphical representations of semi-empirical methods in AC assessment by chiroptical methods. **a:** Diene helicity rule. **b:** Disulfide helicity rule. **c:** Biphenyl helicity rule. **d:** Carbonyl sector rule (octant rule): the front sectors are omitted. **e:** β-Lactam sector rule. **f:** Benzene sector rule.

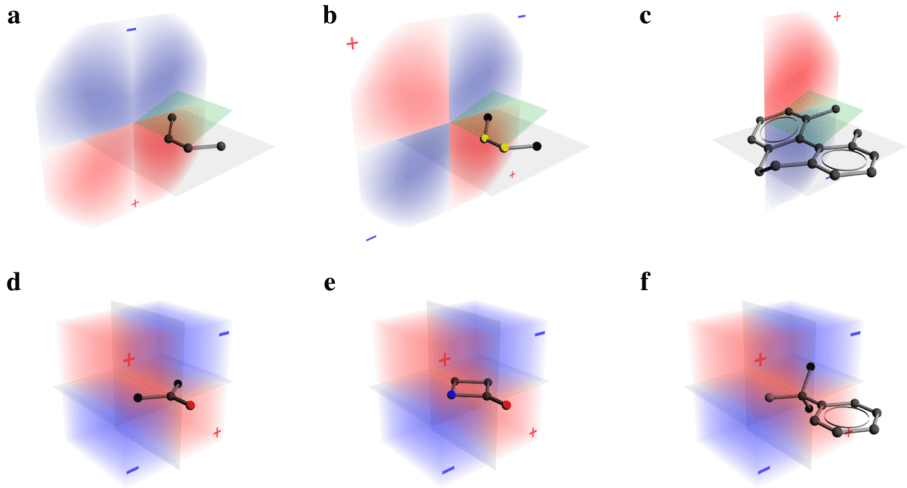

Despite the larger applicability with respect to empirical methods and the improved predictive power, semi-empirical methods have known limitations and should be employed judiciously. These methods are only valid when the largest contribution to the CE of a transition is due to the specific perturbation generalised by the method: different mechanisms or contributions from different chromophores may interfere or even overshadow this contribution, resulting in incorrect predictions.[10] For example, the conformation of 9,10-dihydrophenanthrenes may be tentatively determined by means of the biphenyl helicity rule, which predicts a positive CE for the Suzuki *A* band ($^1L_a \leftarrow {}^1A$ according to Platt's notation,[44] $\sim$ 260 nm) of 2,2′-bridged biphenyl systems having *M* configuration[45–47] (Figure 3.2c).

However, the (9*R*,10*R*)-*trans*-9,10-dihydroxy derivative, which is the main metabolite of phenanthrene, shows a negative CE for this transition,[48] irrespective of the axial conformation of the biphenyl moiety. This behaviour is explained by the presence of the hydroxyl groups on the benzylic carbons: their influence on the underlying $^1L_b \leftarrow {}^1A$ transition overshadows the contribution due the helicity of the biphenyl, and the resulting CE is negative according to the benzene sector rule.[49] Interestingly, the *M*/*P* conformation of the biphenyl moiety

may still be determined by the sign of the exciton-type CE due to the shorter-wavelength Suzuki *B* band ($^1B_b \leftarrow {}^1A$, $\sim$ 210–230 nm), which is negative for *M* configurations and positive for *P* configurations.[48]

3.2.1 Helicity rules

Inherently chiral chromophores, such as helicenes, biaryls, disulfides, cyclic 1,3-dienes and enones, are chromophores lacking symmetry in their structures. The rotational strength of their transitions is generally intense, and the sign of the CE is directly connected to the sense of handedness of the chromophoric system itself; consequently, helicity rules (also called chirality rules) have been developed for some of these systems, such as the diene helicity rule,[50–52] the disulfide helicity rule[53,54] and the aforementioned biphenyl helicity rule[45–47] (Figure 3.2a–c).

Dienes may exist in two limiting planar conformations: *s-cis* ($\theta = 0$) and *s-trans* ($\theta = \pi$), with θ being the dihedral bond between the two double bonds. In ring systems, however, dienes are often twisted: the diene helicity rule correlates the sign of the CE for the lowest-energy $\pi \rightarrow \pi^*$ ($^1B \leftarrow {}^1A$) transition of a diene chromophore to θ, and therefore to the handedness of the twisted system (Figure 3.2a). Dienes having *P* conformations (positive θ) should show positive CEs, while *M* conformations (negative θ) should elicit negative CEs. This rule generally proves valid for moderately twisted, homoannular dienes, and alternative helicity rules have been proposed in order to account for the chiral perturbations due to allylic axial substituents.[55]

3.2.2 Sector rules

Inherently non-chiral chromophores, such as the carbonyl and aryl groups, have a higher degree of symmetry and only display chiroptical properties when substituents induce chiral perturbations to their transitions. Sector rules attempt to establish a relationship between the spatial disposition of substituents around the chromophore and the resulting perturbations on its transition, which are responsible for the observed CEs. The three-dimensional space around the chromophore is therefore divided into sectors, whose contribution to the final CE is either positive or negative. Substituents lying in a specific sector (positive or negative) are expected to induce a corresponding perturbation to the rotational strength.

Several sector rules have been developed for the carbonyl chromophore: arguably, the most famous and successful application is the octant rule for the stereochemical characterisation of saturated ketones[56–59] (Figure 3.2d). The original formulation of the octant rule divides the three-dimensional space around the carbonyl group in eight sectors (octants), delimited by the nodal planes of the n and π^* orbitals. The sign of the CE for the $n \rightarrow \pi^*$ transition is then influenced by the disposition of substituents in the different octants, which have alternate contributions. Observing the carbonyl group from the oxygen side along the C=O bond axis, the upper-left and the lower-right back octants give positive contributions, while the upper-right and the lower-left back octants give negative contributions; opposite contributions arise from the front octants.

Sector rules for the amide chromophore of β-lactam rings[60–63] (Figure 3.2e) are closely connected to the octant rule, and have been successfully applied to assign the correct AC to some alkyl- and aryl-substituted 3-hydroxy-β-lactams.[64] At the same time, the β-lactam amide chromophore is a representative example to explain the weak boundaries in the definition of inherently chiral and inherently non-chiral chromophores. The β-lactam sector rules are based on the assumption that the amide chromophore is inherently non-chiral; nevertheless, the strain of the four-membered β-lactam ring introduces a small inherent helicity to the chromophore. Consequently, a dedicated class of helicity rules was developed,[65,66] which was successfully applied to a series of chiral β-lactam derivatives.[67,68] The two different approaches (sector and helicity rules) are both legitimate, and their combination even serves to describe the chiral perturbations in a more accurate fashion.[10]

Similar sector rules have been developed for the oxygen $n \rightarrow 3s$ Rydberg transition of oxiranes[69] and for the lowest-energy $\pi \rightarrow \pi^*$ ($^1L_b \leftarrow {}^1A$) transition of chiral benzene derivatives.[49] The benzene sector rule (Figure 3.2f) rationalises the vibronic perturbations acting on the ^1L_b band of a monosubstituted benzene chromophore due to the AC of the chiral substituent. The induced perturbations due to further substitutions on the benzene chromophore are considered by means of a separate semi-empirical rule, the benzene chirality rule,[49] which takes into the account the chemical nature and position of the substituent. The benzene sector and chirality rules have been successfully applied to establish the (2*S*,3*S*) AC of (+)-*cis*-2,3-dihydro-2-[(methylamino)methyl]-1-[4-(trifluoromethyl)phenoxy]-1*H*-indene hydrochloride, the most active stereoisomer of a serotonin uptake inhibitor,[70] and to determine the stereochemistry of the stereoisomers of fenoterol, a well-known selective β_2-adrenergic receptor (β_2-AR) agonist, which is used as a bronchodilator in the treatment of asthma.[71]

3.3 Non-empirical methods

Non-empirical methods are able to determine the relevant information about the stereochemistry of a given compound from its chiroptical properties, without empirical comparison with a reference compound (empirical) or class of compounds (semi-empirical); by employment of these methods, the theoretical chiroptical properties are calculated at a suitable level of complexity for selected molecular geometries and subsequently compared with the experimental properties. Non-empirical methods may be roughly classified as follows:

a. *independent systems* (IS) theoretical methods,

b. *quantum mechanical* (QM) calculations.

3.3.1 Independent systems theory

Independent systems (IS) theoretical methods are based on the assumption that the different chromophores of a molecule may be treated as independent electronic entities, coupled through space by Coulombic interactions.[72] Upon excitation, the transitions of a chromophore are influenced to some extent by the electronic perturbations due to the other chromophores, which are dependent on the mutual disposition and orientation of chromophores. The theoretical determination of these interactions may therefore serve to determine the stereochemistry of compounds with interacting chromophores.

The exciton chirality method[73] is based on the physical phenomenon of exciton coupling.[74] The excited states of two interacting chromophores are split in two transition levels, one at lower energy (α) and one at a higher energy (β) with respect to the original transition levels of the single chromophores. In chiral molecules, an additional feature of the interaction is the onset of a distinctive bisignate CD profile, in which the opposite CEs correspond to the α and β energy levels and the sign pattern is related to the AC of the compound: the lowest-energy CE is positive if the interaction between chromophores occurs along a clockwise path (Figure 3.3), negative if it occurs along an anticlockwise direction.

The first application of this approach regarded the AC determination of the alkaloid calycanthine;[75,76] a more general dibenzoate chirality method was then developed, by which the AC of diols could be assessed by derivatisation with 4-bromobenzoic acid to yield the corresponding esters.[77,78] The exciton chirality rule was successfully applied to the determination of the glycosidic linkages

Figure 3.3. Application of the exciton chirality rule for a generic *bis*-4-bromobenzoate derivative with clockwise orientation of interacting chromophores.

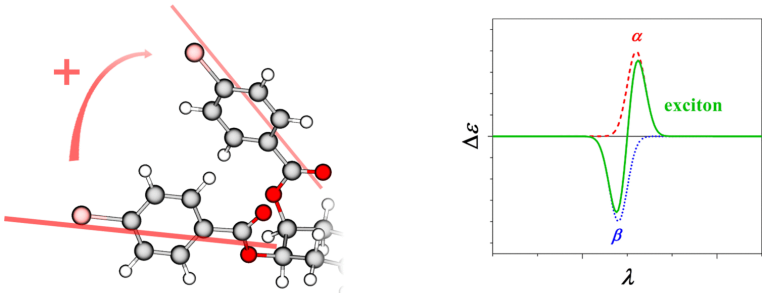

in oligosaccharides, to stereochemical studies on the metabolism of polycyclic aromatic hydrocarbons, and to the stereochemical characterisation of natural products and drugs, such as taxinine, chromomycins, cervicarcin, carbamazepine, cycloxilic acid, vinblastine derivatives, pinellic acid and phorboxazoles.[73,79–83]

IS methods may also be applied at a quantitative level to reproduce the intensity of the observed CEs. For instance, the DeVoe polarisability model[84–86] considers the electric dipole transition moments of chromophores as classical linear oscillators. Upon excitation, the oscillators are polarised by the external electric field of the incident radiation and by the electric field induced by the oscillation of the other chromophores: the latter phenomenon is responsible for the coupling between chromophores.

The resulting induced polarisability tensor is used to calculate the theoretical optical and chiroptical properties of molecules (absorption, refraction, ORD and CD), which are subsequently compared to the experimental properties. DeVoe calculations have been applied to several classes of molecules,[87–90] and even to systems as large as globular proteins.[91] The relatively lower accuracy of IS methods with respect to QM calculations is a limiting factor when dealing with small molecules, but the lower computational requirements of these methods are beneficial in the conformational analysis of large, flexible macromolecules.

3.3.2 Quantum mechanical calculations

The application of QM calculations to the theoretical determination of chiroptical properties is a constantly growing field of research, whose origin dates back to the first formulations of the quantum theory for optical activity.[31] The background assumption is that, once the exact solutions to the Schrödinger equation for the

complete set of wavefunctions are known, all the electronic properties, including excitation energies, dipole transition moments, polarisabilities and rotational strengths, may be exactly calculated and used to determine the theoretical chiroptical properties. These properties may be then compared to the experimental properties in order to assess the AC and equilibrium conformation of molecules, without any empirical comparison to a reference system.

Unfortunately, the Schrödinger equation can only be solved using various degrees of approximation, depending on the size of the system under investigation. However, the steady development of increasingly accurate QM theories for the calculations of the electronic structure of molecules and the parallel evolution of computing technologies, which are the basis of the success of computational chemistry in the last decades,[92] have also greatly contributed to revive the interest in the chiroptical methods for stereochemical analysis.[5]

Virtually all the QM linear response methods have been applied over the years to assess the AC of several molecules,[93–96] ranging from the semi-empirical methods such as the complete neglect of differential overlap approximation for spectroscopy (CNDO/S),[97–99] the Parisier–Pople–Parr method (PPP)[100] and the Hückel methods,[101–106] to the uncorrelated *ab initio* methods such as time-dependent Hartree–Fock theory (TD-HF).[107,108] In recent years, time-dependent density functional theory (TD-DFT)[29] and electron correlation methods such as linear response coupled cluster theory (LR-CC)[109] have become the standard for electronic structure calculations for different reasons. TD-DFT calculations are able to combine a reasonable degree of accuracy in the prediction of excitation energies and rotational strengths with a relatively low computational demand, which is fundamental when dealing with large systems. Coupled cluster calculations, on the other hand, provide the highest degree of accuracy but require a higher computational effort, which limits their applicability to small systems.

Further details on the theoretical formulations and on the main advantages and shortcomings of all the different QM methods may be found in a series of dedicated publications;[27–29,110,111] a schematic representation of stereochemical analysis by HPLC-CD and QM calculations is given in Figure 3.4, based on the AC assessment of a fluorinated propionic acid derivative.[7]

Some practical aspects need to be pointed out for a complete coverage of the application of QM methods in stereochemical analysis:

a. the stereochemistry of a compound of unknown AC can be assessed only if QM calculations have been performed on all the possible stereoisomers. For compounds having a single stereogenic centre, QM calculations need to be

Figure 3.4. Graphical scheme of a typical protocol for the stereochemical characterisation by combination of HPLC-CD methods and QM calculations, involving the AC assessment of the enantiomers of **3**.[7]

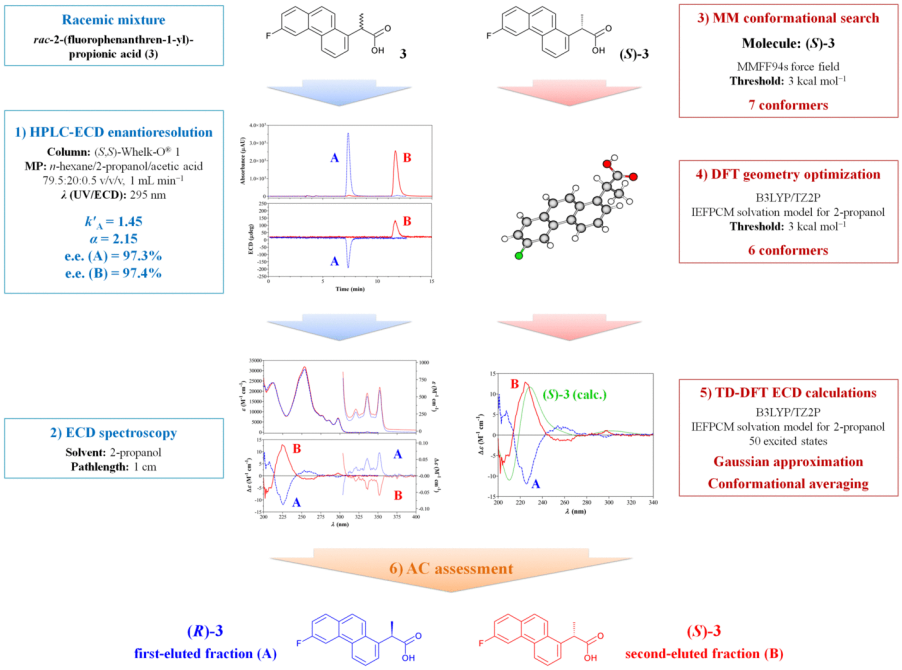

performed for only one enantiomer, since the ECD spectra of enantiomers are in a mirror-image relationship. For compounds having n stereogenic centres, on the other hand, QM calculations need to be performed on one enantiomer of each of the 2^{n-1} possible enantiomeric pairs before a safe AC assignment can be made.[112]

b. the theoretical ECD spectrum for a given compound should be calculated as the weighted average of the contributions from all the equilibrium conformers, based on their Boltzmann population.[28] Therefore, the preliminary steps of conformational search, geometry optimisation and free energy calculations are critical for a reliable prediction of the chiroptical properties: errors in these steps (e.g., failing to identify equilibrium conformers during the conformational search, or failing to optimise the structure of conformers to a local minimum of the potential energy surface) directly affect the quality of the calculated ECD profile, potentially leading to incorrect AC assignments.

c. the theoretical ECD spectrum for a given structure is calculated using a sum-over-state (SOS) expression which takes into account the rotational strengths

for the transitions to all the excited states (R_j). These values are then generally approximated to Gaussian curves to reproduce the actual profile of ECD spectra.[113] As a consequence, accurate ECD predictions may require the calculation of an adequate number of excited states at higher frequencies than the spectral range of interest: the balance between accuracy and computational cost must be found for each system under investigation.

d. solvent effects play a paramount role in the definition of chiroptical properties. One of the most successful approaches to account for solvent effects in QM calculation is represented by the implementation of continuum solvation models, such as the polarisable continuum model (PCM),[114] which account for long-range perturbations to the electronic structure of solutes by electrostatic interactions. However, these models do not account for short-range solvent–solute interactions, such as hydrogen bonding, which may be responsible for large modifications to the chiroptical properties. Whenever solvent effects become relevant, different approaches should be considered, such as QM calculations on solvent–solute clusters (solvated supermolecule approach).[115]

e. the accuracy of QM calculations clearly depends on the level of theory and the depth of the basis set used for the calculations; to simplify the correlation between theoretical and experimental data, the calculated values of excitation energies may need to be shifted to fit the experimental bands. Many different approaches have been proposed to perform such empirical corrections, none of which can be used systematically for every system.[112] As a general trend, these procedures should be performed with extreme care, taking into account that linear corrections are only possible in the frequency scale (not in the wavelength scale, which is inversely proportional to energy), and that the same procedure should be performed on all calculations, in order to avoid spurious or misleading correlations.

Part II

Stereochemical characterisation

Show me how you do it
And I promise you
I promise that
I'll run away with you

— The Cure, *Just Like Heaven*

Chapter 4

2-(fluoroaryl)propionic acids

This chapter is based on a peer-reviewed publication:
Carlo Bertucci, Marco Pistolozzi, Daniele Tedesco, Riccardo Zanasi, Renzo Ruzziconi, Anna Maria Di Pietra (**2012**). Stereochemical characterization of fluorinated 2-(phenanthren-1-yl)propionic acids by enantioselective high performance liquid chromatography analysis and electronic circular dichroism detection. *Journal of Chromatography A 1232*, 128–133.

Abstract: Enantioselective high performance liquid chromatography (HPLC) coupled with a detection system based on the simultaneous measurement of UV absorption and electronic circular dichroism (ECD) allows a complete stereochemical characterization of chiral compounds, once the relationship between sign of the chiroptical properties and absolute configuration is determined. In the present communication, the development of enantioselective HPLC methods for the resolution of a series of fluorinated 2-phenanthrenylpropionic acids (**1–6**) is reported. Different chiral stationary phases (CSPs) were tested: Chiralcel OJ, Chiralcel OD, Chiralpak AD, (*S*,*S*)-Whelk-O 1, Chirobiotic T and α_1-acid glycoprotein (AGP). The results allow the application of the methods to a reliable determination of the enantiomeric excess for all the examined compounds; the highest enantioselectivity values were obtained with the Hibar [(*S*,*S*)-Whelk-O 1] column for some of the examined compounds. In the case of *rac*-2-(6-fluorophenanthren-1-yl)propionic acid (**1**), the relationship between circular dichroism and absolute configuration of the enantiomeric fractions was determined by ECD analysis and time-dependent density functional theory (TD-DFT) calculations. The experimental ECD spectrum of the second-eluted fraction of **1** on the Hibar [(*S*,*S*)-Whelk-O 1] column was found to be in excellent agreement with the theoretical ECD spectrum of (*S*)-**1**; therefore, the absolute configuration of the first- and second-eluted enantiomers on the (*S*,*S*)-Whelk-O 1 CSP was assessed as (*R*) and (*S*), respectively, and the elution orders of the enantiomeric forms of 1 were determined on all the different CSPs.

Acknowledgements: The authors are grateful for financial support from the Universities of Bologna, Salerno and Perugia and from MIUR, Italy (PRIN 2008 National Program).

Fluorinated profens have received particular consideration in reference to their biological activity as successful non-steroidal anti-inflammatory drugs (NSAIDs), especially in connection with the presence of fluorine in the molecule. In fact, once placed in a specific position of a bioactive molecule, fluorine can substantially affect its chemical stability,[116–121] thus slackening the related metabolic processes. Moreover, since the C–F bond is stronger than the C–H bond and exhibits reverse polarity, replacement of the α-hydrogen with the quasi-isosteric fluorine conveys a higher configurational stability to the chiral centre of profens,[122] thus allowing the drug pharmacodynamics, as well as the stereochemical matching with the biological target, to be investigated. Since the biological activity of 2-(phenanthren-1-yl)propionic acid as a NSAID was reported to be similar to that of fenbufen,[123] a number of nucleus and/or side-chain fluorinated 2-phenantrylpropionic acids were prepared,[124] in order to assess the effect of fluorine on the structure/activity relationship with respect to its position and to the configuration of the chiral carbon. Nevertheless, a reliable study on the relationship between stereochemistry and biological activity requires a full stereochemical characterisation of the compounds under investigation.

In this article, the development of enantioselective high performance liquid chromatography (HPLC) methods for the resolution of a series of 2-(fluorophenanthren-1-yl)propionic acids (**1–6**, Figure 4.1) is reported; these methods may be applied for the determination of the enantiomeric excess (e.e.). For one of these compounds, 2-(6-fluorophenanthren-1-yl)-propionic acid (**1**), the enantioselective method has been scaled up to allow the collection of the enantiomeric fractions, before their stereochemical characterisation. The e.e. value was determined through the same chromatographic assay, and the absolute configuration was assessed by electronic circular dichroism (ECD) spectroscopy and time-dependent density functional theory (TD-DFT) computations.

Figure 4.1. Chemical structures of 2-(fluorophenanthren-1-yl)propionic acids.

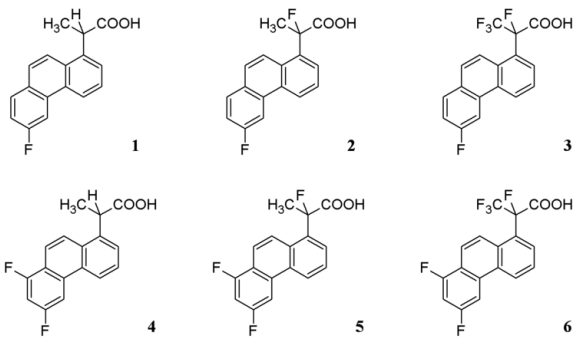

4.1 Materials and methods

Details on the materials and methods used for the enantioselective HPLC analysis on 2-(fluorophenanthren-1-yl)propionic acids **1–6** are reported in Bertucci *et al.* (**2012**), *J. Chromatogr. A 1232*, 128.

4.1.1 Experimental spectroscopy

UV spectra of compounds **1–6** were carried out on a spectrophotometer Jasco V-520, in 2-propanol at room temperature, using 1 cm pathlength cells. ECD spectra (370–210 nm spectral range) of the single enantiomeric fractions of **1** were recorded on a Jasco J-810 spectropolarimeter, in 2-propanol at room temperature, using a 1 cm pathlength cell. Concentrations were adjusted to keep the absorbance in the optimum photometric range. Spectra were recorded at 0.5 nm intervals using a 2 nm spectral bandwidth, a 20 nm min^{-1} scan rate and a 4 s time constant. The actual concentration of the fractions of **1** was determined by UV analysis.

4.1.2 Computational spectroscopy

Molecular mechanics (MM) calculations were carried out for a preliminary conformational analysis of (*S*)-**1**. The conformer distribution was determined at the MMFF94s[125] level using the Spartan'02 software,[126] and the relative energies (ΔE_{MM}) with respect to the lowest-energy conformation were calculated for each conformer.

Full quantum mechanical (QM) geometry optimisations were then performed through density functional theory (DFT)[127,128] calculations on the MM conformers having $\Delta E_{MM} \leq 3$ kcal mol^{-1}, using the Gaussian 09 software package.[129] The hybrid B3LYP exchange-correlation functional[130–133] was used in combination with the triple-ζ plus double-polarisation TZ2P basis set;[134,135] solvent effects were accounted for 2-propanol by adopting the polarisable continuum model (PCM) in its integral equation formalism,[114,136] as implemented within the Gaussian 09 package. The Boltzmann distribution of conformers at 298.15 K and 1 atm was calculated from relative self-consistent field energies (ΔE_{QM}), and relative free energies (ΔG).

Time-dependent DFT (TD-DFT)[137] calculations of the chiroptical properties of (*S*)-**1** were performed at the B3LYP/TZ2P level on the optimised geometries of conformers with $\Delta E_{QM} \leq 3$ kcal mol^{-1}; excitation wave numbers (σ_j) and

rotational strengths (R_j) were determined for the lowest 50 excited states of each conformer. Theoretical ECD spectra as a function of wave number, $\Delta\varepsilon(\sigma)$, were derived for (*S*)-**1** by approximation of all R_j values to Gaussian functions ($\Delta\sigma =$ 0.3 eV), summation over all excited states and conformational averaging, according to the Boltzmann distribution of conformers.[28,113] Theoretical spectra were converted in wavelength scale for a convenient comparison with experimental data; the correlation between the theoretical ECD spectrum of (*S*)-**1** and the experimental ECD spectra of the enantiomeric fractions of **1** was then evaluated by the Pearson product-moment correlation coefficient (r).[138]

4.2 Results and discussion

Results for the enantioselective HPLC analysis on 2-(fluorophenanthren-1-yl)propionic acids **1–6** are reported in Bertucci *et al.* (**2012**), *J. Chromatogr. A 1232*, 128.

The enantiomeric fractions of compound **1** were obtained by preparative enantioselective HPLC on a Chiralcel OD column. Repetitive injections and collection of the enantiomeric fractions yielded about 0.3 mg of each enantiomer. The e.e. resulted 97.3 and 97.4% for the first- and second-eluted fraction, respectively, as determined by the chromatographic assay developed on the Hibar [(*S*,*S*)-Whelk-O 1] column (Figure 4.2). The experimental ECD spectra were carried out by analysing the reconstituted solutions in 2-propanol. The UV absorption spectra, as well as the specular ECD spectra, (Figure 4.3) show three structured bands, the lowest-energy one in the 350–320 nm spectral region, the second one in the 280–250 nm region, and the highest energy one centred at about 230 nm. The absolute configuration of the enantiomers of compound **1** was then determined by comparison of the experimental ECD spectra of the two fractions with the theoretical ECD spectrum calculated for (*S*)-**1**.[28] The latter was obtained by conformational averaging, taking into account the contributions of the lowest-energy conformations and their populations.

The conformational flexibility of the propionic moiety may be conveniently described by two dihedral angles: ϕ_1 (C1–C2–C1′–C2′), describing the rotation about the C2–C1′ bond and the mutual orientation of the propionic and fluorophenanthrenyl moieties, and ϕ_2 (O4–C1–C2–C1′), describing the rotation about the C1–C2 bond and the orientation of the carboxyl group. The conformational analysis at the MM level led to the identification of seven conformers (**1a–g**, Table 4.1) with $\Delta E_{MM} \leq 3$ kcal mol^{-1}. DFT geometry optimisation caused some

Figure 4.2. Enantiomeric excess determination for the enantiomeric fractions of **1**. *Dashed:* First-eluted fraction. *Solid:* Second-eluted fraction. 1 mg mL^{-1}, obtained on the Hibar column. Mobile phase: *n*-hexane/2-propanol/acetic acid 79.5:20:0.5, v/v/v, flow 1 mL min^{-1}; simultaneous UV and ECD detection (λ = 295 nm).

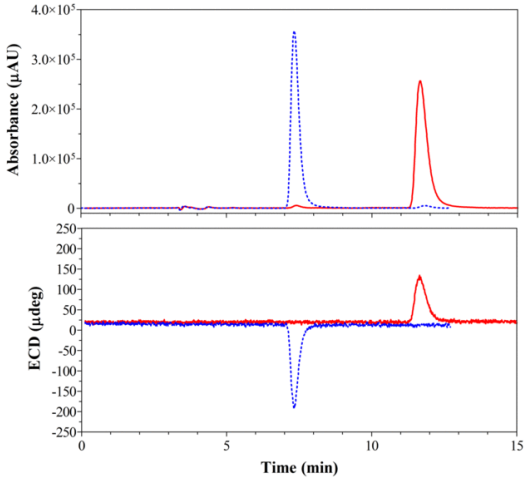

Figure 4.3. UV and ECD spectra for the enantiomeric fractions of **1** in 2-propanol (pathlength: 1 cm). (Dashed) First-eluted fraction (400–300 nm: 711 μM; 350–200 nm: 17.8 μM). *Solid:* Second-eluted fraction (400–300 nm: 646 μM; 350–200 nm: 16.2 μM). Elution order determined on the Hibar column.

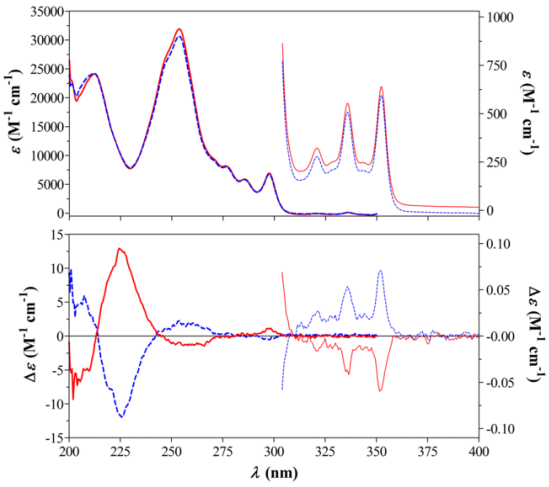

MM conformers to converge to the same geometry: conformational clustering was carried out with a threshold RMSD value of 0.01 Å (Tables 4.7 and 4.8). As a result, four conformers (**1h–k**, Table 4.2) were obtained by calculations without solvation models (gas phase), while six conformers (**1l–q**, Table 4.3) were obtained by calculations with IEFPCM for 2-propanol. Graphical representations of the different conformers are reported in Figures 4.5 and 4.6.

Table 4.1. Geometric parameters, energy values and Boltzmann equilibrium populations at 298.15 K and 1 atm for the conformers of (*S*)-**1**, as obtained after MM conformational analysis.

Conf. ID	ϕ_1 (deg)	ϕ_2 (deg)	E_{MM} (kcal mol^{-1})	ΔE_{MM} (kcal mol^{-1})	χ_{MM} (%)
(*S*)-**1a**	−96.543	57.372	49.432	0.000	30.64
(*S*)-**1b**	123.030	121.692	49.503	0.071	27.18
(*S*)-**1c**	−45.365	99.875	49.824	0.392	15.81
(*S*)-**1d**	−101.334	−114.372	49.868	0.436	14.68
(*S*)-**1e**	121.244	−40.141	50.395	0.963	6.03
(*S*)-**1f**	−46.781	−11.567	50.455	1.023	5.45
(*S*)-**1g**	125.385	141.077	52.379	2.947	0.21

Table 4.2. Geometric parameters, energy values and Boltzmann equilibrium populations at 298.15 K and 1 atm for the conformers of (*S*)-**1**, as obtained after DFT geometry optimisation (B3LYP/TZ2P) in gas phase.

Conf. ID	ϕ_1 (deg)	ϕ_2 (deg)	E_{QM} (Ha)	ΔE_{QM} (kcal mol^{-1})	χ_{QM} (%)	G (Ha)	ΔG (kcal mol^{-1})	χ_G (%)
(*S*)-**1h**	−41.419	−81.720	−906.29110978	0.000	53.04	−906.078785	0.000	72.50
(*S*)-**1i**	122.935	130.731	−906.29042587	0.429	25.70	−906.077137	1.034	12.65
(*S*)-**1j**	−104.315	−119.335	−906.29017972	0.584	19.81	−906.077240	0.970	14.11
(*S*)-**1k**	120.133	−43.138	−906.28771135	2.133	1.45	−906.074447	2.722	0.73

Table 4.3. Geometric parameters, energy values and Boltzmann equilibrium populations at 298.15 K and 1 atm for the conformers of (*S*)-**1**, as obtained after DFT geometry optimisation (B3LYP/TZ2P) in 2-propanol (IEFPCM solvation model).

Conf. ID	ϕ_1 (deg)	ϕ_2 (deg)	E_{QM} (Ha)	ΔE_{QM} (kcal mol^{-1})	χ_{QM} (%)	G (Ha)	ΔG (kcal mol^{-1})	χ_G (%)
(*S*)-**1l**	−41.796	106.466	−906.30098721	0.000	40.37	−906.088983	0.000	62.03
(*S*)-**1m**	122.927	135.824	−906.30034049	0.406	20.35	−906.087263	1.079	10.03
(*S*)-**1n**	−104.913	37.596	−906.30030519	0.428	19.60	−906.087626	0.852	14.74
(*S*)-**1o**	−105.572	−127.412	−906.29999385	0.623	14.09	−906.087346	1.027	10.95
(*S*)-**1p**	120.389	−37.949	−906.29879378	1.376	3.95	−906.085608	2.118	1.74
(*S*)-**1q**	121.161	142.346	−906.29795970	1.900	1.63	−906.084450	2.845	0.51

The optimised conformers showed different theoretical ECD profiles (Figures 4.7 and 4.8; rotational strengths and excitation energies in the 340–200 nm range are reported in Tables 4.4 and 4.5); this behaviour is consistent with the different orientations of the phenanthryl chromophore with respect to the propionic moiety. Conformationally averaged ECD spectra differ when Boltzmann populations are calculated from ΔE_{QM} or ΔG; a stronger contribution of the lowest-energy conformer is observed for ΔG-based calculations, leading to increased

intensities of the short-wavelength ECD bands. Implementation of IEFPCM for long-range solvent effects in TD-DFT calculations caused minimal changes in the conformationally averaged ECD spectrum of (*S*)-**1** (Fig. S.5), mainly consisting in a slight shift towards shorter wavelengths.

The comparison between the theoretical ECD spectrum of (*S*)-**1** and the experimental spectra of the enantiomeric fractions of **1** (Figure 4.4) on the (*S*,*S*)-Whelk-O 1 CSP shows a positive correlation between theoretical and experimental data for the second-eluted fraction, and a negative correlation for the first-eluted fraction (Table 4.6). Better r values are obtained when ΔE_{QM}-based Boltzmann populations are used for the conformational averaging of the theoretical ECD spectrum. Further improvement in correlation coefficients would be obtained by shifting the theoretical ECD spectrum of (*S*)-**1** towards shorter wavelengths, which is consistent with the tendency of TD-DFT calculations to underestimate transition energies.[28] On this basis, the first- and second-eluted fractions on the (*S*,*S*)-Whelk-O 1 CSP are identified as the (*R*)- and (*S*)-enantiomers of **1**, respectively.

Figure 4.4. Theoretical ECD spectrum for (*S*)-**1** and comparison with experimental data. *Thin:* Theoretical ECD spectrum in 2-propanol (IEFPCM solvation model, ΔE_{QM}-based conformational averaging, $\Delta\sigma = 0.3$ eV). *Dashed:* First-eluted enantiomeric fraction of **1**. *Solid:* Second-eluted enantiomeric fraction of **1**. Elution order determined on the Hibar column.

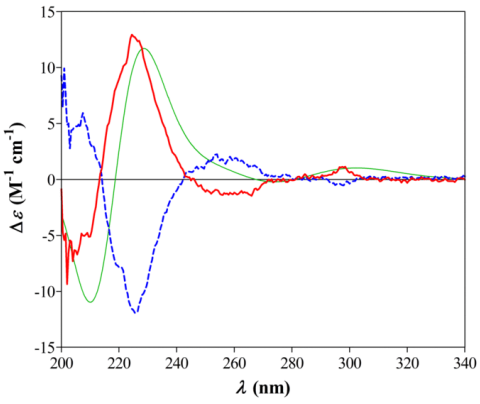

Once the relationship between ECD and absolute configuration was established, it was possible to determine the elution orders for compound **1** not only on the (*S*,*S*)-Whelk-O 1 CSP, but also on the other CSPs employed in the present investigation. In particular, the absolute configuration (*S*) can be assigned to

the first-eluted enantiomer of **1** on Chiralcel OJ and Chiralcel OD, and to the second-eluted enantiomer on Chiral-AGP.

4.3 Conclusions

The developed enantioselective HPLC methods resulted efficient for the resolution of all the racemic mixtures under examination. Relatively high values of enantioselectivity were obtained on the Hibar [(*S*,*S*)-Whelk-O 1] and Chiral-AGP columns. The method was successfully scaled-up on the Chiralcel OD column, allowing to collect the enantiomeric fractions of **1** with high values of enantiomeric excess. Full stereochemical characterisation of **1** was carried out by a combination of experimental ECD spectroscopy and theoretical TD-DFT calculations, which allowed to assign (*R*) and (*S*) absolute configuration to the first- and second-eluted enantiomers of **1** on the (*S*,*S*)-Whelk-O 1 CSP, respectively. The elution order on the different CSPs was determined according to the detected ECD sign at 295 nm, which is negative for the (*R*)-enantiomer and positive for the (*S*)-enantiomer. This multi-technique approach proves to be very promising and may be applied for the stereochemical characterisation of several compounds of biological and pharmaceutical interest.

Figure 4.5. Graphical representation of DFT optimised conformers of (*S*)-**1** in gas phase. **a:** (*S*)-**1h**; **b:** (*S*)-**1i**; **c:** (*S*)-**1j**; **d:** (*S*)-**1k**.

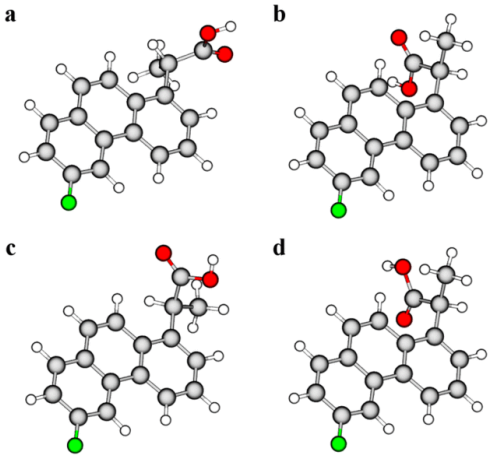

Figure 4.6. Graphical representation of DFT optimised conformers of (*S*)-**1** in 2-propanol (IEFPCM solvation model). **a:** (*S*)-**1l**; **b:** (*S*)-**1m**; **c:** (*S*)-**1n**; **d:** (*S*)-**1o**; **e:** (*S*)-**1p**; **f:** (*S*)-**1q**.

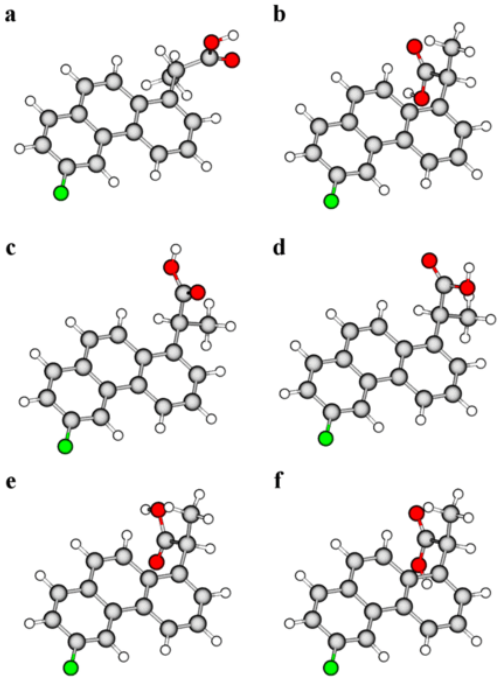

Figure 4.7. Theoretical ECD spectra and rotational strengths for the conformers of (*S*)-**1**, as obtained by TD-DFT calculations (B3LYP/TZ2P) in gas phase ($\Delta\sigma = 0.3$ eV).

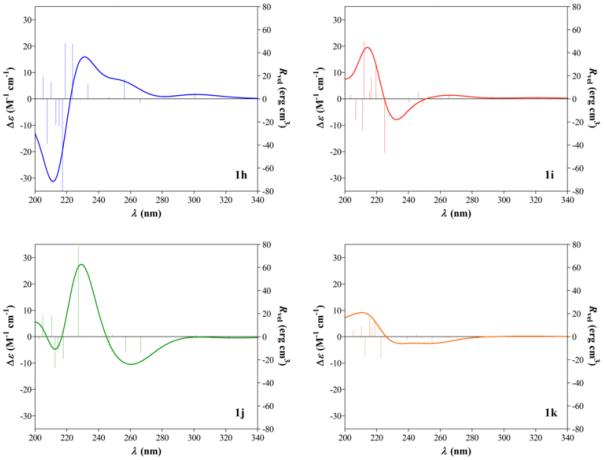

Figure 4.8. Theoretical ECD spectra and rotational strengths for the conformers of (*S*)-**1**, as obtained by TD-DFT calculations (B3LYP/TZ2P) in 2-propanol (IEFPCM solvation model, $\Delta\sigma = 0.3$ eV).

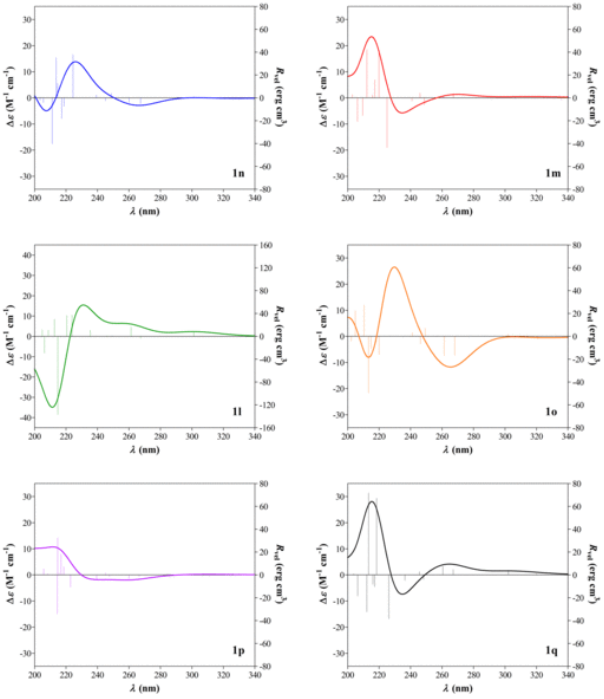

Table 4.4. Rotational strengths in dipole velocity formalism and excitation wavelengths for the lowest-energy electronic transitions of the conformers of (*S*)-**1**, as obtained by TD-DFT calculations (B3LYP/TZ2P) in gas phase.

j	R_j, 10^{-40} erg cm^3 (λ_j, nm)			
	(*S*)-**1h**	(*S*)-**1i**	(*S*)-**1j**	(*S*)-**1k**
1	0.1337 (320.75)	1.2554 (320.86)	−1.8990 (321.79)	0.4353 (319.50)
2	4.9525 (300.43)	0.1091 (300.14)	1.0068 (301.37)	0.1964 (299.34)
3	−3.5216 (266.17)	3.5369 (265.46)	−13.6002 (266.48)	−1.2146 (264.93)
4	17.0375 (256.16)	0.6265 (255.62)	−13.2636 (256.98)	−4.8383 (254.83)
5	−0.1441 (249.26)	−4.2410 (248.83)	1.5084 (248.85)	−1.2527 (247.78)
6	1.3913 (246.27)	5.3840 (246.10)	−7.6488 (246.55)	1.9957 (245.27)
7	13.0064 (233.25)	−2.8185 (240.59)	0.0847 (239.90)	−3.1846 (239.08)
8	47.7800 (223.49)	−46.5049 (224.95)	77.2437 (227.22)	−18.6472 (222.62)
9	47.1041 (218.96)	30.5798 (219.48)	−0.5812 (218.59)	12.9824 (218.82)
10	−78.9071 (217.30)	17.3703 (216.58)	−18.0182 (217.85)	0.3812 (218.17)
11	−23.6000 (215.12)	6.1466 (215.47)	−11.5658 (214.25)	7.9133 (217.03)
12	−22.5019 (213.12)	48.8653 (212.01)	−26.5584 (212.62)	15.8661 (215.47)
13	14.6508 (210.09)	−27.2141 (211.02)	18.0359 (210.49)	−16.9817 (212.76)
14	−38.3972 (207.58)	−17.7532 (206.76)	18.0429 (204.91)	8.5744 (210.45)
15	19.0149 (205.05)	3.3993 (203.62)	−2.4401 (202.34)	5.8247 (205.34)
16	−11.3015 (198.28)	24.1696 (196.88)	−1.0753 (196.39)	12.0754 (197.63)
17	−5.2005 (194.67)	0.2236 (193.50)	−7.7772 (193.22)	−17.6783 (193.10)
18	3.0403 (188.69)	−17.6219 (191.03)	17.2470 (191.46)	13.4326 (191.70)
19	−0.1624 (188.16)	−1.2297 (187.70)	6.1617 (187.62)	6.5899 (187.55)
20	−0.3575 (187.09)	12.4957 (187.18)	−14.2824 (186.91)	−4.7287 (186.34)
21	−6.5469 (185.67)	−8.4962 (186.14)	2.3620 (186.40)	−3.7539 (185.26)
22	2.7632 (184.18)	0.6626 (184.74)	−0.9007 (185.06)	−0.0879 (184.65)
23	−2.9744 (183.00)	11.7132 (182.73)	4.8526 (182.20)	19.7030 (183.37)
24	6.9008 (180.03)	−0.0032 (181.46)	−7.2466 (181.92)	1.8221 (182.06)
25	−16.7052 (179.69)	0.2763 (180.59)	−5.8061 (180.58)	12.2385 (181.19)
26	−1.4204 (179.63)	−15.6249 (178.95)	7.9761 (179.96)	0.0309 (180.50)
27	1.4548 (178.62)	24.6149 (178.19)	1.7512 (178.13)	5.8872 (180.20)
28	−1.3711 (176.56)	4.1361 (176.96)	−0.4065 (177.10)	−1.4799 (178.27)
29	−2.1246 (176.41)	17.5186 (176.06)	−11.8169 (175.41)	−1.4130 (176.92)
30	0.8248 (175.86)	−7.8686 (175.56)	0.6706 (175.15)	5.1278 (176.68)
31	−0.1137 (174.57)	5.2611 (174.08)	1.7893 (174.78)	−2.9295 (174.47)
32	−10.0466 (173.73)	0.2179 (173.28)	0.4607 (172.79)	2.7172 (173.93)
33	2.1416 (171.13)	−5.5719 (171.97)	7.3439 (171.79)	−4.0121 (171.58)
34	−11.0366 (170.49)	20.5365 (169.49)	−4.5534 (168.65)	40.0913 (169.61)
35	2.3311 (167.56)	−23.2025 (168.01)	−1.1959 (168.20)	−2.9984 (168.47)
36	−1.3347 (166.45)	6.2280 (167.39)	4.5159 (167.37)	−35.8166 (168.07)
37	1.5229 (165.67)	−6.1635 (165.64)	0.2660 (166.64)	1.9497 (167.19)
38	21.6267 (164.46)	−7.6250 (163.76)	0.8703 (165.67)	−4.3558 (164.52)
39	2.6453 (164.18)	−9.6484 (163.31)	2.2289 (164.70)	3.6092 (164.26)
40	−11.3205 (163.71)	−1.3853 (163.18)	1.9715 (164.56)	−1.9751 (163.82)
41	25.2747 (163.56)	0.5810 (162.96)	−1.7280 (163.52)	−5.4087 (163.29)
42	0.3586 (162.65)	11.7961 (162.17)	−3.1625 (162.53)	5.5567 (162.40)
43	−2.2476 (162.48)	−21.4566 (162.02)	−11.2725 (162.10)	0.7937 (161.57)
44	31.7590 (161.81)	−14.4831 (161.22)	17.6397 (160.89)	−9.2328 (161.38)
45	−6.8119 (161.35)	−14.4927 (160.67)	1.1915 (160.40)	−44.5114 (161.01)
46	1.0919 (160.77)	13.3781 (160.10)	−1.7254 (159.82)	10.5456 (160.21)
47	−8.7521 (159.59)	−14.1978 (159.71)	8.0128 (158.54)	25.6164 (159.88)
48	3.4455 (159.07)	0.4147 (159.01)	−21.9747 (157.97)	−19.3566 (158.94)
49	8.6104 (158.76)	11.1628 (158.83)	38.9702 (157.39)	−3.0271 (158.55)
50	−6.6399 (158.46)	−18.8483 (157.85)	0.7224 (157.21)	−11.0998 (158.11)

Table 4.5. Rotational strengths in dipole velocity formalism and excitation wavelengths for the lowest-energy electronic transitions of the conformers of (*S*)-**1**, as obtained by TD-DFT calculations (B3LYP/TZ2P) in 2-propanol (IEFPCM solvation model).

j	R_j, 10^{-40} erg cm^3 (λ_j, nm)					
	(*S*)-**1l**	(*S*)-**1m**	(*S*)-**1n**	(*S*)-**1o**	(*S*)-**1p**	(*S*)-**1q**
1	0.1087 (321.15)	1.2549 (320.28)	−1.0025 (319.24)	−2.3491 (320.86)	0.3722 (319.31)	0.9549 (320.05)
2	6.7767 (301.20)	0.3727 (300.97)	0.9934 (301.17)	1.5649 (301.92)	0.4183 (300.15)	3.8521 (302.08)
3	−3.1227 (267.36)	3.5420 (267.16)	−5.1103 (267.35)	−16.5327 (268.05)	−1.2400 (266.42)	4.6227 (267.08)
4	16.3473 (261.35)	1.0574 (260.76)	−3.8942 (260.07)	−16.8451 (261.40)	−3.2774 (260.05)	7.4237 (260.49)
5	1.2734 (249.19)	−5.9826 (248.66)	4.1198 (248.67)	6.9773 (249.25)	−1.3323 (247.54)	−3.7531 (248.21)
6	1.0788 (246.07)	4.2166 (245.95)	−2.5440 (245.03)	−6.4981 (246.22)	1.5676 (245.15)	2.8482 (245.63)
7	10.8674 (235.33)	−2.6585 (240.84)	2.4803 (239.26)	3.1911 (241.01)	−3.2893 (239.46)	−4.6598 (236.40)
8	37.0189 (223.78)	−43.2446 (224.97)	37.6642 (224.40)	81.7275 (226.54)	−10.5218 (222.79)	−38.1663 (226.17)
9	36.2182 (220.42)	40.0022 (219.83)	−7.2202 (218.76)	−15.8828 (219.93)	7.1870 (218.48)	66.7473 (218.34)
10	−1.0133 (216.56)	15.7266 (217.15)	−17.7673 (217.29)	−4.8488 (217.99)	18.0115 (216.78)	−10.2030 (217.13)
11	−135.8149 (214.77)	2.5401 (215.68)	12.5777 (214.57)	−10.4949 (214.82)	1.1732 (215.34)	−8.1956 (215.98)
12	29.8838 (212.64)	41.9022 (212.19)	34.7402 (213.63)	−49.2555 (213.20)	32.1240 (214.64)	71.1986 (213.27)
13	10.7705 (208.72)	−15.3698 (209.55)	−39.7193 (211.19)	27.1274 (210.40)	−33.7795 (214.40)	−31.9946 (212.15)
14	−29.1621 (206.24)	−20.5786 (206.19)	−4.1728 (205.58)	22.2217 (204.80)	1.2071 (208.26)	−18.2671 (206.37)
15	11.3963 (204.86)	2.8056 (202.92)	−1.9794 (203.46)	−4.0228 (202.29)	5.3854 (205.76)	0.9436 (203.90)
16	−12.6364 (199.20)	30.4514 (197.88)	5.5897 (198.13)	−2.1190 (197.46)	14.6823 (198.74)	22.5794 (198.48)
17	−5.0814 (194.90)	−4.8328 (193.60)	19.5066 (193.67)	−0.3606 (193.41)	−14.9275 (193.24)	−1.6215 (193.95)
18	1.0981 (189.50)	−14.4976 (190.83)	−11.4609 (191.15)	13.7375 (191.65)	17.9384 (191.64)	−19.8027 (189.14)
19	0.5501 (188.75)	0.3011 (187.68)	−3.5107 (188.77)	2.7925 (187.51)	3.0304 (187.67)	1.7180 (188.01)
20	−0.7357 (188.24)	16.7426 (187.29)	−1.7900 (187.27)	−6.9808 (186.99)	−0.5313 (187.61)	9.3439 (186.83)
21	1.1024 (186.37)	−20.0855 (186.55)	−5.6247 (186.93)	−6.0961 (186.75)	−4.3003 (186.53)	−10.4483 (186.44)
22	−5.3109 (185.57)	1.2742 (184.34)	3.5446 (184.41)	0.2578 (184.59)	11.6944 (184.71)	6.4612 (185.19)
23	−1.2433 (183.71)	15.7842 (183.85)	−8.5421 (183.69)	−6.5412 (183.32)	3.3435 (184.33)	11.9355 (183.75)
24	−0.2692 (180.30)	0.2586 (182.44)	1.2137 (182.47)	0.7852 (182.95)	2.3084 (182.92)	−2.5023 (183.29)
25	1.5938 (179.93)	0.0716 (181.25)	−2.1405 (180.28)	−7.9936 (181.08)	−1.4674 (181.31)	1.8430 (181.54)
26	1.9752 (179.26)	0.2183 (179.30)	7.4204 (177.84)	12.2860 (178.31)	3.5188 (179.13)	−3.1424 (180.02)
27	−9.0787 (175.41)	12.5867 (175.71)	−4.3656 (176.16)	−8.2247 (176.69)	−7.0036 (178.31)	5.7446 (178.02)
28	−9.8298 (174.33)	19.6181 (175.13)	−0.1722 (175.68)	−11.8133 (175.19)	6.0612 (176.50)	2.9585 (177.08)
29	2.3460 (174.11)	−7.7007 (174.72)	−7.5116 (175.56)	0.2793 (174.74)	9.2272 (176.23)	0.7224 (176.90)
30	−3.0733 (172.89)	−0.0144 (172.87)	−1.2634 (172.65)	0.0636 (172.89)	−2.5534 (173.96)	0.8750 (174.49)
31	−1.7272 (172.54)	0.4190 (172.24)	0.7304 (172.55)	−0.9585 (172.62)	1.1365 (172.96)	−3.7474 (171.66)
32	−3.0553 (171.84)	0.6682 (172.05)	3.4693 (171.82)	9.3316 (172.04)	−3.2374 (171.50)	0.8647 (171.50)
33	−8.2109 (171.54)	14.2514 (170.20)	−8.3005 (169.86)	1.3918 (170.65)	39.7153 (170.14)	−18.0808 (169.97)
34	−2.0322 (169.64)	−1.2984 (168.79)	−19.3232 (169.06)	−8.4975 (169.13)	−51.8619 (168.98)	−3.4696 (169.12)
35	20.5713 (166.66)	−32.6212 (168.34)	15.6954 (167.89)	8.4932 (167.57)	−1.3817 (168.53)	0.0535 (167.49)
36	1.0162 (164.59)	−0.8801 (164.35)	0.0296 (166.26)	1.0892 (165.59)	−5.9756 (164.64)	9.0356 (166.58)
37	−2.4964 (164.34)	−24.6760 (163.75)	−0.8502 (165.55)	−12.7673 (165.46)	−1.9625 (164.24)	−3.9728 (164.30)
38	17.2457 (163.70)	0.5939 (163.46)	17.3351 (164.27)	21.0950 (165.18)	6.9200 (163.92)	3.3379 (163.81)
39	10.4152 (163.50)	−25.2590 (163.36)	−1.7388 (163.49)	−0.0176 (163.82)	−17.4515 (163.52)	1.3626 (163.09)
40	7.5549 (162.70)	13.7149 (162.61)	2.8769 (162.12)	−9.5865 (162.22)	20.5586 (162.60)	3.2044 (162.55)
41	−6.3760 (162.22)	10.0440 (162.17)	−1.9507 (161.82)	3.8157 (161.47)	−4.3305 (162.33)	−11.9440 (162.10)
42	22.2958 (161.76)	−3.0118 (161.02)	−31.8601 (161.57)	−1.0456 (161.28)	−31.6357 (161.93)	−12.4264 (161.44)
43	3.7993 (160.98)	6.0364 (160.67)	−1.6657 (160.61)	2.5615 (160.76)	16.0563 (160.71)	−8.1093 (161.01)
44	7.3818 (160.76)	−5.1432 (160.07)	−1.0320 (160.21)	6.5734 (160.12)	9.5417 (160.59)	15.3764 (160.41)
45	−1.6293 (160.31)	1.5540 (159.96)	20.8190 (159.89)	3.9881 (159.94)	−2.3108 (160.36)	−7.0668 (159.94)
46	−16.5687 (160.04)	−9.6781 (159.65)	−3.6176 (159.35)	−4.6864 (159.51)	6.1928 (159.60)	−0.9782 (159.31)
47	9.3611 (159.48)	−15.5388 (159.49)	−4.4679 (159.01)	2.5060 (158.72)	−1.0817 (159.41)	2.0982 (159.11)
48	−0.4684 (159.40)	7.8316 (158.87)	5.5575 (158.52)	−23.5490 (158.43)	−10.2430 (159.11)	12.3178 (158.66)
49	4.6429 (159.14)	1.6616 (158.54)	−2.6786 (158.09)	8.9204 (157.76)	−14.6849 (158.63)	−10.1062 (158.56)
50	−4.3024 (158.61)	−15.2452 (157.92)	−0.9636 (157.61)	−0.2811 (157.00)	−1.2522 (158.12)	4.4814 (158.17)

Figure 4.9. Theoretical ECD spectra for (*S*)-**1** ($\Delta\sigma = 0.3$ eV). *Blue:* gas phase, ΔE_{QM}-based conformational averaging. *Green:* 2-propanol (IEFPCM), ΔE_{QM}-based conformational averaging. *Red:* gas phase, ΔG-based conformational averaging. *Orange:* 2-propanol (IEFPCM), ΔG-based conformational averaging.

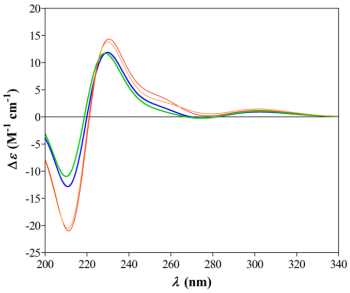

Table 4.6. Correlation coefficients (*r*) between theoretical ECD spectra of (*S*)-**1** and experimental ECD spectra for the enantiomeric fractions of **1**.

	gas phase		2-propanol (IEFPCM)	
	ΔE_{QM}-based	ΔG-based	ΔE_{QM}-based	ΔG-based
First-eluted on Hibar	−0.6229	−0.4969	−0.7271	−0.5293
Second-eluted on Hibar	0.6530	0.5264	0.7566	0.5573

Table 4.7. RMSD values obtained by comparison between the conformers of (*S*)-**1**, as obtained after DFT geometry optimisation (B3LYP/TZ2P) in gas phase. RMSD threshold value for conformational clustering: 0.01 Å.

MM Conf. ID	ΔE_{QM} (kcal mol^{-1})	RMSD, Å							QM Conf. ID
		(*S*)-**1a**	(*S*)-**1c**	(*S*)-**1f**	(*S*)-**1b**	(*S*)-**1d**	(*S*)-**1e**	(*S*)-**1g**	
(*S*)-**1a**	0.000	–	0.001	0.001	1.670	0.976	1.559	1.664	(*S*)-**1h**
(*S*)-**1c**	0.000	0.001	–	0.001	1.671	0.976	1.559	1.665	=
(*S*)-**1f**	0.000	0.001	0.001	–	1.670	0.976	1.559	1.664	=
(*S*)-**1b**	0.429	1.670	1.671	1.670	–	1.448	0.727	0.074	(*S*)-**1i**
(*S*)-**1d**	0.584	0.976	0.976	0.976	1.448	–	1.518	1.461	(*S*)-**1j**
(*S*)-**1e**	2.133	1.559	1.559	1.559	0.727	1.518	–	0.724	(*S*)-**1k**
(*S*)-**1g**	3.280	1.664	1.665	1.664	0.074	1.461	0.724	–	

Table 4.8. RMSD values obtained by comparison between the conformers of (*S*)-**1**, as obtained after DFT geometry optimisation (B3LYP/TZ2P) in 2-propanol (IEFPCM solvation model). RMSD threshold value for conformational clustering: 0.01 Å.

MM Conf. ID	ΔE_{QM} (kcal mol^{-1})	RMSD, Å							QM Conf. ID
		(*S*)-**1c**	(*S*)-**1b**	(*S*)-**1a**	(*S*)-**1f**	(*S*)-**1d**	(*S*)-**1e**	(*S*)-**1g**	
(*S*)-**1c**	0.000	–	1.661	1.034	1.034	0.967	1.576	1.661	(*S*)-**1l**
(*S*)-**1b**	0.406	1.661	–	1.509	1.509	1.455	0.726	0.040	(*S*)-**1m**
(*S*)-**1a**	0.428	1.034	1.509	–	0.001	0.721	1.433	1.516	(*S*)-**1n**
(*S*)-**1f**	0.428	1.034	1.509	0.001	–	0.721	1.433	1.516	=
(*S*)-**1d**	0.623	0.967	1.455	0.721	0.721	–	1.522	1.469	(*S*)-**1o**
(*S*)-**1e**	1.376	1.576	0.726	1.433	1.433	1.522	–	0.722	(*S*)-**1p**
(*S*)-**1g**	1.900	1.661	0.040	1.516	1.516	1.469	0.722	–	(*S*)-**1q**

Chapter 5

Difenoconazole

This chapter is based on a peer-reviewed publication:
Fengshou Dong, Jing Li, Bezhan Chankvetadze, Yongpu Cheng, Jun Xu, Xingang Liu, Yuanbo Li, Xiu Chen, Carlo Bertucci, Daniele Tedesco, Riccardo Zanasi, Yongquan Zheng (**2013**). Chiral triazole fungicide difenoconazole: Absolute stereochemistry, stereoselective bioactivity, aquatic toxicity, and environmental behavior in vegetables and soil. *Environmental Science and Technology* 47, 3386–3394.

Abstract: In this study, the systemic assessments of the stereoisomers of triazole fungicide difenoconazole are reported for the first time, including absolute stereochemistry, stereoselective bioactivity toward pathogens (*Alternaria sonali*, *Fulvia fulva*, *Botrytis cinerea*, and *Rhizoctonia solani*), and toxicity toward aquatic organisms (*Scenedesmus obliquus*, *Daphnia magna*, and *Danio rerio*). Moreover, the stereoselective degradation of difenoconazole in vegetables (cucumber, *Cucumis sativus* and tomato, *Lycopersicon esculentum*) under field conditions and in soil under laboratory-controlled conditions (aerobic and anaerobic) was investigated. There were 1.33–24.2-fold and 1.04–6.78-fold differences in bioactivity and toxicity, respectively. Investigations on the stereoselective degradation of difenoconazole in vegetables showed that the highest-toxic and lowest-bioactive (2*S*,4*S*)-stereoisomer displays a different enrichment behavior in different plant species. Under aerobic or anaerobic conditions, (2*R*,4*R*)- and (2*R*,4*S*)-difenoconazole were preferentially degraded in the soil. Moreover, difenoconazole was configurationally stable in the test soil matrices. On the basis of biological activity, ecotoxicity, and environmental behavior, it is likely that the use of pure (2*R*,4*S*)-difenoconazole instead of the commercial stereoisomer mix may help to increase the bioactivity and reduce environmental pollution.

Acknowledgements: This work was financially supported by the Nature Science Foundation of China (NSFC, 31071706 and 31272071), the foundation of the National Basic Research Program of China (The 973 Program, Grant no. 2009CB119000), the Italian PRIN 2008 program (Italian Ministry of Education, University and Research). Some QM calculations were carried out on the CINECA HPC facilities based in Casalecchio di Reno, Italy; access was provided through the ISCRA Class C Project IsC08_SCCFPM (ID no. HP10CU0YHL). NMR experiments were performed at the Institute of Organic Synthesis and Photoreactivity (ISOF) of the National Research Center (CNR) in Bologna, Italy, under the supervision of Dr. Greta Varchi.

Difenoconazole (compound **1**, Figure 5.1A; *cis*,*trans*-3-chloro-4-[4-methyl-2-(1*H*-1,2,4-triazol-1-ylmethyl)-1,3-dioxolan-2-yl]phenyl-4-chloro phenyl ether), is a broad-spectrum 1,2,4-triazole fungicide used for the control of fungal diseases on fruits, vegetables, cereals, and other field crops.[139,140] The compound was synthesized as a novel demethylation inhibitor (DMI) fungicide and was widely applied for its excellent fast-acting and prominent systemic activity. This fungicide was associated with an increase in the incidence of hepatocellular adenomas and carcinomas in the group of male and female mice following long-term dietary exposure;[141] moreover, **1** was identified as an inhibitor of aromatase activity in human adrenocortical carcinoma cell line H295R.[142,143]

Figure 5.1. A: Chemical structure and atom numbering of **1**. **B:** Structures of the four stereoisomers of **1**. **C:** enantioselective HPLC analysis on the stereoisomer mix of **1** (Chiralcel OJ-H column, mobile phase: *n*-hexane/ethanol 90:10 (v/v), 0.8 mL min^{-1}, 20 °C; DAD detection at 220 nm).

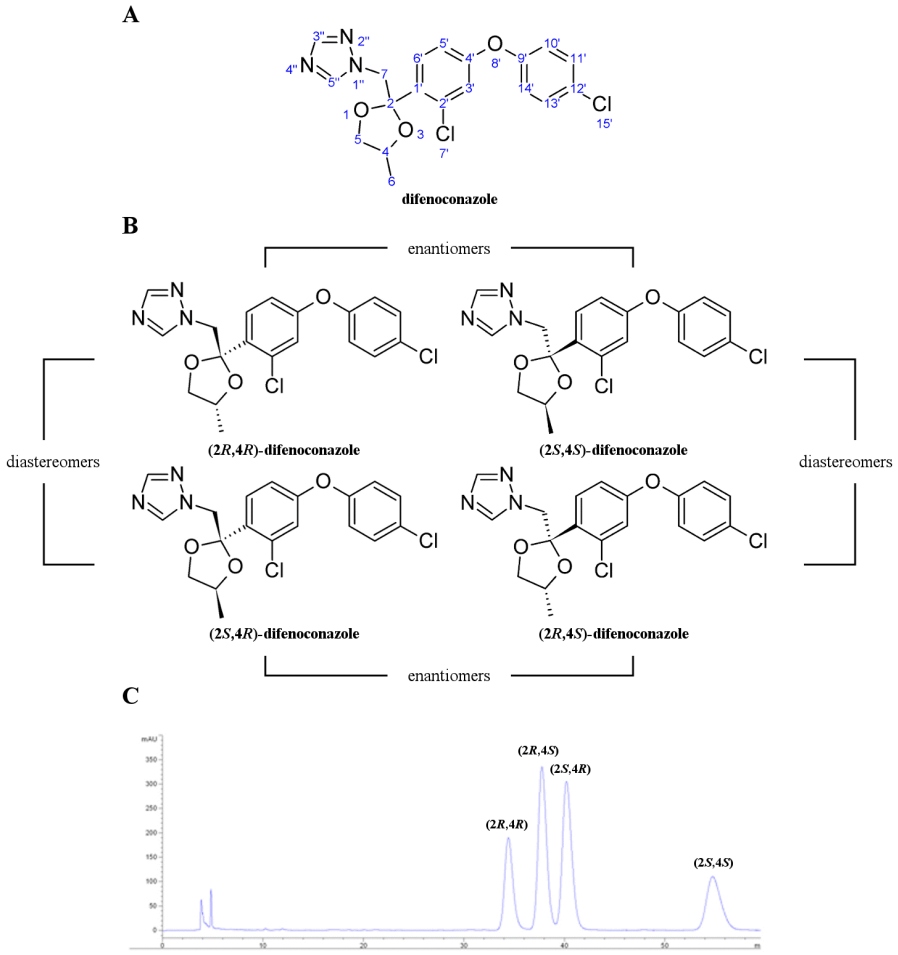

Compared with other triazole fungicides, **1** is reported to possess relatively high acute toxicity to a wide range of aquatic organisms.[141] With respect to its wide application on crops (especially on rice), the contamination of surface aquatic ecosystems by **1** is of a great environmental concern. However, since this fungicide is used worldwide as foliage-spray or seed-treatment to control vegetables (e.g., tomato and cucumber) diseases, it is essential to understand the fate of **1** in vegetables and soil for accurate assessment of its stress to food and environment.

As **1** possesses two chiral centres, it can exist in four stereoisomeric forms (Figure 5.1B). Because of their different molecular configurations, stereoisomers of chiral pesticides may differ in their binding to structure-sensitive biological receptors and naturally occurring chiral biomolecules. Several chiral pesticides also have stereoselective toxicity, such as cytotoxicity, endocrine disruption, and carcinogenesis, to non-target biota.[144–146] The processes of absorption, distribution, and degradation in organisms and the environment are often stereoselective.[147–151] Stereoselectivity in these processes may result in ecotoxicological effects that cannot be predicted from our existing knowledge. The stereospecific toxicities and degradation rates of chiral pesticides indicate that the traditional practice of treating them as single compounds in risk assessment may well be inappropriate. Therefore, the role of stereoselectivity in environmental safety of current chiral pesticides should be taken into account in risk assessment and regulatory decisions. However, until now, stereoselectivity in biological activity, ecotoxicological effects, and environmental fate of **1** is still unknown. Thus, it is essential to get stereospecific information in order to make a more accurate benefit-risk evaluation. The presence of multiple stereoisomers complicates chemical analysis, interpretation of activity, toxicity, degradation, and risk assessment.

In this study, the four stereoisomers of **1** were separated and collected, and their stereochemistry was fully characterised in order to assign the correct absolute configuration to each stereoisomer. Subsequently, the bioactivity toward pathogens (*Alternaria sonali*, *Fulvia fulva*, *Botrytis cinerea*, and *Rhizoctonia solani*), and the acute toxicity toward freshwater green algae *Scenedesmus obliquus* (Chlorophyceae), water fleas *Daphnia magna* (Branchiopoda), and tropical fish *Danio rerio* (Actinopterygii) were determined for the parent pesticide and for the single stereoisomers of **1**. Stereoselectivity was further evaluated during biodegradation in vegetables (cucumber, *Cucumis sativus* and tomato, *Lycopersicon esculentum*) and soil under greenhouse and laboratory conditions. Meanwhile, the stabilities of the four individual pure stereoisomers of **1** in soil were also assessed. The results of this study will be relevant for the assessment of a possible substitution

of the commercial stereoisomer mix with stereoisomerically enriched **1**, which may be more effective and less toxic toward nontarget organisms.

5.1 Materials and methods

> Details on the materials and methods used for the enantioselective HPLC analysis and biological tests on the stereoisomers of **1** are reported in Dong *et al.* (**2013**), *Environ. Sci. Technol.* *47*, 3386.

Previous assignments of ^{1}H-NMR peaks[152] left the relative configuration of diastereomers unclear; the relative configuration of the diastereomers of **1** was therefore determined by ^{1}H-nuclear magnetic resonance (NMR) spectroscopy, one-dimensional ^{1}H-^{1}H nuclear Overhauser effect correlation spectroscopy (^{1}H-^{1}H 1D-NOESY) and two-dimensional ^{1}H-^{1}H rotating-frame Overhauser effect correlation spectroscopy (^{1}H-^{1}H 2D-ROESY) performed on the pure stereoisomers. The absolute configuration of the four stereoisomers was then determined by electronic circular dichroism (ECD) spectroscopy and quantum mechanical (QM) calculations based on time-dependent density functional theory (TD-DFT).

5.1.1 Experimental spectroscopy

NMR spectra of the diastereomers of **1** in $CDCl_3$ ($\sim$ 10 mg mL^{-1}) were measured on a Varian Mercury 400 MHz NMR spectrometer. The experimental ECD spectrum of each stereoisomer was measured in 2-propanol (concentration 0.5 mM) using a 10 mm pathlength in the 350–255 nm spectral range and a 0.5 mm pathlength in the 255–200 nm range. Measurements were carried out at 25 °C on a Jasco (Tōkyō, Japan) J-810 spectropolarimeter equipped with a PTC-423S Peltier-type temperature control system, using a 1 nm spectral bandwidth, a 0.2 nm data interval, a 20 nm min^{-1} scan rate and a 2 sec time constant.

5.1.2 Computational spectroscopy

QM calculations were performed on one enantiomer for each enantiomeric pair, namely on (2*S*,4*S*)-**1** and (2*S*,4*R*)-**1**. A preliminary conformational search was performed at a molecular mechanics (MM) level using the MMFF94s force field[125] and the Spartan'02 software;[126] an energy threshold of 2 kcal mol^{-1} was set for

the indentification of the low-energy conformers (Tables 5.1 and 5.2). DFT geometry optimisation at the B97D/TZ2P level[153,154] (Tables 5.3–5.6) and TD-DFT calculations at the PBE0/TZ2P level[155–157] were performed on the identified MM conformers using the Gaussian 09 software package.[158] Each calculation was carried out implementing the IEFPCM solvation model for 2-propanol.[114,136] The TZ2P basis set consisted in consisted in Dunning's $[5s3p/3s]$ contraction[135] of Huzinaga's primitive $[10s6p/5s]$ set[134] with 2 sets of polarisation functions (α_p = 1.5, 0.375 for H; α_d = 1.5, 0.375 for C; α_d = 1.6, 0.4 for N; α_d = 1.7, 0.425 for O); for chlorine, McLean and Chandler's $[6s5p]$ contraction[159] of Huzinaga's primitive $[12s9p]$ set[160] with 2 sets of polarisation functions (α_d = 1.072, 0.357)[161] was used.

TD-DFT calculations were performed to determine the rotational strengths (R_j) and excitation wavelengths (λ_j) for the first 50 excited states of each optimised conformer (Tables 5.7 and 5.8). The theoretical ECD spectra were then determined by Gaussian approximation of all R_j values for each conformer ($\Delta\sigma = 0.4$ eV), and by conformational averaging based on the relative population of conformers, as calculated by Boltzmann statistics at 298.15 K and 1 atm using the relative free energies (ΔG).[28,113]

5.2 Results and discussion

Results for the enantioselective HPLC analysis and biological tests on the stereoisomers of **1** are reported in Dong *et al.* **(2013)**, *Environ. Sci. Technol. 47*, 3386.

5.2.1 Nuclear magnetic resonance spectroscopy

The main differences in the ^{1}H-NMR spectra of diastereomers are due to the chemical shifts of hydrogen atoms on the dioxolane ring. The H atom on C4 (d5) is coupled with the C6-methyl H atoms (^3J = 6 Hz) and with the diastereotopic H atoms on C5 ($^3J_{cis}$ = 6 Hz; $^3J_{trans}$ = 8 Hz); this signal is significantly more upfield in Figure 5.2 (δ_H = 3.83) than in Figure 5.3 (δ_H = 4.09). On the other hand, the H atom on C5 lying on the same side of the methyl group (t) is coupled with its vicinal H atom (^2J = 8 Hz) and with the H atom on C4 ($^3J_{trans}$ = 8 Hz); this signal is significantly more downfield in Figure 5.2 (δ_H = 3.30) than in Figure 5.3 (δ_H = 3.09).

Figure 5.2. ^{1}H-NMR spectrum in $CDCl_3$ of the fourth-eluted stereoisomer of **1**.

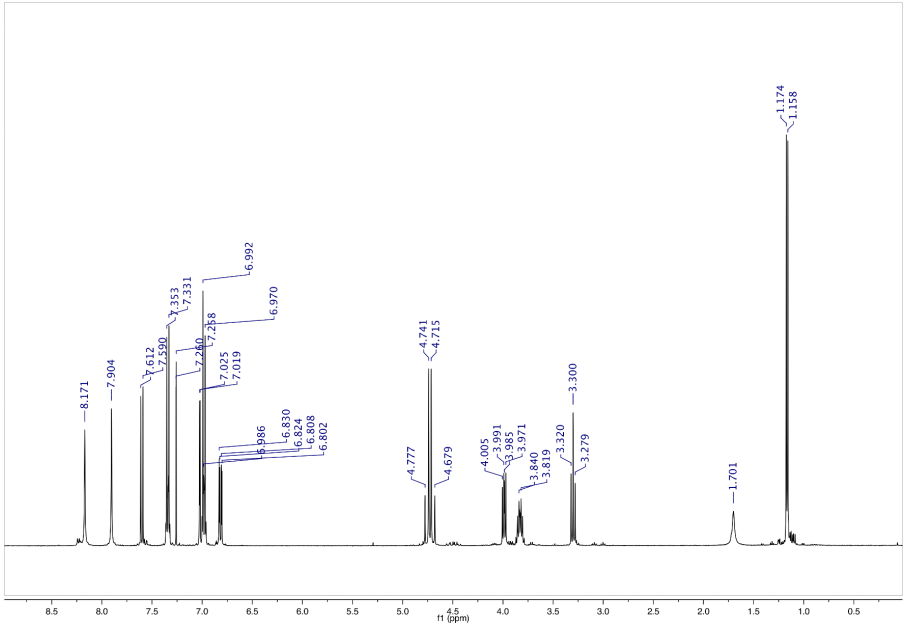

Figure 5.3. ^{1}H-NMR spectrum in $CDCl_3$ of the second-eluted stereoisomer of **1**.

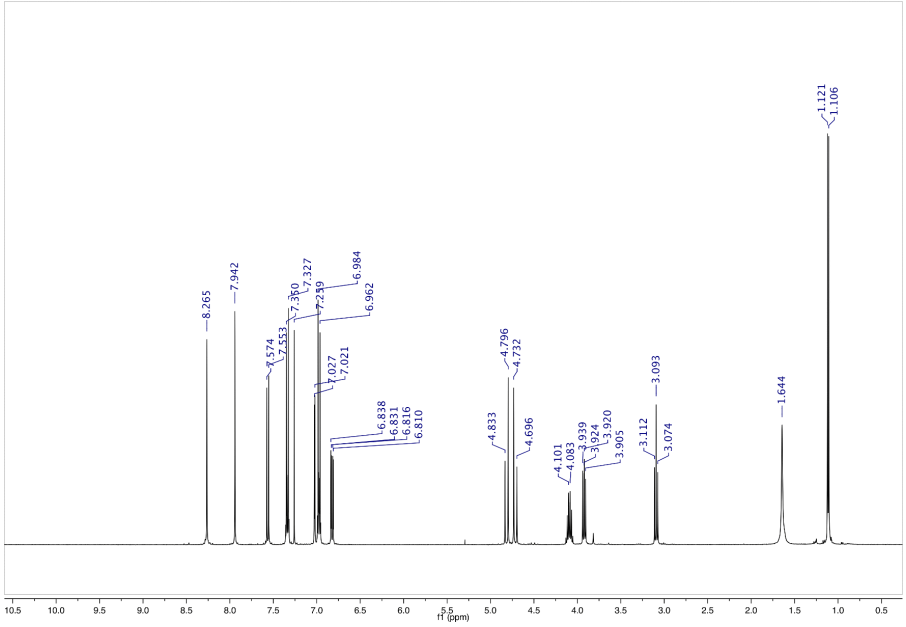

Figure 5.4. ^{1}H-^{1}H 1D-NOESY spectrum in $CDCl_3$ of the fourth-eluted stereoisomer of **1**.

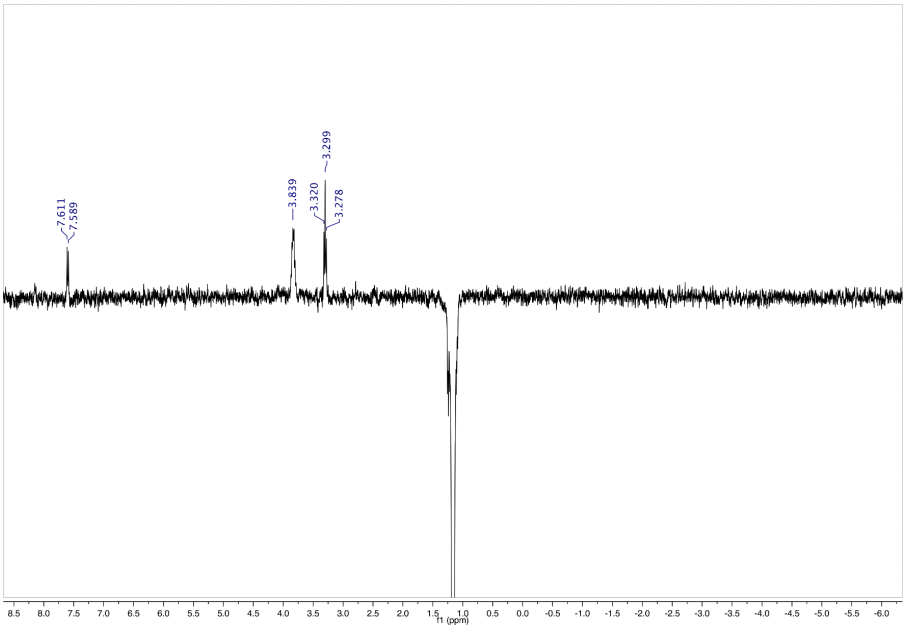

Figure 5.5. ^{1}H-^{1}H 1D-NOESY spectrum in $CDCl_3$ of the second-eluted stereoisomer of **1**.

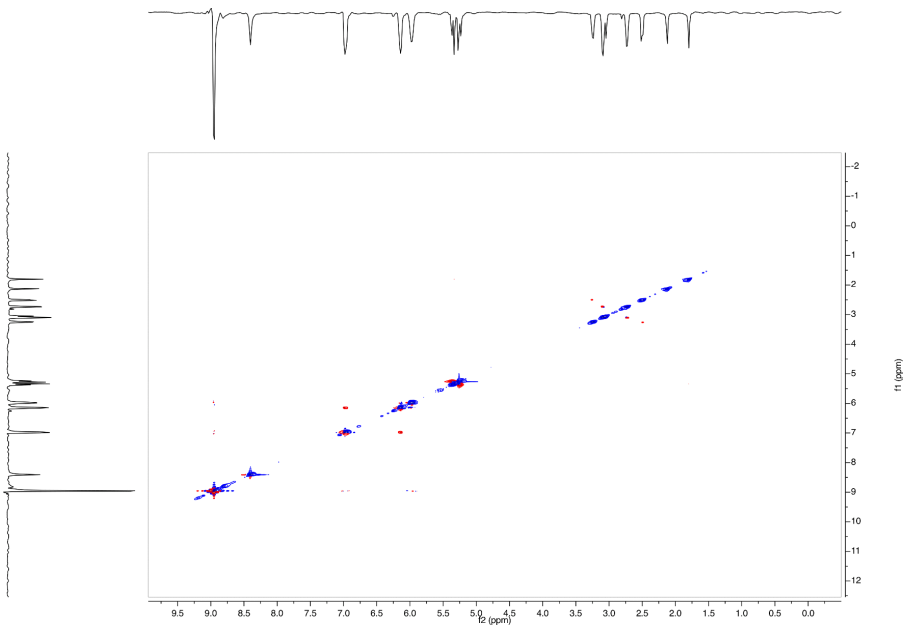

^{1}H-^{1}H 1D-NOESY analysis on the fourth-eluted stereoisomer (Figure 5.4) showed a positive NOE on the C6′-aromatic H atom (δ_H = 7.60) when the C6-methyl H atoms (δ_H = 1.16) are selectively irradiated, suggesting that the methyl group and the 2-chlorophenyl moiety lie on the same side of the dioxolane ring. For the second-eluted stereoisomer, no NOE signals are observed for aromatic H atoms: this was confirmed by ^{1}H-^{1}H 2D-ROESY analysis (Figure 5.5). On this basis, the fourth-eluted stereoisomer can be assigned to the (2*S*,4*S*)/(2*R*,4*R*) enantiomeric pair, and the second-eluted stereoisomer to the (2*S*,4*R*)/(2*R*,4*S*) pair.

5.2.2 Electronic circular dichroism spectroscopy

The experimental ECD spectra of the stereoisomers of **1** (Figure 5.6) clearly show the stereochemical relationship between the different fractions: the ECD spectra are opposite for first- and fourth-eluted fractions on the Chiralcel OJ-H column, and the same holds for the second- and third-eluted fractions. Experimental UV spectra are reported in Figure 5.7.

5.2.3 Quantum mechanical calculations

The comparison between the calculated ECD spectra for (2*S*,4*S*)-**1** and (2*S*,4*R*)-**1** and the experimental ECD spectra (Figure 5.6) allows to assign the absolute configuration to each stereoisomer. The extreme weakness of the experimental ECD signals centred at around 285 nm ($\Delta\varepsilon \sim \pm 0.05$) does not allow a reliable calculation of theoretical properties for these bands; therefore, the low-energy region is not considered in the comparison between calculated and experimental ECD spectra. TD-DFT calculations tend to underestimate excitation energies,[111] resulting in a shift of calculated ECD bands towards longer wavelengths with respect to the experimental spectra. Considering this known issue, the profiles of experimental ECD bands in the high-energy region are reproduced by TD-DFT calculations; the experimental ECD spectra of the third- and fourth-eluted fractions have the same signs and shapes as the calculated ECD spectra of (2*S*,4*R*)-**1** and (2*S*,4*S*)-**1**, respectively. On this basis, the opposite absolute configurations can also be assigned to the respective enantiomers, and the elution order of the stereoisomers of **1** on the Chiralcel OJ-H column under the optimised chromatographic conditions can be assessed (Figure 5.1C): (2*R*,4*R*), (2*R*,4*S*), (2*S*,4*R*), (2*S*,4*S*).

Figure 5.6. Experimental and calculated ECD spectra for the stereoisomers of **1**. *Solid:* experimental, 0.5 mm pathlength (left Y axis). *Dashed:* experimental, 10 mm pathlength (right Y axis). *Dotted:* calculated (left Y axis). **A:** Experimental spectra of the first-eluted (*blue*) and fourth-eluted (*red*) stereoisomers compared to the calculated spectrum of (2*S*,4*S*)-**1** (*green*). **B:** Experimental spectra of the second-eluted (*red*) and third-eluted (*blue*) stereoisomers compared to the calculated spectrum of (2*S*,4*R*)-**1** (*green*).

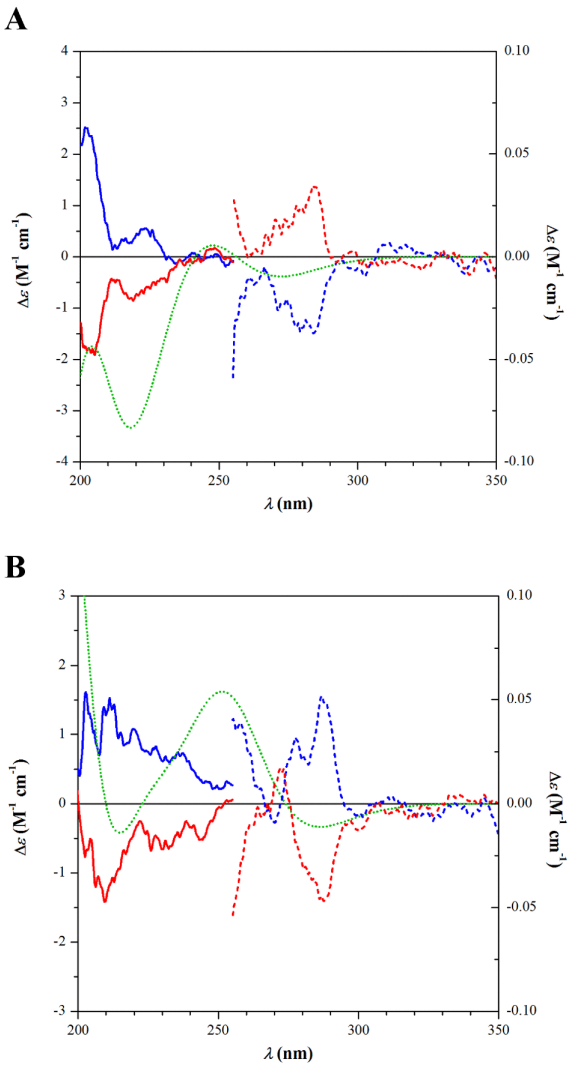

Figure 5.7. Experimental UV spectra for the stereoisomers of **1**. *Solid:* experimental, 0.5 mm pathlength (left Y axis). *Dashed:* experimental, 10 mm pathlength (right Y axis). **A:** (2*R*,4*R*)-**1** (*blue*) and (2*S*,4*S*)-**1** (*red*). **B:** (2*R*,4*S*)-**1** (*red*) and (2*S*,4*R*)-**1** (*blue*).

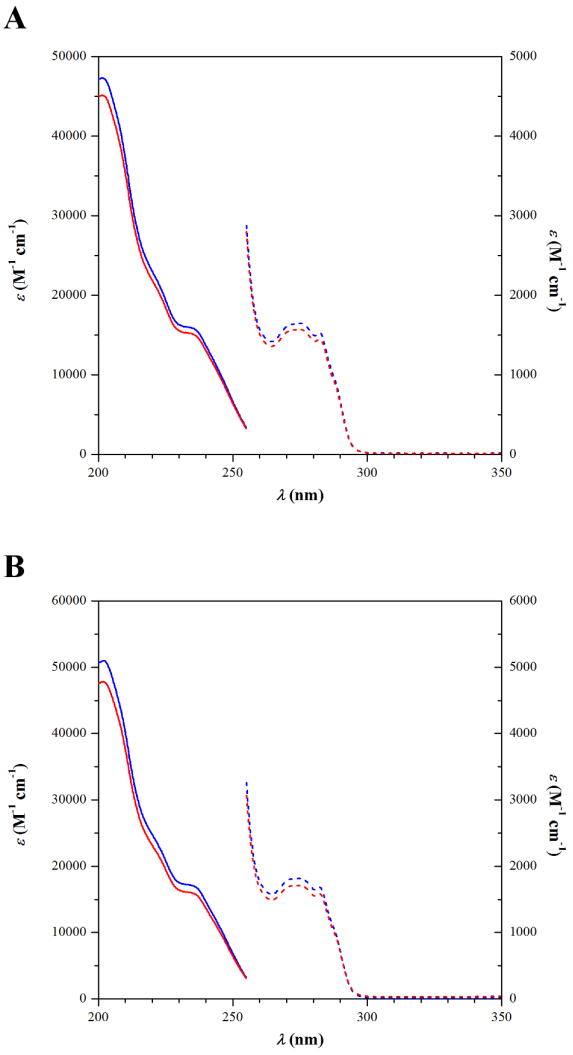

5.3 Conclusions

In the present study, the four stereoisomers of **1** exhibit obvious differences in activity to the target species and toxicity to nontarget species, respectively. The result showed that (2*R*,4*S*)-**1** is the stereoisomer with the highest bioactivity and the lowest ecotoxicity. In contrast, the (2*S*,4*S*)-**1** exhibits the highest ecotoxicity and lowest bioactivity. The higher activity of (2*R*,4*S*)-**1** enriched in the plants will bring about greater fungicidal activity, which would help in protecting against plant disease. Moreover, the stereoselective degradation of **1** in soil showed that the (2*R*,4*S*)-**1** preferentially degraded in the soil. Furthermore, no evidence of interconversion was observed among the four stereoisomers. A potential substitution of the stereoisomer mix with stereoisomer-enriched compounds should always be considered as it may lower application rates at similar field performance, may result in lower residues in crops and environment, and may lead to reduced side effects on nontarget species. Overall, results from this study provide an important justification for potential substitution of the commercial mix with (2*R*,4*S*)-**1**. Meanwhile, (2*R*,4*S*)-**1** should be persistent enough for efficient target kill. From the perspective of fungicidal activity, toxicity, and behaviour in plants and soil, additional efforts for the production of enantiomer enriched **1** would thus be supported.

Table 5.1. Energies and selected dihedral angles for the conformers of (2*S*,4*S*)-**1**, as obtained after MMFF94s conformational search. θ_1: O1–C5–C4–O3 dihedral; θ_2: C2–O3–C4–C6 dihedral; ϕ_1: C3–C2–C1′–C2′ dihedral; ϕ_2: C3′–C4′–C8′–C9′ dihedral; ψ_1: C3–C2–C7–N1″ dihedral; ψ_2: C2–C7–N1″–N2″ dihedral.

MM ID	E_{MM} (kcal mol^{-1})	ΔE_{MM} (kcal mol^{-1})	θ_1 (deg)	θ_2 (deg)	ϕ_1 (deg)	ϕ_2 (deg)	ψ_1 (deg)	ψ_2 (deg)	QM ID
mol001	66.003	0.000	−35.207	−93.533	50.233	53.566	−176.590	107.473	**a**
mol012	66.038	0.035	−35.216	−93.513	50.134	128.467	−176.474	107.523	**b**
mol034	66.148	0.145	−35.750	−94.887	−168.237	−53.619	−68.307	−107.728	**c**
mol045	66.179	0.176	−35.756	−94.862	−168.155	−128.380	−68.416	−107.758	**d**
mol056	66.434	0.430	−35.268	−93.640	49.903	−47.875	−176.752	108.511	**e**
mol059	66.457	0.453	−35.267	−93.638	50.027	−135.298	−176.670	108.666	**f**
mol060	66.566	0.563	−35.784	−94.966	−167.788	47.794	−68.245	−108.728	**g**
mol061	66.574	0.571	−35.790	−94.935	−167.835	135.370	−68.294	−108.866	**h**
mol003	66.678	0.675	−33.243	−95.318	45.962	−49.112	54.140	106.678	**i**
mol004	66.716	0.712	−33.238	−95.325	46.149	−134.766	54.130	106.697	**j**
mol009	66.828	0.825	−33.147	−95.314	46.422	47.606	54.410	107.089	**k**
mol006	66.886	0.882	−33.159	−95.305	46.304	136.932	54.382	107.118	**l**
mol008	67.383	1.380	−35.644	−95.243	50.007	56.405	−171.346	−90.091	**m**
mol010	67.465	1.462	−35.677	−95.202	49.506	132.196	−171.898	−90.352	**n**
mol014	67.724	1.721	−35.777	−95.542	48.384	−48.839	−178.228	−95.691	**o**
mol015	67.727	1.724	−35.785	−95.524	48.458	−136.078	−178.301	−95.737	**p**
mol016	67.750	1.747	−35.511	−96.251	−167.635	−56.960	−74.948	88.989	**q**
mol017	67.831	1.828	−32.012	−96.093	−163.636	49.087	68.201	−97.308	**r**
mol018	67.832	1.829	−35.528	−96.171	−167.158	−131.147	−74.491	89.142	**s**
mol019	67.850	1.847	−32.014	−96.078	−163.746	134.777	68.199	−97.339	**t**

Table 5.2. Energies and selected dihedral angles for the conformers of (2*S*,4*R*)-**1**, as obtained after MMFF94s conformational search. θ_1: O1–C5–C4–O3 dihedral; θ_2: C2–O3–C4–C6 dihedral; ϕ_1: C3–C2–C1′–C2′ dihedral; ϕ_2: C3′–C4′–C8′–C9′ dihedral; ψ_1: C3–C2–C7–N1″ dihedral; ψ_2: C2–C7–N1″–N2″ dihedral.

MM ID	E_{MM} (kcal mol^{-1})	ΔE_{MM} (kcal mol^{-1})	θ_1 (deg)	θ_2 (deg)	ϕ_1 (deg)	ϕ_2 (deg)	ψ_1 (deg)	ψ_2 (deg)	QM ID
mol001	64.871	0.000	−39.330	158.293	51.437	53.509	−176.678	106.359	**a**
mol012	64.909	0.038	−39.329	158.296	51.326	128.415	−176.559	106.424	**b**
mol023	65.029	0.158	−39.668	156.373	−168.788	−53.510	−67.875	−106.485	**c**
mol034	65.066	0.195	−39.668	156.389	−168.690	−128.302	−67.977	−106.518	**d**
mol045	65.360	0.489	−39.440	158.103	51.170	−47.002	−176.784	107.369	**e**
mol056	65.386	0.515	−39.431	158.107	51.259	−136.025	−176.718	107.520	**f**
mol058	65.491	0.620	−39.742	156.225	−168.429	47.091	−67.854	−107.482	**g**
mol060	65.509	0.639	−39.741	156.247	−168.484	135.803	−67.903	−107.620	**h**
mol002	65.605	0.734	−38.204	155.616	47.219	−48.343	55.500	107.544	**i**
mol003	65.642	0.771	−38.196	155.616	47.366	−135.510	55.505	107.563	**j**
mol004	65.693	0.822	−38.159	155.784	47.724	47.712	55.866	108.101	**k**
mol005	65.753	0.882	−38.163	155.781	47.588	136.834	55.840	108.129	**l**
mol007	66.535	1.664	−40.070	156.073	51.020	56.541	−169.626	−88.642	**m**
mol008	66.608	1.737	−36.793	154.904	−164.779	48.313	65.623	−101.407	**n**
mol010	66.626	1.755	−40.078	156.074	50.494	131.222	−170.102	−88.857	**o**
mol013	66.638	1.767	−36.794	154.917	−164.897	135.324	65.616	−101.435	**p**
mol014	66.724	1.853	−36.698	155.003	−165.142	−47.555	65.204	−102.094	**q**
mol055	66.784	1.913	−36.701	155.013	−165.014	−136.826	65.231	−102.134	**r**

Table 5.3. Electronic energies, free energies and Boltzmann populations at 298.15 K and 1 atm for the conformers of (2*S*,4*S*)-**1**, as obtained after B97D/TZ2P/IEFPCM(2-propanol) optimisation.

Conf. ID	E_{QM} (Ha)	ΔE_{QM} (kcal mol^{-1})	χ_{QM} (%)	G (Ha)	ΔG (kcal mol^{-1})	χ_G (%)
(*S*,*S*)-**1a**	−2044.22059349	0.156	6.11	−2043.952726	0.495	5.22
(*S*,*S*)-**1b**	−2044.22060824	0.147	6.21	−2043.953013	0.315	7.08
(*S*,*S*)-**1c**	−2044.22035681	0.305	4.76	−2043.952773	0.466	5.49
(*S*,*S*)-**1d**	−2044.22031867	0.329	4.57	−2043.952995	0.326	6.94
(*S*,*S*)-**1e**	−2044.22040992	0.271	5.03	−2043.952500	0.637	4.11
(*S*,*S*)-**1f**	−2044.22025237	0.370	4.26	−2043.953292	0.140	9.51
(*S*,*S*)-**1g**	−2044.22009244	0.471	3.60	−2043.952761	0.473	5.42
(*S*,*S*)-**1h**	−2044.22010556	0.462	3.65	−2043.952099	0.889	2.69
(*S*,*S*)-**1i**	−2044.22084224	0.000	7.96	−2043.951870	1.032	2.11
(*S*,*S*)-**1j**	−2044.22071056	0.083	6.92	−2043.952442	0.673	3.87
(*S*,*S*)-**1k**	−2044.22071774	0.078	6.97	−2043.952659	0.537	4.86
(*S*,*S*)-**1l**	−2044.22056832	0.172	5.95	−2043.952832	0.429	5.84
(*S*,*S*)-**1m**	−2044.22012631	0.449	3.73	−2043.953051	0.291	7.37
(*S*,*S*)-**1n**	−2044.22011398	0.457	3.68	−2043.953515	0.000	12.05
(*S*,*S*)-**1o**	−2044.21990672	0.587	2.95	−2043.952759	0.474	5.41
(*S*,*S*)-**1p**	−2044.21978655	0.662	2.60	−2043.951994	0.954	2.41
(*S*,*S*)-**1q**	−2044.21983927	0.629	2.75	−2043.951604	1.199	1.59
(*S*,*S*)-**1r**	−2044.22083386	0.005	7.89	−2043.951833	1.055	2.03
(*S*,*S*)-**1s**	−2044.21995209	0.559	3.10	−2043.951752	1.106	1.86
(*S*,*S*)-**1t**	−2044.22076313	0.050	7.32	−2043.952507	0.633	4.14

Table 5.4. Electronic energies, free energies and Boltzmann populations at 298.15 K and 1 atm for the conformers of (2*S*,4*R*)-**1**, as obtained after B97D/TZ2P/IEFPCM(2-propanol) optimisation. Conformer (*S*,*R*)-**1n** was not considered because the optimised structure showed an imaginary frequency.

Conf. ID	E_{QM} (Ha)	ΔE_{QM} (kcal mol^{-1})	χ_{QM} (%)	G (Ha)	ΔG (kcal mol^{-1})	χ_G (%)
(*S*,*R*)-**1a**	−2044.22107094	0.201	6.39	−2043.953062	0.749	4.03
(*S*,*R*)-**1b**	−2044.22103251	0.225	6.14	−2043.953883	0.233	9.61
(*S*,*R*)-**1c**	−2044.22083346	0.350	4.97	−2043.954142	0.071	12.65
(*S*,*R*)-**1d**	−2044.22087985	0.321	5.22	−2043.953461	0.498	6.15
(*S*,*R*)-**1e**	−2044.22075896	0.397	4.59	−2043.953610	0.405	7.20
(*S*,*R*)-**1f**	−2044.22068169	0.445	4.23	−2043.953022	0.774	3.86
(*S*,*R*)-**1g**	−2044.22058255	0.508	3.81	−2043.954255	0.000	14.26
(*S*,*R*)-**1h**	−2044.22053627	0.537	3.63	−2043.953399	0.537	5.76
(*S*,*R*)-**1i**	−2044.22113832	0.159	6.87	−2043.952604	1.036	2.48
(*S*,*R*)-**1j**	−2044.22106274	0.206	6.34	−2043.952522	1.087	2.27
(*S*,*R*)-**1k**	−2044.22113023	0.164	6.81	−2043.952661	1.000	2.63
(*S*,*R*)-**1l**	−2044.22100614	0.242	5.97	−2043.952923	0.836	3.48
(*S*,*R*)-**1m**	−2044.22070746	0.429	4.35	−2043.953536	0.451	6.66
(*S*,*R*)-**1o**	−2044.22081508	0.362	4.88	−2043.952151	1.320	1.54
(*S*,*R*)-**1p**	−2044.22134218	0.031	8.52	−2043.953066	0.746	4.05
(*S*,*R*)-**1q**	−2044.22139141	0.000	8.98	−2043.953552	0.441	6.77
(*S*,*R*)-**1r**	−2044.22131862	0.046	8.31	−2043.953529	0.456	6.61

Table 5.5. Selected dihedral angles for the conformers of (2*S*,4*S*)-**1**, as obtained after B97D/TZ2P/IEFPCM(2-propanol) optimisation. θ_1: O1–C5–C4–O3 dihedral; θ_2: C2–O3–C4–C6 dihedral; ϕ_1: C3–C2–C1′–C2′ dihedral; ϕ_2: C3′–C4′–C8′–C9′ dihedral; ψ_1: C3–C2–C7–N1″ dihedral; ψ_2: C2–C7–N1″–N2″ dihedral.

Conf. ID	θ_1 (deg)	θ_2 (deg)	ϕ_1 (deg)	ϕ_2 (deg)	ψ_1 (deg)	ψ_2 (deg)
(*S*,*S*)-**1a**	−37.455	−90.400	53.135	45.678	−176.501	95.867
(*S*,*S*)-**1b**	−37.889	−90.711	51.729	148.076	−176.653	96.601
(*S*,*S*)-**1c**	−36.788	−92.063	−173.219	−35.241	−64.139	−94.767
(*S*,*S*)-**1d**	−36.931	−90.746	−172.081	−144.656	−65.007	−94.849
(*S*,*S*)-**1e**	−37.650	−90.703	51.816	−25.388	−177.579	95.997
(*S*,*S*)-**1f**	−37.318	−89.626	52.022	−152.126	−178.009	97.684
(*S*,*S*)-**1g**	−36.778	−91.733	−171.641	29.187	−63.591	−94.196
(*S*,*S*)-**1h**	−36.815	−91.639	−172.638	152.102	−64.025	−94.506
(*S*,*S*)-**1i**	−36.054	−89.918	50.201	−26.559	59.320	93.919
(*S*,*S*)-**1j**	−35.793	−90.413	50.727	−156.086	58.614	93.946
(*S*,*S*)-**1k**	−35.911	−90.385	51.222	25.798	58.859	93.902
(*S*,*S*)-**1l**	−35.725	−90.642	50.427	152.024	59.018	93.284
(*S*,*S*)-**1m**	−37.648	−90.748	53.197	40.490	−170.427	−81.311
(*S*,*S*)-**1n**	−37.879	−90.316	51.061	145.965	−172.555	−83.421
(*S*,*S*)-**1o**	−37.754	−90.725	51.431	−25.464	−172.162	−83.806
(*S*,*S*)-**1p**	−37.192	−90.026	50.423	−153.487	−177.690	−88.974
(*S*,*S*)-**1q**	−36.663	−89.184	−171.648	−28.533	−70.328	86.323
(*S*,*S*)-**1r**	−35.864	−91.669	−171.193	27.531	68.764	−88.340
(*S*,*S*)-**1s**	−12.173	122.311	172.779	114.567	77.367	38.315
(*S*,*S*)-**1t**	−35.745	−91.756	−171.783	153.384	68.695	−89.337

Table 5.6. Selected dihedral angles for the conformers of (2*S*,4*R*)-**1**, as obtained after B97D/TZ2P/IEFPCM(2-propanol) optimisation. θ_1: O1–C5–C4–O3 dihedral; θ_2: C2–O3–C4–C6 dihedral; ϕ_1: C3–C2–C1′–C2′ dihedral; ϕ_2: C3′–C4′–C8′–C9′ dihedral; ψ_1: C3–C2–C7–N1″ dihedral; ψ_2: C2–C7–N1″–N2″ dihedral.

Conf. ID	θ_1 (deg)	θ_2 (deg)	ϕ_1 (deg)	ϕ_2 (deg)	ψ_1 (deg)	ψ_2 (deg)
(*S*,*R*)-**1a**	−17.061	157.338	53.053	31.657	−177.201	97.120
(*S*,*R*)-**1b**	−13.711	155.418	52.100	145.241	−176.500	97.088
(*S*,*R*)-**1c**	−30.183	160.902	−171.904	−41.248	−71.167	−96.457
(*S*,*R*)-**1d**	−29.804	160.812	−171.151	−141.905	−70.674	−97.709
(*S*,*R*)-**1e**	−15.915	156.673	52.717	−26.683	−178.871	96.118
(*S*,*R*)-**1f**	−14.756	156.102	52.924	−156.485	−177.950	97.699
(*S*,*R*)-**1g**	−29.263	160.669	−169.647	30.645	−69.355	−96.746
(*S*,*R*)-**1h**	−30.647	160.766	−171.279	155.586	−68.238	−95.917
(*S*,*R*)-**1i**	−35.847	154.472	50.749	−33.725	58.128	93.444
(*S*,*R*)-**1j**	−35.520	153.758	51.507	−158.917	57.359	92.679
(*S*,*R*)-**1k**	−35.883	153.845	51.876	27.057	58.123	92.551
(*S*,*R*)-**1l**	−35.561	153.683	51.575	151.031	57.752	93.012
(*S*,*R*)-**1m**	−15.715	156.548	52.995	30.959	−170.747	−82.055
(*S*,*R*)-**1o**	−7.546	151.507	51.872	144.129	−167.461	−80.349
(*S*,*R*)-**1p**	−35.329	156.861	−171.670	157.440	64.432	−94.320
(*S*,*R*)-**1q**	−35.649	155.704	−172.573	−32.397	65.197	−92.683
(*S*,*R*)-**1r**	−34.760	157.164	−171.207	−157.042	63.314	−95.048

Table 5.7. Rotational strengths in dipole velocity formalism and excitation wavelengths for the lowest-energy electronic transitions of the conformers of (2*S*,4*S*)-**1**, as obtained by PBE0/TZ2P//B97D/TZ2P calculations in 2-propanol (IEFPCM solvation model).

j	R_j, 10^{-40} erg cm^3 (λ_j, nm)				
	(*S*,*S*)-**1a**	(*S*,*S*)-**1b**	(*S*,*S*)-**1c**	(*S*,*S*)-**1d**	(*S*,*S*)-**1e**
1	68.2919 (265.58)	−82.6844 (265.17)	−74.6778 (265.18)	85.2801 (265.51)	−75.0598 (263.66)
2	−138.3965 (251.19)	97.8088 (251.05)	171.2934 (249.78)	−92.1587 (251.42)	60.9707 (248.40)
3	−35.8354 (247.02)	31.9756 (247.45)	35.0918 (247.09)	−34.8492 (247.23)	62.7191 (245.42)
4	−7.2846 (228.93)	0.8296 (225.99)	0.8802 (226.97)	−3.2462 (226.52)	−2.4057 (227.14)
5	−2.2495 (223.14)	6.9626 (223.10)	−12.1305 (223.17)	−5.9649 (223.02)	−3.9032 (223.21)
6	18.3082 (220.09)	−16.8090 (220.92)	−14.7615 (220.30)	26.7096 (220.92)	−44.3390 (220.25)
7	−9.4691 (216.46)	−6.8449 (216.24)	−5.9342 (217.31)	−15.3909 (217.98)	6.9360 (217.79)
8	8.3172 (214.97)	27.1977 (214.68)	19.1553 (215.73)	7.4949 (214.56)	−1.2447 (213.97)
9	−4.7182 (214.18)	−25.2062 (212.64)	7.9092 (214.84)	−8.2436 (214.25)	−17.2374 (212.04)
10	−19.3599 (210.30)	−6.1070 (211.06)	14.8847 (210.55)	10.8500 (210.57)	7.0659 (210.85)
11	7.9643 (209.61)	−7.6072 (209.03)	−9.0856 (209.24)	8.2158 (208.72)	−4.0329 (209.67)
12	0.6994 (204.26)	−0.1927 (203.63)	−27.6449 (203.84)	0.3462 (203.80)	−11.5581 (204.60)
13	45.5035 (203.06)	29.2878 (202.87)	1.6472 (202.97)	−16.7101 (202.92)	−24.8144 (204.25)
14	5.3754 (202.19)	18.3484 (202.04)	−13.0351 (202.69)	7.4777 (201.89)	−1.5278 (202.21)
15	−4.0912 (200.84)	−4.2119 (201.68)	−6.8542 (200.73)	−22.5831 (200.90)	3.0342 (201.18)
16	−9.6769 (199.29)	−12.4119 (200.61)	−0.4747 (199.35)	15.4715 (200.02)	−9.8579 (200.31)
17	−2.1114 (199.17)	3.9071 (197.63)	−4.2508 (198.19)	−24.5459 (197.21)	−57.5489 (197.83)
18	107.9922 (198.16)	−2.5479 (196.79)	9.7778 (196.79)	0.4822 (196.40)	2.9569 (197.03)
19	−53.1314 (196.71)	−74.9262 (195.03)	−24.5852 (195.69)	10.3770 (195.85)	−75.9997 (194.58)
20	−8.1232 (195.32)	29.7538 (194.59)	−10.9393 (195.19)	91.6838 (195.08)	12.9224 (194.05)
21	−2.0572 (193.86)	23.5008 (193.90)	−6.1962 (194.09)	11.8885 (193.86)	−59.4804 (193.68)
22	−26.4573 (192.97)	55.1599 (193.09)	36.8687 (192.76)	−70.2415 (193.16)	93.8699 (192.36)
23	−7.5754 (191.90)	−5.3122 (191.90)	33.6618 (192.01)	20.6268 (192.20)	−26.3089 (191.54)
24	−13.7107 (191.43)	42.5135 (191.74)	32.4507 (191.36)	−134.2181 (191.37)	−2.1751 (191.30)
25	21.7483 (190.74)	38.0168 (190.26)	−37.9101 (190.75)	38.9186 (190.43)	30.9311 (190.56)
26	−108.7745 (190.34)	−118.3817 (189.43)	8.3957 (189.51)	26.5335 (189.62)	34.9516 (189.05)
27	19.3894 (189.50)	11.7483 (188.87)	−12.9266 (189.41)	2.9073 (188.79)	61.5111 (188.47)
28	−133.6730 (188.46)	−41.9250 (188.30)	217.4589 (188.36)	−6.2041 (188.19)	−14.1271 (188.22)
29	11.6620 (186.18)	35.0167 (186.30)	−92.0104 (187.50)	6.4686 (187.23)	85.0186 (187.58)
30	36.3917 (185.98)	1.4280 (185.94)	2.7420 (185.55)	0.7174 (186.22)	8.6972 (185.24)
31	25.5108 (184.06)	9.1633 (185.33)	6.0756 (183.46)	−10.6279 (184.84)	21.4992 (183.49)
32	75.6911 (183.88)	19.7947 (183.78)	8.5908 (182.76)	−2.3489 (183.21)	13.4162 (182.91)
33	−146.0702 (183.28)	−18.0520 (183.28)	2.0787 (182.40)	2.6224 (182.88)	8.6255 (182.63)
34	21.7882 (183.14)	−15.1731 (182.81)	−25.4364 (182.28)	26.9756 (182.71)	−1.0606 (181.69)
35	93.6902 (181.42)	−72.0556 (181.79)	−65.5436 (181.10)	76.8808 (181.77)	−112.3576 (181.50)
36	17.8490 (180.27)	4.7097 (180.38)	−27.5921 (180.37)	−6.0761 (180.85)	4.8671 (180.06)
37	8.0861 (177.76)	13.3083 (177.73)	−4.4340 (176.79)	−4.0656 (177.40)	−7.1951 (177.82)
38	2.4399 (176.98)	−4.7003 (177.33)	0.6218 (176.15)	−21.8021 (177.29)	22.1385 (176.82)
39	−7.7637 (176.35)	−6.2678 (176.78)	0.3814 (175.76)	11.9360 (175.84)	−1.4879 (175.91)
40	−4.2805 (176.18)	12.1938 (176.23)	−11.3336 (175.58)	−2.0869 (175.62)	6.5260 (175.81)
41	2.1953 (175.64)	−1.7621 (175.59)	−10.9641 (175.24)	−1.1163 (175.61)	−0.3660 (175.20)
42	57.6858 (175.40)	1.8703 (175.10)	0.1365 (174.89)	−0.7428 (175.15)	19.8207 (174.99)
43	−1.4212 (174.58)	50.6914 (174.88)	−27.9240 (174.42)	−2.6967 (174.24)	10.5084 (174.60)
44	−2.1878 (174.40)	9.9094 (174.05)	1.8685 (174.01)	−42.7458 (174.05)	−8.9077 (174.24)
45	−7.9178 (173.65)	−4.1369 (173.96)	−5.8092 (173.62)	−0.2880 (173.99)	0.3884 (174.02)
46	2.9851 (173.51)	−0.2365 (173.51)	7.6980 (173.44)	−3.8053 (173.43)	23.8244 (173.28)
47	0.8021 (172.90)	0.6480 (172.78)	−3.1714 (173.29)	0.8583 (173.35)	5.8793 (172.30)
48	−1.2379 (172.14)	−0.6018 (172.10)	−1.0759 (173.08)	0.4014 (172.51)	−0.0574 (171.85)
49	13.9890 (172.11)	3.6356 (171.64)	−0.9019 (171.85)	1.5769 (172.33)	0.2380 (171.83)
50	−1.1452 (171.58)	−2.4119 (171.53)	−9.0643 (170.61)	−0.7140 (171.53)	−0.9163 (171.42)

Table 5.7. (*Continued*)

j	R_j, 10^{-40} erg cm^3 (λ_j, nm)				
	(*S*,*S*)-**1f**	(*S*,*S*)-**1g**	(*S*,*S*)-**1h**	(*S*,*S*)-**1i**	(*S*,*S*)-**1j**
1	76.4997 (264.68)	77.9776 (264.57)	−80.0715 (264.53)	−77.4603 (263.79)	73.3513 (263.38)
2	−85.9200 (249.92)	−70.6949 (249.00)	79.5635 (249.70)	111.5356 (248.58)	−111.1039 (248.41)
3	−29.3847 (247.34)	−51.0389 (246.63)	31.4135 (247.04)	67.4210 (245.64)	−31.7602 (246.34)
4	−6.0020 (225.82)	2.5405 (226.70)	5.5346 (226.12)	−2.0186 (227.04)	−6.7328 (226.30)
5	−11.2011 (223.26)	7.7345 (223.35)	18.7280 (223.01)	−0.8896 (223.64)	−10.7420 (223.59)
6	−22.4808 (220.36)	48.5624 (220.28)	26.1407 (220.08)	−28.2934 (220.48)	−2.1760 (219.39)
7	4.0217 (216.77)	−8.3460 (217.60)	−6.6306 (217.98)	11.8986 (217.01)	−12.2997 (216.80)
8	10.4749 (213.90)	−7.7792 (215.60)	11.9588 (214.90)	5.1355 (212.55)	15.7617 (212.51)
9	−33.5842 (212.15)	7.1490 (213.95)	−4.0569 (213.33)	−8.1549 (212.16)	−22.1888 (211.97)
10	−1.2893 (209.95)	−3.2797 (210.56)	19.5145 (209.33)	2.0167 (209.99)	10.8205 (209.14)
11	7.8073 (209.31)	2.0907 (208.99)	−19.4724 (209.10)	−2.4609 (205.99)	4.7439 (205.52)
12	−9.8543 (203.31)	28.9944 (204.12)	11.7013 (203.35)	−25.0661 (203.93)	−3.0877 (203.19)
13	12.0167 (202.94)	20.3498 (203.69)	3.8683 (202.78)	−7.6746 (202.75)	3.9671 (202.55)
14	3.6680 (202.28)	10.0874 (202.21)	−5.1169 (202.29)	1.4168 (201.29)	−3.3409 (201.27)
15	0.4952 (201.42)	−0.4745 (201.53)	−3.5986 (201.28)	−10.2750 (200.13)	−14.4948 (200.13)
16	−9.5217 (200.48)	8.9152 (199.18)	11.7261 (199.30)	−15.3204 (199.73)	−0.3642 (199.57)
17	8.6190 (197.28)	52.4942 (197.83)	−0.9737 (196.80)	−0.1644 (198.39)	7.0949 (197.56)
18	9.9835 (196.55)	23.9836 (196.02)	−5.3423 (195.81)	−28.4696 (197.53)	22.9282 (196.76)
19	105.4215 (194.80)	6.2294 (195.52)	−11.6479 (195.47)	−142.0611 (195.16)	148.7483 (194.98)
20	−54.2360 (194.23)	84.6299 (194.39)	−126.0439 (194.75)	34.2345 (193.89)	−118.3807 (194.08)
21	−47.6448 (193.62)	−21.8085 (193.51)	274.8113 (193.60)	125.3550 (193.27)	−28.0284 (193.45)
22	−46.2510 (193.11)	−57.9844 (192.78)	−70.1403 (192.96)	−0.4903 (192.34)	−20.5509 (193.04)
23	−52.6084 (191.66)	28.9349 (191.89)	34.0039 (192.01)	29.0912 (191.41)	−21.8799 (191.63)
24	40.5502 (191.40)	8.0327 (191.33)	−73.2191 (191.03)	12.4032 (189.98)	−43.7267 (190.74)
25	0.1970 (191.00)	−68.4945 (190.57)	−41.6375 (190.85)	109.0111 (189.63)	−0.5091 (190.07)
26	−99.0202 (189.39)	−11.3126 (189.21)	145.7063 (189.74)	−17.8468 (189.13)	−13.1796 (189.28)
27	−10.5718 (188.78)	15.6865 (188.95)	6.6798 (188.77)	−1.5438 (187.90)	−1.5651 (187.94)
28	−19.9084 (187.46)	−92.3719 (188.25)	−3.8054 (187.81)	−0.3372 (185.51)	−14.4807 (185.36)
29	21.2176 (186.67)	−89.4550 (187.75)	3.5175 (187.57)	−5.0143 (183.67)	−71.3466 (183.47)
30	1.3230 (185.37)	−2.9862 (185.07)	0.3131 (185.32)	7.8582 (183.21)	15.8153 (183.05)
31	0.3454 (184.04)	−33.0192 (183.44)	47.1494 (183.21)	45.4806 (183.00)	78.5086 (182.53)
32	−69.2017 (183.31)	−37.9975 (181.97)	−37.2568 (183.02)	−164.6907 (181.94)	91.1852 (181.90)
33	57.1517 (182.90)	17.6336 (181.75)	−62.8310 (182.26)	−1.2804 (180.79)	3.8348 (180.64)
34	64.9574 (182.18)	7.8643 (181.56)	−40.2258 (181.82)	35.1596 (180.24)	13.5686 (180.44)
35	25.0827 (181.91)	115.3073 (181.21)	9.9283 (181.67)	4.2271 (179.84)	−1.5147 (179.63)
36	3.3059 (180.22)	−4.6594 (180.32)	−1.3668 (180.48)	−0.5381 (178.34)	−15.2223 (178.75)
37	9.4187 (177.20)	−8.7723 (176.48)	−3.6653 (176.82)	−3.9802 (176.59)	−4.8952 (176.50)
38	−2.4570 (176.73)	−0.2121 (176.10)	−0.3703 (175.78)	11.1854 (176.19)	2.5691 (176.06)
39	19.5725 (176.19)	1.1823 (175.82)	−4.5172 (175.66)	3.0768 (176.08)	−2.4251 (175.91)
40	0.8867 (175.64)	−14.3717 (175.35)	1.0209 (175.55)	3.2800 (175.42)	4.2389 (175.40)
41	14.9132 (175.43)	2.1716 (175.07)	−19.4141 (175.44)	3.6066 (175.06)	2.4778 (175.13)
42	−0.1118 (175.34)	−20.5656 (174.60)	−16.6131 (174.91)	0.1598 (174.84)	−3.8306 (174.76)
43	20.9027 (174.97)	1.1622 (174.29)	−7.7801 (174.17)	−5.7547 (174.24)	9.2969 (174.29)
44	10.4064 (174.07)	−5.7923 (174.02)	−11.3732 (174.10)	−2.5450 (173.93)	−1.3122 (174.05)
45	−3.4995 (173.68)	0.7498 (173.90)	−9.2693 (173.77)	−0.5000 (173.43)	−9.6166 (173.11)
46	−1.3234 (173.13)	6.1685 (173.61)	2.5033 (173.68)	14.9674 (172.89)	17.2290 (173.00)
47	14.9766 (172.04)	−23.5323 (172.77)	−6.1378 (172.48)	6.1036 (171.63)	1.8921 (171.64)
48	2.1000 (172.03)	0.7077 (172.37)	−5.6849 (171.98)	3.6211 (171.33)	9.7923 (171.20)
49	−2.1075 (171.70)	0.1565 (171.44)	−0.3572 (171.77)	−7.3353 (171.29)	6.3753 (170.85)
50	−25.4246 (170.60)	−0.1018 (171.34)	17.6995 (170.44)	−0.8409 (170.62)	−0.9885 (170.30)

Table 5.7. (*Continued*)

j	R_j, 10^{-40} erg cm^3 (λ_j, nm)				
	(*S*,*S*)-**1k**	(*S*,*S*)-**1l**	(*S*,*S*)-**1m**	(*S*,*S*)-**1n**	(*S*,*S*)-**1o**
1	74.1439 (263.51)	−78.4196 (264.36)	69.1545 (265.82)	−82.9128 (265.69)	−74.7260 (263.78)
2	−79.7828 (248.47)	90.2990 (249.96)	−135.8405 (250.87)	101.1548 (251.78)	65.0222 (248.22)
3	−49.3740 (245.47)	31.4162 (246.98)	−35.1405 (247.10)	34.3442 (247.56)	61.9984 (245.59)
4	1.5813 (226.93)	5.0178 (226.07)	−1.6327 (228.55)	−2.4793 (227.51)	−1.5636 (226.70)
5	4.8384 (223.36)	10.4531 (223.34)	2.7534 (223.54)	1.2052 (223.20)	−5.3436 (223.53)
6	28.3585 (220.38)	−19.8692 (219.94)	−1.0648 (220.76)	−4.7813 (221.03)	−2.2433 (220.28)
7	−38.8029 (216.85)	1.9955 (215.99)	28.7689 (219.58)	27.3152 (219.17)	−38.7894 (219.90)
8	2.1570 (212.88)	19.9542 (213.07)	−15.1937 (218.62)	−31.7416 (218.46)	−26.7421 (216.63)
9	−4.0869 (212.01)	−20.6746 (212.25)	−14.2692 (214.88)	−0.2217 (213.47)	27.8131 (214.95)
10	−2.1875 (210.17)	4.2822 (208.91)	−12.9565 (210.39)	−12.8180 (211.36)	−8.0995 (210.50)
11	−0.2124 (205.94)	−2.1693 (205.51)	−13.9387 (209.96)	8.3431 (208.17)	4.1442 (209.61)
12	56.4021 (204.32)	17.7769 (203.04)	5.7763 (203.19)	0.2030 (203.27)	−24.6930 (204.37)
13	29.1446 (203.37)	8.1224 (202.44)	26.0703 (202.84)	3.3850 (202.88)	−30.6244 (203.84)
14	−2.8290 (200.99)	−5.0453 (201.66)	−1.1043 (202.38)	−11.8024 (202.27)	−12.0387 (202.04)
15	8.3474 (200.27)	−24.7119 (200.56)	1.1445 (200.47)	−2.4792 (200.85)	0.6558 (200.99)
16	6.0958 (199.48)	−0.6112 (199.54)	10.3927 (199.84)	−13.4342 (199.97)	−19.4549 (199.88)
17	40.9760 (198.39)	1.0801 (197.47)	29.3041 (199.25)	23.6562 (198.22)	−61.9041 (198.85)
18	−37.7580 (197.37)	−6.9404 (196.86)	13.7335 (198.18)	5.7654 (197.14)	27.5036 (196.62)
19	165.9142 (195.15)	−80.6698 (195.33)	−27.8017 (197.17)	−1.2761 (196.80)	−14.0032 (195.96)
20	4.7503 (193.88)	66.0801 (194.06)	12.8801 (196.40)	−26.1538 (195.75)	−133.1067 (195.17)
21	−116.4326 (193.11)	90.2828 (193.34)	2.1378 (194.33)	−15.4035 (194.48)	34.2058 (194.15)
22	−5.4984 (192.53)	19.3356 (192.27)	−73.1850 (193.63)	−1.5250 (193.96)	6.5829 (193.04)
23	−5.3910 (190.92)	−23.5757 (191.78)	−4.0422 (193.26)	−47.8985 (192.61)	61.8563 (192.73)
24	−130.7617 (190.69)	−1.1761 (191.01)	7.1652 (192.45)	162.9373 (191.83)	−18.9198 (191.89)
25	−7.0789 (189.93)	0.7888 (190.36)	21.3951 (192.07)	−125.8689 (191.17)	−3.7656 (191.12)
26	−52.1544 (188.61)	−20.5086 (188.81)	−29.1299 (191.43)	27.8487 (190.66)	74.1467 (191.03)
27	−7.5953 (187.88)	3.3799 (188.01)	−2.3485 (190.28)	25.0232 (190.34)	−18.8942 (189.88)
28	−6.9516 (185.92)	−1.0481 (184.93)	74.2724 (189.25)	67.9584 (189.56)	41.1266 (189.00)
29	−60.7149 (183.84)	2.4780 (183.39)	−173.2412 (187.96)	15.9476 (187.58)	172.0827 (188.75)
30	−14.6763 (183.42)	45.1768 (183.22)	−0.0291 (186.82)	−0.8962 (186.99)	0.4701 (185.90)
31	49.8703 (183.32)	8.5449 (182.65)	−2.3160 (184.09)	−44.3235 (185.11)	9.5573 (183.54)
32	105.5846 (182.00)	−137.3049 (182.07)	−120.0815 (183.67)	−8.4215 (183.45)	28.4907 (182.71)
33	0.4319 (180.82)	2.6649 (180.86)	80.3575 (183.42)	2.6575 (183.39)	−107.6901 (182.09)
34	6.6431 (179.86)	22.9974 (180.39)	1.8841 (182.14)	−27.6500 (182.73)	−14.3692 (182.00)
35	77.3511 (179.75)	2.1613 (179.88)	147.1125 (181.96)	−59.0052 (182.25)	−6.2172 (181.71)
36	−29.9981 (178.39)	2.3223 (178.01)	4.3639 (180.86)	−2.4153 (181.33)	−10.5422 (180.99)
37	−13.0723 (177.03)	3.4123 (176.74)	4.1384 (179.10)	−2.3265 (178.50)	12.2547 (178.04)
38	−2.3277 (176.20)	14.4249 (176.30)	4.2716 (178.27)	7.1571 (178.21)	−1.9949 (177.27)
39	−0.3647 (176.08)	1.6853 (175.86)	6.8239 (176.99)	12.9280 (177.13)	−5.4006 (176.27)
40	2.5190 (175.37)	−4.0589 (175.48)	1.2553 (175.96)	−0.5862 (176.11)	−1.0211 (176.10)
41	3.7658 (175.29)	1.3649 (175.01)	1.9817 (175.60)	4.1303 (175.94)	−1.8069 (176.01)
42	−0.8125 (174.80)	2.0667 (174.85)	−3.6517 (175.34)	−0.2193 (175.73)	21.1712 (175.78)
43	3.4886 (174.28)	−10.0255 (174.01)	4.5038 (175.02)	2.8829 (174.71)	1.5772 (174.54)
44	2.1942 (173.80)	3.4555 (173.84)	−22.8753 (174.50)	−4.2667 (174.53)	−4.7753 (174.48)
45	−21.8821 (173.35)	4.8256 (173.47)	2.7477 (173.83)	−9.5725 (173.78)	−6.6880 (174.30)
46	9.5634 (172.57)	11.9557 (172.67)	−8.2180 (173.61)	4.4930 (173.61)	3.3318 (173.91)
47	2.6454 (171.78)	1.8583 (171.62)	8.9449 (173.53)	−4.7748 (173.33)	−11.1081 (173.52)
48	4.7339 (171.32)	−5.6800 (171.28)	−9.3452 (173.02)	−0.7629 (172.87)	−0.4549 (171.85)
49	−2.4632 (171.27)	1.8817 (170.66)	−0.9652 (172.49)	0.3750 (172.34)	−0.4478 (171.30)
50	4.0825 (170.83)	37.3986 (169.85)	−1.8516 (171.85)	6.2377 (171.77)	−1.6060 (171.23)

Table 5.7. (*Continued*)

j	R_j, 10^{-40} erg cm^3 (λ_j, nm)				
	(*S*,*S*)-**1p**	(*S*,*S*)-**1q**	(*S*,*S*)-**1r**	(*S*,*S*)-**1s**	(*S*,*S*)-**1t**
1	76.9101 (264.53)	−72.7228 (264.06)	78.5609 (264.00)	86.0056 (265.68)	−80.0939 (264.06)
2	−88.0337 (249.64)	138.1800 (248.26)	−119.9058 (248.69)	−98.2628 (251.61)	109.8782 (249.45)
3	−29.8332 (247.24)	57.2541 (246.04)	−56.7012 (246.12)	−35.4585 (247.49)	33.7789 (246.69)
4	−6.3483 (226.20)	−1.0731 (226.86)	2.0483 (226.60)	3.4136 (227.27)	4.2994 (226.18)
5	−7.4165 (223.33)	−10.4987 (223.53)	0.1072 (223.77)	−2.6382 (223.11)	9.2861 (223.17)
6	−27.5670 (221.20)	6.0944 (220.61)	28.2341 (220.07)	15.9369 (222.17)	7.6428 (219.47)
7	3.5849 (219.05)	−32.6353 (219.76)	−8.3537 (216.30)	−20.5234 (219.03)	5.8851 (216.52)
8	21.5530 (217.01)	33.0532 (216.93)	−21.1214 (213.96)	13.9888 (217.95)	−11.4611 (213.82)
9	−34.2226 (214.22)	23.0573 (215.39)	−3.2167 (212.30)	−2.7776 (213.93)	−1.4807 (211.53)
10	−21.1924 (209.83)	26.5397 (210.89)	−5.1817 (209.68)	20.5735 (210.73)	−5.5479 (208.66)
11	11.7942 (208.70)	−11.1769 (209.69)	0.2604 (206.01)	−9.5381 (208.30)	−4.5705 (205.72)
12	−13.4667 (203.35)	−19.6218 (204.04)	41.1453 (203.80)	2.7756 (203.05)	8.9114 (202.84)
13	18.0523 (202.36)	−18.6169 (203.30)	12.7120 (202.14)	−3.8786 (202.98)	5.1631 (202.12)
14	−1.4491 (202.09)	−0.0164 (201.70)	0.4504 (201.59)	7.9101 (202.11)	−0.5826 (201.23)
15	17.1069 (201.15)	−5.7150 (201.01)	12.2447 (200.16)	−32.9514 (200.25)	−0.6204 (200.01)
16	−1.5374 (200.13)	−0.0349 (199.78)	2.1612 (198.87)	4.1475 (200.21)	3.6023 (198.50)
17	16.3720 (197.47)	9.6595 (199.10)	17.0089 (197.64)	5.8905 (198.41)	−20.3811 (197.02)
18	19.7314 (197.10)	−4.3076 (196.93)	95.3845 (195.89)	0.7900 (197.17)	−60.3407 (195.61)
19	17.9774 (196.36)	−59.1858 (196.02)	37.6221 (195.04)	−3.6742 (196.05)	−31.0945 (194.73)
20	−47.9845 (194.94)	−45.4608 (195.37)	−48.1118 (194.34)	9.5961 (195.60)	15.7595 (194.28)
21	−50.5564 (194.52)	0.9682 (194.22)	−73.8756 (193.26)	10.0081 (194.98)	7.8858 (193.27)
22	−1.1356 (193.81)	−36.1841 (193.70)	−3.9237 (192.81)	27.9692 (194.17)	84.5752 (193.14)
23	−77.2793 (192.70)	130.0929 (193.06)	−14.4026 (191.76)	37.4734 (192.75)	17.3651 (191.84)
24	34.3064 (192.15)	19.0060 (192.15)	−5.7480 (190.94)	−200.6692 (191.83)	1.3376 (191.57)
25	−2.1087 (191.50)	−8.8296 (191.20)	−33.3749 (189.49)	64.0493 (191.24)	83.2509 (190.26)
26	−7.7175 (190.96)	−5.2632 (191.08)	−70.9671 (188.94)	37.8054 (190.97)	6.5297 (189.19)
27	−17.4588 (190.49)	8.8146 (190.89)	2.1812 (188.62)	−24.1977 (190.32)	8.2852 (188.76)
28	39.8811 (188.19)	−79.1987 (189.91)	−14.6598 (185.62)	−3.0136 (188.79)	−0.6799 (185.19)
29	−57.2676 (187.89)	189.5783 (188.49)	10.8368 (184.46)	18.9110 (188.00)	87.7416 (183.51)
30	1.1565 (186.07)	1.2559 (186.66)	−25.2616 (183.47)	0.5150 (187.34)	−111.2491 (182.74)
31	−37.3487 (183.99)	−86.7599 (183.52)	40.0949 (182.05)	−4.4301 (184.90)	−35.4967 (182.56)
32	61.6010 (183.35)	116.0827 (183.38)	111.8094 (181.41)	5.9078 (183.48)	−40.2807 (181.41)
33	58.0882 (182.65)	6.1896 (182.64)	−0.8435 (180.65)	4.4695 (183.42)	3.5816 (180.66)
34	−4.9057 (182.40)	−26.9175 (182.27)	−33.3346 (179.75)	45.9425 (182.85)	−15.5281 (180.24)
35	2.4581 (182.14)	−115.4412 (181.79)	−12.2058 (179.63)	30.6316 (182.39)	−4.2490 (179.76)
36	−1.0946 (181.02)	−4.2762 (181.24)	2.5845 (177.62)	12.0851 (181.50)	9.4459 (177.63)
37	4.2366 (178.24)	−7.5384 (178.72)	1.0682 (176.36)	−3.3043 (178.89)	0.5958 (176.32)
38	5.0739 (177.71)	3.3298 (177.16)	2.4690 (176.04)	2.4516 (177.56)	3.3273 (176.08)
39	1.0843 (176.45)	−4.4159 (176.33)	3.9829 (175.64)	−10.7691 (176.56)	−0.8188 (175.83)
40	0.1430 (175.85)	−0.1501 (176.13)	0.6486 (175.31)	2.5882 (175.99)	−0.2922 (175.67)
41	2.7076 (175.51)	−0.3320 (175.92)	−14.9364 (175.21)	−1.3868 (175.72)	0.6855 (174.71)
42	0.1945 (175.23)	−2.4526 (175.66)	2.9923 (174.23)	−8.7214 (174.92)	−5.5197 (174.08)
43	−12.1795 (174.53)	10.5320 (174.72)	0.8682 (174.10)	−0.0905 (174.77)	−0.4569 (173.92)
44	−9.7881 (174.14)	9.4327 (174.26)	4.1859 (173.93)	7.6168 (174.06)	−13.5286 (173.82)
45	0.0536 (173.98)	5.7621 (174.20)	−9.4374 (173.46)	3.6835 (173.88)	−0.6732 (173.66)
46	15.4053 (173.74)	−5.2138 (173.84)	8.6742 (172.87)	9.4926 (173.73)	7.4438 (172.66)
47	5.6492 (173.40)	0.8511 (173.52)	−4.6266 (172.41)	−1.6425 (173.72)	−7.2699 (172.27)
48	1.0836 (172.08)	−0.1245 (173.02)	−2.3651 (171.86)	−0.6302 (173.65)	−7.9940 (171.67)
49	−2.8087 (171.75)	2.8473 (172.52)	2.6327 (171.09)	5.0383 (172.47)	−2.1113 (170.98)
50	−0.3734 (171.01)	−3.1371 (171.56)	−2.8697 (170.83)	−0.1910 (171.92)	0.7920 (169.92)

Table 5.8. Rotational strengths in dipole velocity formalism and excitation wavelengths for the lowest-energy electronic transitions of the conformers of (2*S*,4*R*)-**1**, as obtained by PBE0/TZ2P//B97D/TZ2P calculations in 2-propanol (IEFPCM solvation model).

j	R_j, 10^{-40} erg cm^3 (λ_j, nm)					
	(*S*,*R*)-**1a**	(*S*,*R*)-**1b**	(*S*,*R*)-**1c**	(*S*,*R*)-**1d**	(*S*,*R*)-**1e**	(*S*,*R*)-**1f**
1	73.7760 (264.55)	−83.2799 (265.43)	−73.0775 (265.99)	82.7437 (265.82)	−74.3997 (263.71)	74.9493 (263.42)
2	−148.6769 (249.02)	95.7677 (251.64)	152.9109 (251.18)	−90.1349 (252.08)	63.9155 (248.25)	−84.1224 (248.55)
3	−41.3682 (246.61)	32.5919 (247.25)	33.4080 (247.56)	−36.2669 (247.31)	56.0569 (245.67)	−31.7893 (246.32)
4	0.9878 (226.66)	1.7507 (226.30)	3.3765 (228.32)	−1.7835 (227.09)	−2.5231 (226.70)	−6.5116 (225.93)
5	10.1755 (223.00)	0.9820 (223.08)	−1.5888 (223.29)	−2.3005 (223.54)	−6.3094 (223.13)	−15.5258 (222.90)
6	25.3787 (220.06)	−4.1032 (220.34)	−30.5655 (219.70)	4.1345 (220.42)	−40.1131 (220.09)	−1.6414 (219.46)
7	−34.4261 (216.14)	3.0848 (214.25)	11.3849 (216.07)	−5.3262 (215.82)	20.2777 (216.39)	−15.1717 (216.06)
8	−26.0469 (211.26)	−8.5718 (211.35)	3.2182 (214.52)	−12.6417 (214.68)	−16.0054 (211.55)	−8.9523 (210.49)
9	2.2459 (210.61)	8.1893 (211.07)	5.5581 (213.64)	10.7688 (212.45)	−0.4004 (210.40)	6.3296 (209.67)
10	1.0551 (209.80)	−18.1180 (209.60)	0.4450 (210.91)	5.2356 (211.79)	−1.8833 (209.08)	−10.8110 (209.45)
11	8.6850 (207.12)	0.8993 (206.66)	11.4679 (210.72)	13.2378 (209.07)	−9.4094 (206.46)	12.8063 (206.17)
12	47.5828 (203.85)	0.0785 (203.70)	−8.2940 (203.99)	−0.2184 (204.08)	−15.2012 (203.84)	−7.5367 (203.27)
13	10.4014 (202.60)	8.8733 (202.76)	−30.3926 (203.29)	−24.1712 (202.93)	−17.8176 (203.50)	−2.2415 (202.64)
14	0.6983 (202.30)	−20.3725 (201.02)	−9.3380 (202.42)	−27.9095 (201.55)	−6.5152 (201.55)	−2.2063 (201.45)
15	1.8609 (200.48)	39.8259 (200.40)	−0.2836 (200.14)	10.0035 (201.37)	2.9316 (200.95)	0.3375 (200.70)
16	−9.2045 (199.02)	−14.7451 (200.22)	−3.6973 (199.30)	30.7110 (200.39)	4.1279 (199.11)	0.7011 (199.14)
17	36.6360 (198.20)	−6.2042 (197.93)	−44.3503 (198.56)	−22.1335 (197.36)	−37.6687 (197.91)	−0.0471 (197.06)
18	−2.2641 (197.47)	36.1941 (197.12)	−26.0315 (198.06)	−24.8024 (197.24)	−4.4178 (197.19)	18.3060 (196.67)
19	−8.6706 (195.75)	−9.0058 (196.05)	36.7564 (196.57)	84.7288 (195.71)	−47.8579 (195.23)	−40.7048 (195.04)
20	8.0675 (195.29)	−26.4178 (195.10)	14.2208 (194.85)	−24.3370 (193.86)	−64.3966 (194.59)	131.2845 (194.41)
21	58.1363 (195.03)	−21.0436 (194.96)	11.3546 (193.60)	−20.3371 (193.68)	−22.5614 (193.90)	26.0692 (193.80)
22	−3.2889 (193.82)	3.6231 (193.56)	16.9953 (192.98)	−22.7894 (193.54)	9.0118 (193.23)	−12.5350 (193.07)
23	−73.3563 (192.47)	74.2308 (192.71)	19.8187 (191.92)	−3.5232 (192.07)	92.4470 (191.94)	−209.8658 (192.81)
24	12.2681 (191.06)	8.7309 (191.55)	7.0690 (191.15)	−1.4414 (190.38)	−37.8019 (190.86)	29.0133 (191.78)
25	−0.6491 (190.82)	−26.6136 (190.69)	16.0529 (190.60)	4.1120 (189.91)	9.2971 (190.51)	−17.9410 (190.41)
26	−93.8294 (190.02)	10.9079 (189.21)	147.9791 (189.02)	33.9743 (189.07)	11.6161 (190.36)	0.1286 (190.36)
27	−155.1954 (188.59)	8.3561 (188.87)	−62.7778 (188.43)	−42.3313 (188.38)	102.7321 (188.44)	−25.2804 (188.55)
28	1.4172 (186.02)	−0.1860 (186.66)	88.9027 (187.49)	3.2612 (187.57)	41.1571 (185.77)	−44.1087 (186.09)
29	7.4481 (185.89)	−5.1970 (186.22)	−5.8911 (186.05)	0.8632 (186.50)	5.0708 (185.55)	−0.3599 (185.68)
30	136.4305 (184.00)	−13.5663 (184.59)	−74.4150 (185.56)	5.5295 (186.38)	45.0984 (184.43)	35.9838 (184.57)
31	−109.1239 (183.38)	25.4652 (183.64)	−2.3957 (184.43)	−23.0948 (185.31)	58.6451 (183.40)	−106.4780 (183.14)
32	−25.3805 (182.65)	−68.5379 (183.10)	−6.4138 (183.59)	−13.4376 (183.52)	23.6752 (181.97)	79.8283 (182.71)
33	20.7975 (182.63)	−4.9161 (183.07)	76.6225 (183.30)	51.9305 (183.08)	−10.3959 (181.72)	79.8450 (182.34)
34	13.4005 (181.72)	−6.9425 (182.54)	−55.0845 (182.39)	−2.2916 (182.93)	−74.7425 (181.48)	2.6045 (181.84)
35	138.8093 (181.53)	−36.5659 (182.07)	−29.4724 (181.54)	38.4063 (182.01)	−65.4651 (181.40)	3.4692 (181.57)
36	−1.6753 (179.11)	−1.0949 (179.04)	−55.0689 (180.33)	32.8899 (180.80)	−4.3246 (179.33)	1.2671 (179.67)
37	−1.9221 (178.70)	−0.6718 (178.77)	4.3189 (178.61)	−13.9030 (178.41)	1.0964 (179.03)	2.8954 (179.09)
38	−3.3275 (178.31)	−7.3770 (178.47)	−2.7192 (177.27)	−6.2291 (178.03)	−1.4175 (177.59)	−1.0140 (177.49)
39	4.5035 (176.47)	20.4940 (178.04)	−6.5486 (176.80)	3.7429 (177.73)	2.5925 (176.31)	2.1739 (176.44)
40	8.6220 (176.00)	2.9009 (176.90)	−1.3734 (175.71)	2.9159 (175.62)	0.1479 (175.97)	0.3198 (175.80)
41	1.7757 (175.88)	−0.7052 (175.66)	9.0939 (175.44)	22.8134 (175.55)	−7.2510 (175.09)	6.8952 (175.27)
42	16.5203 (175.11)	10.0461 (175.10)	−3.5002 (174.29)	−13.0020 (174.56)	28.5709 (174.65)	17.5473 (174.72)
43	−0.4109 (174.00)	−11.8389 (173.91)	−39.8772 (173.91)	−5.2408 (174.34)	−0.0061 (174.48)	13.4648 (174.25)
44	4.2791 (173.82)	6.4145 (173.63)	2.9743 (173.88)	8.9437 (173.99)	−4.2342 (174.16)	−3.7679 (174.06)
45	−0.6345 (173.61)	6.5386 (173.56)	−7.2042 (173.51)	−63.6932 (173.67)	4.5788 (173.86)	−4.4263 (173.95)
46	2.1397 (173.25)	−3.0536 (173.45)	−6.2722 (173.39)	2.1091 (173.22)	−1.9078 (173.78)	3.3330 (173.59)
47	−18.8579 (173.05)	1.0086 (173.35)	3.9120 (173.22)	−9.7521 (172.41)	28.9292 (173.06)	15.4000 (172.81)
48	11.5840 (172.71)	3.8832 (172.26)	−2.3012 (171.94)	−1.9025 (172.39)	−0.8343 (172.60)	5.4798 (172.48)
49	24.2429 (172.55)	−0.5216 (172.16)	−5.3985 (171.70)	1.1836 (172.33)	−0.4738 (171.86)	3.2789 (172.42)
50	−22.2870 (170.89)	21.9401 (171.86)	−13.2333 (171.41)	7.5440 (171.58)	0.7751 (171.31)	−17.1707 (170.28)

Table 5.8. (*Continued*)

j	R_j, 10^{-40} erg cm^3 (λ_j, nm)					
	(*S*,*R*)-**1g**	(*S*,*R*)-**1h**	(*S*,*R*)-**1i**	(*S*,*R*)-**1j**	(*S*,*R*)-**1k**	(*S*,*R*)-**1l**
1	77.8723 (265.04)	−73.5503 (264.01)	−78.4847 (264.78)	73.7865 (262.27)	76.7120 (263.55)	−80.9355 (264.27)
2	−87.9639 (249.54)	69.9338 (248.94)	132.8143 (249.71)	−98.9942 (247.59)	−93.4429 (248.55)	97.6703 (250.20)
3	−47.6961 (247.05)	29.5563 (246.73)	37.3482 (246.80)	−43.8749 (245.39)	−43.3486 (245.69)	32.6880 (246.81)
4	2.8278 (226.93)	6.3062 (226.53)	−3.4244 (226.75)	−8.9601 (226.29)	1.5525 (226.46)	5.0257 (225.93)
5	5.5357 (223.47)	18.2893 (223.47)	−2.5818 (223.75)	−11.7441 (223.31)	5.9514 (223.25)	7.8116 (223.03)
6	44.7412 (220.31)	1.6045 (219.46)	−30.0356 (220.02)	6.9202 (218.90)	30.1678 (220.20)	−16.4261 (219.86)
7	−3.7225 (216.72)	21.0433 (216.68)	7.9755 (216.14)	−17.7987 (216.65)	−36.7939 (216.46)	4.1918 (215.41)
8	−0.5346 (213.89)	−6.5183 (214.30)	−14.0082 (212.07)	15.7782 (211.49)	1.3028 (212.19)	15.1692 (212.48)
9	19.8358 (212.03)	17.7935 (211.43)	3.7633 (211.70)	−14.5683 (211.06)	−3.1081 (211.68)	−17.0140 (211.25)
10	−14.4785 (210.90)	−1.5215 (210.57)	17.7327 (209.49)	6.4988 (208.55)	−1.6078 (209.51)	3.5282 (208.32)
11	6.0283 (210.50)	−8.6921 (209.91)	0.3332 (205.42)	6.0098 (205.12)	−0.7470 (205.50)	−2.1745 (205.14)
12	27.0510 (204.05)	9.1371 (203.67)	−26.1524 (203.27)	−2.0905 (203.37)	59.7297 (204.10)	21.6885 (202.94)
13	11.0994 (203.85)	−13.8166 (203.48)	−2.3783 (202.31)	2.4205 (202.51)	24.4459 (203.02)	15.5654 (202.40)
14	2.3770 (202.31)	2.9075 (201.72)	−9.7555 (201.61)	−13.1484 (200.82)	−2.2874 (201.20)	2.3104 (201.79)
15	−0.9303 (201.26)	0.2081 (201.46)	−27.0447 (200.94)	−0.2589 (200.73)	4.6552 (200.94)	−44.9359 (201.17)
16	23.1913 (199.47)	24.9236 (199.45)	−23.9417 (199.41)	−3.5757 (199.22)	9.2307 (199.37)	2.2684 (199.44)
17	39.2686 (197.66)	−66.1316 (197.14)	−3.9467 (199.06)	−3.7529 (197.83)	46.9582 (198.45)	4.4742 (198.16)
18	−8.3543 (197.35)	−10.2125 (196.04)	−2.0930 (198.29)	31.2285 (196.92)	−43.7201 (198.10)	5.6244 (197.00)
19	68.8039 (194.83)	−123.2441 (194.45)	−78.9042 (196.08)	152.1398 (194.79)	166.5327 (195.23)	−80.8806 (195.29)
20	−6.1798 (193.61)	−15.4585 (194.00)	26.1027 (193.78)	−159.9552 (193.97)	8.3317 (193.86)	56.8965 (193.83)
21	−26.2347 (193.26)	233.9292 (193.58)	84.8502 (193.67)	24.1309 (193.50)	−128.8364 (193.28)	79.8602 (193.30)
22	−21.3056 (192.67)	−4.7123 (193.10)	1.2359 (192.02)	−40.0047 (192.76)	−10.6973 (192.15)	22.9097 (191.63)
23	21.8179 (192.08)	33.7243 (191.98)	29.7615 (191.05)	−15.1630 (191.32)	−101.2809 (190.82)	−12.5790 (191.58)
24	−0.8129 (191.46)	−5.7340 (190.75)	1.8211 (189.82)	−30.1847 (190.69)	−13.5775 (190.50)	−3.0122 (190.96)
25	−5.5295 (189.85)	5.3969 (189.87)	37.3523 (189.63)	−0.2575 (189.96)	−3.4131 (189.74)	1.9751 (190.35)
26	80.7821 (188.40)	76.3696 (188.92)	77.3142 (188.60)	−32.8097 (188.83)	−78.8279 (188.41)	−26.6894 (188.42)
27	−76.9824 (187.85)	−24.5434 (188.17)	−17.2486 (187.70)	−1.9263 (187.50)	−29.1095 (187.32)	2.5273 (187.26)
28	−127.4589 (187.31)	26.0172 (187.47)	0.8756 (184.45)	−14.5149 (184.96)	−4.5726 (185.07)	−6.4416 (184.04)
29	−23.4231 (186.50)	−25.7944 (187.29)	16.0953 (183.72)	−27.8542 (183.94)	−15.3041 (183.86)	9.6060 (183.66)
30	−4.6980 (185.26)	0.3063 (185.24)	−19.0993 (183.22)	−24.9718 (183.03)	−78.6200 (183.61)	29.1886 (183.18)
31	−65.3105 (183.48)	8.2239 (184.60)	41.0144 (182.74)	96.4700 (182.77)	86.6563 (183.23)	38.0834 (182.53)
32	−6.5490 (183.22)	27.5698 (183.06)	−164.4985 (181.74)	75.3620 (181.88)	109.2912 (181.90)	−176.7372 (182.16)
33	−16.1721 (182.33)	−41.9292 (182.54)	1.1017 (180.84)	−9.1489 (180.72)	0.0932 (180.87)	2.3203 (181.01)
34	40.5330 (182.07)	−12.5084 (181.80)	42.1513 (180.30)	7.5067 (180.35)	43.9209 (179.87)	31.7185 (180.21)
35	36.0444 (181.33)	−24.9634 (181.71)	4.5342 (179.86)	−2.8821 (179.42)	21.2007 (179.86)	0.7447 (179.95)
36	45.9110 (180.68)	−19.7300 (180.76)	−5.3265 (178.02)	−9.3323 (179.18)	−10.5147 (178.51)	3.3302 (178.52)
37	0.8807 (177.62)	−1.1500 (177.24)	−2.5097 (177.22)	2.1582 (177.06)	−12.2847 (177.49)	5.6863 (176.94)
38	−3.6810 (176.69)	−3.0934 (176.60)	7.0344 (176.58)	3.1467 (175.94)	−2.6711 (176.34)	8.8896 (176.54)
39	5.1200 (175.88)	1.4933 (175.77)	−0.4073 (175.95)	−0.3642 (175.92)	−0.3056 (176.06)	0.3506 (175.82)
40	2.1548 (175.82)	1.2557 (175.69)	6.2290 (175.71)	−1.5888 (175.59)	−2.3954 (175.46)	−3.0652 (175.48)
41	−13.3273 (175.47)	−10.4077 (175.62)	−0.7695 (174.75)	2.7413 (174.89)	3.9328 (174.94)	−1.7718 (175.01)
42	−26.3251 (174.18)	−12.0205 (174.94)	2.4771 (174.64)	4.2264 (174.55)	4.2264 (174.82)	4.0379 (174.59)
43	6.5156 (173.92)	−8.7856 (174.48)	−3.8136 (173.92)	1.1304 (174.39)	2.7364 (174.26)	−7.7007 (173.93)
44	−9.4194 (173.88)	−43.4446 (174.05)	5.0482 (173.78)	−0.7242 (174.16)	9.1948 (173.64)	1.6082 (173.76)
45	4.5782 (173.69)	2.3309 (173.89)	−9.2822 (173.31)	4.2939 (173.22)	−33.9776 (173.32)	3.4639 (173.52)
46	−30.9821 (173.23)	1.4214 (172.80)	20.4218 (172.58)	3.7087 (172.75)	10.2369 (172.42)	13.2344 (172.46)
47	0.7963 (172.37)	−0.3514 (171.98)	4.5493 (171.61)	−1.6119 (171.07)	2.5093 (171.56)	−0.3381 (171.30)
48	1.6860 (171.44)	−11.2611 (171.60)	−1.3759 (170.73)	1.9242 (170.49)	0.3076 (170.94)	−5.9068 (170.74)
49	−6.1755 (171.34)	−9.1300 (171.59)	−4.5964 (170.50)	10.9071 (170.41)	5.0382 (170.81)	0.6616 (170.19)
50	−0.2954 (171.21)	0.5318 (170.67)	0.4552 (169.95)	7.5073 (170.09)	4.3103 (170.48)	60.0189 (169.63)

Table 5.8. (*Continued*)

j	R_j, 10^{-40} erg cm^3 (λ_j, nm)				
	(*S*,*R*)-**1m**	(*S*,*R*)-**1o**	(*S*,*R*)-**1p**	(*S*,*R*)-**1q**	(*S*,*R*)-**1r**
1	71.1563 (264.46)	−80.6374 (265.57)	−75.0627 (263.05)	−76.0430 (264.82)	77.5231 (263.29)
2	−140.0188 (248.63)	103.1136 (251.75)	94.1196 (248.09)	99.0508 (249.42)	−93.3636 (248.52)
3	−38.6137 (246.30)	33.4371 (247.02)	38.4576 (245.94)	36.6677 (246.70)	−33.2204 (246.23)
4	1.2020 (226.93)	1.9143 (227.35)	6.6348 (226.59)	−1.2620 (226.97)	−7.3421 (226.46)
5	7.5206 (223.17)	1.6487 (223.21)	11.9413 (223.32)	−2.1635 (223.41)	−15.2110 (223.24)
6	30.8411 (219.59)	−5.0180 (219.38)	−10.7066 (218.99)	−37.2641 (219.95)	22.6012 (219.09)
7	−49.4050 (215.86)	−0.0432 (213.99)	21.1559 (216.33)	28.4102 (215.82)	−15.8587 (216.08)
8	1.1368 (212.08)	−4.3468 (211.60)	−17.9476 (211.92)	−16.0276 (212.99)	−9.6025 (211.70)
9	−22.1028 (210.55)	−1.9283 (211.30)	1.4491 (210.15)	4.4463 (211.52)	−0.2314 (210.24)
10	15.0098 (210.08)	12.0979 (208.24)	−5.7921 (208.31)	−0.4757 (209.73)	3.4450 (208.02)
11	−11.6360 (207.78)	−6.5311 (207.03)	−5.8856 (205.34)	2.1772 (205.56)	1.9861 (205.16)
12	30.9927 (203.51)	−22.9926 (203.20)	7.9998 (203.27)	−47.2435 (203.76)	−12.9284 (203.46)
13	−0.5331 (202.65)	−6.5263 (203.01)	−2.7261 (202.43)	−32.1977 (202.47)	16.7113 (202.73)
14	−4.2824 (201.77)	7.8941 (202.51)	3.0841 (200.98)	−7.6150 (201.77)	−1.8346 (201.11)
15	−0.5304 (201.14)	−7.1420 (201.54)	3.5465 (199.56)	−12.8471 (199.48)	6.1725 (199.74)
16	1.7613 (200.75)	4.6887 (201.05)	8.6002 (199.05)	0.9990 (198.82)	−0.5489 (199.01)
17	8.1379 (200.33)	−3.2786 (199.75)	−40.0446 (197.38)	−28.7825 (198.24)	14.9584 (197.10)
18	17.9716 (199.03)	−4.7152 (197.89)	−22.9955 (196.02)	1.2714 (196.97)	1.6054 (196.12)
19	6.9415 (197.67)	49.2340 (197.86)	−118.8462 (194.60)	−50.9809 (195.73)	89.7872 (194.66)
20	27.8594 (197.07)	23.6361 (197.81)	108.6990 (193.75)	−21.4731 (193.94)	−14.6629 (193.66)
21	57.2729 (195.78)	−68.5532 (196.20)	12.2189 (193.47)	68.1805 (193.19)	−101.1103 (193.15)
22	−10.8963 (193.09)	22.2376 (193.13)	94.2785 (192.18)	−0.6802 (192.49)	−43.5232 (192.03)
23	−107.9606 (193.03)	35.5891 (192.54)	−8.7869 (191.66)	38.3922 (190.82)	−3.2531 (191.38)
24	13.2365 (191.79)	−53.8718 (191.44)	2.6538 (190.54)	2.3208 (190.61)	−18.0728 (190.87)
25	−29.6129 (190.82)	−0.7771 (190.01)	36.2136 (190.10)	−4.5018 (190.03)	23.3482 (190.24)
26	−4.3287 (190.24)	−1.1650 (189.78)	22.3965 (188.97)	169.6530 (189.30)	19.8556 (189.04)
27	−173.2063 (188.57)	138.1308 (188.58)	8.1436 (187.39)	52.0995 (186.95)	1.2521 (186.55)
28	1.0650 (186.99)	3.7133 (187.72)	2.6354 (184.40)	1.1582 (184.64)	11.0101 (184.55)
29	176.7200 (185.31)	2.3752 (186.12)	108.3058 (183.26)	61.1591 (184.44)	−25.9164 (183.37)
30	−49.9807 (184.09)	14.7920 (184.11)	−50.5924 (183.01)	−37.7501 (183.41)	−29.3097 (183.15)
31	−112.9619 (183.63)	−25.0909 (184.05)	13.3628 (182.37)	−34.1028 (182.55)	28.1752 (182.68)
32	32.6110 (183.38)	−163.3530 (184.01)	−168.7451 (182.21)	−66.9826 (181.45)	112.1767 (182.15)
33	−0.2471 (183.26)	10.7319 (183.35)	4.8046 (180.85)	−5.3021 (181.12)	−1.3888 (181.02)
34	3.5904 (183.23)	8.4725 (182.56)	−19.2672 (180.50)	−20.9725 (180.21)	−18.0106 (180.38)
35	141.2768 (181.89)	−32.3064 (181.98)	−0.7253 (180.03)	−69.2702 (179.65)	−4.4772 (180.12)
36	7.0791 (180.85)	4.4922 (180.23)	8.4615 (177.94)	−0.6860 (177.30)	6.6504 (177.61)
37	0.4082 (179.53)	−0.4774 (179.96)	2.7860 (176.67)	35.1608 (176.90)	2.0658 (176.74)
38	−2.6893 (179.31)	2.5658 (179.55)	4.0127 (176.55)	3.8630 (176.44)	−1.4598 (176.22)
39	4.9668 (176.90)	4.4981 (177.20)	−0.7555 (175.86)	1.6064 (176.00)	−8.0198 (175.84)
40	−2.9270 (176.18)	3.1298 (176.50)	−0.9037 (175.53)	2.9455 (175.63)	−20.3289 (175.73)
41	−1.2715 (176.07)	−0.1967 (175.88)	6.4666 (175.36)	10.0771 (175.49)	−8.9015 (175.33)
42	3.7490 (175.36)	−0.4358 (175.66)	−3.5101 (174.74)	−2.3068 (174.78)	−0.6000 (175.20)
43	−7.1035 (174.97)	8.0643 (174.91)	−21.4685 (174.36)	−2.0887 (174.02)	13.7388 (174.32)
44	1.1125 (174.60)	2.1420 (174.34)	2.4224 (174.10)	13.0322 (173.45)	−4.5055 (174.10)
45	−8.3132 (174.31)	−7.0788 (173.79)	−9.4537 (173.16)	−30.8157 (173.32)	−5.2022 (172.92)
46	2.3916 (174.17)	−3.5366 (173.76)	3.7830 (172.17)	−1.5617 (172.90)	0.0549 (171.76)
47	3.1759 (173.64)	4.4498 (173.66)	−5.5595 (171.51)	−3.0526 (171.50)	−1.0434 (170.91)
48	−2.0232 (173.55)	0.5715 (173.53)	−2.3682 (170.77)	−1.2027 (171.11)	4.8858 (170.68)
49	0.5726 (173.25)	−4.5393 (173.16)	−6.8826 (170.61)	−3.7833 (170.74)	1.6996 (170.57)
50	−2.8848 (171.38)	−0.5551 (173.02)	−0.0976 (170.42)	0.2024 (170.34)	0.8642 (170.42)

Chapter 6

Mycoleptone A

This chapter is based on a peer-reviewed publication:
Willian J. Andrioli, Raphael Conti, Magali J. Araújo, Riccardo Zanasi, Bruno C. Cavalcanti, Viviane Manfrim, Juliano S. Toledo, Daniele Tedesco, Manoel O. de Moraes, Cláudia Pessoa, Angela K. Cruz, Carlo Bertucci, José Sabino, Dhammika N.P. Nanayakkara, Mônica. T. Pupo, Jairo K. Bastos (**2013**). Mycoleptones A–C and polyketides from the endophyte *Mycoleptodiscus indicus*. *Journal of Natural Products* *77*, 70-78.

Abstract: Three new azaphilones with an unusual methylene bridge, named mycoleptones A, B and C (**2**, **4** and **5**), were isolated from cultures of *Mycoleptodiscus indicus*, a fungus associated with the South American medicinal plant *Borreria verticillata* (Rubiaceae). Additionally, four known polyketides, austdiol (**1**), eugenitin (**3**), 6-methoxyeugenin (**6**) and 9-hydroxyeugenin (**7**), were also isolated. The structural characterization of compounds was carried out by nuclear magnetic resonance (NMR) spectroscopy, high-resolution mass spectrometry (HRMS), electronic circular dichroism (ECD) spectroscopy, time-dependent density functional theory (TD-DFT) calculations and X-ray crystallography. Compounds **1–9** were weakly active when tested in anti-leishmanial and cytotoxicity assays.

Acknowledgements: The authors thank the São Paulo Research Foundation (FAPESP) grants 04/07935-6 and 07/58650-0, CAPES, CNPq, the PRIN 2008 project 2008LYSEBR_005 (MIUR, Italy) and the University of Bologna for financial support.

Endophytic microorganisms live inside the tissues of host plants without apparently harming them, and are a promising source of bioactive compounds.[162–165] Species of *Mycoleptodiscus*, such as *M. indicus*, *M. terrestris* and *M. sphericus* are commonly isolated as endophytes; they are probably latently phytopathogenic and may become phytopathogenic when the host plant is subjected to stress.[166] *M. indicus*, a tropical-to-subtropical species, occurs in leaves of different host plants, mainly monocotyledons. *M. indicus* is associated with large spreading lesions on leaves of *Zamia* spp., an American cycad, and other monocotyledonous plants.[167] *M. indicus* has occasionally been reported to infect humans and canines, causing septic arthritis and skin infections.[168]

In this paper, the isolation, structural characterisation and biological activity of secondary metabolites from cultures of *Mycoleptodiscus indicus*, an endophytic fungus isolated from the leaves from *Borreria verticillata*, are reported. Three new azaphilones, named mycoleptones A, B and C (**2**, **4** and **5**), were isolated and fully characterised; in addition, four known polyketides, namely austdiol (**1**), eugenitin (**3**), 6-methoxyeugenin (**6**), 9-hydroxyeugenin (**7**), were isolated and identified, and the acetylated derivatives of austdiol (**8**) and mycoleptone A (**9**) were synthesized (Figure 6.1).

Figure 6.1. Mycoleptones A–C and polyketides from *Mycoleptodiscus indicus*.

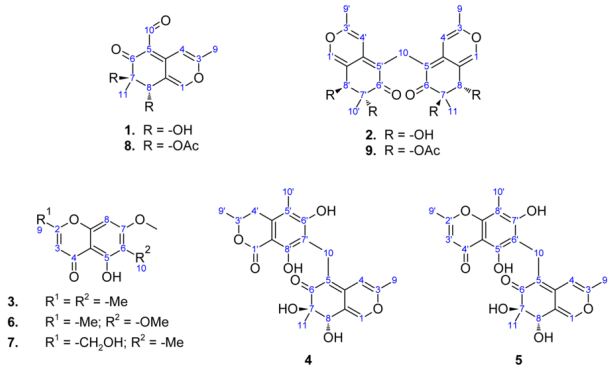

6.1 Results and discussion

Seven secondary metabolites of *Mycoleptodiscus indicus* were isolated, four of which were identified as austdiol, eugenitin, 6-methoxyeugenin and 9-hydroxyeugenin by comparison of experimental spectroscopic data with literature val-

ues.[169–174] Three of the isolated metabolites are previously unreported azaphilones and were named mycoleptones A, B and C (**2**, **4** and **5**).

> Results from the structural analysis and biological tests on mycoleptones A–C are reported in Andrioli *et al.* (**2014**), *J. Nat. Prod.* *77*, 70.

Compounds **1–9** exhibit no significant activity against *Leishmania donovani* and *Leishmania major* compared to the standard anti-leishmanial drugs geneticin (*L. major*), amphotericin B and pentamidin (*L. donovani*). Mycoleptone B (**4**) was the most cytotoxic metabolite (PC3 cells: IC_{50} = 7.1±3.8 μM), but its activity was lower than that of doxorubicin, the reference compound for cytotoxicity assays.

6.1.1 Austdiol

Austdiol (**1**; (7*R*,8*S*)-7,8-dihydroxy-3,7-dimethyl-6-oxo-7,8-dihydro-6*H*-isochromene-5carbaldehyde) is the main toxic component of a mixture of compounds produced in mouldy maize meal by *Aspergillus ustus* and belongs to a class of compounds known generically as azaphilones.[175,176] Azaphilones are yellow or orange pigments produced by fungi: their pyran oxygen atoms are easily exchanged to nitrogen atoms with ammonia, and the name is derived from the ready reaction of these metabolites with ammonia to yield vinylogous γ-pyridones.[177] The skeleton of austdiol is derived from a single pentaketide chain, composed of head-to-tail acetate units, and possesses two C_1 units introduced from *S*-adenosyl-methionine.[178] A wide range of interesting biological activities of azaphilones, such as antimicrobial, antifungal, antiviral, antioxidant, cytotoxic, nematicidal and anti-inflammatory, have been reported in the literature;[175,178] their non-selective biological activities may be related to the production of vinylogous γ-pyridones.[179]

6.1.2 Mycoleptone A

Mycoleptone A (**2**) was isolated as a yellow powder, and the complete structural characterisation was carried out by nuclear magnetic resonance (NMR) spectroscopy, high-resolution mass spectrometry (HRMS), electronic circular dichroism (ECD) spectroscopy, time-dependent density functional theory (TD-DFT) calculations and single-crystal X-ray diffraction studies (Figure 6.2).

The structure of mycoleptone A (**2**) was elucidated as (7*R*,8*S*,7′*R*,8′*S*)-5-[(7′,8′-dihydroxy-3′,7′-dimethyl-6′-oxo-7′,8′-dihydro-6′*H*-isochromen-5′-yl)methyl]-7,8-dihydroxy-3,7-dimethyl-7,8-dihydro-6*H*-isochromen-6-one. The UV spectrum

Figure 6.2. ORTEP representation of mycoleptone A (atom displacement at 30% probability). Hydrogen atoms are represented by spheres of arbitrary radius.

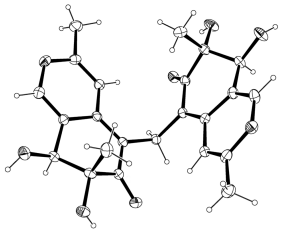

of **2** displays maximum absorptions at 254 nm ($\log \varepsilon$ 2.90) and 361 nm ($\log \varepsilon$ 2.83), revealing the presence of an extended conjugated system, characteristic of azaphilones. Compound **2** displays similar ^{1}H and ^{13}C NMR spectra to austdiol,[169,170] with the replacement of the aldehyde signals (δ_H 9.99 and δ_C 189.3) by methylene signals (δ_H 3.26 and δ_C 18.5) at position C-5.

Compound **2** is a chiral molecule having four asymmetric carbons and a formal binary symmetry axis. An accurate analysis of the eight enantiomeric pairs of **2** reveals that two pairs are formed by non-optically active *meso* structures and two more pairs are repeated twice; as a result, four pairs of enantiomers and two *meso* structures are possible (Table 6.1). Since the reliable assessment of the absolute configuration of a compound is achieved when the theoretical chiroptical properties[28] of all the possible optically-active diastereomers are determined,[112] quantum-mechanical (QM) calculations were performed on four diastereomers of **2** (Figure 6.3): (7*R*,8*S*,7′*R*,8′*S*)-**2** (**2A**), (7*R*,8*S*,7′*R*,8′*R*)-**2** (**2B**), (7*R*,8*S*,7′*S*,8′*S*)-**2** (**2C**) and (7*S*,8*S*,7′*S*,8′*S*)-**2** (**2D**). QM calculations were carried out using density functional theory (DFT) and its time-dependent extension (TD-DFT).

DFT geometry optimisation (Table 6.3) yielded two equilibrium conformers having $\Delta E_{QM} \leq 2$ kcal mol^{-1} for diastereomers **2A**, **2B** and **2C**, while a single equilibrium conformer within the same threshold energy was found for diastereomer **2D**. The most populated conformers of **2A** (Figure 6.4) display similar geometric features: the azaphilone units are oriented in an 'open folder' conformation, the pyran oxygen atoms are pointing toward opposite directions, all the hydroxyl groups are equatorial and form intramolecular hydrogen bonds with each other and with the ketone carbonyl groups. The main difference lies in the direction of the axial methyl groups on C-7 and C-7′, which point outside the molecular cavity for **2A-e** and inside for **2A-b**. Conformer **2A-b** shows a close resemblance to the crystal structure of **2** (Figure 6.2).

Figure 6.3. Diastereomers of mycoleptone A.

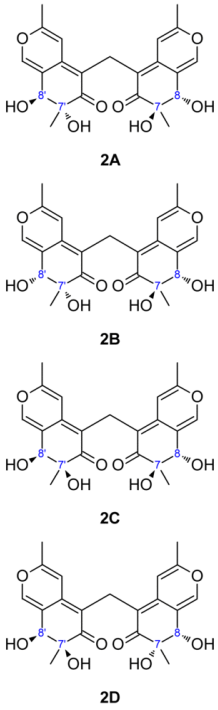

Figure 6.4. Most populated equilibrium conformers of **2A**. The most populated equilibrium conformers of **2B**, **2C** and **2D** are depicted in Figures 6.8–6.10.

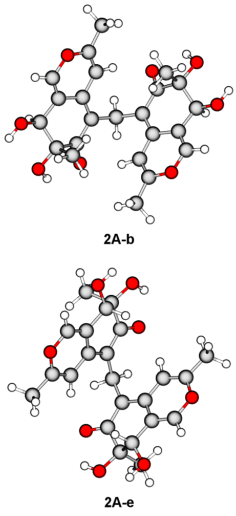

Figure 6.5. Experimental UV and ECD spectra of mycoleptone A (19 μM in MeOH, 1 cm pathlength).

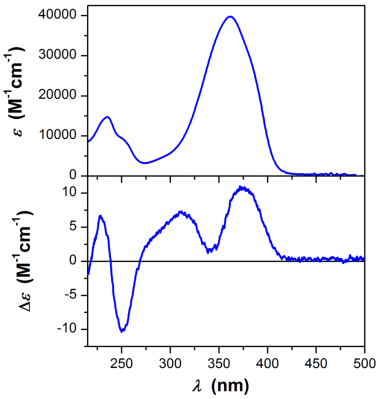

Figure 6.6. Theoretical ECD spectra of the diastereomers of mycoleptone A at the PBE0/6-311++G(2*d*,2*p*)/IEFPCM(MeOH)//B97D/6-311++G(2*d*,2*p*)/IEFPCM(MeOH) level (χ_{QM}-based conformational averaging, $\Delta\sigma = 0.3$ eV). *Solid:* **2A**. *Dash-dotted:* **2B**. *Dotted:* **2C**. *Dashed:* **2D**.

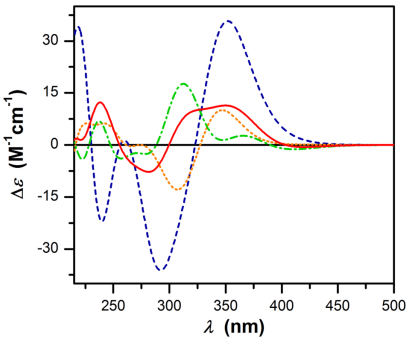

The experimental ECD spectrum of **2** in methanol (Figure 6.5) shows four bands. The broad positive band centered at 372 nm has a strong contribution from the $n \rightarrow \pi^*$ transitions of the ketone carbonyls, which are affected by the chiral environment around these groups. The positive band at 311 nm with a shoulder around 285 nm, the sharp negative peak at 252 nm and the positive peak at 228 nm are due to $\pi \rightarrow \pi^*$ transitions of the conjugated system, which are affected by the chirality of the rings and by the mutual orientation of the azaphilone units.

The theoretical ECD spectra of the diastereomers of **2** (Figure 6.6) displayed different patterns, reflecting their different stereochemistry. The comparison be-

tween the calculated spectrum of **2A** and the experimental spectrum of **2** (Figure 6.7) shows that TD-DFT calculations are able to reproduce the experimental pattern of the transitions in the high-energy region, considering that transition energies are usually underestimated by PBE0.[111] The transitions in the low-energy region are not reproduced, suggesting that QM calculations are unable to describe the chiral environment of the ketone moieties, e.g. hydrogen bonding interactions with hydroxyl groups and solvent molecules, with adequate accuracy. However, the theoretical ECD spectra of the remaining diastereomers (Figures 6.12–6.14) are unable to reproduce the experimental ECD pattern in the high-energy region: on this basis, a (7*R*,8*S*,7′*R*,8′*S*) stereochemistry can be predicted for **2**.

Figure 6.7. Theoretical ECD spectrum of **2A** and comparison with experimental data. *Solid:* experimental ECD spectrum of **2** (19 μM in MeOH, 1 cm pathlength). *Dotted:* theoretical ECD spectrum of **2A** at the PBE0/6-311++G(2*d*,2*p*)/IEFPCM(MeOH)//B97D/6-311++G-(2*d*,2*p*)/IEFPCM(MeOH) level (χ_{QM}-based conformational averaging, $\Delta\sigma = 0.3$ eV).

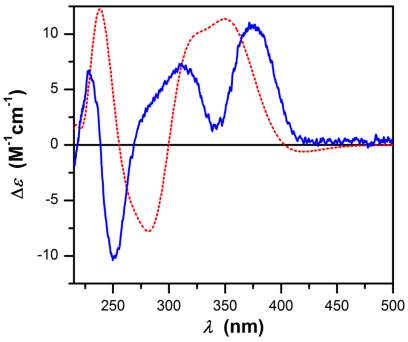

The presence of a methylene bridge is very uncommon among natural compounds, and only few azaphilone dimers have been reported showing such a feature.[176] Dicitrinones A–C[180] were isolated from *Penicillium citrinum*, a volcano ash-derived fungus: the presence of a single sp^3 carbon bridge, either a methine or methylene group, was proposed to derive from the carboxyl group of citrinin through decarboxylation, reduction and Friedel-Crafts alkylation mediated by a polyketide biosynthetic pathway. The methylene bridge in aspergilone B,[181] an azaphilone dimer which was isolated from a marine-derived fungus of the *Aspergillus* species, was hypothesized to derive from a formaldehyde biosynthetic pathway; the same hypothesis was proposed for the biosynthesis of xyloketal F,[182] a dimer isolated from a mangrove fungus of the *Xylaria* species.

The condensation of two austdiol units to form mycoleptone A (**2**) is consistent with a possible biosynthetic pathway similar to the one proposed for dicitrinone C[180] (Figure 6.11). One austdiol unit may undergo decarbonylation, while the

aldehyde group of the second austdiol unit may be reduced to a reactive carbocation species: the two units may then react by Friedel-Crafts alkylation. Similar pathways may also explain the condensation of the dihydroisocoumarin and chromone units with an austdiol unit in mycoleptones B (**4**) and C (**5**), respectively. Due to the limited number of methylene-bridged azaphilones discovered to date, however, a general biosynthetic pathway cannot be postulated, and the biologically-mediated mechanisms of such reactions are unknown.

6.2 Materials and methods

Details on the materials and methods used for the extraction of mycoleptones A–C, their structural characterisation and the evaluation of their biological activity are reported in Andrioli *et al.* (**2014**), *J. Nat. Prod.* 77, 70.

UV and ECD spectra of **2** in MeOH (sample concentration: 19 μM) were recorded in the 500–215 nm spectral range on a Jasco J-810 spectropolarimeter, using a 1 cm pathlength cell at room temperature: measurements were carried out at 0.2 nm intervals using a 1 nm spectral bandwidth, a 20 nm min^{-1} scan rate and a 4 sec time constant.

Conformational analysis on the selected diastereomers of **2** was performed in two steps. In the first step, a preliminary conformer distribution was determined by molecular mechanics (MM) calculations at the MMFF94s[125] level using the Spartan'02 software.[126] In the second step, DFT[127,128] geometry optimisations were performed on the MM conformers having relative energies (ΔE_{MM}) within a threshold value of 3 kcal mol^{-1} (Table 6.2). DFT calculations were carried out at the B97D/6-311++G(2*d*,2*p*) level[153,154,183–185] using the Gaussian 09 software package.[129] The Boltzmann distribution of conformers at 298.15 K and 1 atm was then calculated from the relative electronic energies (ΔE_{QM}). TD-DFT[137] calculations were carried out at the PBE0/6-311++G(2*d*,2*p*) level[155–157,183–185] using the Gaussian 09 software package.[129] All calculations were performed using the IEFPCM continuum solvation model[114,136] for MeOH. Rotational strengths (R_j) and excitation wavelengths (λ_j) were calculated for the lowest 50 excited states on the optimised geometries having $\Delta E_{QM} \leq 2$ kcal mol^{-1} (Tables 6.4 and 6.5). Theoretical ECD spectra were then obtained by approximation of R_j values to Gaussian functions with a half-bandwidth at $\Delta\varepsilon_{max}/e$ ($\Delta\sigma$) of 0.3 eV, summation over all excited states and conformational averaging (Figure 6.15), according to the Boltzmann distribution of conformers (χ_{QM}).[113]

Table 6.1. Enantiomer pairs of **2**.

Enantiomer pair		Stereochemical relationship
(7*R*,8*S*,7′*R*,8′*S*)-**2** (**2A**)	(7*S*,8*R*,7′*S*,8′*R*)-**2**	enantiomers
(7*R*,8*S*,7′*R*,8′*R*)-**2** (**2B**)	(7*S*,8*R*,7′*S*,8′*S*)-**2**	enantiomers
(7*R*,8*S*,7′*S*,8′*S*)-**2** (**2C**)	(7*S*,8*R*,7′*R*,8′*R*)-**2**	enantiomers
(7*R*,8*S*,7′*S*,8′*R*)-**2**	(7*S*,8*R*,7′*R*,8′*S*)-**2**	*meso* structures
(7*R*,8*R*,7′*R*,8′*R*)-**2**	(7*S*,8*S*,7′*S*,8′*S*)-**2** (**2D**)	enantiomers
(7*R*,8*R*,7′*R*,8′*S*)-**2** (=**2B**)	(7*S*,8*S*,7′*S*,8′*R*)-**2**	enantiomers
(7*R*,8*R*,7′*S*,8′*R*)-**2**	(7*S*,8*S*,7′*R*,8′*S*)-**2** (=**2C**)	enantiomers
(7*R*,8*R*,7′*S*,8′*S*)-**2**	(7*S*,8*S*,7′*R*,8′*R*)-**2**	*meso* structures

Figure 6.8. Most populated equilibrium conformers of **2B**. *Left:* conformer **2B-b**. *Right:* conformer **2B-f**.

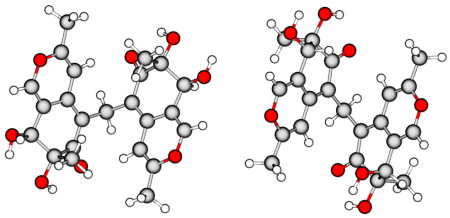

Figure 6.9. Most populated equilibrium conformers of **2C**. *Left:* conformer **2C-e**. *Right:* conformer **2C-f**.

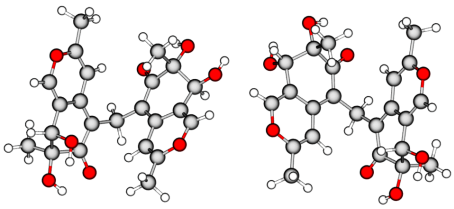

Figure 6.10. Most populated equilibrium conformer of **2D**, **2D-b**.

Table 6.2. Geometric parameters, energies and Boltzmann populations at 298.15 K and 1 atm for the most populated equilibrium conformers of the diastereomers of mycoleptone A, as obtained after MMFF94s conformational analysis. α_1: C-10–C-5–C-12–C-5′ dihedral. α_2: C-10′–C-5′–C-12–C-5 dihedral. β: O-2–C-5–C-5′–O-2′ dihedral. d: O-2–O-2′ distance.

	Conf. ID	α_1 (deg)	α_2 (deg)	β (deg)	d (Å)	E_{MM} (kcal mol^{-1})	ΔE_{MM}	χ_{MM} (%)
2A	**2A-a**	104.133	104.133	145.786	9.835	120.826	0.000	47.78
	2A-b	85.747	85.747	117.739	8.789	120.887	0.061	43.09
	2A-c	63.706	−123.003	−53.149	7.644	122.062	1.236	5.93
	2A-d	−112.477	−112.477	179.272	10.346	122.756	1.931	1.84
	2A-e	−61.264	−61.264	−97.952	7.984	123.193	2.367	0.88
	2A-f	130.976	−57.885	47.728	7.536	123.591	2.765	0.45
2B	**2B-a**	107.576	107.354	152.043	9.988	120.758	0.000	42.96
	2B-b	81.956	81.874	112.549	8.544	120.901	0.142	33.79
	2B-c	−123.727	63.437	−53.799	7.670	121.676	0.917	9.13
	2B-d	62.067	−124.427	−55.849	7.725	121.704	0.945	8.71
	2B-e	127.960	−64.608	44.628	7.395	122.498	1.740	2.28
	2B-f	−60.796	−59.880	−96.696	7.930	122.891	2.133	1.17
	2B-g	−110.191	−110.341	−175.254	10.313	123.072	2.313	0.87
	2B-h	80.855	82.003	111.906	8.529	123.467	2.709	0.44
	2B-i	−57.254	129.772	47.317	7.495	123.646	2.888	0.33
	2B-j	104.966	105.184	147.804	9.895	123.659	2.901	0.32
2C	**2C-a**	127.965	−59.652	51.038	7.319	121.060	0.000	31.23
	2C-b	59.734	−126.237	−49.766	7.255	121.197	0.137	24.79
	2C-c	111.482	106.010	162.168	10.173	121.230	0.170	23.43
	2C-d	−110.770	−114.688	−171.479	10.284	121.588	0.528	12.80
	2C-e	70.744	66.783	100.667	8.059	122.397	1.336	3.27
	2C-f	−66.042	−69.672	−99.582	7.986	122.523	1.463	2.64
	2C-g	−122.837	69.747	−45.360	7.751	123.229	2.169	0.80
	2C-h	91.554	94.510	130.262	9.321	123.376	2.316	0.63
	2C-i	−61.250	129.008	52.835	7.975	123.634	2.573	0.41
2D	**2D-a**	−110.448	−110.448	−158.114	10.109	120.773	0.000	47.96
	2D-b	−79.124	−79.124	−108.855	8.366	121.094	0.320	27.93
	2D-c	−62.506	124.760	55.302	7.732	121.319	0.545	19.10
	2D-d	64.235	−126.841	−44.160	7.362	122.335	1.562	3.43
	2D-e	102.093	112.588	159.515	10.127	123.275	2.501	0.70
	2D-f	−110.293	−110.209	−157.743	10.107	123.458	2.684	0.52
	2D-g	−82.069	−80.937	−112.358	8.553	123.685	2.912	0.35

Table 6.3. Geometric parameters, energies and Boltzmann populations at 298.15 K and 1 atm for the most populated equilibrium conformers of the diastereomers of mycoleptone A, as obtained after DFT geometry optimisation at the B97D/6-311++G(2*d*,2*p*)/IEFPCM(MeOH) level. α_1: C-10–C-5–C-12–C-5′ dihedral. α_2: C-10′–C-5′–C-12–C-5 dihedral. β: O-2–C-5–C-5′–O-2′ dihedral. d: O-2–O-2′ distance.

	Conf. ID	α_1 (deg)	α_2 (deg)	β (deg)	d (Å)	E_{QM} (Ha)	ΔE_{QM} (kcal mol^{-1})	χ_{QM} (%)
2A	**2A-e**	−57.348	−57.348	−95.326	7.453	−1492.14731609	0.000	59.34
	2A-b	66.788	66.788	101.136	7.806	−1492.14692907	0.243	39.39
	2A-f	−51.452	123.033	49.122	6.992	−1492.14309718	2.647	0.68
	2A-a	111.962	111.962	168.029	10.249	−1492.14257458	2.975	0.39
	2A-c	−118.093	65.960	−41.364	7.034	−1492.14163779	3.563	0.14
	2A-d	−101.750	−101.750	−159.334	10.111	−1492.14067396	4.168	0.05
2B	**2B-f**	−56.583	−55.703	−92.428	7.308	−1492.14939496	0.000	65.40
	2B-b	68.871	69.671	105.736	8.045	−1492.14875818	0.400	33.32
	2B-i	−52.015	123.267	49.618	7.069	−1492.14480866	2.878	0.51
	2B-a	110.637	111.089	166.773	10.236	−1492.14453399	3.050	0.38
	2B-d	65.879	−117.358	−39.934	6.952	−1492.14351203	3.692	0.13
	2B-c	−118.940	65.287	−42.642	7.111	−1492.14348219	3.710	0.12
	2B-h	68.788	69.613	105.285	8.016	−1492.14331039	3.818	0.10
	2B-g	−101.334	−100.982	−157.261	10.080	−1492.14204632	4.611	0.03
	2B-j	110.524	110.357	165.342	10.218	−1492.14061049	5.512	0.01
	2B-e	129.869	−57.582	54.017	7.112	−1492.14009469	5.836	0.00
2C	**2C-e**	62.947	57.866	94.503	7.444	−1492.14938642	0.000	58.86
	2C-f	−60.999	−66.239	−101.552	7.806	−1492.14901068	0.236	39.53
	2C-a	122.789	−63.145	41.897	6.976	−1492.14520399	2.625	0.70
	2C-b	62.990	−122.707	−43.272	6.987	−1492.14509552	2.693	0.63
	2C-i	−54.099	118.890	47.630	7.035	−1492.14338140	3.768	0.10
	2C-d	−102.904	−110.476	−163.217	10.181	−1492.14330924	3.813	0.09
	2C-c	110.660	103.455	162.699	10.173	−1492.14315665	3.909	0.08
	2C-h	69.193	67.197	103.855	7.959	−1492.14097434	5.279	0.01
	2C-g	−125.289	60.090	−52.050	7.134	−1492.13867788	6.720	0.00
2D	**2D-b**	−68.275	−68.275	−104.848	8.007	−1492.15018572	0.000	97.09
	2D-a	−110.238	−110.238	−166.366	10.237	−1492.14649001	2.319	1.94
	2D-c	−65.526	117.723	40.294	7.005	−1492.14533746	3.042	0.57
	2D-g	−69.683	−69.600	−106.345	8.063	−1492.14491169	3.310	0.36
	2D-f	−110.788	−111.069	−167.115	10.248	−1492.14250601	4.819	0.03
	2D-d	57.261	−129.194	−54.002	7.103	−1492.14158992	5.394	0.01
	2D-e	100.647	108.985	155.438	9.992	−1492.13699803	8.275	0.00

Table 6.4. Rotational strengths in dipole velocity formalism and excitation wavelengths for the lowest-energy electronic transitions of the conformers of **2A** and **2B**, as obtained by TD-DFT calculations at the PBE0/6-311++G(2*d*,2*p*)/IEFPCM(MeOH)//B97D/6-311++G-(2*d*,2*p*)/IEFPCM(MeOH) level.

j	R_j, 10^{-40} erg cm^3 (λ_j, nm)			
	2A-f	**2A-b**	**2B-f**	**2B-b**
1	−11.8627 (388.20)	−2.3228 (380.45)	−8.1261 (390.54)	−6.2926 (381.98)
2	−0.8655 (386.41)	1.5367 (379.27)	−6.1430 (384.54)	−1.5810 (378.53)
3	306.4914 (350.34)	−266.715 (347.22)	289.3154 (349.57)	−220.201 (346.06)
4	−214.797 (344.77)	231.4787 (341.07)	−262.8130 (344.51)	163.2161 (340.12)
5	48.7161 (311.54)	1.8770 (307.48)	93.5159 (312.86)	13.6244 (309.14)
6	16.7494 (310.74)	−35.4868 (307.43)	17.8819 (310.17)	−25.6249 (306.96)
7	−161.4120 (283.26)	158.4988 (279.03)	−43.5191 (289.72)	65.7500 (286.51)
8	82.7628 (281.86)	−83.6351 (278.47)	−29.5673 (282.13)	15.0886 (279.35)
9	−4.4171 (265.44)	18.7194 (262.82)	12.1380 (269.12)	1.3810 (264.06)
10	−30.2226 (265.18)	−9.1462 (262.73)	−4.3166 (265.10)	−0.8975 (262.82)
11	−30.4686 (262.42)	−25.1264 (258.59)	10.3538 (264.06)	−7.0032 (261.09)
12	44.6761 (261.00)	−15.4280 (257.79)	2.6154 (260.16)	−9.1265 (257.14)
13	91.2995 (258.87)	−58.1413 (257.03)	−19.0188 (258.77)	9.2947 (256.36)
14	−99.3923 (257.77)	98.2885 (255.42)	−8.4613 (250.15)	0.6452 (248.15)
15	5.9954 (244.88)	0.6066 (243.57)	−12.8770 (245.59)	0.7904 (244.01)
16	−2.0603 (244.61)	−1.1951 (243.54)	0.8369 (238.51)	40.2244 (239.36)
17	−0.1035 (238.73)	54.7496 (235.78)	−11.0921 (237.87)	19.0611 (235.66)
18	−50.1214 (235.57)	−7.7795 (235.49)	20.5525 (235.73)	−0.0412 (234.58)
19	79.4270 (235.46)	−1.2362 (234.23)	10.0082 (232.81)	2.6310 (231.86)
20	−6.6618 (234.19)	−1.7342 (231.35)	3.4361 (232.61)	−2.3991 (230.01)
21	−0.8256 (226.12)	−34.2275 (223.46)	−6.2545 (225.61)	−26.5278 (224.83)
22	0.9751 (223.71)	−13.6118 (223.34)	1.1054 (225.29)	−5.4805 (223.85)
23	−1.6706 (223.61)	1.4444 (223.24)	2.0651 (224.94)	3.2987 (223.44)
24	10.2845 (222.10)	4.8909 (221.24)	−6.9646 (223.05)	−25.1564 (222.51)
25	3.7887 (219.08)	0.9891 (218.50)	−0.9708 (220.97)	0.2346 (220.51)
26	2.4888 (218.82)	−11.5434 (218.47)	−4.4970 (218.55)	−2.9781 (218.27)
27	−5.7478 (218.70)	17.3107 (217.59)	7.5770 (218.34)	8.4638 (217.49)
28	−18.9606 (215.91)	0.4967 (217.56)	−20.2139 (216.84)	−2.6049 (215.92)
29	−14.7608 (215.37)	−0.5645 (214.20)	−1.9206 (215.32)	0.1566 (214.97)
30	59.6110 (212.53)	0.0514 (212.15)	−2.3974 (214.87)	−1.4237 (212.80)
31	1.1552 (212.33)	−10.5776 (211.48)	8.8786 (213.30)	−11.4886 (212.37)
32	−11.1260 (208.75)	2.4815 (209.03)	58.8806 (211.27)	−1.5396 (211.44)
33	28.0978 (208.68)	10.5860 (206.18)	−2.5356 (209.58)	−2.7039 (208.47)
34	22.3023 (208.32)	−61.8899 (205.94)	12.2739 (208.02)	3.4177 (206.44)
35	4.1014 (207.48)	5.6392 (205.61)	0.6789 (206.54)	−13.9937 (206.21)
36	0.0059 (206.62)	−11.9652 (203.45)	−21.9707 (206.24)	−0.6379 (204.61)
37	−10.4592 (204.80)	−1.0949 (202.38)	4.1421 (206.08)	−17.7215 (204.01)
38	−3.3698 (204.65)	−1.9639 (202.28)	−4.0058 (205.86)	−8.1654 (203.45)
39	0.7854 (203.48)	−32.1118 (201.47)	2.8864 (204.48)	−1.6027 (202.37)
40	−7.4461 (203.46)	−45.0073 (201.07)	−2.3743 (204.30)	14.4358 (202.26)
41	−14.8326 (203.25)	31.4616 (200.75)	−1.4176 (203.79)	−10.0038 (201.17)
42	4.7589 (202.93)	65.2460 (199.94)	−6.3511 (202.89)	−3.1231 (200.00)
43	−62.7396 (202.49)	−41.5590 (199.75)	1.0640 (202.13)	−21.2851 (199.34)
44	41.1215 (200.22)	−5.1701 (199.32)	6.6757 (200.71)	−1.3573 (198.78)
45	96.7164 (200.04)	97.7091 (198.17)	32.5641 (199.84)	29.5197 (198.55)
46	−147.3337 (199.48)	−18.3309 (198.02)	−38.8989 (199.28)	26.8917 (197.74)
47	34.2083 (198.90)	−82.1598 (197.04)	−12.7570 (198.01)	−49.8847 (196.88)
48	−5.7447 (198.28)	26.2399 (196.87)	−3.1815 (197.97)	20.4329 (196.55)
49	−7.8041 (197.24)	4.2789 (195.88)	−0.3341 (197.25)	6.0651 (195.75)
50	−3.8260 (196.85)	0.7657 (195.81)	−6.6401 (196.69)	7.0831 (195.54)

Table 6.5. Rotational strengths in dipole velocity formalism and excitation wavelengths for the lowest-energy electronic transitions of the conformers of **2C** and **2D**, as obtained by TD-DFT calculations at the PBE0/6-311++G(2*d*,2*p*)/IEFPCM(MeOH)//B97D/6-311++G-(2*d*,2*p*)/IEFPCM(MeOH) level.

j	R_j, 10^{-40} erg cm^3 (λ_j, nm)		
	2C-e	**2C-f**	**2D-b**
1	1.5285 (388.29)	0.7501 (385.72)	8.1326 (381.81)
2	−2.0519 (381.11)	2.6710 (383.72)	0.8473 (379.18)
3	−193.539 (349.97)	207.1990 (349.53)	260.5551 (344.41)
4	200.2323 (343.02)	−109.3724 (341.61)	−148.019 (339.16)
5	−90.7482 (312.48)	41.6476 (311.48)	−12.4128 (309.90)
6	−3.0468 (308.72)	−23.9856 (310.89)	−15.7669 (309.86)
7	36.0748 (290.17)	−93.8881 (287.44)	−189.2505 (287.33)
8	34.2680 (278.66)	8.6524 (282.66)	99.7377 (285.45)
9	−2.7638 (268.30)	−10.8551 (266.56)	−10.5236 (263.40)
10	−9.0818 (265.38)	9.4849 (265.17)	5.0605 (262.68)
11	−2.4284 (263.40)	9.3724 (263.81)	27.9198 (262.16)
12	2.8694 (258.15)	14.6820 (259.42)	−13.7403 (261.53)
13	−13.5407 (258.04)	−32.9258 (258.79)	45.5109 (248.41)
14	21.1145 (250.63)	9.8562 (248.04)	−27.7822 (248.02)
15	7.6645 (247.14)	2.8270 (243.58)	−13.8291 (239.89)
16	17.2808 (238.04)	−37.4889 (238.84)	−59.2329 (238.82)
17	6.7557 (235.48)	0.3108 (237.01)	7.0725 (233.52)
18	0.1787 (235.12)	15.3744 (235.84)	−0.2977 (232.47)
19	0.1801 (231.86)	−4.1845 (233.93)	−7.4959 (231.79)
20	−3.1667 (231.74)	−2.1972 (231.50)	−6.8990 (228.91)
21	−2.0600 (226.33)	−0.7150 (225.47)	−4.1539 (224.36)
22	−1.3720 (224.19)	0.5390 (223.65)	−0.2614 (223.90)
23	10.3668 (223.84)	5.5005 (223.16)	5.5582 (223.44)
24	1.5609 (223.09)	5.7528 (222.17)	2.2323 (222.95)
25	0.6348 (220.26)	−22.5071 (219.61)	66.5343 (222.25)
26	−2.6574 (219.03)	18.2131 (219.14)	0.1673 (219.27)
27	−0.1964 (217.42)	10.5947 (218.42)	−2.5398 (216.68)
28	4.2055 (215.77)	8.2378 (217.23)	3.4280 (215.46)
29	−1.2962 (215.58)	−2.2093 (213.94)	6.1730 (215.29)
30	−6.0979 (215.13)	2.7938 (213.64)	0.2509 (213.13)
31	1.3671 (212.72)	46.5541 (213.57)	0.5293 (212.95)
32	−38.5102 (211.62)	0.7169 (212.89)	7.9919 (212.35)
33	2.7249 (208.69)	7.6454 (209.23)	7.9064 (211.98)
34	4.5434 (207.24)	−4.4375 (207.77)	2.1634 (207.96)
35	−26.3837 (206.21)	−0.0322 (206.42)	−0.3505 (205.04)
36	0.2109 (205.80)	0.8288 (206.32)	0.0131 (205.04)
37	−21.2337 (205.00)	−6.0575 (205.05)	7.6147 (204.81)
38	14.7381 (204.40)	−1.6228 (203.93)	2.9373 (204.64)
39	0.5535 (204.34)	−11.7620 (203.39)	−12.6903 (203.32)
40	−8.7942 (203.29)	4.3413 (203.29)	−0.3947 (201.71)
41	4.7457 (202.74)	−2.6452 (202.94)	−9.4550 (200.70)
42	0.4342 (201.48)	−4.8493 (201.99)	−7.9653 (200.40)
43	−23.7488 (200.69)	6.6432 (201.06)	12.3095 (199.34)
44	−11.0727 (199.97)	−3.2448 (200.57)	3.0313 (198.76)
45	−0.5058 (199.64)	−22.0420 (199.57)	−29.3246 (197.90)
46	97.5397 (198.33)	8.6798 (198.97)	50.0501 (196.92)
47	−56.7747 (198.09)	6.0051 (198.35)	−24.8339 (196.85)
48	−11.3728 (197.33)	0.0303 (197.27)	29.4857 (196.83)
49	3.4840 (196.52)	−2.8820 (196.88)	−8.9621 (196.41)
50	−13.1370 (195.81)	−5.6427 (196.59)	−3.2572 (195.13)

Figure 6.11. Possible pathway for the biosynthesis of mycoleptone A.

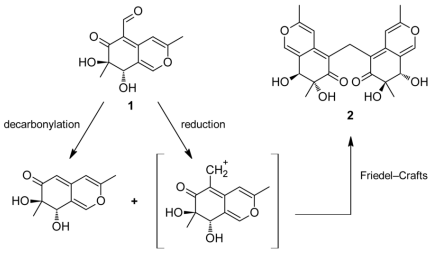

Figure 6.12. Theoretical ECD spectrum of **2B** and comparison with experimental data. *Blue:* experimental ECD spectrum of **2** (19 μM in MeOH, 1 cm pathlength). *Green:* theoretical ECD spectrum of **2B** at the PBE0/6-311++G(2*d*,2*p*)/IEFPCM(MeOH)//B97D/6-311++G-(2*d*,2*p*)/IEFPCM(MeOH) level (χ_{QM}-based conformational averaging, $\Delta\sigma = 0.3$ eV).

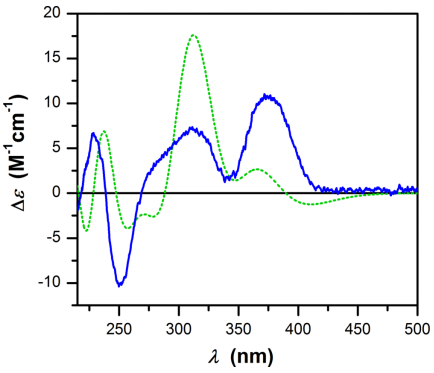

Figure 6.13. Theoretical ECD spectrum of **2C** and comparison with experimental data. *Blue:* experimental ECD spectrum of **2** (19 μM in MeOH, 1 cm pathlength). *Orange:* theoretical ECD spectrum of **2C** at the PBE0/6-311++G(2*d*,2*p*)/IEFPCM(MeOH)//B97D/6-311++G-(2*d*,2*p*)/IEFPCM(MeOH) level (χ_{QM}-based conformational averaging, $\Delta\sigma = 0.3$ eV).

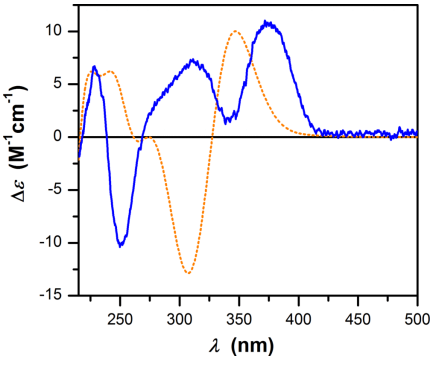

Figure 6.14. Theoretical ECD spectrum of **2D** and comparison with experimental data. *Blue:* experimental ECD spectrum of **2** (19 μM in MeOH, 1 cm pathlength). *Green:* theoretical ECD spectrum of **2D-b** at the PBE0/6-311++G(2*d*,2*p*)/IEFPCM(MeOH)//B97D/6-311++G-(2*d*,2*p*)/IEFPCM(MeOH) level ($\Delta\sigma$ = 0.3 eV).

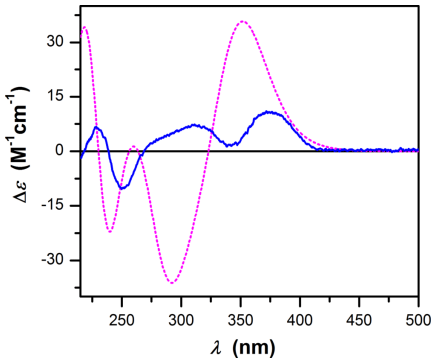

Figure 6.15. Theoretical ECD spectrum of **2A** and weighed contributions from conformers at the PBE0/6-311++G(2*d*,2*p*)/IEFPCM(MeOH)//B97D/6-311++G(2*d*,2*p*)/IEFPCM(MeOH) level ($\Delta\sigma$ = 0.3 eV). *Red:* theoretical ECD spectrum of **2A** (χ_{QM}-based conformational averaging). *Green:* weighed theoretical ECD spectrum of **2A-e** (χ_{QM} = 59.34%). *Orange:* weighed theoretical ECD spectrum of **2A-b** (χ_{QM} = 39.39%).

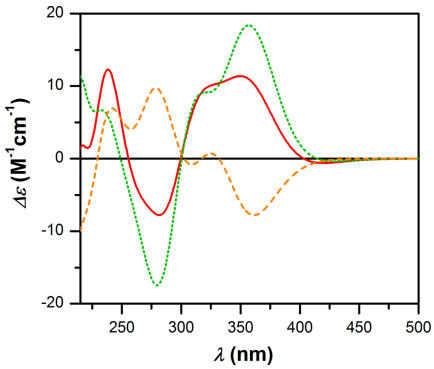

Part III

Conformational flexibility

If something has to change
Then it always does

— Editors, *Bullets*

Chapter 7

β-lactam derivatives

This chapter is based on a peer-reviewed publication:
Daniele Tedesco, Riccardo Zanasi, Andrea Guerrini, Carlo Bertucci (**2012**). Conformational flexibility and absolute stereochemistry of (3*R*)-3-hydroxy-4-aryl-β-lactams investigated by chiroptical properties and TD-DFT calculations. *Chirality* 24, 741–750.

Abstract: The effect of conformational flexibility on the chiroptical properties of a series of synthetic (3*R*)-3-hydroxy-4-aryl-β-lactams of known stereochemistry (**1–6**) was investigated by means of electronic circular dichroism (ECD) measurements and time-dependent density functional theory (TD-DFT) calculations. The application of the β-lactam sector rules allowed a correct stereochemical characterization of these compounds, with the exception of a thienyl-substituted derivative (*cis*-**6**). TD-DFT calculations yielded accurate predictions of experimental ECD spectra and $[\alpha]_D$ values, allowing us to assign the correct absolute configuration to all the investigated compounds. A detailed analysis of the β-lactam ring equilibrium geometry on optimized conformers identified regular patterns for the arrangement of atoms around the amide chromophore, confirming the validity of the β-lactam sector rules. However, relevant variations in theoretical chiroptical properties were found for compounds bearing a heterocyclic substituent at C4 or a phenyl substituent at C3, whose conformers deviate from these regular geometric patterns. This behaviour explains the failure of the β-lactam sector rules in *cis*-**6**. This study showed the importance of conformational flexibility for the determination of chiroptical properties and highlighted the strengths and weaknesses of the different methods for the stereochemical characterization of chiral molecules in solution.

β-Lactam rings play a fundamental role in medicinal chemistry. β-Lactam derivatives have been widely used in therapy as antibiotics,[186–191] cholesterol absorption inhibitors,[192–194] and prostate-specific antigen inhibitors.[195] Moreover, their employment as precursors for the asymmetric synthesis of a variety of compounds of medicinal interest, such as proteinogenic and non-proteinogenic amino acids for peptides and peptidomimetics, taxanes, statines, and norstatines, is well documented in literature under the name of β-lactam synthon method.[196–200]

A series of (3*R*)-3-hydroxy-4-aryl-β-lactam derivatives (Figures 7.1 and 7.2) was previously synthesised for this purpose[201–204] through the synthetic method of self-regeneration of stereocentres,[205] consisting in addition reactions of arylimines to lithium enolates of (2*S*,5*S*)-dioxolan-4-ones, which allowed full control of stereochemistry at C3. Stereochemical characterisation is therefore crucial in the employment of these β-lactam derivatives as chiral intermediates. For these derivatives, it is mainly concerned with the confirmation of the absolute configuration at C3 and the determination of the relative configuration at C3 and C4, which allows the overall absolute stereochemistry to be consequently deduced.

Figure 7.1. General structure of (3*R*)-3-hydroxy-4-aryl-β-lactams.

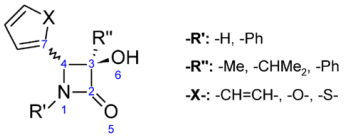

Several methods have been developed and applied to relate the chiroptical properties of β-lactams to their stereochemistry. β-Lactam sector rules are semi-empirical methods for predicting the Cotton effect (CE) arising from the amide chromophore of the lactam ring on the basis of the spatial disposition of atoms around the carbonyl group.[60–63] These methods are closely related to the octant rule for the carbonyl chromophore of ketones[56,57,59] and proved to be very effective in correlating the absolute configuration of stereogenic atoms around the chromophore to the experimental chiroptical properties, that is, optical rotation (OR) and electronic circular dichroism (ECD).

A semi-empirical helicity rule was proposed, suggesting a strong contribution of the intrinsic chirality of non-planar β-lactam rings to the CE of the amide moiety.[65] This method was successfully used to characterise the stereochemistry of small chiral β-lactam derivatives.[67] Another helicity rule was proposed

Figure 7.2. Selected (3*R*)-3-hydroxy-4-aryl-β-lactam derivatives.

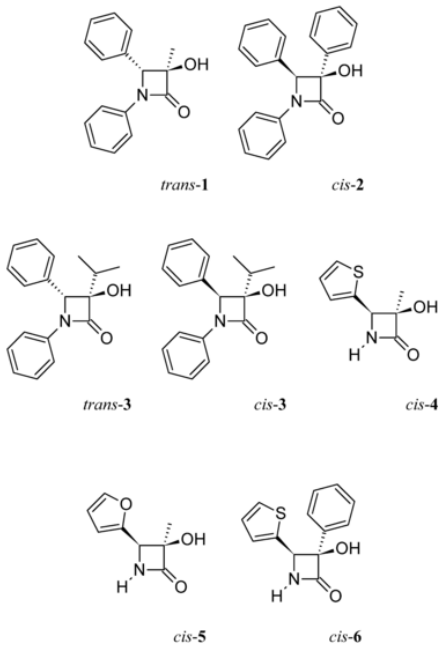

for bicyclic β-lactam derivatives, relating the CE for the amide chromophore to the absolute stereochemistry at the ring junction carbon atom.[66] The effect of conformational flexibility on the chiroptical properties of these derivatives was also investigated by means of molecular dynamics and quantum mechanical (QM) calculations.[68] Moreover, the absolute configuration of a different series of 4-substituted (3*R*)-3-hydroxy-β-lactam derivatives was reliably determined by the application of the exciton-coupled-based zinc-porphyrin tweezer methodology[73,206] combined with molecular mechanical (MM) and QM calculations.[207,208]

By applying the β-lactam sector rules to the series of (3*R*)-3-hydroxy-4-aryl-β-lactam derivatives under investigation, the signs of the specific rotatory power at the sodium D line ($[\alpha]_D$) and the lowest-energy band of the ECD spectra reflect the relative configuration of substituents at C3 and C4. Since the substituents at C3 lie on sectors having opposite contributions to the chiroptical properties, the most important contribution is ultimately due to the configuration of the aryl-substituted C4. In the specific case of (3*R*)-diastereomers, the hydroxyl group at C3 lies on a negative sector, and the hydrocarbon substituent at C3 lies on a positive sector. Compounds having the aryl substituent at C4 on the same

side of the hydroxyl group at C3 (*cis* configuration), therefore lying on a positive sector, are expected to show positive signs of chiroptical properties, whereas compounds having the opposite (*trans*) configuration should show negative signs because the aryl substituent at C4 lies on a negative sector. A full stereochemical characterisation by means of X-ray crystallography, ECD, and nuclear magnetic resonance (NMR) spectroscopies showed that the β-lactam sector rules successfully predicted the correct relative and absolute stereochemistry for the series.[64] Nevertheless, these semi-empirical methods failed to predict the correct signs of chiroptical properties for a 4-(thien-2-yl)-substituted derivative (compound *cis*-**6** in Figure 2), whose relative stereochemistry was determined by the nuclear Overhauser effect (NOE) and heteronuclear single quantum coherence spectroscopies.[204]

In the present study, the effects of geometric perturbations induced by conformational flexibility on the chiroptical properties of the β-lactam ring will be investigated in order to clarify the reasons behind the failure of β-lactam sector rules for the stereochemical characterisation of *cis*-**6** and to have a better insight on the close relationship between molecular geometry and optical activity for this class of molecules. The theoretical chiroptical properties of some selected (3*R*)-3-hydroxy-4-aryl-β-lactam derivatives were determined by full QM calculations by using the time-dependent density functional theory (TD-DFT)[137] and were compared to experimental data. The effect of conformational flexibility was subsequently investigated by analysing the variation of theoretical properties as a function of the geometric parameters of the β-lactam ring on the QM-optimised conformers as obtained with the density functional theory (DFT)[127,128] conformational analysis.

7.1 Materials and methods

Experimental measurements and QM calculations were performed on the following (3*R*)-3-hydroxy-4-aryl-β-lactam derivatives (Figure 7.2):

- (3*R*,4*R*)-3-hydroxy-3-methyl-1,4-diphenylazetidin-2-one (*trans*-**1**);
- (3*R*,4*S*)-3-hydroxy-1,3,4-triphenylazetidin-2-one (*cis*-**2**);
- (3*R*,4*R*)-3-hydroxy-1,4-diphenyl-3-(propan-2-yl)azetidin-2-one (*trans*-**3**);
- (3*R*,4*S*)-3-hydroxy-1,4-diphenyl-3-(propan-2-yl)azetidin-2-one (*cis*-**3**);
- (3*R*,4*R*)-3-hydroxy-3-methyl-4-(thiophen-2-yl)azetidin-2-one (*cis*-**4**);

- (3*R*,4*S*)-4-(furan-2-yl)-3-hydroxy-3-methylazetidin-2-one (*cis*-**5**);
- (3*R*,4*R*)-3-hydroxy-3-phenyl-4-(thiophen-2-yl)-azetidin-2-one (*cis*-**6**).

These derivatives were synthesised according to reported procedures. Experimental $[\alpha]_D$ values were also already reported and are summarised in Table 7.1.[64,201–204]

Table 7.1. Experimental and calculated $[\alpha]_D$ values (conformational averages according to Boltzmann statistics at 298.15 K and 1 atm) for (3*R*)-3-hydroxy-4-aryl-*β*-lactam derivatives **1-6**.[201,202,204]

	trans-**1**	*cis*-**2**	*trans*-**3**	*cis*-**3**	*cis*-**4**	*cis*-**5**	*cis*-**6**
experimental $[\alpha]_D$ **(deg cm^3 g^{-1} dm^{-1})**	−134.0	+52.6	−64	+180	+70	+70	−71
solvent	chloroform	chloroform	chloroform	chloroform	acetone	acetone	chloroform
temperature (°C)	19	19	22	22	22	22	20
calculated $[\alpha]_D$ **(deg cm^3 g^{-1} dm^{-1})**							
ΔE_{QM}-based average	−104.9	+111.2	−27	+147	+14	−29	−70
difference with exp.	+29.1	+58.6	+37	−33	−56	−99	+1
ΔG-based average	−105.9	+106.9	−25	+150	+14	−1	−102
difference with exp.	+28.1	+54.3	+39	−30	−56	−71	−31
conformers	2	5	4	9	6	5	7
SSM, ΔE_{QM}-based average					+69	+106	
difference with exp.					−1	+36	
SSM, ΔG-based average					+88	+180	
difference with exp.					+18	+110	
conformers					7	6	

7.1.1 Experimental spectroscopy

The ultraviolet (UV) and ECD spectra of *trans*-**1** (concentration: 0.4 mM; pathlength: 0.1 cm; range: 350–200 nm), *trans*-**3** (3.5 mM; 0.01 cm; 350–200 nm), *cis*-**3** (3.5 mM; 0.01 cm; 350–220 nm), and *cis*-**4** (5.5 mM; 0.01 cm; 300–190 nm) were recorded in 2-propanol (Sigma-Aldrich, Milan, Italy) on a Jasco (Tōkyō, Japan) J-720 spectropolarimeter at room temperature. The UV and ECD spectra of *cis*-**6** (1.0 mM; 0.1 cm; 350–220 nm) were recorded in 2-propanol (Sigma-Aldrich, Milan, Italy) on a Jasco (Tōkyō, Japan) J-810 spectropolarimeter at room temperature.

7.1.2 Computational spectroscopy

Conformational analysis

A preliminary conformational analysis on all the β-lactam derivatives under examination was carried out through MM calculations using the Spartan'02 software package.[126] A conformational search was performed using the systematic algorithm, and the conformer distribution was determined at the MMFF94s level.[125] Conformers having relative energies (ΔE_{MM}) within a threshold value of 5 kcal mol^{-1} were considered for geometry optimisation at the QM level.

DFT geometry optimisation calculations were carried out using B97D, a generalised gradient approximation functional with semi-empirical corrections for dispersion,[153,154] as implemented in the Gaussian 09 software package.[129] A triple-ζ double polarisation (TZ2P) basis set of Gaussian-type orbitals was employed in the calculations. For hydrogen and first-row atoms, the basis set consisted in Dunning's $[5s3p/3s]$ contraction[135] of Huzinaga's primitive $[10s6p/5s]$ set[134] with two sets of polarisation functions (α_p = 1.5, 0.375 for H; α_d = 1.5, 0.375 for C; α_d = 1.6, 0.4 for N; ad = 1.7, 0.425 for O) was used. For sulfur, McLean and Chandler's $[6s5p]$ contraction[159] of Huzinaga's primitive $[12s9p]$ set[160] with two sets of polarisation functions (α_d = 1.4, 0.35) was used.

Long-range solvent effects were taken into account by using the polarisable continuum model in its integral equation formalism (IEFPCM),[114,136] as implemented in the Gaussian 09 software package. The suitable solvation model was chosen depending on the environment of experimental data: chloroform for $[\alpha]_D$ calculations on *trans*-**1**, *cis*-**2**, *trans*-**3**, *cis*-**3**, and *cis*-**6**; acetone for $[\alpha]_D$ calculations on *cis*-**4** and *cis*-**5**; and 2-propanol for ECD calculations on *trans*-**1**, *trans*-**3**, *cis*-**3**, *cis*-**4**, and *cis*-**6**.

Conformational clustering was performed for optimised geometries having root mean square distances (RMSD) below 0.01 Åfor heavy atoms, as obtained after alignment of the azetidinone skeleton. Geometry alignment and RMSD determination were carried out using the VMD molecular graphics software.[209] The Boltzmann distribution of conformers in a given solvent, at 298.15 K and 1 atm, was subsequently calculated for each compound on the basis of the relative electronic energies (ΔE_{QM}) and relative free energies (ΔG).

Solvation clusters

A method of explicit treatment of solvent molecules around a solute in QM calculations, referred to in literature as the solvated supermolecule (SSM) approach,[114] was employed in the determination of the solvent-induced conformational flexibility and its effect on the chiroptical properties of *β*-lactam derivatives. SSM calculations were carried out on *cis*-**4** and *cis*-**5**, following the same protocol used for standard calculations. An MM conformational search was performed on solute–solvent clusters (labelled *cis*-**4*** and *cis*-**5***, respectively), obtained by placing a molecule of acetone close to each of the 2 H-bond donor groups (the lactam NH group and the hydroxyl group at C3), and with the carbonyl group oriented to interact through hydrogen bonding (Figure 7.3). Conformations having $\Delta E_{\mathrm{MM}} \leq 5$ kcal mol^{-1} were considered for DFT geometry optimisation.

Figure 7.3. Input geometry for the MM conformational search on *cis*-**5***.

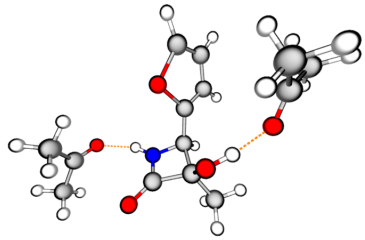

An early optimisation step using the B97D functional and the 6-31G* basis set[185,210–213] was introduced for *cis*-**5*** in order to reduce the time for analysis because the 6-31G* basis set is less expensive than the TZ2P in terms of computational time. B97D/6-31G* conformers having $\Delta E_{\mathrm{QM}} \leq 2.5$ kcal mol^{-1} were subsequently optimised at the B97D/TZ2P level. On the other hand, MM conformers of *cis*-**4*** were directly optimised at the B97D/TZ2P level. The IEFPCM solvation model for acetone was employed in DFT calculations in order to account for bulk effects.

TD-DFT calculations

The determination of theoretical chiroptical properties[28] was carried out by means of TD-DFT calculations using the Gaussian 09 software package.[129] Calculations were performed on the B97D/TZ2P optimised geometries of compounds **1–6** and on the solute–solvent clusters *cis*-**4*** and *cis*-**5***, employing the PBE0 exchange-correlation functional[155–157] and the TZ2P basis set. Theoretical

$[\alpha]_D$ values, as well as the excitation wave numbers (σ_j) and rotational strengths (R_j) for the lowest 50 excited states, were calculated on each optimised conformer by using the same IEFPCM solvation model employed in the optimisation process. Theoretical ECD spectra as a function of wave number, $\Delta\varepsilon(\sigma)$, were derived for each conformer by approximating the R_j values to the Gaussian functions and the summation over all excited states.[113] In this study, the half-bandwidth of the Gaussian functions ($\Delta\sigma$) was set to 0.4 eV. Conformational averaging, on the basis of the Boltzmann distribution of conformers, was subsequently performed to obtain the theoretical properties of the β-lactam derivatives at equilibrium.[28] Calculated ECD spectra were then converted in the wavelength scale for a convenient comparison with the experimental data.

7.2 Results and Discussion

7.2.1 Structural features of β-lactam derivatives

The (3*R*)-3-hydroxy-4-aryl-β-lactams under investigation show the following structural patterns (Figure 7.1):

a. the aromatic substituent at C4 is either a phenyl ring (X = –CH=CH– for *trans*-**1**, *cis*-**2**, *trans*-**3**, and *cis*-**3**), or a five-membered heterocycle (X = –S– for *cis*-**4** and *cis*-**6**; X = –O– for *cis*-**5**);

b. non-heteroaromatic derivatives are all phenyl-substituted at N1 (R′ = –Ph), whereas heteroaromatic derivatives are unsubstituted (R′ = –H);

c. the hydrocarbon substituent at C3 may either be aliphatic (R″ = –Me, –CHMe2) or aromatic (R″ = –Ph).

The four-membered β-lactam ring is a non-planar structure subject to a significant angle strain, which causes the geometry of the amide chromophore to deviate from planarity.[67] The conformational strain of the β-lactam ring may be conveniently characterised by a set of four dihedral angles: ψ_1 (O5–C2–N1–R′1) describes the torsion and intrinsic chirality of the amide C–N bond; ψ_2 (O5–C3–N1–C2) and ψ_3 (R′1–C2–C4–N1) describe the pyramidalisation of C2 and N1, respectively; and ψ_4 (O5–C2–N1–C4) describes the deviation of C4 from the hypothetical plane of the carbonyl group (O5–C2–N1 plane).

Additional conformational flexibility arises from the orientation of substituents at C3 and C4: ϕ_1 (C3–C4–C7–X) describes the orientation of the aromatic substituent at C4 (XC for phenyl, O for furyl, S for thienyl); ϕ_2 (C4–C3–R″1–R″2)

describes the orientation of hydrocarbon substituents other than methyl groups at C3 (R″2H for isopropyl, C for phenyl); and ω (C4–C3–O6–H6) describes the orientation of the O–H bond for the hydroxyl group at C3.

7.2.2 Conformational analysis

Relative energies and fractional populations for the MM conformers of *cis*-**6** are reported in Table 7.2; full details on the geometric parameters, energies, and fractional populations for the MM conformers of all the *β*-lactam derivatives are given in Tables 7.7–7.8.

Table 7.2. Relative energies and Boltzmann equilibrium populations at 298.15 K and 1 atm for the conformers of *cis*-**6**, as obtained after MM conformational analysis.

Conf. ID	ΔE_{MM} (kcal mol^{-1})	χ_{MM} (%)
cis-**6a**	0.000	65.96
cis-**6b**	0.878	14.97
cis-**6c**	1.438	5.82
cis-**6d**	1.493	5.30
cis-**6e**	1.584	4.55
cis-**6f**	1.801	3.15
cis-**6g**	3.528	0.17
cis-**6h**	4.038	0.07

As a result, two conformers for *trans*-**1** (labelled *trans*-**1a–b**), eight for *cis*-**2** (*cis*-**2a–h**), four for *trans*-**3** (*trans*-**3a–d**), nine for *cis*-**3** (*cis*-**3a–i**), six for *cis*-**4** (*cis*-**4a–f**), eight for *cis*-**4*** (*cis*-**4*a–h**), six for *cis*-**5** (*cis*-**5a–f**), twenty-three for *cis*-**5*** (*cis*-**5*a–w**), and eight for *cis*-**6** (*cis*-**6a–h**) were found below the energy threshold value of 5 kcal mol^{-1} and were optimised at the DFT level.

Relative electronic and free energies, and corresponding Boltzmann populations for the DFT conformers of *cis*-**6** are reported in Table 7.3; full details are given in Tables 7.9–7.18, while graphical representations of the most populated conformers are reported in Figures 7.8–7.16.

The preliminary B97D/6-31G* optimisation step for *cis*-**5*** identified sixteen SSM conformations having $\Delta E_{QM} \leq 2.5$ kcal mol^{-1}. After RMSD analysis, some optimised geometries were clustered: *cis*-**2b/f**, *cis*-**2c/d/e**, *cis*-**5e/f**, *cis*-**5*l/p**, *cis*-**5*r/u**, *cis*-**5*b/v**, *cis*-**5*c/q**, *cis*-**5*m/o**, and *cis*-**6e/f**. The B97D/TZ2P optimisation step reduced the number of SSM conformations to seven for *cis*-**4*** and six for *cis*-**5*** because the interaction between acetone and H-bond donor groups was lost during the optimisation process for some conformers (Tables 7.14 and 7.17).

Table 7.3. Relative energies and Boltzmann equilibrium populations at 298.15 K and 1 atm for the conformers of *cis*-**6**, as obtained after DFT geometry optimisation (B97D/TZ2P) in chloroform and 2-propanol (IEFPCM solvation models). RMSD values for *cis*-**6e/f**: 0.0050 Å (chloroform), 0.0004 Å (2-propanol).

Solvent	Conf. ID	ΔE_{QM} (kcal mol^{-1})	χ_{QM} (%)	ΔG (kcal mol^{-1})	χ_G (%)
Chloroform	*cis*-**6c**	0.000	56.16	0.000	45.83
	cis-**6f**	0.492	24.48	0.390	23.74
	cis-**6g**	1.487	4.56	1.099	7.16
	cis-**6h**	1.527	4.27	1.092	7.25
	cis-**6b**	1.534	4.21	1.209	5.95
	cis-**6d**	1.698	3.19	1.279	5.29
	cis-**6a**	1.713	3.11	1.340	4.78
2-Propanol	*cis*-**6c**	0.000	62.71	0.000	34.27
	cis-**6e**	0.679	19.94	0.136	27.26
	cis-**6g**	1.429	5.62	0.919	7.27
	cis-**6h**	1.649	3.88	0.299	20.68
	cis-**6b**	1.797	3.02	1.260	4.09
	cis-**6d**	1.909	2.50	1.293	3.87
	cis-**6a**	1.950	2.33	1.536	2.57

7.2.3 Chiroptical properties

The comparison between conformationally averaged $[\alpha]_D$ calculations and experimental data is shown in Table 7.1, whereas the comparison between the experimental and theoretical ECD data for *trans*-**1**, *trans*-**3**, *cis*-**3**, *cis*-**4**, and *cis*-**6** are reported in Table 7.4 and Figure 7.4. The experimental UV and ECD spectra are reported in Figures 7.17–7.20, the calculated R_j values for the first 25 low-energy electronic transitions of each conformer in Tables 7.20–7.22, and the Pearson correlation coefficients (r)[138] for the comparison between the experimental and theoretical ECD spectra in Table 7.19.

Table 7.4. Experimental and calculated values (conformational averages according to Boltzmann statistics at 298.15 K and 1 atm) for the ECD bands of (3*R*)-3-hydroxy-4-aryl-β-lactam derivatives **1-6** in the 350–200 nm range.

	trans-**1**	*trans*-**3**	*cis*-**3**	*cis*-**4**	*cis*-**6**
experimental $\Delta\varepsilon_{max}$, M^{-1} cm^{-1} (λ_{max}, nm)	−8.4 (246) +2.7 (212)	−13.7 (248)	+10.6 (248)	−1.4 (245) +11.9 (223)	−4.5 (246) +2.0 (219) −4.2 (205)
experimental $\Delta\varepsilon_{max}$, M^{-1} cm^{-1} (λ_{max}, nm)					
ΔE_{QM}-based average	−9.6 (251) –	−7.2 (255)	+13.8 (257)	– +12.2 (227)	−5.1 (244) +3.5 (220) −3.2 (206)
ΔG-based average	−9.6 (251) –	−7.2 (255)	+14.2 (256)	– +12.5 (228)	−13.2 (246) +5.9 (219) −0.6 (205)
conformers	2	4	9	6	7

As a general trend, a good agreement between experimental and theoretical properties was found for all the examined compounds, irrespective of the type

Figure 7.4. Comparison between experimental and theoretical ECD spectra for selected (3*R*)-3-hydroxy-4-aryl-*β*-lactam derivatives. *Solid:* experimental in 2-propanol; *Dashed:* theoretical (PBE0/TZ2P//B97D/TZ2P, IEFPCM solvation model for 2-propanol), ΔE_{QM}-based averaging, $\Delta\sigma = 0.4$ eV; *Dotted:* theoretical (PBE0/TZ2P//B97D/TZ2P, IEFPCM solvation model for 2-propanol), ΔG-based averaging, $\Delta\sigma = 0.4$ eV. **a:** *trans*-**1**; **b:** *cis*-**3** (*thin*) and *trans*-**3** (*bold*); **c:** *cis*-**4**; **d:** *cis*-**6**.

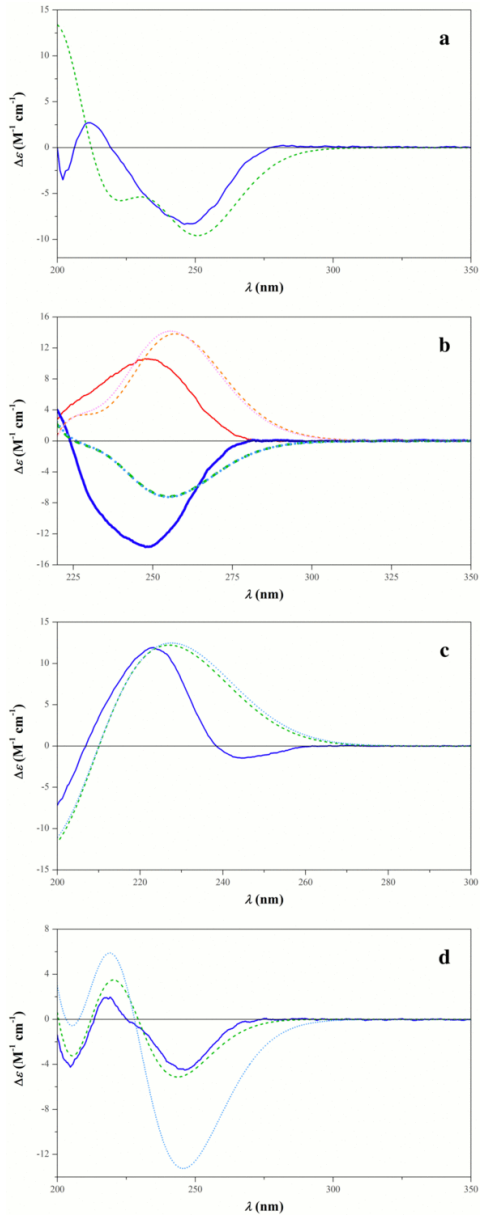

of relative energy used in the conformational averaging process. Although ΔG-based Boltzmann populations are usually preferred in the description of conformationally averaged chiroptical properties,[28,214] the accuracy of calculated ΔG values is strongly dependent upon the size of the molecular system and other factors limiting the ability to calculate the appropriate entropy terms and enthalpy corrections. ΔE_{QM}-based populations may perform better when errors in the calculation of ΔG values become relevant.[28] In the specific case of the TD-DFT calculations on *cis*-**6**, ΔE_{QM}-based conformational averaging yielded better correlation with experimental data, which were reproduced in a very accurate fashion (difference between calculated and experimental values $[\alpha]_D$: $+1$; r = 0.9264 for the ECD comparison; Figure 7.4d).

TD-DFT calculations using IEFPCM solvation models, without treatment of solvent molecules at a QM level, were sufficient to yield a good agreement with the experimental data in the chloroform and 2-propanol. A poor correlation with the experimental data in the acetone was found for *cis*-**4** and *cis*-**5** (differences between ΔE_{QM}-averaged calculations and experimental $[\alpha]_D$ values were $-56°$ and $-99°$, respectively). For the latter compound, calculated and experimental $[\alpha]_D$ values had opposite signs. The application of the SSM approach was then limited to $[\alpha]_D$ calculations in acetone for three reasons:

a. single-wavelength $[\alpha]_D$ calculations are more sensitive than full-spectrum ECD calculations to systematic errors because of the approximations made in the TD-DFT calculations;[28]

b. the poor correlation between the theoretical and experimental data for $[\alpha]_D$ calculations in acetone with respect to chloroform could suggest a stronger effect of hydrogen bonding on the conformational flexibility;

c. $[\alpha]_D$ calculations are less expensive than ECD calculations in terms of computational time.

A better description of short-range interactions between solute and solvent, obtained through the SSM approach, improved the accuracy of the calculations (differences between ΔE_{QM}-averaged SSM calculations and experimental $[\alpha]_D$ values were $-1°$ and $+34°$for *cis*-**4** and *cis*-**5**, respectively). TD-DFT calculations are therefore able to confirm the stereochemistry of all the β-lactam derivatives under investigation, including compound *cis*-**6**, for which the β-lactam sector rules were unable to predict the correct absolute configuration at C4.

7.2.4 Effect of conformational flexibility

Once the predictive capability of TD-DFT calculations was tested and validated, DFT geometries were thoroughly analysed to explore a possible correlation between the variation of geometric features among different optimised conformations and the variation of theoretical chiroptical properties, that is, calculated $[\alpha]_D$ values. Tables 7.5 and 7.6 list the geometric parameters of all the relevant DFT conformers, sorted by decreasing order of theoretical $[\alpha]_D$ values.

Table 7.5. Theoretical $[\alpha]_D$ values (sorted in decreasing order) and geometric parameters for the conformers of *trans*-**1**, *cis*-**2**, *trans*-**3**, *cis*-**3** and *cis*-**6**, as obtained after PBE0/TZ2P//B97D/TZ2P calculations in chloroform (IEFPCM solvation model).

Conf. ID	χ_{QM} (%)	$[\alpha]_D$ (deg cm^3 g^{-1} dm^{-1})	ψ_1 (deg)	ψ_2 (deg)	ψ_3 (deg)	ψ_4 (deg)	ϕ_1 (deg)	ϕ_2 (deg)	ω (deg)
trans-**1a**	73.77	**−90.2**	+2.23	−0.47	−2.39	+176.55	+79.05		+173.52
trans-**1b**	26.23	**−148.5**	+2.12	−0.02	−2.22	+175.99	+78.84		−99.56
cis-**2a**	6.23	**+167.6**	−4.48	−0.28	+1.13	+178.22	+107.48	+87.28	+176.97
cis-**2c**	38.25	**+165.3**	−4.16	−0.24	+0.16	+175.61	+103.54	+71.06	+38.99
cis-**2b**	42.14	**+134.3**	−4.42	−0.19	+0.50	+176.18	+102.14	+83.90	+37.55
cis-**2g**	5.37	**+42.9**	−4.07	+0.09	+1.36	+178.64	+109.40	+46.65	−90.09
cis-**2h**	8.01	**−266.6**	−2.64	+0.38	+1.05	+178.88	+105.54	+137.43	−68.04
trans-**3a**	69.54	**−8.9**	+2.04	−0.83	−2.66	+176.32	+71.16	−46.79	+168.79
trans-**3b**	2.29	**−31.4**	+6.15	−1.06	−4.70	+176.02	+87.96	−176.17	+169.28
trans-**3d**	26.44	**−63.8**	+1.41	−0.25	−2.42	+175.04	+71.91	−43.81	−95.13
trans-**3c**	1.73	**−194.5**	+9.11	−1.09	−6.79	+173.68	+105.15	+54.82	+163.31
cis-**3c**	1.88	**+226.5**	−5.76	+0.17	+1.60	+176.98	+104.53	−175.15	+171.98
cis-**3b**	1.37	**+205.3**	−5.08	+0.13	+1.28	+176.99	+108.48	−49.33	+168.57
cis-**3h**	3.89	**+180.7**	−5.10	+0.53	+2.28	+179.12	+106.49	−173.82	−65.61
cis-**3d**	55.48	**+161.3**	−6.01	+0.23	+1.12	+175.18	+101.66	−175.34	+39.49
cis-**3e**	2.71	**+144.1**	−3.99	+0.44	+1.92	+179.67	+109.34	−46.43	−72.90
cis-**3a**	24.97	**+142.1**	−5.11	+0.22	+0.73	+175.05	+102.78	−47.55	+41.69
cis-**3g**	0.47	**+107.8**	−4.53	+0.16	+0.74	+175.94	+106.89	+66.16	+160.68
cis-**3i**	0.42	**+67.2**	−3.59	+0.56	+1.45	+178.49	+105.88	+67.45	−77.92
cis-**3f**	8.83	**+36.7**	−4.72	+0.45	+0.34	+173.82	+103.22	+68.86	+41.22
cis-**6c**	56.16	**+60.9**	−0.68	−0.13	−1.14	+175.65	+100.45	+83.06	+36.00
cis-**6d**	3.19	**−6.6**	−4.83	+0.13	+2.14	−179.48	+107.85	+47.32	−90.69
cis-**6a**	3.11	**−181.9**	+2.78	−0.22	−1.95	+177.58	+102.95	+119.54	+165.46
cis-**6f**	24.48	**−224.6**	−5.30	−0.10	+1.08	+176.92	−72.60	+72.44	+42.70
cis-**6h**	4.27	**−284.9**	−7.39	+0.10	+3.84	−177.16	−62.14	+43.26	−87.70
cis-**6g**	4.56	**−309.4**	+0.05	+0.03	+0.18	−179.85	+106.38	+135.98	−66.32
cis-**6b**	4.21	**−417.5**	−1.07	−0.24	+0.18	+179.75	−68.59	+108.86	+167.84

Geometry of the β-lactam ring

Excluding *cis*-**6** and the SSM conformations (*cis*-**4*** and *cis*-**5***), regular patterns in the non-planarity features of the β-lactam ring can be identified among optimised conformers with the same relative configuration. All *trans* conformers show positive values for the torsion angle of the amide (ψ_1) and negative values for the pyramidalisation of C2 (ψ_2) and N1 (ψ_3). Conversely, most of the *cis* conformers show the opposite pattern, that is, negative for ψ_1 and positive for ψ_2 and ψ_3. A notable exception is represented by *cis*-**2**, whose geometric properties will be discussed later.

Table 7.6. Theoretical $[\alpha]_D$ values (sorted in decreasing order) and geometric parameters for the conformers of *cis*-**4**, *cis*-**5**, *cis*-**4*** and *cis*-**5***, as obtained after PBE0/TZ2P//B97D/TZ2P calculations in acetone (IEFPCM solvation model).

Conf. ID	χ_{QM} (%)	$[\alpha]_D$ (deg cm^3 g^{-1} dm^{-1})	ψ_1 (deg)	ψ_2 (deg)	ψ_3 (deg)	ψ_4 (deg)	ϕ_1 (deg)	ω (deg)
cis-**4a**	0.54	+**203.4**	−3.38	+0.44	+0.95	+177.78	+98.40	−179.07
cis-**4e**	1.80	+**185.8**	−5.74	+0.66	+2.53	+179.49	+98.20	−83.36
cis-**4c**	58.91	+**120.1**	−3.09	+0.53	+0.42	+176.21	+100.92	+39.55
cis-**4d**	0.83	−**67.9**	−6.39	+0.45	+2.44	+178.88	−70.06	+179.31
cis-**4f**	2.88	−**136.5**	−8.04	+0.64	+3.69	−179.62	−68.89	−84.03
cis-**4b**	35.03	−**162.5**	−6.77	+0.60	+2.19	+177.18	−71.77	+44.60
cis-**5c**	0.65	+**218.8**	−3.36	+0.46	+0.85	+177.43	+95.74	−178.26
cis-**5f**	1.70	+**179.1**	−5.56	+0.71	+2.16	+178.40	+95.34	−90.02
cis-**5d**	51.76	+**127.1**	−3.80	+0.50	+0.81	+176.66	+100.70	+39.55
cis-**5b**	0.67	−**130.4**	−2.48	+0.49	+0.29	+176.63	−62.90	−176.00
cis-**5a**	45.23	−**217.6**	−4.00	+0.46	+0.79	+176.40	−54.31	+48.29
cis-**4*c**	0.43	+**251.2**	+0.72	+0.62	−0.32	+178.49	+96.01	+143.37
cis-**4*b**	0.98	+**139.4**	−14.47	+1.06	+7.31	−177.40	−72.92	+77.88
cis-**4*h**	21.22	+**119.5**	−0.88	+0.58	−0.20	+176.90	−69.30	−79.92
cis-**4*d**	14.23	+**117.5**	+5.05	+0.26	−3.02	+175.98	+108.15	−81.68
cis-**4*f**	50.35	+**56.6**	−5.36	+0.60	+2.14	+179.03	+112.28	−81.76
cis-**4*a**	1.27	+**34.7**	−0.06	+0.04	−0.81	+177.15	−123.72	+52.40
cis-**4*e**	11.52	−**39.1**	+1.36	+0.45	−1.53	+175.75	−97.95	+68.61
cis-**5*a**	9.32	+**313.6**	−1.64	+0.54	+0.36	+177.88	+101.11	−80.12
cis-**5*e**	8.96	+**222.0**	+0.48	+0.21	−0.15	+179.67	+111.42	−66.71
cis-**5*b**	0.40	+**211.5**	−0.32	+0.31	−0.04	+178.74	+96.80	+163.33
cis-**5*u**	36.16	+**156.8**	+3.79	+0.66	−2.59	+174.70	−62.15	−78.96
cis-**5*i**	1.34	+**4.2**	+9.30	+0.46	−5.23	+173.70	−64.01	+146.43
cis-**5*p**	43.82	−**2.2**	−8.87	+0.42	+4.40	−177.43	+111.30	−67.08

The helicity rule,[67] which predicts a negative contribution to $[\alpha]_D$ for positive torsion angles of the amide (ψ_1) and a positive contribution to $[\alpha]_D$ for negative ψ_1 angles, is also consistent with the regular geometric patterns observed for DFT conformers: positive ψ_1 angles for *trans* conformers and negative ψ_1 angles for *cis* conformers. Moreover, almost all conformers show positive values for the deviation of C4 from the plane of the carbonyl group (ψ_4), irrespective of the relative configuration. Orientation of aromatic substituents at C4. Theoretical $[\alpha]_D$ values for the conformers of non-heteroaromatic derivatives are in agreement with the β-lactam sector rules, that is, *trans* conformers show negative $[\alpha]_D$ values and *cis* conformers show positive $[\alpha]_D$ values.

On the other hand, $[\alpha]_D$ values for the conformers of heteroaromatic derivatives show a strong dependence upon the orientation of the heterocycle (ϕ_1; Figure 7.5). Conformers having the heteroatom oriented on the opposite side with respect to the β-lactam ring (positive ϕ_1 values) follow the general trend, and their $[\alpha]_D$ is correctly predicted by the β-lactam sector rules. Conformers having the heteroatom oriented towards the β-lactam ring (negative ϕ_1 values) show an opposite trend, and the calculated $[\alpha]_D$ values are in discordance with the β-lactam sector rules.

Figure 7.5. B97D/TZ2P-optimised conformers of *cis*-**5**. Solvation model: acetone (IEFPCM). *Left:* conformers with positive values of ϕ_1 (*cis*-**5c**, *cis*-**5d** and *cis*-**5f**); *Right:* conformers with negative values of phi_2 (*cis*-**5a** and *cis*-**5b**). Dihedral angles are reported in Table 7.6.

Conformational flexibility of *cis*-2

The geometric features of *cis*-**2** deserve a deeper analysis. This derivative bears a phenyl substituent at C3, similar to *cis*-**6**, and shows a different trend in the non-planarity of the β-lactam ring, denoting a higher conformational flexibility of the system. Conformers *cis*-**2a**, *cis*-**2b**, and *cis*-**2c** show negative ψ_2 values, unlike other *cis* conformers, but show positive $[\alpha]_D$, which is consistent with the β-lactam sector rules. Conformer *cis*-**2g** shows a different orientation of the hydroxyl group (negative o value) and a positive $[\alpha]_D$ of lower magnitude. Finally, conformer *cis*-**2h** shows a negative o value and a different orientation of the phenyl ring at C3 ($\phi_2 \sim 135°$). This conformer shows a negative $[\alpha]_D$, in contrast to the β-lactam sector rules (Figure 7.6).

Figure 7.6. B97D/TZ2P-optimised conformers of *cis*-**2h** and *cis*-**2b**. Solvation model: chloroform (IEFPCM). Dihedral angles are reported in Table 7.5.

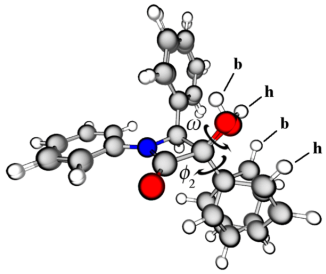

Solvent-induced flexibility

Regular patterns are not observed for the SSM conformations (*cis*-**4*** and *cis*-**5***). The introduction of solvent molecules, interacting with the solute through hydrogen bonding, describes the molecular geometry of a solution in a more accurate

fashion and induces a more complex pattern for the geometric features of the β-lactam ring, which is not possible to rationalise with semi-empirical rules. Another limiting factor is the presence of solvent molecules in TD-DFT calculations. The analysis of their direct and indirect contributions to the final values of theoretical $[\alpha]_D$ is beyond the aims of the present study and makes the correlation of chiroptical properties to the geometry of the solute very difficult.

Conformational flexibility of *cis*-6

Interestingly, the same behaviour is observed for the geometry of the β-lactam ring of *cis*-**6**, even in the absence of explicit solvent molecules in the calculations. The conformational flexibility of the system is therefore much higher than for the other derivatives. A deeper analysis, however, allows us to identify the reasons behind the failure of the β-lactam sector rules in predicting the stereochemistry for this compound.

Conformers, having the thienyl substituent at C4 oriented with the sulfur atom towards the β-lactam ring (negative ϕ_1 values), all show negative $[\alpha]_D$ values, which is consistent with the observations made on *cis*-**4** and *cis*-**5**. Among the conformers with the opposite orientation of the heterocycle (positive ϕ_1 values, Figure 7.7), only *cis*-**6c** shows a negative torsion angle of the amide (ψ_1) and a positive $[\alpha]_D$ value, as expected by the helicity rule. Conformers *cis*-**6a** and *cis*-**6g** show a positive ψ_1 value and, similar to what was observed for *cis*-**2h**, a different orientation of the phenyl ring at C3, thus, showing a negative $[\alpha]_D$. Finally, conformer *cis*-**6d** shows a different orientation of the hydroxyl group (negative ω value) and a negative $[\alpha]_D$ value of low magnitude, which is in accordance with the negative contribution to the $[\alpha]_D$ observed for *cis*-**2g**.

Figure 7.7. B97D/TZ2P-optimised conformers of *cis*-**6** with positive values of ϕ_1. *Left: cis*-**6a** and *cis*-**6c**; *Right: cis*-**6d** and *cis*-**6g**. Solvation model: chloroform (IEFPCM). Dihedral angles are reported in Table 7.6.

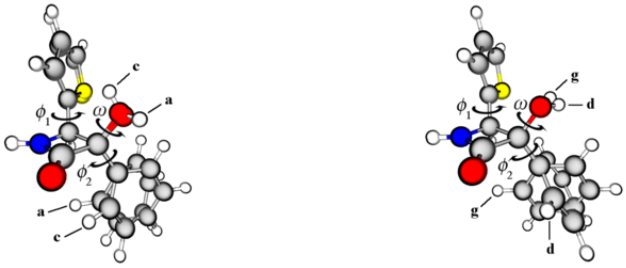

Therefore, the presence of a phenyl substituent at C3 has a double effect:

a. the regular trend in the geometric features of the *β*-lactam ring is perturbed and the conformational flexibility is increased, as observed for the optimised conformers of *cis*-**2** and *cis*-**6**;

b. similar to the orientation of heteroaromatic substituents, the orientation of the phenyl ring affects the chiroptical properties of these *β*-lactam derivatives to a great extent, resulting in a strong negative contribution to the calculated $[\alpha]_D$ values for some specific orientations (e.g., conformers *cis*-**2h**, *cis*-**6a**, and *cis*-**6g**).

Because these additional contributions are not considered in the definition of general chiroptical properties given by the semi-empirical *β*-lactam sector rules, the latter are unable to describe this behaviour appropriately and fail in the prediction of the correct relative configuration of *cis*-**6**.

7.3 Conclusions

TD-DFT calculations on a series of selected (3*R*)-3-hydroxy-4-aryl-*β*-lactam derivatives were successfully employed to confirm their absolute configuration and allowed us to verify the validity of the semi-empirical *β*-lactam sector rules for the stereochemical characterisation of these compounds. The close relationship between the presence of regular patterns in the geometric parameters of *β*-lactam rings and the applicability of sector rules was identified, and the reasons behind their failure for the characterisation of a specific derivative, *cis*-**6**, were unveiled. The presence of a heterocyclic substituent at C4 and a phenyl substituent at C3 introduces additional complexity to the geometric and electronic features of this derivative, increasing its conformational flexibility and affecting its chiroptical properties.

Semi-empirical rules for the determination of the absolute configuration of chiral molecules are very useful tools because the correlation between chiroptical properties and stereochemistry may be easily found by a fast and simple analysis of the position of substituents around a particular chromophore. However, these rules may fail when the nature of substituents affects the molecular geometry and electronic properties of the chromophore. This was the case for *cis*-**6**, where both the aromatic substituents at C3 and C4 induced large modifications to the general chiroptical properties predicted by the *β*-lactam sector rules.

First-principles methods, such as TD-DFT calculations, are very powerful tools for the determination of theoretical chiroptical properties, and their predictive power is becoming increasingly accurate and efficient as more complex theoretical models are being developed and the needed computational power is becoming available. Nevertheless, particular attention must be paid to the description of molecular geometry at equilibrium. A standard conformational analysis using an implicit solvation may not reproduce faithfully the system when perturbations, due to short-range interactions with the solvent, become relevant. Higher levels of complexity, such as the SSM approach, should be considered in the calculation of chiroptical properties, especially in $[\alpha]_D$ calculations, whenever hydrogen bonding between solute and solvent may affect the chemical environment of the chromophore.

The present study highlighted the great importance of conformational flexibility for stereochemical characterisation. A detailed description of even small modifications in the molecular geometry is fundamental for a reliable correlation between the experimental chiroptical properties and the chemical structures of chiral molecules in solution.

Figure 7.8. Graphical representation of *trans*-**1a**, the most populated conformer of *trans*-**1** at the B97D/TZ2P level in chloroform (IEFPCM solvation model).

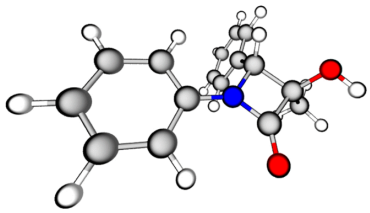

Figure 7.9. Graphical representation of *cis*-**2b**, the most populated conformer of *cis*-**2** at the B97D/TZ2P level in chloroform (IEFPCM solvation model).

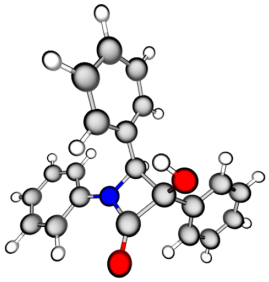

Figure 7.10. Graphical representation of *trans*-**3a**, the most populated conformer of *trans*-**3** at the B97D/TZ2P level in chloroform (IEFPCM solvation model).

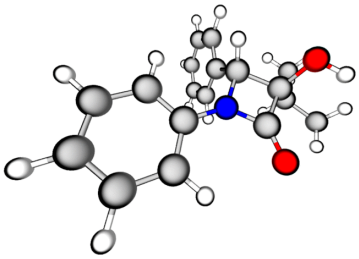

Figure 7.11. Graphical representation of *cis*-**3d**, the most populated conformer of *cis*-**3** at the B97D/TZ2P level in chloroform (IEFPCM solvation model).

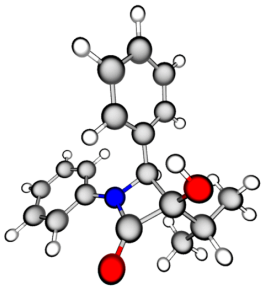

Figure 7.12. Graphical representation of *cis*-**4c**, the most populated conformer of *cis*-**4** at the B97D/TZ2P level in acetone (IEFPCM solvation model).

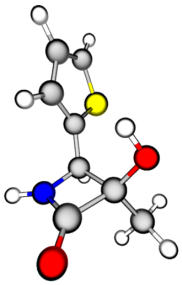

Figure 7.13. Graphical representation of *cis*-**5d**, the most populated conformer of *cis*-**5** at the B97D/TZ2P level in acetone (IEFPCM solvation model).

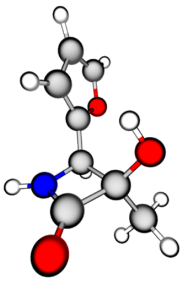

Figure 7.14. Graphical representation of *cis*-**6c**, the most populated conformer of *cis*-**6** at the B97D/TZ2P level in chloroform (IEFPCM solvation model).

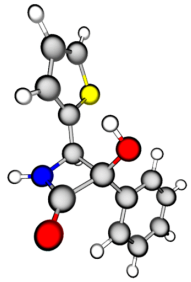

Figure 7.15. Graphical representation of *cis*-**4*f**, the most populated conformer of *cis*-**4*** at the B97D/TZ2P level in acetone (IEFPCM solvation model).

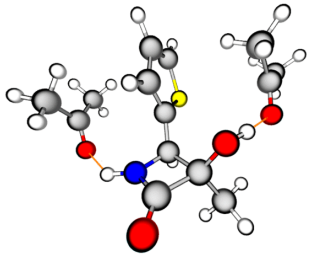

Figure 7.16. Graphical representation of *cis*-**5*p**, the most populated conformer of *cis*-**5*** at the B97D/TZ2P level in acetone (IEFPCM solvation model).

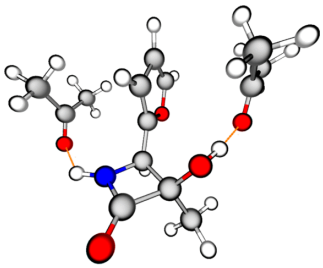

Figure 7.17. Experimental UV and ECD spectra of *cis*-**6**.

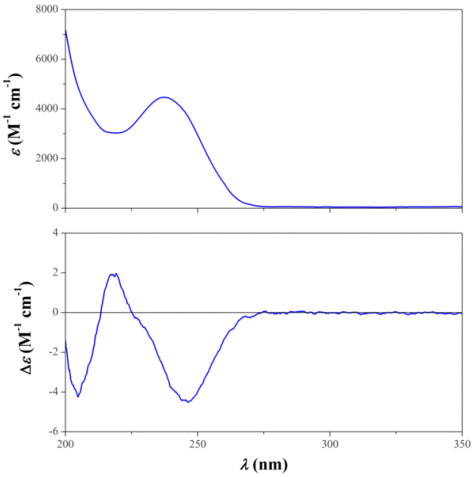

Figure 7.18. Experimental UV and ECD spectra of *cis*-**4**.

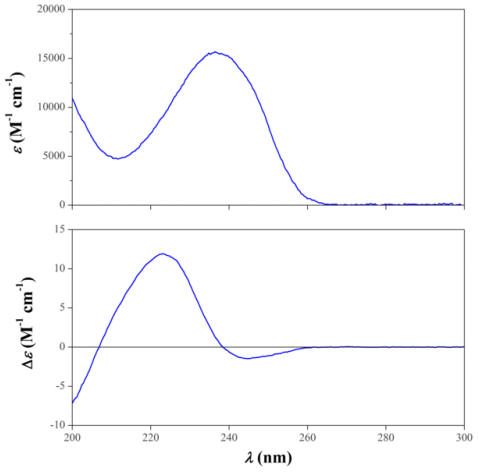

Figure 7.19. Experimental UV and ECD spectra of *trans*-**3**.

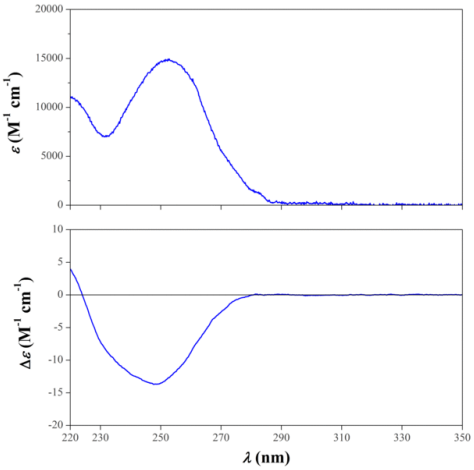

Figure 7.20. Experimental UV and ECD spectra of *cis*-**3**.

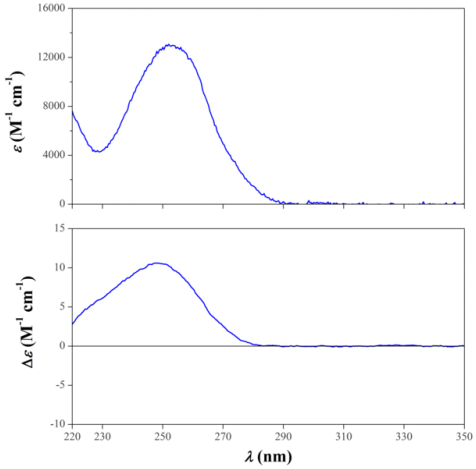

Table 7.7. Geometric parameters, energies and Boltzmann populations at 298.15 K and 1 atm for the conformers of *trans*-**1**, *cis*-**2**, *trans*-**3**, *cis*-**3** and *cis*-**6**, as obtained after MMFF94s conformational analysis.

Conf. ID	ψ_1 (deg)	ψ_2 (deg)	ψ_3 (deg)	ψ_4 (deg)	ϕ_1 (deg)	ϕ_2 (deg)	ω (deg)	E_{MM} (kcal mol^{-1})	ΔE_{MM} (kcal mol^{-1})	χ_{MM} (%)
trans-**1a**	3.968	−0.669	−2.418	179.598	86.432		146.508	77.190	0.000	99.84
trans-**1b**	5.020	0.199	−1.903	−179.497	82.977		−79.309	80.991	3.801	0.16
cis-**2a**	−4.015	−0.081	0.987	177.834	108.242	71.753	158.767	112.273	0.000	74.37
cis-**2b**	−6.569	−0.255	0.773	174.214	92.617	58.867	55.789	113.876	1.603	4.97
cis-**2c**	−7.730	0.045	1.064	172.874	90.175	70.793	56.354	113.934	1.661	4.50
cis-**2d**	−7.350	−0.186	1.366	174.791	86.490	57.496	54.787	113.944	1.671	4.43
cis-**2e**	−7.274	−0.122	1.070	173.868	86.059	55.682	54.704	113.946	1.673	4.41
cis-**2f**	−7.819	−0.090	1.212	173.500	85.539	55.351	54.652	113.946	1.673	4.41
cis-**2g**	−2.676	−0.019	2.061	−177.351	111.377	44.401	−76.270	114.265	1.993	2.57
cis-**2h**	−3.112	0.374	1.632	179.910	106.898	140.002	−60.198	115.496	3.223	0.32
trans-**3a**	2.754	−1.217	−1.785	−178.865	76.661	103.196	138.614	80.819	0.000	99.57
trans-**3b**	5.007	−1.079	−3.474	178.870	93.186	−23.910	141.080	84.604	3.785	0.17
trans-**3c**	5.761	−1.006	−5.047	175.134	104.395	−162.618	134.876	84.669	3.851	0.15
trans-**3d**	4.389	−0.280	−1.079	−176.779	74.674	101.909	−67.534	84.850	4.031	0.11
cis-**3a**	−5.853	0.181	0.712	173.984	92.350	−46.653	54.794	80.235	0.000	49.77
cis-**3b**	−4.237	0.032	0.565	176.017	105.692	−46.334	138.677	80.371	0.136	39.57
cis-**3c**	−4.252	0.225	0.681	175.896	104.520	−173.430	143.183	81.787	1.552	3.62
cis-**3d**	−6.147	0.288	0.965	174.109	90.655	−173.441	53.740	81.809	1.574	3.49
cis-**3e**	−2.162	0.476	1.908	−178.257	108.834	−47.438	−49.875	82.079	1.844	2.22
cis-**3f**	−6.390	0.351	0.719	172.926	89.590	68.791	55.925	82.740	2.504	0.73
cis-**3g**	−4.877	0.233	0.227	173.706	101.803	68.041	134.029	83.038	2.803	0.44
cis-**3h**	−2.458	0.580	1.787	−179.256	107.138	−173.899	−48.778	83.741	3.505	0.13
cis-**3i**	−2.383	0.651	1.574	−179.945	108.382	68.196	−57.357	84.619	4.384	0.03
cis-**6a**	0.343	−0.758	−0.218	−178.629	113.966	61.007	159.882	66.215	0.000	65.96
cis-**6b**	5.819	−0.740	−3.719	177.267	−134.993	58.206	152.445	67.094	0.878	14.97
cis-**6c**	−6.587	−0.865	3.618	−175.294	87.386	52.178	52.756	67.654	1.438	5.82
cis-**6d**	−3.091	−0.317	3.559	−171.926	107.282	44.030	−77.970	67.709	1.493	5.30
cis-**6e**	−2.029	−1.181	1.578	−175.114	−129.762	47.672	56.357	67.800	1.584	4.55
cis-**6f**	0.200	−0.985	−0.174	−178.220	−78.386	55.854	53.876	68.017	1.801	3.15
cis-**6g**	1.178	−0.190	0.075	−177.795	107.082	148.896	−65.027	69.743	3.528	0.17
cis-**6h**	2.625	−0.294	0.324	−174.840	−80.487	43.867	−76.915	70.254	4.038	0.07

Table 7.8. Geometric parameters, energies and Boltzmann populations at 298.15 K and 1 atm for the conformers of *cis*-**4**, *cis*-**4***, *cis*-**5** and *cis*-**5***, as obtained after MMFF94s conformational analysis.

Conf. ID	ψ_1 (deg)	ψ_2 (deg)	ψ_3 (deg)	ψ_4 (deg)	ϕ_1 (deg)	ω (deg)	E_{MM} (kcal mol^{-1})	ΔE_{MM} (kcal mol^{-1})	χ_{MM} (%)
cis-**4a**	2.925	−0.475	−1.739	179.231	118.462	146.792	30.211	0.000	28.91
cis-**4b**	1.253	−0.613	−0.131	−177.447	−125.343	57.863	30.221	0.010	28.44
cis-**4c**	−4.134	−0.322	2.613	−176.344	89.343	53.766	30.247	0.036	27.20
cis-**4d**	7.716	−0.486	−4.770	175.855	−133.057	137.862	30.677	0.466	13.16
cis-**4e**	−0.919	0.259	2.546	−173.518	108.086	−57.474	31.728	1.517	2.23
cis-**4f**	3.465	0.225	0.448	−174.424	−79.035	−49.696	33.990	3.779	0.05
cis-**4*a**	−0.482	0.215	2.297	−173.749	−143.387	61.746	14.120	0.000	48.49
cis-**4*b**	1.788	−0.156	0.083	−177.033	−139.779	60.082	14.398	0.278	30.35
cis-**4*c**	2.587	−0.021	−1.752	177.800	131.213	159.665	15.031	0.911	10.41
cis-**4*d**	4.337	0.149	−2.032	178.913	130.651	−69.326	15.409	1.289	5.50
cis-**4*e**	−5.109	1.071	3.794	−176.954	−134.800	62.755	15.554	1.434	4.31
cis-**4*f**	5.751	0.186	−3.847	174.654	138.759	−68.390	16.852	2.732	0.48
cis-**4*g**	10.779	0.333	−6.754	171.716	−62.028	152.585	17.149	3.029	0.29
cis-**4*h**	8.890	0.155	−4.977	175.593	−59.482	−66.726	17.521	3.401	0.16
cis-**5a**	7.184	−0.296	−4.192	176.685	−46.742	48.204	28.904	0.000	73.41
cis-**5b**	12.387	−0.557	−7.819	172.419	−125.411	136.691	29.680	0.776	19.81
cis-**5c**	3.296	−0.486	−1.961	179.007	130.768	148.610	30.548	1.644	4.58
cis-**5d**	−3.566	−0.423	2.036	−177.210	96.258	56.221	31.378	2.474	1.13
cis-**5e**	−1.623	0.335	3.650	−171.165	35.733	−36.792	31.630	2.726	0.74
cis-**5f**	−0.796	0.290	2.220	−174.462	105.953	−59.220	32.078	3.175	0.35
cis-**5*a**	6.679	0.144	−3.942	175.923	132.027	−68.736	15.598	0.000	27.11
cis-**5*b**	6.098	0.487	−3.848	174.526	−137.760	158.646	15.731	0.133	21.65
cis-**5*c**	13.889	−0.093	−7.817	173.411	−97.949	154.741	16.110	0.512	11.42
cis-**5*d**	8.150	−0.261	−6.356	171.194	−41.510	47.470	16.159	0.562	10.51
cis-**5*e**	6.920	−0.216	−4.707	174.564	133.364	−69.861	16.507	0.909	5.85
cis-**5*f**	−0.537	−0.241	0.271	−179.295	−126.226	61.951	16.713	1.115	4.13
cis-**5*g**	1.462	−0.011	−0.580	−179.891	−8.510	35.403	16.800	1.202	3.57
cis-**5*h**	−6.388	0.477	5.352	−171.956	−131.871	63.144	16.840	1.242	3.33
cis-**5*i**	9.344	0.206	−6.335	171.440	−124.211	157.800	17.164	1.566	1.93
cis-**5*j**	5.123	−0.228	−3.657	175.196	−121.988	62.613	17.187	1.590	1.85
cis-**5*k**	−2.394	−0.181	3.500	−171.273	−49.661	42.995	17.246	1.648	1.68
cis-**5*l**	5.416	0.333	−3.409	175.288	136.066	−68.837	17.400	1.802	1.29
cis-**5*m**	9.558	−0.212	−5.058	176.593	−137.899	159.047	17.581	1.983	0.95
cis-**5*n**	−6.483	−0.391	6.780	−165.549	−116.486	53.933	17.612	2.014	0.90
cis-**5*o**	11.089	−0.123	−6.496	173.823	−131.594	159.746	17.756	2.158	0.71
cis-**5*p**	4.153	0.401	−2.542	176.246	125.762	−69.586	17.786	2.188	0.67
cis-**5*q**	13.767	0.354	−8.855	169.061	−54.673	154.179	17.867	2.269	0.59
cis-**5*r**	13.460	0.081	−8.472	170.937	−47.583	−63.656	17.965	2.367	0.50
cis-**5*s**	7.944	−0.782	−6.666	171.081	−75.166	57.459	18.050	2.453	0.43
cis-**5*t**	11.649	0.088	−6.576	174.048	−57.390	63.858	18.209	2.611	0.33
cis-**5*u**	11.387	−0.026	−6.383	174.880	−78.460	−67.868	18.385	2.787	0.25
cis-**5*v**	10.071	0.224	−6.194	172.966	−132.390	157.627	18.557	2.959	0.18
cis-**5*w**	−12.031	0.282	7.897	−170.956	61.213	45.017	18.580	2.982	0.18

Table 7.9. Energies and Boltzmann populations at 298.15 K and 1 atm for the conformers of *trans*-**1**, as obtained after B97D/TZ2P geometry optimisation.

IEFPCM	Conf. ID	E_{QM} (Ha)	ΔE_{QM} (kcal mol^{-1})	χ_{QM} (%)	G (Ha)	ΔG (kcal mol^{-1})	χ_G (%)
Chloroform	*trans*-**1a**	−823.63235784	0.000	73.77	−823.410216	0.000	72.11
	trans-**1b**	−823.63138140	0.613	26.23	−823.409319	0.563	27.89
2-Propanol	*trans*-**1a**	−823.63500206	0.000	58.15	−823.412722	0.000	57.13
	trans-**1b**	−823.63469160	0.195	41.85	−823.412451	0.170	42.87

Table 7.10. Energies and Boltzmann populations at 298.15 K and 1 atm for the conformers of *cis*-**2**, as obtained after B97D/TZ2P geometry optimisation. RMSD values: 0.0015 Å (*cis*-**2b/f**), 0.0010 Å (*cis*-**2c/d**), 0.0009 Å (*cis*-**2c/e**), 0.0008 Å (*cis*-**2d/e**).

IEFPCM	Conf. ID	E_{QM} (Ha)	ΔE_{QM} (kcal mol^{-1})	χ_{QM} (%)	G (Ha)	ΔG (kcal mol^{-1})	χ_G (%)
Chloroform	*cis*-**2b**	−1015.27665282	0.000	42.14	−1015.007885	0.004	–
	cis-**2f**	−1015.27665232	0.000	–	−1015.007891	0.000	35.12
	cis-**2c**	−1015.27656143	0.057	38.25	−1015.007871	0.013	–
	cis-**2e**	−1015.27656143	0.057	–	−1015.007868	0.014	–
	cis-**2d**	−1015.27656111	0.058	–	−1015.007885	0.004	34.90
	cis-**2h**	−1015.27508507	0.984	8.01	−1015.006507	0.868	8.11
	cis-**2a**	−1015.27484854	1.132	6.23	−1015.006817	0.674	11.26
	cis-**2g**	−1015.27470732	1.221	5.37	−1015.006762	0.708	10.62

Table 7.11. Energies and Boltzmann populations at 298.15 K and 1 atm for the conformers of *trans*-**3**, as obtained after B97D/TZ2P geometry optimisation.

IEFPCM	Conf. ID	E_{QM} (Ha)	ΔE_{QM} (kcal mol^{-1})	χ_{QM} (%)	G (Ha)	ΔG (kcal mol^{-1})	χ_G (%)
Chloroform	*trans*-**3a**	−902.23150204	0.000	69.54	−901.956698	0.000	73.88
	trans-**3d**	−902.23058888	0.573	26.44	−901.955618	0.678	23.53
	trans-**3b**	−902.22827878	2.023	2.29	−901.952853	2.413	1.26
	trans-**3c**	−902.22801716	2.187	1.73	−901.952907	2.379	1.33
2-Propanol	*trans*-**3a**	−902.23402935	0.000	54.21	−901.959233	0.000	49.30
	trans-**3d**	−902.23380975	0.138	42.96	−901.959233	0.000	49.30
	trans-**3b**	−902.23077458	2.042	1.73	−901.955498	2.344	0.94
	trans-**3c**	−902.23034764	2.310	1.10	−901.954833	2.761	0.47

Table 7.12. Energies and Boltzmann populations at 298.15 K and 1 atm for the conformers of *cis*-**3**, as obtained after B97D/TZ2P geometry optimisation.

IEFPCM	Conf. ID	E_{QM} (Ha)	ΔE_{QM} (kcal mol^{-1})	χ_{QM} (%)	G (Ha)	ΔG (kcal mol^{-1})	χ_G (%)
Chloroform	*cis*-**3d**	−902.23411161	0.000	55.48	−901.958756	0.169	28.04
	cis-**3a**	−902.23335781	0.473	24.97	−901.959026	0.000	37.33
	cis-**3f**	−902.23237612	1.089	8.83	−901.957449	0.990	7.02
	cis-**3h**	−902.23160177	1.575	3.89	−901.958207	0.514	15.68
	cis-**3e**	−902.23126150	1.788	2.71	−901.956967	1.292	4.22
	cis-**3c**	−902.23091520	2.006	1.88	−901.956734	1.438	3.29
	cis-**3b**	−902.23061891	2.192	1.37	−901.956557	1.549	2.73
	cis-**3g**	−902.22960462	2.828	0.47	−901.954927	2.572	0.49
	cis-**3i**	−902.22949431	2.897	0.42	−901.955778	2.038	1.20
2-Propanol	*cis*-**3d**	−902.23692630	0.000	53.48	−901.961830	0.000	29.95
	cis-**3a**	−902.23616627	0.477	23.91	−901.961771	0.037	28.13
	cis-**3f**	−902.23516699	1.104	8.30	−901.960407	0.893	6.63
	cis-**3h**	−902.23477336	1.351	5.47	−901.961414	0.261	19.27
	cis-**3e**	−902.23447363	1.539	3.98	−901.960422	0.884	6.74
	cis-**3c**	−902.23392171	1.885	2.22	−901.960002	1.147	4.32
	cis-**3b**	−902.23352943	2.132	1.46	−901.959397	1.527	2.28
	cis-**3i**	−902.23285866	2.552	0.72	−901.959340	1.562	2.14
	cis-**3g**	−902.23243651	2.817	0.46	−901.958030	2.385	0.53

Table 7.13. Energies and Boltzmann populations at 298.15 K and 1 atm for the conformers of *cis*-**4**, as obtained after B97D/TZ2P geometry optimisation.

IEFPCM	Conf. ID	E_{QM} (Ha)	ΔE_{QM} (kcal mol^{-1})	χ_{QM} (%)	G (Ha)	ΔG (kcal mol^{-1})	χ_G (%)
Acetone	*cis*-**4c**	−913.50296842	0.000	58.91	−913.385121	0.000	52.53
	cis-**4b**	−913.50247763	0.308	35.03	−913.384602	0.326	30.31
	cis-**4f**	−913.50011966	1.788	2.88	−913.383328	1.125	7.86
	cis-**4e**	−913.49967656	2.066	1.80	−913.382800	1.456	4.49
	cis-**4d**	−913.49894652	2.524	0.83	−913.382297	1.772	2.64
	cis-**4a**	−913.49854044	2.779	0.54	−913.382111	1.889	2.17
2-Propanol	*cis*-**4c**	−913.50289719	0.000	58.96	−913.385047	0.000	52.52
	cis-**4b**	−913.50240642	0.308	35.06	−913.384532	0.323	30.44
	cis-**4f**	−913.50003370	1.797	2.84	−913.383246	1.130	7.80
	cis-**4e**	−913.49959227	2.074	1.78	−913.382712	1.465	4.43
	cis-**4d**	−913.49886980	2.527	0.83	−913.382217	1.776	2.62
	cis-**4a**	−913.49846419	2.782	0.54	−913.382051	1.880	2.20

Table 7.14. Energies and Boltzmann populations at 298.15 K and 1 atm for the conformers of *cis*-**4***, as obtained after B97D/TZ2P geometry optimisation.

IEFPCM	Conf. ID	E_{QM} (Ha)	ΔE_{QM} (kcal mol^{-1})	χ_{QM} (%)	G (Ha)	ΔG (kcal mol^{-1})	χ_G (%)
Acetone	*cis*-**4***f	−1299.74000177	0.000	50.35	−1299.477750	0.000	33.87
	cis-**4***h	−1299.73918600	0.512	21.22	−1299.477226	0.329	19.44
	cis-**4***d	−1299.73880904	0.748	14.23	−1299.477724	0.016	32.95
	cis-**4***e	−1299.73860917	0.874	11.52	−1299.476179	0.986	6.41
	cis-**4***a	−1299.73652982	2.179	1.27	−1299.474381	2.114	0.96
	cis-**4***b	−1299.73628232	2.334	0.98	−1299.476076	1.050	5.75
	cis-**4***c	−1299.73549545	2.828	0.43	−1299.473958	2.380	0.61
		Not considered in TD-DFT calculations (non-interacting solvent molecule in the optimised geometry).					
	cis-**4***g	−1299.73485278	3.231	–	−1299.475879	1.174	–

Table 7.15. Energies and Boltzmann populations at 298.15 K and 1 atm for the conformers of *cis*-**5**, as obtained after B97D/TZ2P geometry optimisation. RMSD values for *cis*-**5e/f**: 0.0020 Å.

IEFPCM	Conf. ID	E_{QM} (Ha)	ΔE_{QM} (kcal mol^{-1})	χ_{QM} (%)	G (Ha)	ΔG (kcal mol^{-1})	χ_G (%)
Acetone	*cis*-**5d**	−590.48380545	0.000	51.76	−590.362196	0.000	51.14
	cis-**5a**	−590.48367819	0.080	45.23	−590.361896	0.188	37.22
	cis-**5f**	−590.48057843	2.025	1.70	−590.360215	1.243	6.27
	cis-**5e**	−590.48057817	2.025	–	−590.360215	1.243	–
	cis-**5b**	−590.47969450	2.580	0.67	−590.359288	1.825	2.35
	cis-**5c**	−590.47966881	2.596	0.65	−590.359522	1.678	3.01

Table 7.16. Energies and Boltzmann populations at 298.15 K and 1 atm for the conformers of *cis*-**5***, as obtained after B97D/6-31G* geometry optimisation. RMSD values: 0.0003 Å (*cis*-**5*l/p**), 0.0041 Å (*cis*-**5*r/u**), 0.0002 Å (*cis*-**5*b/v**), 0.0012 Å (*cis*-**5*c/q**), 0.0023 Å (*cis*-**5*m/o**).

IEFPCM	Conf. ID	E_{QM} (Ha)	ΔE_{QM} (kcal mol^{-1})	χ_{QM} (%)	G (Ha)	ΔG (kcal mol^{-1})	χ_G (%)
Acetone	*cis*-**5*p**	−976.35101592	0.000	52.13	−976.081131	0.013	28.84
	cis-**5*l**	−976.35101586	0.000	–	−976.081151	0.000	–
	cis-**5*u**	−976.34981799	0.752	14.66	−976.081004	0.092	24.68
	cis-**5*r**	−976.34981183	0.756	–	−976.080660	0.308	–
	cis-**5*e**	−976.34933979	1.052	8.83	−976.078666	1.559	2.07
	cis-**5*a**	−976.34909799	1.204	6.84	−976.080853	0.187	21.03
	cis-**5*i**	−976.34897478	1.281	6.00	−976.078707	1.534	2.17
	cis-**5*b**	−976.34812201	1.816	2.43	−976.080192	0.602	10.48
	cis-**5*v**	−976.34812196	1.816	–	−976.080195	0.600	–
	cis-**5*t**	−976.34790686	1.951	1.94	−976.079339	1.137	4.23
	cis-**5*w**	−976.34780103	2.017	1.73	−976.077592	2.233	0.66
	cis-**5*c**	−976.34764311	2.116	1.46	−976.078388	1.734	1.54
	cis-**5*q**	−976.34764290	2.117	–	−976.077989	1.984	–
	cis-**5*k**	−976.34761438	2.134	1.42	−976.078502	1.662	1.74
	cis-**5*m**	−976.34741420	2.260	1.15	−976.076394	2.985	0.19
	cis-**5*o**	−976.34741398	2.260	–	−976.076330	3.025	–
	cis-**5*j**	−976.34639748	2.898	0.39	−976.075075	3.813	0.05
	cis-**5*f**	−976.34609777	3.086	0.28	−976.077604	2.226	0.67
	cis-**5*h**	−976.34585361	3.239	0.22	−976.075853	3.325	0.11
	cis-**5*g**	−976.34584191	3.247	0.22	−976.078055	1.943	1.09
	cis-**5*n**	−976.34561527	3.389	0.17	−976.074874	3.939	0.04
	cis-**5*d**	−976.34540286	3.522	0.14	−976.077155	2.508	0.42
	cis-**5*s**	−976.34540281	3.522	–	−976.077165	2.501	–

Table 7.17. Energies and Boltzmann populations at 298.15 K and 1 atm for the conformers of *cis*-**5***, as obtained after B97D/TZ2P geometry optimisation.

IEFPCM	Conf. ID	E_{QM} (Ha)	ΔE_{QM} (kcal mol^{-1})	χ_{QM} (%)	G (Ha)	ΔG (kcal mol^{-1})	χ_G (%)
Acetone	*cis*-**5*p**	−976.72016710	0.000	43.82	−976.453249	0.789	10.27
	cis-**5*u**	−976.71998581	0.114	36.16	−976.454507	0.000	38.94
	cis-**5*a**	−976.71870566	0.917	9.32	−976.453870	0.400	19.83
	cis-**5*e**	−976.71866837	0.940	8.96	−976.454081	0.267	24.80
	cis-**5*i**	−976.71687665	2.065	1.34	−976.452613	1.189	5.24
	cis-**5*b**	−976.71574233	2.777	0.40	−976.450972	2.218	0.92
	Not considered in TD-DFT calculations (non-interacting solvent molecule in the optimised geometry).						
	cis-**5*w**	−976.71744412	1.709	–	−976.453096	0.885	–
	cis-**5*k**	−976.71731616	1.789	–	−976.452613	1.189	–
	cis-**5*c**	−976.71518664	3.125	–	−976.452986	0.954	–
	cis-**5*t**	−976.71514456	3.152	–	−976.452666	1.155	–
	cis-**5*m**	−976.71511894	3.168	–	−976.452223	1.433	–

Table 7.18. Energies and Boltzmann populations at 298.15 K and 1 atm for the conformers of *cis*-**6**, as obtained after B97D/TZ2P geometry optimisation. RMSD values for *cis*-**6e/f**: 0.0050 Å (chloroform), 0.0004 Å (2-propanol).

IEFPCM	Conf. ID	E_{QM} (Ha)	ΔE_{QM} (kcal mol^{-1})	χ_{QM} (%)	G (Ha)	ΔG (kcal mol^{-1})	χ_G (%)
Chloroform	*cis*-**6c**	−1105.14213243	0.000	56.16	−1104.978867	0.000	45.83
	cis-**6f**	−1105.14134858	0.492	24.48	−1104.978246	0.390	23.74
	cis-**6e**	−1105.14134835	0.492	–	−1104.978307	0.351	–
	cis-**6g**	−1105.13976249	1.487	4.56	−1104.977115	1.099	7.16
	cis-**6h**	−1105.13969906	1.527	4.27	−1104.977126	1.092	7.25
	cis-**6b**	−1105.13968752	1.534	4.21	−1104.976940	1.209	5.95
	cis-**6d**	−1105.13942571	1.698	3.19	−1104.976828	1.279	5.29
	cis-**6a**	−1105.13940205	1.713	3.11	−1104.976732	1.340	4.78
2-Propanol	*cis*-**6c**	−1105.14596922	0.000	62.71	−1104.981930	0.000	34.27
	cis-**6e**	−1105.14488766	0.679	19.94	−1104.981714	0.136	27.26
	cis-**6f**	−1105.14488766	0.679	–	−1104.981712	0.137	–
	cis-**6g**	−1105.14369177	1.429	5.62	−1104.980466	0.919	7.27
	cis-**6h**	−1105.14334204	1.649	3.88	−1104.981453	0.299	20.68
	cis-**6b**	−1105.14310569	1.797	3.02	−1104.979922	1.260	4.09
	cis-**6d**	−1105.14292743	1.909	2.50	−1104.979870	1.293	3.87
	cis-**6a**	−1105.14286158	1.950	2.33	−1104.979483	1.536	2.57

Table 7.19. Pearson correlation coefficients (r) for the comparison between experimental ECD spectra and conformationally-averaged theoretical ECD spectra.

Compound	ΔE_{QM}-based	ΔG-based
trans-**1**	0.6381	0.6390
trans-**3**	0.7478	0.7491
cis-**3**	0.7587	0.8106
cis-**4**	0.8481	0.8360
cis-**6**	0.9264	0.7630

Table 7.20. Rotational strengths in dipole velocity formalism and excitation wavelengths for the lowest-energy electronic transitions of the conformers of *cis*-**3**, as obtained by PBE0/TZ2P//B97D/TZ2P calculations in 2-propanol (IEFPCM solvation model).

j	R_j, 10^{-40} erg cm^3 (λ_j, nm)				
	cis-**3a**	*cis*-**3b**	*cis*-**3c**	*cis*-**3d**	*cis*-**3e**
1	39.0621 (255.96)	5.7962 (253.76)	14.6511 (253.94)	38.5022 (255.73)	7.7670 (253.40)
2	13.2409 (254.74)	45.6096 (252.65)	53.0113 (252.46)	27.4114 (253.94)	59.0517 (249.71)
3	−5.3658 (250.72)	4.2727 (248.83)	−6.7908 (247.96)	−13.4269 (249.73)	−15.9894 (244.38)
4	−2.9741 (243.57)	−1.8805 (240.40)	0.5161 (239.38)	−1.1847 (243.15)	1.3134 (240.91)
5	−17.8506 (236.46)	−6.6321 (235.12)	−8.2771 (234.86)	−14.6491 (236.21)	−5.7022 (235.11)
6	6.7435 (234.32)	−2.6202 (229.08)	−2.2151 (228.78)	5.0790 (233.94)	−2.1473 (229.74)
7	10.5257 (219.75)	2.9627 (220.83)	6.5462 (221.08)	9.9350 (219.00)	7.0286 (221.44)
8	8.2665 (218.09)	4.0985 (217.12)	−4.1539 (216.78)	3.8943 (218.18)	−3.2913 (216.45)
9	51.3965 (212.06)	37.1197 (213.40)	47.2735 (213.32)	67.2589 (211.91)	56.2176 (212.91)
10	−38.3638 (209.93)	−49.6206 (210.58)	−49.1658 (210.91)	−51.3782 (209.66)	−81.6449 (208.21)
11	−67.7094 (206.96)	27.2341 (205.42)	−47.4079 (204.82)	−65.5514 (206.67)	−25.3693 (205.03)
12	3.1491 (205.01)	−73.8020 (204.86)	−0.3829 (203.92)	2.3771 (204.28)	31.2642 (201.01)
13	35.8188 (204.16)	32.0796 (201.78)	40.7084 (201.48)	27.6223 (203.60)	44.1780 (199.02)
14	0.6515 (201.96)	13.6944 (200.27)	7.7681 (199.58)	3.5189 (201.73)	−68.4217 (196.91)
15	−61.8965 (199.25)	−64.4458 (198.30)	−68.5627 (198.05)	−57.9759 (199.33)	−3.2051 (195.95)
16	−22.5394 (195.17)	−16.9689 (197.32)	−17.3386 (196.94)	−23.2118 (194.74)	68.3660 (194.16)
17	59.0081 (194.03)	24.2882 (195.89)	38.8227 (195.45)	59.2114 (194.03)	−1.1957 (193.74)
18	−40.1926 (192.62)	10.3575 (191.41)	5.9715 (191.26)	−28.5629 (192.50)	−169.0318 (191.64)
19	144.5522 (186.84)	220.7555 (186.76)	226.7541 (186.52)	145.7222 (186.72)	84.1843 (190.69)
20	29.1107 (185.34)	−127.1883 (185.26)	−163.2596 (184.92)	17.2009 (185.28)	93.4537 (188.96)
21	−32.8512 (184.95)	−3.7817 (183.97)	−4.3406 (183.72)	−76.9172 (184.49)	156.4979 (185.83)
22	−76.1153 (183.85)	−87.0032 (182.58)	−79.8867 (182.02)	−35.9561 (183.23)	−228.4647 (184.90)
23	−35.6730 (181.00)	12.5442 (178.96)	9.6279 (178.71)	−40.1715 (180.38)	−41.6634 (178.90)
24	−19.9472 (172.95)	−5.5593 (171.95)	−4.4773 (171.90)	−16.9127 (172.45)	28.2669 (177.38)
25	−17.7042 (172.46)	−16.9068 (170.47)	−2.6807 (169.77)	−1.2271 (171.73)	−15.8994 (176.80)

j	R_j, 10^{-40} erg cm^3 (λ_j, nm)			
	cis-**3f**	*cis*-**3g**	*cis*-**3h**	*cis*-**3i**
1	42.7819 (255.89)	5.4221 (253.63)	10.1878 (253.18)	5.9883 (253.62)
2	1.2329 (255.23)	49.4449 (252.09)	62.6983 (249.01)	55.9225 (249.49)
3	−5.0395 (250.65)	−7.2294 (248.65)	−15.0977 (243.04)	−17.0422 (245.38)
4	−0.7774 (243.70)	0.4903 (239.57)	4.9940 (240.40)	2.9058 (239.72)
5	−10.7666 (236.22)	−5.0492 (234.81)	−6.2530 (234.80)	−6.7191 (234.75)
6	2.6462 (234.03)	−1.7505 (228.22)	−1.8517 (229.63)	−0.5524 (229.09)
7	13.2835 (219.65)	5.8900 (221.64)	6.8701 (221.24)	8.6085 (221.75)
8	5.3285 (218.03)	−2.5840 (216.79)	−6.7855 (215.72)	−6.4707 (216.49)
9	66.4538 (212.19)	52.1234 (213.51)	61.3791 (212.34)	63.7863 (213.12)
10	−46.1954 (210.05)	−49.8033 (210.43)	−80.2516 (207.92)	−64.6491 (208.77)
11	−76.0766 (207.14)	−30.1985 (205.19)	−25.2766 (204.78)	−45.0754 (205.26)
12	−0.8028 (204.97)	−27.6738 (204.62)	17.6495 (200.64)	52.1743 (200.25)
13	31.3659 (204.21)	30.2219 (201.23)	44.5575 (198.99)	28.2275 (199.05)
14	1.3708 (202.04)	17.5882 (199.93)	−48.9238 (196.97)	−61.8169 (196.82)
15	−63.1288 (199.23)	−8.6176 (198.06)	4.8675 (195.73)	6.5418 (195.53)
16	−27.0219 (195.15)	−80.2189 (197.30)	35.9025 (194.05)	−5.0396 (194.98)
17	71.8903 (194.12)	36.1144 (195.50)	10.0841 (193.89)	23.0627 (193.97)
18	−50.8298 (192.68)	−2.1816 (191.22)	−91.8391 (191.47)	−122.7322 (191.43)
19	145.6060 (186.93)	159.6013 (187.13)	43.3048 (190.06)	76.1703 (190.60)
20	118.5246 (185.26)	68.4849 (185.83)	70.8006 (188.53)	83.0086 (188.40)
21	−84.3069 (185.12)	−106.0634 (184.65)	146.0166 (185.68)	64.8364 (185.70)
22	−99.1255 (183.99)	−113.1199 (183.54)	−229.1927 (184.82)	−141.5987 (184.14)
23	−46.1382 (181.25)	8.8617 (179.55)	−43.1561 (178.50)	−38.2146 (179.59)
24	−24.7351 (173.17)	−11.9717 (172.25)	23.9937 (177.05)	19.2889 (178.76)
25	−22.8690 (172.75)	−27.8449 (171.37)	−9.1923 (176.15)	−10.1095 (177.47)

Table 7.21. Rotational strengths in dipole velocity formalism and excitation wavelengths for the lowest-energy electronic transitions of the conformers of *trans*-**1**, *trans*-**3** and *cis*-**4**, as obtained by PBE0/TZ2P//B97D/TZ2P calculations in 2-propanol (IEFPCM solvation model).

j	R_j, 10^{-40} erg cm^3 (λ_j, nm)					
	trans-**1a**	*trans*-**1b**	*trans*-**3a**	*trans*-**3b**	*trans*-**3c**	*trans*-**3d**
1	9.1785 (253.55)	10.8593 (253.51)	8.1004 (254.17)	17.1978 (253.84)	22.9173 (252.93)	9.5056 (253.84)
2	−35.6583 (250.84)	−67.6998 (249.28)	−37.1371 (252.80)	−53.5754 (251.87)	−53.8920 (251.31)	−62.6794 (250.42)
3	−4.9226 (248.26)	21.2276 (245.84)	1.5342 (248.60)	11.5393 (247.84)	9.3549 (246.51)	25.5639 (245.87)
4	−1.7174 (241.27)	−4.5236 (241.47)	2.4136 (243.51)	−1.5511 (242.58)	0.2015 (238.83)	−0.7939 (243.80)
5	8.6865 (234.85)	12.7608 (235.97)	7.1426 (236.37)	11.2150 (236.39)	4.8313 (234.11)	8.2515 (237.62)
6	−0.3213 (231.13)	−2.1147 (231.10)	0.8871 (232.32)	−0.2037 (230.38)	1.3719 (229.60)	−0.6532 (232.41)
7	−10.2253 (217.68)	−16.5258 (219.84)	−4.4487 (219.36)	−10.6243 (221.55)	−18.7837 (221.64)	−10.7512 (222.73)
8	−6.7750 (216.08)	0.3385 (217.58)	−0.5986 (218.57)	−1.9833 (218.38)	−10.0548 (213.36)	6.0893 (220.18)
9	−34.7322 (211.42)	−37.9635 (211.96)	−19.6052 (211.96)	2.0528 (212.48)	−15.2711 (211.79)	−18.3704 (212.24)
10	15.7527 (210.43)	28.0068 (210.97)	13.5853 (210.80)	−20.7021 (211.85)	7.6286 (210.09)	18.2001 (211.07)
11	39.4237 (204.40)	59.4111 (204.69)	−12.0749 (206.70)	2.0715 (205.62)	47.1850 (204.94)	35.3842 (205.09)
12	−21.1092 (203.00)	−4.6649 (201.25)	8.9262 (204.94)	−26.5860 (204.21)	0.1816 (204.02)	−0.3089 (203.49)
13	−23.9971 (201.27)	−56.5046 (200.75)	7.6507 (202.97)	18.6168 (202.86)	−64.5273 (203.11)	−25.0812 (200.65)
14	−6.4986 (199.52)	1.6478 (197.06)	1.5893 (202.04)	7.3426 (201.24)	−59.2026 (199.98)	46.8444 (197.94)
15	103.8987 (198.49)	−23.0178 (194.59)	121.1277 (199.30)	114.7839 (199.11)	135.4936 (197.33)	−55.9196 (196.28)
16	−28.5729 (195.84)	38.1244 (192.59)	−20.3362 (196.86)	−44.2859 (196.73)	−51.6824 (196.54)	26.1213 (195.49)
17	52.7902 (193.82)	89.6470 (192.37)	−0.4858 (196.14)	21.7315 (195.64)	29.9218 (195.75)	116.8499 (193.39)
18	−65.7049 (191.74)	28.3297 (189.63)	−52.8835 (192.60)	−72.9135 (192.58)	−45.5129 (193.13)	−14.4993 (191.96)
19	−236.0635 (186.14)	−87.8832 (187.46)	−284.1199 (187.62)	−244.3919 (187.78)	−318.5836 (187.65)	−118.4638 (189.50)
20	296.4893 (183.97)	−105.6379 (185.60)	204.8354 (186.82)	197.0641 (185.99)	324.1356 (185.36)	18.5863 (188.48)
21	−21.9405 (183.05)	123.5038 (184.03)	95.0592 (184.67)	95.2244 (184.99)	98.5852 (184.82)	−79.3107 (185.99)
22	13.3653 (181.59)	36.6312 (181.15)	29.0709 (183.38)	35.5764 (183.41)	−27.4007 (183.77)	137.7328 (184.81)
23	6.5638 (177.24)	−16.9210 (179.35)	0.2014 (179.07)	3.9369 (179.58)	−4.3114 (180.46)	−19.1897 (180.20)
24	−0.6449 (172.18)	−1.6546 (173.97)	4.4944 (172.70)	8.9344 (173.54)	10.0675 (174.74)	29.2968 (176.56)
25	−36.7166 (168.71)	27.8987 (172.99)	−39.3543 (170.14)	16.8954 (170.46)	7.1184 (171.71)	25.0747 (174.60)

j	R_j, 10^{-40} erg cm^3 (λ_j, nm)					
	cis-**4a**	*cis*-**4b**	*cis*-**4c**	*cis*-**4d**	*cis*-**4e**	*cis*-**4f**
1	48.5176 (236.97)	−57.6542 (240.31)	54.4929 (238.15)	−54.2615 (237.59)	53.1463 (236.45)	48.5176 (236.97)
2	4.5723 (224.80)	14.9396 (227.78)	11.0435 (227.03)	2.0460 (225.08)	3.0847 (220.97)	4.5723 (224.80)
3	8.1330 (218.55)	38.6492 (218.46)	6.5247 (218.01)	47.1175 (219.20)	31.5879 (217.76)	8.1330 (218.55)
4	−0.4318 (210.60)	8.0650 (209.84)	−2.5951 (210.11)	2.3621 (210.71)	−4.4830 (211.09)	−0.4318 (210.60)
5	−4.2762 (209.37)	−4.1572 (208.64)	−1.7112 (208.68)	−1.4803 (204.98)	−23.8377 (200.02)	−4.2762 (209.37)
6	−7.4230 (198.85)	4.5936 (202.44)	2.7707 (201.27)	4.1137 (199.91)	3.0291 (198.69)	−7.4230 (198.85)
7	−12.5904 (198.16)	−46.2322 (199.21)	−32.7745 (198.30)	−30.9509 (198.10)	1.0302 (197.30)	−12.5904 (198.16)
8	5.9988 (197.09)	−1.8288 (193.69)	5.5915 (195.62)	−1.0661 (193.51)	−1.3216 (196.65)	5.9988 (197.09)
9	−5.4235 (181.06)	−19.4675 (183.21)	−15.0303 (182.26)	−14.9050 (183.83)	−7.8931 (185.13)	−5.4235 (181.06)
10	1.5292 (176.49)	−3.4400 (174.49)	−16.7503 (177.49)	−16.9083 (172.96)	−3.2271 (182.19)	1.5292 (176.49)
11	−24.8036 (171.01)	31.1244 (172.86)	−71.5094 (172.08)	13.5206 (170.68)	−24.4856 (176.74)	−24.8036 (171.01)
12	−43.6745 (169.83)	16.5462 (172.15)	−33.8446 (171.30)	−6.4654 (169.20)	0.4783 (171.37)	−43.6745 (169.83)
13	99.2901 (166.76)	−37.0669 (171.43)	−2.7349 (170.99)	47.6200 (168.76)	−59.7638 (169.77)	99.2901 (166.76)
14	−23.5392 (165.54)	51.5195 (169.48)	129.4276 (165.81)	42.1817 (166.42)	−4.3739 (165.85)	−23.5392 (165.54)
15	20.2698 (164.81)	20.3524 (165.17)	39.7094 (165.15)	−110.8616 (165.45)	95.9228 (165.54)	20.2698 (164.81)
16	−162.3880 (164.13)	−5.0554 (165.10)	−166.6932 (164.32)	61.1915 (164.00)	−146.8423 (164.25)	−162.3880 (164.13)
17	30.0887 (161.33)	−18.9771 (164.47)	2.9152 (163.91)	43.4048 (161.79)	−1.7374 (162.69)	30.0887 (161.33)
18	−10.1338 (160.53)	34.9206 (162.09)	2.2358 (161.58)	16.7210 (159.85)	−1.6653 (160.74)	−10.1338 (160.53)
19	66.2339 (158.88)	−14.5971 (159.34)	61.2565 (160.91)	1.8401 (158.10)	2.8070 (157.71)	66.2339 (158.88)
20	2.0770 (157.99)	−12.7409 (157.38)	−11.7556 (158.89)	−14.3925 (156.64)	−3.3382 (154.48)	2.0770 (157.99)
21	−32.4015 (154.79)	39.6893 (153.77)	22.6967 (154.67)	19.8884 (154.61)	3.2890 (153.31)	−32.4015 (154.79)
22	−3.8490 (154.40)	31.4621 (151.85)	6.8975 (153.67)	−1.5263 (154.42)	−9.0520 (152.84)	−3.8490 (154.40)
23	−1.5578 (152.85)	−6.8317 (151.59)	−7.0537 (151.60)	−3.7928 (152.85)	60.6013 (152.27)	−1.5578 (152.85)
24	30.8870 (150.85)	−10.8822 (151.32)	8.6683 (149.29)	10.4011 (150.87)	8.7688 (151.71)	30.8870 (150.85)
25	−4.8416 (149.91)	5.4884 (149.82)	−0.6229 (148.97)	43.6416 (149.79)	−7.0139 (151.30)	−4.8416 (149.91)

Table 7.22. Rotational strengths in dipole velocity formalism and excitation wavelengths for the lowest-energy electronic transitions of the conformers of *cis*-**6**, as obtained by PBE0/TZ2P//B97D/TZ2P calculations in 2-propanol (IEFPCM solvation model).

j	R_j, 10^{-40} erg cm^3 (λ_j, nm)			
	cis-**6a**	*cis*-**6b**	*cis*-**6c**	*cis*-**6d**
1	−47.1823 (252.32)	−154.9284 (251.47)	33.8296 (252.39)	47.7171 (246.07)
2	11.3834 (240.65)	3.3047 (240.12)	0.2446 (237.84)	−28.9582 (235.66)
3	49.0939 (229.67)	−15.5633 (228.07)	−28.9594 (232.36)	−7.2221 (234.25)
4	7.1399 (224.53)	58.5792 (225.98)	6.4094 (223.40)	−9.5974 (225.86)
5	17.0480 (223.82)	43.6996 (223.34)	−13.8214 (220.26)	25.6451 (221.48)
6	17.1597 (220.72)	2.1997 (220.87)	19.7041 (218.17)	1.7317 (220.75)
7	−38.7004 (218.32)	7.8910 (219.12)	1.1920 (215.74)	−3.8509 (215.00)
8	3.3509 (211.89)	2.3529 (209.30)	−0.9349 (215.47)	2.4918 (212.55)
9	−4.2457 (208.62)	8.0380 (205.58)	4.9999 (210.16)	−0.2745 (208.39)
10	−14.4917 (205.40)	−7.1024 (204.88)	−0.3822 (208.52)	−1.3383 (206.83)
11	1.3210 (204.08)	3.5832 (203.62)	5.2134 (204.56)	1.6642 (204.61)
12	−1.8190 (201.79)	−1.2825 (202.42)	−48.9397 (202.55)	16.7878 (202.83)
13	−0.9783 (200.78)	7.6511 (202.08)	5.5051 (201.65)	1.1057 (201.17)
14	−3.5840 (200.25)	6.8499 (200.39)	10.9375 (197.62)	−0.5025 (201.01)
15	−7.9425 (198.47)	−26.6636 (199.75)	4.2821 (195.88)	9.6181 (197.99)
16	−6.4218 (197.54)	−12.7862 (197.92)	6.5126 (195.09)	−11.9938 (196.24)
17	−15.4300 (196.58)	−10.9706 (194.49)	−6.4578 (193.92)	30.3435 (194.84)
18	0.8277 (192.79)	−3.5766 (193.80)	9.5209 (189.09)	34.2890 (193.16)
19	20.4684 (186.43)	12.3087 (187.81)	0.7945 (188.38)	−0.0717 (192.27)
20	1.3626 (186.11)	45.1126 (185.85)	49.3257 (187.84)	−20.9480 (189.89)
21	35.6892 (184.06)	10.6209 (185.56)	−30.0974 (184.79)	32.2882 (189.45)
22	−11.5760 (183.00)	8.2395 (184.29)	47.2467 (183.05)	−117.0362 (187.67)
23	9.7768 (181.94)	11.7174 (183.18)	−42.6381 (182.33)	−5.1565 (185.31)
24	−43.2094 (180.63)	−56.2765 (181.86)	34.2312 (181.65)	18.2650 (182.72)
25	−117.2354 (179.36)	102.1415 (181.12)	−76.2072 (180.63)	−0.5539 (179.18)

j	R_j, 10^{-40} erg cm^3 (λ_j, nm)		
	cis-**6e**	*cis*-**6g**	*cis*-**6h**
1	−96.2811 (250.72)	−57.7406 (249.79)	6.5412 (244.47)
2	−9.8875 (236.73)	5.2992 (239.28)	−131.4035 (236.06)
3	−2.9025 (235.97)	69.9609 (230.22)	−0.7546 (234.37)
4	67.4385 (221.52)	18.7484 (222.71)	−3.8614 (225.14)
5	31.1947 (219.69)	7.8515 (220.65)	48.5781 (221.56)
6	−36.8561 (218.16)	23.0499 (218.95)	2.0273 (220.65)
7	−0.9549 (217.10)	−19.4526 (216.62)	9.0484 (213.82)
8	−4.7625 (215.71)	−16.1054 (210.66)	−9.7216 (211.19)
9	−1.7985 (210.09)	−4.8046 (206.49)	−0.5233 (207.88)
10	0.9301 (209.17)	−31.8986 (204.57)	−0.8923 (203.92)
11	10.5851 (206.07)	2.1035 (202.27)	−12.1446 (203.09)
12	−1.7300 (204.20)	10.0237 (201.38)	7.5875 (201.68)
13	−23.9395 (203.69)	−8.7674 (200.17)	1.2316 (200.80)
14	−25.8976 (197.84)	4.5766 (197.46)	1.1758 (199.90)
15	23.8210 (195.22)	−2.3311 (196.82)	−3.0759 (194.52)
16	−11.8398 (194.48)	−2.2872 (196.45)	39.9631 (194.37)
17	−11.4041 (194.10)	−36.3416 (191.91)	28.2508 (193.23)
18	12.7024 (189.06)	−58.1784 (188.37)	−5.5403 (192.87)
19	42.4096 (188.90)	−14.8173 (187.15)	−9.6933 (191.25)
20	23.3078 (188.21)	−8.5926 (186.51)	24.1053 (189.12)
21	3.8124 (187.25)	7.0110 (185.36)	−12.3885 (188.32)
22	14.2662 (182.38)	21.9213 (184.12)	−10.5777 (186.70)
23	163.6883 (181.12)	−5.3093 (182.07)	−7.1984 (184.77)
24	−108.2871 (179.51)	−13.9457 (179.72)	5.0661 (180.85)
25	36.8126 (179.31)	257.4887 (178.94)	31.5375 (179.97)

Chapter 8

Fenoterol

This chapter is based on a peer-reviewed publication:
Daniele Tedesco, Riccardo Zanasi, Irving W. Wainer, Carlo Bertucci (**2014**). Stereochemical and conformational study on fenoterol by ECD spectroscopy and TD-DFT calculations. *Journal of Pharmaceutical and Biomedical Analysis 91*, 92–96.

Abstract: Fenoterol and its derivatives are selective β_2-adrenergic receptor (β_2-AR) agonists whose stereoselective biological activities have been extensively investigated in the past decade; a complete stereochemical characterization of fenoterol derivatives is therefore crucial for a better understanding of the effects of stereochemistry on β_2-AR binding. In the present project, the relationship between chiroptical properties and absolute stereochemistry of the stereoisomers of fenoterol (**1**) was investigated by experimental ECD spectroscopy and time-dependent density functional theory (TD-DFT). DFT geometry optimizations were carried out at the RI-B97D/TZVP/IEFPCM(MeOH) level and subsequent TD-DFT calculations were performed using the PBE0 hybrid functional. Despite the large pool of equilibrium conformers found for the investigated compounds and the known limitations of the level of theory employed, the computational protocol was able to reproduce the experimental ECD spectra of the stereoisomers of **1**. The main contribution to the overall chiroptical properties was found to arise from the absolute configuration of the chiral centre in α-position to the resorcinol moiety. Based on this evidence, a thorough conformational analysis was performed on the optimized DFT conformers, which revealed the occurrence of a different equilibrium between conformational patterns for the diastereomers of fenoterol: the (R,R')/(S,S') enantiomeric pair showed a higher population of folded conformations than the (R,S')/(S,R') pair.

Acknowledgements: Financial support was provided by the University of Bologna and by MIUR (Rome, Italy) through the PRIN 08 funding program (project number: 2008LYSEBR_005) and by the Intramural Research Program of the NIA/NIH. High-performance computing resources were provided by CINECA (Casalecchio di Reno, Italy) through the ISCRA funding program (class C08 project number: HP10CU0YHL).

Fenoterol (**1**, Figure 8.1a) is a resorcinolamine derivative acting as an agonist of the β_2-adrenergic receptor (β_2-AR), widely known for its pharmacological application as a bronchodilator in the treatment of asthma. Fenoterol is a chiral molecule possessing two chiral centres, and the binding of fenoterol to β_2-AR is highly stereoselective: the (*R*,*R*′)/(*S*,*S*′) racemate is about 20 times more active than the (*R*,*S*′)/(*S*,*R*′) racemate, and stereoisomers with (*R*)-configuration in α-position to the resorcinol moiety display greater affinity to β_2-AR than the corresponding enantiomorphs.[215]

Figure 8.1. Chemical structures of fenoterol derivatives and arbitrary atom numbering used in this article. **a:** Fenoterol (**1**); **b:** (*R*,*R*′)-**1**; **c:** (*R*,*S*′)-**1**; **d:** (*S*)-1′-desmethyl-4″-methoxy)fenoterol (**2**).

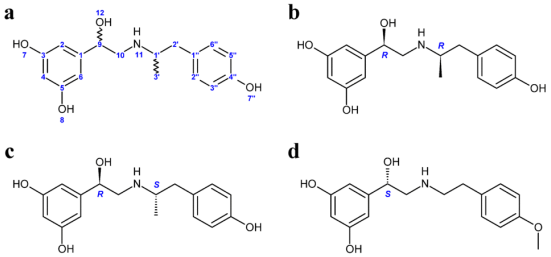

Recently, a large series of fenoterol derivatives was synthesized[216,217] and tested to determine their stereoselective activity toward β_2-AR and other pharmacological targets. β_2-AR agonists, for instance, are promising drugs in the treatment of congestive heart failure[218] and (*R*,*R*′)-**1** is currently under scrutiny as a new therapeutic agent for this application. Moreover, fenoterol derivatives elicit an inhibitory action toward the growth of 1321N1 astrocytoma cells,[219] while (*R*,*R*′)-(4″-methoxy-1″-naphthyl)fenoterol was found to stimulate apoptosis in HepG2 hepatocarcinoma cells through activation of the cannabinoid receptor pathway.[220] The effect of stereochemistry on the binding affinity of fenoterol derivatives to β_2-AR has been extensively investigated by comparative molecular field analysis (CoMFA)[216,217] and a three-dimensional quantitative structure-activity relationship model (3D-QSAR) was developed in order to be used as a predictive tool for the rational drug design of new β_2-AR agonists. The absolute stereochemistry of the stereoisomers of fenoterol derivatives, however, was determined by chemical correlation with the synthetic precursors and no further characterisation carried out. Due to the great influence of stereochemistry on the activity of β_2-AR agonists, a complete stereochemical characterisation of fenoterol derivatives is crucial for a better understanding of the biorecognition mechanism involved in the binding to β_2-AR.

Previously, the absolute stereochemistry of (*R*,*R*′)- and (*S*,*S*′)-**1** was assessed by electronic circular dichroism (ECD) spectroscopy[71] using the Brewster-Buta/Smith-Fontana sector rule,[221,222] a semi-empirical method which predicts the ECD sign for the ^1L_b transition of chiral α-substituted benzylic derivatives. As for all sector rules, however, the stereochemical assessment on new derivatives is not straightforward and relies on specific conditions at the molecular level which must be strictly fulfilled, such as the absence of relevant modifications to the chromophore systems.

In the past decades, quantum mechanical (QM) calculations became the standard method for stereochemical characterisation,[5] thanks to the improvements in accuracy and efficiency of theoretical models and the availability of increasingly powerful computational resources. In particular, the recent advances in density functional theory (DFT)[127,128] and time-dependent DFT (TD-DFT)[29,137] allow the application of these methods to chemical systems of increasing size and complexity, which is fundamental when dealing with molecules of pharmaceutical interest.[111]

The aim of the present study was to investigate the relationship between the absolute stereochemistry and the chiroptical properties of the stereoisomers of fenoterol by means of experimental ECD spectroscopy and TD-DFT calculations, in order to assess the accuracy of the assigned absolute stereochemistry. Once the reliability of the computational protocol was assessed, a thorough conformational analysis was performed on the optimised DFT geometries of conformers, in order to characterise the conformational space of fenoterol and identify possible stereoselective differences in the conformational patterns at equilibrium.

8.1 Material and methods

The study was performed on the stereoisomers of two compounds (Figure 8.1): (*R*,*R*′)- and (*R*,*S*′)-fenoterol (**1**), and (*S*)-(1′-desmethyl-4″-methoxy)fenoterol (**2**). Compounds were kindly provided as fumarate salts by SRI International (Menlo Park, CA, USA) and prepared as previously described.[216] HPLC-grade solvents methanol (MeOH; Sigma-Aldrich, Milan, Italy) was used to prepare the samples for spectroscopic analysis in a 100–400 μM concentration range.

8.1.1 Experimental spectroscopy

ECD and UV spectroscopic analysis was carried out at 25 °C on a Jasco (Tōkyō, Japan) J-810 spectropolarimeter equipped with a PTC-423S Peltier-type temperature control system, using a 2 nm spectral bandwidth, a 50 nm min^{-1} scanning speed and a 2 s data integration time; spectra were averaged over 3 accumulation cycles. Quartz cells (Hellma, Milan, Italy) with a 10 mm pathlength were used to measure spectra in the 350–225 nm spectral range, while a 1 mm pathlength was used in the 250–200 nm range.

8.1.2 Computational spectroscopy

The determination of the theoretical chiroptical properties by TD-DFT was performed on the conjugate acids of the diastereomers of compound **1**, (*R*,*R*′)-**1** and (*R*,*S*′)-**1**, in order to reproduce the experimental conditions in solution. The conformational search on all the compounds was performed according to a standard protocol, consisting in a preliminary identification of conformers by molecular mechanics (MM) calculations and a subsequent DFT geometry optimisation on the identified conformers.

The MMFF94s force field[125] and the Spartan'02[126] software were used for MM calculations. A large energy window was chosen in the selection of input structures for DFT geometry optimisations, in order to increase the accuracy of the conformational search: all MM conformers within a relative energy (ΔE_{MM}) threshold of 10 kcal mol^{-1} were considered.

DFT calculations were carried out using the Gaussian 09 software.[158] The B97D functional[153,154] was used in combination with the Ahlrichs-type triple-ζ valence plus polarisation basis set TZVP[223] in order to improve the description of long-range dispersion interactions by means of semi- classical corrections to the calculated interaction potential.[224] The resolution of identity (RI) approximation, also known as density fitting,[225,226] was used to reduce the computational effort of the calculations. Geometry optimisation and frequency calculations were therefore carried out at the RI-B97D/TZVP level; the IEFPCM solvation model[114,136] for methanol was used to account for long-range solvation effects.

TD-DFT calculations were also carried out using the Gaussian 09 software. The PBE0 global hybrid functional,[155–157] which provides a reasonable balance between accuracy of calculated chiroptical properties and computational cost, was employed in combination with the TZVP basis set and the IEFPCM solvation

model for methanol. Calculations were performed on all optimised conformers having a Boltzmann equilibrium population at 298.15 K and 1 atm (either derived from electronic energies, χ_{QM}, or free energies, χ_G) above 1%.

Theoretical values of oscillator strength (f_j), rotational strength in dipole velocity formalism (R_j) and excitation energies (expressed as wavelengths, λ_j) were calculated for the 30 lowest-energy electronic transitions of each optimised conformer; the number of calculated transition was selected in order to obtain full spectra above 200 nm.

The theoretical UV and ECD spectra of optimised conformers were derived by approximation of f_j and R_j values to Gaussian bands with a $\Delta\sigma$ value (defined as the half-bandwidth at $\Delta\varepsilon_{max}/$ e) of 0.25 eV.[113] The theoretical UV and ECD spectra of compounds were derived as the weighted average of the contribution of all conformers according to their Boltzmann equilibrium populations at 298.15 K and 1 atm derived from free energies (χ_G), and compared to the corresponding experimental spectra.

8.1.3 Conformational analysis

The conformational space of fenoterol can be described by a set of geometric parameters (Table 8.1, Figure 8.2) defining the flexibility of the alkylic linker (dihedral angles α, β, γ and δ), the orientation of the resorcinol and phenol moieties (dihedral angles φ_1 and φ_2, respectively), the orientation of hydroxyl groups (dihedral angles ω_1, ω_2, ω_3 and κ), and the distances between the O7″ atom and the remaining oxygen atoms (distances d_1, d_2 and d_3). The stereochemical descriptors used to describe dihedral angles are summarised in Figure 8.3.

Figure 8.2. Graphical representation of the dihedral angles listed in Table 8.1.

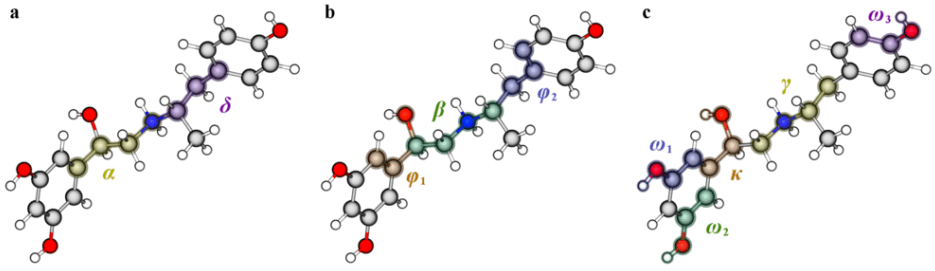

Figure 8.3. Stereochemical descriptors of dihedral angles. *sp*: *syn*-periplanar; *sc*: *syn*-clinal; *ac*: *anti*-clinal; *ap*: *anti*-periplanar.

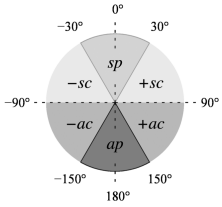

Table 8.1. Relevant geometric parameters defining the conformational flexibility of fenoterol.

Label	Parameter
α	C1–C9–C10–N11
β	C9–C10–N11–C1
γ	C10–N11–C1′–C2′
δ	N11–C1′–C2′–C1′
φ_1	C2–C1–C9–O12
φ_2	C2″–C1″–C2′–C1′
ω_1	C2–C3–O7–H7
ω_2	C6–C5–O8–H8
ω_3	C3″–C4″–O7″–H7′
κ	C1–C9–O12–H12
d_1	O7″–O7
d_2	O7″–O8
d_3	O7″–O12

8.2 Results and discussion

8.2.1 Spectroscopic analysis

The UV spectra of the diastereomers of **1** (Figure 8.4) shows the typical features of the substituted aromatic chromophores,[14] showing a broad absorption band at 279 nm ($\varepsilon \sim 3700$ M^{-1} cm^{-1}) due to the overlapping ^1L_b transitions of the resorcinol and phenol chromophores, with the former lying at a slightly lower energy. The bands of the ^1L_a transitions are centred at 224 nm ($\varepsilon \sim 19000$ M^{-1} cm^{-1}) and are almost covered by the broad ^1B_b transitions at shorter wavelengths. The ECD spectra of the diastereomers of **1** in the 250–200 nm range (Figure 8.4) are very similar to each other, revealing that the strongest contribution to the overall chiroptical properties of fenoterol is given by the absolute configuration of the chiral centre in α-position to the resorcinol chromophore (C9 atom). The strongest Cotton effect (CE) belongs to the ^1B_b transitions and is observed below 210 nm; the CE is negative for (*R*)-configurations at C9. The ^1L_a transitions give rise to weak CEs in the 235–215 nm range, which are respectively negative and positive for (*R*)- and (*S*)-configurations at C1′.

Figure 8.4. Comparison between experimental and calculated UV and ECD spectra of the stereoisomers of **1**. *Solid:* experimental in methanol, 10 mm (320–225 nm) and 1 mm (250–200 nm) pathlengths. *Dashed:* theoretical, PBE0/TZVP/IEFPCM(MeOH)//RI-B97D/TZVP/IEFPCM(MeOH), ΔG-based conformational average, $\Delta\sigma = 0.25$ eV. **a:** (*R*,*R*′)-**1**. **b:** (*R*,*S*′)-**1**.

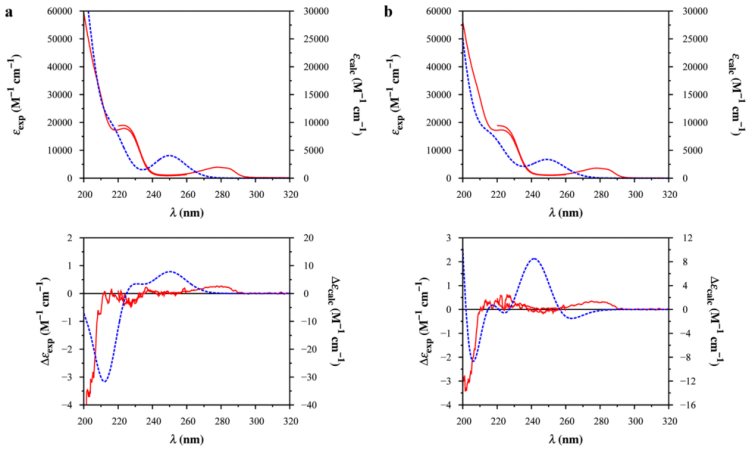

The UV and ECD spectra of **1** and **2** in the 300–250 nm range (Figures 8.5 and 8.8) confirm that the chiroptical properties of fenoterol are mainly defined by the absolute configuration at C9. The comparison between the CEs of the ^1L_b transitions of (*R*,*R*′)-**1** and (*S*)-**2** shows that the absence of a chiral centre at C1′ does not affect the intensity and sign of the ECD band at 279 nm, which is negative for (*S*)-configurations at C9 and positive for (*R*)-configurations. These findings are in agreement with the Brewster-Buta/Smith-Fontana sector rule for chiral α-substituted benzylic derivatives,[221,222] which can therefore be applied to determine the absolute stereochemistry of fenoterol at C9; this approach was already employed for the chiral discrimination of (*R*,*R*′)- and (*S*,*S*′)-**1**.[71]

Figure 8.5. Experimental ECD spectra (320–225 nm) of the stereoisomers of **1** and **2** in methanol. *Solid:* (*R*,*R*′)-**1**. *Dashed:* (*R*,*S*′)-**1**. *Dotted:* (*S*)-**2**.

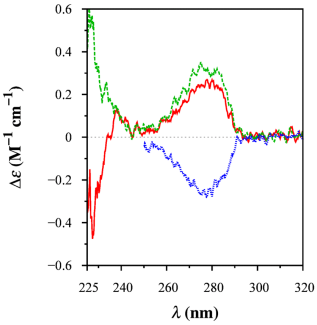

8.2.2 Conformational search

Results from MM calculations are reported in Tables 8.4 and 8.9. According to the 10 kcal mol^{-1} energy threshold for the MM conformational search, DFT calculations were performed on 68 conformers for (*R*,*R*′)-**1** and 57 conformers for (*R*,*S*′)-**1**. Geometric parameters for all optimised conformers are reoprted in Tables 8.5 and 8.10; the corresponding energies and Boltzmann equilibrium populations are reported in Tables 8.6 and 8.11. Conformers (*R*,*R*′)-**1.19**, (*R*,*R*′)-**1.26** and (*R*,*S*′)-**1.22** were found to have an imaginary frequency and were discarded; conformers (*R*,*S*′)-**1.12** and (*R*,*S*′)-**1.13** were found to converge to the same geometry (RMSD = 0.000377 Å). Considering the defined energy thresholds, TD-DFT calculations were performed on 18 conformers for each diastereomer.

8.2.3 TD-DFT calculations

Calculated f_j, R_j and λ_j values for all the low-energy conformers of the diastereomers of **1** are reported in Tables 8.7, 8.8, 8.12 and 8.13, while graphical representations of optimised geometries and theoretical ECD spectra are reported in Figures 8.6 and 8.7.

The comparison between theoretical and experimental spectra of the diastereomers of **1** (Figure 8.4) shows a moderate degree of correlation. The main feature of the experimental ECD profiles in the high-energy spectral range, i.e. the sign of the CE for the ^1B_b transitions, is correctly predicted by PBE0 for the stereoisomers under investigation. A shift toward longer wavelengths and an overestimation of the CE intensity are however observed for the ^1B_b transitions, while the ^1L_a transitions are shifted toward shorter wavelengths and are almost hidden beneath the ^1B_b transitions. TD-DFT calculations also predict a positive CE for the ^1L_b transition of the resorcinol chromophore, even though the calculated R_j values are systematically more intense and shifted toward shorter wavelengths when compared to the experimental band.

Despite the large number of conformers used to average the theoretical UV and ECD spectra and the intrinsic approximations of the PBE0/TZVP level, TD-DFT calculations are able to reproduce the chiroptical properties of the stereoisomers of fenoterol. However, the weak intensity of the experimental ECD bands for the ^1L_a transitions and the overlap of the ^1L_a and ^1B_b transitions in the conformationally-averaged theoretical spectra would not allow a complete discrimination between (*R*,*R*′)-**1** and (*R*,*S*′)-**1** if other information on the stereochemistry were not available.

8.2.4 Conformational analysis

The conformational analysis on the optimised DFT geometries of the investigated compounds allowed to identify the occurrence of seven general patterns for the conformational flexibility of the alkylic linker, which were labeled *A* to *G* (Table 8.2). The classification relies on the regularity shown by the alkylic linker to adopt specific spatial arrangements: dihedral angles α and δ, for instance, adopted either a *syn*-clinal or *anti*-periplanar conformation in almost every conformer. A more detailed classification in sub-patterns can be found in Table 8.3. It should be noted that, in several occasions, conformers belonging to the same sub-pattern only differ in the orientation of hydroxyl groups, and therefore their energies and ECD spectra are very similar (e.g., Figures 8.7a–b).

Table 8.2. Conformational patterns for the alkylic linker of **1** and corresponding Boltzmann equilibrium populations based on relative free energies at the RI-B97D/TZVP/IEFPCM(MeOH) level.

Pattern	α	β	γ	δ	(*R*,*R*′)-**1**		(*R*,*S*′)-**1**	
					Conf.	χ_G (%)	Conf.	χ_G (%)
A	$-sc$	ap/ac	*X*	*sc*	31	78.9	25	92.5
B	$-sc$	*sc*	*X*	*sc*	–	–	7	2.3
C	*ap*	*X*	$\pm(sc/ac)$	$\mp sc$	5	0.5	7	2.7
D	*ap*	*X*	*Y*	*sc*	19	17.2	5	1.3
E	*ap*	*X*	*Y*	*ap*	4	0.7	2	0.5
F	$-sc$	ap/ac	*X*	*ap*	6	1.3	9	0.7
G	$+sc$	*X*	*Y*	*Z*	1	1.4	–	–

The aforementioned classification is useful to draw some general considerations about the overall conformational space of fenoterol. When both dihedral angles α and δ (Figure 8.2a) are *syn*- clinal (patterns *A* and *B*), the alkylic linker is folded and the aromatic moieties are closer to each other; consequently, the average distance between the O7″ atom and the other oxygen atoms ($\bar{d}$) is relatively small. On the other hand, when α and/or δ are *anti*-periplanar (patterns *D*, *E* and *F*), the alkylic linker is extended and the aromatic moieties are more distant (larger $\bar{d}$ values). An exception is represented by pattern *C*, where γ and δ are *syn*-clinal and of opposite sign: when this happens, the alkylic linker is folded (small $\bar{d}$ values). Fenoterol conformers can therefore be divided in three main conformational arrangements: folded ($\bar{d}$ < 6.5 Å), partially-folded (6.5 Å < $\bar{d}$ < 7.5 Å) and extended conformations ($\bar{d}$ > 7.5 Å). Boltzmann populations derived from free energies (χ_G) suggest a preference for folded and partially-folded conformations for the conjugate acid of fenoterol in methanol; however, the contribution of folded conformers differs among diastereomers, accounting for 43.0% and 9.3% of the equilibrium conformers of (*R*,*R*′)-**1** and (*R*,*S*′)-**1**, respectively. The popula-

tion of partially-folded conformations, on the other hand, is higher for (*R*,*S*′)-**1** (71.3%) than for (*R*,*R*′)-**1** (35.5%), while no significant differences are observed for the weight of extended conformations: 21.5% for (*R*,*R*′)-**1**, 19.4% for (*R*,*S*′)-**1**.

8.3 Conclusions

The combination of experimental ECD spectroscopy and theoretical TD-DFT calculations allowed a full characterisation of the UV and ECD profiles for the diastereomers of **1**, whose absolute stereochemistry was confirmed. The present study gave interesting insights on the independent contribution of the two aromatic chromophores to the observed chiroptical properties of fenoterol, revealing that the absolute configuration of the chiral centre in α-position to the resorcinol chromophore is the dominant feature defining the overall ECD spectrum of fenoterol. The main effect of the chiral centre in β-position to the phenol moiety is a modification in the conformational arrangement of the alkylic linker which leads to a different equilibrium between partially-folded and folded conformations among diastereomers, with the (*R*,*R*′)/(*S*,*S*′) enantiomeric pair showing a higher preference for folded conformations.

Table 8.3. Conformational sub-patterns for the alkylic linker of **1** and corresponding Boltzmann equilibrium populations based on relative free energies at the RI-B97D/TZVP/IEFPCM(MeOH) level.

Pattern	α	β	γ	δ	(*R*,*R*′)-**1**		(*R*,*S*′)-**1**	
					Conf.	χ_G **(%)**	**Conf.**	χ_G **(%)**
A_1	$-sc$	ap	ap	$+sc$	5	2.84	6	81.77
A_2	$-sc$	ap	ap	$-sc$	7	37.57	4	1.10
A_3	$-sc$	ap	$+sc$	$+sc$	4	1.98	4	3.69
A_4	$-sc$	ap	$-sc$	$-sc$	4	34.53	–	–
A_5	$-sc$	ap	$+sc$	$-sc$	–	–	1	0.01
A_6	$-sc$	ap	$-sc$	$+sc$	–	–	1	0.00
A_7	$-sc$	ap	$+ac$	$-sc$	5	1.56	–	–
A_8	$-sc$	ap	$-ac$	$+sc$	1	0.01	6	5.82
A_9	$-sc$	$+ac$	ap	$-sc$	–	–	2	0.08
A_{10}	$-sc$	$+ac$	$+sc$	$+sc$	4	0.37	–	–
A_{11}	$-sc$	$+ac$	$+sc$	$-sc$	1	0.04	–	–
A_{12}	$-sc$	ap	ap	sp	–	–	1	0.00
B_1	$-sc$	$-sc$	$-sc$	$+sc$	–	–	2	0.02
B_2	$-sc$	$-sc$	$-ac$	$+sc$	–	–	2	0.02
B_3	$-sc$	$+sc$	ap	$+sc$	–	–	2	2.03
B_4	$-sc$	$-sc$	$-sc$	$-sc$	–	–	1	0.21
C_1	ap	ap	$+sc$	$-sc$	1	0.05	1	0.01
C_2	ap	ap	$-sc$	$+sc$	3	0.16	2	1.26
C_3	ap	ap	$+ac$	$-sc$	1	0.25	1	0.00
C_4	ap	ap	$-ac$	$+sc$	–	–	2	1.08
C_5	ap	$-sc$	$-sc$	$+sc$	–	–	1	0.38
D_1	ap	ap	ap	$+sc$	5	0.96	–	–
D_2	ap	ap	ap	$-sc$	4	13.47	–	–
D_3	ap	ap	$+sc$	$+sc$	4	1.60	2	1.15
D_4	ap	ap	$-sc$	$-sc$	1	0.27	–	–
D_5	ap	$-sc$	ap	$+sc$	4	0.37	–	–
D_6	ap	$-sc$	$-sc$	$-sc$	–	–	1	0.11
D_7	ap	$-sc$	$+ac$	$-sc$	1	0.53	–	–
D_8	ap	$-ac$	ap	$-sc$	–	–	2	0.03
E_1	ap	ap	ap	ap	–	–	2	0.52
E_2	ap	ap	$+sc$	ap	3	0.61	–	–
E_3	ap	ap	$-sc$	ap	1	0.13	–	–
F_1	$-sc$	ap	ap	ap	1	0.10	4	0.34
F_2	$-sc$	ap	$+sc$	ap	3	0.64	1	0.05
F_3	$-sc$	ap	$-sc$	ap	2	0.52	3	0.19
F_4	$-sc$	$+ac$	ap	ap	–	–	1	0.13
G_1	$+sc$	ap	ap	$-sc$	1	1.43	–	–

Table 8.4. Energies for the conformers of (*R*,*R*′)-**1**, as obtained after MM conformational search at the MMFF94s level.

MM ID	E_{MM} (kcal mol^{-1})	ΔE_{MM} (kcal mol^{-1})	QM ID	MM ID	E_{MM} (kcal mol^{-1})	ΔE_{MM} (kcal mol^{-1})	QM ID
mol001	41.8571	0.0000	**01**	**mol080**	47.0457	5.1886	**35**
mol079	42.4842	0.6271	**02**	**mol033**	47.2246	5.3675	**36**
mol025	42.5122	0.6551	**03**	**mol036**	47.3937	5.5366	**37**
mol024	42.6506	0.7935	**04**	**mol037**	47.5024	5.6453	**38**
mol035	42.6544	0.7973	**05**	**mol040**	47.5843	5.7272	**39**
mol046	42.7819	0.9248	**06**	**mol041**	47.6621	5.8050	**40**
mol050	42.9352	1.0782	**07**	**mol043**	47.8125	5.9554	**41**
mol002	44.2493	2.3922	**08**	**mol045**	47.8606	6.0035	**42**
mol015	44.4106	2.5536	**09**	**mol089**	48.1015	6.2444	**43**
mol006	44.5755	2.7184	**10**	**mol059**	48.1332	6.2761	**44**
mol038	44.5811	2.7240	**11**	**mol051**	48.5055	6.6484	**45**
mol007	44.6823	2.8253	**12**	**mol082**	48.5881	6.7310	**46**
mol008	44.7081	2.8510	**13**	**mol054**	48.6026	6.7456	**47**
mol009	44.7931	2.9360	**14**	**mol058**	48.6360	6.7790	**48**
mol098	44.8472	2.9902	**15**	**mol055**	48.6796	6.8225	**49**
mol019	44.8473	2.9902	**16**	**mol061**	48.9099	7.0528	**50**
mol011	45.0667	3.2096	**17**	**mol062**	48.9269	7.0698	**51**
mol012	45.2209	3.3638	**18**	**mol097**	49.1773	7.3202	**52**
mol088	45.2587	3.4016	**19**	**mol064**	49.1820	7.3249	**53**
mol027	45.5652	3.7081	**20**	**mol065**	49.2223	7.3652	**54**
mol091	45.6356	3.7785	**21**	**mol067**	49.3660	7.5089	**55**
mol072	45.7118	3.8547	**22**	**mol069**	49.4403	7.5832	**56**
mol020	46.1887	4.3317	**23**	**mol070**	49.6001	7.7430	**57**
mol021	46.2771	4.4200	**24**	**mol073**	49.8581	8.0010	**58**
mol063	46.3647	4.5076	**25**	**mol074**	49.8592	8.0022	**59**
mol022	46.3967	4.5396	**26**	**mol076**	49.9807	8.1236	**60**
mol023	46.4597	4.6026	**27**	**mol081**	50.1003	8.2432	**61**
mol042	46.4882	4.6312	**28**	**mol083**	50.3555	8.4984	**62**
mol044	46.4958	4.6387	**29**	**mol084**	50.5175	8.6604	**63**
mol066	46.8505	4.9934	**30**	**mol085**	50.5733	8.7162	**64**
mol087	46.8618	5.0047	**31**	**mol086**	50.6205	8.7634	**65**
mol026	46.8815	5.0244	**32**	**mol095**	51.4833	9.6262	**66**
mol028	46.9714	5.1143	**33**	**mol096**	51.4860	9.6289	**67**
mol029	47.0021	5.1451	**34**	**mol003**	51.7773	9.9202	**68**

Table 8.5. Geometric parameters for the conformers of (*R*,*R*′)-**1**, as obtained after DFT geometry optimisation at the RI-B97D/TZVP/IEFPCM(MeOH) level.

Pattern	ID	α (deg)	β (deg)	γ (deg)	δ (deg)	d_1 (Å)	d_2 (Å)	d_3 (Å)	$\bar{d}$ (Å)
A_1	(*R*,*R*′)-**1.03**	−59.542	−178.211	−177.389	60.037	4.550	5.838	7.951	6.113
	(*R*,*R*′)-**1.04**	−59.127	−178.225	−176.531	59.748	4.662	5.716	7.990	6.123
	(*R*,*R*′)-**1.07**	−65.804	165.477	167.702	47.877	3.154	7.700	6.583	5.812
	(*R*,*R*′)-**1.16**	−59.713	−178.474	−177.477	60.139	4.534	5.777	7.943	6.085
	(*R*,*R*′)-**1.62**	−60.509	169.453	−178.896	53.186	3.106	5.396	7.039	5.180
A_2	(*R*,*R*′)-**1.05**	−62.123	−173.491	169.323	−55.824	7.697	11.109	5.781	8.196
	(*R*,*R*′)-**1.06**	−62.096	−173.894	169.413	−56.406	7.856	11.219	5.853	8.309
	(*R*,*R*′)-**1.12**	−62.074	−173.795	169.334	−55.813	7.716	11.132	5.789	8.212
	(*R*,*R*′)-**1.13**	−62.027	−174.103	169.439	−56.342	7.861	11.236	5.856	8.318
	(*R*,*R*′)-**1.15**	−58.355	−168.541	178.651	−49.864	6.206	10.148	5.802	7.385
	(*R*,*R*′)-**1.20**	−61.680	−173.849	169.729	−56.226	7.917	11.181	5.852	8.317
	(*R*,*R*′)-**1.57**	−58.565	−166.213	176.651	−52.465	6.483	10.327	5.751	7.520
A_3	(*R*,*R*′)-**1.08**	−61.151	179.125	71.173	59.744	8.775	11.730	6.214	8.906
	(*R*,*R*′)-**1.14**	−61.229	−179.770	71.550	59.077	8.702	11.732	6.221	8.885
	(*R*,*R*′)-**1.33**	−61.050	179.696	71.486	59.202	8.727	11.763	6.242	8.911
	(*R*,*R*′)-**1.61**	−61.339	−179.874	71.339	58.971	8.854	11.731	6.215	8.933
A_4	(*R*,*R*′)-**1.01**	−67.035	176.608	−67.298	−49.245	3.561	4.794	7.366	5.240
	(*R*,*R*′)-**1.02**	−68.395	175.729	−68.048	−47.740	3.196	4.904	7.225	5.108
	(*R*,*R*′)-**1.11**	−67.100	176.662	−67.364	−49.211	3.554	4.732	7.365	5.217
	(*R*,*R*′)-**1.45**	−65.781	177.162	−65.284	−48.704	3.808	4.593	7.434	5.278
A_7	(*R*,*R*′)-**1.09**	−62.585	177.165	93.090	−56.637	10.546	10.272	5.616	8.811
	(*R*,*R*′)-**1.10**	−62.693	177.434	92.671	−57.446	10.624	10.261	5.719	8.868
	(*R*,*R*′)-**1.25**	−62.611	177.339	93.402	−56.549	10.534	10.387	5.603	8.841
	(*R*,*R*′)-**1.29**	−62.726	177.681	92.921	−57.398	10.614	10.377	5.706	8.899
	(*R*,*R*′)-**1.66**	−62.383	177.337	92.868	−57.099	10.693	10.368	5.692	8.918
A_8	(*R*,*R*′)-**1.64**	−70.623	−179.763	−97.980	45.462	6.412	3.176	7.047	5.545
A_{10}	(*R*,*R*′)-**1.17**	−58.534	96.426	72.698	56.995	10.735	11.265	8.518	10.173
	(*R*,*R*′)-**1.22**	−58.572	96.399	72.648	56.975	10.726	11.275	8.568	10.190
	(*R*,*R*′)-**1.38**	−59.220	95.321	72.458	57.247	10.844	11.224	8.568	10.212
	(*R*,*R*′)-**1.44**	−59.345	95.313	72.285	57.148	10.837	11.235	8.607	10.226
A_{11}	(*R*,*R*′)-**1.31**	−64.578	90.376	82.506	−67.988	9.622	6.112	7.702	7.812
C_1	(*R*,*R*′)-**1.27**	166.546	−176.145	87.709	−56.151	6.195	3.079	6.765	5.346
C_2	(*R*,*R*′)-**1.42**	−172.690	168.869	−84.422	56.728	2.973	7.390	5.525	5.296
	(*R*,*R*′)-**1.48**	−167.324	168.607	−83.257	58.525	3.026	6.386	5.706	5.039
	(*R*,*R*′)-**1.53**	−177.859	168.702	−84.976	61.139	3.823	8.201	5.836	5.953
C_3	(*R*,*R*′)-**1.46**	169.940	−174.388	96.306	−50.000	7.324	2.955	6.762	5.680
D_1	(*R*,*R*′)-**1.35**	179.080	177.227	177.424	61.447	10.694	12.339	6.381	9.805
	(*R*,*R*′)-**1.39**	178.830	178.049	177.165	61.397	10.735	12.410	6.452	9.866
	(*R*,*R*′)-**1.52**	179.515	176.762	177.935	61.460	10.635	12.384	6.354	9.791
	(*R*,*R*′)-**1.55**	179.830	176.446	178.190	61.413	10.717	12.307	6.337	9.787
	(*R*,*R*′)-**1.59**	179.512	177.299	177.917	61.496	10.762	12.379	6.411	9.851
D_2	(*R*,*R*′)-**1.18**	178.779	177.186	167.031	−55.418	11.911	9.494	7.805	9.737
	(*R*,*R*′)-**1.36**	179.071	175.170	165.551	−57.165	11.881	9.641	7.938	9.820
	(*R*,*R*′)-**1.40**	178.811	176.788	166.751	−55.559	11.952	9.486	7.822	9.753
	(*R*,*R*′)-**1.68**	179.613	175.814	166.488	−56.336	11.974	9.672	7.911	9.852
D_3	(*R*,*R*′)-**1.21**	179.498	177.683	69.901	57.438	11.821	9.252	7.983	9.685
	(*R*,*R*′)-**1.24**	179.628	177.657	69.997	57.371	11.895	9.369	8.021	9.762
	(*R*,*R*′)-**1.43**	179.115	177.638	69.704	57.380	11.845	9.210	7.993	9.683
	(*R*,*R*′)-**1.49**	179.221	177.659	69.795	57.280	11.919	9.320	8.027	9.755
D_4	(*R*,*R*′)-**1.23**	−176.495	175.202	−61.655	−47.146	7.560	10.701	5.223	7.828
D_5	(*R*,*R*′)-**1.28**	−177.889	−61.134	−179.385	62.439	12.099	12.181	9.003	11.094
	(*R*,*R*′)-**1.32**	−178.282	−61.371	−177.983	60.617	12.002	12.201	9.002	11.068
	(*R*,*R*′)-**1.50**	−177.878	−61.325	−179.314	62.386	12.162	12.180	9.000	11.114
	(*R*,*R*′)-**1.56**	−177.817	−61.186	−179.328	62.286	12.218	12.169	9.034	11.140
D_7	(*R*,*R*′)-**1.47**	179.348	−78.438	142.107	−57.068	8.385	8.979	4.308	7.224
E_2	(*R*,*R*′)-**1.51**	−178.791	163.494	62.793	−175.422	12.065	13.016	10.238	11.773
	(*R*,*R*′)-**1.54**	−179.637	162.879	61.791	−175.911	12.018	13.222	10.262	11.834
	(*R*,*R*′)-**1.67**	−178.955	163.326	62.953	−175.373	12.165	12.985	10.236	11.795
E_3	(*R*,*R*′)-**1.60**	178.673	169.946	−67.095	−166.863	12.395	13.996	9.961	12.117
F_1	(*R*,*R*′)-**1.30**	−63.034	−177.969	170.294	−170.889	11.624	12.902	10.314	11.613
F_2	(*R*,*R*′)-**1.34**	−62.478	174.258	72.023	−172.031	12.261	12.221	10.320	11.601
	(*R*,*R*′)-**1.37**	−62.561	174.858	71.126	−173.231	12.268	12.347	10.330	11.648
	(*R*,*R*′)-**1.58**	−61.713	170.627	67.213	−172.963	12.227	11.923	10.403	11.518
F_3	(*R*,*R*′)-**1.41**	−64.334	173.976	−65.086	−166.654	10.899	11.145	10.650	10.898
	(*R*,*R*′)-**1.65**	−64.310	173.895	−64.898	−166.578	10.960	11.091	10.653	10.901
G_1	(*R*,*R*′)-**1.63**	50.490	−171.289	160.030	−57.444	3.132	5.214	7.627	5.324

Table 8.5. (*Continued*)

Pattern	ID	φ_1 (deg)	φ_2 (deg)	ω_1 (deg)	ω_2 (deg)	ω_3 (deg)	κ (deg)
A_1	(*R*,*R*′)-**1.03**	−19.341	83.271	−179.038	−178.955	0.186	−54.037
	(*R*,*R*′)-**1.04**	−18.939	82.711	179.717	−178.871	179.147	−54.457
	(*R*,*R*′)-**1.07**	−27.549	79.455	−4.546	−179.816	0.886	−54.426
	(*R*,*R*′)-**1.16**	−19.297	83.357	−178.966	0.190	−0.073	−53.881
	(*R*,*R*′)-**1.62**	−12.435	77.780	6.259	0.316	−160.983	−58.868
A_2	(*R*,*R*′)-**1.05**	−28.920	−73.356	−179.564	−179.090	0.673	−50.513
	(*R*,*R*′)-**1.06**	−28.976	−73.256	−179.523	−179.106	−179.432	−50.757
	(*R*,*R*′)-**1.12**	−28.658	−73.561	−179.517	0.166	0.638	−50.587
	(*R*,*R*′)-**1.13**	−28.710	−73.336	−179.472	0.142	−179.418	−50.748
	(*R*,*R*′)-**1.15**	−24.728	−69.708	0.670	179.600	−0.260	−52.755
	(*R*,*R*′)-**1.20**	−28.327	−73.081	0.872	−179.079	−179.387	−52.088
	(*R*,*R*′)-**1.57**	−27.524	−73.489	1.004	−0.555	−179.604	−51.368
A_3	(*R*,*R*′)-**1.08**	−26.218	87.248	−179.786	179.685	−0.184	−53.274
	(*R*,*R*′)-**1.14**	−28.165	85.934	−179.984	−178.789	179.468	−52.636
	(*R*,*R*′)-**1.33**	−27.264	86.136	−179.847	0.405	179.504	−52.853
	(*R*,*R*′)-**1.61**	−27.735	85.794	0.519	−178.930	179.379	−54.119
A_4	(*R*,*R*′)-**1.01**	−33.953	−59.338	−176.199	−179.910	−2.168	−50.073
	(*R*,*R*′)-**1.02**	−35.997	−54.709	−162.807	−179.116	−175.430	−50.372
	(*R*,*R*′)-**1.11**	−33.994	−59.451	−176.257	−0.349	−1.914	−50.010
	(*R*,*R*′)-**1.45**	−33.220	−59.844	−0.304	−0.061	178.693	−51.787
A_7	(*R*,*R*′)-**1.09**	−24.772	−71.420	−179.233	179.898	0.051	−53.618
	(*R*,*R*′)-**1.10**	−24.857	−70.982	−179.323	−179.993	−179.410	−53.449
	(*R*,*R*′)-**1.25**	−25.333	−71.533	−179.532	0.187	0.013	−53.439
	(*R*,*R*′)-**1.29**	−25.453	−71.024	−179.632	0.105	−179.412	−53.253
	(*R*,*R*′)-**1.66**	−24.056	−71.068	1.087	0.398	−179.364	−54.857
A_8	(*R*,*R*′)-**1.64**	−32.115	75.681	1.338	−9.604	−171.246	−52.224
A_{10}	(*R*,*R*′)-**1.17**	−21.652	84.071	179.931	−178.933	−0.321	−51.979
	(*R*,*R*′)-**1.22**	−21.673	84.012	179.996	−178.925	179.247	−51.914
	(*R*,*R*′)-**1.38**	−21.182	84.439	0.582	−178.889	0.368	−53.255
	(*R*,*R*′)-**1.44**	−21.226	84.631	0.507	−178.921	179.104	−53.202
A_{11}	(*R*,*R*′)-**1.31**	−17.825	−66.652	−179.218	−1.473	−0.187	−51.548
C_1	(*R*,*R*′)-**1.27**	−33.601	−71.804	−179.455	−178.768	161.943	−67.326
C_2	(*R*,*R*′)-**1.42**	−52.018	73.278	−7.760	−179.421	9.663	−67.831
	(*R*,*R*′)-**1.48**	−30.073	73.688	177.934	179.957	−158.137	−69.585
	(*R*,*R*′)-**1.53**	−50.810	75.718	179.978	−179.113	−1.321	−67.915
C_3	(*R*,*R*′)-**1.46**	−16.585	−73.144	−178.936	9.408	−170.544	−68.000
D_1	(*R*,*R*′)-**1.35**	−41.857	84.504	180.000	−179.237	0.094	−65.441
	(*R*,*R*′)-**1.39**	−41.489	84.340	−179.998	−179.250	179.667	−65.060
	(*R*,*R*′)-**1.52**	−41.376	84.496	−179.862	0.534	0.113	−65.504
	(*R*,*R*′)-**1.55**	−41.549	84.354	0.372	−179.321	0.218	−66.348
	(*R*,*R*′)-**1.59**	−41.341	84.325	0.424	−179.288	179.588	−65.914
D_2	(*R*,*R*′)-**1.18**	−38.779	−72.052	179.604	−179.645	−0.427	−65.493
	(*R*,*R*′)-**1.36**	−45.023	−74.498	−179.558	−0.158	−0.345	−65.715
	(*R*,*R*′)-**1.40**	−38.808	−71.884	0.549	−179.717	−0.384	−66.194
	(*R*,*R*′)-**1.68**	−41.057	−69.918	0.567	0.306	−179.484	−65.951
D_3	(*R*,*R*′)-**1.21**	−40.234	84.755	−179.386	−179.211	0.047	−66.141
	(*R*,*R*′)-**1.24**	−40.182	84.444	−179.350	−179.210	179.651	−66.126
	(*R*,*R*′)-**1.43**	−39.675	84.727	0.031	−179.147	−0.081	−66.812
	(*R*,*R*′)-**1.49**	−39.410	84.390	0.105	−179.094	179.641	−66.807
D_4	(*R*,*R*′)-**1.23**	−41.400	−57.287	179.834	−179.290	−0.122	−65.087
D_5	(*R*,*R*′)-**1.28**	−37.594	84.936	−179.989	179.876	0.012	−65.918
	(*R*,*R*′)-**1.32**	−40.236	84.060	−179.867	−179.816	179.766	−65.898
	(*R*,*R*′)-**1.50**	−37.641	84.891	0.084	179.965	0.017	−66.599
	(*R*,*R*′)-**1.56**	−37.260	84.700	0.257	179.936	179.336	−66.559
D_7	(*R*,*R*′)-**1.47**	−34.681	−64.970	0.444	−179.376	−0.570	−95.226
E_2	(*R*,*R*′)-**1.51**	−38.390	76.147	−179.476	−179.989	179.634	−68.718
	(*R*,*R*′)-**1.54**	−42.866	75.876	−179.806	−179.190	0.136	−68.666
	(*R*,*R*′)-**1.67**	−37.469	76.198	0.671	179.964	179.654	−69.351
E_3	(*R*,*R*′)-**1.60**	−41.126	75.159	−179.795	−179.007	179.676	−67.372
F_1	(*R*,*R*′)-**1.30**	−27.569	77.379	−179.762	−178.869	−0.292	−51.710
F_2	(*R*,*R*′)-**1.34**	−25.601	76.554	−179.730	−179.094	179.435	−53.875
	(*R*,*R*′)-**1.37**	−25.713	76.467	−179.813	−179.025	0.329	−53.816
	(*R*,*R*′)-**1.58**	−23.871	77.067	1.004	−179.813	178.904	−55.360
F_3	(*R*,*R*′)-**1.41**	−26.483	77.150	−179.976	−179.348	179.172	−53.807
	(*R*,*R*′)-**1.65**	−25.497	77.054	0.504	−179.524	179.187	−55.508
G_1	(*R*,*R*′)-**1.63**	−56.365	−71.343	−165.723	−179.830	−9.932	−59.828

Table 8.6. Free and electronic energies for the conformers of (*R*,*R*′)-**1**, as obtained after DFT geometry optimisation at the RI-B97D/TZVP/IEFPCM(MeOH) level.

Pattern	ID	E_{QM} (Ha)	ΔE_{QM} (kcal mol^{-1})	χ_{QM} (%)	G (Ha)	ΔG (kcal mol^{-1})	χ_G (%)
A_1	(*R*,*R*′)-**1.03**	−1016.23808882	2.265	0.64	−1015.924440	1.796	0.69
	(*R*,*R*′)-**1.04**	−1016.23802156	2.307	0.60	−1015.924857	1.534	1.07
	(*R*,*R*′)-**1.07**	−1016.23827061	2.151	0.78	−1015.924191	1.952	0.53
	(*R*,*R*′)-**1.16**	−1016.23820259	2.194	0.72	−1015.924084	2.019	0.47
	(*R*,*R*′)-**1.62**	−1016.23874926	1.850	1.29	−1015.922419	3.064	0.08
A_2	(*R*,*R*′)-**1.05**	−1016.23732407	2.745	0.29	−1015.927302	0.000	14.22
	(*R*,*R*′)-**1.06**	−1016.23738567	2.706	0.30	−1015.926014	0.808	3.63
	(*R*,*R*′)-**1.12**	−1016.23749682	2.636	0.34	−1015.927005	0.186	10.38
	(*R*,*R*′)-**1.13**	−1016.23756692	2.592	0.37	−1015.925989	0.824	3.54
	(*R*,*R*′)-**1.15**	−1016.23726358	2.783	0.27	−1015.925293	1.261	1.69
	(*R*,*R*′)-**1.20**	−1016.23732390	2.745	0.29	−1015.925906	0.876	3.24
	(*R*,*R*′)-**1.57**	−1016.23717122	2.841	0.24	−1015.924667	1.653	0.87
A_3	(*R*,*R*′)-**1.08**	−1016.23600327	3.574	0.07	−1015.924559	1.721	0.78
	(*R*,*R*′)-**1.14**	−1016.23602191	3.562	0.07	−1015.923768	2.218	0.34
	(*R*,*R*′)-**1.33**	−1016.23615998	3.475	0.08	−1015.924268	1.904	0.57
	(*R*,*R*′)-**1.61**	−1016.23602523	3.560	0.07	−1015.923632	2.303	0.29
A_4	(*R*,*R*′)-**1.01**	−1016.24135977	0.212	20.50	−1015.926987	0.198	10.18
	(*R*,*R*′)-**1.02**	−1016.24169815	0.000	29.34	−1015.926085	0.764	3.92
	(*R*,*R*′)-**1.11**	−1016.24134672	0.221	20.22	−1015.927069	0.146	11.11
	(*R*,*R*′)-**1.45**	−1016.24129109	0.255	19.06	−1015.926903	0.250	9.32
A_7	(*R*,*R*′)-**1.09**	−1016.23450441	4.514	0.01	−1015.923725	2.245	0.32
	(*R*,*R*′)-**1.10**	−1016.23457462	4.470	0.02	−1015.923524	2.371	0.26
	(*R*,*R*′)-**1.25**	−1016.23469919	4.392	0.02	−1015.923782	2.209	0.34
	(*R*,*R*′)-**1.29**	−1016.23477687	4.343	0.02	−1015.923264	2.534	0.20
	(*R*,*R*′)-**1.66**	−1016.23444914	4.549	0.01	−1015.924029	2.054	0.44
A_8	(*R*,*R*′)-**1.64**	−1016.23657702	3.214	0.13	−1015.920376	4.346	0.01
A_{10}	(*R*,*R*′)-**1.17**	−1016.23528737	4.023	0.03	−1015.922147	3.235	0.06
	(*R*,*R*′)-**1.22**	−1016.23526156	4.039	0.03	−1015.922163	3.225	0.06
	(*R*,*R*′)-**1.38**	−1016.23525179	4.045	0.03	−1015.923005	2.696	0.15
	(*R*,*R*′)-**1.44**	−1016.23522284	4.063	0.03	−1015.922626	2.934	0.10
A_{11}	(*R*,*R*′)-**1.31**	−1016.23619054	3.456	0.09	−1015.921717	3.505	0.04
C_1	(*R*,*R*′)-**1.27**	−1016.23616454	3.472	0.08	−1015.921992	3.332	0.05
C_2	(*R*,*R*′)-**1.42**	−1016.23779872	2.447	0.47	−1015.922932	2.742	0.14
	(*R*,*R*′)-**1.48**	−1016.23455496	4.482	0.02	−1015.920230	4.438	0.01
	(*R*,*R*′)-**1.53**	−1016.23367117	5.037	0.01	−1015.920649	4.175	0.01
C_3	(*R*,*R*′)-**1.46**	−1016.23852193	1.993	1.01	−1015.923487	2.394	0.25
D_1	(*R*,*R*′)-**1.35**	−1016.23344895	5.176	0.00	−1015.923185	2.583	0.18
	(*R*,*R*′)-**1.39**	−1016.23340827	5.202	0.00	−1015.923428	2.431	0.23
	(*R*,*R*′)-**1.52**	−1016.23357499	5.097	0.01	−1015.922660	2.913	0.10
	(*R*,*R*′)-**1.55**	−1016.23367852	5.032	0.01	−1015.923196	2.577	0.18
	(*R*,*R*′)-**1.59**	−1016.23363312	5.061	0.01	−1015.923558	2.349	0.27
D_2	(*R*,*R*′)-**1.18**	−1016.23494623	4.237	0.02	−1015.925490	1.137	2.09
	(*R*,*R*′)-**1.36**	−1016.23504323	4.176	0.03	−1015.926116	0.744	4.05
	(*R*,*R*′)-**1.40**	−1016.23514860	4.110	0.03	−1015.925979	0.830	3.50
	(*R*,*R*′)-**1.68**	−1016.23503742	4.180	0.03	−1015.926064	0.777	3.83
D_3	(*R*,*R*′)-**1.21**	−1016.23471427	4.382	0.02	−1015.923280	2.524	0.20
	(*R*,*R*′)-**1.24**	−1016.23468034	4.404	0.02	−1015.923502	2.385	0.25
	(*R*,*R*′)-**1.43**	−1016.23490030	4.266	0.02	−1015.924091	2.015	0.47
	(*R*,*R*′)-**1.49**	−1016.23487061	4.284	0.02	−1015.924427	1.804	0.68
D_4	(*R*,*R*′)-**1.23**	−1016.23524900	4.047	0.03	−1015.923548	2.356	0.27
D_5	(*R*,*R*′)-**1.28**	−1016.23382868	4.938	0.01	−1015.922739	2.863	0.11
	(*R*,*R*′)-**1.32**	−1016.23379650	4.958	0.01	−1015.922322	3.125	0.07
	(*R*,*R*′)-**1.50**	−1016.23404188	4.804	0.01	−1015.922665	2.910	0.10
	(*R*,*R*′)-**1.56**	−1016.23401143	4.823	0.01	−1015.922543	2.986	0.09
D_7	(*R*,*R*′)-**1.47**	−1016.23686203	3.035	0.17	−1015.924189	1.953	0.53
E_2	(*R*,*R*′)-**1.51**	−1016.23256129	5.733	0.00	−1015.923281	2.523	0.20
	(*R*,*R*′)-**1.54**	−1016.23261661	5.699	0.00	−1015.922073	3.281	0.06
	(*R*,*R*′)-**1.67**	−1016.23276162	5.608	0.00	−1015.923796	2.200	0.35
E_3	(*R*,*R*′)-**1.60**	−1016.23210745	6.018	0.00	−1015.922876	2.777	0.13
F_1	(*R*,*R*′)-**1.30**	−1016.23406669	4.789	0.01	−1015.922579	2.964	0.10
F_2	(*R*,*R*′)-**1.34**	−1016.23359828	5.083	0.01	−1015.923653	2.290	0.30
	(*R*,*R*′)-**1.37**	−1016.23358843	5.089	0.01	−1015.923133	2.616	0.17
	(*R*,*R*′)-**1.58**	−1016.23349965	5.145	0.00	−1015.923148	2.607	0.17
F_3	(*R*,*R*′)-**1.41**	−1016.23341326	5.199	0.00	−1015.923829	2.179	0.36
	(*R*,*R*′)-**1.65**	−1016.23337076	5.226	0.00	−1015.923064	2.659	0.16
G_1	(*R*,*R*′)-**1.63**	−1016.23914410	1.603	1.96	−1015.925131	1.362	1.43

Figure 8.6. Optimised structures and theoretical ECD spectra ($\Delta\sigma$ = 0.25 eV) for the conformers of (*R*,*R*′)-**1**, as obtained after DFT geometry optimisation at the RI-B97D/TZVP/IEFPCM(MeOH) level and TD-DFT calculations at the PBE0/TZVP/IEFPCM(MeOH) level.

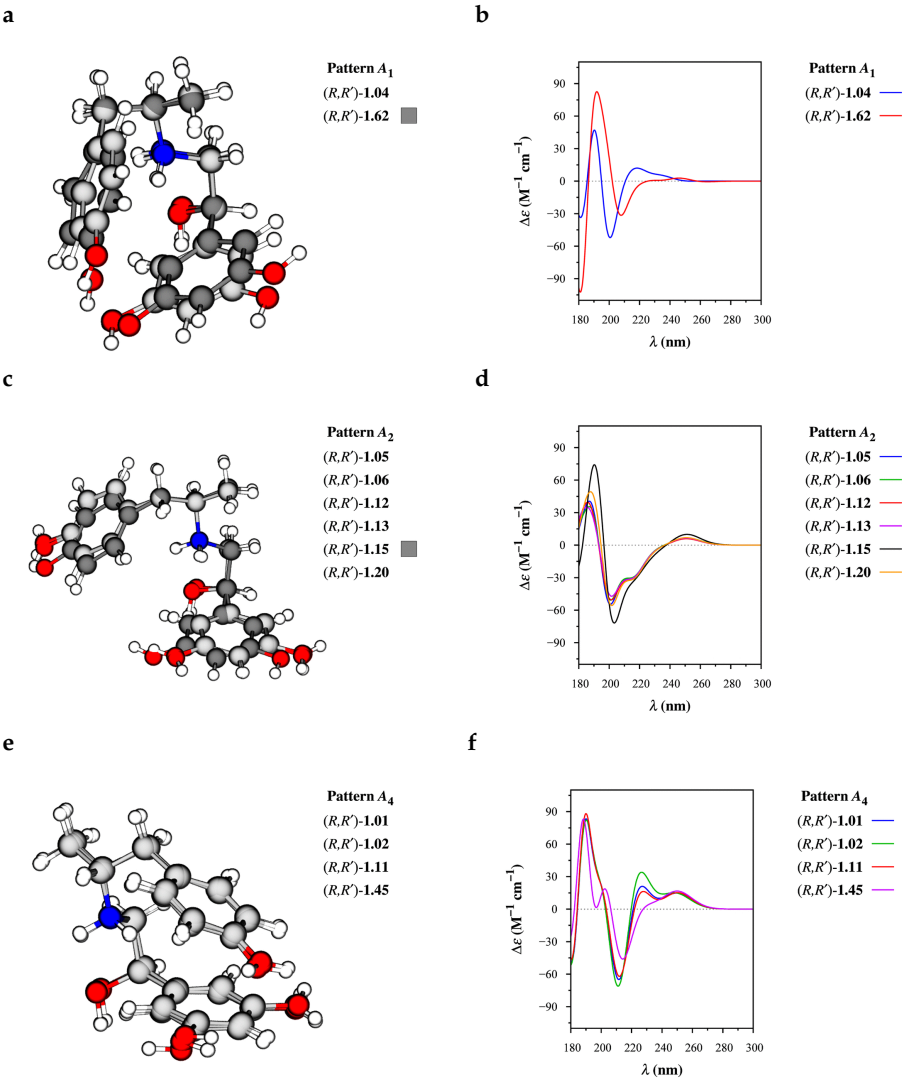

Figure 8.6. (*Continued*)

g

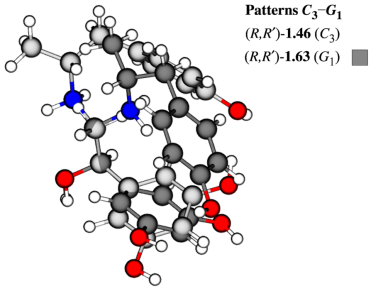

h

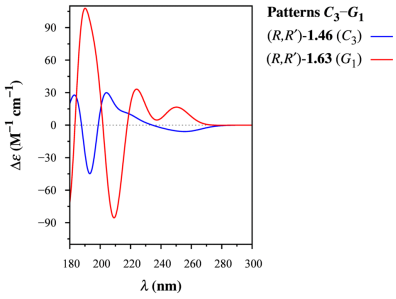

i

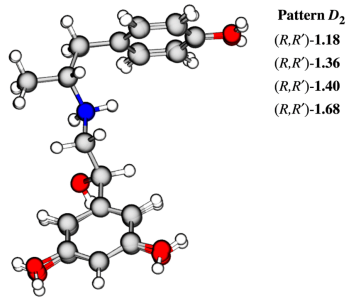

j

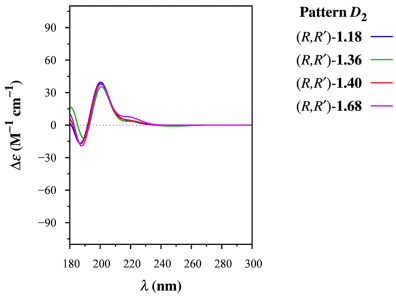

Table 8.7. Rotational strengths (in dipole velocity form) and excitation wavelengths for the conformers of (*R*,*R*′)-**1**, as obtained by TD-DFT calculations at the PBE0/TZVP/IEFPCM(MeOH) level.

j	R_j, 10^{-40} erg cm^3 (λ_j, nm)				
	(*R*,*R*′)-**1.01**	(*R*,*R*′)-**1.02**	(*R*,*R*′)-**1.04**	(*R*,*R*′)-**1.05**	(*R*,*R*′)-**1.06**
1	5.7767 (252.02)	5.4965 (253.20)	5.2981 (251.55)	17.7294 (250.37)	17.8230 (250.36)
2	23.5849 (249.74)	21.2592 (249.22)	−6.5945 (249.68)	−5.0308 (248.13)	−4.1343 (247.99)
3	5.8208 (239.05)	9.0387 (239.88)	7.7517 (234.99)	2.1873 (225.92)	2.9785 (225.54)
4	−3.7054 (238.50)	−2.4832 (238.23)	2.1425 (232.78)	−7.1271 (225.32)	−7.8677 (225.29)
5	24.6298 (222.27)	12.2104 (224.85)	4.3381 (218.44)	−0.5133 (217.33)	−0.3658 (217.32)
6	54.3411 (221.31)	79.9766 (222.54)	−5.0564 (217.08)	−46.5442 (215.68)	−46.8196 (215.54)
7	0.9597 (218.72)	−4.2512 (219.42)	28.3452 (216.31)	−0.1480 (210.56)	0.1025 (210.40)
8	8.0591 (218.35)	7.4180 (218.34)	−11.3176 (212.44)	−1.1865 (207.01)	−1.1075 (207.05)
9	−122.9486 (214.60)	−104.2956 (213.71)	2.6408 (211.78)	3.7079 (204.69)	3.1896 (204.34)
10	−68.3831 (206.68)	−82.8072 (207.54)	42.1539 (202.39)	−61.7964 (200.70)	−59.1638 (200.70)
11	−14.5851 (202.06)	−3.6782 (203.92)	−116.7997 (199.78)	−48.7571 (197.39)	−45.6923 (197.32)
12	135.2125 (200.16)	136.1034 (200.20)	−11.3865 (197.52)	9.8152 (193.77)	10.9936 (193.91)
13	−61.4529 (194.92)	−110.7483 (195.73)	−47.0571 (197.02)	6.6186 (192.91)	7.8380 (192.94)
14	−78.3235 (193.48)	−10.2932 (193.29)	25.5493 (195.09)	7.7845 (192.14)	7.0423 (192.04)
15	−3.0584 (192.51)	7.5334 (191.23)	27.2274 (190.79)	17.0269 (190.15)	21.7347 (190.14)
16	239.9047 (189.41)	232.8673 (189.50)	95.3620 (190.25)	83.6960 (186.11)	67.8463 (186.00)
17	27.7697 (188.24)	−90.5411 (187.72)	137.5252 (187.15)	−52.0517 (184.63)	−49.3339 (184.88)
18	42.3663 (185.15)	119.2813 (185.98)	−92.1975 (186.82)	17.2793 (180.94)	16.7972 (180.91)
19	−40.5230 (184.37)	−51.4056 (184.07)	−123.4120 (184.49)	0.6206 (180.72)	7.0169 (180.31)
20	−136.2990 (183.09)	−97.5031 (183.35)	39.6937 (181.50)	4.7144 (179.65)	2.7120 (179.70)
21	−16.5782 (182.18)	−1.6106 (180.50)	−16.4955 (180.99)	−20.3101 (179.38)	−13.7274 (179.53)
22	0.8410 (179.77)	−36.8668 (178.89)	−15.2266 (179.38)	24.8183 (179.03)	19.4109 (179.00)
23	6.8486 (178.86)	7.4334 (176.65)	−3.7633 (179.23)	−1.8585 (177.78)	−1.8349 (177.75)
24	5.1204 (177.65)	−1.0884 (176.43)	−12.6815 (176.95)	−13.3016 (175.20)	0.6803 (175.88)
25	7.5953 (176.39)	7.0022 (175.35)	20.8681 (175.85)	−2.9261 (174.54)	−12.4378 (175.15)
26	−4.0603 (173.68)	1.2326 (173.75)	−1.9694 (173.63)	4.3191 (170.03)	4.7263 (170.21)
27	−4.3408 (172.64)	−3.3228 (171.07)	−4.0574 (171.84)	1.1034 (169.44)	−19.8506 (169.44)
28	5.2971 (171.13)	−3.0859 (169.97)	25.7223 (170.52)	−28.0139 (169.26)	−0.5652 (168.77)
29	−11.6665 (170.06)	8.1668 (168.95)	−6.6279 (168.64)	2.6906 (168.50)	1.8977 (167.95)
30	20.6936 (168.41)	−0.9025 (168.67)	0.5806 (168.33)	2.8599 (168.14)	−3.5022 (167.50)

j	R_j, 10^{-40} erg cm^3 (λ_j, nm)				
	(*R*,*R*′)-**1.11**	(*R*,*R*′)-**1.12**	(*R*,*R*′)-**1.13**	(*R*,*R*′)-**1.15**	(*R*,*R*′)-**1.18**
1	6.1507 (251.50)	18.6574 (249.88)	18.6740 (249.88)	35.3067 (250.09)	0.1843 (251.76)
2	25.7087 (249.86)	−6.6088 (248.12)	−5.5467 (247.99)	−15.0492 (248.70)	−1.2323 (247.96)
3	−4.1676 (239.44)	−5.3184 (225.89)	−5.6087 (225.93)	0.6572 (228.36)	0.4059 (226.99)
4	4.0205 (237.18)	0.3539 (224.58)	0.6489 (224.17)	−12.8801 (226.68)	2.2579 (219.44)
5	66.1680 (221.87)	−0.0580 (217.84)	−0.2486 (217.82)	−0.9328 (218.31)	1.6094 (217.06)
6	−4.6333 (221.06)	−47.8375 (215.68)	−47.7707 (215.54)	−39.1075 (215.78)	2.9878 (215.52)
7	13.0254 (219.19)	−0.0970 (209.36)	0.1593 (209.21)	−9.0667 (212.73)	0.0397 (211.51)
8	0.2591 (218.70)	−1.2812 (206.51)	−1.2565 (206.55)	4.7676 (208.93)	1.8790 (205.21)
9	−114.0345 (214.94)	2.4205 (206.17)	2.1927 (205.83)	−7.7616 (207.15)	79.8904 (199.29)
10	−69.7638 (206.83)	−73.3568 (200.85)	−71.1169 (200.84)	−107.4703 (200.42)	−12.5078 (197.05)
11	−11.3920 (203.25)	−20.1996 (197.06)	−16.6558 (197.00)	−64.4282 (200.11)	4.4082 (193.30)
12	125.5080 (200.70)	6.4585 (194.13)	6.3122 (194.30)	−16.2321 (196.02)	−7.2692 (192.49)
13	−72.0391 (195.14)	11.5417 (193.51)	11.8731 (193.42)	79.5814 (195.83)	−16.6455 (192.46)
14	−38.5188 (193.40)	−5.3941 (193.02)	−4.8369 (193.06)	33.4588 (194.97)	1.8683 (188.87)
15	−24.2473 (192.38)	6.3104 (190.37)	12.2410 (190.36)	60.8753 (190.29)	64.7458 (188.25)
16	238.5770 (189.48)	82.3954 (186.10)	66.0315 (185.98)	100.2476 (186.67)	−192.4130 (185.74)
17	38.3228 (188.20)	−49.7229 (184.64)	−47.3359 (184.89)	−129.3438 (185.01)	117.2546 (184.38)
18	−7.7156 (184.86)	30.3051 (181.82)	30.1856 (181.79)	45.0143 (184.49)	−3.8374 (180.90)
19	9.4106 (183.72)	0.4244 (180.71)	6.5715 (180.29)	7.0620 (182.41)	−5.9874 (180.66)
20	−28.7890 (183.25)	3.2929 (179.93)	2.9326 (179.99)	2.4270 (182.16)	10.3355 (180.03)
21	−126.3473 (182.84)	−9.0449 (179.03)	−8.9763 (179.19)	7.4602 (179.47)	9.5105 (179.95)
22	1.3359 (180.05)	−1.1971 (178.74)	−1.5503 (178.71)	−26.3322 (179.40)	1.7402 (176.26)
23	13.3253 (179.61)	15.7401 (177.71)	15.4218 (177.68)	−13.6909 (178.32)	−3.4935 (174.16)
24	−1.9856 (178.63)	−17.4841 (174.81)	0.4725 (175.88)	−0.6516 (178.17)	−6.5289 (173.48)
25	8.0494 (174.08)	−2.9032 (174.53)	−16.6667 (174.76)	5.7951 (175.92)	−6.6207 (172.11)
26	−0.6666 (173.49)	−2.1418 (169.48)	−19.4677 (169.53)	−27.1412 (173.24)	−3.3821 (171.64)
27	3.8396 (171.78)	−26.2012 (169.30)	7.2470 (169.16)	5.4761 (171.56)	−0.2020 (169.11)
28	−12.8620 (170.52)	7.1822 (168.96)	−2.9942 (168.87)	−2.6530 (169.79)	−29.5527 (168.76)
29	−24.1734 (169.19)	1.9757 (168.57)	0.0434 (167.79)	−0.7268 (169.36)	−3.3869 (168.54)
30	13.1348 (168.10)	1.4619 (167.97)	−5.4142 (167.54)	−4.6089 (169.27)	1.2937 (167.71)

Table 8.7. (*Continued*)

j	R_j, 10^{-40} erg cm^3 (λ_j, nm)			
	(R,R')-**1.20**	(R,R')-**1.36**	(R,R')-**1.40**	(R,R')-**1.45**
1	19.6845 (249.93)	0.1300 (251.73)	0.4571 (251.20)	8.1994 (252.47)
2	−5.6385 (248.05)	−2.0610 (248.17)	−0.9487 (247.97)	24.7402 (250.13)
3	−5.0112 (225.56)	0.4139 (225.91)	0.3289 (225.71)	−0.1675 (242.20)
4	−1.0203 (224.83)	3.3737 (220.60)	3.4989 (219.89)	5.4539 (236.94)
5	−0.7638 (217.91)	4.4086 (218.22)	4.0666 (217.83)	39.4386 (221.10)
6	−48.4908 (215.59)	−2.9388 (215.50)	−0.1923 (215.53)	−22.7662 (220.19)
7	−0.5233 (209.91)	0.3291 (210.36)	0.2278 (210.38)	−5.1888 (219.18)
8	−0.9494 (206.57)	1.2091 (206.60)	1.2184 (206.76)	19.9425 (217.70)
9	1.7296 (206.22)	74.3399 (199.43)	78.2410 (199.29)	−89.6708 (215.45)
10	−27.4687 (201.55)	−9.8053 (196.96)	−13.2374 (196.68)	−73.5210 (206.91)
11	−97.4832 (198.69)	−2.7733 (193.56)	−5.5097 (193.89)	37.0287 (204.00)
12	17.5591 (194.61)	9.2800 (192.59)	14.3836 (192.87)	101.1576 (201.94)
13	8.7715 (193.83)	−43.3917 (191.61)	−23.6298 (192.53)	85.7576 (195.13)
14	13.4521 (193.78)	4.4720 (189.66)	2.4462 (189.17)	−195.0767 (194.38)
15	49.1178 (191.03)	57.5620 (188.03)	54.2486 (188.36)	−92.8733 (193.37)
16	23.0669 (186.30)	−172.6813 (185.76)	−188.6199 (185.77)	285.6452 (189.37)
17	−35.9279 (185.02)	113.8579 (184.52)	115.3300 (184.39)	5.1417 (184.92)
18	46.0319 (183.76)	10.0759 (181.86)	1.5932 (182.33)	45.6009 (184.06)
19	12.9402 (182.08)	19.5155 (181.23)	11.9624 (180.25)	−131.5147 (183.07)
20	5.8245 (180.31)	5.1698 (179.93)	8.1184 (179.93)	20.6393 (182.58)
21	0.8843 (179.90)	−5.0202 (178.98)	−4.5950 (179.00)	−8.0340 (181.11)
22	−2.0354 (179.67)	−0.9189 (176.52)	1.2847 (177.36)	−15.0782 (181.04)
23	−8.0211 (179.01)	−7.2078 (173.53)	−4.2148 (174.15)	0.0149 (178.70)
24	−12.1820 (176.67)	0.3194 (173.21)	−5.0796 (173.47)	3.1146 (178.10)
25	−2.0716 (175.15)	−10.3156 (171.96)	−7.2393 (171.83)	−10.8252 (173.83)
26	−2.3481 (171.42)	−5.9216 (170.37)	−3.8043 (170.73)	7.0905 (171.99)
27	−15.3329 (170.72)	1.3843 (168.97)	0.7920 (169.19)	4.2493 (170.67)
28	0.7023 (169.57)	−1.1752 (168.28)	−28.7423 (168.80)	−6.7347 (170.56)
29	−5.0918 (168.43)	−33.2427 (167.96)	−2.0337 (168.28)	−1.1130 (170.33)
30	−6.0093 (168.28)	−0.5277 (167.70)	−2.8114 (167.12)	−1.8123 (169.33)

j	R_j, 10^{-40} erg cm^3 (λ_j, nm)			
	(R,R')-**1.46**	(R,R')-**1.62**	(R,R')-**1.63**	(R,R')-**1.68**
1	−14.2905 (256.71)	−21.0583 (251.23)	−10.8596 (256.39)	0.1761 (250.97)
2	11.1888 (249.48)	26.5594 (248.90)	46.6771 (250.17)	−0.1762 (247.82)
3	−12.8512 (245.97)	−6.7796 (235.17)	−7.9072 (237.69)	0.2085 (224.09)
4	1.0222 (235.30)	4.2429 (231.57)	−5.3675 (236.43)	6.3469 (220.61)
5	1.0562 (228.90)	10.5132 (223.67)	0.0944 (225.61)	3.8872 (219.02)
6	7.2540 (217.87)	−15.1569 (220.48)	26.8991 (223.19)	3.1662 (215.35)
7	11.0404 (216.36)	1.8706 (218.42)	59.4275 (220.03)	0.4189 (209.27)
8	−0.4379 (213.29)	0.1877 (214.46)	18.9339 (214.92)	0.8181 (207.89)
9	0.1685 (212.02)	11.7590 (211.10)	−112.8237 (211.11)	80.6093 (199.23)
10	88.7517 (200.17)	−61.6630 (205.99)	−92.5861 (207.15)	−14.9918 (196.43)
11	−42.6098 (194.13)	−85.8495 (201.83)	0.8160 (203.85)	−2.4126 (195.13)
12	−48.4809 (193.10)	132.3808 (198.82)	96.3514 (198.11)	26.6252 (192.74)
13	−60.4231 (192.54)	59.4280 (197.30)	32.0511 (193.64)	−42.3907 (192.45)
14	−91.3587 (188.07)	−35.1392 (194.84)	−12.0245 (192.68)	2.3664 (189.85)
15	233.7152 (187.23)	−118.9455 (192.42)	−49.0018 (189.87)	29.0791 (188.42)
16	−27.9615 (185.40)	425.8230 (188.37)	23.4675 (188.66)	−160.1414 (185.59)
17	−62.9342 (185.12)	−314.1426 (185.13)	78.6727 (187.76)	93.8542 (184.55)
18	34.7879 (181.73)	−0.2883 (183.62)	251.5186 (185.63)	12.6964 (183.78)
19	−3.1656 (180.55)	4.0108 (182.86)	−32.1267 (183.59)	14.3695 (180.98)
20	13.5370 (179.12)	−39.0424 (181.57)	−172.3389 (183.01)	11.1255 (179.74)
21	2.2420 (178.61)	−6.8414 (180.42)	−48.9051 (182.34)	−1.9618 (178.72)
22	−3.1010 (178.34)	6.8358 (179.63)	−0.8920 (181.91)	3.9572 (177.18)
23	0.9684 (177.97)	−29.1927 (179.23)	−6.4101 (177.26)	−5.2910 (173.84)
24	−9.5079 (175.18)	−2.0637 (177.15)	−39.4232 (176.67)	−1.1792 (172.98)
25	−14.0933 (173.91)	1.0107 (172.41)	−1.9021 (176.06)	−9.2294 (171.84)
26	−1.0455 (171.55)	3.6128 (171.37)	−11.5175 (173.39)	7.7629 (170.25)
27	0.7152 (171.04)	19.6995 (170.89)	−3.6927 (172.54)	−7.1995 (169.10)
28	−0.1641 (168.63)	5.3538 (169.86)	1.7096 (170.67)	−12.5593 (168.86)
29	−4.3304 (167.09)	−5.1787 (168.97)	7.9310 (169.80)	−14.0276 (168.74)
30	−0.9330 (166.91)	−4.7909 (168.10)	0.7534 (168.91)	0.0965 (166.01)

Table 8.8. Oscillator strengths and excitation wavelengths for the conformers of (*R*,*R*′)-**1**, as obtained by TD-DFT calculations at the PBE0/TZVP/IEFPCM(MeOH) level.

j	f_j (λ_j, nm)				
	(*R*,*R*′)-**1.01**	(*R*,*R*′)-**1.02**	(*R*,*R*′)-**1.04**	(*R*,*R*′)-**1.05**	(*R*,*R*′)-**1.06**
1	0.0312 (252.02)	0.0249 (253.20)	0.0395 (251.55)	0.0491 (250.37)	0.0491 (250.36)
2	0.0243 (249.74)	0.0275 (249.22)	0.0343 (249.68)	0.0397 (248.13)	0.0400 (247.99)
3	0.0016 (239.05)	0.0029 (239.88)	0.0084 (234.99)	0.0071 (225.92)	0.0031 (225.54)
4	0.0019 (238.50)	0.0015 (238.23)	0.0045 (232.78)	0.0064 (225.32)	0.0103 (225.29)
5	0.0111 (222.27)	0.0083 (224.85)	0.0060 (218.44)	0.0024 (217.33)	0.0021 (217.32)
6	0.0263 (221.31)	0.0331 (222.54)	0.0089 (217.08)	0.1549 (215.68)	0.1523 (215.54)
7	0.0215 (218.72)	0.0286 (219.42)	0.0840 (216.31)	0.0006 (210.56)	0.0002 (210.40)
8	0.0264 (218.35)	0.0150 (218.34)	0.0124 (212.44)	0.0050 (207.01)	0.0065 (207.05)
9	0.0404 (214.60)	0.0347 (213.71)	0.0372 (211.78)	0.0208 (204.69)	0.0220 (204.34)
10	0.1010 (206.68)	0.1012 (207.54)	0.1186 (202.39)	0.5488 (200.70)	0.5525 (200.70)
11	0.0037 (202.06)	0.0049 (203.92)	0.0757 (199.78)	0.1184 (197.39)	0.1200 (197.32)
12	0.1148 (200.16)	0.1243 (200.20)	0.0051 (197.52)	0.0553 (193.77)	0.0516 (193.91)
13	0.1510 (194.92)	0.1387 (195.73)	0.0339 (197.02)	0.0417 (192.91)	0.0469 (192.94)
14	0.0407 (193.48)	0.0089 (193.29)	0.1525 (195.09)	0.0082 (192.14)	0.0065 (192.04)
15	0.0072 (192.51)	0.0152 (191.23)	0.2330 (190.79)	0.4541 (190.15)	0.4555 (190.14)
16	0.2976 (189.41)	0.3863 (189.50)	0.2553 (190.25)	0.6328 (186.11)	0.6287 (186.00)
17	0.1548 (188.24)	0.0626 (187.72)	0.2518 (187.15)	0.3289 (184.63)	0.3277 (184.88)
18	0.2297 (185.15)	0.1700 (185.98)	0.0636 (186.82)	0.0181 (180.94)	0.0177 (180.91)
19	0.2464 (184.37)	0.4014 (184.07)	0.4702 (184.49)	0.0032 (180.72)	0.0035 (180.31)
20	0.5785 (183.09)	0.4909 (183.35)	0.2848 (181.50)	0.0106 (179.65)	0.0113 (179.70)
21	0.0495 (182.18)	0.0025 (180.50)	0.0524 (180.99)	0.0589 (179.38)	0.0644 (179.53)
22	0.0046 (179.77)	0.0411 (178.89)	0.0121 (179.38)	0.0253 (179.03)	0.0225 (179.00)
23	0.0052 (178.86)	0.0055 (176.65)	0.0151 (179.23)	0.0002 (177.78)	0.0002 (177.75)
24	0.0268 (177.65)	0.0011 (176.43)	0.0084 (176.95)	0.0117 (175.20)	0.0060 (175.88)
25	0.0062 (176.39)	0.0114 (175.35)	0.0097 (175.85)	0.0044 (174.54)	0.0095 (175.15)
26	0.0077 (173.68)	0.0231 (173.75)	0.0059 (173.63)	0.0091 (170.03)	0.0088 (170.21)
27	0.0049 (172.64)	0.0069 (171.07)	0.0067 (171.84)	0.0019 (169.44)	0.0044 (169.44)
28	0.0086 (171.13)	0.0059 (169.97)	0.0242 (170.52)	0.0067 (169.26)	0.0021 (168.77)
29	0.0050 (170.06)	0.0147 (168.95)	0.0070 (168.64)	0.0016 (168.50)	0.0047 (167.95)
30	0.0195 (168.41)	0.0044 (168.67)	0.0016 (168.33)	0.0052 (168.14)	0.0044 (167.50)

j	f_j (λ_j, nm)				
	(*R*,*R*′)-**1.11**	(*R*,*R*′)-**1.12**	(*R*,*R*′)-**1.13**	(*R*,*R*′)-**1.15**	(*R*,*R*′)-**1.18**
1	0.0284 (251.50)	0.0443 (249.88)	0.0443 (249.88)	0.0534 (250.09)	0.0484 (251.76)
2	0.0245 (249.86)	0.0395 (248.12)	0.0396 (247.99)	0.0322 (248.70)	0.0391 (247.96)
3	0.0009 (239.44)	0.0034 (225.89)	0.0033 (225.93)	0.0066 (228.36)	0.0004 (226.99)
4	0.0026 (237.18)	0.0089 (224.58)	0.0087 (224.17)	0.0100 (226.68)	0.0060 (219.44)
5	0.0334 (221.87)	0.0008 (217.84)	0.0010 (217.82)	0.0003 (218.31)	0.0051 (217.06)
6	0.0012 (221.06)	0.1562 (215.68)	0.1532 (215.54)	0.1288 (215.78)	0.1514 (215.52)
7	0.0326 (219.19)	0.0007 (209.36)	0.0002 (209.21)	0.0238 (212.73)	0.0013 (211.51)
8	0.0107 (218.70)	0.0082 (206.51)	0.0087 (206.55)	0.0232 (208.93)	0.0051 (205.21)
9	0.0467 (214.94)	0.0144 (206.17)	0.0161 (205.83)	0.0129 (207.15)	0.7072 (199.29)
10	0.0961 (206.83)	0.5664 (200.85)	0.5698 (200.84)	0.3351 (200.42)	0.0127 (197.05)
11	0.0014 (203.25)	0.1194 (197.06)	0.1218 (197.00)	0.1203 (200.11)	0.0664 (193.30)
12	0.1303 (200.70)	0.0403 (194.13)	0.0385 (194.30)	0.0603 (196.02)	0.0178 (192.49)
13	0.1663 (195.14)	0.0095 (193.51)	0.0082 (193.42)	0.1652 (195.83)	0.0550 (192.46)
14	0.0314 (193.40)	0.0452 (193.02)	0.0472 (193.06)	0.0356 (194.97)	0.0073 (188.87)
15	0.0122 (192.38)	0.4414 (190.37)	0.4431 (190.36)	0.3985 (190.29)	0.3541 (188.25)
16	0.2835 (189.48)	0.6407 (186.10)	0.6389 (185.98)	0.6736 (186.67)	0.6933 (185.74)
17	0.1630 (188.20)	0.3354 (184.64)	0.3315 (184.89)	0.2048 (185.01)	0.4867 (184.38)
18	0.4073 (184.86)	0.0305 (181.82)	0.0307 (181.79)	0.0536 (184.49)	0.0006 (180.90)
19	0.1504 (183.72)	0.0032 (180.71)	0.0048 (180.29)	0.0086 (182.41)	0.0038 (180.66)
20	0.1798 (183.25)	0.0121 (179.93)	0.0118 (179.99)	0.0219 (182.16)	0.0126 (180.03)
21	0.3527 (182.84)	0.0561 (179.03)	0.0588 (179.19)	0.0073 (179.47)	0.0070 (179.95)
22	0.0054 (180.05)	0.0005 (178.74)	0.0006 (178.71)	0.0405 (179.40)	0.0047 (176.26)
23	0.0132 (179.61)	0.0160 (177.71)	0.0157 (177.68)	0.0572 (178.32)	0.0010 (174.16)
24	0.0306 (178.63)	0.0128 (174.81)	0.0060 (175.88)	0.0414 (178.17)	0.0107 (173.48)
25	0.0050 (174.08)	0.0026 (174.53)	0.0088 (174.76)	0.0027 (175.92)	0.0022 (172.11)
26	0.0017 (173.49)	0.0020 (169.48)	0.0042 (169.53)	0.0094 (173.24)	0.0138 (171.64)
27	0.0041 (171.78)	0.0061 (169.30)	0.0066 (169.16)	0.0020 (171.56)	0.0004 (169.11)
28	0.0077 (170.52)	0.0072 (168.96)	0.0020 (168.87)	0.0055 (169.79)	0.0067 (168.76)
29	0.0072 (169.19)	0.0019 (168.57)	0.0041 (167.79)	0.0062 (169.36)	0.0008 (168.54)
30	0.0077 (168.10)	0.0044 (167.97)	0.0034 (167.54)	0.0009 (169.27)	0.0003 (167.71)

Table 8.8. (*Continued*)

j	f_j (λ_j, nm)			
	(*R*,*R*′)-**1.20**	(*R*,*R*′)-**1.36**	(*R*,*R*′)-**1.40**	(*R*,*R*′)-**1.45**
1	0.0460 (249.93)	0.0456 (251.73)	0.0444 (251.20)	0.0391 (252.47)
2	0.0392 (248.05)	0.0399 (248.17)	0.0392 (247.97)	0.0089 (250.13)
3	0.0029 (225.56)	0.0007 (225.91)	0.0003 (225.71)	0.0005 (242.20)
4	0.0097 (224.83)	0.0078 (220.60)	0.0081 (219.89)	0.0033 (236.94)
5	0.0009 (217.91)	0.0184 (218.22)	0.0149 (217.83)	0.0155 (221.10)
6	0.1510 (215.59)	0.1460 (215.50)	0.1508 (215.53)	0.0186 (220.19)
7	0.0009 (209.91)	0.0013 (210.36)	0.0018 (210.38)	0.0031 (219.18)
8	0.0129 (206.57)	0.0037 (206.60)	0.0027 (206.76)	0.0339 (217.70)
9	0.0156 (206.22)	0.6788 (199.43)	0.6829 (199.29)	0.0479 (215.45)
10	0.4066 (201.55)	0.0140 (196.96)	0.0133 (196.68)	0.0837 (206.91)
11	0.2122 (198.69)	0.0113 (193.56)	0.0136 (193.89)	0.0459 (204.00)
12	0.0741 (194.61)	0.0874 (192.59)	0.0828 (192.87)	0.0640 (201.94)
13	0.0057 (193.83)	0.1036 (191.61)	0.0713 (192.53)	0.0377 (195.13)
14	0.0168 (193.78)	0.0071 (189.66)	0.0079 (189.17)	0.1361 (194.38)
15	0.4961 (191.03)	0.2916 (188.03)	0.3399 (188.36)	0.0860 (193.37)
16	0.6088 (186.30)	0.7737 (185.76)	0.7003 (185.77)	0.5027 (189.37)
17	0.3127 (185.02)	0.4170 (184.52)	0.4825 (184.39)	0.1558 (184.92)
18	0.0762 (183.76)	0.0064 (181.86)	0.0010 (182.33)	0.2070 (184.06)
19	0.0123 (182.08)	0.0222 (181.23)	0.0142 (180.25)	0.2985 (183.07)
20	0.0044 (180.31)	0.0049 (179.93)	0.0058 (179.93)	0.2920 (182.58)
21	0.0115 (179.90)	0.0025 (178.98)	0.0008 (179.00)	0.0316 (181.11)
22	0.0021 (179.67)	0.0038 (176.52)	0.0063 (177.36)	0.0631 (181.04)
23	0.0643 (179.01)	0.0130 (173.53)	0.0026 (174.15)	0.0193 (178.70)
24	0.0045 (176.67)	0.0007 (173.21)	0.0099 (173.47)	0.0050 (178.10)
25	0.0085 (175.15)	0.0045 (171.96)	0.0024 (171.83)	0.0052 (173.83)
26	0.0129 (171.42)	0.0128 (170.37)	0.0111 (170.73)	0.0012 (171.99)
27	0.0044 (170.72)	0.0005 (168.97)	0.0003 (169.19)	0.0014 (170.67)
28	0.0002 (169.57)	0.0004 (168.28)	0.0068 (168.80)	0.0046 (170.56)
29	0.0094 (168.43)	0.0082 (167.96)	0.0002 (168.28)	0.0041 (170.33)
30	0.0026 (168.28)	0.0007 (167.70)	0.0031 (167.12)	0.0118 (169.33)

j	f_j (λ_j, nm)			
	(*R*,*R*′)-**1.46**	(*R*,*R*′)-**1.62**	(*R*,*R*′)-**1.63**	(*R*,*R*′)-**1.68**
1	0.0374 (256.71)	0.0167 (251.23)	0.0239 (256.39)	0.0409 (250.97)
2	0.0262 (249.48)	0.0374 (248.90)	0.0411 (250.17)	0.0390 (247.82)
3	0.0185 (245.97)	0.0031 (235.17)	0.0058 (237.69)	0.0002 (224.09)
4	0.0030 (235.30)	0.0012 (231.57)	0.0018 (236.43)	0.0143 (220.61)
5	0.0083 (228.90)	0.0257 (223.67)	0.0022 (225.61)	0.0275 (219.02)
6	0.0007 (217.87)	0.0237 (220.48)	0.0394 (223.19)	0.1507 (215.35)
7	0.0712 (216.36)	0.0184 (218.42)	0.0333 (220.03)	0.0026 (209.27)
8	0.0034 (213.29)	0.0013 (214.46)	0.0269 (214.92)	0.0014 (207.89)
9	0.0105 (212.02)	0.0546 (211.10)	0.0446 (211.11)	0.6505 (199.23)
10	0.4193 (200.17)	0.0546 (205.99)	0.0515 (207.15)	0.0184 (196.43)
11	0.0512 (194.13)	0.0126 (201.83)	0.0055 (203.85)	0.0082 (195.13)
12	0.0632 (193.10)	0.1621 (198.82)	0.2842 (198.11)	0.0865 (192.74)
13	0.4010 (192.54)	0.0329 (197.30)	0.0941 (193.64)	0.1168 (192.45)
14	0.4157 (188.07)	0.1107 (194.84)	0.0147 (192.68)	0.0055 (189.85)
15	0.3580 (187.23)	0.1377 (192.42)	0.0771 (189.87)	0.3134 (188.42)
16	0.1315 (185.40)	0.5128 (188.37)	0.0051 (188.66)	0.6900 (185.59)
17	0.2278 (185.12)	0.7020 (185.13)	0.1673 (187.76)	0.4726 (184.55)
18	0.0681 (181.73)	0.0160 (183.62)	0.4640 (185.63)	0.0173 (183.78)
19	0.0052 (180.55)	0.0102 (182.86)	0.0549 (183.59)	0.0177 (180.98)
20	0.0079 (179.12)	0.0783 (181.57)	0.5809 (183.01)	0.0072 (179.74)
21	0.0038 (178.61)	0.0573 (180.42)	0.0477 (182.34)	0.0052 (178.72)
22	0.0230 (178.34)	0.0092 (179.63)	0.0577 (181.91)	0.0035 (177.18)
23	0.0007 (177.97)	0.0305 (179.23)	0.0375 (177.26)	0.0102 (173.84)
24	0.0169 (175.18)	0.0197 (177.15)	0.0239 (176.67)	0.0002 (172.98)
25	0.0334 (173.91)	0.0106 (172.41)	0.0033 (176.06)	0.0025 (171.84)
26	0.0169 (171.55)	0.0084 (171.37)	0.0071 (173.39)	0.0113 (170.25)
27	0.0012 (171.04)	0.0073 (170.89)	0.0184 (172.54)	0.0018 (169.10)
28	0.0027 (168.63)	0.0020 (169.86)	0.0013 (170.67)	0.0014 (168.86)
29	0.0025 (167.09)	0.0023 (168.97)	0.0042 (169.80)	0.0058 (168.74)
30	0.0027 (166.91)	0.0056 (168.10)	0.0051 (168.91)	0.0004 (166.01)

Table 8.9. Energies for the conformers of (*R*,*S*′)-**1**, as obtained after MM conformational search at the MMFF94s level.

MM ID	E_{MM} (kcal mol^{-1})	ΔE_{MM} (kcal mol^{-1})	QM ID	MM ID	E_{MM} (kcal mol^{-1})	ΔE_{MM} (kcal mol^{-1})	QM ID
mol001	41.4512	0.0000	**01**	**mol087**	46.8680	5.4167	**30**
mol006	41.6851	0.2339	**02**	**mol037**	46.8838	5.4326	**31**
mol016	42.6809	1.2297	**03**	**mol050**	47.2060	5.7547	**32**
mol020	43.0615	1.6103	**04**	**mol040**	47.2330	5.7818	**33**
mol081	43.0776	1.6264	**05**	**mol043**	47.5807	6.1294	**34**
mol057	43.5627	2.1114	**06**	**mol044**	47.8637	6.4125	**35**
mol025	43.7658	2.3146	**07**	**mol048**	48.2210	6.7698	**36**
mol079	43.8001	2.3489	**08**	**mol071**	48.2217	6.7705	**37**
mol023	43.9716	2.5204	**09**	**mol084**	48.4644	7.0131	**38**
mol075	44.0893	2.6381	**10**	**mol053**	48.4743	7.0230	**39**
mol014	44.2640	2.8128	**11**	**mol056**	48.5575	7.1062	**40**
mol018	44.4280	2.9767	**12**	**mol058**	48.5792	7.1280	**41**
mol094	44.4280	2.9767	**13**	**mol060**	48.6145	7.1633	**42**
mol004	44.4993	3.0481	**14**	**mol080**	48.6978	7.2466	**43**
mol093	44.6622	3.2110	**15**	**mol063**	48.9049	7.4537	**44**
mol031	44.6995	3.2483	**16**	**mol064**	49.0302	7.5790	**45**
mol007	44.8746	3.4234	**17**	**mol066**	49.2194	7.7681	**46**
mol022	44.9653	3.5141	**18**	**mol067**	49.3585	7.9073	**47**
mol039	44.9918	3.5406	**19**	**mol069**	49.3874	7.9362	**48**
mol008	45.0694	3.6181	**20**	**mol070**	49.3948	7.9435	**49**
mol009	45.3825	3.9313	**21**	**mol073**	49.5365	8.0853	**50**
mol076	45.4051	3.9539	**22**	**mol083**	50.3354	8.8841	**51**
mol012	45.4839	4.0326	**23**	**mol086**	50.4762	9.0250	**52**
mol034	45.6112	4.1600	**24**	**mol091**	50.6293	9.1781	**53**
mol088	46.0674	4.6162	**25**	**mol092**	50.6679	9.2167	**54**
mol028	46.5053	5.0541	**26**	**mol096**	50.8182	9.3669	**55**
mol077	46.6614	5.2101	**27**	**mol100**	51.1947	9.7434	**56**
mol032	46.7324	5.2812	**28**	**mol003**	51.3744	9.9232	**57**
mol036	46.8673	5.4161	**29**				

Table 8.10. Geometric parameters for the conformers of (*R*,*S*′)-**1**, as obtained after DFT geometry optimisation at the RI-B97D/TZVP/IEFPCM(MeOH) level.

Pattern	ID	α (deg)	β (deg)	γ (deg)	δ (deg)	d_1 (Å)	d_2 (Å)	d_3 (Å)	$\bar{d}$ (Å)
A_1	(*R*,*S*′)-**1.01**	−55.382	176.673	−152.619	55.460	5.153	3.201	7.680	5.345
	(*R*,*S*′)-**1.02**	−60.068	164.536	−168.232	50.867	3.118	5.441	7.263	5.274
	(*R*,*S*′)-**1.09**	−59.980	166.454	−165.787	50.420	3.059	5.014	7.143	5.072
	(*R*,*S*′)-**1.10**	−54.548	174.356	−155.151	53.986	4.850	3.141	7.611	5.201
	(*R*,*S*′)-**1.11**	−60.257	164.527	−168.218	50.884	3.121	5.376	7.264	5.254
	(*R*,*S*′)-**1.16**	−55.149	176.618	−152.844	55.630	5.062	3.198	7.685	5.315
A_2	(*R*,*S*′)-**1.06**	−60.401	−175.686	−167.681	−53.264	6.197	10.375	6.326	7.633
	(*R*,*S*′)-**1.08**	−60.328	−175.565	−167.634	−53.089	6.275	10.435	6.356	7.689
	(*R*,*S*′)-**1.17**	−51.383	−160.475	−158.304	−34.151	3.098	7.295	6.404	5.599
	(*R*,*S*′)-**1.24**	−60.223	−175.490	−167.485	−53.112	6.149	10.329	6.334	7.604
A_3	(*R*,*S*′)-**1.12**	−62.858	179.535	64.165	48.928	8.964	11.366	5.443	8.591
	(*R*,*S*′)-**1.13**	−62.859	179.531	64.158	48.931	8.965	11.366	5.444	8.592
	(*R*,*S*′)-**1.15**	−62.773	179.562	64.336	49.057	8.925	11.388	5.492	8.602
	(*R*,*S*′)-**1.26**	−62.732	179.423	64.199	48.956	8.960	11.411	5.448	8.606
	(*R*,*S*′)-**1.31**	−63.021	179.256	63.925	48.847	9.134	11.377	5.454	8.655
A_5	(*R*,*S*′)-**1.28**	−63.469	179.963	87.132	−57.669	10.734	10.260	5.856	8.950
A_6	(*R*,*S*′)-**1.27**	−68.222	−165.291	−85.980	56.984	9.168	6.076	7.523	7.589
A_8	(*R*,*S*′)-**1.03**	−65.713	−177.522	−101.819	48.153	6.740	3.023	6.861	5.541
	(*R*,*S*′)-**1.04**	−66.839	−179.602	−104.701	48.351	6.426	3.134	7.091	5.550
	(*R*,*S*′)-**1.05**	−65.427	−179.717	−97.515	53.320	7.260	3.879	7.275	6.138
	(*R*,*S*′)-**1.07**	−63.479	−177.910	−102.017	48.669	6.932	2.984	6.985	5.634
	(*R*,*S*′)-**1.18**	−65.926	−177.555	−102.093	48.390	6.690	3.011	6.862	5.521
	(*R*,*S*′)-**1.37**	−63.766	−177.998	−101.999	48.831	6.900	2.971	6.988	5.620
A_9	(*R*,*S*′)-**1.19**	−58.176	97.117	−161.796	−59.087	9.340	11.554	8.216	9.703
	(*R*,*S*′)-**1.21**	−58.907	96.232	−164.881	−58.442	9.565	11.584	8.278	9.809
A_{12}	(*R*,*S*′)-**1.20**	−59.906	−163.127	−164.215	−27.983	2.973	7.446	5.570	5.330
B_1	(*R*,*S*′)-**1.43**	−51.524	−81.088	−89.945	56.454	10.928	10.116	6.415	9.153
	(*R*,*S*′)-**1.56**	−51.466	−81.186	−89.795	56.380	11.005	10.112	6.415	9.177
B_2	(*R*,*S*′)-**1.38**	−51.485	−81.092	−90.042	56.102	10.951	10.098	6.486	9.178
	(*R*,*S*′)-**1.52**	−51.463	−81.149	−90.016	56.146	10.949	10.204	6.485	9.213
B_3	(*R*,*S*′)-**1.14**	−67.874	85.230	−170.032	58.151	5.395	9.490	5.460	6.782
	(*R*,*S*′)-**1.29**	−68.184	85.207	−169.807	58.000	5.414	9.488	5.443	6.782
B_4	(*R*,*S*′)-**1.40**	−48.549	−74.181	−70.334	−57.708	10.605	10.845	8.958	10.136
C_1	(*R*,*S*′)-**1.55**	173.475	−171.108	87.212	−53.895	7.299	2.982	6.908	5.730
C_2	(*R*,*S*′)-**1.25**	−169.457	169.318	−81.803	62.990	3.042	6.425	5.823	5.097
	(*R*,*S*′)-**1.44**	−171.889	168.715	−87.751	60.819	2.963	7.344	5.554	5.287
C_3	(*R*,*S*′)-**1.50**	178.408	−174.825	90.015	−51.588	7.608	3.869	6.935	6.137
C_4	(*R*,*S*′)-**1.23**	−169.165	171.761	−94.634	54.412	2.936	7.376	5.245	5.186
	(*R*,*S*′)-**1.36**	−177.807	172.634	−91.389	58.412	3.798	8.122	5.540	5.820
C_5	(*R*,*S*′)-**1.48**	179.637	−64.731	−63.999	81.867	7.483	3.021	6.930	5.811
D_3	(*R*,*S*′)-**1.39**	177.359	−177.382	64.994	48.482	10.951	7.873	7.424	8.749
	(*R*,*S*′)-**1.41**	177.546	−177.300	64.924	48.330	11.011	7.976	7.429	8.805
D_6	(*R*,*S*′)-**1.49**	−177.917	−73.621	−70.838	−57.007	11.251	11.774	8.901	10.642
D_8	(*R*,*S*′)-**1.51**	−176.479	−96.406	177.290	−64.327	10.920	11.169	5.944	9.344
	(*R*,*S*′)-**1.54**	−176.412	−95.945	176.941	−63.682	10.896	11.157	5.933	9.329
E_1	(*R*,*S*′)-**1.46**	−179.403	164.334	−173.179	171.107	12.714	14.329	10.050	12.364
	(*R*,*S*′)-**1.57**	−179.910	165.733	−173.055	170.801	12.802	14.317	10.076	12.398
F_1	(*R*,*S*′)-**1.33**	−62.440	174.984	−168.746	172.379	10.996	11.771	10.640	11.136
	(*R*,*S*′)-**1.34**	−63.206	173.869	−173.008	169.968	10.950	11.755	10.634	11.113
	(*R*,*S*′)-**1.47**	−62.280	174.749	−168.295	172.237	10.993	11.743	10.644	11.127
	(*R*,*S*′)-**1.53**	−65.312	178.692	−171.497	170.754	13.629	10.080	10.541	11.417
F_2	(*R*,*S*′)-**1.35**	−64.428	170.527	59.067	171.105	11.983	12.431	10.395	11.603
F_3	(*R*,*S*′)-**1.30**	−63.244	−176.857	−68.088	174.576	11.876	11.821	10.495	11.397
	(*R*,*S*′)-**1.42**	−63.344	−176.929	−68.099	174.605	11.883	11.892	10.471	11.415
	(*R*,*S*′)-**1.45**	−63.324	−176.950	−67.973	174.756	11.849	11.878	10.498	11.408
F_4	(*R*,*S*′)-**1.32**	−60.673	95.681	−163.301	173.532	6.899	7.441	9.944	8.095

Table 8.10. (*Continued*)

Pattern	ID	φ_1 (deg)	φ_2 (deg)	ω_1 (deg)	ω_2 (deg)	ω_3 (deg)	κ (deg)
A_1	(*R*,*S*′)-**1.01**	−11.293	68.455	−179.426	167.654	6.789	−57.349
	(*R*,*S*′)-**1.02**	−17.517	54.544	−166.590	−179.291	171.285	−56.710
	(*R*,*S*′)-**1.09**	−18.161	61.051	−160.516	−1.117	3.565	−55.980
	(*R*,*S*′)-**1.10**	−8.571	65.334	2.284	162.218	174.005	−60.313
	(*R*,*S*′)-**1.11**	−17.580	54.919	−167.208	−0.767	171.708	−56.656
	(*R*,*S*′)-**1.16**	−11.964	68.429	1.884	167.750	6.456	−58.604
A_2	(*R*,*S*′)-**1.06**	−27.871	−83.862	−178.923	−179.510	0.029	−50.841
	(*R*,*S*′)-**1.08**	−27.857	−83.702	−178.930	−179.518	−179.433	−51.009
	(*R*,*S*′)-**1.17**	−17.206	−74.154	−0.328	−179.682	178.614	−54.669
	(*R*,*S*′)-**1.24**	−28.110	−83.805	−179.097	−0.306	−0.105	−50.807
A_3	(*R*,*S*′)-**1.12**	−26.433	60.274	−179.660	−179.580	−0.262	−52.918
	(*R*,*S*′)-**1.13**	−26.410	60.268	−179.647	−179.586	−0.280	−52.961
	(*R*,*S*′)-**1.15**	−26.357	60.375	−179.651	−179.630	179.566	−52.711
	(*R*,*S*′)-**1.26**	−26.520	60.098	−179.674	0.261	−0.274	−52.884
	(*R*,*S*′)-**1.31**	−25.893	60.146	1.087	−179.600	−0.132	−54.725
A_5	(*R*,*S*′)-**1.28**	−26.018	−77.378	−179.047	−179.804	0.397	−52.358
A_6	(*R*,*S*′)-**1.27**	49.750	64.525	178.463	−179.894	0.056	−21.930
A_8	(*R*,*S*′)-**1.03**	−29.107	71.740	179.812	−175.030	−159.829	−51.479
	(*R*,*S*′)-**1.04**	−32.045	70.795	−179.888	−7.445	−170.846	−50.778
	(*R*,*S*′)-**1.05**	−33.795	71.816	−179.943	−179.813	0.481	−49.679
	(*R*,*S*′)-**1.07**	−22.047	67.849	−179.608	22.955	0.705	−52.078
	(*R*,*S*′)-**1.18**	−28.872	71.590	0.442	−175.149	−159.392	−52.821
	(*R*,*S*′)-**1.37**	−21.306	67.766	0.737	23.169	0.648	−53.403
A_9	(*R*,*S*′)-**1.19**	−22.011	−86.259	−179.906	−179.689	0.148	−52.374
	(*R*,*S*′)-**1.21**	−21.786	−85.443	−179.093	−179.191	−179.935	−51.933
A_{12}	(*R*,*S*′)-**1.20**	−20.448	−69.623	−7.827	−178.924	−1.407	−51.107
B_1	(*R*,*S*′)-**1.43**	−25.132	72.220	−179.552	−179.245	−179.731	−56.113
	(*R*,*S*′)-**1.56**	−24.712	72.422	1.246	−179.294	−179.859	−57.509
B_2	(*R*,*S*′)-**1.38**	−25.215	72.676	−179.475	−179.310	0.014	−56.006
	(*R*,*S*′)-**1.52**	−25.286	72.691	−179.477	−0.068	−0.011	−55.922
B_3	(*R*,*S*′)-**1.14**	−8.287	73.563	−179.852	−179.521	179.662	−53.690
	(*R*,*S*′)-**1.29**	−8.655	73.734	−179.541	−0.192	179.686	−53.516
B_4	(*R*,*S*′)-**1.40**	−29.083	−84.974	−179.638	−179.805	−179.256	−56.310
C_1	(*R*,*S*′)-**1.55**	−14.377	−74.911	−179.724	11.339	−8.916	−68.666
C_2	(*R*,*S*′)-**1.25**	−35.150	64.577	178.434	−179.922	−157.846	−66.779
	(*R*,*S*′)-**1.44**	−53.231	67.345	−7.300	0.332	10.482	−66.828
C_3	(*R*,*S*′)-**1.50**	−31.892	−78.340	−179.832	−179.467	1.130	−66.103
C_4	(*R*,*S*′)-**1.23**	−50.631	69.738	−5.081	179.621	171.007	−65.624
	(*R*,*S*′)-**1.36**	−49.134	70.472	−179.267	0.354	−1.437	−66.389
C_5	(*R*,*S*′)-**1.48**	−31.832	60.661	−179.659	4.848	11.699	−68.252
D_3	(*R*,*S*′)-**1.39**	−34.085	64.119	0.400	−179.842	−0.007	−66.737
	(*R*,*S*′)-**1.41**	−34.120	63.314	0.431	−179.838	179.796	−66.678
D_6	(*R*,*S*′)-**1.49**	−41.396	−83.971	−179.836	0.259	−179.773	−66.748
D_8	(*R*,*S*′)-**1.51**	−43.307	−86.720	−179.772	−0.059	0.210	−70.632
	(*R*,*S*′)-**1.54**	−42.460	−86.123	−179.675	0.086	−179.791	−70.925
E_1	(*R*,*S*′)-**1.46**	−44.655	−73.691	−179.720	−178.810	−0.122	−67.923
	(*R*,*S*′)-**1.57**	−42.420	−73.980	−179.555	0.129	0.049	−67.538
F_1	(*R*,*S*′)-**1.33**	−27.056	−76.360	−179.591	−178.750	−179.574	−53.208
	(*R*,*S*′)-**1.34**	−27.028	−77.882	−179.737	−178.690	0.809	−53.061
	(*R*,*S*′)-**1.47**	−26.862	−76.211	−179.448	−0.007	−179.538	−53.233
	(*R*,*S*′)-**1.53**	47.771	−75.040	178.471	−179.798	−179.707	−52.662
F_2	(*R*,*S*′)-**1.35**	−26.154	−77.088	−179.686	−178.900	0.182	−54.674
F_3	(*R*,*S*′)-**1.30**	−26.461	−77.527	−179.840	−179.528	−0.236	−51.921
	(*R*,*S*′)-**1.42**	−26.919	−77.129	−179.885	0.202	−179.763	−51.872
	(*R*,*S*′)-**1.45**	−26.865	−77.393	−179.837	0.176	−0.218	−51.844
F_4	(*R*,*S*′)-**1.32**	−19.310	−77.363	−179.972	−179.378	−179.508	−51.948

Table 8.11. Free and electronic energies for the conformers of (*R*,*S*′)-**1**, as obtained after DFT geometry optimisation at the RI-B97D/TZVP/IEFPCM(MeOH) level.

Pattern	ID	E_{QM} (Ha)	ΔE_{QM} (kcal mol^{-1})	χ_{QM} (%)	G (Ha)	ΔG (kcal mol^{-1})	χ_G (%)
A_1	(*R*,*S*′)-**1.01**	−1016.24083412	0.878	7.47	−1015.926753	0.993	6.98
	(*R*,*S*′)-**1.02**	−1016.24104087	0.748	9.29	−1015.927649	0.430	18.04
	(*R*,*S*′)-**1.09**	−1016.24223264	0.000	32.84	−1015.926953	0.867	8.63
	(*R*,*S*′)-**1.10**	−1016.24115418	0.677	10.48	−1015.925969	1.485	3.04
	(*R*,*S*′)-**1.11**	−1016.24104215	0.747	9.31	−1015.928335	0.000	37.30
	(*R*,*S*′)-**1.16**	−1016.24073566	0.939	6.73	−1015.926855	0.929	7.78
A_2	(*R*,*S*′)-**1.06**	−1016.23568067	4.111	0.03	−1015.923977	2.735	0.37
	(*R*,*S*′)-**1.08**	−1016.23570939	4.093	0.03	−1015.923561	2.996	0.24
	(*R*,*S*′)-**1.17**	−1016.23484541	4.636	0.01	−1015.919818	5.344	0.00
	(*R*,*S*′)-**1.24**	−1016.23582299	4.022	0.04	−1015.924237	2.572	0.49
A_3	(*R*,*S*′)-**1.12**	−1016.23625571	3.751	0.06	−1015.924780	2.231	0.86
	(*R*,*S*′)-**1.15**	−1016.23633545	3.701	0.06	−1015.924536	2.384	0.67
	(*R*,*S*′)-**1.26**	−1016.23641930	3.648	0.07	−1015.924945	2.127	1.03
	(*R*,*S*′)-**1.31**	−1016.23618670	3.794	0.05	−1015.925030	2.074	1.13
A_5	(*R*,*S*′)-**1.28**	−1016.23276288	5.942	0.00	−1015.920405	4.976	0.01
A_6	(*R*,*S*′)-**1.27**	−1016.23095327	7.078	0.00	−1015.919111	5.788	0.00
A_8	(*R*,*S*′)-**1.03**	−1016.24053111	1.068	5.42	−1015.925011	2.086	1.10
	(*R*,*S*′)-**1.04**	−1016.24015202	1.306	3.63	−1015.925141	2.004	1.27
	(*R*,*S*′)-**1.05**	−1016.23816641	2.552	0.44	−1015.924969	2.112	1.06
	(*R*,*S*′)-**1.07**	−1016.23973069	1.570	2.32	−1015.924950	2.124	1.03
	(*R*,*S*′)-**1.18**	−1016.24053413	1.066	5.43	−1015.924537	2.383	0.67
	(*R*,*S*′)-**1.37**	−1016.23943149	1.758	1.69	−1015.924572	2.361	0.69
A_9	(*R*,*S*′)-**1.19**	−1016.23417363	5.057	0.01	−1015.921884	4.048	0.04
	(*R*,*S*′)-**1.21**	−1016.23413812	5.079	0.01	−1015.921888	4.046	0.04
A_{12}	(*R*,*S*′)-**1.20**	−1016.23584773	4.007	0.04	−1015.919909	5.287	0.00
B_1	(*R*,*S*′)-**1.43**	−1016.23271356	5.973	0.00	−1015.920648	4.824	0.01
	(*R*,*S*′)-**1.56**	−1016.23276664	5.940	0.00	−1015.920392	4.984	0.01
B_2	(*R*,*S*′)-**1.38**	−1016.23275564	5.947	0.00	−1015.920142	5.141	0.01
	(*R*,*S*′)-**1.52**	−1016.23289727	5.858	0.00	−1015.920438	4.955	0.01
B_3	(*R*,*S*′)-**1.14**	−1016.23746381	2.992	0.21	−1015.924678	2.295	0.78
	(*R*,*S*′)-**1.29**	−1016.23757907	2.920	0.24	−1015.925131	2.011	1.25
B_4	(*R*,*S*′)-**1.40**	−1016.23408349	5.114	0.01	−1015.923433	3.076	0.21
C_1	(*R*,*S*′)-**1.55**	−1016.23671524	3.462	0.10	−1015.920597	4.856	0.01
C_2	(*R*,*S*′)-**1.25**	−1016.23582823	4.019	0.04	−1015.922606	3.595	0.09
	(*R*,*S*′)-**1.44**	−1016.23918068	1.915	1.30	−1015.925063	2.053	1.17
C_3	(*R*,*S*′)-**1.50**	−1016.23322115	5.655	0.00	−1015.919745	5.390	0.00
C_4	(*R*,*S*′)-**1.23**	−1016.23915025	1.934	1.25	−1015.924825	2.203	0.91
	(*R*,*S*′)-**1.36**	−1016.23507689	4.490	0.02	−1015.923222	3.208	0.17
C_5	(*R*,*S*′)-**1.48**	−1016.23915845	1.929	1.27	−1015.924010	2.714	0.38
D_3	(*R*,*S*′)-**1.39**	−1016.23537484	4.303	0.02	−1015.924547	2.377	0.67
	(*R*,*S*′)-**1.41**	−1016.23543305	4.267	0.02	−1015.924226	2.578	0.48
D_6	(*R*,*S*′)-**1.49**	−1016.23431380	4.969	0.01	−1015.922851	3.441	0.11
D_8	(*R*,*S*′)-**1.51**	−1016.23222307	6.281	0.00	−1015.921017	4.592	0.02
	(*R*,*S*′)-**1.54**	−1016.23226445	6.255	0.00	−1015.920943	4.639	0.01
E_1	(*R*,*S*′)-**1.46**	−1016.23266390	6.004	0.00	−1015.920724	4.776	0.01
	(*R*,*S*′)-**1.57**	−1016.23276682	5.940	0.00	−1015.924290	2.538	0.51
F_1	(*R*,*S*′)-**1.33**	−1016.23393677	5.206	0.01	−1015.922915	3.401	0.12
	(*R*,*S*′)-**1.34**	−1016.23387828	5.242	0.00	−1015.922278	3.801	0.06
	(*R*,*S*′)-**1.47**	−1016.23407758	5.117	0.01	−1015.923192	3.227	0.16
	(*R*,*S*′)-**1.53**	−1016.22866425	8.514	0.00	−1015.916933	7.155	0.00
F_2	(*R*,*S*′)-**1.35**	−1016.23328738	5.613	0.00	−1015.922151	3.881	0.05
F_3	(*R*,*S*′)-**1.30**	−1016.23385840	5.255	0.00	−1015.921934	4.017	0.04
	(*R*,*S*′)-**1.42**	−1016.23400289	5.164	0.01	−1015.922674	3.552	0.09
	(*R*,*S*′)-**1.45**	−1016.23398268	5.177	0.01	−1015.922278	3.801	0.06
F_4	(*R*,*S*′)-**1.32**	−1016.23550079	4.224	0.03	−1015.922985	3.357	0.13

Figure 8.7. Optimised structures and theoretical ECD spectra ($\Delta\sigma$ = 0.25 eV) for the conformers of (*R*,*S*′)-**1**, as obtained after DFT geometry optimisation at the RI-B97D/TZVP/IEFPCM(MeOH) level and TD-DFT calculations at the PBE0/TZVP/IEFPCM(MeOH) level.

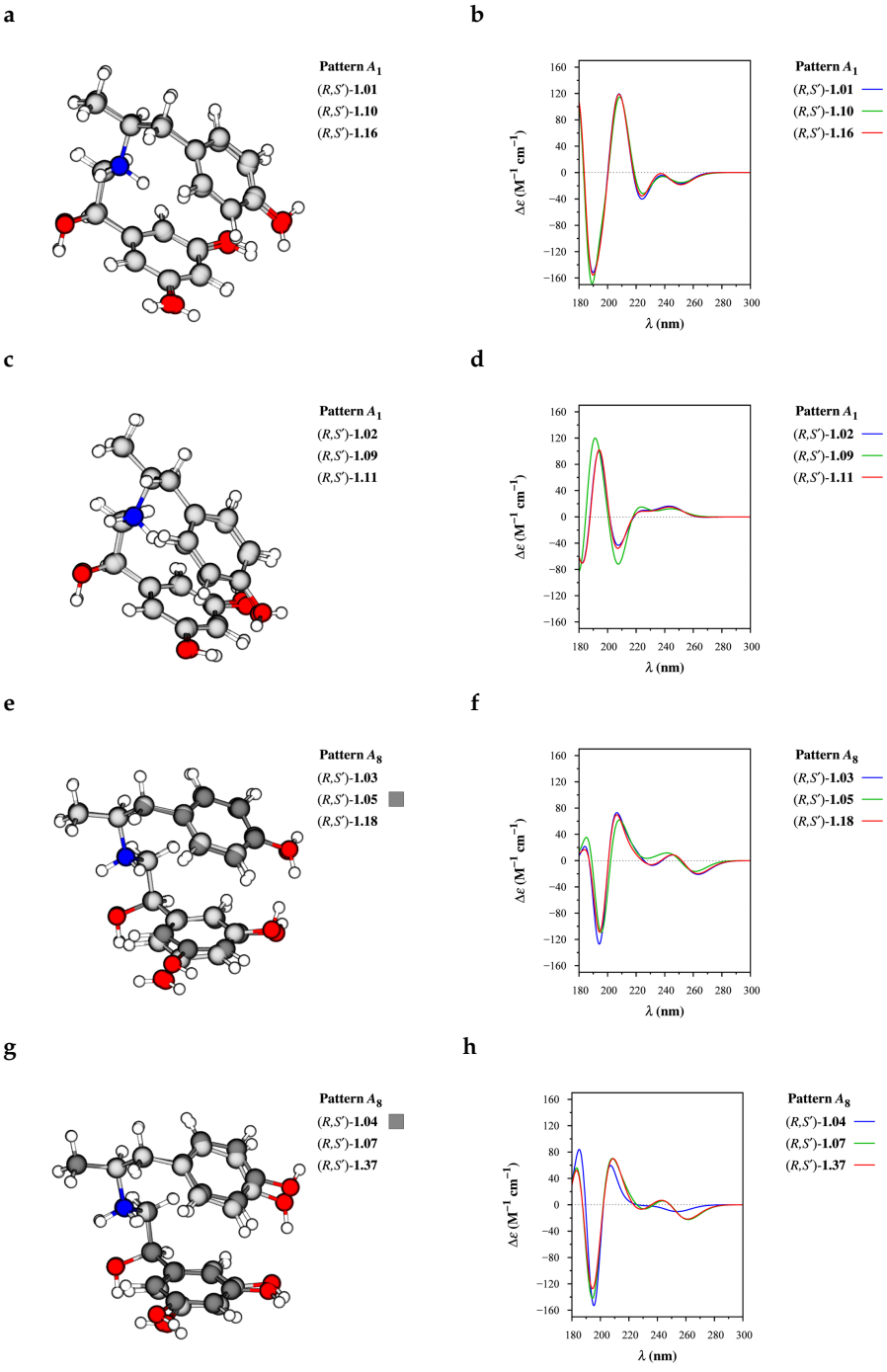

Figure 8.7. (*Continued*)

i

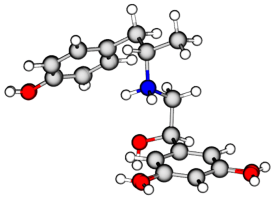

j

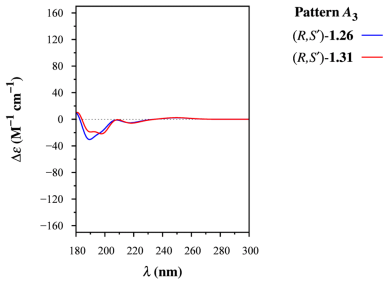

k

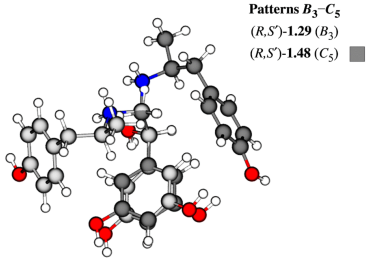

l

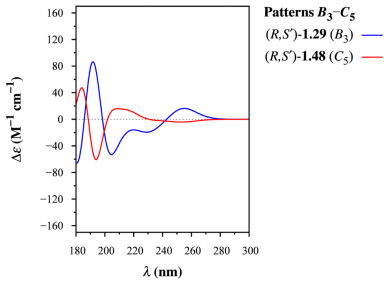

m

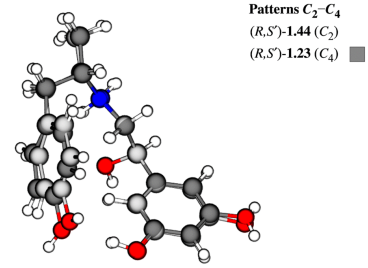

n

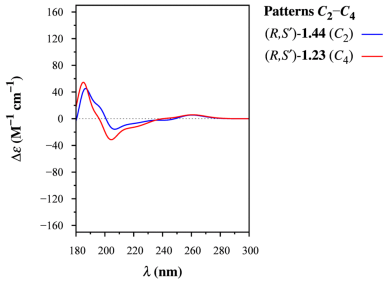

Table 8.12. Rotational strengths (in dipole velocity form) and excitation wavelengths for the conformers of (*R*,*S*′)-**1**, as obtained by TD-DFT calculations at the PBE0/TZVP/IEFPCM(MeOH) level.

j	R_j, 10^{-40} erg cm^3 (λ_j, nm)				
	(*R*,*S*′)-**1.01**	(*R*,*S*′)-**1.02**	(*R*,*S*′)-**1.03**	(*R*,*S*′)-**1.04**	(*R*,*S*′)-**1.05**
1	23.0685 (254.98)	−25.1127 (251.93)	−83.4287 (258.57)	17.8383 (254.59)	−88.5547 (255.50)
2	−59.3817 (251.27)	46.6094 (247.93)	64.1371 (251.37)	−39.4607 (254.23)	73.7126 (250.62)
3	11.6441 (237.12)	8.8040 (236.92)	−5.3593 (238.15)	1.6138 (237.56)	1.1225 (237.33)
4	9.1031 (231.62)	2.9198 (232.40)	8.9707 (231.83)	−2.2700 (233.49)	9.0880 (233.38)
5	−7.9521 (225.29)	−3.4603 (223.85)	−46.7075 (227.71)	−14.8060 (225.02)	−22.0744 (222.40)
6	−43.7369 (223.75)	11.7406 (220.55)	39.8997 (222.76)	16.8392 (223.49)	17.0092 (221.02)
7	−60.0908 (219.69)	31.7206 (217.41)	−13.3957 (217.13)	−4.6791 (216.79)	−5.3363 (216.67)
8	−5.5456 (214.64)	−0.1722 (215.48)	43.7531 (212.93)	−3.1007 (215.89)	25.6039 (213.54)
9	125.3554 (211.01)	−52.4707 (212.58)	−5.4988 (211.23)	18.7163 (212.20)	18.2832 (213.16)
10	109.6056 (205.72)	46.0611 (205.34)	19.0824 (205.29)	9.5973 (205.34)	168.9237 (203.25)
11	49.3342 (202.09)	−119.6166 (204.17)	185.9088 (201.59)	135.5414 (202.16)	−25.2798 (201.69)
12	−94.3658 (196.67)	41.5957 (197.26)	32.4748 (197.84)	136.9325 (200.11)	−2.2848 (198.37)
13	−131.9846 (195.01)	−48.4361 (196.02)	−187.6952 (196.63)	−318.5659 (196.88)	−215.4565 (196.41)
14	−26.8652 (192.11)	182.0305 (193.61)	−188.8667 (193.51)	−170.1631 (194.58)	−82.0174 (192.65)
15	189.6592 (191.92)	41.3083 (191.93)	−4.8085 (191.04)	9.2289 (190.33)	88.4909 (189.07)
16	−136.7277 (188.55)	−40.9965 (187.71)	1.7679 (188.03)	18.1156 (188.02)	23.2262 (187.69)
17	−291.8126 (186.19)	−91.9874 (185.25)	105.2026 (186.53)	52.3470 (187.30)	124.4934 (185.22)
18	−2.3392 (184.00)	104.7738 (184.44)	159.9378 (186.12)	253.9900 (186.29)	−86.2438 (184.24)
19	116.9204 (183.01)	−56.8297 (183.11)	−167.2993 (184.72)	−126.9956 (184.95)	−8.5996 (183.89)
20	−21.4815 (182.31)	−77.6385 (182.11)	10.2960 (181.07)	−22.2649 (181.30)	−18.6862 (183.21)
21	197.7209 (181.56)	2.8639 (181.74)	−13.5480 (180.94)	8.6988 (180.73)	−10.5173 (181.31)
22	1.1427 (179.10)	19.3994 (180.41)	6.9197 (177.70)	−11.3610 (178.80)	7.7090 (180.75)
23	23.0812 (178.78)	−12.1731 (179.12)	−6.6567 (176.59)	16.0819 (177.08)	16.3148 (177.04)
24	7.2401 (178.04)	6.2746 (175.26)	15.3852 (175.73)	19.4471 (176.34)	1.1375 (176.50)
25	0.7426 (175.28)	−2.4307 (174.07)	−4.7978 (172.36)	−1.0329 (174.03)	5.9960 (175.61)
26	2.2967 (172.24)	−1.1142 (171.59)	5.7070 (171.48)	2.2939 (171.97)	−5.6210 (171.58)
27	−0.5116 (171.45)	−5.5508 (171.01)	−4.2464 (170.49)	−1.8854 (169.31)	−3.1473 (169.96)
28	0.2263 (170.94)	0.3983 (170.48)	−2.9799 (169.44)	8.8071 (168.90)	1.4004 (169.24)
29	−4.6625 (170.16)	9.2795 (169.33)	−3.2032 (168.49)	−3.6067 (168.74)	−0.8988 (168.82)
30	−0.3156 (168.67)	−8.3706 (168.64)	−9.4527 (167.77)	17.1327 (167.46)	−1.5189 (168.60)

j	R_j, 10^{-40} erg cm^3 (λ_j, nm)				
	(*R*,*S*′)-**1.07**	(*R*,*S*′)-**1.09**	(*R*,*S*′)-**1.10**	(*R*,*S*′)-**1.11**	(*R*,*S*′)-**1.16**
1	−74.2884 (257.82)	−9.7212 (251.42)	3.0315 (253.66)	−28.0891 (251.22)	27.9791 (254.76)
2	46.1924 (249.75)	29.5627 (247.83)	−36.2592 (250.91)	49.9322 (247.98)	−67.4185 (251.68)
3	0.6931 (241.22)	7.9809 (236.50)	6.8894 (237.68)	8.0084 (235.27)	15.7336 (235.80)
4	−18.1615 (229.40)	−1.8642 (232.75)	3.2134 (233.23)	1.0880 (233.04)	9.0009 (232.25)
5	−11.4691 (224.58)	5.8305 (225.26)	−22.7941 (225.09)	6.8809 (222.94)	−9.6787 (225.81)
6	2.7803 (224.39)	−21.6487 (221.68)	−6.0346 (224.34)	−11.0007 (220.81)	−30.1636 (223.38)
7	30.0048 (219.57)	53.9781 (219.83)	−61.0481 (220.45)	30.5701 (217.66)	−60.8621 (220.47)
8	−10.3435 (214.74)	6.1160 (215.95)	12.3577 (215.23)	12.2236 (215.95)	−4.2636 (214.69)
9	65.7974 (210.20)	−20.4975 (210.65)	90.1660 (210.54)	−41.5881 (212.67)	107.5580 (211.15)
10	1.1633 (207.19)	−67.8337 (208.05)	101.5314 (207.05)	25.5936 (206.17)	97.9601 (206.26)
11	257.0065 (201.67)	−78.4037 (204.10)	73.7955 (203.01)	−118.8011 (204.46)	81.8039 (202.82)
12	−274.4923 (199.10)	143.0427 (197.22)	−146.4332 (197.78)	64.6826 (197.08)	−75.8401 (197.34)
13	24.9986 (197.22)	−54.9748 (196.69)	−55.8813 (196.25)	−45.4031 (196.62)	−150.1612 (195.67)
14	−207.9273 (192.81)	−30.0877 (193.60)	51.3484 (192.50)	147.3008 (193.80)	−19.9797 (193.27)
15	−3.3352 (188.00)	59.6310 (191.72)	168.2025 (192.10)	54.6070 (192.52)	167.0602 (192.11)
16	−36.7194 (186.94)	330.8893 (187.37)	−441.8648 (188.33)	−46.8917 (187.65)	−131.3633 (188.54)
17	130.8592 (186.26)	−298.8613 (185.11)	−41.8286 (184.80)	−65.5561 (185.26)	−310.7843 (186.24)
18	58.0040 (183.66)	54.6906 (183.77)	75.2791 (182.94)	79.1187 (184.46)	64.7812 (183.08)
19	4.8779 (183.44)	14.8193 (182.31)	84.5383 (181.10)	−55.8624 (183.13)	62.9945 (182.09)
20	−1.8623 (181.18)	19.9417 (181.21)	23.7946 (181.01)	−53.5237 (182.24)	183.3482 (181.61)
21	3.3438 (180.34)	−107.9626 (180.48)	56.2585 (180.08)	−6.0305 (181.03)	25.6205 (180.41)
22	−15.6599 (179.86)	−8.0917 (179.44)	30.1348 (179.28)	6.7117 (180.46)	5.7709 (179.92)
23	−20.3297 (177.85)	−20.8338 (177.72)	17.3469 (179.15)	−10.3659 (179.33)	0.5540 (179.37)
24	0.4488 (175.67)	1.7458 (172.85)	−5.3833 (174.49)	10.6757 (174.24)	1.1172 (175.01)
25	5.1841 (171.90)	−2.8970 (172.15)	−0.5921 (173.08)	−1.5744 (172.63)	−6.3994 (174.03)
26	0.0504 (171.57)	1.2554 (171.42)	−7.9712 (172.17)	−1.5724 (171.17)	−5.3209 (172.37)
27	−14.8575 (170.76)	7.8098 (169.65)	−0.4039 (170.92)	−6.4531 (170.09)	3.1566 (171.26)
28	4.5387 (168.09)	10.7512 (169.32)	6.4149 (170.54)	11.8739 (169.74)	−3.1202 (171.21)
29	0.3470 (167.44)	−6.4081 (168.55)	−3.3688 (169.97)	−11.0323 (168.96)	−0.4632 (170.22)
30	−3.3611 (167.07)	4.9054 (167.95)	−7.3915 (168.52)	−1.4603 (167.61)	44.2476 (167.84)

Table 8.12. (*Continued*)

j	R_j, 10^{-40} erg cm^3 (λ_j, nm)			
	(*R*,*S*′)-**1.18**	(*R*,*S*′)-**1.23**	(*R*,*S*′)-**1.26**	(*R*,*S*′)-**1.29**
1	−79.8390 (258.37)	17.5226 (258.17)	5.2903 (249.60)	68.9044 (252.22)
2	63.0754 (251.15)	−15.5481 (248.74)	−0.7673 (248.35)	−37.3571 (249.54)
3	−5.8598 (238.28)	10.9563 (244.71)	−0.0324 (224.26)	−14.0905 (231.41)
4	8.7572 (231.21)	0.3198 (232.14)	−0.9676 (222.63)	−19.7030 (229.24)
5	−39.8789 (227.31)	−11.2485 (226.25)	−1.3135 (218.30)	−5.8246 (219.90)
6	37.6201 (222.26)	−0.1951 (219.97)	−8.6992 (215.43)	8.1940 (216.26)
7	−20.1556 (217.77)	−1.7382 (217.23)	1.8287 (207.33)	−47.7773 (213.39)
8	19.5893 (213.38)	−16.5299 (215.64)	5.4618 (205.60)	40.6389 (211.97)
9	12.4888 (211.63)	2.5043 (209.40)	−8.0487 (205.30)	−27.9291 (208.72)
10	5.8800 (205.69)	−93.9441 (201.08)	29.1292 (201.37)	−115.1798 (201.12)
11	174.4766 (202.18)	30.5367 (196.03)	−96.3729 (196.91)	8.0328 (198.92)
12	61.4891 (198.85)	104.1820 (195.31)	95.8642 (193.55)	81.8350 (197.18)
13	−155.3643 (197.40)	−43.8997 (193.74)	6.0242 (192.69)	−103.9676 (196.27)
14	−219.7976 (194.04)	−152.9574 (189.43)	−12.8589 (192.24)	113.9532 (193.66)
15	30.9791 (190.80)	271.4652 (186.38)	−49.3135 (190.55)	75.9092 (191.01)
16	18.1935 (188.85)	−93.1624 (185.72)	−70.6945 (186.07)	63.0865 (187.02)
17	244.2257 (186.45)	32.9117 (184.44)	20.8431 (184.03)	−80.6502 (184.68)
18	−16.3482 (185.49)	2.7340 (183.77)	58.4821 (181.81)	−17.9665 (183.63)
19	−183.4328 (185.35)	−45.6128 (180.75)	−0.7659 (180.08)	8.8500 (182.29)
20	8.7853 (181.23)	20.1424 (180.51)	−11.8127 (179.89)	−8.3017 (181.88)
21	1.0330 (180.25)	−13.3654 (179.44)	−0.8554 (178.93)	−53.7818 (180.61)
22	8.9146 (177.85)	2.3260 (177.23)	−8.4209 (178.57)	−7.3982 (180.42)
23	9.6791 (176.43)	1.1457 (175.97)	8.7818 (176.84)	−0.3542 (178.56)
24	−2.1268 (175.11)	−4.9702 (175.13)	−10.7060 (175.72)	−12.6237 (175.59)
25	−8.4244 (172.37)	4.3910 (173.11)	−1.5279 (174.56)	0.5208 (175.17)
26	7.9292 (171.72)	−10.4076 (172.18)	7.2477 (172.68)	6.3553 (173.27)
27	−6.7593 (171.13)	−0.6849 (169.46)	6.6529 (170.30)	6.2525 (171.98)
28	7.2526 (168.46)	−1.1757 (168.28)	1.8897 (169.47)	−28.9486 (170.62)
29	−8.7552 (168.39)	−0.0985 (167.68)	2.4385 (169.08)	57.2146 (170.10)
30	14.5036 (167.78)	−0.3699 (167.37)	7.6638 (168.66)	−4.1463 (169.69)

j	R_j, 10^{-40} erg cm^3 (λ_j, nm)			
	(*R*,*S*′)-**1.31**	(*R*,*S*′)-**1.37**	(*R*,*S*′)-**1.44**	(*R*,*S*′)-**1.48**
1	4.7949 (249.65)	−71.9733 (257.39)	20.4346 (256.15)	−15.3672 (252.91)
2	0.1725 (248.36)	44.6316 (249.41)	−14.7073 (249.00)	12.6760 (249.83)
3	0.0040 (223.81)	1.3787 (240.64)	1.0761 (242.21)	−6.3228 (247.01)
4	−1.3930 (223.10)	−1.4570 (228.96)	0.6914 (228.39)	−2.4533 (233.93)
5	−2.2122 (218.43)	−19.7194 (226.05)	−4.4824 (225.85)	−0.9887 (224.73)
6	−9.2146 (215.44)	−2.9571 (224.56)	−1.7908 (222.78)	2.9185 (220.44)
7	1.9281 (207.78)	16.3477 (219.85)	−2.4366 (218.28)	−1.5346 (218.25)
8	9.4510 (205.54)	−18.6033 (214.69)	−6.4757 (215.60)	18.7520 (216.03)
9	−11.1632 (205.44)	91.2268 (210.55)	0.5451 (208.55)	3.9407 (211.66)
10	45.4407 (201.81)	−1.2926 (208.56)	−55.5094 (202.03)	59.0996 (200.65)
11	−127.4069 (197.75)	225.3957 (201.84)	34.9154 (197.07)	−27.7223 (198.29)
12	115.0113 (193.78)	−273.4080 (199.43)	63.1656 (195.58)	−35.5516 (195.96)
13	6.5232 (192.54)	58.5446 (198.02)	−12.0856 (193.88)	16.6116 (192.00)
14	−23.1977 (192.44)	−192.4005 (193.11)	−98.3698 (190.15)	−193.2742 (190.42)
15	−32.8656 (191.01)	−2.3212 (188.40)	4.2537 (186.32)	−21.4307 (187.30)
16	−87.6749 (186.12)	−42.6807 (186.79)	161.2736 (186.22)	253.8300 (186.22)
17	26.6779 (184.07)	134.5971 (185.96)	7.5839 (184.86)	−5.1844 (183.77)
18	73.5695 (182.50)	−13.0801 (184.42)	10.7284 (183.76)	−40.1249 (183.08)
19	−10.1540 (179.89)	63.8497 (183.17)	−57.7269 (181.85)	−15.3114 (182.00)
20	−2.2229 (179.83)	−4.2351 (182.44)	−22.8355 (181.28)	−1.3199 (180.64)
21	−8.1523 (178.49)	−6.0961 (180.08)	8.2467 (178.53)	−3.2043 (179.95)
22	−0.6187 (177.44)	−6.0392 (179.91)	−11.8338 (178.40)	6.8075 (179.13)
23	−2.5896 (176.70)	−23.1067 (177.44)	1.3169 (174.60)	2.4800 (177.97)
24	−9.0571 (174.78)	0.8658 (174.14)	0.9087 (174.29)	−5.3881 (174.37)
25	−4.1735 (174.57)	4.6931 (171.74)	4.2292 (174.09)	−6.7593 (174.16)
26	0.4094 (172.78)	−7.4153 (171.23)	−5.3513 (172.22)	5.0486 (172.71)
27	5.1895 (172.33)	−10.8243 (170.79)	11.0814 (170.38)	0.3011 (170.57)
28	0.6019 (169.80)	−1.0632 (168.62)	0.1294 (168.00)	3.7981 (169.56)
29	4.0560 (169.04)	−9.4881 (167.95)	−3.3358 (166.63)	1.8802 (168.29)
30	8.6238 (167.96)	11.6862 (167.00)	0.3794 (166.35)	−4.6980 (167.99)

Table 8.13. Oscillator strengths and excitation wavelengths for the conformers of (*R*,*S*′)-**1**, as obtained by TD-DFT calculations at the PBE0/TZVP/IEFPCM(MeOH) level.

j	f_j (λ_j, nm)				
	(*R*,*S*′)-**1.01**	(*R*,*S*′)-**1.02**	(*R*,*S*′)-**1.03**	(*R*,*S*′)-**1.04**	(*R*,*S*′)-**1.05**
1	0.0092 (254.98)	0.0145 (251.93)	0.0651 (258.57)	0.0135 (254.59)	0.0609 (255.50)
2	0.0448 (251.27)	0.0416 (247.93)	0.0140 (251.37)	0.0533 (254.23)	0.0274 (250.62)
3	0.0038 (237.12)	0.0075 (236.92)	0.0017 (238.15)	0.0054 (237.56)	0.0041 (237.33)
4	0.0011 (231.62)	0.0075 (232.40)	0.0068 (231.83)	0.0057 (233.49)	0.0071 (233.38)
5	0.0038 (225.29)	0.0008 (223.85)	0.0429 (227.71)	0.0391 (225.02)	0.0181 (222.40)
6	0.0354 (223.75)	0.0142 (220.55)	0.0515 (222.76)	0.0470 (223.49)	0.0506 (221.02)
7	0.0438 (219.69)	0.0567 (217.41)	0.0214 (217.13)	0.0150 (216.79)	0.0203 (216.67)
8	0.0168 (214.64)	0.0264 (215.48)	0.0148 (212.93)	0.0190 (215.89)	0.0584 (213.54)
9	0.0484 (211.01)	0.0360 (212.58)	0.0231 (211.23)	0.0290 (212.20)	0.0095 (213.16)
10	0.0470 (205.72)	0.0345 (205.34)	0.0107 (205.29)	0.0239 (205.34)	0.0415 (203.25)
11	0.0160 (202.09)	0.0568 (204.17)	0.1964 (201.59)	0.1198 (202.16)	0.2938 (201.69)
12	0.0317 (196.67)	0.0337 (197.26)	0.0671 (197.84)	0.0624 (200.11)	0.0054 (198.37)
13	0.1744 (195.01)	0.1914 (196.02)	0.0634 (196.63)	0.1455 (196.88)	0.0749 (196.41)
14	0.0353 (192.11)	0.1619 (193.61)	0.0989 (193.51)	0.0878 (194.58)	0.0629 (192.65)
15	0.2158 (191.92)	0.0690 (191.93)	0.1226 (191.04)	0.0084 (190.33)	0.2673 (189.07)
16	0.1817 (188.55)	0.1363 (187.71)	0.2785 (188.03)	0.1034 (188.02)	0.0429 (187.69)
17	0.4096 (186.19)	0.4860 (185.25)	0.2187 (186.53)	0.1712 (187.30)	0.7181 (185.22)
18	0.0700 (184.00)	0.4296 (184.44)	0.3833 (186.12)	0.6770 (186.29)	0.2872 (184.24)
19	0.3886 (183.01)	0.2624 (183.11)	0.3801 (184.72)	0.3989 (184.95)	0.0302 (183.89)
20	0.1244 (182.31)	0.0928 (182.11)	0.0152 (181.07)	0.0341 (181.30)	0.1156 (183.21)
21	0.2513 (181.56)	0.0019 (181.74)	0.0290 (180.94)	0.0219 (180.73)	0.0154 (181.31)
22	0.0067 (179.10)	0.0319 (180.41)	0.0134 (177.70)	0.0400 (178.80)	0.0302 (180.75)
23	0.0177 (178.78)	0.0240 (179.12)	0.0116 (176.59)	0.0504 (177.08)	0.0205 (177.04)
24	0.0078 (178.04)	0.0044 (175.26)	0.0236 (175.73)	0.0144 (176.34)	0.0154 (176.50)
25	0.0062 (175.28)	0.0085 (174.07)	0.0164 (172.36)	0.0117 (174.03)	0.0061 (175.61)
26	0.0077 (172.24)	0.0041 (171.59)	0.0019 (171.48)	0.0026 (171.97)	0.0099 (171.58)
27	0.0002 (171.45)	0.0057 (171.01)	0.0072 (170.49)	0.0017 (169.31)	0.0066 (169.96)
28	0.0098 (170.94)	0.0005 (170.48)	0.0021 (169.44)	0.0063 (168.90)	0.0038 (169.24)
29	0.0024 (170.16)	0.0027 (169.33)	0.0053 (168.49)	0.0024 (168.74)	0.0008 (168.82)
30	0.0002 (168.67)	0.0066 (168.64)	0.0168 (167.77)	0.0120 (167.46)	0.0023 (168.60)

j	f_j (λ_j, nm)				
	(*R*,*S*′)-**1.07**	(*R*,*S*′)-**1.09**	(*R*,*S*′)-**1.10**	(*R*,*S*′)-**1.11**	(*R*,*S*′)-**1.16**
1	0.0586 (257.82)	0.0168 (251.42)	0.0183 (253.66)	0.0102 (251.22)	0.0068 (254.76)
2	0.0079 (249.75)	0.0280 (247.83)	0.0254 (250.91)	0.0427 (247.98)	0.0450 (251.68)
3	0.0074 (241.22)	0.0056 (236.50)	0.0034 (237.68)	0.0071 (235.27)	0.0037 (235.80)
4	0.0278 (229.40)	0.0038 (232.75)	0.0016 (233.23)	0.0080 (233.04)	0.0014 (232.25)
5	0.0224 (224.58)	0.0038 (225.26)	0.0087 (225.09)	0.0062 (222.94)	0.0157 (225.81)
6	0.0007 (224.39)	0.0241 (221.68)	0.0219 (224.34)	0.0123 (220.81)	0.0229 (223.38)
7	0.0190 (219.57)	0.0542 (219.83)	0.0415 (220.45)	0.0506 (217.66)	0.0423 (220.47)
8	0.0693 (214.74)	0.0091 (215.95)	0.0139 (215.23)	0.0210 (215.95)	0.0094 (214.69)
9	0.0274 (210.20)	0.0256 (210.65)	0.0334 (210.54)	0.0392 (212.67)	0.0527 (211.15)
10	0.0050 (207.19)	0.0147 (208.05)	0.0589 (207.05)	0.0099 (206.17)	0.0408 (206.26)
11	0.1066 (201.67)	0.0754 (204.10)	0.0219 (203.01)	0.0798 (204.46)	0.0215 (202.82)
12	0.1871 (199.10)	0.1523 (197.22)	0.0562 (197.78)	0.0522 (197.08)	0.0258 (197.34)
13	0.0314 (197.22)	0.0640 (196.69)	0.0677 (196.25)	0.1919 (196.62)	0.1935 (195.67)
14	0.1821 (192.81)	0.1010 (193.60)	0.0895 (192.50)	0.1531 (193.80)	0.0177 (193.27)
15	0.3240 (188.00)	0.0774 (191.72)	0.1940 (192.10)	0.0679 (192.52)	0.2411 (192.11)
16	0.3508 (186.94)	0.4399 (187.37)	0.5306 (188.33)	0.1414 (187.65)	0.1644 (188.54)
17	0.4057 (186.26)	0.5974 (185.11)	0.1178 (184.80)	0.4858 (185.26)	0.4366 (186.24)
18	0.1300 (183.66)	0.1332 (183.77)	0.4524 (182.94)	0.4362 (184.46)	0.4924 (183.08)
19	0.0736 (183.44)	0.0197 (182.31)	0.1985 (181.10)	0.2313 (183.13)	0.0733 (182.09)
20	0.0653 (181.18)	0.0761 (181.21)	0.0717 (181.01)	0.1325 (182.24)	0.1755 (181.61)
21	0.0066 (180.34)	0.2245 (180.48)	0.0662 (180.08)	0.0133 (181.03)	0.0789 (180.41)
22	0.0366 (179.86)	0.0221 (179.44)	0.0212 (179.28)	0.0083 (180.46)	0.0140 (179.92)
23	0.0577 (177.85)	0.0103 (177.72)	0.0157 (179.15)	0.0224 (179.33)	0.0063 (179.37)
24	0.0010 (175.67)	0.0012 (172.85)	0.0056 (174.49)	0.0089 (174.24)	0.0011 (175.01)
25	0.0060 (171.90)	0.0030 (172.15)	0.0031 (173.08)	0.0026 (172.63)	0.0048 (174.03)
26	0.0115 (171.57)	0.0036 (171.42)	0.0056 (172.17)	0.0011 (171.17)	0.0044 (172.37)
27	0.0075 (170.76)	0.0051 (169.65)	0.0046 (170.92)	0.0047 (170.09)	0.0017 (171.26)
28	0.0022 (168.09)	0.0099 (169.32)	0.0044 (170.54)	0.0065 (169.74)	0.0095 (171.21)
29	0.0025 (167.44)	0.0021 (168.55)	0.0033 (169.97)	0.0042 (168.96)	0.0037 (170.22)
30	0.0079 (167.07)	0.0035 (167.95)	0.0142 (168.52)	0.0031 (167.61)	0.0135 (167.84)

Table 8.13. (*Continued*)

j	f_j (λ_j, nm)			
	(*R*,*S*′)-**1.18**	(*R*,*S*′)-**1.23**	(*R*,*S*′)-**1.26**	(*R*,*S*′)-**1.29**
1	0.0623 (258.37)	0.0597 (258.17)	0.0382 (249.60)	0.0485 (252.22)
2	0.0138 (251.15)	0.0217 (248.74)	0.0372 (248.35)	0.0335 (249.54)
3	0.0025 (238.28)	0.0083 (244.71)	0.0014 (224.26)	0.0196 (231.41)
4	0.0067 (231.21)	0.0012 (232.14)	0.0028 (222.63)	0.0185 (229.24)
5	0.0349 (227.31)	0.0131 (226.25)	0.0002 (218.30)	0.0032 (219.90)
6	0.0562 (222.26)	0.0006 (219.97)	0.1498 (215.43)	0.0463 (216.26)
7	0.0323 (217.77)	0.0081 (217.23)	0.0057 (207.33)	0.0432 (213.39)
8	0.0137 (213.38)	0.0777 (215.64)	0.0026 (205.60)	0.0506 (211.97)
9	0.0152 (211.63)	0.0010 (209.40)	0.0330 (205.30)	0.0623 (208.72)
10	0.0117 (205.69)	0.3976 (201.08)	0.5307 (201.37)	0.1876 (201.12)
11	0.1694 (202.18)	0.0846 (196.03)	0.1665 (196.91)	0.1952 (198.92)
12	0.0580 (198.85)	0.2861 (195.31)	0.1157 (193.55)	0.1220 (197.18)
13	0.0902 (197.40)	0.0657 (193.74)	0.0036 (192.69)	0.1821 (196.27)
14	0.1093 (194.04)	0.2528 (189.43)	0.0112 (192.24)	0.0585 (193.66)
15	0.1178 (190.80)	0.4219 (186.38)	0.3660 (190.55)	0.3497 (191.01)
16	0.1869 (188.85)	0.3896 (185.72)	0.5337 (186.07)	0.3637 (187.02)
17	0.4584 (186.45)	0.1279 (184.44)	0.4819 (184.03)	0.1635 (184.68)
18	0.0803 (185.49)	0.0133 (183.77)	0.0650 (181.81)	0.1668 (183.63)
19	0.5385 (185.35)	0.0965 (180.75)	0.0116 (180.08)	0.0221 (182.29)
20	0.0205 (181.23)	0.0325 (180.51)	0.0062 (179.89)	0.0079 (181.88)
21	0.0164 (180.25)	0.0119 (179.44)	0.0094 (178.93)	0.1372 (180.61)
22	0.0276 (177.85)	0.0041 (177.23)	0.0137 (178.57)	0.0739 (180.42)
23	0.0237 (176.43)	0.0148 (175.97)	0.0034 (176.84)	0.0249 (178.56)
24	0.0020 (175.11)	0.0003 (175.13)	0.0051 (175.72)	0.0067 (175.59)
25	0.0153 (172.37)	0.0243 (173.11)	0.0044 (174.56)	0.0014 (175.17)
26	0.0009 (171.72)	0.0139 (172.18)	0.0102 (172.68)	0.0064 (173.27)
27	0.0093 (171.13)	0.0001 (169.46)	0.0035 (170.30)	0.0029 (171.98)
28	0.0073 (168.46)	0.0020 (168.28)	0.0008 (169.47)	0.0044 (170.62)
29	0.0052 (168.39)	0.0038 (167.68)	0.0026 (169.08)	0.0375 (170.10)
30	0.0234 (167.78)	0.0014 (167.37)	0.0028 (168.66)	0.0014 (169.69)

j	f_j (λ_j, nm)			
	(*R*,*S*′)-**1.31**	(*R*,*S*′)-**1.37**	(*R*,*S*′)-**1.44**	(*R*,*S*′)-**1.48**
1	0.0396 (249.65)	0.0565 (257.39)	0.0512 (256.15)	0.0491 (252.91)
2	0.0366 (248.36)	0.0078 (249.41)	0.0284 (249.00)	0.0124 (249.83)
3	0.0012 (223.81)	0.0065 (240.64)	0.0051 (242.21)	0.0185 (247.01)
4	0.0036 (223.10)	0.0221 (228.96)	0.0071 (228.39)	0.0041 (233.93)
5	0.0009 (218.43)	0.0158 (226.05)	0.0166 (225.85)	0.0102 (224.73)
6	0.1497 (215.44)	0.0179 (224.56)	0.0066 (222.78)	0.0229 (220.44)
7	0.0054 (207.78)	0.0104 (219.85)	0.0072 (218.28)	0.0129 (218.25)
8	0.0158 (205.54)	0.0704 (214.69)	0.0611 (215.60)	0.0578 (216.03)
9	0.0178 (205.44)	0.0392 (210.55)	0.0003 (208.55)	0.0060 (211.66)
10	0.4529 (201.81)	0.0040 (208.56)	0.3396 (202.03)	0.4113 (200.65)
11	0.2142 (197.75)	0.0827 (201.84)	0.0976 (197.07)	0.0192 (198.29)
12	0.1121 (193.78)	0.1979 (199.43)	0.2534 (195.58)	0.1199 (195.96)
13	0.0110 (192.54)	0.0351 (198.02)	0.1255 (193.88)	0.1457 (192.00)
14	0.0231 (192.44)	0.1878 (193.11)	0.2534 (190.15)	0.2599 (190.42)
15	0.3718 (191.01)	0.2760 (188.40)	0.1986 (186.32)	0.2205 (187.30)
16	0.5345 (186.12)	0.5204 (186.79)	0.6614 (186.22)	0.7926 (186.22)
17	0.4574 (184.07)	0.2901 (185.96)	0.0052 (184.86)	0.0093 (183.77)
18	0.1041 (182.50)	0.0949 (184.42)	0.0571 (183.76)	0.1263 (183.08)
19	0.0049 (179.89)	0.0495 (183.17)	0.1686 (181.85)	0.0316 (182.00)
20	0.0118 (179.83)	0.1295 (182.44)	0.0495 (181.28)	0.0096 (180.64)
21	0.0138 (178.49)	0.0365 (180.08)	0.0127 (178.53)	0.0041 (179.95)
22	0.0022 (177.44)	0.0022 (179.91)	0.0100 (178.40)	0.0052 (179.13)
23	0.0006 (176.70)	0.0503 (177.44)	0.0095 (174.60)	0.0262 (177.97)
24	0.0028 (174.78)	0.0022 (174.14)	0.0127 (174.29)	0.0299 (174.37)
25	0.0057 (174.57)	0.0060 (171.74)	0.0034 (174.09)	0.0095 (174.16)
26	0.0115 (172.78)	0.0022 (171.23)	0.0080 (172.22)	0.0080 (172.71)
27	0.0061 (172.33)	0.0105 (170.79)	0.0095 (170.38)	0.0098 (170.57)
28	0.0008 (169.80)	0.0006 (168.62)	0.0037 (168.00)	0.0005 (169.56)
29	0.0030 (169.04)	0.0091 (167.95)	0.0028 (166.63)	0.0003 (168.29)
30	0.0031 (167.96)	0.0038 (167.00)	0.0020 (166.35)	0.0064 (167.99)

Figure 8.8. Experimental UV spectra of the stereoisomers of **1** and **2**.

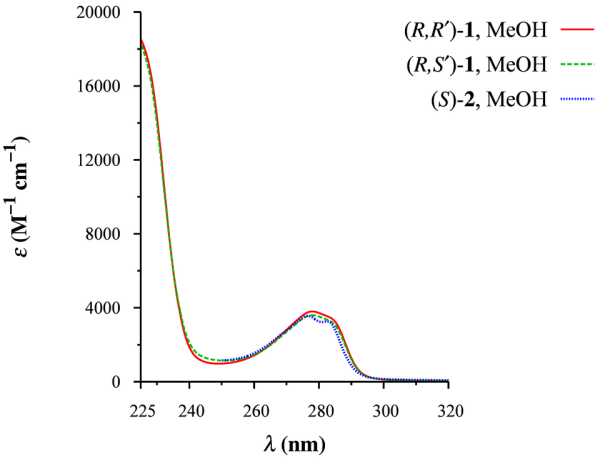

Part IV

Solvation effects

Time is overrated
Momentum carries me

— Maxïmo Park, *I Haven't Seen Her In Ages*

Chapter 9

Austdiol

(7*R*,8*S*)-Austdiol (**1**, Figure 9.1) is the main secondary metabolite produced by the mould *Aspergillus ustus*;[170] the chemical structure of **1** shows a 2-methyl-4*H*-pyran ring condensed with a cyclohexenone ring, which is functionalised with an aldehyde moiety, two *trans*-vicinal hydroxyl groups in α and β positions to the ketone moiety and a methyl group in α position to the ketone moiety. The extended conjugate system endows **1** with a large degree of planarity, and ring puckering is only slightly possible for the stereogenic carbon atoms. However, the *trans* relative configuration of the hydroxyl groups seems to favour a bi-equatorial conformation.[227,228] The stereochemistry of **1** has been characterised by ^{1}H-NMR analysis,[170] Horeau's partial resolution method with racemic α-phenylbutyric acid[229] and X-ray analysis on the 5-bromo-derivative.[230] A collection of physico-chemical data, including specific rotatory powers ($[\alpha]_D$), electronic circular dichroism (ECD), UV, IR and mass spectra, is also available in literature.[231]

Figure 9.1. Molecular structure, crystal structure and atom numbering scheme of **1**.[227]

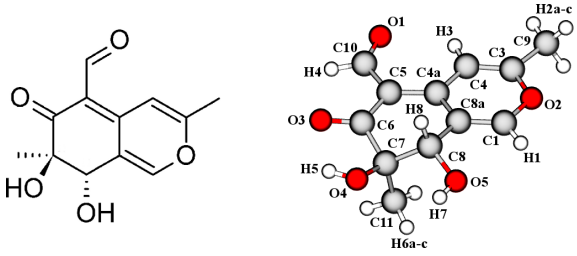

The intramolecular and intermolecular interactions of **1** have been thoroughly investigated by a combined experimental and theoretical study on its crystal packing: a total of 5 intramolecular and 9 intermolecular X−H···O interactions were characterised by means of their geometric parameters and topological analysis of the experimental and calculated electron distribution, $\rho(\mathbf{r})$.[228] Interestingly, the experimental and calculated properties of the intramolecular O−H···O interactions formed by the hydroxyl groups were found to differ significantly. In particular, density functional theory (DFT) gas-phase optimisation at the B3LYP/6-31G(*p*,*d*) level on the isolated structure of **1** resulted in shorter H···O distances, larger O−H distances and larger O−H···O angles with respect to crystallographic structures. Moreover, the topological analysis of the calculated $\rho(\mathbf{r})$ identifies a bond critical point for the O4–H5$\cdots$O3 interaction which is not found in the experimental $\rho(\mathbf{r})$ for the crystal, where the H5 atom is involved in intermolecular hydrogen bonds even though the geometric parameters might suggest an intramolecular interaction.

A new series of naturally-occurring derivatives of **1**, named mycoleptones A–C, was recently isolated and characterised from cultures of *Mycoleptodiscus indicus*;[9] the chemical structure of mycoleptone A shows two units of **1**, linked by a methylene bridge deriving from the condensation of the aldehyde moieties. The stereochemistry of mycoleptone A was investigated by ECD spectroscopy and time-dependent density functional theory (TD-DFT) calculations, in order to confirm the (7*R*,8*S*) absolute configuration of the two units of **1**;[9] the high-energy region of the ECD spectrum in methanol was correctly predicted, while TD-DFT calculations failed to reproduce the low-energy region. This behaviour was hypothesized to derive from a wrong description of the chiral environment around the carbonyl chromophores in solution: methanol, for instance, may induce perturbations to the electronic structure of **1** through intermolecular hydrogen bonding with carbonyl and hydroxyl groups, and may also induce small conformational changes which are not possible to describe without explicit treatment of solvent molecules in quantum mechanical (QM) calculations.

Short-range solvation effects on the spectroscopic and chiroptical properties can be described explicitly by performing QM calculations on solvation clusters (sometimes called 'solvated supermolecules').[114,115,232] This method has been used extensively over the years: nevertheless, a standard method for the generation of input structures has not been established yet, and several different strategies can be employed. The limiting factor in the choice of the proper strategy is the scaling of the computational effort with the size of the system: a reasonable balance between the need for chemical accuracy and the high com-

putational requirements for QM calculations on large clusters is crucial. Input structures can be either generated by direct optimisation of solvation clusters at the QM level or by extraction of sample geometries from molecular dynamics (MD) simulations on solvation boxes. The number and position of solvent molecules included in the cluster usually depends on the nature of the system: the general trend is to consider the solvent molecules closest to strong interacting groups of the solute (e.g., H-bond acceptors in alcohols or H-bond donors in acetone), or the first solvation shell(s).

Once the appropriate solvation clusters are generated, solvent molecules can be either included in or excluded from chiroptical properties calculations: the inclusion of solvent molecules at this stage is still an open matter of debate. Optical rotatory dispersion (ORD) and $[\alpha]_D$ calculations are likely to benefit the most from the inclusion of solvent molecules, due to the dispersive nature of optical rotation; non-chiral UV-absorbing solvents may directly contribute to the observed optical rotation of the system (or even be the main source of it) if the first solvation shells are highly organised and their chromophores absorb at lower energies than the chromophores of the solute. This phenomenon, defined 'chiral imprint',[233,234] was crucial to rationalise the ORD profile of 2-methyloxirane in benzene. On the other hand, ECD calculations may be relatively less sensitive to the inclusion of solvent molecules than ORD calculations: ECD is not affected by direct contributions of the solvation shells to the observed spectrum, since solvents in ECD spectroscopy are typically transparent in the UV region, but the inclusion of solvent molecules may result in a better description of the local perturbations to the electronic structure of chromophores, which is particularly important for the $n \rightarrow \pi^*$ transition of carbonyl groups.

The present project investigates the effect of solvation on the chiroptical properties of **1** in methanol through a combination of ECD spectroscopy, polarimetry, QM calculations at the DFT and TD-DFT level and *ab initio* MD simulations; the different computational strategies currently available were applied and compared. Although the combination of *ab initio* MD and TD-DFT calculations has been proposed as a possible strategy to investigate solvation effects on chiroptical properties, this is the first situation where such a strategy has been successfuly employed on a system of this size for the purpose; the advantages, the shortcomings and the perspective on the future development of reliable protocols for the description of solvation effects in stereochemical analysis will be discussed.

9.1 Results and discussion

9.1.1 TD-DFT calculations without explicit solvation

The main geometric parameters defining the conformational flexibility of **1** (Table 9.1, Figure 9.S1) are the dihedral angles describing the orientation of the O−H bonds of the α- and β-hydroxyl groups (dihedrals α and β, respectively), the mutual position of the vicinal hydroxyl groups (dihedral γ), which reflects the puckering of the cyclohexenone ring, and the twist of the α,β-unsaturated aldehyde moiety (dihedral δ).

Table 9.1. Main geometric parameters of **1**.

Label	Dihedral
α	C6–C7–O4–H5
β	C7–C8–O5–H7
γ	O4–C7–C8–O5
δ	C4a–C5–C10–O1

Standard DFT optimisation (Table 9.2, Figure 9.2) showed that the conformational flexibility of **1** is rather limited, with conformer **1.01** being the only significantly populated conformer at equilibrium; the bi-equatorial arrangement of hydroxyl groups ($\gamma \sim 60°$) and the *cis* orientation of the aldehyde moiety ($\delta \sim 0°$) are thus largely favoured, with the hydroxyl groups oriented to form intramolecular hydrogen bonds.

Table 9.2. Calculated energies, $[\alpha]_D$ values and geometric parameters for the lowest-energy conformers of **1**, as obtained by standard DFT optimisation and TD-DFT calculations.

Conf. ID	ΔE_{MM} (kcal mol^{-1})	ΔG (kcal mol^{-1})	χ_G (%)	$[\alpha]_D$ (deg cm^3 g^{-1} dm^{-1})	α (deg)	β (deg)	γ (deg)	δ (deg)
1.01	0.000	0.000	99.63	**−30.89**	13.700	−60.727	61.382	−1.792
1.02	3.168	4.231	0.08	**356.25**	66.963	177.346	178.085	3.253
1.03	4.914	3.456	0.29	**505.01**	10.622	−60.010	60.641	170.554

Unfortunately, TD-DFT calculations (Table 9.2) predict a negative $[\alpha]_D$ value for conformer **1.01**, leading to a conformationally-averaged value for **1** (−29) not in agreement with the experimental value in methanol (+147), even though the calculated $[\alpha]_D$ values for conformers **1.02** (bi-axial arrangement of the hydroxyl groups) and **1.03** (*trans* orientation of the aldehyde moiety) are both positive. The influence of ring puckering and aldehyde orientation is clearly evident from the theoretical spectra of the conformers of **1** (Figure 9.S2): in particular, the ECD

Figure 9.2. Graphical representation of conformers **1.01** (*left*), **1.02** (*center*) and **1.03** (*right*), as obtained by standard DFT optimisation.

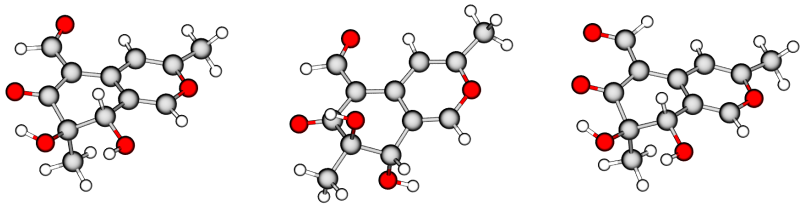

spectra of conformers **1.01** and **1.02** are almost opposite, although the absolute stereochemistry of chiral centers is retained.

The conformationally-averaged spectra of **1** (Figure 9.3) show a better correlation with experimental data, mainly in the high-energy region ($\lambda < 300$ nm) where the effect of the chiral centers on the $\pi \rightarrow \pi^*$ transitions of the conjugated system is strongest; nevertheless, the low-energy region of the spectra ($\lambda > 300$ nm), where the $n \rightarrow \pi^*$ transitions of carbonyl chromophores are observed, show a lower degree of correlation. Both behaviours are consistent to what previously observed with mycoleptone A.[9]

9.1.2 Effect of the orientation of hydroxyl groups

The strong influence of small geometric perturbations on the chiroptical properties of **1** was confirmed by DFT conformational scans on the orientation of hydroxyl groups (Table 9.S3).

Figure 9.3. Theoretical spectra of **1**, as obtained by standard DFT optimisation and TD-DFT calculations. *Red:* experimental spectra. *Blue:* theoretical spectra. *Left:* ECD spectra. *Center:* ORD spectra. *Right:* UV spectra.

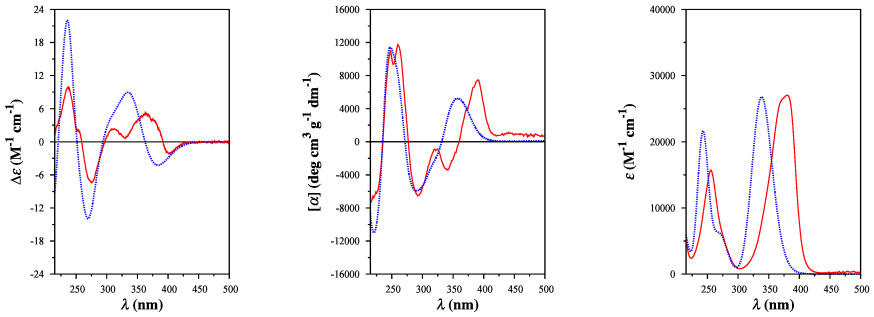

Figure 9.4. Dependence of calculated $[\alpha]_D$ values and orientation of the β-hydroxyl group upon rotation of the α-hydroxyl group of conformer **1.01**, as obtained by DFT conformational scan and TD-DFT calculations. Conformer **1.01** is marked with a dotted line.

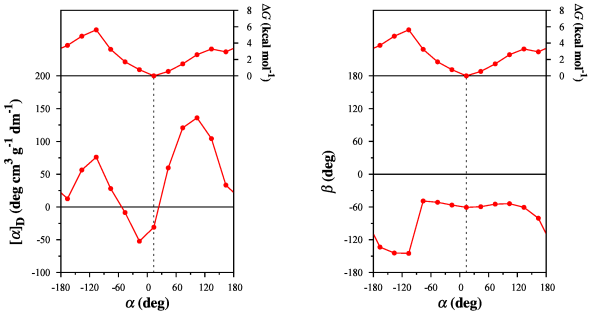

The rotation of the α-hydroxyl group elicits a dramatic change in the calculated $[\alpha]_D$ values for different rotamers (Figure 9.4), due to its direct perturbation of the electronic properties of the ketone chromophore; moreover, most of the rotamers display positive $[\alpha]_D$ values. On the other hand, the orientation of the β-hydroxyl group affects the overall chiroptical properties of **1** to a relatively smaller extent (Figure 9.S3), and most of the rotamers display negative $[\alpha]_D$ values.

The theoretical properties of rotamer **1.01c** (Figure 9.S4) display a particularly good agreement with the experimental data for **1** in solution: the calculated $[\alpha]_D$ (+136) is very close to the experimental value (+147), and the description of the ECD spectrum in the low-energy region (Figure 9.5) is improved.

Figure 9.5. Theoretical spectra of conformer **1.01** and rotamer **1.01c**, as obtained by DFT conformational scan and TD-DFT calculations. *Red:* experimental spectra. *Blue:* theoretical spectra of **1.01**. *Green:* theoretical spectra of **1.01c**. *Left:* ECD spectra. *Center:* ORD spectra. *Right:* UV spectra.

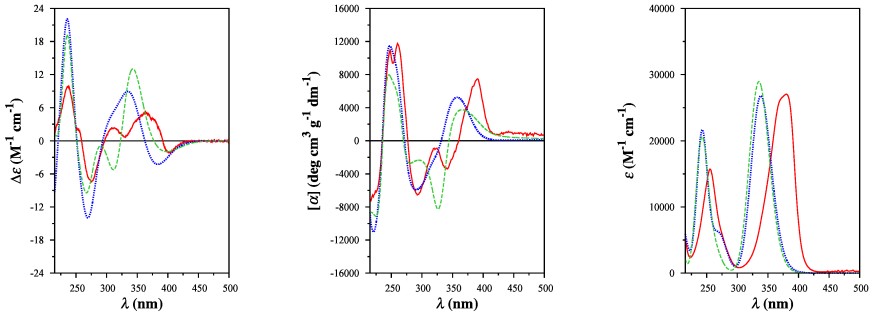

9.1.3 TD-DFT calculations with explicit solvation

A preliminary calculation with explicit treatment of solvation was carried out by direct DFT optimisation of a solvation cluster of **1** with 6 molecules of methanol (Figure 9.S7). Such a strategy fails to sample the possible arrangements of the solute and solvent molecules in solution, and therefore does not describe the dynamic nature of solvation properly. However, calculated properties were clearly improved when TD-DFT calculations were performed on the solute without solvent molecules (calculated $[\alpha]_D = +210$; spectra reported in Figure 9.S8); this behaviour can be explained by the conformational perturbations on the hydroxyl groups due to the interaction with methanol in the solvation cluster, in agreement to what was observed by DFT conformational scan. TD-DFT calculations on the whole cluster did not perform as well (calculated $[\alpha]_D = 0$; spectra reported in Figure 9.S9), since the conformational sampling was inadequate: the direct contribution of solvent molecules to $[\alpha]_D$ was negligible (+1) and did not justify the huge difference between the calculated $[\alpha]_D$ values for the cluster and for the solute alone. These results prompted the application of MD simulations in order to increase the number and quality of solvation clusters for TD-DFT calculations.

The conformational analysis of classical and *ab initio* MD simulations performed on cubic solvation boxes of **1** and 128 molecules of methanol (dihedral distribution functions are reported in Figure 9.6) showed that the two techniques describe the orientation of hydroxyl groups in a different fashion. While results from classical MD are similar to the DFT optimised geometry of **1**, where hydroxyl groups are oriented to favour intramolecular interactions, the *ab initio* MD simulation predicts the occurrence of different orientations for both the α- and the β-hydroxyl groups, consistent with intermolecular interactions with the solvent. The puckering of the cyclohexenone ring and the orientation of the aldehyde moiety are described in the same fashion by both techniques, confirming the limited conformational flexibility of **1** observed in standard DFT optimisations.

The theoretical chiroptical properties of **1** in methanol were then determined as an average over 100 TD-DFT calculations on solvation clusters of **1** with 5 molecules of methanol, randomly sampled from the *ab initio* MD simulation (Figure 9.S10). The inclusion of solvation effects by this technique allows a clear improvement in the agreement between experimental properties of **1** and TD-DFT calculations on the solute (calculated $[\alpha]_D = +88$, spectra reported in Figure 9.7), which is further improved when solvent molecules are included in TD-DFT calculations (calculated $[\alpha]_D = +111$, spectra reported in Figure 9.8).

Figure 9.6. Dihedral distribution functions (DDF) of the main geometric features of **1** in methanol, as obtained by classical (*blue*) and *ab initio* (*red*) MD simulations.

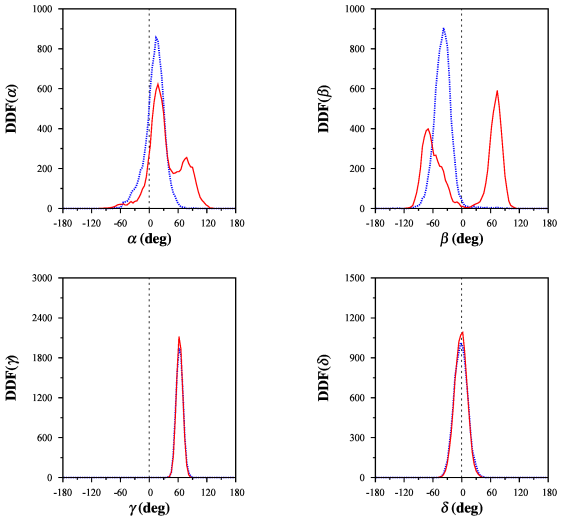

Figure 9.7. Theoretical spectra of **1**, as obtained by TD-DFT calculations performed on **1** alone and taken from the *ab initio* MD trajectory. *Red:* experimental spectra. *Blue:* theoretical spectra. *Left:* ECD spectra. *Center:* ORD spectra. *Right:* UV spectra.

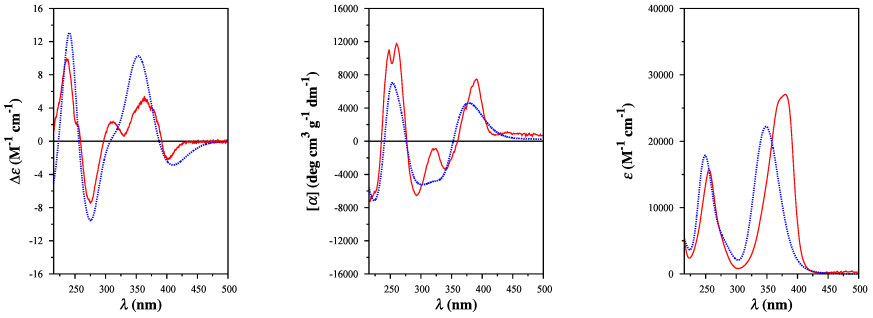

9.2 Conclusions

The present study investigated the performance of different computational methods in the description of solvation effects on theoretically determined chiroptical properties. The study was performed on **1**, a molecule whose absolute stereochemistry was already characterised and whose conformational flexibility was very limited, which is usually an ideal situation for standard TD-DFT calculations. However, very small perturbations to the electronic structure and molecular geometry of **1** induced by solvation result in a dramatic change of chiroptical properties for this system (Table 9.3): standard TD-DFT calculations would have

Figure 9.8. Theoretical spectra of **1**, as obtained by TD-DFT calculations performed on the solvation clusters and taken from the *ab initio* MD trajectory. *Red:* experimental spectra. *Blue/green:* theoretical spectra. *Left:* ECD spectra. *Center:* ORD spectra. *Right:* UV spectra. ORD spectra were calculated with two different molecular weights (236.22 for **1**, *green*; 396.43 for the cluster, *blue*).

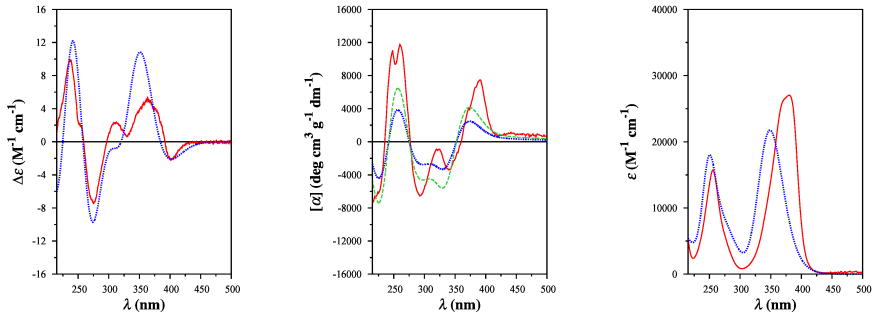

led to an ambiguous or wrong assessment of the absolute configuration of **1**, had the stereochemistry of the system not been fully characterised before. This behaviour is a very powerful example showing the paramount importance of a proper and accurate description of the system for stereochemical studies on chiral molecules of unknown stereochemistry.

The extreme sensitivity of the chiroptical properties of **1** to solvation effects is due to the presence of two hydroxyl groups in α- and β-position to a ketone moiety: the chiral environment of the carbonyl chromophore in solution is dramatically influenced by the network of short-range interactions with solvent molecules, e.g. hydrogen bonds in the case of methanol, involving both the chromophore and the hydroxyl groups. Such interactions cannot be described

Table 9.3. Calculated $[\alpha]_D$ values and orientation of hydroxyl groups for the different computational protocols employed in the generation of input structures for TD-DFT calculations on **1**.

Protocol	$[\alpha]_D$ (deg cm^3 g^{-1} dm^{-1})	α (deg)	β (deg)	γ (deg)	δ (deg)
Experimental in MeOH	+147				
Standard DFT optimisation	−29.03				
Standard DFT optimisation, conformer **1.01**	−30.87	13.700	−60.727	61.382	−1.792
DFT solvation cluster (**1.01***)	+0.03				
DFT solvation cluster, **1** only (**1.01#**)	+210.38	103.552	−74.139	63.756	−12.921
DFT solvation cluster, MeOH only	+1.42				
DFT conformational scan, rotamer **1.01c**	+135.98	103.700	−53.941	62.136	−3.208
Ab initio MD solvation cluster (**md***)	+110.55				
Ab initio MD solvation cluster, **1** only (**md#**)	+87.55		Figure 9.6		

by continuum solvation models, and an explicit treatment of solvent molecules is necessary, which was obtained by an *ab initio* MD simulation of the solvation dynamics of **1**.

The size of the system represented a very challenging task for *ab initio* MD; unfortunately, the huge computational requirements of the technique are still preventing the applicability of *ab initio* MD to stereochemical studies on solvated systems. However, the present study on **1** showed that the accuracy of *ab initio* MD in the description of short-range solute-solvent interactions may become necessary in order to fully understand and characterise very small solvent-related perturbations to the calculated chiroptical properties of molecules.

9.3 Materials and methods

9.3.1 Experimental spectroscopy

Compound **1** was extracted from cultures of *Mycoleptodiscus indicus* according to a recently reported procedure[9] and kindly provided by the research group led by Prof. Jairo K. Bastos (Faculty of Pharmaceutical Sciences of Ribeirão Preto, University of São Paulo, Brazil). The experimental ECD and UV spectra of **1** (concentration: 44.4 μM; pathlength: 1 cm; λ: 500–215 nm) were recorded in methanol (Sigma-Aldrich, Milan, Italy) at room temperature on a Jasco (Tōkyō, Japan) J-810 spectropolarimeter, using a 1 nm spectral bandwidth, a 0.2 nm data interval, a 20 nm min^{-1} scan rate and a 4 s time constant. The ORD spectrum was derived from the ECD spectrum by Kronig-Kramers (KK) transformation, which was performed with the built-in function of the Jasco Spectra Manager 2 software.

The experimental $[\alpha]_D$ value of **1** (concentration: 0.401 g L^{-1}; pathlength: 1 dm; λ: 589 nm) was measured in methanol at room temperature (measured temperature: 22.8 °C) on a Jasco P-2000 polarimeter, using a 5 s time constant over 350 acquisition cycles. $[\alpha]_D^{22.8}$ (MeOH): +147 deg cm^3 g^{-1} dm^{-1} (relative standard deviation: 2.1%).

9.3.2 TD-DFT calculations

TD-DFT calculations for the theoretical determination of $[\alpha]_D$ values and electronic spectra were carried out using the PBE0 functional[155–157] and the TZ2P

basis set, consisting in Dunning's $[5s3p/3s]$ contraction[135] of Huzinaga's primitive $[10s6p/5s]$ set[134] with 2 sets of polarisation functions (α_p = 1.5, 0.375 for H; α_d = 1.5, 0.375 for C; α_d = 1.7, 0.425 for O); the IEFPCM continuum solvation model[114,136] for methanol was employed. Input geometries for TD-DFT calculations were generated using the protocols described in the next sections.

Rotational strengths in dipole velocity formalism (R_j), oscillator strengths (f_j) and excitation wavelengths (λ_j) were determined for the first lowest-energy excited states of each input structure; the theoretical spectra were then determined by approximation of all R_j and f_j values to Gaussian (for UV and ECD) or Lorentzian (for ORD) band shapes centered at the corresponding λ_j values and summation over all calculated excited states, with a spectral damping ($\Delta\sigma$) of 0.25 eV.[28,113]

9.3.3 Standard DFT optimisation

A preliminary conformational search was performed at the MM level using the MMFF94s force field.[125] DFT geometry optimisation was performed on MM conformers within a relative energy (ΔE_{MM}) threshold of 5 kcal mol^{-1} using the B97D functional[153,154] and the TZ2P[134,135] basis set; the IEFPCM continuum solvation model[114,136] for methanol was employed.

TD-DFT calculations were carried out on the optimised geometries of the resulting 3 conformers for the first 50 excited states (Tables 9.S1–9.S2); the overall theoretical spectra of **1** were derived by conformational averaging according to the Boltzmann population of conformers at 298.15 K and 1 atm based on relative free energies (χ_{G}).

9.3.4 DFT conformational scans

The effect of the orientation of O–H bonds on the chiroptical properties of **1** was investigated by two independent conformational scans at the DFT level, one on the hydroxyl group in α position to the ketone chromophore and one on the hydroxyl group in β position. The optimised structure of conformer **1.01** was systematically modified by rotation of the O–H bond by steps of +30°, yielding 11 new rotamers for each conformational scan.

After DFT optimisation at the B97D/TZ2P level, TD-DFT calculations for the first 50 excited states were performed on all the rotamers (Figures 9.S5–9.S6,

Tables 9.S4–9.S7), which were labelled **1.01a–k** for the rotation of the α-hydroxyl group and **1.01l–v** for the rotation of the β-hydroxyl group.

9.3.5 DFT optimisation on a solvation cluster

The input structure for a solvation cluster of **1** with methanol was generated by a preliminary MMFF94s energy minimisation on a system consisting of conformer **1.01** and 50 methanol molecules randomly distributed around the solute; molecules of methanol not interacting with **1** were removed. Repeated cycles of energy minimisation and removal of redundant solvent molecules led to the identification of a solvation cluster with 6 molecules of methanol interacting with **1** through hydrogen bonding: the selected input structure was then optimised at the B97D/TZ2P level.

After DFT optimisation, TD-DFT calculations were performed on the whole solvation cluster and separately on **1** and methanol, in order to evaluate their separate contribution to the calculated properties of the solvation cluster; the first 50 excited states were considered.

9.3.6 Classical MD simulation

Preliminary classical MD simulations[235] were used to create the starting structure of the subsequent *ab initio* MD simulation[236,237] of the solvation dynamics of **1** in methanol. The system consisted of one molecule of **1** inside cubic solvation boxes of different sizes under periodic boundary conditions (PBC). 5 ns (Δt = 0.8 fs) simulations were carried out in a NVT ensemble, using a velocity rescaling thermostat[238] at different temperatures ranging from 273 K to 323 K (τ_T = 0.05 ps). The OPLS-AA force field[239] was employed in combination with PME electrostatics.[240] The standard parameters for methanol were previously employed for accurate simulations of the solvent bulk properties,[241] while several sets of customised OPLS-AA parameters for **1** were prepared and tested for their accuracy in reproducing the main geometric features of **1**; the best combination, reported in the Supplementary Information, was chosen for further calculations. RESP charges[242] for **1** were determined by HF/6-311++G**[159,184,243] calculations.

After the optimisation of force field parameters, a PBC cubic box consisting of **1** and 128 molecules of methanol was employed for a 5 ns (Δt = 2 fs) simulation in a NPT ensemble, using the Nosé-Hoover (NH) thermostat[244–246] at 298 K (τ_T

= 1 ps) and the Parrinello-Rahman barostat[247,248] at 1 bar (τ_P = 5 ps), in order to obtain a starting structure for the *ab initio* MD simulation.

9.3.7 *Ab initio* MD simulation

The *ab initio* MD simulation (Δt = 0.5 fs) was carried out in a NVT ensemble, using the NH thermostat at 300 K (τ_T = 50 ps), on a PBC cubic box consisting of **1** and 128 molecules of methanol, which was taken from the optimised classical MD simulation. Born-Oppenheimer molecular dynamics (BOMD) based on the Gaussian and plane wave (GPW) method[249] was performed using the BLYP[131,250] functional with the DFT-D3[251] empirical corrections for dispersion in combination with GTH pseudopotentials[252–254] for core electrons and nuclei and the DZVP-MOLOPT-SR basis set[255] for valence Kohn-Sham orbitals. The cut-off for the plane wave representation of electron density was set to 280 Ry, while the SCF convergence criterion was set to 10^{-6}.[256] Massive equilibration (5.09 ps) was carried out with chains of 3 NH thermostats coupled to each degree of freedom; subsequently, a single NH chain was used for global equilibration (5.00 ps) and production runs (51.97 ps). Despite the size of the system, the tight SCF convergence criterion ensured a good conservation of energy throughout the trajectory (Figure 9.S11).

TD-DFT calculations of chiroptical properties were subsequently carried out on 100 solvation clusters randomly sampled from the production run of the *ab initio* MD simulation (Table 9.S8). Each solvation cluster consisted in **1** and the 5 molecules of methanol closest to the oxygen atoms of **1**. Similarly to the previous protocol for the DFT solvation cluster, TD-DFT calculations for the first 30 excited states were performed on the whole cluster and separately on **1** (Tables 9.S9–9.S12). The overall chiroptical properties of **1** were finally determined by averaging over all 100 input structures.

9.3.8 Software

DFT and TD-DFT calculations were performed using Gaussian 09,[158] while *ab initio* MD simulations and RESP fit calculations were carried out using CP2K.[257] Preliminary MM and MD calculations were performed using Spartan'02[126] and GROMACS,[258,259] respectively. Computational data from DFT and TD-DFT calculations were processed by self-developed UNIX shell scripts, while MD trajectories were analysed with TRAVIS.[260] Plots were created with GNUplot;[261] optimised geometries were rendered with VMD.[209]

Acknowledgements

DFT and TD-DFT calculations were performed on the computing clusters of Prof. Riccardo Zanasi's research group (University of Salerno, Italy); additional high-performance computing resources were provided by CINECA (Casalecchio di Reno, Italy) through the ISCRA funding programme (Class C projects HP10CU0YHL and HP10CRFD44). The classical and *ab initio* MD study was performed on the computing clusters of Prof. Dr. Barbara Kirchner's research group at the University of Leipzig, Germany, as part of the Marco Polo exchange programme funded by the Department of Pharmacy and Biotechnology of the University of Bologna, Italy.

Supplementary material

Standard DFT optimisation

Figure 9.S1. Main geometric parameters of **1**. **a:** dihedral α; **b:** dihedral β; **c:** dihedral γ; **d:** dihedral δ.

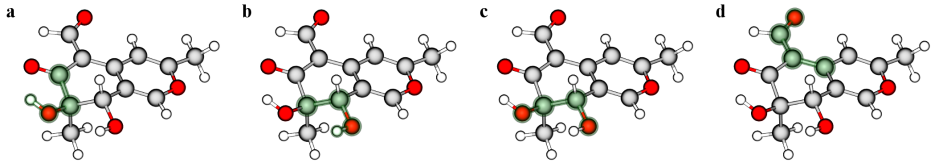

Figure 9.S2. Theoretical spectra of the conformers of **1**, as obtained by standard DFT optimisation and TD-DFT calculations. *Red:* conformer **1.01**. *Blue:* conformer **1.02**. *Green:* conformer **1.03**. *Left:* ECD spectra. *Center:* ORD spectra. *Right:* UV spectra.

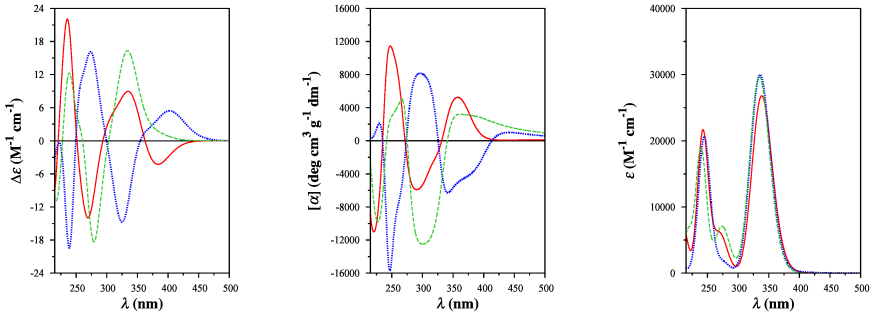

Table 9.S1. Rotational strengths in dipole velocity formalism and excitation wavelengths for the conformers of **1**, as obtained by TD-DFT calculations, and for the DFT solvation cluster of **1** with methanol, as obtained by TD-DFT calculations on the whole cluster (**1.01***) and on **1** alone (**1.01#**).

j	R_j, 10^{-40} erg cm^3 (λ_j, nm)				
	1.01	**1.02**	**1.03**	**1.01***	**1.01#**
1	−15.0330 (378.99)	17.8010 (402.96)	4.3050 (377.74)	−23.0665 (372.99)	−17.0535 (398.99)
2	24.0592 (338.52)	50.1522 (336.48)	41.3631 (334.77)	54.8967 (341.86)	98.6172 (342.10)
3	9.4220 (308.67)	−82.5716 (330.40)	4.7967 (320.38)	−23.9831 (314.86)	−56.0680 (327.08)
4	−14.2381 (274.20)	4.8254 (283.30)	−23.3838 (278.99)	0.3679 (300.20)	3.4420 (283.09)
5	−3.5730 (268.81)	31.9659 (273.75)	−35.1152 (274.52)	0.0066 (284.98)	−40.1875 (272.80)
6	−14.8593 (266.03)	−8.3792 (253.20)	22.6305 (268.31)	0.8702 (277.71)	1.1926 (262.71)
7	−7.4009 (247.98)	96.0265 (248.26)	16.8786 (245.11)	−58.1392 (270.78)	125.8931 (248.90)
8	4.8582 (242.61)	−4.2624 (247.48)	−35.0980 (243.37)	5.7625 (264.53)	−117.8577 (245.11)
9	35.0508 (237.16)	−58.2076 (245.82)	42.0860 (239.80)	−0.6894 (256.27)	3.6601 (243.43)
10	2.5076 (234.17)	−48.1810 (241.16)	0.6301 (233.38)	−0.1359 (253.48)	43.2141 (237.58)
11	9.1960 (227.25)	5.0154 (229.29)	−2.0242 (226.42)	1.5281 (249.44)	−9.2190 (229.18)
12	−21.5263 (211.81)	−8.6450 (208.82)	−19.0839 (217.56)	79.0708 (248.66)	9.5494 (209.31)
13	12.4381 (201.34)	−3.1589 (205.66)	16.0275 (199.67)	69.8517 (244.86)	−18.2399 (203.79)
14	−12.3112 (198.90)	13.4049 (198.43)	−9.5680 (198.03)	−112.6651 (242.59)	−5.8188 (198.42)
15	−6.6207 (196.97)	−11.3308 (195.10)	0.4083 (196.87)	28.2181 (238.77)	−35.3308 (194.28)
16	1.7364 (194.36)	18.1574 (191.24)	−21.3622 (194.74)	3.0426 (231.71)	−3.5267 (192.39)
17	0.2705 (188.67)	−4.5283 (188.75)	4.2247 (187.94)	−7.7042 (229.59)	0.2614 (190.18)
18	12.3003 (183.91)	5.8335 (185.80)	7.8061 (186.12)	−6.3184 (225.87)	7.9007 (187.39)
19	−7.8598 (181.67)	−14.3795 (182.24)	6.6209 (181.97)	−0.8048 (216.36)	9.4220 (183.97)
20	0.2019 (181.26)	−5.3550 (181.87)	−8.5901 (181.34)	−9.7614 (212.63)	16.9233 (179.71)
21	2.0393 (179.21)	7.1967 (178.48)	−13.7224 (177.91)	−2.9691 (210.81)	0.9095 (178.70)
22	−2.8652 (174.14)	3.7637 (175.78)	−2.2525 (176.82)	16.8290 (210.19)	5.9825 (177.52)
23	26.3516 (173.81)	−0.3897 (175.40)	11.7733 (173.08)	0.0569 (207.18)	−2.9607 (174.73)
24	−15.3557 (172.62)	−2.7448 (173.99)	−3.2009 (172.12)	−1.7414 (206.86)	−13.9418 (174.24)
25	11.2065 (168.44)	21.2196 (170.49)	25.5765 (167.64)	−0.1357 (204.45)	−8.2307 (169.67)
26	−21.7944 (167.54)	−19.4134 (167.83)	−11.3259 (167.44)	0.8681 (202.96)	9.0049 (168.89)
27	3.4838 (164.92)	6.5460 (166.06)	−1.4646 (165.95)	4.3320 (202.62)	9.9603 (165.90)
28	7.5486 (162.87)	−1.2899 (163.86)	−15.6259 (165.33)	0.6979 (201.87)	−1.0647 (164.83)
29	−3.3587 (161.90)	10.5737 (163.47)	4.1892 (162.89)	0.5651 (198.72)	14.1649 (164.10)
30	−21.1218 (160.15)	−49.4862 (161.52)	1.3489 (162.55)	1.6538 (197.60)	−14.6878 (163.39)
31	21.5390 (158.92)	8.3004 (160.67)	21.9045 (159.97)	−2.3784 (195.12)	12.0585 (161.87)
32	19.9544 (157.45)	−12.7168 (160.19)	−4.9267 (158.82)	−8.7613 (193.71)	5.3290 (160.70)
33	−9.9787 (156.88)	0.8405 (159.25)	−2.7547 (158.24)	−0.8221 (192.56)	8.2504 (159.72)
34	5.7390 (155.94)	8.0957 (158.75)	17.5138 (157.76)	−23.8034 (191.85)	−19.1244 (157.38)
35	−4.6968 (155.63)	19.2625 (156.89)	18.7057 (155.84)	3.3821 (189.94)	19.4887 (156.66)
36	−4.5708 (154.53)	−0.6344 (154.80)	−10.5710 (155.01)	1.1411 (188.55)	19.6184 (156.15)
37	−3.0172 (153.21)	24.5097 (154.47)	−5.6498 (154.69)	−3.3068 (187.79)	−5.8621 (154.60)
38	2.2145 (152.77)	−0.0582 (153.96)	−1.6912 (153.73)	0.8800 (186.95)	−15.5078 (154.00)
39	−9.8559 (152.17)	6.7424 (153.23)	−0.9947 (153.27)	7.2032 (185.63)	−1.6422 (153.75)
40	5.8089 (151.34)	−3.9143 (152.68)	−13.4196 (152.70)	−0.4519 (185.02)	4.0304 (152.93)
41	−16.9819 (150.67)	−10.9483 (152.29)	−8.8843 (151.88)	−5.5937 (182.67)	−13.4753 (151.93)
42	−13.8159 (150.44)	−26.1342 (150.98)	−7.0510 (151.17)	1.9968 (181.09)	11.8651 (151.15)
43	9.5310 (149.27)	15.0414 (149.79)	−13.3808 (150.14)	13.8720 (179.77)	−25.0841 (150.67)
44	−0.5020 (148.04)	2.9489 (149.44)	−5.1429 (149.29)	2.0003 (178.05)	−4.2480 (150.10)
45	1.0574 (147.79)	−22.7859 (148.96)	−2.7213 (148.64)	−10.7307 (175.88)	−8.5237 (149.88)
46	−21.5434 (147.72)	−6.8207 (148.01)	−3.5815 (148.43)	5.6463 (173.79)	−1.2610 (149.50)
47	9.2701 (147.11)	−1.4875 (147.59)	7.7000 (147.09)	8.3253 (173.03)	−5.1014 (148.56)
48	13.3613 (146.19)	5.5189 (147.44)	28.7698 (146.53)	11.3050 (171.88)	4.4455 (148.18)
49	19.6148 (145.40)	9.1806 (146.60)	−8.5323 (146.17)	−2.2294 (170.44)	3.8238 (148.04)
50	8.3947 (145.21)	4.4086 (145.99)	−5.2196 (145.75)	−23.0978 (169.53)	−20.0681 (147.31)

Table 9.S2. Oscillator strengths and excitation wavelengths for the conformers of **1**, as obtained by TD-DFT calculations, and for the DFT solvation cluster of **1** with methanol, as obtained by TD-DFT calculations on the whole cluster (**1.01***) and on **1** alone (**1.01#**).

j	f_j (λ_j, nm)				
	1.01	**1.02**	**1.03**	**1.01***	**1.01#**
1	0.0015 (378.99)	0.0021 (402.96)	0.0001 (377.74)	0.0058 (372.99)	0.0024 (398.99)
2	0.4132 (338.52)	0.4209 (336.48)	0.4535 (334.77)	0.3641 (341.86)	0.4008 (342.10)
3	0.0010 (308.67)	0.0451 (330.40)	0.0087 (320.38)	0.0099 (314.86)	0.0285 (327.08)
4	0.0514 (274.20)	0.0028 (283.30)	0.0391 (278.99)	0.0109 (300.20)	0.0011 (283.09)
5	0.0087 (268.81)	0.0240 (273.75)	0.0415 (274.52)	0.0035 (284.98)	0.0202 (272.80)
6	0.0358 (266.03)	0.0056 (253.20)	0.0370 (268.31)	0.0091 (277.71)	0.0351 (262.71)
7	0.0336 (247.98)	0.1110 (248.26)	0.0309 (245.11)	0.0555 (270.78)	0.0904 (248.90)
8	0.2859 (242.61)	0.0088 (247.48)	0.0039 (243.37)	0.0647 (264.53)	0.1424 (245.11)
9	0.0171 (237.16)	0.0817 (245.82)	0.2310 (239.80)	0.0011 (256.27)	0.0345 (243.43)
10	0.0054 (234.17)	0.1319 (241.16)	0.0404 (233.38)	0.0003 (253.48)	0.0948 (237.58)
11	0.0156 (227.25)	0.0207 (229.29)	0.0158 (226.42)	0.0019 (249.44)	0.0211 (229.18)
12	0.0929 (211.81)	0.0073 (208.82)	0.0878 (217.56)	0.0887 (248.66)	0.0473 (209.31)
13	0.0490 (201.34)	0.0049 (205.66)	0.0533 (199.67)	0.1201 (244.86)	0.0693 (203.79)
14	0.0089 (198.90)	0.1016 (198.43)	0.0027 (198.03)	0.0665 (242.59)	0.0023 (198.42)
15	0.0142 (196.97)	0.0450 (195.10)	0.0750 (196.87)	0.0711 (238.77)	0.0620 (194.28)
16	0.0239 (194.36)	0.0186 (191.24)	0.0280 (194.74)	0.0293 (231.71)	0.0585 (192.39)
17	0.0118 (188.67)	0.0059 (188.75)	0.0104 (187.94)	0.0060 (229.59)	0.0022 (190.18)
18	0.0582 (183.91)	0.0928 (185.80)	0.0171 (186.12)	0.0064 (225.87)	0.0047 (187.39)
19	0.0584 (181.67)	0.0034 (182.24)	0.0401 (181.97)	0.0024 (216.36)	0.0866 (183.97)
20	0.0273 (181.26)	0.0079 (181.87)	0.0053 (181.34)	0.0445 (212.63)	0.0191 (179.71)
21	0.0010 (179.21)	0.0012 (178.48)	0.0016 (177.91)	0.0065 (210.81)	0.0153 (178.70)
22	0.0219 (174.14)	0.0037 (175.78)	0.0004 (176.82)	0.0546 (210.19)	0.0048 (177.52)
23	0.0093 (173.81)	0.0072 (175.40)	0.0250 (173.08)	0.0001 (207.18)	0.0062 (174.73)
24	0.0232 (172.62)	0.0227 (173.99)	0.0018 (172.12)	0.0064 (206.86)	0.0298 (174.24)
25	0.0233 (168.44)	0.0718 (170.49)	0.0811 (167.64)	0.0039 (204.45)	0.0333 (169.67)
26	0.1426 (167.54)	0.3145 (167.83)	0.0224 (167.44)	0.0106 (202.96)	0.0065 (168.89)
27	0.0023 (164.92)	0.0261 (166.06)	0.0732 (165.95)	0.0034 (202.62)	0.1877 (165.90)
28	0.1057 (162.87)	0.0086 (163.86)	0.1280 (165.33)	0.0106 (201.87)	0.0224 (164.83)
29	0.0906 (161.90)	0.0011 (163.47)	0.0586 (162.89)	0.0065 (198.72)	0.0635 (164.10)
30	0.0485 (160.15)	0.0308 (161.52)	0.1068 (162.55)	0.0012 (197.60)	0.0076 (163.39)
31	0.0925 (158.92)	0.1434 (160.67)	0.0309 (159.97)	0.0299 (195.12)	0.0244 (161.87)
32	0.0132 (157.45)	0.0286 (160.19)	0.0120 (158.82)	0.0076 (193.71)	0.0385 (160.70)
33	0.0124 (156.88)	0.0094 (159.25)	0.0060 (158.24)	0.0095 (192.56)	0.0298 (159.72)
34	0.0016 (155.94)	0.0416 (158.75)	0.0255 (157.76)	0.0301 (191.85)	0.0105 (157.38)
35	0.0015 (155.63)	0.0030 (156.89)	0.0173 (155.84)	0.0114 (189.94)	0.0939 (156.66)
36	0.0582 (154.53)	0.0017 (154.80)	0.0154 (155.01)	0.0004 (188.55)	0.0550 (156.15)
37	0.0038 (153.21)	0.0157 (154.47)	0.0113 (154.69)	0.0102 (187.79)	0.0014 (154.60)
38	0.0025 (152.77)	0.0234 (153.96)	0.0004 (153.73)	0.0131 (186.95)	0.0056 (154.00)
39	0.0058 (152.17)	0.0120 (153.23)	0.0205 (153.27)	0.0044 (185.63)	0.0012 (153.75)
40	0.0081 (151.34)	0.0197 (152.68)	0.0105 (152.70)	0.0039 (185.02)	0.0007 (152.93)
41	0.0036 (150.67)	0.0024 (152.29)	0.0123 (151.88)	0.0605 (182.67)	0.0242 (151.93)
42	0.0084 (150.44)	0.0648 (150.98)	0.0296 (151.17)	0.0243 (181.09)	0.0369 (151.15)
43	0.0133 (149.27)	0.0121 (149.79)	0.0072 (150.14)	0.0245 (179.77)	0.0109 (150.67)
44	0.0050 (148.04)	0.0003 (149.44)	0.0155 (149.29)	0.0008 (178.05)	0.0020 (150.10)
45	0.0012 (147.79)	0.0186 (148.96)	0.0237 (148.64)	0.0101 (175.88)	0.0101 (149.88)
46	0.0278 (147.72)	0.0051 (148.01)	0.0095 (148.43)	0.0019 (173.79)	0.0024 (149.50)
47	0.0057 (147.11)	0.0020 (147.59)	0.0135 (147.09)	0.0021 (173.03)	0.0082 (148.56)
48	0.0179 (146.19)	0.0074 (147.44)	0.0166 (146.53)	0.0075 (171.88)	0.0016 (148.18)
49	0.0151 (145.40)	0.0150 (146.60)	0.0024 (146.17)	0.0297 (170.44)	0.0019 (148.04)
50	0.0200 (145.21)	0.0112 (145.99)	0.0285 (145.75)	0.0606 (169.53)	0.0218 (147.31)

DFT conformational scans

Table 9.S3. Geometric parameters, energies and $[\alpha]_D$ values for the rotamers of conformer **1.01**, as obtained by DFT conformational scan on the α- and β-hydroxyl groups.

Conf. ID	α (deg)	β (deg)	γ (deg)	δ (deg)	ΔG (kcal mol^{-1})	$[\alpha]_D$ (deg cm^3 g^{-1} dm^{-1})
1.01	13.700	−60.727	61.382	−1.792	0.000	**−30.89**
1.01a	43.700	−59.612	62.739	−2.987	0.538	**+59.70**
1.01b	73.700	−54.795	63.148	−3.239	1.468	**+120.70**
1.01c	103.700	−53.941	62.136	−3.208	2.581	**+135.98**
1.01d	133.700	−60.786	61.841	−3.227	3.287	**+104.34**
1.01e	163.700	−80.654	61.914	−3.294	2.931	**+33.42**
1.01f	−166.300	−133.417	60.600	−3.673	3.717	**+12.45**
1.01g	−136.300	−144.310	57.906	−3.612	4.842	**+56.35**
1.01h	−106.300	−144.874	57.554	−3.522	5.622	**+76.03**
1.01i	−76.300	−49.088	59.470	−3.061	3.239	**+28.09**
1.01j	−46.300	−51.426	57.836	−2.089	1.711	**−8.65**
1.01k	−16.300	−56.473	58.422	−1.100	0.752	**−52.25**
1.01l	14.354	−30.728	59.543	−1.931	0.126	**−26.80**
1.01m	17.102	−0.727	58.791	−2.125	1.742	**−9.13**
1.01n	16.826	29.273	58.825	−1.995	1.497	**+5.27**
1.01o	16.185	59.273	60.061	−1.631	1.130	**−35.63**
1.01p	15.730	89.272	60.249	−1.021	1.834	**−97.43**
1.01q	15.032	119.272	60.459	−0.420	4.160	**−103.33**
1.01r	16.955	149.272	57.756	−2.298	4.807	**−41.91**
1.01s	17.928	179.273	59.935	−2.756	2.926	**−35.16**
1.01t	17.490	−150.728	62.092	−2.348	1.727	**−52.54**
1.01u	16.773	−120.728	63.318	−2.044	1.474	**−56.12**
1.01v	15.776	−90.728	63.223	−1.894	0.578	**−42.87**

Figure 9.S3. Dependence of calculated $[\alpha]_D$ values and orientation of the α-hydroxyl group upon rotation of the β-hydroxyl group of conformer **1.01**, as obtained by DFT conformational scan and TD-DFT calculations. Conformer **1.01** is marked with a dotted line.

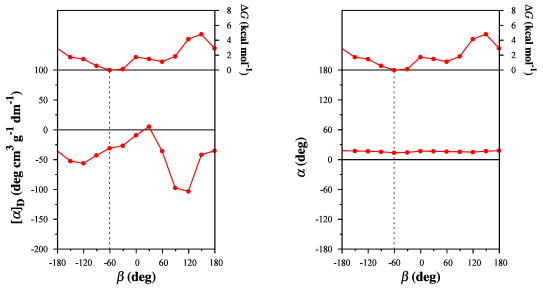

Figure 9.S4. Graphical representation of rotamer **1.01c**, as obtained by DFT conformational scan.

Figure 9.S5. Theoretical ECD and UV spectra of the rotamers of **1.01**, as obtained by TD-DFT calculations after DFT conformational scan on the α-hydroxyl group.

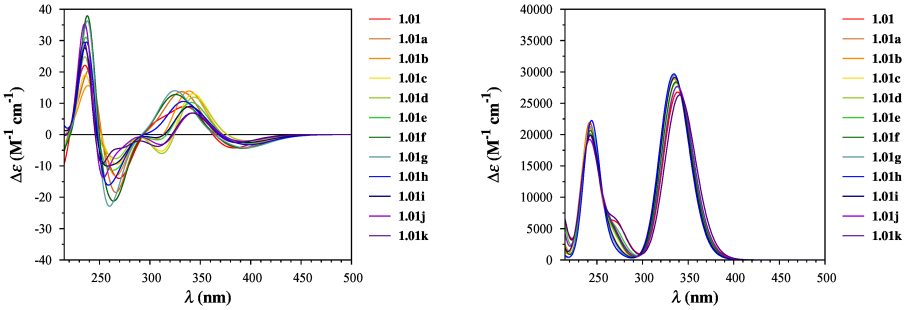

Figure 9.S6. Theoretical ECD and UV spectra of the rotamers of **1.01**, as obtained by TD-DFT calculations after DFT conformational scan on the β-hydroxyl group.

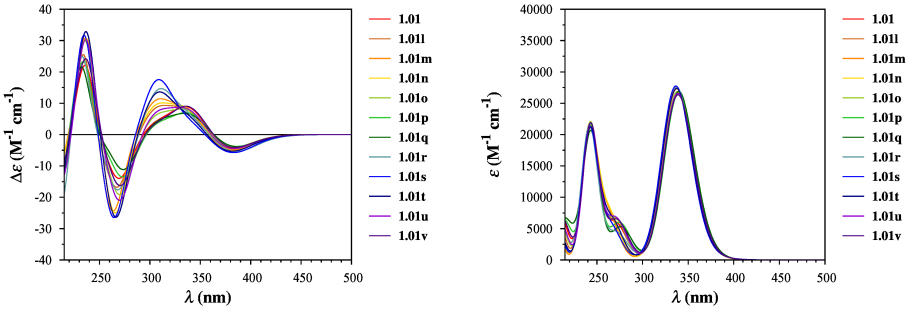

Table 9.S4. Rotational strengths in dipole velocity formalism and excitation wavelengths for the rotamers of **1.01**, as obtained by TD-DFT calculations after DFT conformational scan on the α-hydroxyl group.

j	R_j, 10^{-40} erg cm^3 (λ_j, nm)					
	1.01a	**1.01b**	**1.01c**	**1.01d**	**1.01e**	**1.01f**
1	−14.2837 (387.16)	−9.8491 (393.65)	−6.7912 (395.12)	−6.8342 (392.98)	−10.0647 (390.74)	−14.2784 (391.49)
2	32.2785 (334.94)	53.2032 (334.57)	61.9244 (335.71)	52.1679 (336.99)	35.1534 (338.00)	15.2643 (336.70)
3	9.4603 (316.79)	−22.2262 (322.23)	−41.9723 (323.29)	−36.2909 (321.99)	−13.0985 (320.56)	23.7828 (320.36)
4	−0.4376 (273.81)	1.7777 (277.68)	3.9145 (278.83)	5.6594 (277.95)	5.3946 (276.31)	0.8368 (275.04)
5	−36.2363 (266.32)	−29.0451 (266.54)	−26.2966 (267.14)	−25.4446 (267.97)	−23.9016 (269.30)	−26.9183 (268.38)
6	−3.3105 (264.34)	−1.0094 (259.41)	5.0126 (260.15)	6.8443 (263.47)	−1.1047 (266.75)	−14.4966 (264.26)
7	−23.8192 (246.39)	−33.1870 (244.90)	−13.6341 (245.24)	−9.4411 (246.15)	−32.7768 (247.22)	−53.6010 (247.39)
8	145.2175 (241.56)	50.9710 (243.38)	9.1751 (243.50)	−17.2818 (242.99)	−16.3133 (242.11)	−44.9189 (241.34)
9	−91.1341 (240.74)	0.9679 (241.32)	−1.4431 (241.87)	0.8704 (240.71)	29.9360 (239.67)	153.1361 (240.65)
10	2.6926 (238.20)	9.1322 (236.80)	40.8555 (236.01)	65.0937 (237.05)	62.1585 (238.74)	−0.3939 (239.39)
11	11.3044 (228.75)	5.9825 (229.24)	−3.8760 (225.77)	−6.4969 (221.66)	−0.0221 (214.48)	−2.5275 (225.13)
12	−38.3712 (205.54)	10.2437 (205.34)	11.2230 (206.56)	3.6921 (207.46)	−12.7796 (208.55)	−34.1528 (205.14)
13	9.1958 (202.48)	−41.0171 (200.50)	−25.0245 (200.99)	−12.0270 (203.24)	1.6032 (204.06)	8.7452 (203.54)
14	−7.1308 (198.79)	2.7547 (197.65)	−11.4895 (194.78)	−7.1276 (196.01)	−9.9961 (200.71)	6.3851 (198.16)
15	0.8278 (195.95)	0.5055 (193.28)	3.7952 (192.80)	−23.5731 (193.15)	−16.3294 (196.11)	2.5439 (193.54)
16	1.6770 (193.21)	−6.5515 (190.57)	−17.9451 (189.90)	7.0798 (189.92)	4.3919 (191.31)	5.0546 (189.16)
17	−3.1058 (189.38)	−4.8316 (188.83)	2.3584 (186.59)	7.3457 (185.28)	6.1209 (185.80)	−7.7016 (187.24)
18	7.9232 (184.04)	9.6220 (184.60)	10.5685 (184.73)	−6.6360 (184.37)	5.4929 (181.90)	−4.1358 (183.82)
19	−1.7011 (180.85)	13.2785 (180.16)	11.3919 (182.02)	27.4314 (180.85)	5.3357 (179.83)	6.0185 (180.94)
20	8.9735 (179.05)	11.4402 (178.94)	17.5208 (179.05)	−5.9488 (178.72)	−14.4457 (177.24)	−6.8083 (178.96)
21	0.6713 (178.70)	−3.8100 (178.56)	−9.8750 (178.46)	−4.9548 (178.14)	11.6554 (176.17)	6.8974 (177.58)
22	−11.0292 (174.96)	−6.4622 (175.91)	−3.8684 (176.35)	−0.2364 (176.09)	−11.2139 (174.28)	1.0485 (176.32)
23	23.9099 (174.41)	4.9011 (173.84)	0.2087 (172.57)	5.3849 (171.34)	6.2551 (171.86)	0.7942 (172.25)
24	−15.4675 (172.89)	−13.0545 (171.68)	−5.2334 (170.91)	−2.1247 (170.88)	−10.6200 (170.14)	−4.4966 (171.79)
25	7.1862 (167.84)	−2.1101 (167.79)	−9.2174 (167.84)	−9.3221 (168.50)	4.8758 (167.26)	−3.7301 (170.40)
26	−16.1180 (167.24)	−4.6717 (167.30)	−1.0473 (167.65)	−1.0652 (167.08)	−0.3705 (166.63)	−1.3413 (170.12)
27	−3.0877 (164.42)	−4.2009 (163.91)	−5.8484 (163.85)	−6.7712 (163.98)	−8.2089 (164.89)	6.1813 (165.11)
28	17.1972 (163.02)	12.8723 (162.75)	4.9122 (162.13)	−1.8162 (162.26)	6.6018 (163.48)	−19.9257 (164.09)
29	−2.5940 (161.46)	13.4389 (161.75)	15.8711 (161.61)	29.4160 (161.73)	17.9213 (163.12)	−4.5104 (163.23)
30	−14.4289 (160.29)	3.8818 (160.77)	−12.5080 (160.28)	−19.1614 (161.28)	−0.1077 (161.64)	3.5436 (161.41)
31	6.2007 (159.44)	−21.5193 (160.30)	5.9351 (159.17)	9.7921 (159.59)	4.1809 (160.62)	4.2745 (160.76)
32	28.3277 (158.15)	21.3085 (158.04)	0.3974 (158.03)	−0.9429 (159.02)	0.6727 (160.21)	29.4555 (157.45)
33	3.8648 (157.25)	4.2576 (157.57)	13.0913 (157.63)	−43.5045 (156.94)	−35.4678 (158.65)	1.0812 (156.81)
34	24.4958 (155.98)	27.7551 (155.74)	5.7280 (156.37)	43.3914 (156.33)	15.5217 (157.48)	−23.6802 (156.59)
35	−2.8887 (155.30)	−2.8807 (154.97)	−0.3610 (154.79)	2.2515 (155.63)	21.6336 (156.40)	−3.1285 (155.72)
36	−17.2705 (154.43)	2.6364 (154.65)	6.4335 (154.71)	−1.3645 (154.70)	−1.1878 (154.72)	−2.7957 (154.76)
37	−4.5775 (154.17)	−19.2983 (153.63)	−2.3108 (153.87)	0.5375 (154.01)	−2.9884 (154.23)	0.5892 (154.51)
38	−2.2782 (152.70)	−4.6348 (153.33)	−22.8702 (153.62)	−21.9157 (153.45)	−2.2971 (153.46)	−11.4095 (154.27)
39	−14.5194 (151.86)	−26.2721 (152.07)	−0.4486 (152.06)	0.5400 (152.37)	−5.2167 (152.76)	−11.2785 (152.85)
40	1.0548 (151.00)	2.0746 (151.70)	7.5016 (151.86)	1.5072 (151.86)	1.6550 (152.23)	−4.6363 (151.69)
41	10.1954 (150.43)	10.3024 (150.90)	−0.3465 (151.31)	1.9736 (151.14)	−44.0769 (151.18)	17.6685 (150.97)
42	−4.9225 (149.31)	−0.5296 (150.64)	−5.2968 (151.04)	4.3328 (150.55)	−5.3480 (150.69)	4.8756 (150.74)
43	−19.4839 (148.42)	7.3971 (148.53)	−2.1624 (149.47)	−2.2982 (149.76)	−3.1373 (150.47)	−22.2808 (150.08)
44	5.0723 (148.13)	3.1962 (148.11)	−1.0160 (148.93)	−1.2575 (149.17)	7.0455 (148.97)	−14.1880 (149.91)
45	−6.7715 (147.84)	−3.8551 (147.50)	2.3593 (148.19)	−4.0878 (148.58)	−5.7398 (148.90)	−10.9597 (148.81)
46	1.4324 (147.38)	−11.7223 (147.35)	−7.7097 (147.92)	−8.2231 (148.32)	8.3505 (148.49)	14.3864 (148.56)
47	−12.5396 (146.46)	−2.0374 (146.93)	4.0786 (147.58)	−0.1928 (147.77)	23.0892 (147.16)	−0.7693 (146.91)
48	5.0522 (146.04)	9.7695 (146.18)	−5.1966 (146.82)	0.9814 (146.89)	−2.9161 (146.80)	−0.7221 (146.75)
49	−8.3066 (145.63)	3.2285 (146.04)	−4.3889 (146.66)	−13.4317 (146.48)	−1.9509 (146.54)	−1.8886 (146.01)
50	−0.3244 (145.30)	−8.7910 (145.81)	−1.1137 (146.17)	13.6787 (146.36)	−1.6093 (146.44)	−3.7715 (145.72)

Table 9.S4. (*Continued*)

j	R_j, 10^{-40} erg cm^3 (λ_j, nm)				
	1.01g	**1.01h**	**1.01i**	**1.01j**	**1.01k**
1	−13.6965 (394.78)	−10.6215 (397.38)	−8.4011 (394.80)	−7.3842 (388.23)	−9.6828 (380.68)
2	9.9841 (334.84)	26.7908 (334.31)	35.0328 (335.35)	25.9181 (338.40)	22.2401 (340.78)
3	29.6739 (322.28)	2.7008 (324.06)	−15.0709 (323.24)	−15.5182 (319.56)	−11.9997 (312.45)
4	0.8387 (276.80)	1.8896 (278.58)	2.8516 (278.09)	4.5786 (275.98)	0.9171 (274.68)
5	−23.4010 (267.28)	−21.5365 (267.44)	−21.7212 (268.25)	−20.3144 (268.80)	−22.3602 (269.15)
6	−19.9568 (257.52)	−8.4349 (254.47)	5.5010 (259.40)	10.7842 (263.59)	14.6392 (265.75)
7	−68.4414 (247.02)	−113.1516 (245.42)	−70.2749 (246.18)	−51.3574 (247.73)	−16.3726 (248.22)
8	82.0315 (241.66)	−1.5271 (243.21)	44.1460 (242.88)	−16.1091 (242.14)	−69.2799 (241.89)
9	0.3774 (241.26)	147.3473 (242.16)	14.5506 (242.67)	16.6241 (238.83)	117.6795 (237.95)
10	38.2076 (240.13)	−2.4161 (237.14)	45.4208 (235.70)	85.7071 (237.66)	0.7401 (234.83)
11	−1.1523 (228.86)	9.8266 (233.64)	−2.7828 (223.66)	−3.4796 (223.19)	−2.8659 (224.82)
12	4.0524 (205.07)	7.7894 (206.19)	12.1868 (206.54)	3.9117 (207.28)	−1.9548 (210.30)
13	0.9205 (202.28)	6.3028 (204.73)	−29.5892 (200.84)	−6.7470 (203.08)	9.1089 (202.84)
14	−19.7368 (199.53)	−22.2949 (194.83)	−1.8349 (197.39)	−13.1594 (194.95)	−9.6498 (195.67)
15	4.5824 (191.60)	−5.1580 (193.09)	−2.2377 (193.26)	−2.4558 (191.71)	−21.8028 (194.32)
16	2.7404 (189.90)	1.3712 (188.52)	−12.2654 (189.70)	−9.5672 (191.29)	5.1932 (192.50)
17	−5.6440 (186.20)	0.5443 (187.41)	−1.5421 (185.06)	3.8352 (185.81)	3.8984 (186.71)
18	−0.9542 (183.50)	−3.1077 (182.98)	18.7907 (183.02)	19.0981 (182.41)	14.8486 (182.87)
19	6.0104 (181.86)	9.1066 (182.27)	4.0568 (179.77)	−1.7133 (180.30)	−0.4678 (181.07)
20	−7.3287 (179.91)	−4.0856 (178.59)	−1.5497 (178.71)	0.1205 (179.51)	−2.8307 (180.69)
21	11.8200 (177.77)	6.8331 (178.01)	19.2830 (177.21)	7.2523 (177.69)	0.3199 (178.89)
22	−4.7014 (174.82)	1.1664 (176.03)	−8.7994 (175.78)	−3.8016 (176.23)	1.3380 (175.37)
23	2.3119 (173.06)	−1.3404 (173.76)	0.2152 (172.58)	0.9349 (172.02)	10.4401 (172.43)
24	−26.9459 (172.36)	−39.0976 (172.99)	−22.4795 (170.67)	−15.4091 (170.61)	−4.0798 (172.03)
25	−4.9619 (170.69)	−3.7651 (171.25)	−11.6371 (169.95)	−2.8678 (169.24)	−6.5312 (168.61)
26	10.5928 (169.11)	−19.6698 (168.19)	−1.5121 (165.84)	−0.8436 (168.68)	−1.7567 (168.43)
27	−18.2542 (166.58)	12.9368 (166.91)	4.1179 (165.33)	7.5434 (164.33)	−5.6235 (164.13)
28	0.0248 (164.71)	12.4019 (165.60)	21.6734 (164.15)	−7.1677 (162.04)	14.7411 (163.06)
29	−2.3026 (163.91)	−2.9853 (164.77)	8.8099 (162.15)	23.2409 (161.83)	−19.9367 (160.80)
30	1.7666 (163.43)	−7.0223 (163.23)	−1.5598 (160.80)	−5.6299 (160.51)	24.6634 (159.93)
31	9.8407 (161.46)	10.7565 (162.33)	−1.6784 (160.06)	2.6738 (159.25)	−2.2076 (158.22)
32	24.3435 (159.51)	16.4644 (160.51)	−3.8963 (158.50)	−1.7540 (158.28)	8.1797 (157.67)
33	−10.0620 (157.15)	−12.1374 (157.28)	7.6219 (158.29)	−11.6820 (157.65)	−9.4511 (157.22)
34	−0.8428 (156.31)	0.5416 (156.54)	−3.4380 (156.68)	−2.2961 (156.89)	−24.4258 (156.56)
35	−11.2319 (155.08)	−9.1919 (155.80)	16.7216 (155.57)	−0.9498 (154.98)	−2.8450 (155.34)
36	−0.9877 (154.83)	−0.9403 (154.81)	−2.8629 (154.68)	3.4176 (154.80)	−15.3329 (154.72)
37	39.0235 (154.36)	6.9473 (153.99)	−3.1345 (154.55)	23.7495 (154.15)	14.9188 (154.50)
38	−13.5309 (154.10)	−11.7691 (153.58)	14.2764 (153.99)	−11.3263 (153.70)	3.5965 (153.78)
39	−10.5577 (152.73)	47.4172 (153.38)	−32.7159 (153.25)	−24.2385 (153.24)	−13.5272 (153.12)
40	5.6787 (151.34)	9.1988 (151.52)	−10.6884 (152.05)	−3.7870 (151.36)	−2.9428 (151.56)
41	4.0049 (151.12)	−1.6244 (151.45)	4.4333 (151.46)	19.4105 (151.09)	1.4692 (151.15)
42	14.5595 (151.07)	11.3704 (151.41)	−10.6100 (151.15)	−20.4210 (150.29)	−26.6933 (150.43)
43	−17.2456 (149.03)	10.5144 (149.83)	12.1467 (150.14)	−20.8724 (149.98)	17.1087 (149.76)
44	−4.8846 (148.71)	−3.0012 (148.48)	−0.4254 (149.07)	−8.5803 (149.48)	2.5174 (148.95)
45	−16.9203 (148.44)	−6.3313 (148.04)	−10.8167 (148.45)	−13.7605 (148.89)	−23.2866 (148.22)
46	−7.8722 (148.05)	−13.2016 (147.84)	−12.3862 (147.99)	2.4500 (147.90)	7.5636 (147.88)
47	−4.4620 (146.97)	8.4295 (147.54)	−47.3443 (147.25)	−6.7623 (147.79)	0.1297 (147.11)
48	−5.2671 (146.69)	−26.1117 (147.33)	4.5207 (146.53)	13.1049 (146.70)	21.2270 (146.84)
49	−9.2996 (146.52)	−16.1544 (146.49)	22.4099 (146.38)	3.3458 (146.16)	−8.3801 (145.74)
50	−24.0445 (145.89)	−1.1803 (146.10)	−1.5854 (146.10)	8.0232 (145.54)	1.3723 (145.63)

Table 9.S5. Oscillator strengths and excitation wavelengths for the rotamers of **1.01**, as obtained by TD-DFT calculations after DFT conformational scan on the α-hydroxyl group.

j	f_j (λ_j, nm)					
	1.01a	**1.01b**	**1.01c**	**1.01d**	**1.01e**	**1.01f**
1	0.0013 (387.16)	0.0005 (393.65)	0.0002 (395.12)	0.0002 (392.98)	0.0004 (390.74)	0.0011 (391.49)
2	0.4446 (334.94)	0.4493 (334.57)	0.4351 (335.71)	0.4279 (336.99)	0.4243 (338.00)	0.4369 (336.70)
3	0.0011 (316.79)	0.0064 (322.23)	0.0158 (323.29)	0.0118 (321.99)	0.0033 (320.56)	0.0023 (320.36)
4	0.0006 (273.81)	0.0009 (277.68)	0.0019 (278.83)	0.0044 (277.95)	0.0077 (276.31)	0.0005 (275.04)
5	0.0195 (266.32)	0.0206 (266.54)	0.0188 (267.14)	0.0198 (267.97)	0.0275 (269.30)	0.0199 (268.38)
6	0.0494 (264.34)	0.0388 (259.41)	0.0373 (260.15)	0.0412 (263.47)	0.0427 (266.75)	0.0516 (264.26)
7	0.0708 (246.39)	0.1918 (244.90)	0.2143 (245.24)	0.1915 (246.15)	0.1460 (247.22)	0.1029 (247.39)
8	0.1440 (241.56)	0.0134 (243.38)	0.0015 (243.50)	0.0008 (242.99)	0.0008 (242.11)	0.0861 (241.34)
9	0.1199 (240.74)	0.0131 (241.32)	0.0135 (241.87)	0.0163 (240.71)	0.0665 (239.67)	0.1368 (240.65)
10	0.0081 (238.20)	0.1354 (236.80)	0.1283 (236.01)	0.1457 (237.05)	0.1330 (238.74)	0.0096 (239.39)
11	0.0171 (228.75)	0.0046 (229.24)	0.0030 (225.77)	0.0056 (221.66)	0.0066 (214.48)	0.0010 (225.13)
12	0.1068 (205.54)	0.0420 (205.34)	0.0592 (206.56)	0.1066 (207.46)	0.1299 (208.55)	0.0997 (205.14)
13	0.0066 (202.48)	0.1114 (200.50)	0.0807 (200.99)	0.0239 (203.24)	0.0011 (204.06)	0.0093 (203.54)
14	0.0067 (198.79)	0.0028 (197.65)	0.0386 (194.78)	0.0282 (196.01)	0.0034 (200.71)	0.0307 (198.16)
15	0.0733 (195.95)	0.0343 (193.28)	0.0083 (192.80)	0.0707 (193.15)	0.0641 (196.11)	0.0222 (193.54)
16	0.0026 (193.21)	0.0124 (190.57)	0.0448 (189.90)	0.0053 (189.92)	0.0133 (191.31)	0.0629 (189.16)
17	0.0165 (189.38)	0.0229 (188.83)	0.0336 (186.59)	0.0226 (185.28)	0.0393 (185.80)	0.0085 (187.24)
18	0.0763 (184.04)	0.0893 (184.60)	0.0089 (184.73)	0.0196 (184.37)	0.0685 (181.90)	0.0475 (183.82)
19	0.0526 (180.85)	0.0124 (180.16)	0.0638 (182.02)	0.0697 (180.85)	0.0038 (179.83)	0.0239 (180.94)
20	0.0246 (179.05)	0.0540 (178.94)	0.0173 (179.05)	0.0023 (178.72)	0.0049 (177.24)	0.0121 (178.96)
21	0.0090 (178.70)	0.0014 (178.56)	0.0155 (178.46)	0.0076 (178.14)	0.0036 (176.17)	0.0014 (177.58)
22	0.0123 (174.96)	0.0015 (175.91)	0.0016 (176.35)	0.0005 (176.09)	0.0081 (174.28)	0.0023 (176.32)
23	0.0087 (174.41)	0.0057 (173.84)	0.0013 (172.57)	0.0475 (171.34)	0.0663 (171.86)	0.0005 (172.25)
24	0.0242 (172.89)	0.0326 (171.68)	0.0523 (170.91)	0.0132 (170.88)	0.0975 (170.14)	0.1804 (171.79)
25	0.0655 (167.84)	0.0711 (167.79)	0.0498 (167.84)	0.0576 (168.50)	0.0011 (167.26)	0.0469 (170.40)
26	0.0434 (167.24)	0.0100 (167.30)	0.0064 (167.65)	0.0007 (167.08)	0.0023 (166.63)	0.0017 (170.12)
27	0.0066 (164.42)	0.1730 (163.91)	0.2285 (163.85)	0.2190 (163.98)	0.0703 (164.89)	0.0609 (165.11)
28	0.1507 (163.02)	0.0147 (162.75)	0.0035 (162.13)	0.0096 (162.26)	0.0850 (163.48)	0.0703 (164.09)
29	0.0665 (161.46)	0.0084 (161.75)	0.0376 (161.61)	0.0242 (161.73)	0.0479 (163.12)	0.1010 (163.23)
30	0.0480 (160.29)	0.0515 (160.77)	0.0114 (160.28)	0.0179 (161.28)	0.0042 (161.64)	0.0239 (161.41)
31	0.0069 (159.44)	0.0203 (160.30)	0.0242 (159.17)	0.0141 (159.59)	0.0346 (160.62)	0.0608 (160.76)
32	0.0729 (158.15)	0.0883 (158.04)	0.0280 (158.03)	0.0196 (159.02)	0.0296 (160.21)	0.0430 (157.45)
33	0.0242 (157.25)	0.0289 (157.57)	0.0419 (157.63)	0.1390 (156.94)	0.0748 (158.65)	0.0045 (156.81)
34	0.0097 (155.98)	0.0081 (155.74)	0.0012 (156.37)	0.0645 (156.33)	0.1276 (157.48)	0.0070 (156.59)
35	0.0035 (155.30)	0.0058 (154.97)	0.0007 (154.79)	0.0202 (155.63)	0.0111 (156.40)	0.0047 (155.72)
36	0.0440 (154.43)	0.0468 (154.65)	0.1185 (154.71)	0.0023 (154.70)	0.0021 (154.72)	0.0014 (154.76)
37	0.0022 (154.17)	0.0049 (153.63)	0.0030 (153.87)	0.0030 (154.01)	0.0020 (154.23)	0.0023 (154.51)
38	0.0034 (152.70)	0.0033 (153.33)	0.0328 (153.62)	0.0029 (153.45)	0.0049 (153.46)	0.0030 (154.27)
39	0.0043 (151.86)	0.0082 (152.07)	0.0001 (152.06)	0.0002 (152.37)	0.0003 (152.76)	0.0015 (152.85)
40	0.0235 (151.00)	0.0034 (151.70)	0.0192 (151.86)	0.0033 (151.86)	0.0029 (152.23)	0.0076 (151.69)
41	0.0337 (150.43)	0.1088 (150.90)	0.0378 (151.31)	0.0487 (151.14)	0.0298 (151.18)	0.0617 (150.97)
42	0.0279 (149.31)	0.0031 (150.64)	0.0172 (151.04)	0.0020 (150.55)	0.0264 (150.69)	0.0062 (150.74)
43	0.0055 (148.42)	0.0011 (148.53)	0.0041 (149.47)	0.0127 (149.76)	0.0035 (150.47)	0.0198 (150.08)
44	0.0035 (148.13)	0.0019 (148.11)	0.0004 (148.93)	0.0026 (149.17)	0.0011 (148.97)	0.0478 (149.91)
45	0.0029 (147.84)	0.0086 (147.50)	0.0080 (148.19)	0.0111 (148.58)	0.0094 (148.90)	0.0051 (148.81)
46	0.0022 (147.38)	0.0084 (147.35)	0.0034 (147.92)	0.0008 (148.32)	0.0069 (148.49)	0.0037 (148.56)
47	0.0245 (146.46)	0.0014 (146.93)	0.0021 (147.58)	0.0007 (147.77)	0.0028 (147.16)	0.0059 (146.91)
48	0.0055 (146.04)	0.0072 (146.18)	0.0006 (146.82)	0.0036 (146.89)	0.0031 (146.80)	0.0039 (146.75)
49	0.0395 (145.63)	0.0011 (146.04)	0.0010 (146.66)	0.0015 (146.48)	0.0143 (146.54)	0.0181 (146.01)
50	0.0003 (145.30)	0.0042 (145.81)	0.0010 (146.17)	0.0040 (146.36)	0.0003 (146.44)	0.0012 (145.72)

Table 9.S5. (*Continued*)

j	f_j (λ_j, nm)				
	1.01g	**1.01h**	**1.01i**	**1.01j**	**1.01k**
1	0.0010 (394.78)	0.0005 (397.38)	0.0003 (394.80)	0.0002 (388.23)	0.0004 (380.68)
2	0.4508 (334.84)	0.4570 (334.31)	0.4462 (335.35)	0.4256 (338.40)	0.4058 (340.78)
3	0.0038 (322.28)	0.0012 (324.06)	0.0040 (323.24)	0.0041 (319.56)	0.0033 (312.45)
4	0.0007 (276.80)	0.0005 (278.58)	0.0010 (278.09)	0.0062 (275.98)	0.0343 (274.68)
5	0.0172 (267.28)	0.0162 (267.44)	0.0180 (268.25)	0.0275 (268.80)	0.0365 (269.15)
6	0.0387 (257.52)	0.0303 (254.47)	0.0350 (259.40)	0.0422 (263.59)	0.0281 (265.75)
7	0.0827 (247.02)	0.1556 (245.42)	0.1948 (246.18)	0.1528 (247.73)	0.1069 (248.22)
8	0.2272 (241.66)	0.0172 (243.21)	0.0170 (242.88)	0.0009 (242.14)	0.1208 (241.89)
9	0.0112 (241.26)	0.1552 (242.16)	0.0172 (242.67)	0.0282 (238.83)	0.1107 (237.95)
10	0.0078 (240.13)	0.0029 (237.14)	0.1261 (235.70)	0.1661 (237.66)	0.0071 (234.83)
11	0.0022 (228.86)	0.0073 (233.64)	0.0027 (223.66)	0.0042 (223.19)	0.0049 (224.82)
12	0.0015 (205.07)	0.0100 (206.19)	0.0476 (206.54)	0.1271 (207.28)	0.1258 (210.30)
13	0.0512 (202.28)	0.0273 (204.73)	0.1036 (200.84)	0.0098 (203.08)	0.0131 (202.84)
14	0.0483 (199.53)	0.1450 (194.83)	0.0118 (197.39)	0.0670 (194.95)	0.0264 (195.67)
15	0.1075 (191.60)	0.0019 (193.09)	0.0446 (193.26)	0.0037 (191.71)	0.0329 (194.32)
16	0.0256 (189.90)	0.0741 (188.52)	0.0224 (189.70)	0.0119 (191.29)	0.0106 (192.50)
17	0.0045 (186.20)	0.0038 (187.41)	0.0547 (185.06)	0.0518 (185.81)	0.0236 (186.71)
18	0.0427 (183.50)	0.0131 (182.98)	0.0477 (183.02)	0.0404 (182.41)	0.0680 (182.87)
19	0.0251 (181.86)	0.0518 (182.27)	0.0049 (179.77)	0.0143 (180.30)	0.0041 (181.07)
20	0.0141 (179.91)	0.0018 (178.59)	0.0169 (178.71)	0.0037 (179.51)	0.0096 (180.69)
21	0.0026 (177.77)	0.0031 (178.01)	0.0037 (177.21)	0.0019 (177.69)	0.0001 (178.89)
22	0.0039 (174.82)	0.0058 (176.03)	0.0066 (175.78)	0.0013 (176.23)	0.0025 (175.37)
23	0.0235 (173.06)	0.0093 (173.76)	0.0037 (172.58)	0.0011 (172.02)	0.0391 (172.43)
24	0.2129 (172.36)	0.2371 (172.99)	0.0917 (170.67)	0.0890 (170.61)	0.0147 (172.03)
25	0.0006 (170.69)	0.0016 (171.25)	0.0208 (169.95)	0.0772 (169.24)	0.1763 (168.61)
26	0.0019 (169.11)	0.0715 (168.19)	0.0655 (165.84)	0.0005 (168.68)	0.0021 (168.43)
27	0.1265 (166.58)	0.0043 (166.91)	0.0079 (165.33)	0.1788 (164.33)	0.0475 (164.13)
28	0.0120 (164.71)	0.0031 (165.60)	0.1311 (164.15)	0.0380 (162.04)	0.1283 (163.06)
29	0.0105 (163.91)	0.0159 (164.77)	0.0291 (162.15)	0.0196 (161.83)	0.0515 (160.80)
30	0.0114 (163.43)	0.0149 (163.23)	0.0149 (160.80)	0.0021 (160.51)	0.0592 (159.93)
31	0.0511 (161.46)	0.0136 (162.33)	0.0044 (160.06)	0.1600 (159.25)	0.0661 (158.22)
32	0.0820 (159.51)	0.1177 (160.51)	0.1596 (158.50)	0.0160 (158.28)	0.0359 (157.67)
33	0.0024 (157.15)	0.0028 (157.28)	0.0249 (158.29)	0.0073 (157.65)	0.0107 (157.22)
34	0.0008 (156.31)	0.0046 (156.54)	0.0008 (156.68)	0.0017 (156.89)	0.0113 (156.56)
35	0.0061 (155.08)	0.0057 (155.80)	0.0261 (155.57)	0.0137 (154.98)	0.0025 (155.34)
36	0.0015 (154.83)	0.0008 (154.81)	0.0131 (154.68)	0.0125 (154.80)	0.0091 (154.72)
37	0.0405 (154.36)	0.0060 (153.99)	0.0047 (154.55)	0.0208 (154.15)	0.0429 (154.50)
38	0.0430 (154.10)	0.0108 (153.58)	0.0054 (153.99)	0.0204 (153.70)	0.0048 (153.78)
39	0.0020 (152.73)	0.1192 (153.38)	0.0078 (153.25)	0.0175 (153.24)	0.0138 (153.12)
40	0.0125 (151.34)	0.0109 (151.52)	0.0037 (152.05)	0.0059 (151.36)	0.0013 (151.56)
41	0.0466 (151.12)	0.0043 (151.45)	0.0042 (151.46)	0.0072 (151.09)	0.0034 (151.15)
42	0.0068 (151.07)	0.0468 (151.41)	0.0422 (151.15)	0.0468 (150.29)	0.0098 (150.43)
43	0.0086 (149.03)	0.0033 (149.83)	0.0057 (150.14)	0.0061 (149.98)	0.0203 (149.76)
44	0.0235 (148.71)	0.0275 (148.48)	0.0113 (149.07)	0.0108 (149.48)	0.0008 (148.95)
45	0.0132 (148.44)	0.0139 (148.04)	0.0028 (148.45)	0.0063 (148.89)	0.0182 (148.22)
46	0.0079 (148.05)	0.0015 (147.84)	0.0122 (147.99)	0.0119 (147.90)	0.0009 (147.88)
47	0.0047 (146.97)	0.0095 (147.54)	0.0497 (147.25)	0.0016 (147.79)	0.0006 (147.11)
48	0.0048 (146.69)	0.0059 (147.33)	0.0034 (146.53)	0.0077 (146.70)	0.0106 (146.84)
49	0.0044 (146.52)	0.0029 (146.49)	0.0236 (146.38)	0.0014 (146.16)	0.0077 (145.74)
50	0.0395 (145.89)	0.0084 (146.10)	0.0039 (146.10)	0.0064 (145.54)	0.0056 (145.63)

Table 9.S6. Rotational strengths in dipole velocity formalism and excitation wavelengths for the rotamers of **1.01**, as obtained by TD-DFT calculations after DFT conformational scan on the β-hydroxyl group.

j	R_j, 10^{-40} erg cm^3 (λ_j, nm)					
	1.01l	**1.01m**	**1.01n**	**1.01o**	**1.01p**	**1.01q**
1	−16.2582 (378.40)	−16.8959 (377.87)	−15.7955 (377.47)	−14.0577 (378.92)	−12.9878 (382.10)	−13.0850 (383.37)
2	20.7539 (337.64)	20.0434 (336.97)	21.5560 (337.19)	20.4381 (338.42)	18.6345 (339.80)	17.3271 (339.79)
3	20.1135 (307.50)	25.8793 (307.05)	22.1304 (307.09)	14.7344 (308.16)	8.6053 (309.67)	10.5063 (309.70)
4	−17.3768 (270.26)	5.5227 (268.73)	2.2449 (268.87)	−20.8993 (272.20)	−14.1251 (277.09)	−10.5753 (278.34)
5	−0.9071 (268.45)	−37.5527 (264.92)	−35.8157 (266.24)	−11.7732 (269.41)	−16.8504 (270.52)	−18.8099 (271.11)
6	−19.4655 (264.81)	−19.1489 (263.17)	−20.9240 (264.71)	−10.0527 (267.50)	−0.5406 (269.25)	3.1871 (269.84)
7	−2.7371 (247.66)	8.3184 (248.17)	−3.2947 (249.06)	−6.6846 (248.81)	−6.8839 (249.02)	−7.3425 (249.16)
8	−7.4793 (242.03)	−23.4189 (246.60)	4.4690 (244.71)	−0.5127 (243.31)	−3.6099 (243.29)	6.3168 (243.63)
9	−0.2921 (238.80)	16.6463 (241.12)	30.2703 (237.95)	53.3589 (236.58)	18.9178 (237.30)	−6.6623 (238.35)
10	45.1948 (234.86)	49.9612 (235.43)	26.2515 (235.45)	4.0536 (234.51)	23.1224 (236.26)	17.4726 (236.80)
11	9.5919 (233.39)	3.6118 (233.02)	2.7645 (233.11)	4.9956 (228.54)	20.4066 (224.39)	33.6980 (229.48)
12	−31.1943 (209.12)	−32.5086 (206.00)	−23.1397 (207.60)	−22.8335 (211.68)	−24.6861 (214.50)	−26.4226 (215.39)
13	−2.8714 (198.97)	0.2045 (199.17)	4.2082 (199.76)	5.7853 (201.14)	9.9209 (203.18)	14.6339 (203.90)
14	17.3948 (197.49)	1.5594 (196.40)	3.5044 (196.99)	7.7523 (198.79)	−0.6424 (199.99)	0.1180 (200.69)
15	−4.0672 (196.29)	5.6611 (194.47)	−0.3441 (195.44)	−1.7098 (197.64)	−2.5310 (199.39)	−6.9727 (197.57)
16	−1.9029 (193.25)	9.5524 (193.05)	5.0560 (193.56)	0.0514 (193.42)	−5.9722 (193.77)	−8.7630 (195.01)
17	−3.8111 (189.51)	−4.0380 (191.76)	−4.2636 (189.26)	−6.2886 (188.38)	−7.6868 (188.98)	−2.8527 (190.00)
18	7.6973 (186.02)	−4.9587 (186.40)	−13.8192 (186.33)	−8.2723 (184.14)	4.4702 (187.62)	3.3732 (189.33)
19	8.0031 (181.65)	10.9721 (183.58)	19.6331 (182.32)	10.3122 (182.53)	9.6598 (182.92)	7.6698 (183.98)
20	−4.7641 (180.28)	8.9964 (181.24)	6.1262 (181.78)	−10.4731 (181.73)	−4.2651 (181.86)	−8.5389 (182.91)
21	−0.8463 (179.27)	−9.9983 (180.44)	−7.4333 (178.82)	19.7753 (181.03)	−0.1803 (180.28)	−0.7909 (181.26)
22	−1.3145 (178.31)	4.7835 (177.07)	16.3950 (178.22)	13.1975 (174.39)	3.2638 (174.71)	4.1117 (175.81)
23	37.8231 (173.81)	21.7820 (174.05)	1.0031 (173.52)	−1.2155 (173.55)	0.8952 (173.57)	23.5844 (174.94)
24	−19.9815 (172.93)	−5.5478 (172.45)	4.6566 (171.38)	−11.1708 (171.36)	−2.9769 (171.04)	−17.5579 (173.59)
25	−8.0397 (169.66)	−10.2368 (170.52)	−7.5199 (171.16)	3.1421 (169.02)	−0.7599 (168.47)	−0.1299 (169.65)
26	−16.1503 (167.25)	−23.0722 (167.23)	−38.6171 (167.38)	−45.0513 (167.62)	−23.4498 (167.18)	−29.0474 (167.39)
27	1.6532 (163.38)	−6.1384 (164.21)	−11.7126 (164.81)	−7.0381 (164.69)	0.2824 (164.06)	−5.3143 (164.50)
28	−6.1784 (162.05)	−9.5217 (162.08)	1.3794 (162.39)	1.2130 (162.89)	−9.7346 (163.22)	−2.8640 (162.77)
29	1.2687 (161.05)	−2.7559 (159.57)	−4.4978 (159.35)	−5.4248 (160.03)	−0.5210 (161.42)	10.2848 (161.38)
30	−18.8666 (159.41)	2.4657 (158.75)	−1.3717 (159.08)	13.4405 (159.60)	1.3761 (160.38)	6.7698 (160.81)
31	35.8975 (158.09)	−15.5203 (158.36)	18.9239 (158.20)	5.2189 (158.95)	−8.9995 (159.65)	−13.7291 (160.67)
32	−10.3232 (157.34)	20.2549 (157.30)	2.2015 (157.33)	4.4197 (157.84)	21.4589 (159.15)	−6.9365 (160.08)
33	25.0383 (156.95)	43.9308 (157.07)	26.5920 (156.92)	20.0174 (157.52)	−3.7544 (157.94)	35.0923 (158.87)
34	−0.9300 (155.80)	−0.5766 (155.80)	−0.2854 (155.43)	−5.3273 (155.04)	22.3855 (155.88)	−0.6593 (155.88)
35	12.6713 (155.46)	15.9893 (155.23)	14.5549 (154.57)	27.2144 (154.09)	−0.8639 (155.16)	2.8361 (155.37)
36	−19.9459 (153.94)	−19.8119 (153.42)	−3.4672 (153.23)	−3.0151 (153.79)	11.3324 (154.77)	16.5129 (155.21)
37	−0.6314 (152.66)	−0.5074 (152.70)	−16.9780 (153.06)	−23.0007 (153.69)	−5.1363 (154.10)	−8.2381 (154.02)
38	−1.9012 (152.22)	−1.7552 (151.73)	0.2414 (151.94)	−4.2220 (152.85)	4.3966 (153.78)	3.9060 (153.85)
39	−8.8559 (151.91)	−6.7673 (151.42)	5.0056 (151.13)	8.7891 (152.54)	−1.1941 (153.25)	0.3908 (153.13)
40	6.9859 (150.84)	−11.3506 (150.19)	−33.6334 (150.18)	−9.1409 (152.08)	−4.0967 (152.76)	−6.7535 (152.80)
41	−7.7236 (149.69)	−1.4596 (149.19)	1.2548 (149.85)	−2.4092 (150.72)	−9.0851 (151.65)	−16.8690 (152.01)
42	−17.2899 (149.46)	−25.0626 (148.69)	−7.4300 (149.04)	−6.6567 (150.08)	−10.8071 (150.70)	−0.8877 (151.65)
43	4.6402 (148.94)	9.5469 (148.45)	14.5442 (148.91)	−19.8646 (149.58)	−32.5256 (150.25)	−32.5330 (150.58)
44	−32.3769 (147.93)	2.3210 (147.86)	3.9463 (148.55)	4.7304 (149.31)	6.3011 (149.71)	−5.8129 (150.20)
45	2.2699 (147.68)	9.8682 (147.46)	−1.1215 (147.74)	−1.3040 (148.74)	3.4484 (149.22)	2.5353 (149.15)
46	11.8212 (147.18)	−39.2014 (147.11)	−21.9798 (147.39)	6.4483 (147.49)	7.8467 (147.63)	7.0064 (148.05)
47	0.7734 (146.79)	30.4546 (146.60)	19.0024 (146.99)	15.8526 (147.23)	0.5811 (147.47)	8.6328 (147.91)
48	22.5660 (145.78)	3.4834 (145.83)	−4.4194 (146.15)	−10.8847 (146.74)	5.7104 (147.28)	15.1134 (147.53)
49	−12.5144 (145.12)	−9.9214 (145.57)	−9.2677 (145.68)	4.0646 (145.92)	−4.6498 (146.71)	−8.3074 (147.09)
50	14.6920 (145.05)	2.2840 (144.75)	−2.5182 (145.14)	−0.7050 (145.50)	1.5931 (145.80)	4.9985 (146.66)

Table 9.S6. (*Continued*)

j	R_j, 10^{-40} erg cm^3 (λ_j, nm)				
	1.01r	**1.01s**	**1.01t**	**1.01u**	**1.01v**
1	−17.7542 (383.64)	−18.4585 (381.56)	−17.4823 (379.22)	−15.7053 (378.56)	−14.6039 (379.00)
2	14.7887 (337.45)	9.8699 (336.65)	14.2507 (337.32)	21.1131 (338.60)	24.6312 (338.97)
3	34.9460 (308.91)	42.8958 (307.94)	32.4386 (307.83)	17.2012 (308.49)	8.3313 (309.04)
4	−9.8773 (274.52)	6.0806 (270.70)	1.9803 (270.23)	−21.8013 (273.17)	−16.7360 (275.24)
5	−5.6310 (269.32)	−33.4683 (265.82)	−32.1449 (267.20)	−6.7260 (269.42)	−6.0368 (269.40)
6	−24.7008 (266.45)	−28.2445 (264.41)	−26.7911 (265.92)	−19.3032 (266.95)	−15.5643 (266.93)
7	−12.8313 (247.98)	−12.7219 (248.21)	−6.9956 (248.92)	−7.5463 (248.87)	−7.9107 (248.58)
8	43.3266 (242.91)	9.6979 (246.83)	3.9158 (244.36)	5.7716 (243.54)	7.4546 (243.20)
9	−62.5426 (239.80)	−3.6630 (241.54)	32.6378 (238.35)	52.6672 (237.00)	39.5626 (237.36)
10	0.4798 (236.59)	32.7942 (235.60)	26.1773 (235.43)	1.8726 (234.08)	2.3024 (234.39)
11	74.3463 (234.44)	31.2765 (234.57)	6.4405 (234.01)	5.4587 (228.59)	12.9048 (223.57)
12	−39.7140 (211.66)	−36.7651 (208.15)	−29.7137 (209.24)	−26.8195 (212.14)	−23.2396 (213.08)
13	−4.2568 (200.83)	−1.3019 (200.03)	2.8154 (200.01)	5.3257 (201.41)	9.7415 (202.31)
14	3.3175 (199.61)	0.8266 (198.67)	2.0933 (198.26)	4.7413 (198.71)	−10.1046 (199.53)
15	19.6373 (197.74)	4.7362 (193.94)	3.9258 (196.22)	−1.8414 (197.96)	−3.9429 (197.83)
16	0.4345 (192.62)	16.8868 (192.94)	7.4760 (192.08)	−8.0618 (192.43)	−8.2765 (194.15)
17	−8.0288 (190.41)	−0.2260 (190.93)	0.2067 (189.06)	3.8457 (189.13)	6.0168 (189.24)
18	2.0557 (188.80)	−7.0397 (187.54)	−16.7449 (187.12)	−3.3749 (186.50)	3.1112 (185.43)
19	0.9330 (185.79)	−4.8298 (185.34)	3.1974 (184.24)	0.1361 (182.26)	−0.9685 (182.01)
20	6.1465 (182.06)	16.4508 (182.54)	−0.7121 (182.34)	−4.1759 (181.51)	−0.6380 (180.20)
21	−3.1167 (181.05)	4.2196 (181.87)	13.8093 (181.00)	15.0831 (180.60)	6.1872 (179.84)
22	0.8884 (179.71)	−10.7120 (181.07)	3.1184 (178.60)	17.8964 (174.61)	6.2048 (174.03)
23	19.2333 (174.87)	21.8985 (174.84)	21.3692 (174.50)	7.7220 (173.68)	0.5841 (172.97)
24	−8.5153 (173.40)	−8.3374 (173.27)	−12.8469 (173.09)	−18.5696 (172.21)	−5.0131 (170.85)
25	−8.8378 (170.28)	−4.8226 (170.75)	−4.9265 (171.20)	−4.1439 (171.14)	−16.2978 (169.39)
26	−19.1261 (169.71)	−29.2163 (169.12)	−37.3652 (169.08)	−32.5589 (169.13)	19.0480 (168.01)
27	−4.6321 (164.35)	−19.7876 (164.78)	−25.6766 (164.99)	−31.7275 (164.89)	−9.6509 (166.15)
28	1.3731 (162.96)	−2.2538 (163.05)	3.3813 (163.34)	21.6776 (164.20)	−14.0338 (164.01)
29	0.7697 (162.14)	17.4649 (162.24)	23.0247 (161.95)	7.6183 (162.48)	4.2336 (162.43)
30	−24.3436 (160.90)	−31.3476 (160.44)	−22.7661 (160.25)	−14.9539 (160.01)	−5.2124 (159.88)
31	−1.4969 (160.31)	36.6893 (159.34)	26.8202 (158.99)	−10.8804 (159.31)	16.1631 (159.39)
32	26.1140 (158.91)	−6.2714 (157.84)	−3.4328 (158.33)	24.2690 (159.10)	−8.7648 (158.35)
33	39.6700 (157.71)	13.3482 (157.39)	1.4761 (157.61)	−4.3254 (157.93)	−16.7308 (157.68)
34	17.9799 (157.12)	−2.1504 (156.01)	−0.7873 (155.72)	2.1216 (155.55)	25.2091 (155.94)
35	−1.9778 (155.93)	5.7106 (155.73)	2.6807 (155.16)	1.7884 (155.36)	0.7902 (155.56)
36	8.2747 (155.22)	22.4394 (154.63)	5.8360 (153.54)	16.7729 (154.15)	11.2009 (155.24)
37	8.6229 (155.13)	26.9701 (153.64)	−7.8739 (153.13)	−11.3414 (153.19)	1.8746 (153.43)
38	−12.2032 (153.03)	−0.0430 (152.74)	4.6073 (152.40)	7.4261 (153.01)	−1.4379 (152.99)
39	−2.1513 (152.75)	−1.1186 (152.13)	10.3982 (152.32)	19.1705 (152.22)	3.2344 (151.90)
40	−6.5036 (152.30)	−26.8904 (151.89)	6.1109 (152.02)	−7.8536 (151.46)	−29.6653 (151.39)
41	−32.7089 (151.91)	−0.2582 (151.31)	6.4929 (151.29)	−23.3918 (151.34)	−18.6572 (151.26)
42	−11.1313 (151.63)	−1.4316 (150.92)	4.8327 (151.07)	15.5658 (150.90)	1.2547 (150.79)
43	−10.5863 (151.15)	11.0768 (149.36)	−9.7195 (149.38)	−8.7727 (150.62)	9.1160 (149.79)
44	12.3577 (150.38)	−8.9707 (148.53)	15.2445 (148.55)	18.8657 (148.58)	5.1219 (148.82)
45	9.0624 (148.66)	0.5106 (148.17)	10.0287 (147.95)	14.7958 (148.34)	−2.3549 (148.08)
46	−18.9112 (147.94)	3.9165 (147.85)	−13.9242 (147.62)	−5.5924 (147.86)	5.5255 (147.83)
47	28.6064 (147.73)	−5.9166 (147.42)	0.9424 (147.40)	1.3086 (147.52)	−2.7870 (147.45)
48	−2.1801 (147.34)	1.0861 (147.19)	−7.8338 (146.81)	−11.9096 (146.84)	3.7508 (146.93)
49	8.6083 (147.14)	−4.1227 (146.65)	−14.7004 (146.17)	0.8188 (146.13)	3.0640 (145.77)
50	−12.8516 (146.99)	−12.8077 (146.15)	−1.3687 (146.05)	−7.7383 (146.02)	−12.6382 (145.53)

Table 9.S7. Oscillator strengths and excitation wavelengths for the rotamers of **1.01**, as obtained by TD-DFT calculations after DFT conformational scan on the β-hydroxyl group.

j	f_j (λ_j, nm)					
	1.01l	**1.01m**	**1.01n**	**1.01o**	**1.01p**	**1.01q**
1	0.0020 (378.40)	0.0023 (377.87)	0.0019 (377.47)	0.0012 (378.92)	0.0008 (382.10)	0.0008 (383.37)
2	0.4212 (337.64)	0.4247 (336.97)	0.4213 (337.19)	0.4145 (338.42)	0.4104 (339.80)	0.4151 (339.79)
3	0.0019 (307.50)	0.0033 (307.05)	0.0024 (307.09)	0.0013 (308.16)	0.0012 (309.67)	0.0012 (309.70)
4	0.0439 (270.26)	0.0062 (268.73)	0.0075 (268.87)	0.0616 (272.20)	0.0669 (277.09)	0.0622 (278.34)
5	0.0031 (268.45)	0.0266 (264.92)	0.0328 (266.24)	0.0058 (269.41)	0.0132 (270.52)	0.0181 (271.11)
6	0.0431 (264.81)	0.0656 (263.17)	0.0612 (264.71)	0.0331 (267.50)	0.0155 (269.25)	0.0045 (269.84)
7	0.0460 (247.66)	0.0133 (248.17)	0.0020 (249.06)	0.0097 (248.81)	0.0114 (249.02)	0.0113 (249.16)
8	0.2725 (242.03)	0.0804 (246.60)	0.2498 (244.71)	0.3095 (243.31)	0.3071 (243.29)	0.2925 (243.63)
9	0.0062 (238.80)	0.2276 (241.12)	0.0830 (237.95)	0.0270 (236.58)	0.0170 (237.30)	0.0067 (238.35)
10	0.0220 (234.86)	0.0170 (235.43)	0.0061 (235.45)	0.0036 (234.51)	0.0052 (236.26)	0.0016 (236.80)
11	0.0070 (233.39)	0.0046 (233.02)	0.0038 (233.11)	0.0012 (228.54)	0.0176 (224.39)	0.0475 (229.48)
12	0.0827 (209.12)	0.0662 (206.00)	0.0597 (207.60)	0.0732 (211.68)	0.0859 (214.50)	0.0899 (215.39)
13	0.0792 (198.97)	0.0402 (199.17)	0.0432 (199.76)	0.0434 (201.14)	0.0320 (203.18)	0.0349 (203.90)
14	0.0071 (197.49)	0.0006 (196.40)	0.0011 (196.99)	0.0056 (198.79)	0.0062 (199.99)	0.0007 (200.69)
15	0.0135 (196.29)	0.0388 (194.47)	0.0048 (195.44)	0.0010 (197.64)	0.0008 (199.39)	0.0015 (197.57)
16	0.0103 (193.25)	0.0478 (193.05)	0.0553 (193.56)	0.0506 (193.42)	0.0654 (193.77)	0.0612 (195.01)
17	0.0087 (189.51)	0.0036 (191.76)	0.0109 (189.26)	0.0045 (188.38)	0.0030 (188.98)	0.0036 (190.00)
18	0.0283 (186.02)	0.0312 (186.40)	0.0162 (186.33)	0.0268 (184.14)	0.0020 (187.62)	0.0070 (189.33)
19	0.1144 (181.65)	0.0249 (183.58)	0.1032 (182.32)	0.0548 (182.53)	0.1069 (182.92)	0.0558 (183.98)
20	0.0112 (180.28)	0.0530 (181.24)	0.0444 (181.78)	0.0229 (181.73)	0.0050 (181.86)	0.0689 (182.91)
21	0.0049 (179.27)	0.0537 (180.44)	0.0071 (178.82)	0.0430 (181.03)	0.0159 (180.28)	0.0011 (181.26)
22	0.0014 (178.31)	0.0103 (177.07)	0.0131 (178.22)	0.0053 (174.39)	0.0029 (174.71)	0.0140 (175.81)
23	0.0241 (173.81)	0.0083 (174.05)	0.0009 (173.52)	0.0007 (173.55)	0.0269 (173.57)	0.0094 (174.94)
24	0.0089 (172.93)	0.0035 (172.45)	0.0031 (171.38)	0.0322 (171.36)	0.0069 (171.04)	0.0184 (173.59)
25	0.0023 (169.66)	0.0078 (170.52)	0.0116 (171.16)	0.0012 (169.02)	0.0003 (168.47)	0.0004 (169.65)
26	0.1631 (167.25)	0.1804 (167.23)	0.2574 (167.38)	0.3127 (167.62)	0.2981 (167.18)	0.2159 (167.39)
27	0.1589 (163.38)	0.1270 (164.21)	0.0488 (164.81)	0.0289 (164.69)	0.0432 (164.06)	0.0803 (164.50)
28	0.0079 (162.05)	0.0560 (162.08)	0.0649 (162.39)	0.0410 (162.89)	0.0562 (163.22)	0.0522 (162.77)
29	0.0223 (161.05)	0.0007 (159.57)	0.0315 (159.35)	0.0100 (160.03)	0.0048 (161.42)	0.0189 (161.38)
30	0.0579 (159.41)	0.0559 (158.75)	0.0346 (159.08)	0.0528 (159.60)	0.0084 (160.38)	0.0081 (160.81)
31	0.1039 (158.09)	0.0068 (158.36)	0.0332 (158.20)	0.0255 (158.95)	0.0244 (159.65)	0.0379 (160.67)
32	0.0107 (157.34)	0.0554 (157.30)	0.0250 (157.33)	0.0183 (157.84)	0.0194 (159.15)	0.0124 (160.08)
33	0.0139 (156.95)	0.0415 (157.07)	0.0253 (156.92)	0.0352 (157.52)	0.0617 (157.94)	0.1441 (158.87)
34	0.0020 (155.80)	0.0057 (155.80)	0.0131 (155.43)	0.0161 (155.04)	0.1143 (155.88)	0.0319 (155.88)
35	0.0041 (155.46)	0.0114 (155.23)	0.0088 (154.57)	0.0046 (154.09)	0.0051 (155.16)	0.0032 (155.37)
36	0.0489 (153.94)	0.0494 (153.42)	0.0212 (153.23)	0.0104 (153.79)	0.0129 (154.77)	0.0091 (155.21)
37	0.0035 (152.66)	0.0049 (152.70)	0.0430 (153.06)	0.0674 (153.69)	0.0058 (154.10)	0.0032 (154.02)
38	0.0037 (152.22)	0.0024 (151.73)	0.0032 (151.94)	0.0235 (152.85)	0.0015 (153.78)	0.0075 (153.85)
39	0.0022 (151.91)	0.0006 (151.42)	0.0012 (151.13)	0.0150 (152.54)	0.0049 (153.25)	0.0007 (153.13)
40	0.0088 (150.84)	0.0075 (150.19)	0.0141 (150.18)	0.0087 (152.08)	0.0094 (152.76)	0.0046 (152.80)
41	0.0010 (149.69)	0.0002 (149.19)	0.0066 (149.85)	0.0045 (150.72)	0.0066 (151.65)	0.0071 (152.01)
42	0.0075 (149.46)	0.0178 (148.69)	0.0183 (149.04)	0.0021 (150.08)	0.0009 (150.70)	0.0048 (151.65)
43	0.0075 (148.94)	0.0289 (148.45)	0.0356 (148.91)	0.0047 (149.58)	0.0066 (150.25)	0.0055 (150.58)
44	0.0425 (147.93)	0.0096 (147.86)	0.0052 (148.55)	0.0334 (149.31)	0.0070 (149.71)	0.0087 (150.20)
45	0.0010 (147.68)	0.0065 (147.46)	0.0127 (147.74)	0.0093 (148.74)	0.0310 (149.22)	0.0236 (149.15)
46	0.0058 (147.18)	0.0205 (147.11)	0.0246 (147.39)	0.0026 (147.49)	0.0117 (147.63)	0.0118 (148.05)
47	0.0070 (146.79)	0.0475 (146.60)	0.0138 (146.99)	0.0207 (147.23)	0.0080 (147.47)	0.0020 (147.91)
48	0.0474 (145.78)	0.0071 (145.83)	0.0073 (146.15)	0.0079 (146.74)	0.0059 (147.28)	0.0246 (147.53)
49	0.0101 (145.12)	0.0051 (145.57)	0.0010 (145.68)	0.0033 (145.92)	0.0014 (146.71)	0.0042 (147.09)
50	0.0191 (145.05)	0.0018 (144.75)	0.0027 (145.14)	0.0015 (145.50)	0.0042 (145.80)	0.0004 (146.66)

Table 9.S7. (*Continued*)

j	f_j (λ_j, nm)				
	1.01r	**1.01s**	**1.01t**	**1.01u**	**1.01v**
1	0.0023 (383.64)	0.0029 (381.56)	0.0023 (379.22)	0.0016 (378.56)	0.0013 (379.00)
2	0.4242 (337.45)	0.4266 (336.65)	0.4214 (337.32)	0.4098 (338.60)	0.4066 (338.97)
3	0.0058 (308.91)	0.0093 (307.94)	0.0049 (307.83)	0.0016 (308.49)	0.0012 (309.04)
4	0.0432 (274.52)	0.0159 (270.70)	0.0220 (270.23)	0.0645 (273.17)	0.0628 (275.24)
5	0.0012 (269.32)	0.0186 (265.82)	0.0236 (267.20)	0.0031 (269.42)	0.0071 (269.40)
6	0.0271 (266.45)	0.0450 (264.41)	0.0479 (265.92)	0.0374 (266.95)	0.0340 (266.93)
7	0.0290 (247.98)	0.0064 (248.21)	0.0047 (248.92)	0.0101 (248.87)	0.0164 (248.58)
8	0.2106 (242.91)	0.0604 (246.83)	0.2549 (244.36)	0.3074 (243.54)	0.3056 (243.20)
9	0.0726 (239.80)	0.2515 (241.54)	0.0731 (238.35)	0.0240 (237.00)	0.0182 (237.36)
10	0.0084 (236.59)	0.0167 (235.60)	0.0072 (235.43)	0.0043 (234.08)	0.0050 (234.39)
11	0.0343 (234.44)	0.0094 (234.57)	0.0038 (234.01)	0.0017 (228.59)	0.0112 (223.57)
12	0.0773 (211.66)	0.0568 (208.15)	0.0601 (209.24)	0.0784 (212.14)	0.0892 (213.08)
13	0.0759 (200.83)	0.0462 (200.03)	0.0502 (200.01)	0.0443 (201.41)	0.0345 (202.31)
14	0.0053 (199.61)	0.0004 (198.67)	0.0005 (198.26)	0.0065 (198.71)	0.0099 (199.53)
15	0.0094 (197.74)	0.0510 (193.94)	0.0065 (196.22)	0.0010 (197.96)	0.0029 (197.83)
16	0.0176 (192.62)	0.0416 (192.94)	0.0595 (192.08)	0.0518 (192.43)	0.0474 (194.15)
17	0.0089 (190.41)	0.0101 (190.93)	0.0150 (189.06)	0.0018 (189.13)	0.0073 (189.24)
18	0.0033 (188.80)	0.0078 (187.54)	0.0243 (187.12)	0.0480 (186.50)	0.0481 (185.43)
19	0.0136 (185.79)	0.0029 (185.34)	0.0288 (184.24)	0.0441 (182.26)	0.0751 (182.01)
20	0.1240 (182.06)	0.0554 (182.54)	0.0083 (182.34)	0.0157 (181.51)	0.0002 (180.20)
21	0.0076 (181.05)	0.0007 (181.87)	0.0950 (181.00)	0.0412 (180.60)	0.0219 (179.84)
22	0.0087 (179.71)	0.0813 (181.07)	0.0055 (178.60)	0.0072 (174.61)	0.0022 (174.03)
23	0.0324 (174.87)	0.0202 (174.84)	0.0080 (174.50)	0.0012 (173.68)	0.0474 (172.97)
24	0.0031 (173.40)	0.0030 (173.27)	0.0049 (173.09)	0.0326 (172.21)	0.0047 (170.85)
25	0.0038 (170.28)	0.0023 (170.75)	0.0096 (171.20)	0.0130 (171.14)	0.0711 (169.39)
26	0.1038 (169.71)	0.1727 (169.12)	0.2433 (169.08)	0.2584 (169.13)	0.1340 (168.01)
27	0.1956 (164.35)	0.1185 (164.78)	0.0773 (164.99)	0.0684 (164.89)	0.0123 (166.15)
28	0.0085 (162.96)	0.0089 (163.05)	0.0165 (163.34)	0.0223 (164.20)	0.0876 (164.01)
29	0.0144 (162.14)	0.0542 (162.24)	0.0248 (161.95)	0.0206 (162.48)	0.0866 (162.43)
30	0.0377 (160.90)	0.0151 (160.44)	0.0180 (160.25)	0.0044 (160.01)	0.0146 (159.88)
31	0.0113 (160.31)	0.0717 (159.34)	0.0657 (158.99)	0.0261 (159.31)	0.0329 (159.39)
32	0.0290 (158.91)	0.0097 (157.84)	0.0091 (158.33)	0.0210 (159.10)	0.0044 (158.35)
33	0.0672 (157.71)	0.0144 (157.39)	0.0308 (157.61)	0.0541 (157.93)	0.0354 (157.68)
34	0.0529 (157.12)	0.0087 (156.01)	0.0007 (155.72)	0.0020 (155.55)	0.0213 (155.94)
35	0.0240 (155.93)	0.0160 (155.73)	0.0246 (155.16)	0.0213 (155.36)	0.0030 (155.56)
36	0.0042 (155.22)	0.0227 (154.63)	0.0141 (153.54)	0.0548 (154.15)	0.0836 (155.24)
37	0.0285 (155.13)	0.0637 (153.64)	0.0080 (153.13)	0.0030 (153.19)	0.0024 (153.43)
38	0.0076 (153.03)	0.0113 (152.74)	0.0055 (152.40)	0.0079 (153.01)	0.0059 (152.99)
39	0.0010 (152.75)	0.0044 (152.13)	0.0659 (152.32)	0.0378 (152.22)	0.0234 (151.90)
40	0.0037 (152.30)	0.0027 (151.89)	0.0107 (152.02)	0.0090 (151.46)	0.0094 (151.39)
41	0.0038 (151.91)	0.0004 (151.31)	0.0095 (151.29)	0.0219 (151.34)	0.0051 (151.26)
42	0.0123 (151.63)	0.0011 (150.92)	0.0029 (151.07)	0.0056 (150.90)	0.0042 (150.79)
43	0.0024 (151.15)	0.0216 (149.36)	0.0135 (149.38)	0.0228 (150.62)	0.0198 (149.79)
44	0.0098 (150.38)	0.0415 (148.53)	0.0315 (148.55)	0.0201 (148.58)	0.0132 (148.82)
45	0.0178 (148.66)	0.0067 (148.17)	0.0403 (147.95)	0.0236 (148.34)	0.0150 (148.08)
46	0.0328 (147.94)	0.0529 (147.85)	0.0111 (147.62)	0.0008 (147.86)	0.0011 (147.83)
47	0.0289 (147.73)	0.0028 (147.42)	0.0043 (147.40)	0.0008 (147.52)	0.0022 (147.45)
48	0.0053 (147.34)	0.0025 (147.19)	0.0094 (146.81)	0.0048 (146.84)	0.0087 (146.93)
49	0.0060 (147.14)	0.0016 (146.65)	0.0024 (146.17)	0.0050 (146.13)	0.0003 (145.77)
50	0.0034 (146.99)	0.0045 (146.15)	0.0033 (146.05)	0.0086 (146.02)	0.0028 (145.53)

DFT optimisation of a solvation cluster

Figure 9.S7. Graphical representation of the solvation cluster of **1** with methanol, as obtained by DFT optimisation.

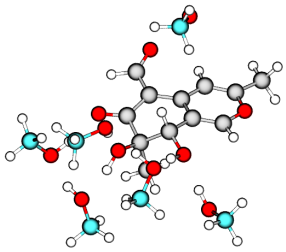

Figure 9.S8. Theoretical spectra of **1**, as obtained by DFT optimisation on a solvation cluster and TD-DFT calculations on **1** alone. *Red:* experimental spectra. *Blue:* theoretical spectra. *Left:* ECD spectra. *Center:* ORD spectra. *Right:* UV spectra.

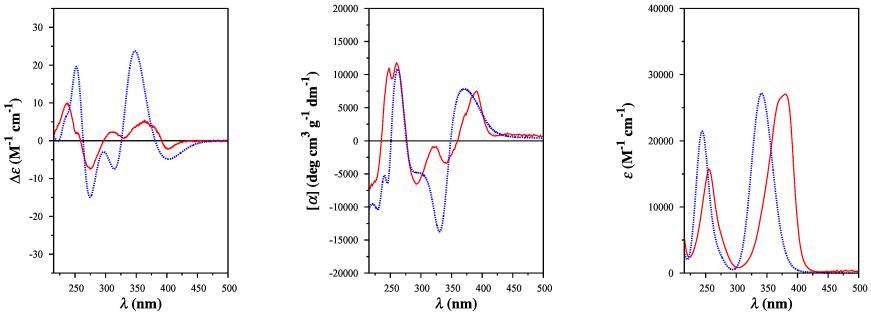

Figure 9.S9. Theoretical spectra of **1**, as obtained by DFT optimisation on a solvation cluster and TD-DFT calculations on the whole cluster. *Red:* experimental spectra. *Blue/green:* theoretical spectra. *Left:* ECD spectra. *Center:* ORD spectra. *Right:* UV spectra. ORD spectra were calculated with two different molecular weights (236.22 for **1**, *green*; 428.48 for the cluster, *blue*).

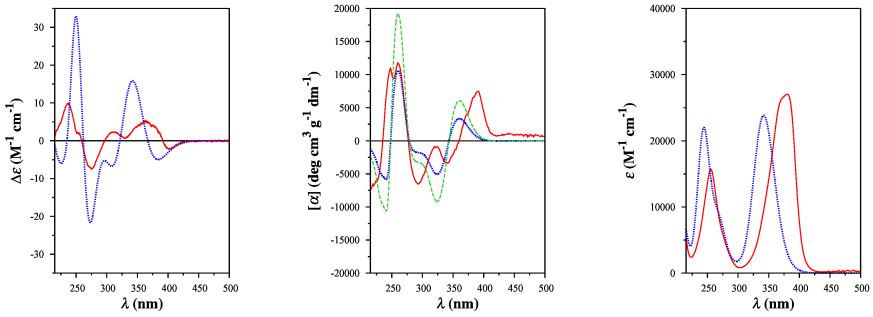

OPLS-AA parameters for austdiol

The OPLS-AA force field does not include default parameters to describe the bond angles and dihedrals for **1**; therefore, a parametrisation for the missing angle and dihedral types was carried out on the basis of the following considerations:

a. the missing angle types were introduced, when possible, with standard parameters for angles between atoms with the same hybridisation;

b. due to the planarity of the pyran ring, the O2 atom was sometimes considered as a sp^2-hybridised atom if no satisfactory parameters involving oxygen were found;

c. the dihedral angles to describe ring puckering and the orientation of hydroxyl groups were described by the standard parameters for the hexopyranose ring of sugars;

Moreover, partial charges were modified according to the values obtained by a RESP fit at the HF/6-311++G** level; bond lengths and angles were also modified according to the optimised geometry of **1** at the HF/6-311++G** level.

The Gromacs topology file for **1** (`austdiol.itp`), containing the optimised force field parameters, is reported below:

```
[ moleculetype ]
; name      nrexcl
austdiol         3

[ atoms ]
; HF/6-311++G** RESP charges are used; standard LJ parameters are also reported.
; Units: q_i (AU), m_i (AU), s_ii (nm), e_ii (KJ mol^-1).
;  i      code res_n  res  name  chgr      q_i       m_i  ; st.q_1 - type          s_ii          e_ii - comments
   1  opls_141     1  AUS     C     1   0.332  12.0110  ;  0.000 - CM    3.55000e-01  3.17984e-01 - C3
   2  opls_142     1  AUS     C     2  -0.285  12.0110  ; -0.115 - CM    3.55000e-01  3.17984e-01 - C4,
        opls_150, C=, same s_ii and e_ii
   3  opls_142     1  AUS     C     1   0.248  12.0110  ; -0.115 - CM    3.55000e-01  3.17984e-01 - C1
   4  opls_141     1  AUS     C     3   0.143  12.0110  ;  0.000 - CM    3.55000e-01  3.17984e-01 - C4a,
        opls_178, C=, same s_ii and e_ii
   5  opls_180     1  AUS     O     1  -0.296  15.9994  ; -0.400 - OS    2.90000e-01  5.85760e-01 - O2
   6  opls_141     1  AUS     C     3  -0.042  12.0110  ;  0.000 - CM    3.55000e-01  3.17984e-01 - C8a,
        opls_178, C=, same s_ii and e_ii
   7  opls_141     1  AUS     C     3  -0.206  12.0110  ;  0.000 - CM    3.55000e-01  3.17984e-01 - C5
   8  opls_280     1  AUS     C     4   0.348  12.0110  ;  0.470 - C_2   3.75000e-01  4.39320e-01 - C6
   9  opls_159     1  AUS     C     5   0.308  12.0110  ;  0.265 - CT    3.50000e-01  2.76144e-01 - C7
  10  opls_158     1  AUS     C     6  -0.182  12.0110  ;  0.205 - CT    3.50000e-01  2.76144e-01 - C8
  11  opls_277     1  AUS     C     7   0.432  12.0110  ;  0.450 - C_2   3.75000e-01  4.39320e-01 - C10
  12  opls_278     1  AUS     O     7  -0.565  15.9994  ; -0.450 - O_2   2.96000e-01  8.78640e-01 - O1
  13  opls_281     1  AUS     O     4  -0.510  15.9994  ; -0.470 - O_2   2.96000e-01  8.78640e-01 - O3
  14  opls_135     1  AUS     C     8  -0.351  12.0110  ; -0.180 - CT    3.50000e-01  2.76144e-01 - C9
  15  opls_169     1  AUS     O     6  -0.589  15.9994  ; -0.700 - OH    3.07000e-01  7.11280e-01 - O5
  16  opls_169     1  AUS     O     5  -0.622  15.9994  ; -0.700 - OH    3.07000e-01  7.11280e-01 - O4
  17  opls_135     1  AUS     C     9  -0.332  12.0110  ; -0.180 - CT    3.50000e-01  2.76144e-01 - C11
  18  opls_279     1  AUS     H     7   0.059   1.0080  ;  0.000 - HC    2.42000e-01  6.27600e-02 - H4
  19  opls_144     1  AUS     H     2   0.191   1.0080  ;  0.115 - HC    2.42000e-01  1.25520e-01 - H3
  20  opls_144     1  AUS     H     1   0.139   1.0080  ;  0.115 - HC    2.42000e-01  1.25520e-01 - H1
  21  opls_140     1  AUS     H     8   0.137   1.0080  ;  0.060 - HC    2.50000e-01  1.25520e-01 - H2a
  22  opls_140     1  AUS     H     8   0.137   1.0080  ;  0.060 - HC    2.50000e-01  1.25520e-01 - H2b
  23  opls_140     1  AUS     H     8   0.137   1.0080  ;  0.060 - HC    2.50000e-01  1.25520e-01 - H2c
  24  opls_140     1  AUS     H     6   0.164   1.0080  ;  0.060 - HC    2.50000e-01  1.25520e-01 - H8
```

```
    25   opls_170     1   AUS     H     6   0.475   1.0080  ;  0.435 - HO    0.00000e+00  0.00000e+00 - H7
    26   opls_140     1   AUS     H     9   0.114   1.0080  ;  0.060 - HC    2.50000e-01  1.25520e-01 - H6a
    27   opls_140     1   AUS     H     9   0.114   1.0080  ;  0.060 - HC    2.50000e-01  1.25520e-01 - H6b
    28   opls_140     1   AUS     H     9   0.114   1.0080  ;  0.060 - HC    2.50000e-01  1.25520e-01 - H6c
    29   opls_170     1   AUS     H     5   0.388   1.0080  ;  0.435 - HO    0.00000e+00  0.00000e+00 - H5

[ pairs ]
; Used to calculate 1-4 interactions. A fudge factor of 0.5 is used for both Coulombic and LJ potentials.
;   i    j  func
     1    6     1
     1    7     1
     2   10     1
     2   11     1
     2   21     1
     2   22     1
     2   23     1
     2    3     1
     2    8     1
     3   15     1
     3   24     1
     3    9     1
     4   12     1
     4   13     1
     4   15     1
     4   18     1
     4   24     1
     4    9     1
     5   10     1
     5   19     1
     5   21     1
     5   22     1
     5   23     1
     5    4     1
     6    1     1
     6   11     1
     6   25     1
     6    8     1
     7   10     1
     7   16     1
     7   17     1
     7    3     1
     8   12     1
     8   15     1
     8   18     1
     8   24     1
     8   26     1
     8   27     1
     8   28     1
     8   29     1
     8    6     1
     9   25     1
    10   26     1
    10   27     1
    10   28     1
    10   29     1
    11   13     1
    11    9     1
    13   10     1
    13   16     1
    13   17     1
    14   19     1
    14    3     1
    14    4     1
    16   15     1
    16   24     1
    16   26     1
    16   27     1
    16   28     1
    16    6     1
    17   15     1
    17   24     1
    17   29     1
    17    6     1
    19    6     1
    19    7     1
    20   10     1
    20    1     1
```

```
  20   4     1
  24  25     1

[ bonds ]
; The potential is expressed as a harmonic function (func 1): V_b = K_b/2*(b-b0)^2. Units: b0 (nm), K_b (KJ mol
      ^-1 nm^-2).
; HF/6-311++G** values are used for b0.
;  i   j  func       b0        K_b   ; st.b0   - type
   1   2     1  0.13380   459403.2  ; 0.13400 - CM CM
   1   5     1  0.13369   376560.0  ; 0.13700 - CM OS
   1  14     1  0.14923   265265.6  ; 0.15100 - CM CT
   2   4     1  0.14437   459403.2  ; 0.13400 - CM CM
   2  19     1  0.10671   284512.0  ; 0.10800 - CM HC
   3   5     1  0.13351   376560.0  ; 0.13700 - CM OS
   3   6     1  0.13290   459403.2  ; 0.13400 - CM CM
   3  20     1  0.10697   284512.0  ; 0.10800 - CM HC
   4   6     1  0.14541   459403.2  ; 0.13400 - CM CM
   4   7     1  0.13766   459403.2  ; 0.13400 - CM CM
   6  10     1  0.15028   265265.6  ; 0.15100 - CM CT
   7   8     1  0.14674   343088.0  ; 0.14440 - CM C_2
   7  11     1  0.14729   343088.0  ; 0.14440 - CM C_2
   8   9     1  0.15330   265265.6  ; 0.15220 - C_2 CT
   8  13     1  0.11994   476976.0  ; 0.12290 - C_2 O_2
   9  10     1  0.15257   224262.4  ; 0.15290 - CT CT
   9  16     1  0.13970   267776.0  ; 0.14100 - CT OH
   9  17     1  0.15328   224262.4  ; 0.15290 - CT CT
  10  15     1  0.13932   267776.0  ; 0.14100 - CT OH
  10  24     1  0.10901   284512.0  ; 0.10900 - CT HC
  11  12     1  0.11951   476976.0  ; 0.12290 - C_2 O_2
  11  18     1  0.10889   284512.0  ; 0.10900 - C_2 HC
  14  21     1  0.10838   284512.0  ; 0.10900 - CT HC
  14  22     1  0.10838   284512.0  ; 0.10900 - CT HC
  14  23     1  0.10838   284512.0  ; 0.10900 - CT HC
  15  25     1  0.09430   462750.4  ; 0.09450 - OH HO
  16  29     1  0.09460   462750.4  ; 0.09450 - OH HO
  17  26     1  0.10837   284512.0  ; 0.10900 - CT HC
  17  27     1  0.10837   284512.0  ; 0.10900 - CT HC
  17  28     1  0.10837   284512.0  ; 0.10900 - CT HC

[ angles ]
; The potential is expressed as a harmonic function (func 1): V_f = K_f/2*(f-f0)^2. Units: f0 (deg), K_f (KJ
      mol^-1 rad^-2).
; HF/6-311++G** values are used for f0.
;  i   j   k  func        f0       K_f  ; st.f0   - type       - comments
   2   1   5     1  122.2575  585.760  ; 123.000 - CM CM OS
   2   1  14     1  125.7201  585.760  ; 124.000 - CM CM CT
   5   1  14     1  112.0211  585.760  ; 123.000 - OS CM CT   - copied from CM CM OS and C= CM OS
   1   2   4     1  120.5581  585.760  ; 124.000 - CM CM CM   - copied from CM C= C= and C= C= CT
   1   2  19     1  119.5265  292.880  ; 120.000 - CM CM HC
   4   2  19     1  119.8833  292.880  ; 120.000 - CM CM HC
   5   3   6     1  123.5495  585.760  ; 123.000 - OS CM CM
   5   3  20     1  112.6723  292.880  ; 114.500 - OS CM HC
   6   3  20     1  123.7776  292.880  ; 120.000 - CM CM HC
   2   4   6     1  114.2648  585.760  ; 124.000 - CM CM CM   - copied from CM C= C= and C= C= CT
   2   4   7     1  124.9715  585.760  ; 124.000 - CM CM CM   - copied from CM C= C= and C= C= CT
   6   4   7     1  120.7636  585.760  ; 124.000 - CM CM CM   - copied from CM C= C= and C= C= CT
   1   5   3     1  119.5220  627.600  ; 111.000 - CM OS CM   - copied from CT OS CM and CM OS CA
   3   6   4     1  119.5402  585.760  ; 124.000 - CM CM CM   - copied from CM C= C= and C= C= CT
   3   6  10     1  121.9782  585.760  ; 124.000 - CM CM CT
   4   6  10     1  118.3900  585.760  ; 124.000 - CM CM CT
   4   7   8     1  119.8895  711.280  ; 120.700 - CM CM C_2
   4   7  11     1  124.1424  711.280  ; 120.700 - CM CM C_2
   8   7  11     1  115.9431  711.280  ; 120.700 - C_2 CM C_2 - copied from C_2 CM CM
   7   8   9     1  118.1668  585.760  ; 116.000 - CM C_2 CT  - copied from C= C_2 CT
   7   8  13     1  123.7819  669.440  ; 125.300 - CM C_2 O_2
   9   8  13     1  117.9913  669.440  ; 125.300 - CT C_2 O_2
   8   9  10     1  107.9693  527.184  ; 111.100 - C_2 CT CT
   8   9  16     1  109.6886  418.400  ; 109.500 - C_2 CT OH
   8   9  17     1  109.3961  527.184  ; 111.100 - C_2 CT CT
  10   9  16     1  106.5363  418.400  ; 109.500 - CT CT OH
  10   9  17     1  113.6121  488.273  ; 112.700 - CT CT CT
  16   9  17     1  109.5551  418.400  ; 109.500 - OH CT CT
   6  10   9     1  110.4398  527.184  ; 112.400 - CM CT CT
   6  10  15     1  112.8384  418.400  ; 109.500 - CM CT OH
   6  10  24     1  107.6148  292.880  ; 109.500 - CM CT HC
   9  10  15     1  112.8384  418.400  ; 109.500 - CT CT OH
   9  10  24     1  106.1940  313.800  ; 110.700 - CT CT HC
```

```
    15   10   24      1  109.5010   292.880  ; 109.500 - OH CT HC
     7   11   12      1  126.1765   669.440  ; 125.300 - CM C_2 O_2
     7   11   18      1  113.6748   292.880  ; 120.000 - CM C_2 HC  - copied from CM CM HC and CM C= HC
    12   11   18      1  120.1487   292.880  ; 123.000 - O_2 C_2 HC
     1   14   21      1  110.0647   292.880  ; 109.500 - CM CT HC
     1   14   22      1  110.0647   292.880  ; 109.500 - CM CT HC
     1   14   23      1  110.0647   292.880  ; 109.500 - CM CT HC
    21   14   22      1  108.8670   276.144  ; 107.800 - HC CT HC
    21   14   23      1  108.8670   276.144  ; 107.800 - HC CT HC
    22   14   23      1  108.8670   276.144  ; 107.800 - HC CT HC
    10   15   25      1  108.6437   460.240  ; 108.500 - CT OH HO
     9   16   29      1  108.5618   460.240  ; 108.500 - CT OH HO
     9   17   26      1  110.2878   313.800  ; 110.700 - CT CT HC
     9   17   27      1  110.2878   313.800  ; 110.700 - CT CT HC
     9   17   28      1  110.2878   313.800  ; 110.700 - CT CT HC
    26   17   27      1  108.6349   276.144  ; 107.800 - HC CT HC
    26   17   28      1  108.6349   276.144  ; 107.800 - HC CT HC
    27   17   28      1  108.6349   276.144  ; 107.800 - HC CT HC

[ dihedrals ]
; In OPLS, torsional potentials are defined by a periodic function expressed as a Fourier series expansion:
; V_w (OPLS) = F1/2*(1+cos(w)) + F2/2*(1-cos(2w)) + F3/2*(1+cos(3w)) + F4/2*(1-cos(4w)).
; In GROMACS, this is implemented in a special form by means of Ryckaert-Bellemans potentials (func 3):
; V_w (GROMACS) = c0 + c1*cos(w-180) + c2*cos^2(w-180) + c3*cos^3(w-180) + c4*cos^4(w-180) + c5*cos^5(w-180).
; Conversions: c0 = F2+(F1+F3)/2 , c1 = (3*F3-F1)/2 , c2 = 4*F4-F2 , c3 = -2*F3 , c4 = -4*F4 , c5 = 0. Units:
      KJ mol^-1.
;  i    j    k    l  func        c0          c1          c2          c3          c4          c5  ; type           - comments
    5    1    2    4     3   58.57600     0.00000   -58.57600    0.00000   0.00000   0.00000  ; OS CM CM CM
    5    1    2   19     3   58.57600     0.00000   -58.57600    0.00000   0.00000   0.00000  ; OS CM CM HC
   14    1    2    4     3   58.57600     0.00000   -58.57600    0.00000   0.00000   0.00000  ; CT CM CM CM
   14    1    2   19     3   58.57600     0.00000   -58.57600    0.00000   0.00000   0.00000  ; CT CM CM HC
    2    1    5    3     3   58.57600     0.00000   -58.57600    0.00000   0.00000   0.00000  ; CM CM OS CM    - copied
      from X CM CM X - alkene
   14    1    5    3     3   58.57600     0.00000   -58.57600    0.00000   0.00000   0.00000  ; CT CM OS CM    - copied
      from X CM CM X - alkene
    2    1   14   21     3   -0.77822    -2.33467    0.00000    3.11290   0.00000   0.00000  ; CM CM CT HC
    2    1   14   22     3   -0.77822    -2.33467    0.00000    3.11290   0.00000   0.00000  ; CM CM CT HC
    2    1   14   23     3   -0.77822    -2.33467    0.00000    3.11290   0.00000   0.00000  ; CM CM CT HC
    5    1   14   21     3   -0.77822    -2.33467    0.00000    3.11290   0.00000   0.00000  ; OS CM CT HC    - copied
      from CM CM CT HC - alkenes all-atom
    5    1   14   22     3   -0.77822    -2.33467    0.00000    3.11290   0.00000   0.00000  ; OS CM CT HC    - copied
      from CM CM CT HC - alkenes all-atom
    5    1   14   23     3   -0.77822    -2.33467    0.00000    3.11290   0.00000   0.00000  ; OS CM CT HC    - copied
      from CM CM CT HC - alkenes all-atom
    1    2    4    6     3   58.57600     0.00000   -58.57600    0.00000   0.00000   0.00000  ; CM CM CM CM
    1    2    4    7     3   58.57600     0.00000   -58.57600    0.00000   0.00000   0.00000  ; CM CM CM CM
   19    2    4    6     3   58.57600     0.00000   -58.57600    0.00000   0.00000   0.00000  ; HC CM CM CM    - copied
      from X CM CM X - alkene
   19    2    4    7     3   58.57600     0.00000   -58.57600    0.00000   0.00000   0.00000  ; HC CM CM CM    - copied
      from X CM CM X - alkene
    6    3    5    1     3   58.57600     0.00000   -58.57600    0.00000   0.00000   0.00000  ; CM CM OS CM    - copied
      from X CM CM X - alkene
   20    3    5    1     3   58.57600     0.00000   -58.57600    0.00000   0.00000   0.00000  ; HC CM OS CM    - copied
      from X CM CM X - alkene
    5    3    6    4     3   58.57600     0.00000   -58.57600    0.00000   0.00000   0.00000  ; OS CM CM CM
    5    3    6   10     3   58.57600     0.00000   -58.57600    0.00000   0.00000   0.00000  ; OS CM CM CT
   20    3    6    4     3   58.57600     0.00000   -58.57600    0.00000   0.00000   0.00000  ; HC CM CM CM    - copied
      from X CM CM X - alkene
   20    3    6   10     3   58.57600     0.00000   -58.57600    0.00000   0.00000   0.00000  ; HC CM CM CT
    2    4    6    3     3   58.57600     0.00000   -58.57600    0.00000   0.00000   0.00000  ; CM CM CM CM
    2    4    6   10     3   58.57600     0.00000   -58.57600    0.00000   0.00000   0.00000  ; CM CM CM CT
    7    4    6    3     3   58.57600     0.00000   -58.57600    0.00000   0.00000   0.00000  ; CM CM CM CM
    7    4    6   10     3   58.57600     0.00000   -58.57600    0.00000   0.00000   0.00000  ; CM CM CM CT
    2    4    7    8     3   58.57600     0.00000   -58.57600    0.00000   0.00000   0.00000  ; CM CM CM C_2
    2    4    7   11     3   58.57600     0.00000   -58.57600    0.00000   0.00000   0.00000  ; CM CM CM C_2
    6    4    7    8     3   58.57600     0.00000   -58.57600    0.00000   0.00000   0.00000  ; CM CM CM C_2
    6    4    7   11     3   58.57600     0.00000   -58.57600    0.00000   0.00000   0.00000  ; CM CM CM C_2
    3    6   10    9     3    0.52719    -6.39734    -1.69452    7.56467   0.00000   0.00000  ; CM CM CT CT
    3    6   10   15     3    1.04600    -1.04600     0.00000    0.00000   0.00000   0.00000  ; CM CM CT OH
    3    6   10   24     3   -0.77822    -2.33467     0.00000    3.11290   0.00000   0.00000  ; CM CM CT HC
    4    6   10    9     3    0.52719    -6.39734    -1.69452    7.56467   0.00000   0.00000  ; CM CM CT CT
    4    6   10   15     3    1.04600    -1.04600     0.00000    0.00000   0.00000   0.00000  ; CM CM CT OH
    4    6   10   24     3   -0.77822    -2.33467     0.00000    3.11290   0.00000   0.00000  ; CM CM CT HC
    4    7    8    9     3    0.83680     0.00000    -0.83680    0.00000   0.00000   0.00000  ; CM CM C_2 CT   - copied
      from CA CA C CT - aryl ketone
    4    7    8   13     3   30.33400    -5.23000   -25.10400    0.00000   0.00000   0.00000  ; CM CM C_2 O_2  - copied
      from CM CM C O - acrolein-like
```

```
  11   7   8   9     3   0.00000    0.00000    0.00000   0.00000  0.00000  0.00000  ; C_2 CM C_2 CT  - copied
        from CM C= C_2 HC - acrolein
  11   7   8  13     3  30.33400    5.23000  -25.10400   0.00000  0.00000  0.00000  ; C_2 CM C_2 O_2 - modified
        from CM CM C O - acrolein-like
   4   7  11  12     3  30.33400   -5.23000  -25.10400   0.00000  0.00000  0.00000  ; CM CM C_2 O_2  - copied
        from CM CM C O - acrolein-like
   4   7  11  18     3   0.83680    0.00000   -0.83680   0.00000  0.00000  0.00000  ; CM CM C_2 HC   - copied
        from CA CA C HC - aryl aldehyde
   8   7  11  12     3  30.33400    5.23000  -25.10400   0.00000  0.00000  0.00000  ; C_2 CM C_2 O_2 - modified
         from CM CM C O - acrolein-like
   8   7  11  18     3   0.00000    0.00000    0.00000   0.00000  0.00000  0.00000  ; C_2 CM C_2 HC  - copied
        from CM C= C_2 HC - acrolein
   7   8   9  10     3   0.81797    7.90567    0.60250  -6.48520  0.00000  0.00000  ; CM C_2 CT CT   - modified
         from CT C_2 CT CT - ketone
   7   8   9  16     3   0.81797   -7.90567    0.60250   6.48520  0.00000  0.00000  ; CM C_2 CT OH   - copied
        from CT C_2 CT CT - ketone
   7   8   9  17     3   0.81797   -7.90567    0.60250   6.48520  0.00000  0.00000  ; CM C_2 CT CT   - copied
        from CT C_2 CT CT - ketone
  13   8   9  10     3   3.10662   -3.77606   -5.13795   5.80739  0.00000  0.00000  ; O_2 C_2 CT CT
  13   8   9  16     3   3.10662   -3.77606   -5.13795   5.80739  0.00000  0.00000  ; O_2 C_2 CT OH  - copied
        from CT CT C_2 O_2 - aldehyde & ketone
  13   8   9  17     3   3.10662   -3.77606   -5.13795   5.80739  0.00000  0.00000  ; O_2 C_2 CT CT
   8   9  10   6     3  -4.23421    7.22159    1.90790  -4.89528  0.00000  0.00000  ; C_2 CT CT CM   - copied
        from C_2 CT CT CT - aldehyde & ketone
   8   9  10  15     3   2.87441    0.58158    2.09200  -5.54799  0.00000  0.00000  ; C_2 CT CT OH
   8   9  10  24     3  -0.15899   -0.47698    0.00000   0.63596  0.00000  0.00000  ; C_2 CT CT HC
  16   9  10   6     3   2.87441    0.58158    2.09200  -5.54799  0.00000  0.00000  ; OH CT CT CM
  16   9  10  15     3  18.96607  -18.96607    0.00000   0.00000  0.00000  0.00000  ; OH CT CT OH    - or
       dih_diols_OH_CT_CT_OH
  16   9  10  24     3   0.97905    2.93716    0.00000  -3.91622  0.00000  0.00000  ; OH CT CT HC
  17   9  10   6     3   2.92880   -1.46440    0.20920  -1.67360  0.00000  0.00000  ; CT CT CT CM
  17   9  10  15     3   2.87441    0.58158    2.09200  -5.54799  0.00000  0.00000  ; CT CT CT OH
  17   9  10  24     3   0.62760    1.88280    0.00000  -2.51040  0.00000  0.00000  ; CT CT CT HC
   8   9  16  29     3  -1.88280    1.88280    0.00000   0.00000  0.00000  0.00000  ; C_2 CT OH HO   - copied
        from C= CT OH HO - allyl alcohols
  10   9  16  29     3  -0.44350    3.83255    0.72801  -4.11705  0.00000  0.00000  ; CT CT OH HO    - or
       dih_hexopyranoses_CT_CT_OH_HO
  17   9  16  29     3  -0.44350    3.83255    0.72801  -4.11705  0.00000  0.00000  ; CT CT OH HO
   8   9  17  26     3  -0.15899   -0.47698    0.00000   0.63596  0.00000  0.00000  ; C_2 CT CT HC
   8   9  17  27     3  -0.15899   -0.47698    0.00000   0.63596  0.00000  0.00000  ; C_2 CT CT HC
   8   9  17  28     3  -0.15899   -0.47698    0.00000   0.63596  0.00000  0.00000  ; C_2 CT CT HC
  10   9  17  26     3   0.62760    1.88280    0.00000  -2.51040  0.00000  0.00000  ; CT CT CT HC
  10   9  17  27     3   0.62760    1.88280    0.00000  -2.51040  0.00000  0.00000  ; CT CT CT HC
  10   9  17  28     3   0.62760    1.88280    0.00000  -2.51040  0.00000  0.00000  ; CT CT CT HC
  16   9  17  26     3   0.97905    2.93716    0.00000  -3.91622  0.00000  0.00000  ; OH CT CT HC
  16   9  17  27     3   0.97905    2.93716    0.00000  -3.91622  0.00000  0.00000  ; OH CT CT HC
  16   9  17  28     3   0.97905    2.93716    0.00000  -3.91622  0.00000  0.00000  ; OH CT CT HC
   6  10  15  25     3  -1.88280    1.88280    0.00000   0.00000  0.00000  0.00000  ; CM CT OH HO
   9  10  15  25     3  -0.44350    3.83255    0.72801  -4.11705  0.00000  0.00000  ; CT CT OH HO    - or
       dih_hexopyranoses_CT_CT_OH_HO
  24  10  15  25     3   0.94140    2.82420    0.00000  -3.76560  0.00000  0.00000  ; HC CT OH HO
; Improper dihedrals to keep groups planar are also defined by Fourier potentials in OPLS (with F1 = F3 = F4 =
    0): V_w (OPLS) = F2*(1-cos(2w)).
; GROMACS defines OPLS impropers as proper dihedrals (func 1): V_w (GROMACS) = K_w*(1+cos(N*w+180-w0)).
; Conversions: K_w = F2 , N = 2. Units: w0 (deg), K_w (KJ mol^-1), N (multiplicity, no units).
; Impropers were not used for austdiol.
;  i   j   k   l  func      w0        K_w  N  ; type
;  13   8   9   7     1  180.0  43.93200  2  ; improper_O_C_X_Y
;  12  11  18   7     1  180.0  43.93200  2  ; improper_O_C_X_Y
;   4   7   6   2     1  180.0  62.76000  2  ; improper_Z_CM_X_Y
;   6   3  10   4     1  180.0  62.76000  2  ; improper_Z_CM_X_Y
;   3   6  20   5     1  180.0  62.76000  2  ; improper_Z_CM_X_Y
;   2   1  19   4     1  180.0  62.76000  2  ; improper_Z_CM_X_Y
;   1   2  14   5     1  180.0  62.76000  2  ; improper_Z_CM_X_Y
; Chirality impropers are not needed in OPLS.
;  10   9   6  15     2     35.000  500.00000     ; chirality restraint
;  10   6   9  24     2     35.000  500.00000     ; chirality restraint
;   9   8  10  17     2     35.000  500.00000     ; chirality restraint
;   9  10   8  16     2     35.000  500.00000     ; chirality restraint

;[ constraints ]
; Constraints were not used for austdiol.
;  i   j  func
;   9  29     2
;  10  25     2
```

Ab initio MD simulation

Figure 9.S10. Graphical representation of a sample solvation cluster of **1** with methanol, as obtained by the *ab initio* MD simulation.

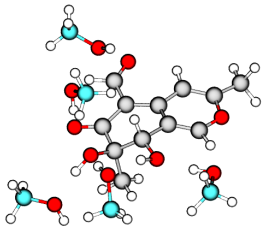

Figure 9.S11. Time evolution of energy and temperature for the *ab initio* MD simulation of **1** in methanol. The blue line represents the linear drift in energy conservation ($3.294 \cdot 10^{-7}$ Ha fs^{-1}).

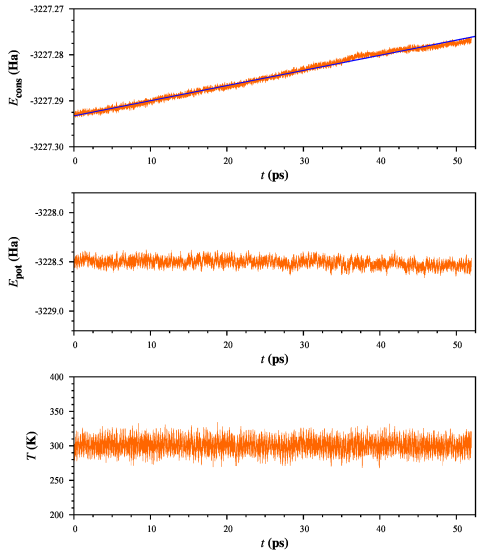

Table 9.S8. Simulation time and calculated $[\alpha]_D$ values for the *ab initio* MD solvation clusters of **1** with methanol, as obtained by TD-DFT calculations on the whole cluster (*) and on **1** alone (#).

Cluster	t (ps)	$[\alpha]_D$ (deg cm^3 g^{-1} dm^{-1}) *	#	Cluster	t (ps)	$[\alpha]_D$ (deg cm^3 g^{-1} dm^{-1}) *	#
md001	0.4790	−129.33	−35.18	**md051**	23.2860	43.98	9.61
md002	0.5765	124.14	351.62	**md052**	23.7175	−116.70	111.97
md003	0.9815	345.57	436.05	**md053**	23.7865	−559.16	−469.75
md004	1.5365	274.80	366.36	**md054**	23.9820	12.56	−73.73
md005	1.6760	289.02	18.66	**md055**	24.6825	401.19	279.74
md006	1.9275	136.20	367.58	**md056**	25.0190	213.46	30.39
md007	2.1840	185.99	173.01	**md057**	25.1185	383.74	310.95
md008	2.5525	431.03	380.03	**md058**	25.2835	452.95	600.85
md009	3.2925	140.03	101.19	**md059**	25.3335	326.94	325.64
md010	3.5390	582.89	513.73	**md060**	25.3795	271.41	514.53
md011	3.8500	−78.33	−207.27	**md061**	26.1835	−161.78	−305.99
md012	3.8830	−156.23	−259.49	**md062**	26.4185	96.88	227.87
md013	4.2670	87.59	−114.58	**md063**	26.6990	−7.51	149.52
md014	4.4900	25.47	3.89	**md064**	26.9690	98.88	19.47
md015	4.6550	−115.58	−177.80	**md065**	27.3330	166.97	14.49
md016	4.9610	83.52	232.77	**md066**	31.2230	181.80	−22.02
md017	5.1645	−64.25	−248.92	**md067**	31.3705	159.56	−48.51
md018	5.2765	335.75	463.10	**md068**	31.9440	412.59	529.70
md019	5.4740	182.87	338.27	**md069**	34.6500	−88.90	15.54
md020	6.2160	22.61	−110.51	**md070**	34.8305	−17.91	−34.15
md021	6.6610	−279.68	−329.10	**md071**	36.7580	199.21	226.28
md022	6.7625	−104.01	91.66	**md072**	37.1350	114.01	95.33
md023	6.7750	−39.93	266.28	**md073**	37.4380	−28.29	−8.86
md024	7.2730	45.93	−79.52	**md074**	37.7085	136.30	396.21
md025	7.3665	−3.63	−343.02	**md075**	38.5785	−124.11	−56.31
md026	7.9755	78.39	−46.53	**md076**	38.5895	−158.77	−276.51
md027	8.3675	381.47	168.34	**md077**	39.8525	61.31	29.27
md028	8.4110	52.88	−80.16	**md078**	40.4135	−253.09	−355.58
md029	8.4275	528.57	835.36	**md079**	40.9230	215.17	127.04
md030	8.4465	97.69	71.06	**md080**	41.2815	357.60	385.41
md031	9.2400	71.05	−78.72	**md081**	41.2865	343.30	414.86
md032	9.3095	−17.89	−334.45	**md082**	41.6780	−23.14	−296.64
md033	10.7230	272.98	630.97	**md083**	41.7370	361.69	314.68
md034	11.5610	−167.90	−582.07	**md084**	41.7905	144.13	265.33
md035	11.8725	28.71	−190.98	**md085**	43.9835	−95.88	−139.22
md036	12.2925	232.54	248.82	**md086**	44.9085	516.24	856.78
md037	13.8155	−0.15	−134.53	**md087**	44.9135	503.95	878.11
md038	13.9820	25.26	−75.44	**md088**	45.2725	437.33	425.13
md039	16.2690	168.56	−7.41	**md089**	45.3305	320.56	396.17
md040	17.3630	−64.57	−247.12	**md090**	45.6070	345.50	464.53
md041	17.7935	257.89	471.58	**md091**	45.7510	−60.08	−294.77
md042	17.8330	−17.48	−434.62	**md092**	45.8265	146.10	297.14
md043	18.7225	478.07	616.64	**md093**	46.5595	112.08	255.24
md044	19.5545	440.08	587.81	**md094**	46.5715	32.49	162.63
md045	19.7660	−371.66	−535.37	**md095**	46.5980	64.64	216.92
md046	20.7525	−9.18	−134.56	**md096**	47.6945	321.81	278.73
md047	20.7960	−83.01	−305.22	**md097**	47.8810	−143.34	−241.86
md048	21.2075	363.36	308.80	**md098**	48.0650	−7.44	−197.34
md049	22.5095	−584.92	−736.45	**md099**	48.3000	237.95	−69.06
md050	22.5905	−17.96	−125.57	**md100**	48.3225	241.95	−70.04

Table 9.S9. Rotational strengths in dipole velocity formalism and excitation wavelengths for the *ab initio* MD solvation clusters of **1** with methanol, as obtained by TD-DFT calculations.

j	R_j, 10^{-40} erg cm^3 (λ_j, nm)									
	md001*	**md002***	**md003***	**md004***	**md005***	**md006***	**md007***	**md008***	**md009***	**md010***
1	−2.9978 (363.28)	36.4328 (361.30)	−2.6172 (374.10)	−15.3201 (417.31)	−41.0387 (395.53)	0.8275 (389.91)	2.4752 (378.63)	−24.0890 (373.48)	−2.5851 (366.84)	5.9303 (411.48)
2	6.4272 (342.35)	−63.8832 (335.51)	119.6299 (337.61)	134.8129 (358.47)	132.9165 (341.88)	−28.2173 (339.47)	11.0254 (352.04)	110.2440 (349.40)	16.3870 (338.58)	83.0705 (362.58)
3	−14.0439 (312.20)	27.1783 (315.56)	−67.6882 (325.30)	−91.6067 (344.78)	−32.4083 (325.52)	56.6904 (321.73)	24.5488 (324.60)	−59.7382 (321.42)	−30.2444 (320.29)	−82.0244 (329.24)
4	0.3821 (298.21)	0.4986 (292.99)	−0.5192 (285.16)	13.4764 (306.27)	−0.5684 (320.81)	0.0279 (293.58)	−19.3183 (284.81)	−18.6990 (291.04)	16.4415 (279.34)	10.1902 (303.38)
5	−1.1995 (294.82)	−0.0080 (292.80)	−30.3639 (280.78)	−2.5856 (299.75)	−0.1689 (297.33)	−0.4623 (292.84)	−11.8568 (282.46)	0.8748 (285.00)	5.5318 (276.87)	−0.1914 (294.37)
6	1.0515 (287.25)	0.8839 (292.02)	−0.4137 (279.61)	−2.9790 (289.23)	−0.5308 (296.91)	3.8104 (285.73)	−23.4875 (280.98)	−0.5332 (280.55)	−23.6712 (276.63)	3.5031 (292.86)
7	3.2631 (283.09)	−25.5265 (280.02)	−9.5971 (271.33)	2.2841 (287.94)	4.2572 (282.52)	13.9392 (278.51)	3.1897 (276.13)	2.1860 (278.56)	−2.7327 (270.80)	8.9666 (289.10)
8	4.4563 (279.07)	53.4926 (279.01)	−1.6665 (264.44)	−13.4199 (283.34)	4.5544 (279.91)	−1.5964 (276.43)	−2.0785 (275.02)	11.2544 (262.78)	0.3601 (267.57)	10.2354 (279.19)
9	−3.3643 (270.18)	4.7015 (270.10)	−0.1743 (257.32)	37.5430 (275.95)	−15.4019 (272.09)	−22.2638 (269.99)	−2.1639 (270.77)	90.0148 (256.06)	−0.5463 (262.15)	1.2607 (275.61)
10	−9.5187 (264.87)	−14.3424 (257.56)	32.3245 (256.23)	−53.5008 (262.95)	−4.0748 (264.40)	−34.2602 (261.60)	15.4567 (260.25)	29.4586 (253.44)	−44.1972 (250.90)	−0.1298 (274.55)
11	−22.4088 (253.48)	−63.2218 (249.88)	68.6790 (250.89)	17.3886 (259.45)	−11.2393 (262.15)	−3.4596 (249.92)	−115.3675 (258.93)	−132.4812 (250.66)	−0.6965 (248.64)	23.0220 (254.67)
12	−2.9144 (242.78)	−8.1454 (246.98)	−70.6284 (247.99)	−0.1688 (257.09)	4.1185 (253.68)	6.0747 (246.33)	109.2586 (257.54)	6.6690 (245.36)	117.6319 (243.94)	−30.0591 (250.52)
13	20.2914 (240.64)	5.6280 (242.83)	−9.1854 (244.50)	−6.8060 (251.59)	−36.6875 (249.96)	12.3955 (239.17)	20.5629 (248.80)	22.1217 (239.72)	32.3218 (234.32)	1.6495 (249.69)
14	9.4481 (237.37)	100.8788 (238.82)	4.2881 (233.55)	14.3047 (243.58)	43.2418 (241.48)	39.6368 (235.98)	−2.0577 (241.13)	11.9418 (238.89)	−3.1067 (230.88)	3.9708 (247.09)
15	6.2844 (232.93)	−0.0472 (237.65)	−8.2569 (232.01)	1.4434 (241.48)	−8.5674 (237.84)	1.5898 (224.18)	−2.3488 (231.31)	2.1593 (232.16)	−5.7633 (229.73)	−12.9043 (246.31)
16	−0.6663 (231.36)	10.2382 (236.50)	18.4322 (230.96)	−2.8947 (236.58)	−0.9153 (231.09)	4.6469 (223.75)	−1.0689 (226.92)	0.4234 (231.81)	−1.2319 (225.81)	−2.2720 (231.65)
17	5.7344 (230.67)	−0.0369 (229.49)	0.3782 (220.03)	2.8109 (232.56)	0.1912 (230.65)	0.0985 (218.01)	0.0559 (226.08)	−0.3190 (226.57)	0.7979 (219.56)	12.2612 (228.01)
18	−0.4386 (227.65)	−0.8447 (225.62)	−0.7146 (214.98)	−13.4395 (227.39)	−3.4412 (230.17)	−1.7629 (215.89)	0.2048 (222.41)	0.4980 (221.02)	0.5461 (215.96)	−3.0263 (220.70)
19	−3.6661 (222.77)	1.6974 (224.89)	0.0401 (212.97)	0.3274 (226.10)	−0.6151 (227.23)	−2.7500 (214.53)	−23.7120 (218.01)	−17.5090 (212.24)	−1.4129 (215.38)	−4.6110 (220.28)
20	−37.5391 (219.54)	−24.3711 (219.92)	−0.5889 (208.07)	−1.8394 (222.93)	6.9569 (226.78)	−2.8813 (212.26)	−3.6385 (212.87)	3.3083 (209.03)	−6.7442 (210.27)	−9.0721 (219.46)
21	9.6100 (218.02)	6.7757 (213.81)	−17.5192 (207.21)	4.7524 (213.96)	2.4393 (224.35)	5.2360 (211.21)	12.3763 (210.80)	−5.5161 (208.66)	−0.5022 (208.88)	8.1141 (219.24)
22	−0.4393 (214.27)	−0.3999 (212.31)	0.4092 (206.21)	−10.7783 (212.98)	2.7667 (221.11)	−0.8698 (210.58)	8.7347 (208.04)	−0.4754 (206.44)	−1.1360 (205.38)	−11.4046 (215.63)
23	8.5554 (211.38)	16.0791 (209.19)	−5.7136 (205.59)	7.5260 (210.55)	0.0490 (216.98)	−6.1720 (206.42)	3.5358 (206.42)	1.6894 (205.47)	1.0281 (203.48)	0.7002 (212.85)
24	0.1483 (209.18)	0.2858 (208.44)	−1.6418 (203.82)	−2.4578 (210.24)	−36.7819 (209.18)	−1.2424 (205.06)	−2.4375 (206.15)	6.4883 (203.90)	1.7946 (202.86)	1.7186 (210.63)
25	2.1358 (208.98)	−6.3356 (207.75)	−5.1779 (201.56)	−5.8375 (209.55)	2.4750 (207.84)	−10.0897 (202.47)	−9.7425 (205.09)	−0.0891 (203.39)	6.7045 (202.25)	−0.9120 (208.78)
26	7.9677 (206.70)	−0.8865 (205.79)	3.7348 (200.44)	0.6477 (207.15)	−5.9459 (206.68)	−7.8142 (200.73)	−0.7559 (204.07)	−12.4906 (202.51)	8.5252 (200.50)	0.9392 (207.81)
27	2.5352 (206.29)	−14.6920 (204.84)	−0.0276 (198.66)	0.8410 (205.01)	−3.9646 (205.90)	−0.4516 (199.72)	−0.0413 (203.62)	0.6934 (198.96)	−10.1631 (198.60)	3.2107 (206.73)
28	−11.3282 (203.63)	−7.4851 (203.03)	6.4837 (198.07)	−1.8390 (203.85)	0.8600 (205.12)	−15.8267 (198.29)	0.7565 (202.40)	5.1253 (198.51)	−8.2655 (196.95)	−14.2031 (205.98)
29	2.0003 (199.34)	−0.5180 (202.61)	−0.3098 (194.39)	−1.9977 (202.41)	3.4548 (202.11)	0.2058 (197.38)	−15.3955 (201.33)	−6.9919 (195.46)	−7.1517 (196.00)	0.2955 (203.74)
30	−4.3995 (198.92)	4.0430 (200.19)	−0.4963 (192.91)	−6.6034 (201.85)	2.0205 (201.44)	7.9168 (196.31)	18.7741 (198.24)	−5.1957 (194.96)	−3.1395 (194.65)	−5.3498 (202.71)

Table 9.S9. (*Continued*)

j	R_j, 10^{-40} erg cm^3 (λ_j, nm)									
	md011*	md012*	md013*	md014*	md015*	md016*	md017*	md018*	md019*	md020*
1	−6.3359 (377.78)	−15.7932 (370.50)	−35.2212 (383.03)	−14.2686 (384.50)	28.4175 (362.72)	15.1196 (393.95)	33.2617 (387.60)	2.9077 (374.70)	13.7078 (395.70)	29.4110 (379.95)
2	38.9031 (346.92)	−16.2161 (341.65)	31.7889 (350.25)	28.3924 (334.64)	−53.2555 (339.26)	−9.5306 (354.11)	−112.0137 (348.02)	66.8729 (341.59)	65.1907 (337.12)	−55.9010 (350.53)
3	−73.6966 (326.23)	−1.2492 (319.42)	37.5451 (321.77)	−11.9863 (317.32)	−7.9182 (307.53)	−3.1453 (335.44)	23.6738 (327.29)	−44.3019 (328.42)	−69.5605 (326.93)	4.7650 (327.66)
4	−3.0632 (299.75)	−0.3379 (300.36)	−0.7596 (303.46)	5.2657 (276.02)	−0.4157 (286.07)	−2.6408 (299.95)	31.9719 (292.56)	−5.9010 (283.37)	4.4668 (289.30)	−0.4549 (293.70)
5	3.5147 (291.33)	5.3145 (280.04)	2.4511 (294.76)	2.8273 (273.77)	0.2999 (272.98)	0.1181 (294.70)	−1.5734 (289.92)	−8.5201 (273.74)	−2.6452 (281.50)	3.4353 (288.13)
6	31.7456 (288.28)	3.6251 (271.56)	−7.2352 (279.92)	0.1102 (271.08)	1.1726 (270.91)	−0.7887 (292.93)	−2.1266 (286.23)	11.2769 (271.40)	0.8984 (280.10)	−0.8292 (279.54)
7	10.7884 (275.47)	0.7932 (271.51)	5.5394 (276.44)	−0.0021 (269.68)	−3.4693 (267.80)	−26.7595 (287.74)	4.0794 (282.78)	−3.1992 (269.80)	0.3684 (278.50)	−3.7529 (274.09)
8	11.9804 (273.61)	22.4460 (268.81)	2.2921 (275.93)	−14.6574 (268.20)	12.0980 (265.88)	13.0626 (282.28)	28.6081 (271.83)	13.8094 (267.02)	−7.6788 (266.07)	−0.8838 (269.68)
9	−1.8303 (267.11)	−0.2955 (264.97)	−44.3901 (273.30)	−1.5409 (266.90)	−0.1059 (263.70)	−14.6729 (274.08)	−36.2956 (269.63)	−4.2412 (265.52)	−18.2124 (263.84)	9.6029 (266.68)
10	−33.1302 (255.73)	8.2503 (259.52)	0.5223 (264.22)	6.1433 (263.79)	−24.7434 (258.89)	6.5737 (265.14)	21.2059 (255.19)	20.7012 (261.92)	−13.7549 (258.34)	−41.8184 (259.50)
11	−68.4067 (254.89)	0.5567 (255.79)	−55.6742 (254.57)	−71.3751 (247.13)	−1.0164 (250.51)	−27.8431 (258.22)	−76.1223 (250.56)	56.4916 (256.73)	−6.7215 (248.68)	−0.5581 (253.09)
12	71.4326 (251.91)	−111.1711 (250.51)	−16.5171 (248.29)	9.6153 (240.01)	−29.1423 (247.55)	−0.4873 (255.79)	87.9396 (242.29)	−81.2383 (248.56)	−8.0331 (246.17)	121.4739 (248.76)
13	46.5745 (246.88)	95.2729 (242.73)	125.3918 (245.63)	23.9434 (239.26)	−9.8646 (241.86)	30.2052 (251.00)	4.6583 (239.81)	3.3584 (242.55)	32.4887 (242.08)	−4.2286 (240.01)
14	−4.7677 (242.37)	63.6009 (237.59)	−4.3142 (242.13)	24.2874 (236.75)	94.5374 (233.89)	−2.1846 (246.95)	4.5898 (231.57)	−11.3264 (231.24)	24.3443 (235.40)	18.5846 (237.10)
15	7.0972 (240.11)	−4.3027 (233.32)	−0.7396 (236.92)	51.6713 (235.77)	−1.0374 (226.45)	33.2388 (244.39)	2.3590 (229.48)	18.4891 (230.04)	3.1030 (229.35)	0.3730 (236.71)
16	−9.4883 (237.04)	2.6016 (228.63)	1.5931 (230.66)	4.6176 (225.16)	−0.1198 (218.39)	0.8526 (238.76)	0.2146 (226.60)	0.5826 (221.13)	4.4940 (228.25)	4.5937 (235.78)
17	−0.2051 (233.67)	2.1860 (219.02)	2.7251 (228.56)	3.3416 (213.77)	−0.2972 (217.09)	0.7601 (236.04)	3.4809 (224.90)	−3.1627 (219.22)	−7.0494 (218.24)	−1.2529 (232.42)
18	0.3212 (225.51)	1.5095 (215.64)	−0.0188 (216.99)	−2.6189 (213.70)	−0.2425 (215.27)	0.0428 (231.77)	−2.1553 (218.38)	−19.7347 (215.86)	−4.7992 (213.57)	0.8159 (220.84)
19	2.9303 (221.09)	3.4643 (210.44)	5.3768 (213.19)	0.1806 (211.24)	0.6544 (208.49)	−1.5438 (223.63)	9.8751 (217.26)	2.6766 (211.40)	−0.2199 (210.46)	−1.9835 (218.49)
20	20.8748 (218.86)	−3.7039 (208.56)	6.0404 (212.81)	0.4580 (207.80)	2.6024 (207.31)	−2.8833 (222.40)	−4.8600 (212.54)	−0.7831 (210.74)	0.0395 (210.13)	0.3471 (217.41)
21	−0.3497 (216.29)	16.6353 (206.87)	0.0634 (210.58)	−2.5914 (205.87)	−13.7155 (205.21)	1.8810 (220.64)	10.2837 (211.25)	0.4407 (208.29)	−1.5519 (208.95)	−12.5805 (212.40)
22	−2.9461 (214.84)	7.2798 (205.81)	1.3357 (210.54)	6.2812 (204.49)	−0.2320 (201.91)	−14.0255 (219.76)	5.0901 (210.58)	4.0887 (205.28)	−14.4852 (205.78)	−1.6264 (211.41)
23	−8.6296 (214.66)	−15.8417 (202.85)	1.4761 (208.70)	9.0239 (201.98)	0.4661 (201.73)	−5.7141 (217.39)	1.7947 (208.67)	7.6273 (205.00)	−5.0131 (205.60)	0.6082 (209.72)
24	−0.4610 (210.03)	−12.1783 (202.22)	−6.6482 (207.07)	2.9658 (200.67)	15.3187 (199.58)	2.7234 (214.89)	−0.1132 (204.34)	−9.0296 (204.54)	−2.4853 (203.55)	0.3675 (208.93)
25	−0.3413 (208.66)	−2.7871 (201.73)	−11.3440 (206.25)	−6.1390 (199.53)	5.8699 (198.39)	−0.1108 (209.71)	5.0351 (202.50)	−5.7694 (203.46)	3.4094 (199.84)	0.0751 (205.68)
26	−1.3053 (208.06)	2.3105 (201.12)	−5.7236 (204.87)	1.5694 (197.89)	0.4867 (197.27)	2.0149 (208.68)	0.3755 (202.03)	−3.7107 (201.11)	0.7921 (198.94)	9.2326 (203.49)
27	−13.9299 (206.48)	−2.6072 (198.70)	−1.4488 (204.65)	1.9218 (197.47)	7.8758 (196.81)	−0.5690 (208.52)	1.2407 (200.98)	−0.2501 (200.13)	−1.1258 (197.64)	−10.1780 (201.26)
28	2.5511 (204.05)	−1.1343 (197.51)	1.2106 (201.33)	0.2045 (196.41)	−0.5419 (196.55)	−1.5063 (205.76)	−3.1562 (198.31)	−3.5502 (199.41)	−0.2987 (197.19)	−11.8508 (200.60)
29	−5.0622 (202.89)	0.2525 (197.07)	−0.6550 (199.51)	−3.0520 (196.23)	−0.2536 (196.22)	0.4345 (203.85)	8.3850 (197.54)	−7.7592 (197.63)	−2.7781 (196.49)	0.1869 (198.94)
30	−1.8467 (200.29)	−3.8505 (196.05)	−4.1376 (198.32)	−8.0035 (195.17)	−1.3648 (195.85)	−0.5212 (203.57)	−7.6514 (194.98)	1.7694 (194.06)	−5.2234 (195.61)	−0.8168 (198.38)

Table 9.S9. (*Continued*)

j	R_j, 10^{-40} erg cm^3 (λ_j, nm)									
	md021*	**md022***	**md023***	**md024***	**md025***	**md026***	**md027***	**md028***	**md029***	**md030***
1	−14.3777 (390.19)	−28.7664 (357.72)	12.5714 (389.78)	−2.5935 (395.06)	−9.7440 (388.60)	−1.6198 (392.93)	−20.3657 (376.23)	−2.2031 (372.85)	22.4260 (435.91)	−12.4715 (391.95)
2	25.6021 (345.20)	25.8132 (347.13)	39.1699 (342.99)	−21.1241 (345.59)	−18.9363 (340.97)	100.1176 (334.67)	72.9823 (344.82)	−38.5141 (341.74)	30.8843 (350.66)	15.0364 (341.88)
3	−23.0094 (332.99)	21.0140 (318.75)	−63.8584 (328.27)	38.2729 (328.47)	30.4360 (333.70)	−90.5114 (325.98)	−24.0668 (328.27)	59.4644 (312.32)	−45.0654 (342.95)	14.4443 (330.60)
4	−0.4986 (287.86)	−5.4237 (289.09)	15.6832 (306.01)	−4.3981 (283.35)	10.3918 (290.59)	−0.4096 (289.08)	−2.5707 (299.42)	6.4391 (288.59)	16.8294 (299.90)	9.2804 (285.12)
5	1.9548 (286.55)	−37.7334 (287.37)	0.1808 (290.62)	−0.1401 (275.23)	0.2431 (284.92)	−0.2490 (285.91)	0.9142 (297.09)	0.0381 (279.25)	−1.0372 (295.04)	−15.7359 (276.48)
6	10.3913 (283.59)	6.8523 (282.78)	30.7136 (287.82)	−7.7183 (273.98)	1.2586 (279.80)	−20.6706 (279.88)	6.9557 (286.78)	4.4931 (277.01)	−22.3455 (281.53)	12.9172 (272.99)
7	2.0364 (279.76)	0.3720 (282.18)	−3.6757 (277.98)	2.6309 (273.42)	1.2977 (273.37)	11.7571 (276.44)	7.1599 (283.10)	4.4246 (273.44)	−0.0673 (279.88)	−5.7115 (269.77)
8	−19.1438 (273.42)	18.5476 (274.07)	13.7936 (274.61)	9.4553 (268.95)	23.7732 (270.67)	5.6180 (272.92)	−30.4535 (271.49)	−21.2007 (269.99)	1.0251 (277.80)	−9.4035 (267.46)
9	−3.0379 (269.28)	−17.3470 (269.29)	−37.6693 (270.52)	−3.1780 (266.57)	−53.1639 (266.14)	−17.3094 (270.54)	−21.0810 (265.97)	−24.7854 (266.85)	13.2777 (268.54)	−0.4190 (257.89)
10	−0.5186 (266.30)	−0.7374 (259.86)	0.3680 (259.13)	−0.4901 (260.26)	−8.6486 (258.00)	0.3063 (264.80)	2.0640 (257.42)	6.1938 (257.44)	−8.3275 (263.43)	−12.9630 (253.99)
11	−9.7510 (262.46)	8.0563 (252.27)	5.1426 (255.97)	−103.2936 (255.22)	−1.1509 (255.24)	6.0033 (259.29)	38.6920 (256.04)	−22.4946 (253.65)	−16.3832 (255.08)	32.6572 (251.40)
12	−48.2488 (253.54)	−31.0067 (248.91)	−110.8610 (251.00)	−23.3734 (251.74)	32.6076 (248.66)	34.5199 (251.08)	−12.2422 (251.13)	5.5724 (245.53)	−8.6725 (254.49)	−1.5691 (247.34)
13	101.9237 (248.62)	46.4285 (246.54)	7.2392 (248.00)	132.4218 (249.62)	−4.2339 (245.16)	11.2080 (248.51)	−4.7502 (245.79)	25.4200 (242.98)	−3.9720 (253.04)	10.1492 (244.44)
14	−1.5847 (244.37)	0.1449 (237.54)	76.3839 (244.57)	4.9707 (245.98)	−7.8160 (244.08)	−75.1677 (243.19)	30.8094 (241.86)	39.3169 (237.56)	−99.5486 (249.38)	−0.4274 (236.74)
15	0.8163 (234.51)	−0.4350 (236.54)	3.6508 (241.34)	−12.9424 (243.12)	−3.5117 (238.02)	19.5232 (232.09)	22.2094 (240.23)	1.5801 (228.09)	0.8778 (246.81)	0.6933 (234.02)
16	0.5823 (232.32)	9.3794 (235.39)	1.0610 (232.54)	8.6968 (232.98)	3.9147 (236.52)	0.0598 (227.98)	0.0634 (236.19)	0.4923 (227.30)	140.9580 (243.19)	2.7200 (227.63)
17	−8.0929 (229.54)	−6.6733 (225.88)	9.6702 (228.17)	−0.0091 (214.43)	−0.3616 (219.95)	−0.8122 (225.94)	0.0355 (234.18)	0.3882 (223.75)	6.7081 (219.65)	−4.4512 (224.04)
18	−6.8423 (222.74)	−13.7974 (221.61)	−2.9550 (226.55)	−2.5811 (212.19)	−0.6163 (216.48)	6.1310 (223.01)	1.5337 (223.49)	−12.0098 (219.94)	0.6782 (215.71)	−8.9956 (215.00)
19	−1.6004 (220.24)	3.3324 (217.26)	−0.7856 (222.74)	9.7256 (211.62)	2.2949 (214.04)	−5.2188 (219.98)	5.7244 (218.63)	0.9859 (217.61)	1.0993 (214.71)	−18.3170 (214.33)
20	−9.6502 (216.23)	−0.0778 (215.41)	−0.6737 (218.48)	13.3807 (209.09)	−1.0318 (213.72)	−2.8894 (216.41)	−3.2633 (217.61)	−3.2739 (216.54)	2.3893 (212.74)	0.6003 (210.85)
21	−16.6586 (210.34)	0.6782 (212.72)	2.0230 (216.09)	−34.0353 (207.69)	13.7412 (212.61)	−1.9529 (216.16)	−9.9084 (212.23)	−1.0294 (212.09)	−2.9652 (210.89)	−2.2047 (206.25)
22	5.4896 (210.20)	−0.8494 (206.87)	−11.2766 (211.32)	−9.4694 (204.57)	−28.6689 (211.31)	−0.8589 (212.11)	−6.0495 (211.91)	−0.4118 (210.23)	−8.2421 (208.43)	−0.0098 (204.99)
23	2.3534 (207.39)	−5.7103 (206.82)	0.8437 (210.29)	6.3893 (201.74)	2.0580 (207.16)	0.5037 (210.22)	−1.1721 (208.91)	−7.1148 (208.69)	−0.0097 (205.63)	−1.0713 (203.97)
24	−8.0347 (206.05)	1.6572 (203.99)	−3.9107 (207.76)	0.1706 (201.06)	5.8312 (206.33)	−0.5071 (209.86)	2.0339 (208.25)	−3.8389 (206.89)	−1.3447 (205.49)	2.7985 (203.33)
25	−3.5775 (205.79)	1.0297 (202.92)	1.5680 (207.24)	0.5398 (200.13)	1.9674 (204.66)	1.9016 (209.15)	2.2342 (203.58)	0.7784 (205.23)	0.1661 (205.03)	0.9995 (201.43)
26	5.0537 (202.24)	5.7100 (201.60)	0.0450 (205.87)	2.5549 (199.28)	−2.5183 (203.49)	13.7483 (208.34)	1.3397 (202.47)	0.9752 (202.92)	−2.6325 (203.97)	−3.8275 (200.97)
27	10.9812 (201.33)	−0.6691 (200.85)	8.1877 (202.25)	3.8552 (198.39)	2.0380 (202.48)	−10.7087 (205.71)	0.8501 (202.05)	1.4541 (201.84)	−6.3731 (202.77)	−6.1754 (198.33)
28	3.7830 (200.49)	−4.9595 (199.49)	−1.8980 (200.73)	−5.0046 (198.16)	0.0227 (199.49)	3.0995 (202.52)	−0.5250 (201.37)	0.1324 (199.61)	3.0774 (200.78)	−6.0114 (196.13)
29	−1.6547 (199.77)	0.6797 (198.85)	0.4171 (200.19)	13.0776 (197.60)	3.1899 (198.85)	5.6089 (201.52)	0.1187 (201.25)	−1.0427 (198.73)	−7.2184 (199.24)	9.2539 (195.47)
30	0.4554 (199.13)	1.3168 (197.55)	0.4049 (198.74)	−9.3197 (196.04)	19.3509 (197.11)	1.6217 (199.81)	−0.0473 (200.64)	−5.3960 (197.95)	1.4104 (198.56)	0.6079 (191.58)

Table 9.S9. (*Continued*)

j	R_j, 10^{-40} erg cm^3 (λ_j, nm)									
	md031*	**md032***	**md033***	**md034***	**md035***	**md036***	**md037***	**md038***	**md039***	**md040***
1	7.5315 (380.56)	−16.0361 (395.20)	4.8903 (398.75)	23.9450 (379.13)	−20.4618 (403.74)	28.1905 (395.47)	−62.1980 (359.18)	−14.4917 (371.58)	−33.1655 (383.06)	79.7310 (360.90)
2	−23.0240 (345.08)	29.8466 (347.71)	87.9551 (331.35)	−29.7840 (352.56)	40.5609 (343.49)	−3.6048 (348.35)	71.0829 (350.08)	28.3869 (350.16)	65.2612 (356.99)	−58.7001 (356.03)
3	10.3580 (316.12)	−10.2240 (327.22)	−70.7554 (319.49)	−24.3875 (323.07)	4.7964 (325.93)	−32.9142 (324.97)	10.4624 (308.80)	2.4931 (313.53)	−24.9249 (326.62)	−53.7827 (311.46)
4	−1.1195 (296.02)	−1.1283 (305.96)	36.6013 (282.70)	−0.6214 (308.23)	−0.0513 (297.68)	−2.3663 (301.57)	−14.7423 (289.51)	−15.8382 (296.34)	26.9030 (290.48)	−0.2749 (300.52)
5	0.6413 (286.95)	8.5139 (286.78)	−7.9866 (277.37)	−0.3816 (299.09)	2.7703 (287.79)	−8.7154 (289.23)	−30.3236 (280.16)	25.9553 (291.30)	−12.5034 (284.68)	11.0205 (294.72)
6	−0.1577 (283.27)	2.9200 (282.85)	−0.0578 (267.14)	−10.0566 (287.61)	−0.3421 (284.16)	−8.4020 (288.51)	15.3997 (278.22)	−2.6969 (286.97)	−0.3999 (284.50)	−3.0131 (289.23)
7	−19.2335 (275.00)	0.7176 (280.83)	−3.9809 (263.86)	−0.9397 (286.24)	4.2716 (282.45)	5.3408 (282.15)	−3.1985 (267.46)	5.2057 (275.78)	−0.3843 (280.67)	−12.2301 (285.94)
8	18.3172 (272.82)	−34.0844 (273.26)	−1.0634 (262.06)	−3.4984 (280.05)	−2.6951 (273.34)	−0.9400 (281.51)	−10.2738 (262.84)	−1.4204 (271.88)	−4.4931 (270.35)	0.3901 (274.20)
9	13.1849 (265.81)	0.2271 (265.84)	−11.8132 (260.16)	11.6622 (274.68)	−12.9246 (269.39)	11.5796 (276.27)	−21.9508 (261.43)	14.8968 (263.73)	1.6067 (266.00)	−5.2608 (266.87)
10	1.5067 (262.44)	21.1928 (264.24)	−0.9122 (259.04)	12.2771 (273.53)	16.7764 (261.29)	−19.6258 (268.45)	−1.9328 (259.46)	−95.4067 (258.58)	−7.7055 (260.24)	−1.9554 (262.23)
11	−65.9014 (254.78)	−68.7935 (254.37)	79.0586 (247.23)	−3.1680 (260.91)	−19.6716 (258.53)	1.6989 (258.12)	1.4196 (256.84)	−5.6385 (256.85)	−58.3867 (254.80)	1.0135 (258.62)
12	−2.8171 (252.39)	−5.0165 (250.43)	−0.8455 (244.01)	−83.2761 (256.55)	−12.4580 (251.00)	0.9674 (252.21)	43.8967 (251.42)	2.0336 (253.64)	91.3133 (252.68)	−1.8499 (256.07)
13	12.4206 (247.45)	32.3369 (248.95)	−8.0508 (242.67)	61.1171 (253.83)	−6.4254 (246.56)	−34.4800 (248.96)	−21.4706 (241.18)	62.0595 (250.44)	1.0301 (250.55)	14.1799 (252.72)
14	48.3777 (240.67)	69.5934 (245.60)	−44.1598 (238.58)	22.6176 (248.12)	−0.3754 (244.93)	64.0405 (246.79)	11.1764 (232.64)	−0.6603 (239.74)	1.6926 (243.57)	−38.9608 (245.56)
15	34.2721 (234.62)	1.8035 (244.83)	−37.9596 (234.41)	5.2599 (240.65)	36.0921 (244.39)	18.6926 (237.30)	−2.0490 (228.17)	5.0057 (235.70)	−1.6479 (241.30)	−17.7760 (243.63)
16	1.5307 (233.02)	2.3140 (239.61)	−0.0262 (218.24)	−3.0006 (239.93)	−2.1883 (239.51)	4.0262 (234.34)	32.5581 (225.92)	2.0360 (233.53)	3.2979 (227.38)	24.6721 (236.75)
17	6.2544 (230.36)	−0.4953 (235.25)	−34.0810 (209.88)	13.2698 (238.99)	6.1238 (226.27)	2.0907 (229.66)	−1.7251 (221.87)	9.3393 (232.81)	10.9654 (220.71)	2.5934 (236.23)
18	−0.2940 (217.90)	0.5583 (220.14)	0.1792 (208.26)	0.1538 (234.97)	3.6124 (224.33)	6.3153 (225.33)	0.0549 (220.70)	9.1189 (230.66)	1.2339 (218.37)	67.6494 (230.34)
19	−0.6274 (217.53)	3.4650 (219.82)	−7.8934 (205.33)	7.1819 (227.70)	0.0566 (220.25)	5.9526 (223.63)	0.2991 (217.79)	0.7978 (220.40)	−2.3515 (215.62)	4.4083 (223.78)
20	−2.5993 (216.97)	−2.9430 (216.51)	4.2124 (202.82)	−0.1708 (224.21)	0.7233 (219.29)	−0.1380 (219.00)	0.6642 (212.11)	0.3850 (218.49)	−21.6493 (214.59)	−0.9548 (222.97)
21	2.7399 (209.84)	−3.3465 (213.83)	0.1327 (202.14)	−0.1199 (220.96)	−12.4542 (212.00)	3.1463 (215.62)	−1.1093 (208.38)	−4.0747 (215.45)	−0.5094 (211.88)	4.1430 (222.32)
22	4.9777 (209.44)	−0.1891 (211.84)	4.7872 (200.10)	0.1695 (217.87)	3.0949 (211.60)	21.3745 (214.67)	2.9447 (206.79)	13.0078 (212.62)	11.3891 (209.15)	0.6864 (216.08)
23	−0.1570 (208.98)	0.5016 (211.47)	5.2945 (199.22)	−2.9010 (216.25)	−7.8718 (211.00)	−23.8724 (212.42)	3.1530 (203.09)	0.7431 (211.52)	14.4509 (208.24)	0.8544 (215.87)
24	−2.9310 (208.72)	1.7542 (210.86)	−8.3226 (197.83)	−20.0962 (215.67)	−2.1995 (209.17)	−7.0846 (211.19)	3.1438 (202.72)	−0.8943 (209.55)	−18.7332 (205.62)	−7.8526 (210.66)
25	−3.1006 (207.19)	−4.5298 (208.63)	−1.8555 (197.31)	0.0685 (212.95)	−0.1759 (208.76)	0.8143 (210.85)	−3.0312 (200.25)	12.5135 (209.07)	−9.3390 (205.00)	3.5160 (210.51)
26	−1.7553 (205.46)	−34.8555 (206.79)	−3.7047 (195.32)	1.9276 (209.80)	4.1589 (208.05)	1.0164 (209.93)	−1.2482 (199.25)	−7.7470 (207.90)	3.2229 (201.88)	0.6610 (208.91)
27	−4.3809 (203.24)	4.7259 (204.90)	0.7715 (194.50)	5.8437 (209.24)	0.5343 (206.92)	−1.5842 (209.79)	0.9991 (198.16)	1.6869 (206.55)	−0.3060 (198.57)	0.4196 (208.57)
28	12.3863 (201.43)	−3.7089 (204.72)	19.2642 (193.68)	3.1575 (208.03)	−7.2779 (203.19)	−4.9538 (206.51)	−0.5783 (195.59)	−7.2549 (201.80)	−0.2094 (195.67)	−4.0091 (207.64)
29	0.5064 (200.89)	1.1844 (201.83)	−0.4530 (193.04)	0.9808 (207.44)	−11.9931 (202.41)	−0.7716 (205.55)	−0.1419 (194.16)	−1.9743 (201.04)	11.1109 (195.24)	−2.1433 (205.65)
30	0.5481 (200.64)	−2.2032 (201.11)	−1.4098 (191.67)	−0.1663 (204.88)	0.2157 (200.02)	−1.5301 (203.52)	−1.4228 (194.00)	−9.0417 (200.55)	−2.8573 (194.56)	−1.6603 (203.24)

Table 9.S9. (*Continued*)

j	R_j, 10^{-40} erg cm^3 (λ_j, nm)									
	md041*	**md042***	**md043***	**md044***	**md045***	**md046***	**md047***	**md048***	**md049***	**md050***
1	−25.7620 (353.06)	−71.4975 (365.47)	−34.9769 (387.86)	−32.9483 (389.18)	−5.4997 (386.71)	11.3010 (382.14)	6.6256 (366.82)	64.1905 (360.60)	−18.3714 (389.65)	−21.3103 (390.03)
2	76.9921 (342.60)	84.5819 (349.90)	132.4811 (349.65)	94.0110 (363.13)	−16.6058 (362.23)	−24.6949 (341.86)	−1.1652 (336.91)	−10.2386 (349.08)	−51.8751 (348.96)	32.2075 (368.80)
3	−33.7035 (306.71)	19.3329 (318.22)	−23.0092 (325.27)	−2.0475 (312.65)	−19.9659 (319.76)	−24.7553 (300.80)	−38.7061 (302.84)	−68.4275 (305.83)	45.2433 (315.46)	−21.5180 (320.01)
4	9.1406 (291.30)	−35.3087 (296.53)	−0.7073 (286.75)	−4.4621 (294.28)	16.2480 (303.38)	−1.3478 (296.04)	1.2641 (290.71)	−0.3297 (288.94)	3.6579 (305.70)	−0.0416 (314.81)
5	−0.9179 (289.50)	6.1720 (291.39)	4.2149 (285.10)	−1.6273 (284.12)	−2.3957 (281.52)	0.2374 (292.92)	6.0767 (283.87)	−1.1287 (286.10)	1.6184 (302.34)	31.4720 (297.20)
6	−27.1329 (282.55)	6.9031 (287.06)	−16.9624 (277.45)	−0.4749 (280.94)	4.7679 (278.79)	12.7856 (291.50)	−3.0987 (277.31)	0.2205 (283.60)	−17.1483 (286.33)	−38.7882 (289.61)
7	5.5884 (276.43)	−23.5935 (284.18)	−34.5212 (272.33)	−58.6426 (279.38)	−8.1897 (277.64)	−30.8188 (277.69)	−9.2137 (274.29)	−20.3913 (277.86)	11.2205 (278.22)	−0.8812 (275.78)
8	−6.4128 (265.47)	−1.7946 (273.77)	1.8917 (267.43)	6.7633 (276.97)	0.5644 (273.12)	25.1361 (274.93)	17.8283 (268.63)	9.2924 (275.87)	−28.3688 (273.71)	9.9577 (273.97)
9	6.7000 (256.96)	−1.6842 (267.60)	0.6802 (261.39)	−0.1411 (272.87)	10.8686 (269.59)	6.4380 (267.77)	3.0401 (264.01)	1.9958 (271.55)	9.5086 (267.28)	3.6882 (271.75)
10	−42.5588 (250.71)	16.1937 (262.51)	27.6155 (259.80)	−0.6315 (263.46)	−21.2668 (266.61)	16.0113 (263.91)	−0.0373 (258.79)	1.9089 (269.09)	31.8442 (260.13)	−1.5321 (260.92)
11	−9.4911 (250.47)	−46.3104 (256.57)	18.1755 (254.86)	−9.9778 (258.02)	22.6234 (262.22)	−27.8038 (248.71)	−0.1011 (255.59)	23.1276 (263.52)	−53.0173 (254.40)	4.8625 (256.96)
12	1.0758 (249.30)	−54.4849 (254.78)	25.5740 (250.18)	55.5724 (252.29)	−79.9726 (248.93)	−4.0589 (246.97)	1.0038 (250.48)	−33.1387 (251.66)	−28.1120 (253.53)	−16.7383 (252.04)
13	56.4069 (247.31)	80.2465 (251.55)	−69.1604 (246.09)	−1.6075 (243.79)	37.9169 (243.98)	2.6426 (239.56)	−37.2651 (246.40)	−52.0571 (249.21)	82.9672 (250.53)	−39.1049 (250.69)
14	7.5358 (239.40)	1.1967 (244.86)	19.2985 (242.25)	−20.5006 (242.81)	24.5659 (239.77)	69.1580 (239.40)	47.4284 (242.92)	94.6538 (243.20)	3.0325 (249.42)	30.6708 (248.43)
15	−2.2178 (237.10)	16.2109 (240.69)	−15.3059 (239.07)	−3.3469 (236.08)	0.1572 (236.22)	1.0111 (234.86)	1.6326 (231.07)	−0.7099 (229.28)	0.6116 (241.43)	−5.7697 (244.32)
16	34.5229 (235.22)	−8.2846 (233.43)	−2.0177 (231.83)	0.2607 (228.63)	0.3171 (229.13)	0.4371 (227.56)	−1.2241 (227.83)	10.9284 (228.03)	−0.1427 (235.55)	37.9169 (235.58)
17	−16.1940 (232.73)	−19.5432 (232.64)	0.2674 (226.20)	−8.3866 (221.14)	33.9030 (227.52)	−0.6117 (227.25)	−3.3030 (226.85)	30.0735 (222.84)	0.9988 (231.21)	3.1845 (230.23)
18	2.2744 (228.56)	15.5906 (232.29)	−4.0068 (223.30)	−9.3072 (215.88)	−0.2857 (216.42)	3.9321 (220.65)	2.2149 (222.35)	38.7194 (221.49)	−0.7152 (226.99)	0.8329 (229.24)
19	0.2087 (217.43)	6.1397 (228.47)	−32.4764 (214.77)	−5.1209 (215.47)	4.9067 (214.05)	−1.0335 (217.61)	0.1880 (221.77)	−0.1665 (221.04)	−32.2600 (226.13)	1.0239 (220.52)
20	−3.2083 (212.07)	−0.3077 (214.96)	−0.4394 (213.29)	5.2936 (213.66)	−3.7374 (212.29)	1.8932 (215.79)	8.8769 (215.83)	−0.5396 (214.89)	−0.1001 (225.25)	−0.5212 (220.22)
21	−3.5412 (211.74)	12.2799 (213.13)	8.9445 (209.29)	2.0045 (212.35)	−14.8380 (211.76)	0.2901 (214.49)	−0.1240 (211.94)	−0.8861 (211.80)	2.9183 (209.96)	0.9251 (212.39)
22	0.7346 (211.59)	2.1950 (210.98)	0.4807 (206.67)	−1.1271 (209.50)	−2.3211 (207.44)	−4.5289 (214.29)	−7.1739 (211.29)	0.2389 (211.38)	−0.9568 (209.34)	−3.2044 (211.63)
23	−17.0649 (209.24)	−0.7987 (210.02)	−1.3008 (205.29)	0.9686 (208.18)	−4.6564 (206.08)	0.3231 (213.98)	14.2007 (208.86)	−11.0634 (210.91)	1.4580 (208.25)	1.7051 (211.22)
24	3.3915 (202.51)	−2.8755 (209.17)	0.6813 (204.19)	−0.1918 (206.81)	3.9282 (205.08)	3.0567 (208.75)	−0.3127 (206.52)	4.4623 (210.27)	4.5477 (207.38)	−0.7478 (206.58)
25	−2.1936 (201.91)	3.0239 (208.88)	−0.1761 (204.11)	2.5107 (206.13)	2.4801 (203.71)	−11.7601 (206.46)	0.2711 (205.96)	0.0021 (209.67)	3.7688 (206.73)	−1.3278 (203.83)
26	−1.9986 (201.39)	3.3270 (208.11)	−1.6861 (201.36)	0.0982 (203.63)	2.4120 (203.36)	−1.5884 (201.90)	−0.7740 (203.59)	−17.2838 (208.79)	6.5128 (205.21)	−2.6544 (203.40)
27	−1.3281 (199.99)	−11.1756 (207.17)	1.0350 (200.47)	2.5801 (202.87)	−1.3788 (201.00)	1.2829 (201.35)	−10.4939 (200.80)	0.1320 (205.09)	1.2248 (204.80)	−5.8655 (201.62)
28	−7.2934 (199.09)	0.1688 (204.52)	−8.4418 (199.56)	−1.3748 (201.76)	−4.3623 (200.29)	4.6049 (200.97)	9.5938 (199.55)	−0.0544 (201.56)	−16.9601 (203.71)	1.1367 (199.46)
29	0.6073 (196.51)	−0.3153 (201.60)	1.0956 (197.86)	−1.9142 (201.31)	0.0081 (198.57)	1.3156 (198.62)	−4.4333 (196.48)	−26.3279 (201.35)	−1.7512 (200.67)	−2.4216 (198.29)
30	−3.1628 (194.55)	−7.1436 (198.15)	3.1352 (196.37)	3.2782 (198.26)	0.4441 (198.32)	−1.3632 (198.31)	3.5402 (194.74)	−0.1282 (199.80)	20.0728 (198.77)	0.7797 (197.37)

Table 9.S9. (*Continued*)

j	R_j, 10^{-40} erg cm^3 (λ_j, nm)									
	md051*	**md052***	**md053***	**md054***	**md055***	**md056***	**md057***	**md058***	**md059***	**md060***
1	−15.4048 (383.65)	−38.5951 (394.86)	−65.7128 (377.74)	−52.8280 (388.14)	−21.9488 (379.50)	−52.8674 (386.56)	−48.4428 (385.65)	−27.1058 (381.31)	−51.9664 (401.14)	−3.5891 (403.09)
2	29.8564 (361.22)	65.2295 (360.26)	41.1134 (351.52)	101.8760 (349.76)	77.7121 (363.21)	98.7161 (355.04)	96.0607 (367.99)	121.4415 (345.50)	113.6269 (357.37)	112.0333 (341.32)
3	−27.3767 (323.26)	−10.6630 (332.11)	37.2778 (316.62)	−8.3438 (322.81)	−46.5593 (323.22)	1.1138 (315.16)	−16.3910 (333.32)	−12.1581 (328.40)	24.5886 (320.44)	−59.0880 (333.87)
4	43.5111 (301.37)	11.0614 (312.94)	−3.6636 (299.69)	1.7788 (309.35)	−0.3041 (307.77)	14.6080 (299.05)	−23.1590 (310.93)	−11.6434 (313.82)	4.7614 (303.80)	12.1032 (303.29)
5	0.0901 (293.33)	−7.6391 (303.14)	−23.7186 (293.78)	−7.1722 (296.85)	38.1988 (301.11)	3.8700 (284.68)	73.6986 (304.05)	−2.1385 (289.67)	9.1139 (300.96)	3.7190 (293.07)
6	2.6330 (278.58)	−15.0228 (279.04)	3.3135 (287.84)	6.0775 (277.70)	3.1028 (282.03)	22.8336 (277.74)	0.0600 (284.46)	−0.9217 (288.42)	−47.4938 (286.44)	1.1124 (291.17)
7	−23.7023 (276.49)	−60.4026 (275.96)	−28.9067 (283.61)	−60.1720 (269.78)	−5.6472 (281.33)	1.1135 (274.21)	−85.6945 (275.18)	3.1683 (281.53)	2.1473 (284.49)	−5.6560 (280.05)
8	−14.7683 (276.05)	42.9310 (274.22)	13.0942 (276.20)	6.1978 (266.81)	−3.3583 (273.72)	−37.5479 (269.50)	−6.7390 (270.62)	−7.3509 (274.55)	18.9861 (273.99)	−57.3662 (265.59)
9	0.1634 (268.36)	−5.8388 (263.91)	−20.8103 (273.58)	4.3785 (260.39)	−51.9034 (271.25)	1.3366 (265.33)	−1.5159 (262.61)	−52.5775 (270.61)	0.2154 (262.83)	−0.8433 (258.37)
10	−2.8347 (264.45)	−7.6895 (259.20)	4.4788 (266.29)	10.2170 (253.97)	−0.8654 (269.20)	12.5542 (258.18)	2.8557 (260.27)	−1.5856 (257.96)	−59.8337 (255.64)	−20.6644 (255.55)
11	−1.1714 (262.94)	−78.8825 (256.01)	7.6028 (258.51)	3.7567 (250.07)	0.5162 (259.22)	−26.9700 (254.38)	14.8232 (259.24)	0.4338 (255.70)	−14.4829 (251.37)	13.9454 (253.83)
12	−15.0227 (256.55)	2.3219 (253.56)	16.9222 (253.57)	−10.4437 (247.64)	−7.6457 (255.60)	−11.4406 (249.07)	−43.4759 (251.88)	0.6301 (253.37)	92.6127 (250.91)	12.3630 (253.30)
13	−5.2815 (246.63)	116.6726 (252.88)	−29.3074 (248.63)	42.0282 (247.29)	73.6088 (251.63)	−6.7498 (243.07)	23.9634 (250.40)	53.3978 (252.11)	2.6461 (250.04)	3.9267 (248.89)
14	17.0778 (244.99)	1.6154 (248.16)	53.7046 (245.38)	3.2790 (239.60)	−44.6668 (245.78)	−0.0867 (240.31)	53.5759 (248.61)	49.6870 (246.40)	44.5813 (245.07)	13.9758 (247.68)
15	14.4206 (237.87)	−9.3287 (241.28)	0.7390 (241.81)	2.0467 (232.34)	20.4496 (243.98)	2.6208 (237.44)	14.7974 (235.68)	−70.3220 (241.67)	−60.9425 (243.82)	−2.7717 (241.43)
16	5.1553 (231.77)	3.2320 (239.05)	5.3583 (236.52)	3.4165 (232.22)	4.4735 (234.02)	−3.2426 (236.95)	−48.1191 (234.21)	−0.3025 (236.49)	−2.0617 (235.24)	−4.0170 (230.15)
17	26.6227 (227.84)	1.0005 (234.18)	−16.4257 (228.69)	−6.8912 (228.96)	2.4420 (233.12)	−16.0695 (223.63)	3.0860 (231.38)	−0.4495 (231.97)	3.3811 (230.36)	−12.8876 (228.85)
18	15.2255 (226.51)	−3.7014 (232.24)	0.3917 (225.60)	−1.3991 (226.95)	−0.3432 (231.51)	−0.7042 (218.02)	25.6091 (229.02)	−7.9048 (230.12)	0.0306 (230.01)	2.6701 (227.89)
19	−8.3464 (218.72)	−2.5510 (215.88)	−2.0220 (224.15)	−0.1217 (219.08)	6.7175 (225.10)	0.9608 (215.73)	−0.4374 (221.88)	−1.7802 (227.38)	−7.6619 (227.50)	−2.1013 (226.14)
20	−11.5579 (215.00)	−4.6509 (214.55)	−12.2918 (215.19)	1.3531 (213.74)	−8.1063 (218.85)	0.0617 (215.56)	5.5081 (220.62)	−24.5607 (223.78)	−0.4275 (223.66)	−25.6265 (221.56)
21	−1.6986 (211.20)	−10.3860 (212.96)	−15.8755 (214.10)	−5.7204 (210.82)	2.7170 (214.07)	3.2849 (212.93)	−1.3860 (219.30)	0.4553 (219.79)	−10.1289 (218.70)	2.0772 (214.91)
22	−0.5097 (210.38)	−5.2980 (211.46)	−4.9130 (209.88)	−18.2867 (209.87)	1.3741 (211.38)	2.2250 (212.57)	−5.6507 (217.18)	1.3181 (219.22)	−26.8008 (217.85)	1.3571 (214.89)
23	−9.9778 (207.83)	−1.7371 (210.81)	−12.6352 (208.91)	−7.8272 (209.29)	−0.0339 (208.46)	0.2271 (207.47)	−22.9801 (210.78)	−1.0939 (211.89)	−0.1976 (214.95)	1.3595 (209.64)
24	−0.0158 (206.75)	−0.0147 (208.24)	−9.4731 (208.36)	−3.3558 (203.28)	−1.8585 (208.06)	−1.6746 (206.56)	1.3843 (205.80)	−2.5042 (207.16)	−10.7771 (210.98)	−2.2300 (205.24)
25	−0.2529 (205.99)	1.6573 (206.45)	5.2659 (206.12)	0.5528 (202.99)	−0.2689 (207.03)	−1.2820 (203.73)	−1.3347 (205.04)	−0.1005 (204.20)	12.2323 (206.80)	−0.4926 (204.42)
26	−0.6733 (205.04)	1.1970 (203.98)	−2.1187 (204.49)	1.1894 (198.84)	0.0956 (205.63)	−4.9839 (203.06)	−0.0248 (203.87)	−8.0326 (203.29)	−4.3038 (206.30)	−1.1649 (204.22)
27	−3.9444 (202.95)	−0.5839 (200.53)	0.3623 (204.30)	−6.0447 (198.17)	−1.0711 (203.88)	0.7762 (201.74)	3.3100 (201.29)	0.5571 (202.55)	−0.4594 (204.91)	4.4106 (202.49)
28	2.6852 (201.93)	1.6402 (199.27)	3.1420 (202.85)	−2.1765 (196.01)	−5.4915 (203.05)	−0.3973 (199.31)	−0.2533 (200.86)	−0.0949 (202.35)	−7.7976 (203.49)	−1.5035 (201.80)
29	−5.2495 (200.40)	−2.2630 (197.70)	−1.1185 (200.49)	0.1213 (195.48)	−0.4185 (202.27)	−0.8512 (198.97)	−5.3062 (195.89)	−3.0617 (201.04)	−7.7824 (197.13)	0.4699 (200.76)
30	−4.4739 (199.70)	0.7853 (197.28)	1.5293 (198.89)	−3.0478 (192.94)	0.2663 (202.02)	−2.4403 (196.26)	−2.5528 (194.61)	−5.3192 (200.41)	1.2103 (196.75)	−4.9419 (199.37)

Table 9.S9. (*Continued*)

j	R_j, 10^{-40} erg cm^3 (λ_j, nm)									
	md061*	**md062***	**md063***	**md064***	**md065***	**md066***	**md067***	**md068***	**md069***	**md070***
1	−25.8180 (369.44)	−24.3895 (383.22)	−0.7479 (388.79)	−19.9161 (380.95)	−11.7561 (381.11)	−62.9468 (369.74)	−37.6368 (397.69)	−38.7217 (392.20)	−33.4264 (386.73)	−9.9587 (364.08)
2	−2.3756 (353.30)	53.4599 (361.21)	2.2704 (352.54)	15.1840 (350.72)	57.3840 (339.49)	91.6931 (360.10)	86.0164 (370.08)	126.7839 (359.76)	50.6480 (373.97)	5.6580 (331.96)
3	75.5781 (311.65)	−9.3845 (320.29)	−15.9002 (325.40)	49.3914 (324.95)	−33.1952 (320.15)	−26.9558 (327.06)	−21.2520 (333.11)	−22.8953 (329.64)	0.3272 (343.33)	17.8312 (302.85)
4	−4.1556 (286.61)	0.6218 (294.21)	−2.3170 (296.10)	2.9872 (302.57)	−6.0086 (313.65)	4.0964 (298.62)	−14.5946 (304.10)	−1.1526 (298.01)	−13.3874 (336.91)	0.4416 (283.97)
5	−55.5106 (283.00)	8.8008 (291.92)	1.2507 (283.48)	−0.6156 (294.76)	27.9870 (287.92)	5.3967 (293.55)	0.6113 (293.27)	−0.2646 (296.36)	0.2626 (308.72)	1.3049 (269.85)
6	−6.6929 (279.01)	3.0246 (288.69)	17.0189 (279.25)	0.0495 (288.33)	−23.6597 (280.63)	−0.7035 (288.75)	1.5295 (291.00)	−22.4952 (290.30)	−6.0152 (303.79)	−11.7574 (266.52)
7	−10.9069 (274.45)	2.3187 (280.88)	−12.1663 (275.30)	−12.9496 (281.39)	−9.6045 (275.33)	36.8944 (282.88)	3.6408 (289.94)	−13.4916 (283.82)	13.1077 (296.53)	−7.6957 (264.70)
8	0.8512 (271.55)	−2.0945 (277.70)	−5.0033 (261.66)	−18.3678 (278.19)	−19.4002 (266.90)	3.0171 (281.99)	−2.7824 (285.27)	−26.0647 (278.71)	−0.0148 (293.88)	−30.3893 (263.19)
9	−2.3442 (269.64)	−15.1058 (277.34)	−6.6277 (260.77)	0.2999 (271.60)	3.6868 (261.19)	13.4532 (280.18)	−37.9337 (276.73)	−0.2327 (276.47)	−11.8548 (289.97)	0.7062 (259.00)
10	−1.3058 (262.17)	−41.1685 (275.61)	2.1046 (256.45)	−43.7894 (266.72)	9.8139 (257.72)	−53.3054 (277.47)	−4.5894 (272.87)	2.7577 (263.54)	−45.5560 (279.87)	−0.0009 (258.71)
11	−8.3523 (258.00)	−21.4715 (258.61)	−50.5371 (251.78)	−0.2645 (260.61)	−0.2744 (249.07)	20.4004 (267.37)	126.8185 (257.36)	97.5227 (258.81)	8.8501 (275.39)	−5.9804 (248.15)
12	−7.0036 (251.77)	46.2764 (251.90)	33.0017 (245.06)	−79.4022 (255.82)	−3.1498 (245.68)	−51.1989 (258.52)	−85.2012 (255.31)	4.2223 (254.77)	−13.3723 (267.19)	55.3485 (241.43)
13	80.3532 (246.79)	61.8044 (245.28)	3.5904 (244.20)	57.5092 (251.57)	73.2717 (242.47)	−18.7705 (253.80)	−26.3623 (249.58)	−70.3422 (253.23)	4.4210 (262.59)	23.4860 (238.27)
14	6.4462 (232.97)	−31.2955 (244.63)	20.5940 (239.28)	69.9230 (247.61)	0.5996 (239.31)	75.1645 (250.22)	22.2956 (245.41)	0.5460 (240.90)	27.3106 (260.61)	−22.5742 (237.70)
15	−0.8070 (226.83)	0.8704 (241.24)	37.1240 (233.61)	−4.3026 (239.24)	−11.6911 (237.51)	0.0736 (241.83)	−4.2169 (243.45)	−1.8999 (232.61)	12.0637 (256.25)	−1.8131 (229.94)
16	−0.2285 (224.21)	−2.8425 (235.86)	0.3325 (229.58)	1.7740 (235.57)	−23.8811 (236.11)	2.4035 (231.06)	0.3756 (236.65)	−3.8127 (231.77)	5.6172 (249.02)	−2.4561 (223.46)
17	−5.5593 (222.08)	−1.6987 (222.21)	17.9764 (219.49)	0.1565 (231.56)	4.2216 (231.46)	−5.4394 (227.38)	−0.8153 (225.27)	2.0658 (227.08)	0.2962 (238.26)	−0.2316 (217.58)
18	0.5710 (221.20)	−13.3382 (219.66)	−4.0158 (216.72)	−0.4174 (221.91)	−2.8737 (220.91)	0.9260 (226.45)	−0.9970 (220.77)	−25.6792 (225.48)	−1.0476 (237.91)	1.7480 (211.33)
19	−1.1258 (217.20)	0.3330 (216.51)	0.9557 (212.39)	−12.0019 (217.37)	−5.7615 (218.10)	−1.1917 (224.20)	−6.2576 (218.90)	0.5365 (220.25)	−1.2285 (233.12)	−16.7829 (207.42)
20	−18.9364 (213.48)	2.4932 (211.10)	14.6895 (204.24)	−1.1475 (216.08)	−0.1766 (215.44)	−0.5100 (223.75)	−1.0901 (217.16)	0.1621 (218.50)	4.4693 (231.30)	−1.3297 (206.95)
21	3.4828 (207.52)	0.3122 (210.72)	0.1646 (203.25)	−1.0501 (215.39)	0.2959 (213.84)	−0.3228 (219.22)	−3.3511 (216.34)	0.2233 (216.86)	−4.3443 (228.13)	1.4174 (202.53)
22	−2.7620 (207.09)	18.6618 (209.98)	−0.9930 (203.06)	−6.7176 (213.75)	−1.5352 (212.86)	0.9881 (217.43)	4.7779 (214.16)	−6.3463 (211.15)	0.0196 (227.80)	1.8672 (200.50)
23	−3.6945 (206.60)	−2.5954 (206.31)	−2.1089 (200.78)	1.1211 (213.13)	−0.0594 (206.33)	0.2477 (216.32)	−1.7141 (213.77)	5.9130 (208.98)	−8.1956 (226.87)	3.8908 (198.50)
24	3.7525 (204.51)	2.3131 (206.02)	−2.9698 (200.11)	−0.2784 (212.33)	10.9210 (205.98)	−1.0206 (213.79)	−0.1213 (209.50)	2.0935 (208.10)	1.9027 (220.70)	−1.4599 (198.36)
25	0.7491 (203.32)	−0.1844 (205.67)	2.8510 (199.67)	−0.7945 (210.36)	8.4411 (203.81)	−6.3480 (211.50)	0.6373 (207.90)	−0.8026 (207.61)	−0.2842 (217.82)	0.1007 (197.53)
26	2.8444 (201.92)	5.1436 (204.19)	4.7822 (199.28)	−0.3621 (209.04)	−2.4354 (201.13)	−4.0687 (208.97)	0.8829 (207.58)	−0.6396 (206.47)	0.0171 (216.65)	0.9391 (196.92)
27	2.0448 (200.16)	−5.9570 (203.75)	−9.6270 (197.86)	−3.8423 (207.56)	−0.2828 (200.78)	0.6249 (207.14)	0.1279 (206.61)	−2.0617 (205.85)	−1.8657 (214.77)	0.1536 (196.40)
28	−0.2026 (199.05)	−0.1540 (202.35)	−1.3559 (197.32)	4.4301 (206.64)	−2.8606 (199.50)	0.2039 (205.47)	7.1143 (204.79)	−7.0248 (200.68)	−1.1397 (213.51)	1.0669 (193.74)
29	−1.2557 (198.43)	−1.8523 (200.68)	−17.0066 (196.10)	−1.9416 (205.14)	−6.5894 (197.90)	−4.7256 (204.70)	5.6503 (204.06)	−0.5730 (200.04)	−9.0453 (212.39)	−10.9852 (191.45)
30	1.7272 (197.52)	−6.7311 (199.68)	−13.8149 (192.96)	−7.6292 (201.62)	−1.0246 (194.04)	1.7704 (202.49)	−2.7461 (201.46)	0.3224 (199.76)	−10.3162 (210.95)	0.0102 (190.67)

Table 9.S9. (*Continued*)

j	R_j, 10^{-40} erg cm^3 (λ_j, nm)									
	md071*	**md072***	**md073***	**md074***	**md075***	**md076***	**md077***	**md078***	**md079***	**md080***
1	−11.2452 (385.28)	−29.8497 (380.48)	−56.3050 (366.24)	−19.3595 (387.17)	−36.2074 (369.35)	−15.6045 (363.13)	38.3750 (377.74)	−12.5467 (366.06)	−29.0681 (403.30)	−61.5996 (389.88)
2	39.8443 (348.59)	57.4557 (349.08)	61.9920 (360.88)	75.3089 (349.49)	43.8523 (349.89)	−12.4248 (342.59)	−55.0031 (347.59)	−5.6427 (352.30)	81.7307 (375.19)	137.4410 (359.48)
3	5.4591 (317.91)	−4.1229 (332.24)	5.9154 (310.74)	−2.6604 (317.79)	−10.6812 (304.69)	8.2058 (307.67)	31.5127 (313.43)	5.9840 (318.07)	−23.3939 (320.67)	−21.1611 (316.58)
4	−12.1961 (283.34)	14.3145 (311.88)	4.1255 (307.75)	−0.2454 (315.19)	−0.0337 (292.56)	−0.2061 (290.85)	−1.4101 (288.61)	−0.8311 (309.88)	−22.1550 (312.26)	18.9820 (304.39)
5	−2.5166 (281.86)	0.2991 (296.81)	0.7433 (292.96)	0.6392 (306.36)	−0.7489 (291.81)	2.6908 (287.95)	−1.9345 (285.57)	−16.1199 (301.25)	−2.0916 (300.23)	1.5576 (298.10)
6	−3.7949 (280.02)	0.0758 (289.05)	−16.4882 (287.11)	−22.1243 (282.64)	−0.2065 (284.77)	0.1015 (285.50)	15.9354 (282.44)	−4.6830 (287.72)	−12.7576 (292.20)	0.5368 (293.56)
7	−25.0296 (274.21)	0.7876 (281.74)	0.5699 (282.50)	−0.6130 (275.44)	−24.4356 (277.86)	0.0591 (269.57)	−4.4470 (279.12)	12.9767 (278.88)	−4.6844 (291.28)	−0.8120 (289.35)
8	60.1016 (271.71)	−0.4639 (276.80)	−7.2289 (273.60)	−1.4763 (274.97)	11.5027 (273.05)	7.7272 (268.96)	−4.9018 (275.56)	−4.8814 (277.02)	9.6598 (276.76)	−41.7709 (274.04)
9	−22.3160 (268.48)	−0.1756 (275.72)	−59.9308 (271.37)	−45.3446 (270.24)	2.0923 (263.31)	−1.2665 (264.12)	−51.4889 (272.20)	−1.0778 (269.54)	−3.0717 (275.51)	−18.7330 (272.34)
10	−37.0618 (267.95)	−61.9287 (268.49)	−0.0499 (268.30)	0.0360 (259.29)	3.1265 (252.44)	4.4558 (262.62)	−1.2892 (265.16)	−0.1902 (262.27)	−62.8848 (272.34)	−5.4279 (258.78)
11	32.8423 (249.91)	1.4729 (258.72)	3.2654 (260.78)	2.2854 (257.80)	−0.8603 (252.04)	−38.8108 (256.51)	13.5649 (260.14)	−54.3057 (258.73)	0.8270 (262.14)	49.5035 (254.55)
12	18.4256 (242.52)	66.0783 (251.01)	11.4276 (254.90)	2.2668 (256.55)	1.9154 (250.68)	−13.3036 (254.21)	−37.0996 (252.07)	56.3310 (249.67)	28.9177 (248.53)	27.6755 (250.48)
13	13.7668 (239.29)	−21.2804 (248.81)	29.3014 (251.56)	114.3576 (249.74)	8.1730 (246.33)	83.0445 (250.36)	−0.0125 (244.46)	−6.7271 (247.56)	67.0486 (248.43)	−65.1577 (242.04)
14	0.3810 (235.71)	−15.8538 (247.64)	−6.0659 (249.30)	−65.6003 (242.68)	50.1135 (232.83)	−0.3237 (239.64)	10.3410 (242.92)	−0.0840 (238.79)	6.3226 (243.85)	−4.6684 (239.44)
15	−0.5582 (229.61)	23.0690 (243.75)	33.9455 (241.88)	5.1482 (240.65)	3.2393 (229.25)	8.8039 (236.60)	59.3376 (239.94)	−1.6169 (237.04)	−24.9603 (240.03)	21.4191 (234.07)
16	3.6659 (227.81)	12.4678 (237.32)	1.0949 (237.54)	−0.7607 (231.49)	−5.7587 (226.56)	0.1404 (234.19)	7.1627 (233.23)	3.1112 (234.07)	−5.1129 (237.45)	−6.2206 (228.67)
17	0.7009 (220.20)	−0.1334 (235.21)	5.8606 (228.01)	0.3085 (230.53)	−1.3146 (221.06)	−6.6085 (229.86)	1.7097 (222.86)	27.9005 (232.88)	−5.5051 (234.81)	−2.8999 (228.21)
18	−17.7083 (218.63)	−7.7302 (229.74)	1.8346 (223.41)	−3.3757 (223.84)	−0.0773 (219.24)	0.2550 (228.50)	2.8331 (219.14)	2.3717 (223.94)	38.6106 (221.58)	0.9705 (225.21)
19	−1.2117 (215.43)	0.1951 (222.02)	−1.7418 (218.24)	−4.4052 (218.30)	−0.1764 (216.02)	−7.9135 (221.33)	−7.1141 (217.10)	−0.5976 (221.32)	−0.1186 (214.73)	−3.9834 (224.44)
20	−1.4369 (212.39)	0.0776 (220.94)	4.5271 (217.21)	0.7694 (217.32)	−6.0407 (211.21)	−16.1786 (218.36)	−20.8850 (214.98)	1.9727 (221.03)	−38.1687 (213.18)	1.2072 (222.64)
21	4.0436 (209.82)	−4.1537 (217.12)	1.5421 (214.13)	−28.9023 (215.65)	−0.1479 (210.70)	−7.1258 (214.98)	2.9116 (213.34)	−14.3383 (216.28)	3.7637 (212.05)	−0.3806 (214.77)
22	1.3363 (206.05)	−12.2782 (216.55)	1.4817 (213.61)	−4.1455 (212.72)	−0.0858 (210.25)	−2.4683 (213.83)	−2.2558 (212.78)	−21.1701 (213.93)	−0.3483 (209.56)	0.1876 (213.99)
23	−4.7931 (205.26)	−0.2808 (212.79)	1.0171 (210.77)	1.6114 (210.34)	−0.0990 (204.80)	−0.3069 (212.82)	15.4077 (210.23)	−13.3832 (212.91)	−0.5676 (208.54)	0.0007 (213.51)
24	−8.3326 (202.27)	−0.8110 (209.25)	−6.5924 (209.37)	−1.5964 (209.78)	−10.4567 (202.44)	0.2355 (211.74)	−0.0732 (208.49)	2.5789 (212.84)	−5.7200 (207.62)	−4.0012 (212.06)
25	−1.6317 (201.59)	0.3737 (208.68)	−3.7824 (206.77)	0.5470 (208.68)	9.2824 (200.50)	0.9820 (211.40)	1.0227 (207.90)	10.9399 (209.47)	0.3735 (207.34)	−4.5290 (210.44)
26	−4.8781 (198.70)	−1.1519 (206.74)	0.4547 (205.50)	−0.0034 (207.80)	0.0063 (199.87)	0.0184 (205.84)	1.5745 (206.38)	−2.8087 (207.31)	5.5843 (204.82)	0.5559 (205.35)
27	−3.5963 (198.33)	−0.6750 (205.79)	−1.3435 (203.59)	3.7905 (201.62)	1.1524 (199.82)	−3.3277 (203.65)	0.9989 (205.07)	0.1799 (206.77)	−0.2855 (203.44)	−0.9633 (203.28)
28	2.7474 (196.05)	−5.7240 (203.38)	−5.0916 (201.91)	−3.2027 (200.65)	−2.4760 (198.51)	0.9862 (202.30)	−3.2893 (204.17)	−5.2752 (204.63)	5.3442 (202.98)	−1.0615 (202.46)
29	−3.8323 (195.55)	−0.5143 (202.40)	−2.0308 (201.28)	−7.2061 (197.30)	1.0622 (196.68)	2.1758 (201.64)	−7.1708 (202.72)	−1.6372 (202.14)	−1.8666 (200.70)	0.0321 (201.30)
30	14.2653 (195.01)	−8.0549 (201.56)	1.5629 (201.11)	−0.1853 (196.85)	−0.2466 (195.59)	−0.6796 (200.77)	0.0576 (200.77)	3.2332 (200.19)	−0.0049 (199.05)	−13.3428 (199.91)

Table 9.S9. (*Continued*)

j	R_j, 10^{-40} erg cm^3 (λ_j, nm)									
	md081*	**md082***	**md083***	**md084***	**md085***	**md086***	**md087***	**md088***	**md089***	**md090***
1	−61.6399 (373.75)	−47.9527 (406.64)	−27.4131 (371.07)	2.6778 (372.43)	−10.4609 (392.91)	−57.1930 (356.74)	−38.9140 (364.03)	−37.9655 (387.54)	−63.7687 (375.10)	−22.9922 (387.42)
2	135.3027 (353.18)	70.0857 (361.32)	82.2976 (342.63)	15.2911 (351.93)	4.8097 (358.64)	187.8119 (345.55)	164.2605 (344.02)	165.8631 (349.94)	120.4684 (358.72)	95.5390 (355.88)
3	−23.3388 (316.01)	35.2237 (320.29)	7.9725 (328.25)	48.1724 (311.74)	21.7967 (314.94)	−51.0314 (323.88)	−34.6231 (322.94)	−68.5340 (325.43)	−34.5892 (315.62)	−26.7142 (323.36)
4	−0.1387 (299.29)	−14.5174 (308.66)	−2.6591 (293.95)	−11.3890 (297.14)	−10.1940 (292.97)	−5.0965 (297.37)	−22.8700 (286.33)	7.0739 (289.99)	8.8477 (304.27)	−0.6413 (310.75)
5	−0.0325 (297.50)	−0.1511 (292.91)	−46.5482 (289.94)	−1.4897 (291.41)	−1.1008 (279.62)	−22.3118 (288.65)	−1.6515 (284.88)	6.7086 (286.28)	3.0287 (300.92)	4.5440 (308.12)
6	25.2770 (293.84)	0.6024 (292.20)	−5.9634 (289.53)	−0.2081 (285.97)	0.0961 (278.80)	1.5980 (284.59)	−15.8076 (282.86)	1.7591 (285.51)	1.2104 (297.41)	0.2822 (295.79)
7	−0.2218 (285.61)	−1.6416 (285.45)	−1.9348 (283.71)	−15.7546 (280.01)	7.7768 (275.93)	−36.7289 (276.01)	−58.9057 (274.13)	−63.0220 (276.67)	−18.1512 (284.92)	6.5143 (282.70)
8	−57.9284 (278.98)	2.0886 (278.00)	−17.2226 (276.68)	4.2791 (278.45)	−3.7743 (274.81)	12.3051 (271.67)	19.7436 (270.90)	11.8978 (276.06)	−2.8450 (279.18)	2.4239 (281.79)
9	−5.2402 (267.12)	−49.0419 (275.17)	−3.5583 (269.97)	−16.3862 (274.78)	−34.8692 (271.86)	0.7993 (265.96)	7.2297 (262.14)	1.6807 (270.10)	0.0814 (274.13)	−82.6920 (276.01)
10	2.2072 (260.33)	−10.3643 (272.61)	24.5022 (264.67)	−60.9956 (268.58)	0.0976 (265.51)	23.9898 (260.92)	89.2667 (261.62)	−1.0646 (265.52)	−0.8543 (264.44)	−7.8400 (270.00)
11	68.0710 (255.03)	7.1160 (259.27)	52.2127 (257.64)	−17.6370 (253.94)	−11.6867 (256.75)	−5.0409 (256.32)	−2.2081 (257.27)	106.7181 (258.90)	−9.2179 (261.01)	−3.9207 (259.48)
12	−64.4454 (245.11)	32.1993 (251.34)	−32.3433 (255.95)	−43.9553 (249.15)	8.2737 (252.11)	−16.3636 (254.66)	−79.7543 (254.72)	−6.6767 (251.69)	109.7232 (255.55)	160.3318 (255.74)
13	−6.0926 (243.22)	4.1695 (247.94)	−1.6644 (248.91)	95.5759 (243.21)	−7.6529 (246.50)	12.1198 (242.72)	−7.8959 (241.06)	−110.6556 (244.04)	−86.8033 (246.03)	−66.2306 (248.74)
14	−6.0844 (234.90)	−21.9885 (242.78)	0.2707 (240.85)	−2.2428 (234.18)	29.8935 (241.33)	−12.2983 (241.56)	5.1625 (234.89)	10.1816 (240.60)	4.5714 (241.53)	−20.8617 (245.19)
15	1.5441 (234.43)	8.8218 (237.67)	−0.4570 (239.68)	0.4448 (232.60)	11.1620 (238.65)	−15.3350 (228.87)	−10.6835 (232.77)	−14.7958 (237.16)	22.9179 (238.73)	−5.2988 (237.96)
16	15.8226 (232.30)	5.8315 (234.11)	4.1811 (237.02)	7.7389 (231.89)	−0.9051 (235.93)	0.6215 (227.81)	−0.5082 (228.85)	−1.1025 (234.58)	−0.2514 (234.01)	−0.2303 (237.11)
17	5.0134 (229.78)	7.7620 (222.28)	4.3659 (231.81)	−2.0208 (225.46)	−15.4087 (219.35)	−6.5863 (226.92)	10.2465 (226.01)	−0.0403 (223.17)	−5.7226 (232.68)	3.8192 (234.62)
18	4.3800 (229.07)	−1.8301 (221.71)	7.2008 (231.64)	−23.5530 (223.04)	−0.0789 (212.21)	8.0941 (224.47)	−2.5246 (223.57)	−19.3809 (216.58)	−0.4487 (231.83)	0.6061 (233.91)
19	−6.5467 (228.27)	2.3524 (217.61)	0.0818 (227.10)	−0.0326 (217.77)	−3.7325 (210.12)	−19.0919 (222.47)	−25.8490 (217.42)	1.0911 (214.16)	1.8750 (225.25)	0.1433 (229.84)
20	1.2539 (226.29)	−0.1216 (216.36)	−17.1856 (223.52)	4.1836 (217.45)	1.2554 (209.26)	3.0206 (213.46)	2.5196 (210.12)	−0.7000 (211.44)	−8.8227 (219.39)	3.2032 (218.45)
21	−1.3200 (219.14)	−4.4397 (215.16)	−4.9614 (219.76)	2.8319 (216.20)	0.4364 (208.32)	0.8122 (211.88)	1.4900 (208.41)	−4.5754 (210.23)	−4.8840 (215.65)	−1.7627 (218.08)
22	−1.9321 (213.83)	2.2823 (213.31)	15.0254 (217.38)	4.5830 (214.84)	5.7731 (207.44)	0.5398 (210.76)	2.4866 (208.21)	−5.1979 (209.70)	−0.1132 (214.81)	0.7123 (215.39)
23	4.0639 (212.79)	−1.5832 (212.51)	3.9788 (213.31)	−5.2398 (214.13)	0.9649 (206.42)	−3.1762 (210.23)	−1.7570 (206.37)	18.6524 (206.28)	−10.2743 (212.50)	−0.1111 (215.10)
24	−0.8665 (209.96)	−21.2580 (207.84)	0.1627 (211.23)	−14.1323 (210.20)	3.5860 (205.16)	1.2980 (208.88)	1.0752 (205.35)	−4.4376 (204.83)	−5.2001 (210.09)	−18.2911 (214.06)
25	−0.3294 (207.22)	−0.5700 (206.94)	−3.8857 (210.64)	−0.7699 (210.05)	−0.0041 (203.18)	0.1003 (207.21)	2.2749 (204.96)	−1.4735 (204.26)	12.4608 (208.03)	−6.7125 (212.64)
26	−15.3845 (206.54)	−6.8134 (205.85)	0.7919 (210.31)	9.7390 (208.01)	−0.3253 (201.00)	−0.3817 (204.24)	−0.8156 (204.06)	−2.2907 (203.58)	3.1652 (207.62)	2.7303 (210.53)
27	0.2614 (202.88)	−7.7853 (204.87)	−0.9152 (206.52)	−1.7565 (203.19)	−4.5941 (200.58)	−4.0506 (203.47)	−12.6558 (201.27)	1.5475 (203.13)	−0.4078 (206.57)	1.4069 (208.83)
28	−0.9431 (200.82)	0.4250 (204.38)	−1.8503 (205.20)	0.9716 (202.71)	−1.1267 (198.55)	−3.8355 (201.97)	−4.6157 (200.02)	0.1893 (202.16)	0.8859 (206.31)	−0.1970 (206.94)
29	−1.9326 (199.54)	0.8415 (203.37)	1.2510 (204.02)	0.0747 (202.54)	0.6658 (198.32)	−13.7419 (199.59)	−0.4940 (197.96)	0.9306 (201.36)	4.5362 (205.24)	3.2551 (206.36)
30	5.1628 (197.21)	−0.7885 (202.81)	0.6616 (202.61)	−0.6817 (200.58)	0.4711 (197.60)	8.6864 (198.50)	1.0073 (195.97)	1.2415 (200.12)	−2.9794 (201.01)	−7.9483 (205.27)

Table 9.S9. (*Continued*)

j	R_j, 10^{-40} erg cm^3 (λ_j, nm)									
	md091*	**md092***	**md093***	**md094***	**md095***	**md096***	**md097***	**md098***	**md099***	**md100***
1	−61.6529 (375.33)	−41.9957 (380.96)	−35.4556 (356.80)	−15.2893 (393.79)	−11.1298 (405.12)	−10.9423 (369.30)	−37.3744 (373.97)	−7.7590 (361.41)	−10.6307 (374.47)	−34.9153 (380.52)
2	82.8278 (350.36)	110.6654 (350.02)	97.8881 (340.12)	54.3164 (358.63)	20.2119 (356.48)	66.6021 (349.72)	52.1894 (345.72)	−5.2109 (343.28)	45.8344 (349.10)	95.4192 (352.29)
3	27.8150 (312.21)	−49.9421 (319.49)	−0.6506 (307.08)	−9.5634 (317.34)	13.4640 (323.04)	−33.7369 (312.02)	−30.5265 (313.54)	16.2393 (313.05)	5.6609 (313.73)	−25.2681 (317.81)
4	−6.6558 (293.64)	−10.9317 (292.40)	−0.9324 (293.02)	−0.5053 (309.48)	0.8259 (308.90)	12.3781 (301.54)	32.2186 (292.48)	2.9078 (293.09)	−0.2800 (298.03)	−1.1139 (313.21)
5	−1.4967 (289.20)	15.4893 (284.97)	−10.1391 (292.21)	15.9585 (304.09)	25.9515 (307.04)	−0.4263 (293.38)	−0.1539 (281.92)	27.5488 (282.93)	−0.7005 (289.76)	−0.1751 (290.02)
6	−22.9267 (285.62)	−9.2962 (281.76)	−10.0201 (283.77)	−20.1303 (289.37)	1.6861 (290.20)	−7.5227 (290.76)	−2.2811 (275.43)	24.7178 (279.89)	−18.0059 (289.26)	0.5217 (285.44)
7	−0.4595 (278.88)	−1.1032 (278.36)	−23.0467 (274.60)	−0.7364 (284.56)	2.1193 (281.52)	−2.1835 (278.00)	−31.8095 (271.10)	0.8509 (273.47)	−7.9074 (283.28)	4.8700 (276.11)
8	−32.9251 (274.94)	−3.2210 (274.86)	5.3162 (271.02)	−7.7438 (278.17)	−22.5972 (273.88)	18.8323 (277.01)	5.6024 (269.75)	−4.2616 (269.59)	−0.7461 (281.59)	−4.1874 (275.51)
9	−2.4444 (273.91)	−7.0136 (273.29)	−37.7707 (267.71)	−36.5024 (268.86)	−47.1771 (263.26)	−19.8028 (272.82)	−0.4496 (265.36)	−2.7931 (264.91)	−6.9460 (275.47)	−9.2072 (273.82)
10	−27.3588 (270.03)	1.0046 (269.15)	−0.2721 (265.06)	−18.6337 (265.62)	−3.1555 (257.30)	2.2246 (266.96)	11.6851 (260.72)	2.2257 (263.87)	−10.1580 (269.91)	−3.1974 (267.91)
11	−7.0081 (253.22)	9.8726 (262.98)	−1.2093 (254.88)	0.9264 (256.37)	−2.1389 (250.77)	−2.6804 (255.37)	1.2666 (252.47)	−55.6630 (258.15)	23.6158 (256.75)	12.7663 (260.13)
12	105.8690 (247.55)	67.5951 (254.90)	88.1613 (248.56)	−4.7190 (250.96)	−4.1685 (247.20)	6.3275 (250.50)	−104.4475 (248.20)	−8.9432 (250.44)	−7.3796 (247.49)	11.5868 (252.23)
13	−53.1354 (241.98)	−77.0389 (244.56)	−59.1177 (244.88)	114.5242 (246.46)	30.3349 (243.47)	−12.5650 (245.19)	104.8411 (244.51)	31.1584 (239.50)	−23.9405 (245.70)	−18.3073 (241.87)
14	10.8020 (235.43)	−8.3185 (241.63)	10.3871 (243.12)	9.0671 (241.95)	32.0046 (240.17)	−0.5602 (241.91)	−0.5275 (239.88)	−0.1037 (236.97)	49.1435 (244.02)	3.4822 (240.49)
15	10.7716 (233.26)	32.9826 (239.68)	4.1795 (233.41)	−22.8186 (240.21)	21.0199 (235.21)	8.3834 (234.52)	−2.5032 (229.83)	−2.1567 (233.54)	2.9776 (236.92)	2.5096 (238.04)
16	6.4042 (229.18)	4.1205 (234.05)	−1.7350 (232.75)	−53.8746 (237.02)	−2.8995 (234.26)	9.6357 (232.39)	4.1383 (227.92)	2.1093 (231.85)	−1.3569 (235.37)	−3.2942 (231.70)
17	−0.0862 (223.79)	−8.8705 (226.05)	−11.5125 (228.47)	0.0196 (227.37)	−1.2343 (227.14)	−1.2495 (229.07)	9.4718 (225.53)	−6.3100 (221.95)	−3.0059 (224.48)	2.7051 (228.36)
18	−41.1937 (219.79)	−5.4738 (220.24)	−17.6376 (222.94)	−25.9680 (221.26)	−2.7097 (221.72)	0.2373 (225.65)	−0.4041 (219.10)	−0.2494 (219.73)	−27.7265 (222.74)	−10.8652 (221.71)
19	−0.4640 (217.84)	0.2684 (217.47)	−7.7883 (221.73)	−15.7578 (215.95)	−16.8514 (218.04)	0.9709 (222.57)	−6.7294 (210.88)	−14.7787 (217.98)	−2.1842 (222.21)	−5.5911 (218.73)
20	−2.9317 (216.51)	−0.1508 (215.03)	−1.9737 (217.06)	0.8401 (214.62)	2.9079 (214.10)	−5.9032 (216.33)	0.2748 (209.87)	1.3204 (213.26)	−3.9891 (216.99)	0.8540 (218.29)
21	0.1453 (212.35)	2.6370 (212.90)	1.0119 (213.83)	1.6882 (212.01)	0.9702 (211.71)	1.1798 (214.32)	0.4623 (209.15)	−4.2825 (212.17)	1.4462 (216.40)	2.8554 (214.19)
22	−0.5884 (210.23)	2.3544 (212.06)	2.0327 (211.76)	−0.5603 (211.94)	−2.1045 (210.92)	1.3644 (212.18)	9.7028 (207.49)	3.6295 (211.15)	3.8524 (216.20)	0.7027 (212.18)
23	−1.4483 (206.38)	−11.5198 (208.65)	2.7132 (208.90)	−0.1455 (211.55)	1.8141 (206.31)	2.9722 (211.84)	4.8933 (203.16)	−1.3046 (210.90)	−0.2401 (209.60)	0.1495 (210.59)
24	−1.8753 (205.00)	−1.1704 (208.14)	−5.7413 (207.30)	1.4484 (208.76)	−2.7261 (205.05)	0.1577 (208.75)	−0.1819 (202.06)	2.1977 (209.86)	3.8666 (208.09)	−0.9235 (210.14)
25	5.6011 (203.53)	−3.7440 (205.34)	0.2371 (203.70)	0.1506 (207.52)	−14.1278 (204.26)	−0.0724 (208.16)	1.4856 (201.60)	−4.5143 (207.27)	2.2517 (207.83)	4.2878 (206.21)
26	1.5954 (202.91)	−3.2181 (202.86)	−5.0775 (203.43)	−2.2904 (204.95)	−4.8293 (202.02)	1.5586 (207.69)	−7.4525 (199.78)	28.3791 (204.89)	5.2586 (205.78)	−3.3695 (204.28)
27	−0.7100 (202.35)	0.9269 (202.44)	−10.7459 (202.04)	1.0256 (203.95)	1.1900 (199.38)	−1.3435 (204.49)	3.1491 (199.04)	−0.3226 (203.19)	4.4479 (205.04)	5.0541 (203.76)
28	4.1793 (201.94)	0.1890 (202.04)	−0.8469 (200.20)	2.2024 (202.12)	11.0826 (197.18)	−3.8119 (204.01)	−0.6676 (198.17)	2.5586 (201.13)	−1.4683 (204.37)	0.8285 (202.52)
29	15.0164 (200.08)	0.9177 (201.42)	−4.2771 (199.31)	1.0621 (201.03)	−1.5199 (196.07)	−6.4056 (201.87)	−6.7728 (197.11)	−6.2164 (199.25)	7.1879 (201.42)	2.1178 (197.01)
30	0.2567 (199.17)	0.8437 (199.55)	3.1676 (196.52)	0.7321 (199.39)	−5.2507 (193.62)	−0.6878 (201.23)	1.1384 (194.14)	−0.9573 (196.98)	−1.7553 (201.04)	0.4569 (195.15)

Table 9.S10. Oscillator strengths and excitation wavelengths for the *ab initio* MD solvation clusters of **1** with methanol, as obtained by TD-DFT calculations.

	f_j (λ_j, nm)									
j	**md001***	**md002***	**md003***	**md004***	**md005***	**md006***	**md007***	**md008***	**md009***	**md010***
1	0.0064 (363.28)	0.0068 (361.30)	0.0002 (374.10)	0.0032 (417.31)	0.0270 (395.53)	0.0000 (389.91)	0.0009 (378.63)	0.0103 (373.48)	0.0020 (366.84)	0.0028 (411.48)
2	0.4183 (342.35)	0.3917 (335.51)	0.4318 (337.61)	0.0886 (358.47)	0.3589 (341.88)	0.4381 (339.47)	0.4184 (352.04)	0.3588 (349.40)	0.3961 (338.58)	0.2962 (362.58)
3	0.0020 (312.20)	0.0036 (315.56)	0.0298 (325.30)	0.3495 (344.78)	0.0091 (325.52)	0.0150 (321.73)	0.0026 (324.60)	0.0268 (321.42)	0.0102 (320.29)	0.0444 (329.24)
4	0.0000 (298.21)	0.0008 (292.99)	0.0035 (285.16)	0.0056 (306.27)	0.0071 (320.81)	0.0001 (293.58)	0.0178 (284.81)	0.0565 (291.04)	0.0063 (279.34)	0.0087 (303.38)
5	0.0013 (294.82)	0.0004 (292.80)	0.0585 (280.78)	0.0079 (299.75)	0.0001 (297.33)	0.0003 (292.84)	0.0330 (282.46)	0.0009 (285.00)	0.0286 (276.87)	0.0007 (294.37)
6	0.0169 (287.25)	0.0031 (292.02)	0.0059 (279.61)	0.0021 (289.23)	0.0008 (296.91)	0.0041 (285.73)	0.0241 (280.98)	0.0010 (280.55)	0.0430 (276.63)	0.0035 (292.86)
7	0.0344 (283.09)	0.0573 (280.02)	0.0017 (271.33)	0.0012 (287.94)	0.0114 (282.52)	0.0050 (278.51)	0.0131 (276.13)	0.0050 (278.56)	0.0755 (270.80)	0.0375 (289.10)
8	0.0578 (279.07)	0.0577 (279.01)	0.0013 (264.44)	0.0024 (283.34)	0.0032 (279.91)	0.0072 (276.43)	0.0016 (275.02)	0.0156 (262.78)	0.0003 (267.57)	0.0605 (279.19)
9	0.0025 (270.18)	0.0013 (270.10)	0.0002 (257.32)	0.1273 (275.95)	0.0295 (272.09)	0.0424 (269.99)	0.0188 (270.77)	0.1095 (256.06)	0.0209 (262.15)	0.0359 (275.61)
10	0.0257 (264.87)	0.0272 (257.56)	0.0270 (256.23)	0.0414 (262.95)	0.0092 (264.40)	0.1417 (261.60)	0.0604 (260.25)	0.0162 (253.44)	0.1353 (250.90)	0.0019 (274.55)
11	0.2366 (253.48)	0.1135 (249.88)	0.0450 (250.89)	0.0308 (259.45)	0.1218 (262.15)	0.0032 (249.92)	0.1225 (258.93)	0.1471 (250.66)	0.0165 (248.64)	0.1421 (254.67)
12	0.0082 (242.78)	0.0309 (246.98)	0.0366 (247.99)	0.0021 (257.09)	0.0678 (253.68)	0.0758 (246.33)	0.1386 (257.54)	0.0226 (245.36)	0.0661 (243.94)	0.0137 (250.52)
13	0.0066 (240.64)	0.0014 (242.83)	0.1070 (244.50)	0.1823 (251.59)	0.0030 (249.96)	0.0026 (239.17)	0.0827 (248.80)	0.0639 (239.72)	0.0411 (234.32)	0.0140 (249.69)
14	0.0021 (237.37)	0.1157 (238.82)	0.0151 (233.55)	0.0535 (243.58)	0.2211 (241.48)	0.0781 (235.98)	0.0020 (241.13)	0.0419 (238.89)	0.0333 (230.88)	0.2416 (247.09)
15	0.0176 (232.93)	0.0006 (237.65)	0.0928 (232.01)	0.0056 (241.48)	0.0210 (237.84)	0.0012 (224.18)	0.0010 (231.31)	0.0104 (232.16)	0.0099 (229.73)	0.0040 (246.31)
16	0.0001 (231.36)	0.0075 (236.50)	0.0377 (230.96)	0.0034 (236.58)	0.0017 (231.09)	0.0070 (223.75)	0.0010 (226.92)	0.0012 (231.81)	0.0022 (225.81)	0.0025 (231.65)
17	0.0216 (230.67)	0.0074 (229.49)	0.0005 (220.03)	0.0043 (232.56)	0.0011 (230.65)	0.0001 (218.01)	0.0001 (226.08)	0.0004 (226.57)	0.0051 (219.56)	0.0089 (228.01)
18	0.0003 (227.65)	0.0093 (225.62)	0.0011 (214.98)	0.0392 (227.39)	0.0102 (230.17)	0.0009 (215.89)	0.0029 (222.41)	0.0013 (221.02)	0.0017 (215.96)	0.0078 (220.70)
19	0.0136 (222.77)	0.0085 (224.89)	0.0001 (212.97)	0.0007 (226.10)	0.0083 (227.23)	0.0022 (214.53)	0.0925 (218.01)	0.1087 (212.24)	0.0649 (215.38)	0.0027 (220.28)
20	0.0696 (219.54)	0.0306 (219.92)	0.0018 (208.07)	0.0061 (222.93)	0.0264 (226.78)	0.0033 (212.26)	0.0093 (212.87)	0.0050 (209.03)	0.0079 (210.27)	0.0394 (219.46)
21	0.0166 (218.02)	0.0095 (213.81)	0.0393 (207.21)	0.0089 (213.96)	0.0041 (224.35)	0.0017 (211.21)	0.0344 (210.80)	0.0113 (208.66)	0.0129 (208.88)	0.0459 (219.24)
22	0.0002 (214.27)	0.0027 (212.31)	0.0083 (206.21)	0.0449 (212.98)	0.0011 (221.11)	0.0144 (210.58)	0.0120 (208.04)	0.0022 (206.44)	0.0022 (205.38)	0.0184 (215.63)
23	0.0140 (211.38)	0.0554 (209.19)	0.0123 (205.59)	0.0083 (210.55)	0.0013 (216.98)	0.0314 (206.42)	0.0044 (206.42)	0.0040 (205.47)	0.0025 (203.48)	0.0003 (212.85)
24	0.0005 (209.18)	0.0016 (208.44)	0.0056 (203.82)	0.0056 (210.24)	0.0625 (209.18)	0.0065 (205.06)	0.0077 (206.15)	0.0040 (203.90)	0.0042 (202.86)	0.0010 (210.63)
25	0.0090 (208.98)	0.0022 (207.75)	0.0327 (201.56)	0.0188 (209.55)	0.0022 (207.84)	0.0260 (202.47)	0.0193 (205.09)	0.0001 (203.39)	0.0262 (202.25)	0.0009 (208.78)
26	0.0046 (206.70)	0.0016 (205.79)	0.0069 (200.44)	0.0019 (207.15)	0.0106 (206.68)	0.0114 (200.73)	0.0083 (204.07)	0.0203 (202.51)	0.0192 (200.50)	0.0018 (207.81)
27	0.0006 (206.29)	0.0185 (204.84)	0.0001 (198.66)	0.0010 (205.01)	0.0020 (205.90)	0.0012 (199.72)	0.0031 (203.62)	0.0043 (198.96)	0.0882 (198.60)	0.0077 (206.73)
28	0.1392 (203.63)	0.0173 (203.03)	0.0026 (198.07)	0.0026 (203.85)	0.0005 (205.12)	0.0320 (198.29)	0.0021 (202.40)	0.0009 (198.51)	0.0041 (196.95)	0.0086 (205.98)
29	0.0073 (199.34)	0.0004 (202.61)	0.0004 (194.39)	0.0120 (202.41)	0.0010 (202.11)	0.0003 (197.38)	0.0225 (201.33)	0.0545 (195.46)	0.0033 (196.00)	0.0008 (203.74)
30	0.0027 (198.92)	0.0110 (200.19)	0.0002 (192.91)	0.0017 (201.85)	0.0028 (201.44)	0.0236 (196.31)	0.0516 (198.24)	0.0125 (194.96)	0.0307 (194.65)	0.0483 (202.71)

Table 9.S10. (*Continued*)

j	f_j (λ_j, nm)									
	md011*	**md012***	**md013***	**md014***	**md015***	**md016***	**md017***	**md018***	**md019***	**md020***
1	0.0006 (377.78)	0.0009 (370.50)	0.0184 (383.03)	0.0008 (384.50)	0.0077 (362.72)	0.0042 (393.95)	0.0201 (387.60)	0.0003 (374.70)	0.0017 (395.70)	0.0095 (379.95)
2	0.3449 (346.92)	0.4464 (341.65)	0.3754 (350.25)	0.4339 (334.64)	0.4042 (339.26)	0.3857 (354.11)	0.3535 (348.02)	0.4047 (341.59)	0.3715 (337.12)	0.3992 (350.53)
3	0.0445 (326.23)	0.0014 (319.42)	0.0052 (321.77)	0.0031 (317.32)	0.0016 (307.53)	0.0016 (335.44)	0.0033 (327.29)	0.0150 (328.42)	0.0376 (326.93)	0.0017 (327.66)
4	0.0035 (299.75)	0.0004 (300.36)	0.0011 (303.46)	0.0170 (276.02)	0.0004 (286.07)	0.0042 (299.95)	0.0174 (292.56)	0.0736 (283.37)	0.0065 (289.30)	0.0020 (293.70)
5	0.0006 (291.33)	0.0012 (280.04)	0.0013 (294.76)	0.0005 (273.77)	0.0004 (272.98)	0.0006 (294.70)	0.0023 (289.92)	0.0091 (273.74)	0.0110 (281.50)	0.0859 (288.13)
6	0.0132 (288.28)	0.0068 (271.56)	0.0094 (279.92)	0.0048 (271.08)	0.0005 (270.91)	0.0005 (292.93)	0.0014 (286.23)	0.0050 (271.40)	0.0047 (280.10)	0.0043 (279.54)
7	0.0713 (275.47)	0.0074 (271.51)	0.0035 (276.44)	0.0088 (269.68)	0.0392 (267.80)	0.0384 (287.74)	0.0167 (282.78)	0.0030 (269.80)	0.0018 (278.50)	0.0126 (274.09)
8	0.0429 (273.61)	0.0564 (268.81)	0.0005 (275.93)	0.0438 (268.20)	0.0721 (265.88)	0.0259 (282.28)	0.0990 (271.83)	0.0148 (267.02)	0.0056 (266.07)	0.0012 (269.68)
9	0.0114 (267.11)	0.0009 (264.97)	0.0550 (273.30)	0.0213 (266.90)	0.0004 (263.70)	0.1586 (274.08)	0.0479 (269.63)	0.0088 (265.52)	0.0104 (263.84)	0.0079 (266.68)
10	0.0123 (255.73)	0.0199 (259.52)	0.0325 (264.22)	0.0397 (263.79)	0.0286 (258.89)	0.0112 (265.14)	0.0229 (255.19)	0.0493 (261.92)	0.1325 (258.34)	0.2164 (259.50)
11	0.0387 (254.89)	0.0005 (255.79)	0.1586 (254.57)	0.1874 (247.13)	0.0032 (250.51)	0.0087 (258.22)	0.1320 (250.56)	0.1568 (256.73)	0.0015 (248.68)	0.0002 (253.09)
12	0.1149 (251.91)	0.1187 (250.51)	0.0012 (248.29)	0.0044 (240.01)	0.0875 (247.55)	0.0006 (255.79)	0.1133 (242.29)	0.0266 (248.56)	0.0053 (246.17)	0.0634 (248.76)
13	0.2138 (246.88)	0.0702 (242.73)	0.2232 (245.63)	0.0192 (239.26)	0.2048 (241.86)	0.1458 (251.00)	0.0090 (239.81)	0.0046 (242.55)	0.2190 (242.08)	0.0025 (240.01)
14	0.0163 (242.37)	0.1989 (237.59)	0.0039 (242.13)	0.0121 (236.75)	0.0473 (233.89)	0.0411 (246.95)	0.0123 (231.57)	0.0375 (231.24)	0.0360 (235.40)	0.0224 (237.10)
15	0.0088 (240.11)	0.0082 (233.32)	0.0203 (236.92)	0.0770 (235.77)	0.0052 (226.45)	0.0902 (244.39)	0.0060 (229.48)	0.0659 (230.04)	0.0057 (229.35)	0.0061 (236.71)
16	0.0097 (237.04)	0.0009 (228.63)	0.0003 (230.66)	0.0065 (225.16)	0.0001 (218.39)	0.0007 (238.76)	0.0001 (226.60)	0.0008 (221.13)	0.0233 (228.25)	0.0035 (235.78)
17	0.0032 (233.67)	0.0039 (219.02)	0.0010 (228.56)	0.0054 (213.77)	0.0014 (217.09)	0.0031 (236.04)	0.0053 (224.90)	0.0028 (219.22)	0.0088 (218.24)	0.0093 (232.42)
18	0.0011 (225.51)	0.0035 (215.64)	0.0001 (216.99)	0.0076 (213.70)	0.0005 (215.27)	0.0000 (231.77)	0.0091 (218.38)	0.0863 (215.86)	0.0025 (213.57)	0.0037 (220.84)
19	0.0013 (221.09)	0.0096 (210.44)	0.0019 (213.19)	0.0014 (211.24)	0.0042 (208.49)	0.0065 (223.63)	0.0532 (217.26)	0.0038 (211.40)	0.0008 (210.46)	0.0045 (218.49)
20	0.1007 (218.86)	0.0131 (208.56)	0.0044 (212.81)	0.1064 (207.80)	0.0009 (207.31)	0.0073 (222.40)	0.0107 (212.54)	0.0033 (210.74)	0.0003 (210.13)	0.0011 (217.41)
21	0.0186 (216.29)	0.0340 (206.87)	0.0007 (210.58)	0.0214 (205.87)	0.1343 (205.21)	0.0005 (220.64)	0.0490 (211.25)	0.0021 (208.29)	0.0038 (208.95)	0.0654 (212.40)
22	0.0012 (214.84)	0.0026 (205.81)	0.0100 (210.54)	0.0063 (204.49)	0.0006 (201.91)	0.0816 (219.76)	0.0086 (210.58)	0.0407 (205.28)	0.0261 (205.78)	0.0039 (211.41)
23	0.0267 (214.66)	0.0483 (202.85)	0.0156 (208.70)	0.0083 (201.98)	0.0003 (201.73)	0.0113 (217.39)	0.0602 (208.67)	0.0042 (205.00)	0.0175 (205.60)	0.0003 (209.72)
24	0.0090 (210.03)	0.0242 (202.22)	0.0584 (207.07)	0.0060 (200.67)	0.0178 (199.58)	0.0030 (214.89)	0.0007 (204.34)	0.0161 (204.54)	0.0216 (203.55)	0.0011 (208.93)
25	0.0006 (208.66)	0.0015 (201.73)	0.0207 (206.25)	0.0131 (199.53)	0.0022 (198.39)	0.0003 (209.71)	0.0228 (202.50)	0.0603 (203.46)	0.0377 (199.84)	0.0062 (205.68)
26	0.0005 (208.06)	0.0075 (201.12)	0.0080 (204.87)	0.0017 (197.89)	0.0019 (197.27)	0.0043 (208.68)	0.0051 (202.03)	0.0247 (201.11)	0.0010 (198.94)	0.0284 (203.49)
27	0.0314 (206.48)	0.0028 (198.70)	0.0020 (204.65)	0.0018 (197.47)	0.0034 (196.81)	0.0237 (208.52)	0.0078 (200.98)	0.0002 (200.13)	0.0009 (197.64)	0.0168 (201.26)
28	0.0027 (204.05)	0.0036 (197.51)	0.0022 (201.33)	0.0007 (196.41)	0.0002 (196.55)	0.0108 (205.76)	0.0024 (198.31)	0.0086 (199.41)	0.0005 (197.19)	0.0137 (200.60)
29	0.0514 (202.89)	0.0014 (197.07)	0.0020 (199.51)	0.0165 (196.23)	0.0005 (196.22)	0.0038 (203.85)	0.0079 (197.54)	0.0585 (197.63)	0.0014 (196.49)	0.0031 (198.94)
30	0.0003 (200.29)	0.0037 (196.05)	0.0046 (198.32)	0.0198 (195.17)	0.0003 (195.85)	0.0006 (203.57)	0.0052 (194.98)	0.0003 (194.06)	0.0037 (195.61)	0.0486 (198.38)

Table 9.S10. (*Continued*)

j	f_j (λ_j, nm)									
	md021*	**md022***	**md023***	**md024***	**md025***	**md026***	**md027***	**md028***	**md029***	**md030***
1	0.0009 (390.19)	0.0088 (357.72)	0.0026 (389.78)	0.0001 (395.06)	0.0003 (388.60)	0.0006 (392.93)	0.0026 (376.23)	0.0002 (372.85)	0.0046 (435.91)	0.0021 (391.95)
2	0.4048 (345.20)	0.4002 (347.13)	0.3678 (342.99)	0.4367 (345.59)	0.4032 (340.97)	0.4461 (334.67)	0.4088 (344.82)	0.4241 (341.74)	0.3974 (350.66)	0.4500 (341.88)
3	0.0105 (332.99)	0.0022 (318.75)	0.0281 (328.27)	0.0069 (328.47)	0.0060 (333.70)	0.0500 (325.98)	0.0051 (328.27)	0.0118 (312.32)	0.0299 (342.95)	0.0016 (330.60)
4	0.0004 (287.86)	0.0133 (289.09)	0.0055 (306.01)	0.0038 (283.35)	0.0022 (290.59)	0.0002 (289.08)	0.0091 (299.42)	0.0207 (288.59)	0.0131 (299.90)	0.0039 (285.12)
5	0.0007 (286.55)	0.0770 (287.37)	0.0005 (290.62)	0.0175 (275.23)	0.0008 (284.92)	0.0001 (285.91)	0.0003 (297.09)	0.0001 (279.25)	0.0006 (295.04)	0.0031 (276.48)
6	0.0202 (283.59)	0.0225 (282.78)	0.0179 (287.82)	0.0087 (273.98)	0.0030 (279.80)	0.0184 (279.88)	0.0093 (286.78)	0.0094 (277.01)	0.0326 (281.53)	0.1382 (272.99)
7	0.0146 (279.76)	0.0016 (282.18)	0.0011 (277.98)	0.0016 (273.42)	0.0047 (273.37)	0.0276 (276.44)	0.0008 (283.10)	0.0449 (273.44)	0.0000 (279.88)	0.0039 (269.77)
8	0.0909 (273.42)	0.1055 (274.07)	0.0185 (274.61)	0.0210 (268.95)	0.0126 (270.67)	0.0035 (272.92)	0.0789 (271.49)	0.0475 (269.99)	0.0032 (277.80)	0.0256 (267.46)
9	0.1122 (269.28)	0.0151 (269.29)	0.0497 (270.52)	0.0188 (266.57)	0.1402 (266.14)	0.0101 (270.54)	0.1396 (265.97)	0.0708 (266.85)	0.0164 (268.54)	0.0008 (257.89)
10	0.0003 (266.30)	0.0022 (259.86)	0.0030 (259.13)	0.0006 (260.26)	0.0056 (258.00)	0.0036 (264.80)	0.0028 (257.42)	0.0030 (257.44)	0.0398 (263.43)	0.0238 (253.99)
11	0.0435 (262.46)	0.0109 (252.27)	0.0127 (255.97)	0.1553 (255.22)	0.0051 (255.24)	0.0094 (259.29)	0.0121 (256.04)	0.0994 (253.65)	0.0403 (255.08)	0.0087 (251.40)
12	0.0097 (253.54)	0.0546 (248.91)	0.2415 (251.00)	0.0161 (251.74)	0.1626 (248.66)	0.2043 (251.08)	0.0171 (251.13)	0.0106 (245.53)	0.0047 (254.49)	0.0018 (247.34)
13	0.1611 (248.62)	0.0175 (246.54)	0.0098 (248.00)	0.1331 (249.62)	0.0134 (245.16)	0.0482 (248.51)	0.0031 (245.79)	0.0145 (242.98)	0.0071 (253.04)	0.2257 (244.44)
14	0.0032 (244.37)	0.0003 (237.54)	0.0800 (244.57)	0.0108 (245.98)	0.1295 (244.08)	0.0195 (243.19)	0.0824 (241.86)	0.0890 (237.56)	0.1639 (249.38)	0.0115 (236.74)
15	0.0010 (234.51)	0.0012 (236.54)	0.0033 (241.34)	0.0104 (243.12)	0.0054 (238.02)	0.0545 (232.09)	0.1448 (240.23)	0.0011 (228.09)	0.0014 (246.81)	0.0034 (234.02)
16	0.0014 (232.32)	0.0877 (235.39)	0.0026 (232.54)	0.0354 (232.98)	0.0164 (236.52)	0.0000 (227.98)	0.0001 (236.19)	0.0008 (227.30)	0.1201 (243.19)	0.0024 (227.63)
17	0.0066 (229.54)	0.0040 (225.88)	0.0089 (228.17)	0.0004 (214.43)	0.0011 (219.95)	0.0003 (225.94)	0.0010 (234.18)	0.0010 (223.75)	0.0055 (219.65)	0.0027 (224.04)
18	0.0045 (222.74)	0.0531 (221.61)	0.0033 (226.55)	0.0532 (212.19)	0.0009 (216.48)	0.0102 (223.01)	0.0059 (223.49)	0.0162 (219.94)	0.0015 (215.71)	0.0053 (215.00)
19	0.0027 (220.24)	0.0020 (217.26)	0.0052 (222.74)	0.0029 (211.62)	0.0009 (214.04)	0.0043 (219.98)	0.0071 (218.63)	0.0019 (217.61)	0.1211 (214.71)	0.0347 (214.33)
20	0.0666 (216.23)	0.0001 (215.41)	0.0287 (218.48)	0.0243 (209.09)	0.0018 (213.72)	0.0029 (216.41)	0.0074 (217.61)	0.0025 (216.54)	0.0010 (212.74)	0.0005 (210.85)
21	0.0090 (210.34)	0.0013 (212.72)	0.0265 (216.09)	0.0547 (207.69)	0.0411 (212.61)	0.0031 (216.16)	0.0152 (212.23)	0.0076 (212.09)	0.0010 (210.89)	0.0017 (206.25)
22	0.0039 (210.20)	0.0054 (206.87)	0.0315 (211.32)	0.0081 (204.57)	0.0485 (211.31)	0.0084 (212.11)	0.0139 (211.91)	0.0092 (210.23)	0.0437 (208.43)	0.0018 (204.99)
23	0.0067 (207.39)	0.0034 (206.82)	0.0003 (210.29)	0.0125 (201.74)	0.0065 (207.16)	0.0040 (210.22)	0.0053 (208.91)	0.0309 (208.69)	0.0004 (205.63)	0.0046 (203.97)
24	0.0085 (206.05)	0.0013 (203.99)	0.0444 (207.76)	0.0002 (201.06)	0.0077 (206.33)	0.0024 (209.86)	0.0016 (208.25)	0.0164 (206.89)	0.0039 (205.49)	0.0020 (203.33)
25	0.0044 (205.79)	0.0020 (202.92)	0.0058 (207.24)	0.0149 (200.13)	0.0017 (204.66)	0.0070 (209.15)	0.0029 (203.58)	0.0001 (205.23)	0.0006 (205.03)	0.0275 (201.43)
26	0.0106 (202.24)	0.0023 (201.60)	0.0049 (205.87)	0.0356 (199.28)	0.0044 (203.49)	0.0938 (208.34)	0.0030 (202.47)	0.0008 (202.92)	0.0006 (203.97)	0.0032 (200.97)
27	0.0443 (201.33)	0.0010 (200.85)	0.0262 (202.25)	0.0010 (198.39)	0.0010 (202.48)	0.0248 (205.71)	0.0084 (202.05)	0.0007 (201.84)	0.0019 (202.77)	0.0248 (198.33)
28	0.0127 (200.49)	0.0436 (199.49)	0.0020 (200.73)	0.0034 (198.16)	0.0005 (199.49)	0.0038 (202.52)	0.0019 (201.37)	0.0018 (199.61)	0.0175 (200.78)	0.0131 (196.13)
29	0.0042 (199.77)	0.0059 (198.85)	0.0296 (200.19)	0.0464 (197.60)	0.0041 (198.85)	0.0155 (201.52)	0.0005 (201.25)	0.0815 (198.73)	0.0110 (199.24)	0.0246 (195.47)
30	0.0039 (199.13)	0.0009 (197.55)	0.0042 (198.74)	0.0161 (196.04)	0.0861 (197.11)	0.0153 (199.81)	0.0044 (200.64)	0.0263 (197.95)	0.0076 (198.56)	0.0006 (191.58)

Table 9.S10. (*Continued*)

j	$f_j(\lambda_j$, nm)										
	md031*	**md032***	**md033***	**md034***	**md035***	**md036***	**md037***	**md038***	**md039***	**md040***
1	0.0034 (380.56)	0.0017 (395.20)	0.0006 (398.75)	0.0116 (379.13)	0.0027 (403.74)	0.0191 (395.47)	0.2976 (359.18)	0.0091 (371.58)	0.0361 (383.06)	0.2184 (360.90)
2	0.4446 (345.08)	0.4226 (347.71)	0.4213 (331.35)	0.3679 (352.56)	0.4075 (343.49)	0.3573 (348.35)	0.0435 (350.08)	0.4113 (350.16)	0.3653 (356.99)	0.1605 (356.03)
3	0.0008 (316.12)	0.0026 (327.22)	0.0488 (319.49)	0.0050 (323.07)	0.0007 (325.93)	0.0114 (324.97)	0.0008 (308.80)	0.0020 (313.53)	0.0112 (326.62)	0.0445 (311.46)
4	0.0022 (296.02)	0.0014 (305.96)	0.0452 (282.70)	0.0001 (308.23)	0.0037 (297.68)	0.0015 (301.57)	0.1128 (289.51)	0.0156 (296.34)	0.0082 (290.48)	0.0016 (300.52)
5	0.0016 (286.95)	0.0012 (286.78)	0.0107 (277.37)	0.0008 (299.09)	0.0003 (287.79)	0.0099 (289.23)	0.0647 (280.16)	0.0743 (291.30)	0.0282 (284.68)	0.0297 (294.72)
6	0.0016 (283.27)	0.0029 (282.85)	0.0001 (267.14)	0.0052 (287.61)	0.0007 (284.16)	0.0038 (288.51)	0.0111 (278.22)	0.0019 (286.97)	0.0083 (284.50)	0.0051 (289.23)
7	0.0358 (275.00)	0.0016 (280.83)	0.0167 (263.86)	0.0013 (286.24)	0.0042 (282.45)	0.0121 (282.15)	0.0015 (267.46)	0.0008 (275.78)	0.0152 (280.67)	0.0441 (285.94)
8	0.0593 (272.82)	0.0776 (273.26)	0.0009 (262.06)	0.0254 (280.05)	0.0047 (273.34)	0.0004 (281.51)	0.0052 (262.84)	0.0010 (271.88)	0.0020 (270.35)	0.0006 (274.20)
9	0.0500 (265.81)	0.0014 (265.84)	0.0577 (260.16)	0.1440 (274.68)	0.0728 (269.39)	0.0196 (276.27)	0.0135 (261.43)	0.0182 (263.73)	0.0006 (266.00)	0.0111 (266.87)
10	0.0047 (262.44)	0.0631 (264.24)	0.0012 (259.04)	0.0521 (273.53)	0.0499 (261.29)	0.0386 (268.45)	0.0025 (259.46)	0.1927 (258.58)	0.0395 (260.24)	0.0287 (262.23)
11	0.1332 (254.78)	0.0246 (254.37)	0.1956 (247.23)	0.0027 (260.91)	0.0014 (258.53)	0.0028 (258.12)	0.0063 (256.84)	0.0100 (256.85)	0.2056 (254.80)	0.0034 (258.62)
12	0.0073 (252.39)	0.1143 (250.43)	0.0017 (244.01)	0.1638 (256.55)	0.0056 (251.00)	0.1944 (252.21)	0.2095 (251.42)	0.0017 (253.64)	0.0655 (252.68)	0.2732 (256.07)
13	0.0317 (247.45)	0.0101 (248.95)	0.0204 (242.67)	0.1124 (253.83)	0.1050 (246.56)	0.0031 (248.96)	0.0039 (241.18)	0.0442 (250.44)	0.0058 (250.55)	0.0174 (252.72)
14	0.0325 (240.67)	0.1855 (245.60)	0.0500 (238.58)	0.0028 (248.12)	0.0169 (244.93)	0.1032 (246.79)	0.0260 (232.64)	0.0024 (239.74)	0.0012 (243.57)	0.0220 (245.56)
15	0.1091 (234.62)	0.0008 (244.83)	0.0058 (234.41)	0.0025 (240.65)	0.1723 (244.39)	0.0589 (237.30)	0.0238 (228.17)	0.0215 (235.70)	0.0190 (241.30)	0.0117 (243.63)
16	0.0025 (233.02)	0.0036 (239.61)	0.0013 (218.24)	0.0029 (239.93)	0.0056 (239.51)	0.0053 (234.34)	0.0444 (225.92)	0.0043 (233.53)	0.0042 (227.38)	0.0176 (236.75)
17	0.0099 (230.36)	0.0231 (235.25)	0.0672 (209.88)	0.0272 (238.99)	0.0089 (226.27)	0.0013 (229.66)	0.0021 (221.87)	0.0056 (232.81)	0.1814 (220.71)	0.0009 (236.23)
18	0.0004 (217.90)	0.0004 (220.14)	0.0004 (208.26)	0.0013 (234.97)	0.0056 (224.33)	0.0149 (225.33)	0.0025 (220.70)	0.0794 (230.66)	0.0010 (218.37)	0.0532 (230.34)
19	0.0008 (217.53)	0.0026 (219.82)	0.0064 (205.33)	0.0064 (227.70)	0.0001 (220.25)	0.0304 (223.63)	0.0000 (217.79)	0.0089 (220.40)	0.0118 (215.62)	0.0150 (223.78)
20	0.0039 (216.97)	0.0019 (216.51)	0.0039 (202.82)	0.0001 (224.21)	0.0017 (219.29)	0.0002 (219.00)	0.0013 (212.11)	0.0004 (218.49)	0.0223 (214.59)	0.0017 (222.97)
21	0.0008 (209.84)	0.0042 (213.83)	0.0004 (202.14)	0.0017 (220.96)	0.0087 (212.00)	0.0054 (215.62)	0.0237 (208.38)	0.0172 (215.45)	0.0044 (211.88)	0.0016 (222.32)
22	0.0442 (209.44)	0.0002 (211.84)	0.0021 (200.10)	0.0010 (217.87)	0.0035 (211.60)	0.0273 (214.67)	0.0104 (206.79)	0.0072 (212.62)	0.0114 (209.15)	0.0005 (216.08)
23	0.0027 (208.98)	0.0013 (211.47)	0.0240 (199.22)	0.0287 (216.25)	0.0040 (211.00)	0.0358 (212.42)	0.0164 (203.09)	0.0003 (211.52)	0.0423 (208.24)	0.0002 (215.87)
24	0.0115 (208.72)	0.0028 (210.86)	0.0748 (197.83)	0.1103 (215.67)	0.0024 (209.17)	0.0178 (211.19)	0.0108 (202.72)	0.0435 (209.55)	0.0303 (205.62)	0.0023 (210.66)
25	0.0625 (207.19)	0.0493 (208.63)	0.0536 (197.31)	0.0002 (212.95)	0.0014 (208.76)	0.0007 (210.85)	0.0227 (200.25)	0.0452 (209.07)	0.0140 (205.00)	0.0037 (210.51)
26	0.0072 (205.46)	0.0529 (206.79)	0.0042 (195.32)	0.0013 (209.80)	0.0122 (208.05)	0.0074 (209.93)	0.0011 (199.25)	0.0655 (207.90)	0.0175 (201.88)	0.0144 (208.91)
27	0.0026 (203.24)	0.0057 (204.90)	0.0005 (194.50)	0.0164 (209.24)	0.0040 (206.92)	0.0026 (209.79)	0.0110 (198.16)	0.0212 (206.55)	0.0006 (198.57)	0.0061 (208.57)
28	0.0561 (201.43)	0.0042 (204.72)	0.0239 (193.68)	0.0009 (208.03)	0.0300 (203.19)	0.0346 (206.51)	0.0002 (195.59)	0.0030 (201.80)	0.0047 (195.67)	0.0128 (207.64)
29	0.0015 (200.89)	0.0017 (201.83)	0.0005 (193.04)	0.0007 (207.44)	0.0198 (202.41)	0.0023 (205.55)	0.0031 (194.16)	0.0026 (201.04)	0.0462 (195.24)	0.0411 (205.65)
30	0.0028 (200.64)	0.0015 (201.11)	0.0122 (191.67)	0.0106 (204.88)	0.0001 (200.02)	0.0081 (203.52)	0.0021 (194.00)	0.0106 (200.55)	0.0074 (194.56)	0.0007 (203.24)

Table 9.S10. (*Continued*)

j	f_j (λ_j, nm)									
	md041*	**md042***	**md043***	**md044***	**md045***	**md046***	**md047***	**md048***	**md049***	**md050***
1	0.0556 (353.06)	0.1370 (365.47)	0.0070 (387.86)	0.0209 (389.18)	0.0002 (386.71)	0.0183 (382.14)	0.0046 (366.82)	0.1491 (360.60)	0.0075 (389.65)	0.0035 (390.03)
2	0.3071 (342.60)	0.2076 (349.90)	0.3974 (349.65)	0.3230 (363.13)	0.2836 (362.23)	0.3425 (341.86)	0.3330 (336.91)	0.1284 (349.08)	0.3870 (348.96)	0.2816 (368.80)
3	0.0062 (306.71)	0.0032 (318.22)	0.0114 (325.27)	0.0019 (312.65)	0.0091 (319.76)	0.0089 (300.80)	0.0110 (302.84)	0.0720 (305.83)	0.0084 (315.46)	0.0049 (320.01)
4	0.0128 (291.30)	0.0873 (296.53)	0.0205 (286.75)	0.0615 (294.28)	0.1346 (303.38)	0.0016 (296.04)	0.0006 (290.71)	0.0055 (288.94)	0.0015 (305.70)	0.0008 (314.81)
5	0.0646 (289.50)	0.0130 (291.39)	0.0238 (285.10)	0.0004 (284.12)	0.0012 (281.52)	0.0011 (292.92)	0.0583 (283.87)	0.0348 (286.10)	0.0010 (302.34)	0.1244 (297.20)
6	0.1050 (282.55)	0.0127 (287.06)	0.0372 (277.45)	0.0008 (280.94)	0.0011 (278.79)	0.0260 (291.50)	0.0076 (277.31)	0.0002 (283.60)	0.0529 (286.33)	0.1332 (289.61)
7	0.0123 (276.43)	0.0617 (284.18)	0.0588 (272.33)	0.0234 (279.38)	0.0058 (277.64)	0.0756 (277.69)	0.0863 (274.29)	0.0433 (277.86)	0.0418 (278.22)	0.0005 (275.78)
8	0.0058 (265.47)	0.0040 (273.77)	0.0055 (267.43)	0.0064 (276.97)	0.0056 (273.12)	0.0219 (274.93)	0.0224 (268.63)	0.0288 (275.87)	0.0884 (273.71)	0.0069 (273.97)
9	0.0514 (256.96)	0.0051 (267.60)	0.0018 (261.39)	0.0005 (272.87)	0.0546 (269.59)	0.0259 (267.77)	0.0148 (264.01)	0.0038 (271.55)	0.0129 (267.28)	0.0025 (271.75)
10	0.0097 (250.71)	0.0107 (262.51)	0.0942 (259.80)	0.0010 (263.46)	0.0533 (266.61)	0.0277 (263.91)	0.0005 (258.79)	0.0029 (269.09)	0.0759 (260.13)	0.0234 (260.92)
11	0.0265 (250.47)	0.0698 (256.57)	0.0354 (254.86)	0.0381 (258.02)	0.0933 (262.22)	0.0561 (248.71)	0.0000 (255.59)	0.0114 (263.52)	0.0197 (254.40)	0.0519 (256.96)
12	0.0019 (249.30)	0.1292 (254.78)	0.0972 (250.18)	0.3221 (252.29)	0.1250 (248.93)	0.0102 (246.97)	0.0421 (250.48)	0.0249 (251.66)	0.0155 (253.53)	0.0723 (252.04)
13	0.1271 (247.31)	0.0741 (251.55)	0.0621 (246.09)	0.0155 (243.79)	0.0429 (243.98)	0.0052 (239.56)	0.0067 (246.40)	0.2051 (249.21)	0.1013 (250.53)	0.0299 (250.69)
14	0.0083 (239.40)	0.0006 (244.86)	0.0029 (242.25)	0.0155 (242.81)	0.0222 (239.77)	0.1736 (239.40)	0.2120 (242.92)	0.1122 (243.20)	0.0216 (249.42)	0.0867 (248.43)
15	0.0026 (237.10)	0.0440 (240.69)	0.0212 (239.07)	0.0042 (236.08)	0.0007 (236.22)	0.0046 (234.86)	0.0017 (231.07)	0.0029 (229.28)	0.0023 (241.43)	0.0047 (244.32)
16	0.0441 (235.22)	0.0130 (233.43)	0.0016 (231.83)	0.0005 (228.63)	0.0085 (229.13)	0.0020 (227.56)	0.0143 (227.83)	0.0303 (228.03)	0.0019 (235.55)	0.0566 (235.58)
17	0.0438 (232.73)	0.0243 (232.64)	0.0005 (226.20)	0.1180 (221.14)	0.0915 (227.52)	0.0008 (227.25)	0.0723 (226.85)	0.0283 (222.84)	0.0028 (231.21)	0.0355 (230.23)
18	0.0091 (228.56)	0.0321 (232.29)	0.0202 (223.30)	0.0126 (215.88)	0.0005 (216.42)	0.0677 (220.65)	0.0070 (222.35)	0.0631 (221.49)	0.0006 (226.99)	0.0022 (229.24)
19	0.0037 (217.43)	0.0333 (228.47)	0.0389 (214.77)	0.0009 (215.47)	0.0424 (214.05)	0.0056 (217.61)	0.0004 (221.77)	0.0003 (221.04)	0.0527 (226.13)	0.0038 (220.52)
20	0.0007 (212.07)	0.0319 (214.96)	0.0019 (213.29)	0.0070 (213.66)	0.0091 (212.29)	0.0138 (215.79)	0.0018 (215.83)	0.0018 (214.89)	0.0004 (225.25)	0.0003 (220.22)
21	0.0132 (211.74)	0.0168 (213.13)	0.0541 (209.29)	0.0126 (212.35)	0.0162 (211.76)	0.0008 (214.49)	0.0003 (211.94)	0.0012 (211.80)	0.0033 (209.96)	0.0573 (212.39)
22	0.0018 (211.59)	0.0163 (210.98)	0.0004 (206.67)	0.0024 (209.50)	0.0020 (207.44)	0.0105 (214.29)	0.0055 (211.29)	0.0005 (211.38)	0.0013 (209.34)	0.0048 (211.63)
23	0.0683 (209.24)	0.0222 (210.02)	0.0010 (205.29)	0.0018 (208.18)	0.0054 (206.08)	0.0016 (213.98)	0.0803 (208.86)	0.0059 (210.91)	0.0031 (208.25)	0.0013 (211.22)
24	0.0035 (202.51)	0.0031 (209.17)	0.0013 (204.19)	0.0012 (206.81)	0.0049 (205.08)	0.0015 (208.75)	0.0064 (206.52)	0.0032 (210.27)	0.0103 (207.38)	0.0201 (206.58)
25	0.0123 (201.91)	0.0024 (208.88)	0.0006 (204.11)	0.0037 (206.13)	0.0027 (203.71)	0.0051 (206.46)	0.0007 (205.96)	0.0000 (209.67)	0.0030 (206.73)	0.0003 (203.83)
26	0.0024 (201.39)	0.0031 (208.11)	0.0130 (201.36)	0.0042 (203.63)	0.0045 (203.36)	0.0037 (201.90)	0.0030 (203.59)	0.0113 (208.79)	0.0250 (205.21)	0.0018 (203.40)
27	0.0023 (199.99)	0.0228 (207.17)	0.0011 (200.47)	0.0037 (202.87)	0.0288 (201.00)	0.0080 (201.35)	0.0030 (200.80)	0.0015 (205.09)	0.0076 (204.80)	0.0151 (201.62)
28	0.0052 (199.09)	0.0033 (204.52)	0.0072 (199.56)	0.0021 (201.76)	0.0040 (200.29)	0.0099 (200.97)	0.0329 (199.55)	0.0003 (201.56)	0.0426 (203.71)	0.0001 (199.46)
29	0.0017 (196.51)	0.0078 (201.60)	0.0112 (197.86)	0.0037 (201.31)	0.0027 (198.57)	0.0045 (198.62)	0.0039 (196.48)	0.0550 (201.35)	0.0017 (200.67)	0.0007 (198.29)
30	0.0008 (194.55)	0.0053 (198.15)	0.0013 (196.37)	0.0160 (198.26)	0.0004 (198.32)	0.0149 (198.31)	0.0021 (194.74)	0.0007 (199.80)	0.0338 (198.77)	0.0006 (197.37)

Table 9.S10. (*Continued*)

j	f_j (λ_j, nm)									
	md051*	**md052***	**md053***	**md054***	**md055***	**md056***	**md057***	**md058***	**md059***	**md060***
1	0.0095 (383.65)	0.0202 (394.86)	0.0898 (377.74)	0.0375 (388.14)	0.0059 (379.50)	0.0367 (386.56)	0.0560 (385.65)	0.0307 (381.31)	0.0886 (401.14)	0.0003 (403.09)
2	0.3859 (361.22)	0.3411 (360.26)	0.3126 (351.52)	0.2884 (349.76)	0.3301 (363.21)	0.2569 (355.04)	0.2461 (367.99)	0.3940 (345.50)	0.2849 (357.37)	0.4511 (341.32)
3	0.0192 (323.26)	0.0032 (332.11)	0.0067 (316.62)	0.0079 (322.81)	0.0455 (323.22)	0.0019 (315.16)	0.0099 (333.32)	0.0041 (328.40)	0.0043 (320.44)	0.0202 (333.87)
4	0.0354 (301.37)	0.0091 (312.94)	0.0069 (299.69)	0.0089 (309.35)	0.0008 (307.77)	0.0938 (299.05)	0.0437 (310.93)	0.0048 (313.82)	0.0016 (303.80)	0.0024 (303.29)
5	0.0026 (293.33)	0.0790 (303.14)	0.0449 (293.78)	0.1040 (296.85)	0.0510 (301.11)	0.0017 (284.68)	0.0542 (304.05)	0.0058 (289.67)	0.0053 (300.96)	0.0127 (293.07)
6	0.0072 (278.58)	0.0127 (279.04)	0.0026 (287.84)	0.0082 (277.70)	0.0010 (282.03)	0.0180 (277.74)	0.0012 (284.46)	0.0250 (288.42)	0.0172 (286.44)	0.0178 (291.17)
7	0.0310 (276.49)	0.0542 (275.96)	0.0772 (283.61)	0.0845 (269.78)	0.0007 (281.33)	0.0008 (274.21)	0.0807 (275.18)	0.0013 (281.53)	0.0315 (284.49)	0.0052 (280.05)
8	0.0325 (276.05)	0.1054 (274.22)	0.0096 (276.20)	0.0182 (266.81)	0.0012 (273.72)	0.0352 (269.50)	0.0114 (270.62)	0.0024 (274.55)	0.0074 (273.99)	0.0521 (265.59)
9	0.0003 (268.36)	0.0011 (263.91)	0.0424 (273.58)	0.0039 (260.39)	0.0568 (271.25)	0.0013 (265.33)	0.0035 (262.61)	0.0950 (270.61)	0.0011 (262.83)	0.0003 (258.37)
10	0.0031 (264.45)	0.0019 (259.20)	0.0079 (266.29)	0.0065 (253.97)	0.0007 (269.20)	0.0287 (258.18)	0.0091 (260.27)	0.0042 (257.96)	0.0332 (255.64)	0.0088 (255.55)
11	0.0067 (262.94)	0.0250 (256.01)	0.0022 (258.51)	0.0014 (250.07)	0.0019 (259.22)	0.0128 (254.38)	0.0600 (259.24)	0.0007 (255.70)	0.1185 (251.37)	0.0016 (253.83)
12	0.2588 (256.55)	0.0064 (253.56)	0.1880 (253.57)	0.2395 (247.64)	0.0102 (255.60)	0.3735 (249.07)	0.0133 (251.88)	0.0003 (253.37)	0.2544 (250.91)	0.0216 (253.30)
13	0.0035 (246.63)	0.1886 (252.88)	0.0336 (248.63)	0.0152 (247.29)	0.2404 (251.63)	0.0059 (243.07)	0.0583 (250.40)	0.0336 (252.11)	0.0081 (250.04)	0.0067 (248.89)
14	0.0330 (244.99)	0.0016 (248.16)	0.0220 (245.38)	0.0133 (239.60)	0.0074 (245.78)	0.0722 (240.31)	0.1906 (248.61)	0.2140 (246.40)	0.0178 (245.07)	0.2935 (247.68)
15	0.0200 (237.87)	0.0036 (241.28)	0.0002 (241.81)	0.0074 (232.34)	0.0918 (243.98)	0.0015 (237.44)	0.0784 (235.68)	0.0567 (241.67)	0.0223 (243.82)	0.0274 (241.43)
16	0.0051 (231.77)	0.0008 (239.05)	0.0026 (236.52)	0.0308 (232.22)	0.0307 (234.02)	0.0067 (236.95)	0.0211 (234.21)	0.0014 (236.49)	0.0035 (235.24)	0.0023 (230.15)
17	0.0231 (227.84)	0.0063 (234.18)	0.0546 (228.69)	0.0342 (228.96)	0.0238 (233.12)	0.0923 (223.63)	0.0016 (231.38)	0.0298 (231.97)	0.0056 (230.36)	0.0062 (228.85)
18	0.0430 (226.51)	0.0585 (232.24)	0.0049 (225.60)	0.0120 (226.95)	0.0003 (231.51)	0.0005 (218.02)	0.0362 (229.02)	0.0086 (230.12)	0.0007 (230.01)	0.0069 (227.89)
19	0.0268 (218.72)	0.0226 (215.88)	0.0306 (224.15)	0.0034 (219.08)	0.0367 (225.10)	0.0055 (215.73)	0.0001 (221.88)	0.0021 (227.38)	0.0032 (227.50)	0.0013 (226.14)
20	0.0056 (215.00)	0.0112 (214.55)	0.0059 (215.19)	0.0106 (213.74)	0.0070 (218.85)	0.0003 (215.56)	0.0176 (220.62)	0.0507 (223.78)	0.0003 (223.66)	0.0532 (221.56)
21	0.0017 (211.20)	0.0057 (212.96)	0.0407 (214.10)	0.0167 (210.82)	0.0073 (214.07)	0.0019 (212.93)	0.0004 (219.30)	0.0030 (219.79)	0.0421 (218.70)	0.0022 (214.91)
22	0.0031 (210.38)	0.0230 (211.46)	0.0043 (209.88)	0.0240 (209.87)	0.0006 (211.38)	0.0019 (212.57)	0.0308 (217.18)	0.0024 (219.22)	0.0348 (217.85)	0.0006 (214.89)
23	0.0085 (207.83)	0.0036 (210.81)	0.0434 (208.91)	0.0297 (209.29)	0.0000 (208.46)	0.0199 (207.47)	0.0212 (210.78)	0.0010 (211.89)	0.0017 (214.95)	0.0239 (209.64)
24	0.0005 (206.75)	0.0031 (208.24)	0.0131 (208.36)	0.0103 (203.28)	0.0009 (208.06)	0.0027 (206.56)	0.0040 (205.80)	0.0506 (207.16)	0.0096 (210.98)	0.0012 (205.24)
25	0.0013 (205.99)	0.0025 (206.45)	0.0084 (206.12)	0.0094 (202.99)	0.0024 (207.03)	0.0042 (203.73)	0.0020 (205.04)	0.0001 (204.20)	0.0102 (206.80)	0.0003 (204.42)
26	0.0018 (205.04)	0.0028 (203.98)	0.0070 (204.49)	0.0020 (198.84)	0.0004 (205.63)	0.0121 (203.06)	0.0002 (203.87)	0.0040 (203.29)	0.0132 (206.30)	0.0036 (204.22)
27	0.0126 (202.95)	0.0044 (200.53)	0.0004 (204.30)	0.0126 (198.17)	0.0019 (203.88)	0.0012 (201.74)	0.0019 (201.29)	0.0097 (202.55)	0.0003 (204.91)	0.0143 (202.49)
28	0.0101 (201.93)	0.0028 (199.27)	0.0013 (202.85)	0.0039 (196.01)	0.0207 (203.05)	0.0008 (199.31)	0.0011 (200.86)	0.0003 (202.35)	0.0045 (203.49)	0.0036 (201.80)
29	0.0041 (200.40)	0.0109 (197.70)	0.0294 (200.49)	0.0010 (195.48)	0.0002 (202.27)	0.0041 (198.97)	0.0111 (195.89)	0.0123 (201.04)	0.0512 (197.13)	0.0007 (200.76)
30	0.0042 (199.70)	0.0026 (197.28)	0.0021 (198.89)	0.0243 (192.94)	0.0004 (202.02)	0.0031 (196.26)	0.0047 (194.61)	0.0177 (200.41)	0.0071 (196.75)	0.0196 (199.37)

Table 9.S10. (*Continued*)

j	f_j (λ_j, nm)									
	md061*	**md062***	**md063***	**md064***	**md065***	**md066***	**md067***	**md068***	**md069***	**md070***
1	0.0425 (369.44)	0.0105 (383.22)	0.0008 (388.79)	0.0095 (380.95)	0.0010 (381.11)	0.1820 (369.74)	0.0071 (397.69)	0.0503 (392.20)	0.0147 (386.73)	0.0064 (364.08)
2	0.3531 (353.30)	0.3373 (361.21)	0.4081 (352.54)	0.3872 (350.72)	0.4190 (339.49)	0.0808 (360.10)	0.2895 (370.08)	0.2615 (359.76)	0.2850 (373.97)	0.4701 (331.96)
3	0.0238 (311.65)	0.0016 (320.29)	0.0054 (325.40)	0.0161 (324.95)	0.0149 (320.15)	0.0171 (327.06)	0.0077 (333.11)	0.0088 (329.64)	0.0035 (343.33)	0.0021 (302.85)
4	0.0042 (286.61)	0.0136 (294.21)	0.0007 (296.10)	0.0006 (302.57)	0.0105 (313.65)	0.0672 (298.62)	0.0103 (304.10)	0.0013 (298.01)	0.0014 (336.91)	0.0010 (283.97)
5	0.0831 (283.00)	0.0297 (291.92)	0.0006 (283.48)	0.0003 (294.76)	0.0127 (287.92)	0.0278 (293.55)	0.0017 (293.27)	0.0019 (296.36)	0.0001 (308.72)	0.0004 (269.85)
6	0.0052 (279.01)	0.0046 (288.69)	0.0031 (279.25)	0.0012 (288.33)	0.0164 (280.63)	0.0053 (288.75)	0.0022 (291.00)	0.0506 (290.30)	0.0109 (303.79)	0.0127 (266.52)
7	0.0098 (274.45)	0.0046 (280.88)	0.0126 (275.30)	0.0065 (281.39)	0.0088 (275.33)	0.0398 (282.88)	0.0130 (289.94)	0.0075 (283.82)	0.0091 (296.53)	0.0061 (264.70)
8	0.0077 (271.55)	0.0016 (277.70)	0.0173 (261.66)	0.0255 (278.19)	0.0947 (266.90)	0.0004 (281.99)	0.0475 (285.27)	0.1402 (278.71)	0.0001 (293.88)	0.0702 (263.19)
9	0.0462 (269.64)	0.0043 (277.34)	0.0122 (260.77)	0.0002 (271.60)	0.0075 (261.19)	0.0101 (280.18)	0.0612 (276.73)	0.0145 (276.47)	0.0398 (289.97)	0.0014 (259.00)
10	0.0054 (262.17)	0.0412 (275.61)	0.0026 (256.45)	0.0706 (266.72)	0.0549 (257.72)	0.0575 (277.47)	0.0099 (272.87)	0.0174 (263.54)	0.1255 (279.87)	0.0003 (258.71)
11	0.1959 (258.00)	0.0112 (258.61)	0.1883 (251.78)	0.0285 (260.61)	0.0003 (249.07)	0.0312 (267.37)	0.0927 (257.36)	0.0498 (258.81)	0.0789 (275.39)	0.0157 (248.15)
12	0.0023 (251.77)	0.3019 (251.90)	0.1082 (245.06)	0.1607 (255.82)	0.2337 (245.68)	0.0132 (258.52)	0.0827 (255.31)	0.0067 (254.77)	0.0011 (267.19)	0.2109 (241.43)
13	0.0389 (246.79)	0.0370 (245.28)	0.0085 (244.20)	0.0363 (251.57)	0.0226 (242.47)	0.2157 (253.80)	0.1920 (249.58)	0.1954 (253.23)	0.0042 (262.59)	0.0029 (238.27)
14	0.0292 (232.97)	0.0379 (244.63)	0.0158 (239.28)	0.1261 (247.61)	0.0024 (239.31)	0.0778 (250.22)	0.0144 (245.41)	0.0010 (240.90)	0.0376 (260.61)	0.1096 (237.70)
15	0.0041 (226.83)	0.0007 (241.24)	0.0802 (233.61)	0.0030 (239.24)	0.0191 (237.51)	0.0005 (241.83)	0.0254 (243.45)	0.0096 (232.61)	0.2392 (256.25)	0.0011 (229.94)
16	0.0008 (224.21)	0.0271 (235.86)	0.0033 (229.58)	0.0030 (235.57)	0.0175 (236.11)	0.0987 (231.06)	0.0015 (236.65)	0.0239 (231.77)	0.0118 (249.02)	0.0084 (223.46)
17	0.0068 (222.08)	0.0022 (222.21)	0.0086 (219.49)	0.0007 (231.56)	0.0031 (231.46)	0.0122 (227.38)	0.0118 (225.27)	0.0032 (227.08)	0.0019 (238.26)	0.0001 (217.58)
18	0.0005 (221.20)	0.0566 (219.66)	0.0082 (216.72)	0.0003 (221.91)	0.0007 (220.91)	0.0044 (226.45)	0.0013 (220.77)	0.0595 (225.48)	0.0067 (237.91)	0.0040 (211.33)
19	0.0015 (217.20)	0.0169 (216.51)	0.0008 (212.39)	0.0090 (217.37)	0.0691 (218.10)	0.0019 (224.20)	0.0473 (218.90)	0.0019 (220.25)	0.0120 (233.12)	0.0416 (207.42)
20	0.0500 (213.48)	0.0025 (211.10)	0.0511 (204.24)	0.0060 (216.08)	0.0002 (215.44)	0.0014 (223.75)	0.0180 (217.16)	0.0008 (218.50)	0.0041 (231.30)	0.0005 (206.95)
21	0.0024 (207.52)	0.0046 (210.72)	0.0012 (203.25)	0.0005 (215.39)	0.0009 (213.84)	0.0019 (219.22)	0.0061 (216.34)	0.0006 (216.86)	0.0021 (228.13)	0.0021 (202.53)
22	0.0023 (207.09)	0.0163 (209.98)	0.0006 (203.06)	0.0235 (213.75)	0.0094 (212.86)	0.0031 (217.43)	0.0117 (214.16)	0.0057 (211.15)	0.0004 (227.80)	0.0024 (200.50)
23	0.0029 (206.60)	0.0042 (206.31)	0.0161 (200.78)	0.0026 (213.13)	0.0023 (206.33)	0.0004 (216.32)	0.0007 (213.77)	0.0187 (208.98)	0.0388 (226.87)	0.0157 (198.50)
24	0.0084 (204.51)	0.0015 (206.02)	0.0272 (200.11)	0.0001 (212.33)	0.0500 (205.98)	0.0134 (213.79)	0.0223 (209.50)	0.0079 (208.10)	0.0026 (220.70)	0.0056 (198.36)
25	0.0011 (203.32)	0.0025 (205.67)	0.0065 (199.67)	0.0048 (210.36)	0.0146 (203.81)	0.0087 (211.50)	0.0067 (207.90)	0.0023 (207.61)	0.0004 (217.82)	0.0016 (197.53)
26	0.0100 (201.92)	0.0012 (204.19)	0.0011 (199.28)	0.0058 (209.04)	0.0017 (201.13)	0.0402 (208.97)	0.0021 (207.58)	0.0038 (206.47)	0.0004 (216.65)	0.0014 (196.92)
27	0.0021 (200.16)	0.0117 (203.75)	0.0117 (197.86)	0.0074 (207.56)	0.0039 (200.78)	0.0075 (207.14)	0.0032 (206.61)	0.0287 (205.85)	0.0010 (214.77)	0.0001 (196.40)
28	0.0006 (199.05)	0.0006 (202.35)	0.0026 (197.32)	0.0202 (206.64)	0.0041 (199.50)	0.0068 (205.47)	0.0134 (204.79)	0.0168 (200.68)	0.0032 (213.51)	0.0026 (193.74)
29	0.0078 (198.43)	0.0011 (200.68)	0.0057 (196.10)	0.0128 (205.14)	0.0175 (197.90)	0.0107 (204.70)	0.0083 (204.06)	0.0004 (200.04)	0.0335 (212.39)	0.0478 (191.45)
30	0.0010 (197.52)	0.0186 (199.68)	0.0197 (192.96)	0.0346 (201.62)	0.0100 (194.04)	0.0048 (202.49)	0.0040 (201.46)	0.0033 (199.76)	0.0140 (210.95)	0.0009 (190.67)

Table 9.S10. (*Continued*)

j	f_j (λ_j, nm)									
	md071*	**md072***	**md073***	**md074***	**md075***	**md076***	**md077***	**md078***	**md079***	**md080***
1	0.0012 (385.28)	0.0431 (380.48)	0.0743 (366.24)	0.0253 (387.17)	0.0218 (369.35)	0.0014 (363.13)	0.0330 (377.74)	0.0025 (366.06)	0.0140 (403.30)	0.0517 (389.88)
2	0.3783 (348.59)	0.3450 (349.08)	0.2886 (360.88)	0.4283 (349.49)	0.4011 (349.89)	0.4347 (342.59)	0.3792 (347.59)	0.3785 (352.30)	0.3238 (375.19)	0.2626 (359.48)
3	0.0016 (317.91)	0.0250 (332.24)	0.0004 (310.74)	0.0014 (317.79)	0.0057 (304.69)	0.0008 (307.67)	0.0044 (313.43)	0.0018 (318.07)	0.0046 (320.67)	0.0168 (316.58)
4	0.0418 (283.34)	0.0011 (311.88)	0.0010 (307.75)	0.0013 (315.19)	0.0001 (292.56)	0.0003 (290.85)	0.0020 (288.61)	0.0004 (309.88)	0.0395 (312.26)	0.0840 (304.39)
5	0.0041 (281.86)	0.0003 (296.81)	0.0096 (292.96)	0.0008 (306.36)	0.0011 (291.81)	0.1043 (287.95)	0.0116 (285.57)	0.0467 (301.25)	0.0005 (300.23)	0.0343 (298.10)
6	0.0098 (280.02)	0.0009 (289.05)	0.0460 (287.11)	0.0140 (282.64)	0.0004 (284.77)	0.0000 (285.50)	0.0047 (282.44)	0.0406 (287.72)	0.0381 (292.20)	0.0003 (293.56)
7	0.0250 (274.21)	0.0297 (281.74)	0.0011 (282.50)	0.0067 (275.44)	0.0382 (277.86)	0.0015 (269.57)	0.0072 (279.12)	0.0017 (278.88)	0.0142 (291.28)	0.0014 (289.35)
8	0.0528 (271.71)	0.0154 (276.80)	0.0052 (273.60)	0.0176 (274.97)	0.0461 (273.05)	0.0219 (268.96)	0.0135 (275.56)	0.0039 (277.02)	0.0014 (276.76)	0.0383 (274.04)
9	0.0156 (268.48)	0.0012 (275.72)	0.1081 (271.37)	0.1125 (270.24)	0.0010 (263.31)	0.0015 (264.12)	0.0433 (272.20)	0.0110 (269.54)	0.0007 (275.51)	0.0456 (272.34)
10	0.0248 (267.95)	0.0963 (268.49)	0.0002 (268.30)	0.0000 (259.29)	0.0056 (252.44)	0.0073 (262.62)	0.0011 (265.16)	0.0005 (262.27)	0.0186 (272.34)	0.0283 (258.78)
11	0.0415 (249.91)	0.0529 (258.72)	0.0324 (260.78)	0.0047 (257.80)	0.0014 (252.04)	0.0390 (256.51)	0.0096 (260.14)	0.2100 (258.73)	0.0623 (262.14)	0.1369 (254.55)
12	0.2143 (242.52)	0.1357 (251.01)	0.0602 (254.90)	0.0023 (256.55)	0.0044 (250.68)	0.1405 (254.21)	0.2558 (252.07)	0.0970 (249.67)	0.0244 (248.53)	0.1208 (250.48)
13	0.0032 (239.29)	0.0123 (248.81)	0.1465 (251.56)	0.2709 (249.74)	0.2829 (246.33)	0.0839 (250.36)	0.0166 (244.46)	0.0057 (247.56)	0.2420 (248.43)	0.0114 (242.04)
14	0.0157 (235.71)	0.1041 (247.64)	0.0673 (249.30)	0.0272 (242.68)	0.0306 (232.83)	0.0002 (239.64)	0.0198 (242.92)	0.0008 (238.79)	0.0369 (243.85)	0.0007 (239.44)
15	0.0142 (229.61)	0.0067 (243.75)	0.0224 (241.88)	0.0019 (240.65)	0.0022 (229.25)	0.0122 (236.60)	0.0263 (239.94)	0.0027 (237.04)	0.0207 (240.03)	0.0132 (234.07)
16	0.0062 (227.81)	0.0230 (237.32)	0.0006 (237.54)	0.0003 (231.49)	0.0039 (226.56)	0.0003 (234.19)	0.0074 (233.23)	0.0173 (234.07)	0.0164 (237.45)	0.0518 (228.67)
17	0.0002 (220.20)	0.0025 (235.21)	0.0103 (228.01)	0.0015 (230.53)	0.0021 (221.06)	0.0077 (229.86)	0.0017 (222.86)	0.0377 (232.88)	0.0007 (234.81)	0.0045 (228.21)
18	0.0468 (218.63)	0.0249 (229.74)	0.0590 (223.41)	0.0079 (223.84)	0.0003 (219.24)	0.0072 (228.50)	0.0028 (219.14)	0.0135 (223.94)	0.0816 (221.58)	0.0026 (225.21)
19	0.0043 (215.43)	0.0002 (222.02)	0.0028 (218.24)	0.0013 (218.30)	0.0004 (216.02)	0.0163 (221.33)	0.0067 (217.10)	0.0023 (221.32)	0.0000 (214.73)	0.0212 (224.44)
20	0.0019 (212.39)	0.0012 (220.94)	0.0057 (217.21)	0.0011 (217.32)	0.0804 (211.21)	0.0294 (218.36)	0.0153 (214.98)	0.0114 (221.03)	0.0500 (213.18)	0.0015 (222.64)
21	0.0034 (209.82)	0.0244 (217.12)	0.0067 (214.13)	0.0281 (215.65)	0.0001 (210.70)	0.0061 (214.98)	0.0032 (213.34)	0.0354 (216.28)	0.0026 (212.05)	0.0015 (214.77)
22	0.0009 (206.05)	0.0238 (216.55)	0.0034 (213.61)	0.0059 (212.72)	0.0004 (210.25)	0.0162 (213.83)	0.0196 (212.78)	0.0383 (213.93)	0.0003 (209.56)	0.0005 (213.99)
23	0.0079 (205.26)	0.0001 (212.79)	0.0018 (210.77)	0.0063 (210.34)	0.0003 (204.80)	0.0005 (212.82)	0.0742 (210.23)	0.0364 (212.91)	0.0015 (208.54)	0.0024 (213.51)
24	0.0036 (202.27)	0.0017 (209.25)	0.0033 (209.37)	0.0014 (209.78)	0.0083 (202.44)	0.0006 (211.74)	0.0037 (208.49)	0.0045 (212.84)	0.0159 (207.62)	0.0150 (212.06)
25	0.0382 (201.59)	0.0005 (208.68)	0.0308 (206.77)	0.0083 (208.68)	0.0112 (200.50)	0.0007 (211.40)	0.0018 (207.90)	0.0250 (209.47)	0.0138 (207.34)	0.0029 (210.44)
26	0.0025 (198.70)	0.0035 (206.74)	0.0140 (205.50)	0.0001 (207.80)	0.0000 (199.87)	0.0002 (205.84)	0.0027 (206.38)	0.0059 (207.31)	0.0091 (204.82)	0.0026 (205.35)
27	0.0039 (198.33)	0.0002 (205.79)	0.0102 (203.59)	0.0320 (201.62)	0.0014 (199.82)	0.0246 (203.65)	0.0819 (205.07)	0.0003 (206.77)	0.0018 (203.44)	0.0030 (203.28)
28	0.0030 (196.05)	0.0344 (203.38)	0.0244 (201.91)	0.0116 (200.65)	0.0397 (198.51)	0.0024 (202.30)	0.0206 (204.17)	0.0083 (204.63)	0.0052 (202.98)	0.0012 (202.46)
29	0.0019 (195.55)	0.0009 (202.40)	0.0108 (201.28)	0.0101 (197.30)	0.0076 (196.68)	0.0041 (201.64)	0.0095 (202.72)	0.0041 (202.14)	0.0078 (200.70)	0.0002 (201.30)
30	0.0063 (195.01)	0.0106 (201.56)	0.0126 (201.11)	0.0003 (196.85)	0.0013 (195.59)	0.0005 (200.77)	0.0003 (200.77)	0.0098 (200.19)	0.0000 (199.05)	0.0239 (199.91)

Table 9.S10. (*Continued*)

j	f_j (λ_j, nm)									
	md081*	**md082***	**md083***	**md084***	**md085***	**md086***	**md087***	**md088***	**md089***	**md090***
1	0.0368 (373.75)	0.0228 (406.64)	0.0283 (371.07)	0.0001 (372.43)	0.0023 (392.91)	0.0766 (356.74)	0.0364 (364.03)	0.0465 (387.54)	0.0701 (375.10)	0.0304 (387.42)
2	0.2670 (353.18)	0.3928 (361.32)	0.4056 (342.63)	0.3818 (351.93)	0.3768 (358.64)	0.2624 (345.55)	0.3281 (344.02)	0.2708 (349.94)	0.2495 (358.72)	0.3230 (355.88)
3	0.0167 (316.01)	0.0076 (320.29)	0.0016 (328.25)	0.0197 (311.74)	0.0030 (314.94)	0.0152 (323.88)	0.0086 (322.94)	0.0464 (325.43)	0.0218 (315.62)	0.0065 (323.36)
4	0.0007 (299.29)	0.0180 (308.66)	0.0064 (293.95)	0.0290 (297.14)	0.0425 (292.97)	0.0037 (297.37)	0.0245 (286.33)	0.0017 (289.99)	0.0784 (304.27)	0.0011 (310.75)
5	0.0005 (297.50)	0.0013 (292.91)	0.0831 (289.94)	0.0055 (291.41)	0.0007 (279.62)	0.0653 (288.65)	0.0028 (284.88)	0.0026 (286.28)	0.0080 (300.92)	0.0171 (308.12)
6	0.1202 (293.84)	0.0004 (292.20)	0.0138 (289.53)	0.0001 (285.97)	0.0006 (278.80)	0.0090 (284.59)	0.0183 (282.86)	0.0022 (285.51)	0.0025 (297.41)	0.0011 (295.79)
7	0.0055 (285.61)	0.0063 (285.45)	0.0043 (283.71)	0.0137 (280.01)	0.0107 (275.93)	0.0556 (276.01)	0.0553 (274.13)	0.0385 (276.67)	0.0465 (284.92)	0.0036 (282.70)
8	0.0715 (278.98)	0.0210 (278.00)	0.0039 (276.68)	0.0011 (278.45)	0.0030 (274.81)	0.0750 (271.67)	0.0358 (270.90)	0.0537 (276.06)	0.0220 (279.18)	0.0032 (281.79)
9	0.0638 (267.12)	0.0042 (275.17)	0.0121 (269.97)	0.0041 (274.78)	0.0213 (271.86)	0.0062 (265.96)	0.0074 (262.14)	0.0137 (270.10)	0.0022 (274.13)	0.0805 (276.01)
10	0.0385 (260.33)	0.0320 (272.61)	0.0274 (264.67)	0.0425 (268.58)	0.0003 (265.51)	0.0029 (260.92)	0.0308 (261.62)	0.0098 (265.52)	0.0008 (264.44)	0.0501 (270.00)
11	0.1418 (255.03)	0.0339 (259.27)	0.1780 (257.64)	0.0115 (253.94)	0.0091 (256.75)	0.0389 (256.32)	0.0002 (257.27)	0.0579 (258.90)	0.0071 (261.01)	0.0224 (259.48)
12	0.0488 (245.11)	0.2801 (251.34)	0.0043 (255.95)	0.2855 (249.15)	0.3103 (252.11)	0.1014 (254.66)	0.1342 (254.72)	0.0054 (251.69)	0.2646 (255.55)	0.2223 (255.74)
13	0.0097 (243.22)	0.0111 (247.94)	0.0928 (248.91)	0.0653 (243.21)	0.0254 (246.50)	0.1191 (242.72)	0.1277 (241.06)	0.2601 (244.04)	0.0482 (246.03)	0.0345 (248.74)
14	0.0049 (234.90)	0.0153 (242.78)	0.0049 (240.85)	0.0043 (234.18)	0.0056 (241.33)	0.0274 (241.56)	0.0401 (234.89)	0.0299 (240.60)	0.0068 (241.53)	0.0357 (245.19)
15	0.0022 (234.43)	0.0068 (237.67)	0.0002 (239.68)	0.0002 (232.60)	0.0051 (238.65)	0.0549 (228.87)	0.0312 (232.77)	0.0393 (237.16)	0.0487 (238.73)	0.0177 (237.96)
16	0.0075 (232.30)	0.0022 (234.11)	0.0172 (237.02)	0.0196 (231.89)	0.0138 (235.93)	0.0110 (227.81)	0.0016 (228.85)	0.0038 (234.58)	0.0115 (234.01)	0.0004 (237.11)
17	0.0329 (229.78)	0.0185 (222.28)	0.0252 (231.81)	0.0025 (225.46)	0.0509 (219.35)	0.0120 (226.92)	0.0300 (226.01)	0.0000 (223.17)	0.0246 (232.68)	0.0163 (234.62)
18	0.0459 (229.07)	0.0008 (221.71)	0.0219 (231.64)	0.0539 (223.04)	0.0040 (212.21)	0.0128 (224.47)	0.0085 (223.57)	0.0344 (216.58)	0.0982 (231.83)	0.0037 (233.91)
19	0.0040 (228.27)	0.0027 (217.61)	0.0015 (227.10)	0.0001 (217.77)	0.0043 (210.12)	0.0357 (222.47)	0.0452 (217.42)	0.0025 (214.16)	0.0010 (225.25)	0.0010 (229.84)
20	0.0029 (226.29)	0.0000 (216.36)	0.0177 (223.52)	0.0070 (217.45)	0.0157 (209.26)	0.0045 (213.46)	0.0072 (210.12)	0.0092 (211.44)	0.0303 (219.39)	0.0034 (218.45)
21	0.0018 (219.14)	0.0071 (215.16)	0.0040 (219.76)	0.0047 (216.20)	0.0021 (208.32)	0.0017 (211.88)	0.0036 (208.41)	0.0143 (210.23)	0.0235 (215.65)	0.0022 (218.08)
22	0.0024 (213.83)	0.0014 (213.31)	0.0140 (217.38)	0.0121 (214.84)	0.0101 (207.44)	0.0011 (210.76)	0.0029 (208.21)	0.0085 (209.70)	0.0001 (214.81)	0.0014 (215.39)
23	0.0307 (212.79)	0.0034 (212.51)	0.0475 (213.31)	0.0019 (214.13)	0.0058 (206.42)	0.0011 (210.23)	0.0027 (206.37)	0.0234 (206.28)	0.0060 (212.50)	0.0007 (215.10)
24	0.0040 (209.96)	0.0324 (207.84)	0.0002 (211.23)	0.0298 (210.20)	0.0043 (205.16)	0.0093 (208.88)	0.0003 (205.35)	0.0018 (204.83)	0.0018 (210.09)	0.0360 (214.06)
25	0.0003 (207.22)	0.0004 (206.94)	0.0144 (210.64)	0.0006 (210.05)	0.0029 (203.18)	0.0018 (207.21)	0.0019 (204.96)	0.0024 (204.26)	0.0130 (208.03)	0.0038 (212.64)
26	0.0212 (206.54)	0.0138 (205.85)	0.0016 (210.31)	0.0097 (208.01)	0.0012 (201.00)	0.0126 (204.24)	0.0101 (204.06)	0.0087 (203.58)	0.0035 (207.62)	0.0064 (210.53)
27	0.0013 (202.88)	0.0125 (204.87)	0.0002 (206.52)	0.0127 (203.19)	0.0017 (200.58)	0.0134 (203.47)	0.0563 (201.27)	0.0038 (203.13)	0.0011 (206.57)	0.0015 (208.83)
28	0.0025 (200.82)	0.0009 (204.38)	0.0347 (205.20)	0.0002 (202.71)	0.0059 (198.55)	0.0249 (201.97)	0.0143 (200.02)	0.0010 (202.16)	0.0009 (206.31)	0.0011 (206.94)
29	0.0008 (199.54)	0.0012 (203.37)	0.0043 (204.02)	0.0000 (202.54)	0.0001 (198.32)	0.0283 (199.59)	0.0022 (197.96)	0.0004 (201.36)	0.0273 (205.24)	0.0084 (206.36)
30	0.0642 (197.21)	0.0007 (202.81)	0.0009 (202.61)	0.0004 (200.58)	0.0007 (197.60)	0.0065 (198.50)	0.0020 (195.97)	0.0008 (200.12)	0.0075 (201.01)	0.0183 (205.27)

Table 9.S10. (*Continued*)

j	f_j (λ_j, nm)									
	md091*	**md092***	**md093***	**md094***	**md095***	**md096***	**md097***	**md098***	**md099***	**md100***
1	0.0757 (375.33)	0.0085 (380.96)	0.0650 (356.80)	0.0019 (393.79)	0.0007 (405.12)	0.0006 (369.30)	0.0274 (373.97)	0.0011 (361.41)	0.0006 (374.47)	0.0089 (380.52)
2	0.2937 (350.36)	0.3579 (350.02)	0.2982 (340.12)	0.3437 (358.63)	0.3931 (356.48)	0.3335 (349.72)	0.2974 (345.72)	0.3792 (343.28)	0.3391 (349.10)	0.3906 (352.29)
3	0.0040 (312.21)	0.0246 (319.49)	0.0007 (307.08)	0.0043 (317.34)	0.0007 (323.04)	0.0087 (312.02)	0.0120 (313.54)	0.0012 (313.05)	0.0006 (313.73)	0.0092 (317.81)
4	0.0114 (293.64)	0.0494 (292.40)	0.0007 (293.02)	0.0000 (309.48)	0.0039 (308.90)	0.0367 (301.54)	0.0817 (292.48)	0.0021 (293.09)	0.0003 (298.03)	0.0001 (313.21)
5	0.0011 (289.20)	0.0156 (284.97)	0.0203 (292.21)	0.0268 (304.09)	0.0253 (307.04)	0.0011 (293.38)	0.0009 (281.92)	0.0708 (282.93)	0.0006 (289.76)	0.0136 (290.02)
6	0.0525 (285.62)	0.0255 (281.76)	0.0198 (283.77)	0.0808 (289.37)	0.0010 (290.20)	0.0114 (290.76)	0.0692 (275.43)	0.0586 (279.89)	0.0593 (289.26)	0.0382 (285.44)
7	0.0014 (278.88)	0.0045 (278.36)	0.0300 (274.60)	0.0095 (284.56)	0.0006 (281.52)	0.0077 (278.00)	0.0088 (271.10)	0.0016 (273.47)	0.0131 (283.28)	0.0041 (276.11)
8	0.0699 (274.94)	0.0039 (274.86)	0.0068 (271.02)	0.0033 (278.17)	0.0610 (273.88)	0.0128 (277.01)	0.0109 (269.75)	0.0014 (269.59)	0.0065 (281.59)	0.0946 (275.51)
9	0.0010 (273.91)	0.0129 (273.29)	0.1687 (267.71)	0.0410 (268.86)	0.0868 (263.26)	0.0410 (272.82)	0.0006 (265.36)	0.0116 (264.91)	0.0027 (275.47)	0.0178 (273.82)
10	0.0104 (270.03)	0.0020 (269.15)	0.0003 (265.06)	0.0243 (265.62)	0.0368 (257.30)	0.0117 (266.96)	0.0090 (260.72)	0.0130 (263.87)	0.0644 (269.91)	0.0006 (267.91)
11	0.0036 (253.22)	0.0475 (262.98)	0.0341 (254.88)	0.0384 (256.37)	0.0021 (250.77)	0.0026 (255.37)	0.0069 (252.47)	0.1131 (258.15)	0.0415 (256.75)	0.0628 (260.13)
12	0.3145 (247.55)	0.2328 (254.90)	0.1399 (248.56)	0.0047 (250.96)	0.0188 (247.20)	0.2477 (250.50)	0.1501 (248.20)	0.1466 (250.44)	0.0188 (247.49)	0.1852 (252.23)
13	0.0206 (241.98)	0.0277 (244.56)	0.0257 (244.88)	0.2828 (246.46)	0.2407 (243.47)	0.0979 (245.19)	0.1572 (244.51)	0.0335 (239.50)	0.3248 (245.70)	0.0020 (241.87)
14	0.0090 (235.43)	0.0086 (241.63)	0.0373 (243.12)	0.0211 (241.95)	0.0045 (240.17)	0.0060 (241.91)	0.0010 (239.88)	0.0009 (236.97)	0.0095 (244.02)	0.0016 (240.49)
15	0.0098 (233.26)	0.0218 (239.68)	0.0060 (233.41)	0.0142 (240.21)	0.0138 (235.21)	0.0071 (234.52)	0.0523 (229.83)	0.0008 (233.54)	0.0028 (236.92)	0.0004 (238.04)
16	0.0401 (229.18)	0.0069 (234.05)	0.0008 (232.75)	0.0129 (237.02)	0.0222 (234.26)	0.0072 (232.39)	0.0150 (227.92)	0.0018 (231.85)	0.0018 (235.37)	0.0032 (231.70)
17	0.0002 (223.79)	0.0834 (226.05)	0.0155 (228.47)	0.0000 (227.37)	0.0002 (227.14)	0.0377 (229.07)	0.0330 (225.53)	0.0415 (221.95)	0.0034 (224.48)	0.0107 (228.36)
18	0.0657 (219.79)	0.0035 (220.24)	0.0287 (222.94)	0.0394 (221.26)	0.0039 (221.72)	0.0005 (225.65)	0.0002 (219.10)	0.0348 (219.73)	0.0440 (222.74)	0.0301 (221.71)
19	0.0043 (217.84)	0.0005 (217.47)	0.0107 (221.73)	0.0738 (215.95)	0.0213 (218.04)	0.0026 (222.57)	0.0176 (210.88)	0.0500 (217.98)	0.0109 (222.21)	0.0336 (218.73)
20	0.0034 (216.51)	0.0009 (215.03)	0.0004 (217.06)	0.0030 (214.62)	0.0017 (214.10)	0.0397 (216.33)	0.0010 (209.87)	0.0017 (213.26)	0.0201 (216.99)	0.0083 (218.29)
21	0.0002 (212.35)	0.0050 (212.90)	0.0014 (213.83)	0.0003 (212.01)	0.0004 (211.71)	0.0088 (214.32)	0.0030 (209.15)	0.0062 (212.17)	0.0044 (216.40)	0.0052 (214.19)
22	0.0004 (210.23)	0.0159 (212.06)	0.0028 (211.76)	0.0002 (211.94)	0.0014 (210.92)	0.0026 (212.18)	0.0129 (207.49)	0.0010 (211.15)	0.0037 (216.20)	0.0006 (212.18)
23	0.0051 (206.38)	0.0224 (208.65)	0.0071 (208.90)	0.0032 (211.55)	0.0075 (206.31)	0.0014 (211.84)	0.0067 (203.16)	0.0014 (210.90)	0.0001 (209.60)	0.0004 (210.59)
24	0.0039 (205.00)	0.0269 (208.14)	0.0068 (207.30)	0.0058 (208.76)	0.0138 (205.05)	0.0045 (208.75)	0.0002 (202.06)	0.0002 (209.86)	0.0028 (208.09)	0.0166 (210.14)
25	0.0113 (203.53)	0.0394 (205.34)	0.0015 (203.70)	0.0001 (207.52)	0.0208 (204.26)	0.0012 (208.16)	0.0015 (201.60)	0.0111 (207.27)	0.0088 (207.83)	0.0280 (206.21)
26	0.0014 (202.91)	0.0136 (202.86)	0.0139 (203.43)	0.0026 (204.95)	0.0065 (202.02)	0.0032 (207.69)	0.0330 (199.78)	0.0414 (204.89)	0.0084 (205.78)	0.0068 (204.28)
27	0.0008 (202.35)	0.0019 (202.44)	0.0218 (202.04)	0.0043 (203.95)	0.0012 (199.38)	0.0019 (204.49)	0.0010 (199.04)	0.0218 (203.19)	0.0112 (205.04)	0.0303 (203.76)
28	0.0055 (201.94)	0.0001 (202.04)	0.0010 (200.20)	0.0009 (202.12)	0.0189 (197.18)	0.0099 (204.01)	0.0006 (198.17)	0.0016 (201.13)	0.0010 (204.37)	0.0300 (202.52)
29	0.0093 (200.08)	0.0023 (201.42)	0.0063 (199.31)	0.0011 (201.03)	0.0062 (196.07)	0.0041 (201.87)	0.0050 (197.11)	0.0162 (199.25)	0.0032 (201.42)	0.0074 (197.01)
30	0.0010 (199.17)	0.0007 (199.55)	0.0048 (196.52)	0.0161 (199.39)	0.0084 (193.62)	0.0101 (201.23)	0.0144 (194.14)	0.0032 (196.98)	0.0023 (201.04)	0.0041 (195.15)

Table 9.S11. Rotational strengths in dipole velocity formalism and excitation wavelengths for the *ab initio* MD solvation clusters of **1** with methanol, as obtained by TD-DFT calculations on **1** alone.

					R_j, 10^{-40} erg cm^3 (λ_j, nm)					
j	md001#	md002#	md003#	md004#	md005#	md006#	md007#	md008#	md009#	md010#
1	−0.7353 (391.63)	29.7752 (379.12)	−4.0924 (381.89)	−11.8863 (429.41)	−31.7670 (416.79)	3.6151 (409.75)	4.7109 (397.06)	−9.3299 (391.06)	−0.5681 (379.74)	0.6428 (425.05)
2	28.4554 (340.50)	−70.3886 (335.42)	113.4710 (336.48)	92.6803 (362.08)	143.9594 (344.60)	−49.5194 (339.47)	−1.1123 (353.41)	97.0732 (351.60)	21.9990 (338.67)	95.2238 (360.36)
3	−29.3462 (323.30)	42.0780 (325.87)	−64.6036 (326.73)	−52.6514 (345.64)	−63.7768 (335.14)	72.6279 (330.77)	30.6868 (329.99)	−75.4677 (327.48)	−34.1692 (326.67)	−92.9913 (332.97)
4	−0.9546 (280.43)	6.7388 (278.54)	−28.1128 (278.96)	5.6799 (306.72)	6.9819 (286.20)	19.5417 (281.86)	−20.7179 (287.87)	−27.4987 (292.41)	15.7495 (280.59)	6.0242 (290.47)
5	−16.9326 (275.92)	3.8112 (273.74)	−25.0596 (275.52)	−23.3039 (283.40)	−17.0742 (274.75)	−15.2138 (271.67)	−29.5756 (282.34)	1.1826 (284.75)	−26.8928 (275.49)	−16.9281 (278.40)
6	−2.0374 (269.40)	18.9688 (260.06)	8.9412 (257.10)	48.1296 (276.44)	−38.4544 (261.70)	−35.5020 (259.71)	−2.5288 (271.30)	18.5026 (261.68)	10.8928 (265.52)	18.8928 (276.20)
7	−40.4471 (252.43)	−106.8511 (251.81)	115.2522 (250.89)	−79.5313 (265.53)	29.8121 (255.82)	−1.6428 (247.91)	−10.2290 (259.39)	94.7418 (256.48)	−80.6038 (253.11)	6.2787 (256.01)
8	24.5080 (246.00)	45.5545 (247.26)	−102.5908 (247.39)	20.6220 (258.17)	−44.3121 (250.35)	−40.9013 (243.50)	8.4445 (257.54)	−105.8806 (250.66)	145.8548 (246.47)	47.6111 (250.60)
9	−6.3386 (242.49)	−20.9164 (242.16)	2.9651 (235.71)	5.6097 (251.63)	−10.3116 (244.15)	91.1087 (240.78)	−4.6777 (249.51)	10.2137 (247.09)	−4.3844 (236.88)	−115.6256 (247.80)
10	42.7978 (241.25)	119.7672 (238.70)	8.5125 (234.43)	24.7969 (247.52)	28.8464 (241.09)	6.8700 (230.96)	30.8334 (246.59)	29.7387 (237.67)	10.4534 (235.08)	75.0170 (243.74)
11	−0.9577 (240.22)	−0.9899 (233.91)	7.3484 (232.28)	−9.4406 (242.08)	27.6888 (235.68)	0.6055 (226.78)	−8.4015 (240.88)	−1.0734 (228.61)	10.0376 (231.25)	−19.5757 (240.43)
12	−10.0021 (209.76)	−20.4203 (209.45)	−23.5031 (207.84)	−9.9088 (224.02)	2.2431 (209.20)	−2.6574 (207.84)	11.3279 (215.25)	13.8899 (213.65)	−2.2741 (210.59)	15.4476 (218.24)
13	−0.6433 (206.80)	−0.4021 (204.39)	6.1257 (200.90)	6.4765 (215.53)	−40.3547 (208.39)	−25.3548 (205.07)	−22.8384 (211.68)	−42.8958 (207.25)	12.5931 (205.51)	−16.0549 (209.35)
14	21.1547 (204.92)	4.1522 (203.02)	−3.6472 (200.46)	−4.4289 (208.04)	7.0526 (205.19)	−9.7495 (202.67)	−1.1168 (205.01)	2.5109 (201.03)	−3.2611 (202.78)	−10.3894 (204.81)
15	−7.2611 (202.11)	−6.6426 (200.89)	1.7938 (196.85)	−5.5832 (203.49)	1.8847 (202.14)	7.5138 (199.62)	−4.9004 (203.06)	6.8054 (196.04)	−25.5805 (197.87)	−2.9637 (203.01)
16	13.0602 (198.90)	5.6390 (198.08)	2.1656 (193.24)	−25.6290 (201.47)	−0.6742 (199.21)	−19.0236 (192.74)	0.7474 (200.96)	−16.5525 (194.99)	15.2383 (195.79)	−20.6654 (200.28)
17	−15.9977 (195.23)	−3.0713 (195.44)	−0.7075 (191.66)	−9.6398 (199.44)	−22.9055 (198.27)	6.3165 (189.93)	−3.9266 (198.63)	4.1668 (192.78)	−40.7211 (191.91)	9.9508 (195.51)
18	8.3940 (193.63)	−14.8184 (193.33)	−21.2367 (189.55)	17.5153 (198.33)	8.7213 (194.82)	5.5476 (187.72)	25.6147 (195.82)	−0.4175 (189.38)	−3.3815 (190.27)	23.4877 (191.28)
19	11.6754 (188.88)	−1.9686 (190.58)	2.3760 (184.73)	7.0203 (197.04)	−5.3692 (192.91)	1.0410 (187.14)	−5.6903 (191.61)	−5.5557 (183.21)	−10.0902 (187.14)	1.9063 (190.99)
20	2.2038 (184.74)	−15.6447 (188.82)	1.4976 (182.36)	−0.6813 (192.36)	−19.8882 (187.77)	−20.9402 (184.10)	17.1010 (188.55)	−0.4398 (181.89)	−28.9169 (183.53)	20.6301 (188.07)
21	1.1499 (183.31)	−1.8620 (184.90)	3.1946 (180.54)	0.1244 (190.67)	6.1987 (186.08)	4.0097 (182.87)	−3.3308 (187.37)	9.0641 (181.33)	15.0532 (180.61)	−23.7136 (185.62)
22	−22.0826 (180.42)	12.6431 (184.27)	−4.5961 (176.61)	24.2385 (189.79)	11.0747 (182.54)	31.2837 (181.29)	−3.1340 (184.25)	−0.5104 (176.00)	6.9693 (179.01)	9.4409 (183.41)
23	6.0061 (178.78)	−2.0315 (182.89)	−1.3420 (175.61)	−28.9994 (187.96)	9.5970 (179.11)	−73.2824 (174.04)	−17.9464 (182.92)	37.6790 (174.54)	−3.8862 (177.73)	−6.4526 (181.08)
24	3.7669 (174.79)	7.1123 (177.07)	6.6716 (174.84)	0.3766 (179.83)	66.3560 (177.09)	−9.8767 (173.51)	5.7255 (178.81)	−3.6710 (171.42)	−14.0611 (173.09)	−1.0009 (179.47)
25	14.1879 (174.31)	−2.1704 (175.35)	−9.4603 (174.02)	16.1974 (177.93)	−5.9877 (175.02)	9.1952 (173.08)	−10.8898 (176.71)	−6.2078 (171.13)	4.2264 (172.44)	21.9721 (176.46)
26	8.0037 (172.57)	−14.1150 (172.12)	6.8217 (171.73)	−13.1775 (176.04)	6.0326 (170.88)	−3.1458 (172.04)	−1.8801 (173.45)	22.1247 (169.19)	46.3106 (170.42)	3.3414 (171.52)
27	3.4228 (170.22)	−6.7612 (171.03)	−10.3392 (169.40)	−15.3718 (174.74)	18.2921 (169.24)	−41.9060 (169.56)	−16.2201 (169.14)	−6.0348 (168.93)	5.6119 (169.21)	4.6976 (171.00)
28	−2.3683 (167.82)	−21.6852 (167.53)	12.1272 (167.97)	−24.6584 (172.98)	4.3495 (168.27)	0.0934 (167.96)	13.0231 (167.74)	−9.3321 (167.36)	−21.6333 (167.69)	−4.7550 (170.48)
29	4.8770 (166.87)	−16.5870 (167.12)	13.7044 (166.27)	2.8490 (171.62)	−16.2053 (167.27)	−0.9604 (166.73)	−7.8277 (167.35)	−5.3437 (165.74)	1.9741 (166.87)	11.9636 (167.23)
30	11.1152 (164.52)	−6.2211 (165.17)	−5.9338 (165.13)	5.2389 (170.57)	−4.9422 (166.31)	−4.3682 (166.20)	0.8094 (166.24)	44.7330 (163.82)	13.2629 (163.87)	−20.6228 (166.21)

Table 9.S11. (*Continued*)

j	R_j, 10^{-40} erg cm^3 (λ_j, nm)									
	md011#	md012#	md013#	md014#	md015#	md016#	md017#	md018#	md019#	md020#
1	−5.5501 (400.83)	−6.2407 (392.68)	−18.3058 (411.77)	−5.4716 (403.01)	16.3828 (387.54)	13.1556 (411.33)	23.9752 (405.74)	0.3970 (390.08)	12.1843 (407.68)	13.6304 (383.95)
2	68.4620 (348.06)	−25.6427 (343.71)	−9.7067 (354.50)	29.9039 (335.51)	−44.8448 (338.93)	−2.9706 (354.60)	−137.4031 (347.31)	85.4999 (342.19)	103.4239 (338.32)	−55.5386 (347.35)
3	−91.2803 (337.10)	2.5696 (331.55)	59.7512 (331.93)	−27.5968 (325.03)	−0.7169 (319.23)	−5.7872 (341.71)	71.3121 (331.69)	−51.6484 (331.03)	−103.4889 (330.78)	21.8929 (327.41)
4	13.8197 (291.46)	6.4893 (284.70)	0.4623 (286.33)	4.6850 (278.63)	−3.7233 (272.63)	−20.2558 (292.82)	6.7334 (284.13)	−19.6710 (282.55)	3.1544 (283.19)	−2.1943 (286.54)
5	7.3098 (278.35)	16.0591 (272.57)	−34.9988 (277.27)	−12.5408 (269.23)	11.1087 (267.92)	10.8460 (280.34)	31.5087 (270.43)	−22.3705 (276.89)	−24.4809 (268.21)	−0.9053 (275.10)
6	10.7155 (270.59)	18.0062 (261.18)	0.8128 (261.46)	14.8164 (264.52)	−22.2997 (258.62)	−8.2199 (273.49)	−16.0697 (265.30)	9.9237 (267.56)	−14.8528 (259.37)	12.1434 (266.67)
7	−78.4301 (261.00)	−110.0951 (253.59)	−94.9417 (254.71)	−52.8652 (248.77)	−43.4890 (247.48)	−58.7124 (261.03)	−64.4533 (255.04)	95.7815 (258.60)	21.3253 (252.68)	−36.8966 (259.60)
8	−0.7440 (252.21)	65.1776 (244.31)	15.0851 (249.32)	3.3644 (247.62)	65.0060 (240.43)	22.2919 (252.47)	−19.4723 (243.68)	−24.2159 (250.29)	−42.1448 (248.52)	77.4151 (246.61)
9	40.4245 (250.59)	−3.4277 (243.44)	94.6932 (247.63)	−5.5442 (243.86)	−55.5123 (238.89)	27.6619 (250.89)	106.3280 (240.42)	−54.5728 (247.42)	21.9851 (243.40)	22.5278 (240.72)
10	49.3029 (242.87)	82.3120 (238.07)	13.2052 (242.06)	49.6379 (237.84)	49.8247 (235.17)	1.3005 (243.76)	−1.0956 (237.38)	−0.0798 (230.96)	41.9331 (235.40)	20.9235 (239.24)
11	−4.9062 (233.85)	−4.3148 (229.34)	8.1474 (228.93)	41.7012 (234.48)	33.0853 (228.65)	25.4787 (242.20)	14.5579 (231.34)	5.0499 (224.51)	2.3606 (233.72)	−0.9590 (227.76)
12	26.3977 (223.28)	24.3342 (214.38)	17.1970 (213.08)	28.3992 (207.64)	29.3884 (205.87)	−19.9679 (214.92)	23.8019 (208.12)	−34.3897 (211.62)	−13.9654 (208.73)	−9.3747 (210.75)
13	−18.1304 (211.25)	−34.4842 (202.15)	−26.0865 (203.62)	−21.4625 (203.88)	−36.6507 (201.50)	10.1216 (208.72)	−6.1932 (203.50)	7.4214 (206.86)	−9.7372 (206.54)	8.0319 (204.22)
14	−14.0377 (203.09)	−2.6732 (197.80)	−5.6017 (202.38)	−10.1629 (199.19)	−0.1315 (197.45)	3.7314 (207.22)	−0.6158 (200.98)	−22.6441 (200.92)	−3.3550 (203.26)	−6.2441 (202.09)
15	−2.5962 (201.27)	−11.8668 (194.00)	−23.3071 (196.95)	−2.7576 (198.74)	17.7569 (194.47)	−2.4779 (205.17)	−7.8223 (196.22)	6.9967 (198.60)	−10.6698 (199.00)	−6.3088 (198.42)
16	10.9135 (198.83)	−9.9233 (191.51)	−5.1930 (192.94)	−4.7893 (194.81)	1.8576 (191.71)	−2.0769 (199.70)	−14.4365 (193.21)	−6.2324 (192.48)	−4.4976 (196.53)	−1.1582 (197.94)
17	−14.7963 (196.88)	−1.1088 (189.12)	9.2719 (190.53)	−11.3313 (192.43)	10.4261 (189.54)	−27.7372 (197.35)	−3.7908 (191.23)	10.1817 (189.23)	−2.4587 (193.56)	−4.8080 (194.88)
18	−5.8738 (193.81)	7.1675 (186.83)	6.0905 (187.86)	5.3468 (191.77)	−1.7171 (187.89)	22.6216 (195.78)	−4.2692 (189.93)	1.8533 (188.39)	−8.5688 (190.60)	−10.2953 (192.28)
19	15.6982 (190.59)	4.2967 (184.12)	10.3802 (182.70)	−17.2606 (187.68)	−17.0747 (186.38)	15.0133 (193.28)	−12.2495 (189.23)	13.6122 (183.88)	14.9066 (183.96)	−26.5496 (188.22)
20	4.6487 (186.66)	6.6606 (182.61)	9.6918 (181.62)	−7.7642 (187.51)	−3.5702 (184.30)	−17.1929 (187.31)	−21.8600 (186.33)	−5.5915 (182.14)	5.4825 (182.76)	5.3482 (185.83)
21	6.1914 (185.40)	0.0843 (181.09)	6.2861 (181.11)	−1.7994 (182.63)	−7.8433 (180.65)	−5.4524 (186.09)	14.0994 (183.63)	−6.8812 (181.87)	−0.9016 (181.19)	−7.2319 (180.83)
22	9.6931 (182.73)	10.0173 (180.03)	10.7857 (180.84)	1.6528 (182.04)	−5.3158 (179.70)	3.6805 (184.90)	1.5609 (179.58)	1.9763 (176.19)	−6.1800 (178.97)	−6.4650 (177.83)
23	0.5916 (181.07)	1.0441 (175.67)	−5.3380 (179.04)	10.8920 (178.96)	7.7134 (175.71)	5.5859 (184.55)	−3.6471 (177.72)	7.3842 (175.43)	−4.2763 (177.86)	−3.7548 (174.26)
24	11.4588 (179.50)	12.2322 (173.43)	−12.1825 (175.80)	−4.0492 (175.54)	−3.9297 (174.25)	−0.4351 (182.01)	−10.6819 (176.79)	−3.8669 (173.23)	−8.4984 (177.44)	−14.7863 (173.87)
25	15.6277 (174.15)	−10.9757 (172.61)	−0.0247 (174.55)	6.8673 (173.76)	4.9285 (173.36)	−16.1244 (174.41)	16.0648 (175.14)	−4.4637 (172.53)	−26.2602 (175.99)	−4.1265 (172.60)
26	−2.0038 (169.34)	−14.8521 (170.91)	−0.4665 (173.97)	−1.6825 (172.08)	−1.3210 (171.65)	−21.0023 (171.80)	1.7740 (172.44)	5.5927 (169.61)	14.8662 (174.28)	31.4958 (170.45)
27	2.8971 (169.00)	5.0900 (168.63)	−14.7649 (170.89)	−8.5791 (169.91)	−8.2271 (169.36)	−3.8854 (169.68)	1.7950 (170.99)	3.1641 (168.67)	0.2503 (172.61)	−24.4998 (169.05)
28	7.9050 (167.30)	−10.2691 (165.17)	7.6001 (169.64)	26.3756 (169.01)	13.8016 (167.60)	22.7156 (169.41)	−22.7275 (168.68)	−3.4621 (166.89)	−16.4683 (169.00)	0.7996 (168.61)
29	−20.5151 (166.99)	1.1405 (164.49)	0.5376 (167.10)	−13.2771 (166.78)	4.3373 (167.47)	0.8441 (168.51)	54.9648 (167.56)	−18.8130 (165.70)	1.0443 (167.33)	14.4330 (166.74)
30	21.4030 (165.73)	12.8581 (163.64)	24.8608 (165.24)	22.5289 (163.61)	5.2281 (163.88)	−10.7330 (166.20)	−25.6232 (166.09)	−21.0362 (163.94)	−6.7098 (165.15)	−39.6574 (166.03)

Table 9.S11. *(Continued)*

j	R_j, 10^{-40} erg cm^3 (λ_j, nm)									
	md021#	**md022#**	**md023#**	**md024#**	**md025#**	**md026#**	**md027#**	**md028#**	**md029#**	**md030#**
1	−12.2506 (398.87)	−9.4213 (376.59)	8.3310 (399.61)	0.0289 (393.97)	−5.7708 (395.13)	−0.3738 (412.21)	−16.2512 (396.95)	1.2109 (389.69)	20.9331 (444.85)	−9.8705 (403.17)
2	32.5138 (343.09)	−8.1818 (343.73)	44.7673 (339.28)	−23.9455 (343.02)	−28.9698 (340.28)	100.9330 (335.89)	84.8174 (344.29)	−53.8919 (340.73)	93.6895 (352.44)	0.4449 (342.14)
3	−32.5568 (333.88)	44.7852 (325.92)	−38.1194 (330.74)	33.2446 (326.88)	21.6801 (334.69)	−97.4831 (330.75)	−53.0843 (337.44)	65.8198 (314.32)	−106.3148 (348.18)	30.6594 (333.08)
4	5.3492 (283.11)	−32.1043 (280.28)	13.9662 (282.50)	−5.1086 (281.71)	11.3981 (289.02)	−6.4632 (281.53)	7.3083 (286.91)	−11.2387 (273.17)	2.2993 (296.30)	2.7837 (284.47)
5	0.7536 (273.94)	−3.3595 (276.18)	−25.5804 (274.25)	−10.1192 (274.30)	22.6053 (269.99)	−21.9128 (275.89)	−49.8152 (268.37)	−15.3121 (270.72)	−12.3250 (276.87)	−31.3674 (273.13)
6	−27.0684 (269.35)	−3.2823 (269.92)	4.8753 (264.66)	5.5682 (268.08)	−55.6056 (265.93)	13.1037 (259.53)	−29.6981 (261.74)	5.0594 (268.36)	8.5273 (272.02)	2.4675 (266.05)
7	−11.6263 (255.70)	−43.9082 (254.26)	−82.6390 (250.95)	−83.8599 (252.90)	−35.2544 (258.39)	2.4260 (256.87)	33.1930 (260.26)	−4.0416 (257.43)	−32.4092 (258.35)	−32.0501 (255.64)
8	−61.5822 (253.08)	73.4998 (249.64)	−2.9490 (248.88)	33.0678 (249.00)	38.6213 (248.31)	31.4528 (249.15)	46.3049 (246.22)	−62.8821 (249.23)	−1.5874 (257.01)	65.2138 (252.99)
9	41.9532 (250.47)	−9.1413 (235.65)	−26.2253 (245.55)	31.7169 (244.96)	5.9710 (243.81)	−72.6791 (245.74)	19.5544 (240.94)	95.0916 (242.99)	−84.6395 (251.66)	0.2475 (241.57)
10	85.7436 (247.00)	3.4321 (229.98)	105.0101 (242.74)	19.1832 (244.75)	−1.5310 (240.61)	28.0039 (237.22)	−0.0659 (234.06)	11.1855 (235.69)	112.0210 (244.49)	1.4109 (239.15)
11	−0.1852 (237.51)	1.4964 (226.16)	0.3761 (237.14)	0.1838 (232.25)	0.1908 (230.01)	−3.0534 (220.05)	0.1567 (231.02)	1.2905 (234.82)	8.4293 (238.43)	0.0010 (230.34)
12	−14.5849 (209.73)	−25.2280 (213.65)	7.4328 (212.69)	0.3253 (212.96)	14.0533 (214.08)	19.2954 (210.54)	9.2115 (210.57)	−26.3169 (211.45)	3.5060 (217.86)	−2.7784 (213.76)
13	−16.7404 (207.38)	7.0700 (201.62)	−3.4862 (205.33)	15.9403 (211.11)	−26.8182 (208.76)	−10.0005 (204.68)	3.4350 (205.00)	−3.3389 (202.55)	8.4698 (213.44)	−31.4166 (208.55)
14	10.3352 (205.40)	17.2134 (197.76)	−10.5236 (204.51)	−35.4833 (206.21)	8.0839 (205.53)	16.6944 (197.57)	−20.1429 (204.69)	0.1320 (199.58)	−16.3676 (206.26)	4.1035 (202.58)
15	−0.9185 (203.02)	−4.2770 (195.77)	0.3528 (198.15)	−7.5036 (198.58)	32.0025 (198.85)	−6.5240 (193.90)	−9.9416 (198.49)	−4.1412 (198.84)	−7.9983 (201.19)	3.2451 (196.96)
16	−2.5702 (200.73)	−6.2992 (193.82)	1.3454 (195.66)	9.7091 (194.25)	−15.0472 (195.11)	20.1265 (191.31)	−5.1969 (193.03)	−4.2131 (197.26)	−8.0016 (197.25)	−8.4849 (195.66)
17	−16.6147 (197.55)	6.3929 (193.22)	24.2919 (192.78)	−5.1736 (191.29)	−2.8159 (193.87)	−9.4931 (187.52)	−5.1658 (189.26)	0.6374 (196.04)	25.6481 (193.93)	−9.6173 (193.16)
18	17.1022 (195.12)	−10.6502 (190.24)	10.5954 (191.21)	2.6015 (187.95)	−3.5917 (189.97)	27.0876 (185.61)	−5.7637 (188.79)	13.5919 (192.76)	24.6588 (192.08)	9.9818 (189.27)
19	11.2278 (190.49)	3.3870 (188.30)	−2.9246 (187.09)	5.1015 (184.27)	17.5583 (189.89)	9.2369 (185.29)	45.0896 (186.59)	6.0991 (190.32)	−7.5816 (190.24)	19.8923 (186.83)
20	7.4748 (187.15)	−14.5488 (184.97)	−27.4023 (185.89)	−13.9519 (181.76)	34.9644 (184.55)	−16.2801 (184.00)	6.0928 (182.25)	5.7740 (187.34)	−33.5685 (189.25)	1.0992 (184.51)
21	1.3528 (186.11)	3.8838 (183.14)	−7.9733 (184.13)	12.1902 (181.40)	−3.6776 (180.87)	−0.9419 (181.19)	−3.2862 (181.13)	−9.9687 (185.09)	−7.2813 (186.14)	1.3979 (183.02)
22	−3.4485 (183.30)	12.9820 (179.34)	−10.5044 (181.67)	−18.6723 (178.75)	−43.7984 (176.94)	−3.4744 (178.76)	−35.7809 (180.21)	−0.8771 (181.14)	5.1324 (182.91)	−23.2805 (180.84)
23	2.0109 (182.64)	−0.1802 (174.05)	5.2188 (179.86)	−3.4122 (177.47)	−4.6820 (175.81)	−0.5496 (174.46)	6.8829 (179.53)	−20.1313 (178.80)	−7.9546 (180.91)	−0.2208 (175.44)
24	−34.6342 (181.79)	5.9424 (173.77)	25.7453 (174.10)	3.9566 (176.75)	4.5694 (173.71)	6.3968 (173.47)	8.5483 (175.19)	−2.2737 (177.94)	−4.9265 (178.45)	3.3301 (173.33)
25	17.2911 (175.10)	2.7792 (170.99)	4.3911 (173.04)	−3.0396 (173.28)	18.3030 (169.88)	6.6829 (172.50)	−14.8823 (174.19)	−3.3881 (173.61)	−1.2327 (176.75)	−4.5473 (172.67)
26	−8.2367 (174.39)	25.7727 (169.83)	−3.9990 (170.99)	−1.0388 (171.83)	−3.7403 (168.43)	−1.3705 (170.12)	−11.1932 (171.17)	12.3692 (172.82)	−22.8070 (174.46)	−6.0065 (171.85)
27	14.0785 (172.43)	−30.2273 (168.78)	−1.6063 (169.22)	−2.4320 (170.85)	1.6529 (166.82)	0.9031 (169.26)	7.2766 (170.53)	−41.5706 (170.69)	0.1995 (169.62)	−9.9134 (171.34)
28	−5.0222 (170.40)	−22.2006 (167.41)	−9.5694 (166.88)	7.5401 (168.18)	2.2010 (165.04)	1.6902 (167.43)	15.3315 (167.55)	−7.3597 (167.88)	11.5210 (169.49)	−3.2318 (170.26)
29	−0.8612 (169.02)	−17.1692 (166.62)	2.6005 (165.89)	0.5565 (165.78)	4.7742 (164.75)	−31.6536 (164.69)	−5.1255 (165.79)	14.8984 (167.34)	−0.8243 (168.54)	30.8835 (165.69)
30	−1.0824 (168.12)	−5.2067 (163.96)	15.4981 (164.22)	22.3988 (165.07)	−12.0836 (163.83)	11.0634 (163.74)	19.3347 (164.32)	−4.3926 (165.47)	−17.9363 (167.59)	−0.3319 (165.30)

Table 9.S11. (*Continued*)

j	R_j, 10^{-40} erg cm^3 (λ_j, nm)									
	md031#	**md032#**	**md033#**	**md034#**	**md035#**	**md036#**	**md037#**	**md038#**	**md039#**	**md040#**
1	4.5988 (401.31)	−11.9608 (408.64)	2.7141 (401.24)	6.5908 (403.93)	−16.0554 (419.79)	19.1363 (407.15)	−66.9530 (365.53)	−11.7680 (386.61)	−25.2973 (397.70)	4.3434 (387.59)
2	−31.4059 (345.10)	18.0564 (347.22)	114.4272 (329.37)	−28.5553 (352.32)	6.5373 (344.37)	−4.8452 (348.08)	58.2185 (351.97)	34.0510 (344.23)	35.2734 (357.47)	−7.0267 (356.67)
3	19.9012 (323.54)	−9.7645 (335.69)	−69.6898 (320.53)	−31.8954 (332.28)	22.0506 (332.39)	−27.3705 (330.51)	26.8312 (314.18)	−1.6258 (322.98)	−10.1766 (332.87)	−10.4622 (312.76)
4	−20.5770 (279.60)	9.2399 (290.12)	4.8058 (276.77)	−12.3839 (286.79)	7.2673 (289.64)	−9.2407 (288.52)	−12.1923 (286.43)	−16.9114 (297.24)	−8.2833 (290.19)	−7.7559 (291.21)
5	11.6360 (273.73)	−39.9253 (273.65)	−23.4005 (266.12)	−5.0335 (278.41)	−21.1885 (271.54)	5.9713 (278.56)	−30.1003 (267.71)	3.0745 (281.93)	6.0787 (286.19)	−15.6404 (286.79)
6	17.6972 (265.81)	31.3643 (262.47)	−11.7075 (261.96)	25.0732 (272.18)	42.4873 (260.40)	−1.7284 (267.86)	3.5922 (266.03)	−5.9811 (268.54)	9.8541 (274.01)	10.0868 (271.15)
7	−66.0247 (255.56)	−114.6083 (255.18)	90.8119 (247.30)	−63.2657 (255.38)	−63.4129 (257.45)	−46.7238 (255.17)	−15.8175 (259.43)	−85.1398 (256.79)	−84.3151 (258.43)	−6.8135 (258.93)
8	41.8096 (243.36)	104.5906 (249.52)	7.1593 (245.18)	51.2610 (253.97)	37.4307 (247.11)	−16.4276 (253.51)	40.2799 (244.23)	101.2961 (249.59)	85.2723 (255.28)	9.3457 (253.06)
9	20.8131 (240.70)	−9.8380 (243.73)	−18.7493 (241.57)	−25.9771 (250.48)	−2.3150 (246.35)	−0.5236 (247.45)	5.5383 (240.11)	−6.1173 (247.13)	7.2291 (248.86)	12.2817 (248.51)
10	−12.0940 (238.16)	23.7711 (243.43)	−76.6854 (237.99)	58.4685 (247.33)	−3.1586 (243.88)	77.3821 (244.54)	−2.3381 (228.36)	8.3978 (236.09)	40.7986 (245.49)	−24.6514 (242.93)
11	34.7858 (233.76)	16.3281 (240.63)	−5.4558 (226.49)	31.5926 (241.43)	19.8755 (240.56)	20.1890 (239.21)	5.7638 (225.91)	−1.3794 (234.64)	1.7179 (226.67)	10.8799 (237.06)
12	15.9406 (207.01)	7.9091 (208.91)	4.0550 (203.94)	18.9346 (214.55)	4.9766 (211.78)	16.9402 (216.72)	−6.1477 (213.12)	39.7279 (216.28)	23.8568 (221.33)	35.5885 (224.99)
13	−9.6768 (203.62)	−6.7238 (206.09)	−32.9866 (201.54)	−28.1842 (210.63)	−12.4127 (208.89)	21.4265 (215.26)	5.6085 (202.27)	−24.3003 (213.32)	5.7729 (213.11)	6.9815 (214.15)
14	3.4675 (197.50)	−9.7423 (203.92)	17.7836 (198.81)	−3.8213 (206.18)	−9.6521 (204.45)	−41.4615 (208.81)	−10.8139 (200.35)	−13.7637 (200.97)	−63.4498 (210.88)	1.3447 (205.67)
15	−10.3568 (196.59)	−27.3366 (200.72)	−6.7335 (196.43)	21.1873 (202.27)	−2.4866 (200.88)	4.4346 (198.29)	−0.3832 (198.53)	6.7877 (200.49)	7.9485 (202.18)	−0.5976 (204.19)
16	−0.5396 (194.07)	−14.3091 (197.96)	−11.5785 (190.24)	0.2912 (200.71)	−16.6363 (199.67)	6.6644 (198.04)	22.4878 (196.56)	−0.5838 (199.46)	−12.4701 (196.60)	−22.0528 (199.38)
17	6.3769 (192.16)	−5.6617 (193.39)	25.0638 (186.94)	−5.9411 (197.63)	3.0094 (193.24)	−7.9766 (195.31)	−4.1945 (194.10)	−8.5473 (199.01)	14.5177 (194.72)	−6.6345 (198.04)
18	6.2440 (190.68)	3.8175 (191.15)	−1.1263 (185.27)	21.2651 (192.40)	7.8531 (192.94)	28.6358 (190.12)	−0.1344 (191.92)	−3.0611 (195.28)	−2.0399 (187.68)	16.5535 (196.73)
19	−4.4804 (189.19)	32.2277 (189.82)	−1.2629 (183.50)	−0.9897 (190.56)	19.6402 (189.12)	1.2602 (188.09)	−14.8992 (189.48)	30.7772 (186.21)	13.3433 (186.30)	−8.8109 (192.96)
20	−43.7904 (187.13)	−1.0977 (184.38)	−4.0252 (182.38)	−2.1847 (188.46)	−14.4855 (188.54)	−8.4421 (186.10)	−1.5893 (186.75)	−27.1300 (183.86)	13.9105 (184.63)	−1.2260 (190.82)
21	−0.4940 (181.36)	10.6572 (183.00)	7.5898 (180.82)	−6.7199 (185.87)	6.6678 (183.13)	1.4408 (183.16)	−13.4543 (184.08)	−0.9652 (182.89)	3.7899 (183.73)	−27.0182 (187.03)
22	11.5041 (180.90)	−27.3157 (181.76)	−6.0642 (178.93)	−15.6341 (184.41)	16.8615 (182.10)	−6.2554 (182.33)	−11.2699 (181.09)	−12.9844 (180.61)	−5.2581 (179.72)	−1.1023 (184.71)
23	1.4432 (178.68)	−1.0871 (181.19)	1.5228 (173.85)	−5.1866 (183.89)	0.4644 (181.94)	−17.0446 (180.51)	17.8244 (174.60)	−15.7703 (178.93)	−39.0518 (178.77)	12.2095 (184.05)
24	6.9259 (175.38)	3.3245 (179.92)	−3.3000 (172.63)	5.7756 (182.10)	3.6281 (180.07)	−35.4754 (180.26)	14.5106 (173.56)	−0.3295 (174.30)	5.4014 (177.62)	−3.1068 (182.06)
25	5.8444 (173.26)	−11.6659 (177.62)	4.5665 (172.14)	30.0346 (177.26)	−17.3077 (174.54)	16.1937 (176.90)	25.3811 (171.28)	−4.2305 (173.86)	−0.6400 (175.81)	14.2279 (177.78)
26	7.8056 (169.68)	48.2005 (172.46)	7.8329 (169.84)	1.1322 (173.71)	−8.3802 (173.44)	23.9041 (174.64)	2.7125 (169.74)	0.0961 (172.16)	−7.2347 (172.12)	0.5246 (175.72)
27	−1.1654 (168.03)	−1.9926 (170.19)	−12.7235 (168.67)	15.0325 (171.56)	24.2047 (172.20)	−9.7733 (173.08)	−11.9180 (168.27)	11.9152 (170.05)	3.3462 (170.90)	−2.6211 (174.75)
28	−4.8573 (166.89)	14.9106 (168.24)	−1.7984 (167.97)	5.8058 (169.11)	−38.5775 (170.98)	−2.3533 (170.77)	7.2265 (165.81)	1.8912 (169.37)	−8.7209 (168.79)	6.7725 (171.48)
29	−5.8992 (164.20)	5.3689 (167.44)	−4.7210 (163.38)	−7.0068 (165.51)	10.1484 (168.30)	9.1519 (168.49)	−2.1067 (164.03)	−15.5473 (167.88)	1.4219 (168.52)	−0.8200 (170.25)
30	−9.2398 (163.82)	−0.9057 (166.10)	7.6921 (163.07)	−26.9585 (165.17)	5.0776 (167.55)	−13.1766 (166.44)	25.0750 (163.21)	−23.9311 (167.42)	12.9258 (167.24)	7.0216 (167.89)

Table 9.S11. (*Continued*)

j	R_j, 10^{-40} erg cm^3 (λ_j, nm)									
	md041#	**md042#**	**md043#**	**md044#**	**md045#**	**md046#**	**md047#**	**md048#**	**md049#**	**md050#**
1	−8.1273 (378.15)	−46.9344 (382.10)	−32.1381 (407.48)	−24.3621 (398.65)	−8.4518 (405.03)	9.8583 (398.14)	2.9688 (384.96)	9.7488 (380.53)	−18.6480 (392.95)	−20.5317 (398.42)
2	49.4932 (339.00)	30.5332 (348.85)	132.0663 (348.21)	74.3826 (361.52)	−11.8850 (361.81)	−16.4701 (343.15)	0.8318 (338.83)	29.3665 (356.12)	−53.5716 (348.35)	21.9907 (366.11)
3	5.8633 (309.89)	23.3907 (324.59)	−25.5901 (331.44)	12.0445 (314.73)	5.1774 (322.75)	−26.9433 (305.22)	−30.7113 (307.05)	−64.2669 (314.00)	57.8082 (315.20)	1.3593 (321.26)
4	−9.1964 (280.29)	−0.0751 (286.79)	2.1452 (279.49)	−14.1825 (286.30)	−13.1814 (296.81)	−38.4083 (278.80)	−28.5640 (279.05)	9.5582 (288.51)	−18.9715 (281.35)	18.4447 (293.23)
5	−19.6287 (273.77)	−9.7993 (282.78)	−33.8867 (276.47)	−31.8531 (280.11)	−6.5381 (281.30)	19.3036 (273.31)	5.1998 (274.76)	−0.3078 (280.54)	21.9689 (277.16)	−30.7467 (287.80)
6	−0.4197 (270.33)	−19.3733 (278.30)	−2.1725 (269.19)	−5.5231 (276.19)	−14.4973 (265.20)	28.9745 (266.02)	14.2438 (268.72)	23.5718 (269.89)	−39.0303 (271.86)	15.3581 (273.91)
7	12.7936 (253.38)	−38.6124 (259.59)	76.9657 (257.54)	−16.6714 (255.94)	28.2635 (259.62)	−0.3778 (252.28)	−4.6307 (250.79)	−18.6672 (251.85)	9.9715 (257.11)	0.5556 (260.28)
8	−36.0226 (249.31)	−31.6393 (252.66)	9.8341 (248.07)	64.3565 (250.17)	−51.8586 (249.47)	−38.3616 (248.17)	42.4651 (244.97)	−103.4868 (249.69)	−21.3058 (252.35)	−69.8997 (251.07)
9	50.2163 (245.61)	87.4814 (247.39)	−74.6238 (246.33)	−4.1862 (247.52)	51.5439 (240.75)	43.3400 (241.60)	−14.5697 (244.21)	106.8620 (244.66)	73.6308 (249.28)	55.0869 (249.44)
10	0.7330 (229.89)	6.7664 (237.87)	1.2777 (240.26)	−35.7190 (237.26)	1.6012 (235.47)	28.7939 (236.61)	3.3584 (236.48)	23.9697 (237.64)	1.1534 (228.75)	27.6197 (233.12)
11	11.1460 (227.71)	22.9912 (231.81)	3.7694 (232.44)	12.2641 (232.66)	12.8719 (232.50)	0.4561 (223.46)	6.4873 (229.90)	32.3059 (225.01)	1.6271 (225.83)	0.7460 (231.02)
12	−13.2044 (222.13)	−29.5918 (219.96)	−19.8767 (208.05)	−19.9738 (215.75)	2.4614 (221.89)	8.3727 (216.37)	−22.6476 (221.84)	44.9185 (222.48)	−35.8599 (222.84)	0.7194 (225.82)
13	−16.8075 (205.52)	11.4909 (209.49)	−21.5826 (207.33)	−14.9033 (210.25)	5.9384 (210.55)	0.1104 (205.92)	15.4429 (206.89)	1.8090 (210.93)	13.5078 (205.44)	−0.7021 (209.42)
14	−1.2616 (202.96)	16.6826 (208.00)	−5.8592 (204.77)	12.1634 (207.81)	−18.1403 (207.88)	−20.2030 (204.38)	−9.7949 (201.30)	−28.5092 (207.58)	−11.5991 (202.95)	−7.1891 (204.64)
15	1.5381 (199.24)	−3.8708 (205.11)	−10.6781 (200.59)	−1.3772 (205.29)	4.4043 (200.06)	2.8066 (198.34)	7.1777 (200.13)	−42.6493 (199.47)	−21.7247 (200.09)	−2.4950 (200.13)
16	−11.5615 (198.12)	−9.8511 (201.75)	−4.9172 (195.56)	0.9975 (201.89)	2.8931 (199.20)	−3.7147 (195.68)	−8.9555 (199.72)	2.0192 (197.40)	11.5738 (197.62)	−1.5962 (196.62)
17	2.4918 (190.54)	5.3727 (194.53)	−0.8598 (191.50)	16.8133 (193.23)	−3.7592 (198.80)	−2.4755 (195.05)	−3.6077 (193.44)	−4.3122 (190.27)	23.5733 (196.53)	−7.9699 (194.37)
18	−11.3034 (188.67)	3.9052 (192.40)	0.4375 (189.56)	8.7037 (189.67)	7.7186 (195.81)	15.6557 (192.83)	9.1569 (191.67)	6.8165 (187.83)	−14.2942 (194.54)	4.7659 (194.06)
19	12.6505 (187.15)	−0.7332 (189.47)	9.3287 (185.00)	2.6898 (187.84)	31.8086 (189.58)	−0.8485 (191.82)	9.3195 (188.79)	−0.9507 (185.71)	15.7733 (190.07)	1.8495 (192.62)
20	5.1971 (186.16)	−4.5685 (186.69)	19.3992 (183.56)	−6.4953 (183.88)	1.2592 (188.58)	−9.5512 (190.05)	29.4667 (185.60)	−4.6013 (183.81)	−0.1345 (186.69)	10.2886 (189.61)
21	−4.6152 (180.65)	−2.7183 (183.53)	11.3220 (182.21)	−4.0046 (182.13)	4.8634 (183.92)	−36.5447 (185.57)	−12.0040 (184.84)	−11.3820 (183.30)	−12.3185 (184.78)	−9.5654 (188.10)
22	29.5532 (177.40)	−5.9341 (182.75)	5.4904 (180.15)	−2.5229 (180.29)	13.4352 (182.23)	−6.9506 (183.47)	−38.6571 (178.90)	−4.0930 (180.13)	20.6490 (182.43)	−7.6128 (185.41)
23	−8.8617 (174.74)	51.6126 (179.75)	−3.7882 (177.65)	4.3043 (179.83)	−8.6990 (181.51)	3.0034 (178.65)	1.1819 (178.35)	41.6439 (177.25)	0.8900 (177.83)	−6.8785 (179.19)
24	−55.9344 (173.70)	16.5981 (177.87)	−19.2268 (176.59)	3.1931 (176.13)	−41.3154 (180.46)	4.9664 (177.25)	−2.9833 (176.27)	−24.4457 (174.09)	40.3295 (173.42)	−3.1887 (178.25)
25	2.7240 (172.49)	−1.6807 (175.96)	−22.8312 (173.18)	−20.3744 (174.19)	31.2929 (176.56)	15.4189 (176.58)	34.1790 (172.98)	3.2156 (172.32)	25.3148 (172.56)	17.7577 (175.05)
26	1.9841 (171.41)	−19.8285 (174.18)	1.5168 (169.96)	7.3055 (170.22)	−4.0793 (173.94)	7.7132 (173.58)	0.3827 (172.43)	8.0886 (171.08)	−2.9335 (172.08)	−5.8609 (172.81)
27	−18.5319 (168.94)	−20.4308 (171.37)	−3.6826 (169.62)	−27.2533 (168.97)	7.6447 (172.63)	45.7383 (172.38)	6.6909 (171.28)	13.0672 (169.93)	−20.4868 (170.52)	1.1839 (172.21)
28	−15.2975 (166.11)	−0.0825 (170.35)	−15.8515 (168.69)	−9.2229 (168.04)	−29.8056 (167.78)	−20.1297 (171.95)	−4.9967 (169.42)	−3.0844 (166.68)	23.5759 (167.10)	8.2840 (170.87)
29	17.7424 (165.70)	19.9775 (168.43)	−1.9476 (165.89)	13.3504 (167.41)	6.5435 (166.46)	−1.8408 (168.34)	−2.0414 (166.39)	0.4454 (166.07)	−9.8989 (165.48)	36.2128 (169.89)
30	1.6266 (163.24)	9.2305 (166.51)	16.1571 (165.14)	−8.2435 (166.26)	9.6984 (164.88)	−2.9378 (164.71)	13.0366 (165.01)	−24.6164 (165.44)	9.0208 (165.22)	−6.7882 (167.54)

Table 9.S11. (*Continued*)

j	R_j, 10^{-40} erg cm^3 (λ_j, nm)									
	md051#	**md052#**	**md053#**	**md054#**	**md055#**	**md056#**	**md057#**	**md058#**	**md059#**	**md060#**
1	−14.1282 (401.04)	−28.8434 (409.05)	−40.2478 (399.58)	−35.8489 (405.80)	−22.8084 (398.64)	−53.0967 (392.72)	−35.5131 (399.99)	−20.9566 (404.49)	−51.7583 (410.76)	−10.3369 (405.86)
2	23.8678 (361.03)	59.7747 (358.47)	12.7359 (354.79)	83.6860 (348.00)	77.2743 (361.49)	91.2138 (352.71)	73.6098 (367.43)	93.8071 (345.98)	102.2134 (360.24)	111.2906 (340.22)
3	−3.6485 (322.30)	13.6932 (330.74)	50.4472 (320.01)	−3.5287 (330.86)	−43.9375 (327.11)	16.0874 (315.70)	−7.5942 (323.00)	−0.6106 (322.65)	37.5816 (318.30)	−35.4637 (330.56)
4	18.5931 (296.09)	−15.7676 (290.11)	−0.5155 (282.43)	−2.6214 (294.83)	21.1662 (293.92)	−3.6422 (287.41)	27.9472 (300.64)	−28.6925 (279.37)	−37.2332 (288.41)	1.1799 (282.03)
5	−13.8487 (277.95)	0.8176 (280.73)	−13.8571 (278.27)	10.5583 (282.92)	0.0733 (280.28)	12.5692 (278.82)	−5.5269 (275.46)	15.6161 (277.94)	−7.7135 (281.82)	−20.9115 (275.76)
6	−3.6106 (277.48)	−37.5201 (273.49)	−19.9735 (273.83)	−49.9533 (268.55)	−37.5440 (273.61)	−21.7189 (269.81)	−56.8556 (275.11)	−38.9797 (271.82)	24.9893 (277.79)	−44.1610 (266.71)
7	−17.7552 (261.92)	0.5443 (260.93)	−32.5394 (260.02)	0.6518 (254.46)	−13.5649 (254.58)	−3.4208 (256.84)	37.8770 (257.88)	80.8584 (251.63)	−61.5840 (255.37)	65.3005 (252.34)
8	−25.2250 (255.12)	46.3544 (254.76)	17.0846 (253.79)	−54.6152 (251.21)	33.7677 (250.50)	17.9244 (248.23)	19.7134 (246.34)	26.1477 (244.24)	108.6116 (250.75)	43.2577 (249.52)
9	27.2369 (245.21)	−13.1285 (249.07)	52.2581 (247.17)	92.6487 (247.85)	4.2894 (250.19)	−4.1103 (243.07)	−32.6952 (242.70)	−93.7145 (243.06)	−5.6884 (246.79)	−90.7913 (245.54)
10	26.0127 (243.04)	2.6982 (239.45)	−1.5614 (234.71)	4.8656 (235.33)	3.3476 (237.86)	−74.3092 (240.89)	−0.9368 (239.49)	−2.4492 (239.61)	−40.8678 (240.78)	−2.0642 (240.67)
11	7.3548 (226.07)	6.4517 (235.47)	23.8170 (233.62)	−20.2312 (227.79)	9.3485 (236.63)	43.1291 (234.53)	6.2485 (225.65)	0.8545 (238.27)	0.4529 (235.16)	−2.0920 (235.76)
12	17.9150 (222.02)	−14.4613 (222.82)	−32.6379 (216.62)	0.6587 (223.73)	14.1517 (219.92)	−30.3775 (216.96)	−0.1765 (223.60)	−25.8761 (216.56)	−40.8388 (216.25)	−35.8363 (213.35)
13	−2.2016 (214.85)	−0.7917 (207.95)	−0.9116 (205.32)	−8.0067 (209.63)	−8.1204 (214.17)	−3.0281 (210.43)	0.7644 (215.93)	−0.0744 (202.39)	−1.1349 (208.80)	4.5849 (204.35)
14	−18.1816 (213.22)	−32.3695 (205.43)	−18.8879 (202.75)	−25.0909 (207.63)	7.1938 (211.94)	−3.9041 (208.65)	−25.8699 (206.83)	−2.9520 (199.33)	3.8409 (207.66)	−6.7003 (203.12)
15	−4.0574 (202.69)	1.6589 (203.98)	−11.2963 (202.16)	3.4830 (200.03)	−11.5044 (202.21)	13.2576 (204.74)	4.8199 (200.98)	−10.0284 (197.28)	6.4091 (204.53)	−0.2933 (202.05)
16	−7.5461 (200.82)	7.4979 (200.34)	−2.0345 (200.99)	−3.6792 (199.46)	−15.4985 (196.73)	−1.8565 (201.11)	−6.2670 (199.86)	12.9429 (196.05)	−12.3025 (202.74)	−2.7564 (199.12)
17	2.9324 (196.67)	−0.1256 (197.70)	0.7393 (198.26)	−2.0107 (196.52)	−3.5284 (194.90)	−9.2051 (196.37)	−3.9253 (190.74)	−0.3106 (193.91)	−6.2363 (196.83)	1.8747 (196.11)
18	1.3568 (194.65)	−0.3524 (195.66)	5.8685 (192.11)	4.5404 (191.78)	−5.8614 (191.44)	2.2067 (192.77)	4.5665 (189.26)	−0.0013 (191.17)	−18.9959 (192.35)	3.2629 (190.74)
19	13.8156 (190.39)	5.7077 (191.55)	0.4274 (190.42)	−5.4961 (187.54)	17.6217 (186.14)	23.7026 (188.70)	16.2771 (185.94)	1.2774 (188.74)	6.3385 (189.11)	6.2930 (188.18)
20	−20.9423 (187.54)	15.7003 (189.24)	−8.8727 (187.53)	−2.9667 (184.86)	−13.2996 (185.60)	0.1493 (186.71)	−1.1101 (182.05)	9.3080 (182.94)	−10.7234 (187.42)	29.9944 (184.89)
21	20.1301 (182.82)	23.2982 (186.32)	−3.1990 (186.34)	−3.3703 (181.95)	6.5574 (184.51)	−21.3840 (186.33)	−12.0008 (180.40)	6.5177 (179.89)	0.3926 (185.23)	−2.9677 (183.65)
22	35.6864 (181.42)	−2.7984 (183.58)	4.5595 (182.68)	3.6903 (181.16)	1.0736 (183.96)	12.7276 (182.14)	0.2708 (178.85)	8.4040 (179.11)	−8.6857 (182.70)	2.5027 (181.94)
23	−28.4465 (178.97)	−3.1594 (182.71)	48.8406 (180.08)	60.5900 (178.54)	6.7719 (177.48)	3.9798 (180.81)	12.1583 (177.43)	6.9614 (178.47)	48.6986 (180.43)	−4.7124 (179.71)
24	−39.3576 (174.76)	−4.6469 (178.80)	3.8609 (177.77)	0.5060 (176.36)	10.9875 (176.65)	−2.4502 (178.95)	24.2586 (175.37)	27.8221 (177.99)	7.0599 (177.68)	4.3783 (177.97)
25	6.5528 (173.59)	−31.9331 (176.21)	5.5128 (174.71)	−12.7553 (172.68)	2.5556 (174.22)	55.4754 (176.50)	−17.7421 (175.33)	0.9059 (175.24)	−16.5053 (174.75)	−7.6861 (176.47)
26	3.8409 (172.68)	24.9552 (175.32)	−14.3767 (174.36)	−29.1124 (171.05)	−11.9069 (173.02)	−32.6148 (172.10)	−12.7075 (174.49)	−7.9089 (174.25)	−10.2690 (173.31)	10.1587 (173.54)
27	−6.1284 (172.44)	0.5431 (170.60)	14.3640 (170.69)	5.3795 (170.10)	0.2095 (170.95)	0.1426 (169.06)	1.4485 (171.93)	−11.5576 (170.24)	−6.8973 (171.96)	−7.0557 (173.03)
28	16.9456 (170.43)	−1.4591 (169.76)	−8.7143 (168.17)	2.5673 (169.43)	2.4496 (170.45)	2.5035 (166.32)	−28.7496 (169.00)	18.8158 (168.22)	9.0203 (171.22)	13.8443 (169.03)
29	20.7400 (168.27)	−2.6054 (167.47)	2.7918 (166.36)	−3.5713 (167.32)	7.6116 (168.69)	−26.2484 (165.86)	13.9616 (167.25)	−31.6581 (166.86)	−11.4913 (169.44)	−1.5369 (167.84)
30	4.0723 (167.11)	18.0550 (166.24)	20.3539 (166.19)	−0.8333 (164.16)	27.8450 (165.77)	−10.3974 (164.61)	11.6886 (165.89)	10.3479 (166.61)	−7.6326 (166.46)	16.8505 (166.82)

Table 9.S11. *(Continued)*

j	R_j, 10^{-40} erg cm^3 (λ_j, nm)									
	md061#	**md062#**	**md063#**	**md064#**	**md065#**	**md066#**	**md067#**	**md068#**	**md069#**	**md070#**
1	−17.7437 (387.06)	−15.7987 (408.96)	−0.2593 (406.62)	−7.7884 (403.49)	−9.9458 (402.38)	−92.6881 (373.45)	−37.2155 (416.78)	−41.5224 (405.19)	−16.3996 (420.26)	−6.3008 (380.89)
2	−21.5314 (355.47)	42.8745 (363.57)	13.9945 (354.20)	−3.1105 (352.77)	56.6592 (340.77)	122.2187 (359.81)	84.6406 (370.29)	128.8804 (359.99)	42.5133 (372.28)	1.4483 (332.61)
3	71.1482 (316.37)	8.7915 (325.58)	−19.8224 (325.46)	52.6287 (329.35)	−41.3276 (330.22)	−24.7893 (330.18)	−24.6666 (340.01)	−16.3188 (333.36)	−2.7106 (345.93)	22.6001 (305.24)
4	−48.2650 (282.91)	−7.3743 (287.39)	5.7796 (282.41)	−9.9413 (286.89)	5.2539 (285.70)	−2.9032 (296.09)	7.0445 (294.61)	−22.9342 (287.99)	4.8379 (302.08)	3.4668 (269.92)
5	−12.4152 (277.92)	−2.2378 (282.25)	−2.1846 (277.98)	−13.4705 (276.98)	−18.0027 (273.55)	46.9419 (284.76)	−29.6768 (279.79)	−5.2099 (284.37)	−16.8134 (287.45)	−31.9343 (265.58)
6	2.6979 (266.03)	−26.1322 (279.56)	8.9620 (260.26)	−26.0226 (268.25)	−25.0201 (270.88)	−47.8999 (277.13)	−9.4997 (278.24)	−38.2070 (277.09)	−34.3765 (276.90)	−14.0266 (261.56)
7	−58.6186 (259.83)	−28.3391 (257.48)	−71.3946 (252.08)	2.1734 (259.75)	1.1552 (252.24)	18.2118 (271.32)	25.6971 (259.02)	100.3334 (260.39)	−5.8188 (266.75)	2.5973 (246.12)
8	113.4310 (250.03)	−59.6488 (251.37)	3.9907 (249.99)	−105.4063 (256.79)	−50.6649 (249.57)	−67.0261 (257.79)	69.5985 (255.66)	53.7667 (256.61)	−1.9987 (263.19)	−20.0218 (241.14)
9	1.3262 (246.10)	129.8526 (248.32)	−30.6868 (242.84)	100.2640 (251.32)	46.2533 (247.19)	38.8626 (252.47)	−93.6235 (251.38)	−109.6233 (253.35)	23.8705 (257.03)	58.2455 (240.23)
10	0.0440 (235.27)	5.7674 (245.36)	102.9852 (240.61)	23.2632 (247.83)	49.6267 (246.17)	49.7531 (247.55)	−16.5802 (250.47)	−6.6849 (237.24)	−4.4912 (250.73)	−2.9267 (230.53)
11	−1.4977 (234.25)	−14.9110 (243.09)	28.9683 (231.81)	5.5586 (243.54)	6.5562 (229.21)	2.3999 (230.37)	34.6216 (243.49)	−0.3165 (230.12)	3.0359 (248.77)	−1.9682 (228.76)
12	−32.9642 (210.57)	−20.8188 (216.75)	20.5744 (213.33)	1.9398 (211.43)	14.3785 (212.61)	−5.4961 (228.74)	2.3785 (214.97)	−28.9367 (220.22)	−12.2366 (222.89)	−21.1390 (206.23)
13	9.3011 (206.39)	8.0659 (210.48)	−2.0117 (200.69)	−18.8540 (211.10)	−18.2319 (209.48)	−1.7052 (217.90)	7.3490 (213.69)	0.1575 (214.55)	1.0182 (219.65)	7.8098 (198.52)
14	5.9894 (204.44)	13.7450 (208.77)	12.2060 (198.02)	2.4553 (206.39)	1.5649 (204.59)	−11.0257 (212.99)	−19.7545 (211.16)	8.8057 (206.66)	5.2388 (213.49)	5.0262 (196.34)
15	1.2113 (199.33)	−5.0737 (204.10)	−30.2718 (196.10)	−14.2943 (200.73)	−4.1352 (200.27)	−11.1123 (210.93)	−1.4041 (201.86)	−13.9386 (203.06)	−6.9205 (208.78)	3.3507 (192.23)
16	23.9394 (194.71)	−4.5391 (196.93)	−12.5423 (192.24)	−3.2522 (198.67)	20.2314 (196.62)	1.6249 (206.60)	14.6412 (200.07)	−1.0541 (201.75)	−2.9749 (205.61)	0.9008 (190.35)
17	−7.6142 (191.73)	12.6804 (193.54)	15.6323 (190.29)	2.0250 (196.62)	−3.5582 (191.15)	9.8648 (202.29)	2.5063 (198.99)	−16.1219 (196.63)	28.3217 (204.92)	−13.9751 (187.30)
18	−6.5753 (190.32)	−6.4615 (192.75)	−0.9931 (186.93)	−10.3873 (194.82)	−10.2896 (190.72)	−12.4045 (198.34)	4.3072 (193.75)	6.5491 (190.72)	−4.5891 (203.11)	−5.7673 (185.57)
19	0.2027 (185.86)	−1.9962 (189.45)	−2.4930 (184.56)	−11.9851 (191.69)	10.5520 (185.55)	−2.7188 (195.79)	−21.3383 (189.96)	−7.0017 (187.63)	0.1902 (197.20)	−8.4550 (183.71)
20	6.9560 (182.45)	−9.0813 (187.48)	−20.3443 (183.65)	28.9676 (188.22)	25.9416 (184.23)	1.3224 (192.14)	0.1030 (187.42)	−5.7610 (186.25)	−2.4268 (194.18)	17.4644 (181.04)
21	−6.7423 (181.12)	22.3738 (186.83)	0.5574 (181.66)	−18.0398 (185.90)	−4.2966 (182.58)	−4.9185 (188.78)	6.6323 (186.07)	−5.0234 (184.52)	−12.1416 (192.81)	8.4339 (175.78)
22	−1.3953 (180.11)	−12.5726 (181.69)	16.6912 (179.63)	1.1356 (185.40)	−20.7237 (181.16)	−1.1471 (187.03)	−2.9435 (181.70)	−8.9788 (183.21)	49.1208 (189.76)	3.9586 (174.14)
23	−3.8614 (179.13)	21.3796 (179.93)	2.3911 (178.16)	−4.5166 (181.35)	−4.5280 (178.48)	19.6007 (184.29)	29.8522 (180.45)	25.7598 (178.65)	−2.0375 (186.04)	−8.3654 (173.74)
24	3.6286 (176.65)	−4.8646 (178.79)	2.5138 (176.50)	−9.0712 (179.90)	−2.0787 (175.46)	−21.3771 (178.32)	18.0970 (178.85)	33.4369 (177.18)	−14.2647 (181.72)	11.3506 (172.91)
25	−4.1772 (174.45)	28.1220 (173.29)	−6.7156 (172.52)	33.4442 (177.61)	−14.0265 (172.04)	4.7751 (177.70)	5.9731 (176.35)	−16.1489 (175.87)	−9.4766 (180.04)	5.5126 (170.91)
26	1.5249 (172.20)	−53.9679 (170.96)	15.1940 (171.08)	−42.8654 (174.66)	15.7311 (171.04)	44.5642 (175.61)	−21.9857 (174.04)	−25.9108 (173.72)	−5.0692 (178.41)	−5.3103 (168.35)
27	31.7970 (171.62)	5.6241 (170.05)	−8.6008 (170.00)	−14.4900 (167.75)	8.4935 (169.51)	−19.9473 (174.20)	−27.9171 (171.47)	−25.4428 (171.50)	−20.9243 (175.79)	0.4825 (165.93)
28	5.7496 (170.08)	12.1045 (167.30)	−4.0829 (167.73)	1.5592 (167.62)	−1.6538 (168.73)	15.4183 (171.70)	−0.2302 (168.97)	18.0556 (170.11)	10.2706 (171.76)	−14.3007 (164.13)
29	−9.4841 (165.56)	−6.2767 (166.59)	22.0495 (167.22)	13.8033 (166.16)	−10.4982 (166.92)	0.4517 (168.96)	5.3544 (166.95)	0.9663 (168.08)	3.2860 (171.29)	45.9178 (161.64)
30	−9.7376 (163.93)	−25.8036 (165.70)	1.3808 (163.80)	−26.2085 (165.17)	6.0314 (165.37)	1.2732 (168.24)	23.0771 (166.66)	6.4838 (165.79)	2.3141 (169.64)	3.4595 (161.48)

Table 9.S11. (*Continued*)

j	R_j, 10^{-40} erg cm^3 (λ_j, nm)									
	md071#	**md072#**	**md073#**	**md074#**	**md075#**	**md076#**	**md077#**	**md078#**	**md079#**	**md080#**
1	−12.7656 (404.11)	−27.2324 (405.15)	−17.7269 (394.24)	−16.0273 (412.25)	−23.6640 (386.69)	−16.8665 (385.47)	22.5610 (396.69)	−12.6881 (387.40)	−22.3922 (429.56)	−53.1169 (403.61)
2	40.9005 (348.00)	47.5213 (353.01)	28.8843 (366.60)	69.5816 (352.06)	40.1976 (351.62)	−3.9246 (344.73)	−41.4101 (346.79)	−3.2369 (347.94)	72.3843 (376.08)	127.1760 (359.37)
3	9.8865 (324.70)	25.7790 (318.46)	8.3913 (317.18)	4.9007 (325.28)	−16.0703 (310.27)	7.7663 (314.38)	26.0912 (318.33)	6.5464 (321.60)	−25.0769 (328.92)	−17.2736 (320.92)
4	−18.0823 (279.01)	−3.0898 (280.77)	−20.1218 (283.85)	1.3529 (284.34)	−20.1467 (280.27)	4.6506 (288.43)	1.1595 (286.81)	10.7754 (287.90)	−15.1354 (299.12)	16.9023 (297.41)
5	−7.3416 (277.79)	−19.6664 (275.13)	−11.7518 (279.05)	−32.0987 (276.75)	7.3323 (279.04)	11.0016 (274.90)	8.0671 (279.89)	7.0818 (278.99)	14.7869 (279.59)	13.8275 (275.69)
6	−40.9120 (269.55)	−18.0475 (271.73)	−25.1821 (274.35)	−40.0890 (272.40)	0.5768 (268.46)	−2.9331 (265.54)	−51.1363 (270.43)	2.7879 (270.42)	−33.7807 (276.65)	−49.9787 (273.28)
7	32.1662 (250.88)	−9.1970 (253.99)	−9.3986 (257.68)	7.2427 (256.37)	6.0011 (251.18)	−25.9721 (260.61)	18.4754 (258.46)	−108.3702 (258.79)	−6.6075 (266.21)	11.6733 (255.04)
8	0.2494 (242.06)	25.4275 (249.66)	35.0661 (252.35)	133.7587 (250.72)	−4.7745 (245.94)	−8.9139 (252.45)	−29.3368 (252.53)	96.4078 (249.81)	3.6589 (251.37)	54.4395 (250.62)
9	37.8340 (241.25)	−12.9320 (243.66)	4.0582 (247.20)	−99.5564 (246.30)	9.8746 (236.62)	72.5729 (250.32)	−12.2097 (247.97)	−19.4026 (246.69)	−12.4259 (248.59)	−72.5923 (242.03)
10	7.4943 (237.11)	13.3339 (240.21)	−0.0411 (242.35)	5.0251 (240.54)	48.7147 (234.52)	1.5103 (238.46)	42.7848 (241.03)	−2.2858 (244.47)	74.2758 (244.52)	3.7994 (233.01)
11	2.6819 (227.52)	15.9873 (232.57)	27.5110 (238.81)	2.2929 (239.31)	−2.6298 (227.45)	−6.0523 (233.94)	34.8832 (238.75)	27.1395 (232.82)	−52.8257 (237.56)	9.9092 (232.55)
12	−25.4923 (213.61)	−8.8365 (212.00)	−8.3923 (216.35)	−30.6390 (212.99)	−4.0749 (215.56)	−19.0235 (222.01)	−16.8111 (214.23)	−24.5267 (215.07)	−24.0014 (214.38)	−10.4411 (221.70)
13	4.0447 (203.60)	−22.3283 (209.76)	7.0494 (212.45)	5.5211 (208.71)	11.3588 (203.27)	−9.0866 (211.54)	−5.8141 (210.47)	4.2461 (213.03)	6.5700 (210.49)	−5.1559 (219.07)
14	10.1272 (199.02)	8.7945 (203.89)	7.7923 (203.26)	−0.2056 (202.86)	−7.1343 (200.20)	−6.1721 (204.27)	9.7340 (209.44)	0.8957 (205.38)	−3.6132 (207.82)	−2.4152 (209.57)
15	−3.1930 (196.06)	0.9636 (200.88)	0.8360 (200.93)	0.2826 (200.34)	−0.5606 (198.44)	4.1541 (200.96)	5.8785 (203.50)	−6.9337 (201.86)	2.7836 (203.51)	−6.0708 (201.34)
16	−10.5988 (195.77)	−1.6080 (196.96)	−2.2346 (197.68)	−12.9656 (197.85)	5.2364 (195.28)	−2.5350 (199.64)	−4.7050 (199.46)	1.9014 (201.40)	−3.0033 (200.47)	−6.7296 (198.32)
17	−0.8433 (191.83)	−3.8782 (194.22)	−2.2223 (193.54)	−2.8905 (196.98)	−6.8271 (192.68)	11.8553 (196.25)	−0.2240 (196.41)	−3.1963 (197.37)	14.4431 (195.84)	1.7967 (196.76)
18	−2.9109 (189.21)	−17.9916 (190.20)	−1.5482 (190.89)	14.8021 (193.11)	−5.0931 (189.27)	−6.3618 (194.71)	−15.3462 (193.47)	7.6050 (194.63)	36.1053 (191.90)	0.1177 (191.86)
19	−0.8612 (186.63)	−8.6977 (186.79)	−11.2676 (188.83)	−21.3885 (187.66)	−8.3767 (186.11)	19.7233 (192.86)	3.1924 (189.31)	11.0910 (188.64)	7.3887 (189.55)	13.8856 (187.98)
20	14.3158 (182.28)	2.8331 (183.74)	11.8532 (185.44)	3.1402 (186.61)	−8.7215 (183.46)	−2.8218 (187.12)	−8.7075 (188.11)	−3.7510 (188.41)	9.5806 (188.68)	6.8501 (187.03)
21	5.9726 (180.57)	36.8322 (182.07)	7.4190 (183.48)	10.9272 (184.70)	1.1517 (182.31)	−0.6519 (184.83)	−3.2742 (185.76)	4.4303 (185.59)	14.9001 (186.69)	2.3312 (183.57)
22	−23.9512 (179.02)	2.8896 (181.59)	5.8997 (181.35)	−9.0059 (182.98)	2.2051 (180.36)	22.4607 (182.52)	−44.0774 (182.76)	−10.3865 (183.10)	−0.1700 (182.45)	39.5828 (180.29)
23	−2.1831 (175.88)	−6.6713 (180.25)	3.1334 (179.16)	31.8892 (181.07)	−52.0539 (172.16)	0.0653 (181.54)	0.2606 (178.94)	18.8160 (182.13)	20.4629 (180.70)	−24.5334 (179.57)
24	−10.0016 (172.02)	2.1203 (176.00)	−3.6719 (176.03)	−2.6197 (177.44)	5.3842 (170.20)	−2.4777 (180.30)	−17.5372 (176.73)	−8.4000 (176.78)	−27.4828 (176.99)	−2.0446 (175.44)
25	2.8226 (171.24)	3.8249 (175.42)	0.5813 (173.63)	−25.2889 (174.03)	9.0399 (168.75)	−72.5471 (176.13)	11.0542 (174.84)	−11.8921 (174.72)	8.5940 (174.94)	−9.3599 (174.71)
26	7.4383 (170.24)	−15.4411 (173.10)	−19.6146 (173.12)	−31.2769 (171.79)	13.7230 (168.69)	32.3299 (175.39)	2.7735 (172.62)	−34.2835 (171.93)	11.4804 (172.96)	−5.5183 (172.19)
27	−17.5334 (167.83)	41.0021 (170.33)	−4.4559 (169.94)	2.8395 (170.12)	3.4597 (167.89)	−7.7535 (172.69)	−25.7376 (170.89)	6.8507 (169.42)	3.4791 (169.67)	3.1110 (171.00)
28	12.6107 (166.77)	−20.4695 (168.78)	−14.1154 (167.38)	−1.4405 (169.35)	4.9661 (166.63)	6.5826 (171.04)	3.4851 (169.59)	−26.0716 (167.06)	0.1232 (168.13)	−59.2160 (169.03)
29	6.5255 (165.61)	−5.8325 (167.92)	0.0841 (165.43)	−3.7037 (167.89)	24.0316 (165.10)	−2.1452 (168.73)	44.1795 (165.75)	3.3387 (165.93)	10.1922 (167.78)	13.4758 (167.67)
30	36.7574 (163.82)	−0.2724 (166.20)	33.7996 (164.90)	2.1799 (167.25)	−9.3173 (164.78)	10.2589 (168.48)	8.2612 (165.02)	−14.5961 (165.18)	0.7699 (164.09)	−0.7009 (165.73)

Table 9.S11. *(Continued)*

j	R_j, 10^{-40} erg cm^3 (λ_j, nm)									
	md081#	md082#	md083#	md084#	md085#	md086#	md087#	md088#	md089#	md090#
1	−52.2221 (385.83)	−33.0622 (427.28)	−21.4923 (395.66)	8.2097 (396.14)	−10.0861 (408.42)	−47.3042 (376.26)	−32.7274 (382.22)	−41.9403 (408.24)	−44.5879 (401.26)	−24.7789 (417.99)
2	125.2541 (352.47)	34.0906 (362.47)	51.5375 (344.43)	6.6548 (353.73)	4.7527 (355.15)	174.6796 (348.20)	153.9663 (347.23)	169.1107 (352.25)	109.7532 (360.25)	95.8382 (359.44)
3	−13.4082 (319.34)	44.5615 (327.35)	27.3247 (335.38)	47.7489 (316.52)	23.5101 (316.62)	−30.9847 (332.25)	−21.7651 (329.66)	−63.0959 (333.17)	−26.7196 (327.16)	−14.5627 (332.24)
4	11.2628 (289.76)	17.1192 (283.26)	−58.0492 (290.47)	−17.3033 (284.33)	−8.8060 (283.31)	−21.7730 (286.11)	−14.2659 (286.63)	8.5841 (290.47)	−6.3215 (302.71)	5.6387 (288.50)
5	−55.8632 (276.91)	−35.5421 (276.91)	0.2975 (283.19)	−18.5194 (279.85)	12.9250 (279.44)	−62.3929 (280.83)	−72.9792 (279.60)	−36.3124 (280.69)	−25.6583 (290.40)	−62.8292 (280.79)
6	9.8740 (269.52)	−24.4408 (273.60)	9.2779 (268.52)	−32.1578 (271.76)	−20.7192 (271.54)	21.5209 (270.41)	2.6980 (270.84)	−5.2481 (271.78)	12.3782 (281.78)	−10.3821 (276.59)
7	2.4581 (256.25)	5.5295 (258.80)	96.0355 (261.06)	−38.0566 (252.83)	−11.0297 (254.06)	63.3778 (266.24)	91.7608 (264.44)	94.5165 (263.85)	4.8871 (264.01)	−16.5446 (261.34)
8	75.7171 (254.14)	−17.5510 (250.45)	−82.6101 (260.19)	−69.4505 (248.11)	−46.4601 (249.75)	−78.0305 (255.39)	−90.3042 (254.04)	−10.5762 (253.59)	61.5466 (253.52)	177.2069 (256.80)
9	−83.5339 (242.19)	17.6318 (249.02)	−9.6549 (250.94)	65.5601 (245.11)	64.2911 (243.86)	5.6548 (240.91)	−8.4422 (241.16)	−86.5497 (245.09)	−33.6336 (250.90)	−40.5746 (249.83)
10	3.2800 (233.21)	4.0333 (239.93)	7.7191 (249.11)	43.7267 (242.60)	3.5526 (241.47)	−11.2293 (236.69)	−2.1604 (239.11)	−46.4194 (243.60)	−33.4423 (246.77)	−76.1213 (249.68)
11	4.0376 (228.82)	7.2226 (234.45)	5.9270 (234.81)	6.2677 (230.48)	2.8342 (236.21)	7.0207 (226.92)	12.6472 (227.47)	18.8005 (239.21)	36.2769 (240.30)	0.5413 (238.63)
12	4.0117 (223.74)	0.2717 (214.03)	−19.5474 (219.64)	−40.9461 (215.25)	−22.2240 (214.23)	−23.9699 (215.97)	−22.7360 (214.20)	4.7134 (215.49)	−10.4394 (230.03)	−12.6432 (217.98)
13	−5.7741 (218.61)	−9.2518 (206.67)	6.3179 (212.84)	16.3045 (211.17)	1.8078 (206.51)	7.1595 (211.25)	3.1951 (212.44)	−30.2950 (212.61)	14.1582 (216.78)	−2.4900 (212.29)
14	−1.6084 (210.60)	−26.4914 (203.57)	4.5160 (211.11)	3.0443 (208.51)	7.5004 (205.61)	−1.5615 (205.35)	−1.7917 (206.18)	−1.0554 (208.98)	−1.8146 (212.35)	4.6785 (209.36)
15	−7.1715 (202.24)	−1.0274 (198.52)	−2.9936 (207.49)	−3.2551 (204.77)	5.5649 (202.90)	−1.7708 (200.42)	−6.4474 (200.58)	8.7133 (203.78)	−4.1627 (210.53)	−2.8969 (203.72)
16	3.3891 (197.16)	34.0148 (195.19)	4.4940 (202.40)	4.0226 (198.26)	−7.2750 (197.40)	−6.6690 (197.73)	−0.0512 (195.74)	1.0318 (200.38)	−3.0665 (203.37)	−2.6410 (201.50)
17	6.6302 (194.52)	−0.9879 (194.60)	18.3237 (198.45)	8.5408 (191.40)	4.2184 (194.71)	3.7394 (192.95)	9.1932 (192.35)	−7.7567 (197.67)	−3.3798 (198.29)	−11.0844 (197.73)
18	15.3644 (191.68)	1.2331 (190.24)	3.7132 (193.60)	−8.1255 (190.12)	−6.6863 (191.62)	13.4867 (190.16)	−1.1654 (188.78)	7.9908 (192.63)	−8.6413 (194.53)	7.1577 (193.59)
19	−8.6804 (190.48)	−11.4078 (189.32)	15.2538 (192.69)	−10.9620 (185.48)	−8.8886 (190.47)	−8.3090 (188.04)	−4.5698 (186.69)	−2.0040 (189.63)	−1.6354 (190.88)	−27.6583 (190.66)
20	10.4648 (186.31)	−20.4424 (187.17)	0.7103 (190.44)	2.9181 (183.64)	8.4230 (186.16)	32.8074 (185.87)	35.5928 (183.62)	−7.3613 (189.45)	−7.0308 (188.84)	−0.3389 (188.42)
21	8.2586 (184.52)	−3.5988 (185.93)	10.0769 (185.95)	5.0305 (182.58)	−1.7487 (182.89)	−17.6734 (182.91)	−24.4262 (180.45)	−10.2787 (187.76)	4.8217 (187.31)	14.9271 (186.61)
22	3.3877 (182.59)	40.9026 (181.70)	22.5942 (182.99)	−39.6271 (177.19)	−5.9298 (179.16)	1.3663 (181.47)	−4.0635 (178.21)	18.0355 (183.67)	−10.0505 (184.56)	−9.0449 (183.72)
23	−4.6587 (177.60)	2.5711 (181.39)	−14.9477 (182.28)	7.7565 (176.25)	40.9213 (176.96)	−2.5903 (178.59)	0.2900 (177.77)	9.2743 (180.39)	24.9854 (182.40)	19.3904 (180.21)
24	−36.9043 (176.47)	−9.8907 (177.17)	−21.0312 (180.58)	−2.7287 (174.75)	−0.4349 (175.81)	4.3770 (175.98)	17.8285 (176.70)	47.2778 (179.27)	−4.2278 (180.38)	28.2400 (179.43)
25	−0.8579 (175.01)	4.1373 (175.62)	−8.1799 (179.98)	3.8364 (173.69)	−15.9876 (174.14)	−15.9150 (173.36)	−13.8909 (171.40)	−1.1102 (175.69)	20.1537 (176.92)	8.5015 (175.76)
26	−2.1899 (174.23)	−4.1963 (173.37)	17.1592 (178.36)	−0.0926 (170.87)	4.3160 (171.05)	27.7406 (172.56)	18.4305 (171.26)	−12.5190 (172.16)	−5.6692 (175.59)	−10.1817 (175.26)
27	14.5873 (172.64)	−40.1768 (172.28)	−36.3718 (174.06)	−13.7088 (169.72)	6.8762 (170.00)	6.9475 (171.17)	−9.9003 (170.32)	−4.1404 (170.79)	−27.7775 (171.01)	−14.0562 (170.71)
28	−4.2782 (171.40)	0.7547 (170.52)	23.2295 (171.17)	1.5730 (168.91)	−13.2756 (167.62)	−4.6546 (170.75)	10.6984 (167.13)	0.8875 (169.86)	−0.2018 (167.49)	1.4972 (169.67)
29	−27.9872 (170.07)	9.4007 (169.26)	11.4935 (170.48)	7.2604 (165.92)	−4.4046 (166.15)	−23.6394 (166.68)	−40.9490 (165.45)	−11.9819 (169.59)	−0.6533 (167.39)	8.3136 (167.71)
30	3.7855 (166.93)	11.3078 (169.11)	7.2920 (168.49)	−11.8910 (164.33)	6.7352 (166.01)	28.7141 (166.34)	18.0743 (163.16)	9.5336 (166.90)	1.8864 (165.60)	2.9863 (167.21)

Table 9.S11. (*Continued*)

j	R_j, 10^{-40} erg cm^3 (λ_j, nm)									
	md091#	**md092#**	**md093#**	**md094#**	**md095#**	**md096#**	**md097#**	**md098#**	**md099#**	**md100#**
1	−41.0616 (402.41)	−33.6355 (393.93)	−25.7461 (382.56)	−12.9219 (421.74)	−12.2290 (429.84)	−9.8757 (387.58)	−29.3629 (391.16)	−6.8738 (393.12)	−7.0557 (399.30)	−24.0950 (401.16)
2	47.7862 (357.17)	106.2789 (350.68)	83.6032 (344.01)	60.5064 (360.19)	35.5519 (355.84)	49.9595 (349.07)	42.0866 (346.02)	−12.3397 (344.98)	19.6886 (347.85)	70.1447 (349.43)
3	30.1337 (321.67)	−48.4597 (324.82)	3.0415 (315.45)	−5.2534 (326.71)	18.9235 (332.83)	−20.5046 (315.52)	−7.6820 (316.24)	20.5995 (322.24)	3.1454 (322.49)	−28.6350 (327.33)
4	−24.6117 (287.82)	6.5343 (290.97)	−32.0601 (284.14)	−32.8553 (287.37)	2.1580 (286.91)	1.5417 (287.86)	14.0201 (287.28)	17.6835 (284.92)	3.2444 (287.54)	−12.4227 (284.59)
5	33.0847 (282.79)	−16.8071 (282.44)	4.0227 (275.57)	10.4072 (283.86)	−25.6114 (272.15)	−19.9971 (274.95)	9.6923 (276.67)	−13.3227 (275.89)	−33.7516 (283.78)	1.8818 (278.88)
6	−57.1438 (275.38)	10.4722 (276.81)	−37.4847 (266.89)	−37.7364 (273.17)	−37.5800 (265.58)	11.7804 (272.03)	−24.6448 (273.87)	18.2484 (269.58)	−14.1364 (269.73)	−7.0123 (274.33)
7	−15.3054 (251.16)	9.2789 (262.02)	17.8895 (254.82)	11.8610 (256.57)	23.0804 (251.80)	−5.5151 (252.88)	−10.9478 (252.21)	−64.5856 (258.66)	25.2644 (253.39)	12.6594 (257.30)
8	92.2780 (246.08)	81.4371 (252.71)	105.8079 (250.09)	9.3187 (251.39)	−67.2710 (244.67)	−8.1899 (246.88)	−78.5626 (248.50)	−5.7748 (249.66)	−0.3921 (246.81)	30.8113 (251.55)
9	−88.2773 (243.12)	−95.4692 (248.37)	−91.9670 (247.69)	99.8967 (245.30)	76.2064 (242.65)	5.0593 (243.24)	89.8811 (243.55)	4.6381 (248.01)	−54.0201 (244.79)	−17.2406 (245.55)
10	22.5376 (239.03)	13.8072 (242.86)	3.3649 (237.66)	−81.6942 (241.14)	11.3079 (242.37)	15.1030 (237.41)	−6.4866 (237.27)	53.6281 (242.05)	81.2660 (243.88)	4.1019 (236.54)
11	27.0736 (234.96)	1.9869 (235.87)	−6.0246 (232.20)	−18.5222 (235.73)	15.3738 (234.28)	7.6207 (231.77)	8.5766 (225.73)	−0.3579 (218.58)	7.7824 (233.10)	2.5684 (226.11)
12	−42.1808 (216.85)	3.0728 (225.71)	−29.7143 (220.64)	−17.8966 (215.05)	3.8090 (210.50)	−1.1125 (219.94)	4.2994 (221.47)	0.4990 (214.46)	−36.5369 (220.03)	−21.1241 (217.93)
13	4.4456 (205.90)	2.6040 (213.39)	1.0524 (210.55)	−8.2332 (210.37)	10.5890 (203.83)	−1.6042 (209.21)	7.0810 (208.23)	3.0037 (205.68)	9.4440 (208.41)	2.5359 (208.87)
14	−1.1371 (204.64)	−3.4182 (210.60)	−10.6762 (204.30)	5.8896 (206.91)	−26.9258 (202.01)	−1.7263 (204.84)	−0.1218 (200.77)	−0.1171 (202.89)	2.0731 (207.63)	3.2364 (203.63)
15	14.9614 (203.87)	−19.0837 (205.45)	3.4856 (200.43)	2.2439 (202.72)	0.0326 (196.70)	−6.9109 (200.83)	3.1282 (198.73)	0.0942 (199.94)	6.8627 (205.34)	−1.9620 (201.08)
16	8.7934 (202.27)	−2.1384 (204.99)	−1.2043 (199.46)	−7.8476 (198.68)	−3.9191 (191.45)	−3.2747 (199.24)	−5.1495 (195.82)	4.1432 (197.15)	7.2134 (198.08)	0.0579 (198.44)
17	4.9324 (194.63)	3.4566 (196.98)	−5.6533 (194.61)	15.3280 (194.99)	5.3213 (190.97)	−4.4679 (196.13)	−1.0461 (190.52)	−6.9661 (193.80)	−16.6894 (193.23)	−7.3449 (195.50)
18	−1.2099 (191.03)	−4.3452 (193.47)	6.3843 (189.59)	2.6827 (191.05)	17.3952 (188.90)	3.4100 (193.46)	−2.6167 (187.22)	5.8898 (191.17)	9.2353 (192.32)	−4.7251 (190.35)
19	−10.3748 (188.46)	−6.5770 (190.85)	−7.4481 (188.49)	4.3763 (187.69)	−1.1155 (187.77)	17.1876 (186.40)	11.8061 (185.98)	−3.4594 (186.22)	−15.1502 (188.99)	−1.5406 (189.27)
20	−1.4810 (185.70)	7.6802 (190.35)	10.2868 (184.24)	−9.6846 (186.28)	−21.8368 (184.47)	10.6985 (185.19)	10.6050 (183.05)	−16.4791 (183.03)	3.0380 (184.98)	12.3478 (188.25)
21	−2.7779 (183.15)	18.6512 (183.82)	15.5527 (183.60)	−5.6400 (183.46)	17.8708 (182.47)	7.7095 (184.07)	2.7321 (182.36)	0.2832 (181.83)	4.4818 (183.19)	16.7760 (182.17)
22	−26.0928 (181.16)	9.7044 (182.95)	−7.8890 (178.81)	12.7191 (180.41)	−48.9821 (182.06)	−0.7342 (179.09)	27.6880 (178.92)	5.9311 (180.59)	−9.3559 (179.17)	−14.0910 (180.97)
23	4.3455 (180.16)	−2.9935 (181.11)	4.8412 (177.20)	−22.4489 (179.26)	1.2080 (179.16)	−7.3075 (176.61)	−13.4521 (174.75)	−1.3619 (179.78)	0.6086 (178.28)	1.0835 (178.69)
24	57.4378 (178.14)	0.8358 (178.36)	20.6308 (175.64)	9.4759 (177.89)	−0.6556 (177.35)	36.1591 (175.90)	−2.2184 (171.50)	−28.9058 (176.60)	8.2607 (175.20)	−30.6186 (177.99)
25	0.2108 (174.60)	−28.4552 (177.33)	18.8220 (173.91)	3.8089 (175.12)	−3.4403 (171.73)	−14.9871 (174.61)	−11.9284 (170.92)	10.7783 (174.39)	−7.3251 (174.05)	−20.1937 (171.97)
26	28.1283 (171.65)	36.6772 (174.87)	−54.3387 (172.24)	−14.6093 (173.64)	8.8940 (171.11)	−67.8234 (170.33)	15.6823 (170.77)	7.7820 (171.06)	−20.9043 (170.36)	4.9785 (170.50)
27	−57.8992 (169.60)	−11.7172 (171.64)	−31.0685 (168.98)	−15.9993 (166.98)	−30.2386 (168.44)	−5.2410 (168.05)	14.2053 (166.94)	2.8057 (167.48)	12.7566 (168.43)	26.9238 (169.09)
28	3.3580 (167.33)	−1.2670 (171.06)	−14.6273 (165.39)	8.2004 (166.83)	20.5075 (167.31)	0.9915 (167.65)	−24.2087 (165.25)	−47.3446 (166.69)	−3.7638 (166.65)	−12.5687 (168.30)
29	6.7552 (166.69)	−3.7320 (169.54)	1.4548 (164.97)	6.1242 (165.89)	−4.3295 (166.72)	14.3434 (166.34)	12.9344 (163.15)	−24.8466 (165.28)	−0.0296 (164.52)	−3.6664 (166.62)
30	12.6422 (165.17)	18.5294 (165.13)	14.3845 (163.95)	7.1856 (164.90)	−5.5872 (163.98)	−1.8807 (165.21)	−0.6155 (162.61)	−4.4023 (164.00)	6.0076 (163.45)	0.0599 (165.16)

Table 9.S12. Oscillator strengths and excitation wavelengths for the *ab initio* MD solvation clusters of **1** with methanol, as obtained by TD-DFT calculations on **1** alone.

j	f_j (Λ_j, nm)										
	md001#	**md002#**	**md003#**	**md004#**	**md005#**	**md006#**	**md007#**	**md008#**	**md009#**	**md010#**
1	0.0021 (391.63)	0.0051 (379.12)	0.0003 (381.89)	0.0024 (429.41)	0.0120 (416.79)	0.0001 (409.75)	0.0007 (397.06)	0.0018 (391.06)	0.0017 (379.74)	0.0017 (425.05)
2	0.4389 (340.50)	0.3911 (335.42)	0.4234 (336.48)	0.0405 (362.08)	0.3265 (344.60)	0.4053 (339.47)	0.4201 (353.41)	0.3527 (351.60)	0.3948 (338.67)	0.3166 (360.36)
3	0.0069 (323.30)	0.0112 (325.87)	0.0281 (326.73)	0.3894 (345.64)	0.0452 (335.14)	0.0325 (330.77)	0.0039 (329.99)	0.0429 (327.48)	0.0135 (326.67)	0.0510 (332.97)
4	0.0080 (280.43)	0.0484 (278.54)	0.0393 (278.96)	0.0020 (306.72)	0.0072 (286.20)	0.0078 (281.86)	0.0108 (287.87)	0.0245 (292.41)	0.0060 (280.59)	0.0182 (290.47)
5	0.0071 (275.92)	0.0110 (273.74)	0.0161 (275.52)	0.0044 (283.40)	0.0251 (274.75)	0.0498 (271.67)	0.0221 (282.34)	0.0056 (284.75)	0.0437 (275.49)	0.0535 (278.40)
6	0.0563 (269.40)	0.0250 (260.06)	0.0102 (257.10)	0.0850 (276.44)	0.0558 (261.70)	0.0776 (259.71)	0.0297 (271.30)	0.0209 (261.68)	0.0584 (265.52)	0.0463 (276.20)
7	0.2065 (252.43)	0.1165 (251.81)	0.0893 (250.89)	0.0295 (265.53)	0.0276 (255.82)	0.0589 (247.91)	0.0014 (259.39)	0.0406 (256.48)	0.1164 (253.11)	0.0226 (256.01)
8	0.0112 (246.00)	0.0205 (247.26)	0.0661 (247.39)	0.0479 (258.17)	0.0058 (250.35)	0.0135 (243.50)	0.3008 (257.54)	0.1955 (250.66)	0.0970 (246.47)	0.0915 (250.60)
9	0.0163 (242.49)	0.0112 (242.16)	0.0188 (235.71)	0.1697 (251.63)	0.0036 (244.15)	0.1036 (240.78)	0.0025 (249.51)	0.0245 (247.09)	0.0124 (236.88)	0.0814 (247.80)
10	0.0101 (241.25)	0.1431 (238.70)	0.1732 (234.43)	0.0658 (247.52)	0.2697 (241.09)	0.0069 (230.96)	0.0727 (246.59)	0.1090 (237.67)	0.0272 (235.08)	0.1431 (243.74)
11	0.0631 (240.22)	0.0146 (233.91)	0.0071 (232.28)	0.0085 (242.08)	0.0599 (235.68)	0.0048 (226.78)	0.0081 (240.88)	0.0013 (228.61)	0.0418 (231.25)	0.0163 (240.43)
12	0.2032 (209.76)	0.1100 (209.45)	0.0873 (207.84)	0.0647 (224.02)	0.0028 (209.20)	0.0120 (207.84)	0.0964 (215.25)	0.0280 (213.65)	0.1063 (210.59)	0.0846 (218.24)
13	0.0133 (206.80)	0.0412 (204.39)	0.0027 (200.90)	0.0242 (215.53)	0.0440 (208.39)	0.0664 (205.07)	0.0488 (211.68)	0.1357 (207.25)	0.0079 (205.51)	0.0572 (209.35)
14	0.0123 (204.92)	0.0012 (203.02)	0.0162 (200.46)	0.0315 (208.04)	0.0076 (205.19)	0.0328 (202.67)	0.0394 (205.01)	0.0012 (201.03)	0.0073 (202.78)	0.0158 (204.81)
15	0.0160 (202.11)	0.0045 (200.89)	0.0050 (196.85)	0.0072 (203.49)	0.0013 (202.14)	0.0183 (199.62)	0.0013 (203.06)	0.0216 (196.04)	0.0327 (197.87)	0.0007 (203.01)
16	0.0805 (198.90)	0.0185 (198.08)	0.0201 (193.24)	0.0411 (201.47)	0.0116 (199.21)	0.1151 (192.74)	0.0118 (200.96)	0.0175 (194.99)	0.0924 (195.79)	0.0422 (200.28)
17	0.0128 (195.23)	0.0009 (195.44)	0.0112 (191.66)	0.0591 (199.44)	0.0684 (198.27)	0.0065 (189.93)	0.0768 (198.63)	0.0021 (192.78)	0.0707 (191.91)	0.0037 (195.51)
18	0.0225 (193.63)	0.0385 (193.33)	0.0752 (189.55)	0.0112 (198.33)	0.0179 (194.82)	0.0051 (187.72)	0.0811 (195.82)	0.0706 (189.38)	0.0098 (190.27)	0.0400 (191.28)
19	0.0218 (188.88)	0.0012 (190.58)	0.0093 (184.73)	0.0670 (197.04)	0.0093 (192.91)	0.0002 (187.14)	0.0271 (191.61)	0.0036 (183.21)	0.0073 (187.14)	0.0423 (190.99)
20	0.0007 (184.74)	0.0227 (188.82)	0.0034 (182.36)	0.0088 (192.36)	0.0401 (187.77)	0.0179 (184.10)	0.0245 (188.55)	0.0119 (181.89)	0.0224 (183.53)	0.0326 (188.07)
21	0.0095 (183.31)	0.0126 (184.90)	0.0076 (180.54)	0.0107 (190.67)	0.0123 (186.08)	0.0084 (182.87)	0.0140 (187.37)	0.0028 (181.33)	0.0043 (180.61)	0.0239 (185.62)
22	0.0085 (180.42)	0.0059 (184.27)	0.0014 (176.61)	0.0367 (189.79)	0.1356 (182.54)	0.0099 (181.29)	0.0020 (184.25)	0.0053 (176.00)	0.0054 (179.01)	0.0151 (183.41)
23	0.0006 (178.78)	0.0028 (182.89)	0.0060 (175.61)	0.0336 (187.96)	0.0144 (179.11)	0.1235 (174.04)	0.0086 (182.92)	0.1653 (174.54)	0.0041 (177.73)	0.0581 (181.08)
24	0.0092 (174.79)	0.0030 (177.07)	0.0371 (174.84)	0.0047 (179.83)	0.0429 (177.09)	0.0062 (173.51)	0.1082 (178.81)	0.0144 (171.42)	0.0736 (173.09)	0.0380 (179.47)
25	0.1416 (174.31)	0.1621 (175.35)	0.0629 (174.02)	0.0104 (177.93)	0.0124 (175.02)	0.0189 (173.08)	0.0118 (176.71)	0.0204 (171.13)	0.0020 (172.44)	0.0689 (176.46)
26	0.0670 (172.57)	0.0180 (172.12)	0.0519 (171.73)	0.1158 (176.04)	0.0430 (170.88)	0.0212 (172.04)	0.0439 (173.45)	0.0934 (169.19)	0.1322 (170.42)	0.0019 (171.52)
27	0.0052 (170.22)	0.0564 (171.03)	0.0176 (169.40)	0.0493 (174.74)	0.0228 (169.24)	0.2210 (169.56)	0.1078 (169.14)	0.0108 (168.93)	0.0414 (169.21)	0.0015 (171.00)
28	0.0428 (167.82)	0.1033 (167.53)	0.0348 (167.97)	0.0866 (172.98)	0.0594 (168.27)	0.0127 (167.96)	0.1077 (167.74)	0.0508 (167.36)	0.0200 (167.69)	0.0843 (170.48)
29	0.0157 (166.87)	0.0375 (167.12)	0.0031 (166.27)	0.0027 (171.62)	0.0388 (167.27)	0.0092 (166.73)	0.0224 (167.35)	0.0040 (165.74)	0.0113 (166.87)	0.0159 (167.23)
30	0.0575 (164.52)	0.0132 (165.17)	0.1095 (165.13)	0.0207 (170.57)	0.0168 (166.31)	0.0055 (166.20)	0.0115 (166.24)	0.0651 (163.82)	0.0290 (163.87)	0.0288 (166.21)

Table 9.S12. (*Continued*)

j	$f_j(\lambda_j$, nm)									
	md011#	**md012#**	**md013#**	**md014#**	**md015#**	**md016#**	**md017#**	**md018#**	**md019#**	**md020#**
1	0.0002 (400.83)	0.0004 (392.68)	0.0036 (411.77)	0.0004 (403.01)	0.0023 (387.54)	0.0026 (411.33)	0.0089 (405.74)	0.0003 (390.08)	0.0014 (407.68)	0.0044 (383.95)
2	0.3264 (348.06)	0.4180 (343.71)	0.3698 (354.50)	0.4086 (335.51)	0.4018 (338.93)	0.3773 (354.60)	0.3468 (347.31)	0.3884 (342.19)	0.3357 (338.32)	0.4009 (347.35)
3	0.0596 (337.10)	0.0010 (331.55)	0.0154 (331.93)	0.0105 (325.03)	0.0010 (319.23)	0.0020 (341.71)	0.0324 (331.69)	0.0272 (331.03)	0.0924 (330.78)	0.0028 (327.41)
4	0.0024 (291.46)	0.0005 (284.70)	0.0034 (286.33)	0.0032 (278.63)	0.0078 (272.63)	0.0200 (292.82)	0.0106 (284.13)	0.0293 (282.55)	0.0068 (283.19)	0.0657 (286.54)
5	0.0268 (278.35)	0.0251 (272.57)	0.0198 (277.27)	0.0311 (269.23)	0.0304 (267.92)	0.0207 (280.34)	0.0423 (270.43)	0.0113 (276.89)	0.0226 (268.21)	0.0100 (275.10)
6	0.0573 (270.59)	0.0134 (261.18)	0.0301 (261.46)	0.0768 (264.52)	0.0490 (258.62)	0.0985 (273.49)	0.0498 (265.30)	0.0179 (267.56)	0.0598 (259.37)	0.0034 (266.67)
7	0.0230 (261.00)	0.0785 (253.59)	0.1100 (254.71)	0.0633 (248.77)	0.0662 (247.48)	0.0143 (261.03)	0.0597 (255.04)	0.2053 (258.60)	0.0193 (252.68)	0.1870 (259.60)
8	0.0072 (252.21)	0.0463 (244.31)	0.0353 (249.32)	0.0334 (247.62)	0.1322 (240.43)	0.1538 (252.47)	0.0241 (243.68)	0.0148 (250.29)	0.0075 (248.52)	0.0247 (246.61)
9	0.1713 (250.59)	0.0204 (243.44)	0.1092 (247.63)	0.0910 (243.86)	0.0523 (238.89)	0.0210 (250.89)	0.1574 (240.42)	0.0188 (247.42)	0.1652 (243.40)	0.0532 (240.72)
10	0.1513 (242.87)	0.2292 (238.07)	0.1133 (242.06)	0.0266 (237.84)	0.0298 (235.17)	0.0113 (243.76)	0.0026 (237.38)	0.1106 (230.96)	0.0889 (235.40)	0.0392 (239.24)
11	0.0059 (233.85)	0.0039 (229.34)	0.0091 (228.93)	0.0596 (234.48)	0.0399 (228.65)	0.0958 (242.20)	0.0219 (231.34)	0.0060 (224.51)	0.0173 (233.72)	0.0026 (227.76)
12	0.0383 (223.28)	0.0374 (214.38)	0.0143 (213.08)	0.0917 (207.64)	0.0737 (205.87)	0.1131 (214.92)	0.1683 (208.12)	0.1381 (211.62)	0.0164 (208.73)	0.1056 (210.75)
13	0.1680 (211.25)	0.1163 (202.15)	0.0689 (203.62)	0.0806 (203.88)	0.0603 (201.50)	0.0244 (208.72)	0.0350 (203.50)	0.0125 (206.86)	0.0207 (206.54)	0.0067 (204.22)
14	0.0304 (203.09)	0.0073 (197.80)	0.0228 (202.38)	0.0090 (199.19)	0.0075 (197.45)	0.0127 (207.22)	0.0095 (200.98)	0.1243 (200.92)	0.0450 (203.26)	0.0128 (202.09)
15	0.0085 (201.27)	0.0025 (194.00)	0.0309 (196.95)	0.0097 (198.74)	0.0203 (194.47)	0.0073 (205.17)	0.0010 (196.22)	0.0033 (198.60)	0.0359 (199.00)	0.0636 (198.42)
16	0.0063 (198.83)	0.0173 (191.51)	0.0051 (192.94)	0.0267 (194.81)	0.0105 (191.71)	0.0237 (199.70)	0.0185 (193.21)	0.0043 (192.48)	0.0035 (196.53)	0.0074 (197.94)
17	0.0076 (196.88)	0.0447 (189.12)	0.1141 (190.53)	0.0513 (192.43)	0.0304 (189.54)	0.1123 (197.35)	0.0039 (191.23)	0.0341 (189.23)	0.0034 (193.56)	0.0099 (194.88)
18	0.0142 (193.81)	0.0299 (186.83)	0.0440 (187.86)	0.0080 (191.77)	0.0120 (187.89)	0.0244 (195.78)	0.0045 (189.93)	0.0006 (188.39)	0.0393 (190.60)	0.0036 (192.28)
19	0.0852 (190.59)	0.0044 (184.12)	0.0086 (182.70)	0.0098 (187.68)	0.0118 (186.38)	0.0281 (193.28)	0.0256 (189.23)	0.0131 (183.88)	0.0253 (183.96)	0.0129 (188.22)
20	0.0006 (186.66)	0.0063 (182.61)	0.0030 (181.62)	0.0048 (187.51)	0.0010 (184.30)	0.0380 (187.31)	0.0131 (186.33)	0.0060 (182.14)	0.0035 (182.76)	0.0058 (185.83)
21	0.0250 (185.40)	0.0103 (181.09)	0.0111 (181.11)	0.0015 (182.63)	0.0038 (180.65)	0.0063 (186.09)	0.0138 (183.63)	0.0143 (181.87)	0.0773 (181.19)	0.0090 (180.83)
22	0.0035 (182.73)	0.0011 (180.03)	0.0080 (180.84)	0.0048 (182.04)	0.0080 (179.70)	0.0025 (184.90)	0.0016 (179.58)	0.0129 (176.19)	0.0103 (178.97)	0.2139 (177.83)
23	0.0183 (181.07)	0.0093 (175.67)	0.0543 (179.04)	0.0107 (178.96)	0.0272 (175.71)	0.0087 (184.55)	0.0252 (177.72)	0.0329 (175.43)	0.0077 (177.86)	0.0313 (174.26)
24	0.0272 (179.50)	0.1189 (173.43)	0.0620 (175.80)	0.1555 (175.54)	0.0108 (174.25)	0.0331 (182.01)	0.0440 (176.79)	0.0285 (173.23)	0.0236 (177.44)	0.0477 (173.87)
25	0.1912 (174.15)	0.0705 (172.61)	0.0021 (174.55)	0.0069 (173.76)	0.0412 (173.36)	0.2102 (174.41)	0.0557 (175.14)	0.0021 (172.53)	0.0411 (175.99)	0.0080 (172.60)
26	0.0010 (169.34)	0.0032 (170.91)	0.0007 (173.97)	0.0285 (172.08)	0.0017 (171.65)	0.0263 (171.80)	0.0089 (172.44)	0.0074 (169.61)	0.0110 (174.28)	0.1209 (170.45)
27	0.0056 (169.00)	0.1451 (168.63)	0.0309 (170.89)	0.0406 (169.91)	0.1027 (169.36)	0.1375 (169.68)	0.0380 (170.99)	0.2009 (168.67)	0.0272 (172.61)	0.0092 (169.05)
28	0.0162 (167.30)	0.0068 (165.17)	0.0257 (169.64)	0.0522 (169.01)	0.1134 (167.60)	0.0103 (169.41)	0.1038 (168.68)	0.0255 (166.89)	0.0123 (169.00)	0.0046 (168.61)
29	0.0082 (166.99)	0.0144 (164.49)	0.1859 (167.10)	0.0783 (166.78)	0.0960 (167.47)	0.0263 (168.51)	0.1235 (167.56)	0.0180 (165.70)	0.0928 (167.33)	0.0095 (166.74)
30	0.0329 (165.73)	0.0081 (163.64)	0.0329 (165.24)	0.0106 (163.61)	0.0067 (163.88)	0.0129 (166.20)	0.0265 (166.09)	0.0082 (163.94)	0.0003 (165.15)	0.0744 (166.03)

Table 9.S12. *(Continued)*

j	f_j (λ_j, nm)									
	md021#	**md022#**	**md023#**	**md024#**	**md025#**	**md026#**	**md027#**	**md028#**	**md029#**	**md030#**
1	0.0006 (398.87)	0.0004 (376.59)	0.0020 (399.61)	0.0001 (393.97)	0.0002 (395.13)	0.0006 (412.21)	0.0021 (396.95)	0.0001 (389.69)	0.0033 (444.85)	0.0009 (403.17)
2	0.4391 (343.09)	0.4396 (343.73)	0.4405 (339.28)	0.4450 (343.02)	0.3979 (340.28)	0.0497 (335.89)	0.3894 (344.29)	0.4015 (340.73)	0.2472 (352.44)	0.4458 (342.14)
3	0.0123 (333.88)	0.0093 (325.92)	0.0100 (330.74)	0.0053 (326.88)	0.0035 (334.69)	0.4213 (330.75)	0.0223 (337.44)	0.0182 (314.32)	0.1800 (348.18)	0.0040 (333.08)
4	0.0068 (283.11)	0.0595 (280.28)	0.0082 (282.50)	0.0059 (281.71)	0.0032 (289.02)	0.0061 (281.53)	0.0011 (286.91)	0.0064 (273.17)	0.0075 (296.30)	0.0018 (284.47)
5	0.0174 (273.94)	0.0073 (276.18)	0.0089 (274.25)	0.0150 (274.30)	0.0224 (269.99)	0.0163 (275.89)	0.0559 (268.37)	0.0451 (270.72)	0.0307 (276.87)	0.0626 (273.13)
6	0.1229 (269.35)	0.0940 (269.92)	0.0221 (264.66)	0.0412 (268.08)	0.0809 (265.93)	0.0150 (259.53)	0.0847 (261.74)	0.0664 (268.36)	0.0095 (272.02)	0.0416 (266.05)
7	0.0023 (255.70)	0.0388 (254.26)	0.0780 (250.95)	0.1463 (252.90)	0.0059 (258.39)	0.0111 (256.87)	0.0129 (260.26)	0.0333 (257.43)	0.0475 (258.35)	0.0572 (255.64)
8	0.0861 (253.08)	0.0345 (249.64)	0.0007 (248.88)	0.0104 (249.00)	0.0940 (248.31)	0.2157 (249.15)	0.0481 (246.22)	0.0746 (249.23)	0.0038 (257.01)	0.0262 (252.99)
9	0.0674 (250.47)	0.1263 (235.65)	0.0877 (245.55)	0.1011 (244.96)	0.2284 (243.81)	0.0191 (245.74)	0.2074 (240.94)	0.1217 (242.99)	0.0411 (251.66)	0.1835 (241.57)
10	0.0667 (247.00)	0.0041 (229.98)	0.1378 (242.74)	0.0861 (244.75)	0.0054 (240.61)	0.0974 (237.22)	0.0004 (234.06)	0.0067 (235.69)	0.2089 (244.49)	0.0049 (239.15)
11	0.0012 (237.51)	0.0009 (226.16)	0.0097 (237.14)	0.0006 (232.25)	0.0014 (230.01)	0.0044 (220.05)	0.0056 (231.02)	0.0006 (234.82)	0.0056 (238.43)	0.0035 (230.34)
12	0.0958 (209.73)	0.0445 (213.65)	0.0351 (212.69)	0.0200 (212.96)	0.0341 (214.08)	0.1069 (210.54)	0.0083 (210.57)	0.0352 (211.45)	0.0772 (217.86)	0.0037 (213.76)
13	0.0125 (207.38)	0.0234 (201.62)	0.0416 (205.33)	0.0637 (211.11)	0.0759 (208.76)	0.0347 (204.68)	0.0224 (205.00)	0.0682 (202.55)	0.0095 (213.44)	0.0456 (208.55)
14	0.0210 (205.40)	0.1542 (197.76)	0.1162 (204.51)	0.1017 (206.21)	0.0076 (205.53)	0.0965 (197.57)	0.0224 (204.69)	0.0614 (199.58)	0.0711 (206.26)	0.0094 (202.58)
15	0.0045 (203.02)	0.0154 (195.77)	0.0252 (198.15)	0.0565 (198.58)	0.0702 (198.85)	0.0229 (193.90)	0.0036 (198.49)	0.0021 (198.84)	0.0167 (201.19)	0.0478 (196.96)
16	0.0152 (200.73)	0.0021 (193.82)	0.0169 (195.66)	0.0293 (194.25)	0.0161 (195.11)	0.0379 (191.31)	0.0031 (193.03)	0.0066 (197.26)	0.0156 (197.25)	0.0049 (195.66)
17	0.0114 (197.55)	0.0034 (193.22)	0.0604 (192.78)	0.0024 (191.29)	0.0410 (193.87)	0.0032 (187.52)	0.0403 (189.26)	0.0215 (196.04)	0.1164 (193.93)	0.0202 (193.16)
18	0.0497 (195.12)	0.0076 (190.24)	0.0108 (191.21)	0.0812 (187.95)	0.0142 (189.97)	0.0156 (185.61)	0.0024 (188.79)	0.0267 (192.76)	0.0121 (192.08)	0.0834 (189.27)
19	0.0751 (190.49)	0.0051 (188.30)	0.0050 (187.09)	0.0093 (184.27)	0.0777 (189.89)	0.0050 (185.29)	0.1652 (186.59)	0.0153 (190.32)	0.0149 (190.24)	0.0204 (186.83)
20	0.0299 (187.15)	0.0443 (184.97)	0.0306 (185.89)	0.0099 (181.76)	0.0547 (184.55)	0.0383 (184.00)	0.0066 (182.25)	0.0014 (187.34)	0.0393 (189.25)	0.0048 (184.51)
21	0.0159 (186.11)	0.0032 (183.14)	0.0061 (184.13)	0.0023 (181.40)	0.0255 (180.87)	0.0032 (181.19)	0.0138 (181.13)	0.0072 (185.09)	0.0099 (186.14)	0.0864 (183.02)
22	0.0073 (183.30)	0.0079 (179.34)	0.0286 (181.67)	0.0483 (178.75)	0.0382 (176.94)	0.0020 (178.76)	0.0140 (180.21)	0.0023 (181.14)	0.0349 (182.91)	0.0096 (180.84)
23	0.0010 (182.64)	0.0487 (174.05)	0.0018 (179.86)	0.0065 (177.47)	0.0007 (175.81)	0.0267 (174.46)	0.0012 (179.53)	0.1861 (178.80)	0.0212 (180.91)	0.0101 (175.44)
24	0.0245 (181.79)	0.0228 (173.77)	0.1948 (174.10)	0.0096 (176.75)	0.0054 (173.71)	0.0259 (173.47)	0.0011 (175.19)	0.0054 (177.94)	0.0035 (178.45)	0.0346 (173.33)
25	0.0568 (175.10)	0.0023 (170.99)	0.0200 (173.04)	0.1145 (173.28)	0.1145 (169.88)	0.0299 (172.50)	0.0577 (174.19)	0.0043 (173.61)	0.0002 (176.75)	0.0036 (172.67)
26	0.0028 (174.39)	0.1352 (169.83)	0.0042 (170.99)	0.0006 (171.83)	0.0901 (168.43)	0.0005 (170.12)	0.1360 (171.17)	0.0493 (172.82)	0.1742 (174.46)	0.0779 (171.85)
27	0.2274 (172.43)	0.1342 (168.78)	0.0820 (169.22)	0.0598 (170.85)	0.0075 (166.82)	0.0425 (169.26)	0.0331 (170.53)	0.1816 (170.69)	0.0087 (169.62)	0.0189 (171.34)
28	0.0087 (170.40)	0.0245 (167.41)	0.0236 (166.88)	0.0201 (168.18)	0.0081 (165.04)	0.1188 (167.43)	0.0337 (167.55)	0.0262 (167.88)	0.0025 (169.49)	0.0297 (170.26)
29	0.0031 (169.02)	0.0143 (166.62)	0.0072 (165.89)	0.0028 (165.78)	0.0170 (164.75)	0.0580 (164.69)	0.0855 (165.79)	0.0526 (167.34)	0.0011 (168.54)	0.1602 (165.69)
30	0.0037 (168.12)	0.0183 (163.96)	0.0878 (164.22)	0.0463 (165.07)	0.0097 (163.83)	0.0196 (163.74)	0.0289 (164.32)	0.0478 (165.47)	0.0115 (167.59)	0.0631 (165.30)

Table 9.S12. (*Continued*)

j	$f_j(\lambda_j$, nm)									
	md031#	md032#	md033#	md034#	md035#	md036#	md037#	md038#	md039#	md040#
1	0.0014 (401.31)	0.0009 (408.64)	0.0002 (401.24)	0.0032 (403.93)	0.0016 (419.79)	0.0090 (407.15)	0.0298 (365.53)	0.0035 (386.61)	0.0160 (397.70)	0.0015 (387.59)
2	0.4359 (345.10)	0.4141 (347.22)	0.4179 (329.37)	0.3511 (352.32)	0.3988 (344.37)	0.3568 (348.08)	0.3276 (351.97)	0.4243 (344.23)	0.3755 (357.47)	0.4175 (356.67)
3	0.0012 (323.54)	0.0022 (335.69)	0.0718 (320.53)	0.0093 (332.28)	0.0018 (332.39)	0.0082 (330.51)	0.0027 (314.18)	0.0022 (322.98)	0.0045 (332.87)	0.0034 (312.76)
4	0.0144 (279.60)	0.0010 (290.12)	0.0050 (276.77)	0.0065 (286.79)	0.0013 (289.64)	0.0092 (288.52)	0.0820 (286.43)	0.0135 (297.24)	0.0062 (290.19)	0.0149 (291.21)
5	0.0350 (273.73)	0.0446 (273.65)	0.0532 (266.12)	0.0468 (278.41)	0.0443 (271.54)	0.0198 (278.56)	0.0296 (267.71)	0.0013 (281.93)	0.0059 (286.19)	0.0300 (286.79)
6	0.0431 (265.81)	0.0233 (262.47)	0.0180 (261.96)	0.1252 (272.18)	0.0085 (260.40)	0.0415 (267.86)	0.0026 (266.03)	0.0639 (268.54)	0.0455 (274.01)	0.0096 (271.15)
7	0.1296 (255.56)	0.0548 (255.18)	0.1289 (247.30)	0.1199 (255.38)	0.0308 (257.45)	0.0571 (255.17)	0.1190 (259.43)	0.1328 (256.79)	0.0840 (258.43)	0.0739 (258.93)
8	0.0391 (243.36)	0.1665 (249.52)	0.0309 (245.18)	0.0506 (253.97)	0.1224 (247.11)	0.0052 (253.51)	0.1601 (244.23)	0.1049 (249.59)	0.0908 (255.28)	0.2337 (253.06)
9	0.0154 (240.70)	0.0127 (243.73)	0.0933 (241.57)	0.1065 (250.48)	0.0058 (246.35)	0.0046 (247.45)	0.0053 (240.11)	0.0108 (247.13)	0.0155 (248.86)	0.0330 (248.51)
10	0.0416 (238.16)	0.0543 (243.43)	0.0236 (237.99)	0.0248 (247.33)	0.1432 (243.88)	0.2479 (244.54)	0.0012 (228.36)	0.0213 (236.09)	0.1278 (245.49)	0.0073 (242.93)
11	0.0808 (233.76)	0.0644 (240.63)	0.0012 (226.49)	0.0270 (241.43)	0.0574 (240.56)	0.0524 (239.21)	0.0154 (225.91)	0.0034 (234.64)	0.0039 (226.67)	0.0183 (237.06)
12	0.1508 (207.01)	0.0135 (208.91)	0.0482 (203.94)	0.1337 (214.55)	0.0031 (211.78)	0.0696 (216.72)	0.0630 (213.12)	0.0977 (216.28)	0.0473 (221.33)	0.1005 (224.99)
13	0.0087 (203.62)	0.0256 (206.09)	0.0763 (201.54)	0.0699 (210.63)	0.0113 (208.89)	0.0120 (215.26)	0.0127 (202.27)	0.1754 (213.32)	0.0335 (213.11)	0.0095 (214.15)
14	0.0069 (197.50)	0.0639 (203.92)	0.0077 (198.81)	0.0044 (206.18)	0.0229 (204.45)	0.1200 (208.81)	0.0248 (200.35)	0.0048 (200.97)	0.1976 (210.88)	0.0648 (205.67)
15	0.0613 (196.59)	0.0144 (200.72)	0.1443 (196.43)	0.0323 (202.27)	0.0028 (200.88)	0.0136 (198.29)	0.0064 (198.53)	0.0081 (200.49)	0.0478 (202.18)	0.0000 (204.19)
16	0.0072 (194.07)	0.0106 (197.96)	0.0158 (190.24)	0.0027 (200.71)	0.0529 (199.67)	0.0088 (198.04)	0.0722 (196.56)	0.0067 (199.46)	0.0499 (196.60)	0.0109 (199.38)
17	0.0196 (192.16)	0.0034 (193.39)	0.0500 (186.94)	0.0087 (197.63)	0.0063 (193.24)	0.0165 (195.31)	0.0144 (194.10)	0.0418 (199.01)	0.0657 (194.72)	0.0355 (198.04)
18	0.0063 (190.68)	0.0017 (191.15)	0.0031 (185.27)	0.0467 (192.40)	0.0151 (192.94)	0.1409 (190.12)	0.0044 (191.92)	0.0076 (195.28)	0.0102 (187.68)	0.0267 (196.73)
19	0.0285 (189.19)	0.1352 (189.82)	0.0029 (183.50)	0.0029 (190.56)	0.0476 (189.12)	0.0068 (188.09)	0.0094 (189.48)	0.0245 (186.21)	0.0435 (186.30)	0.0254 (192.96)
20	0.0221 (187.13)	0.0163 (184.38)	0.0053 (182.38)	0.0146 (188.46)	0.0737 (188.54)	0.0160 (186.10)	0.0047 (186.75)	0.0421 (183.86)	0.0117 (184.63)	0.0002 (190.82)
21	0.0113 (181.36)	0.0035 (183.00)	0.0130 (180.82)	0.0185 (185.87)	0.0414 (183.13)	0.0120 (183.16)	0.0459 (184.08)	0.0004 (182.89)	0.0011 (183.73)	0.0198 (187.03)
22	0.0167 (180.90)	0.0371 (181.76)	0.0027 (178.93)	0.0171 (184.41)	0.0080 (182.10)	0.0034 (182.33)	0.0270 (181.09)	0.0858 (180.61)	0.0048 (179.72)	0.0016 (184.71)
23	0.0264 (178.68)	0.0011 (181.19)	0.0006 (173.85)	0.0064 (183.89)	0.0071 (181.94)	0.0299 (180.51)	0.1682 (174.60)	0.0370 (178.93)	0.1968 (178.77)	0.0115 (184.05)
24	0.1001 (175.38)	0.0060 (179.92)	0.0109 (172.63)	0.0466 (182.10)	0.0109 (180.07)	0.0212 (180.26)	0.0383 (173.56)	0.0048 (174.30)	0.0041 (177.62)	0.0741 (182.06)
25	0.0205 (173.26)	0.0417 (177.62)	0.0115 (172.14)	0.0746 (177.26)	0.1046 (174.54)	0.0344 (176.90)	0.1895 (171.28)	0.0013 (173.86)	0.0033 (175.81)	0.0212 (177.78)
26	0.1243 (169.68)	0.2309 (172.46)	0.0919 (169.84)	0.0002 (173.71)	0.2143 (173.44)	0.0276 (174.64)	0.0030 (169.74)	0.0004 (172.16)	0.0029 (172.12)	0.0063 (175.72)
27	0.0794 (168.03)	0.0015 (170.19)	0.0963 (168.67)	0.0177 (171.56)	0.0292 (172.20)	0.0303 (173.08)	0.0226 (168.27)	0.0219 (170.05)	0.0218 (170.90)	0.0005 (174.75)
28	0.0062 (166.89)	0.0772 (168.24)	0.0015 (167.97)	0.0071 (169.11)	0.0987 (170.98)	0.0002 (170.77)	0.0143 (165.81)	0.0207 (169.37)	0.0035 (168.79)	0.0693 (171.48)
29	0.0046 (164.20)	0.0192 (167.44)	0.0049 (163.38)	0.0313 (165.51)	0.0178 (168.30)	0.1019 (168.49)	0.0042 (164.03)	0.1685 (167.88)	0.0048 (168.52)	0.3135 (170.25)
30	0.0105 (163.82)	0.0009 (166.10)	0.0015 (163.07)	0.0273 (165.17)	0.0167 (167.55)	0.0062 (166.44)	0.0160 (163.21)	0.0098 (167.42)	0.0095 (167.24)	0.0049 (167.89)

Table 9.S12. (*Continued*)

j	f_j (λ_j, nm)									
	md041#	**md042#**	**md043#**	**md044#**	**md045#**	**md046#**	**md047#**	**md048#**	**md049#**	**md050#**
1	0.0051 (378.15)	0.0276 (382.10)	0.0056 (407.48)	0.0085 (398.65)	0.0004 (405.03)	0.0102 (398.14)	0.0013 (384.96)	0.0196 (380.53)	0.0067 (392.95)	0.0042 (398.42)
2	0.3849 (339.00)	0.3584 (348.85)	0.4111 (348.21)	0.3450 (361.52)	0.2990 (361.81)	0.3851 (343.15)	0.3636 (338.83)	0.2733 (356.12)	0.3774 (348.35)	0.2951 (366.11)
3	0.0007 (309.89)	0.0020 (324.59)	0.0155 (331.44)	0.0013 (314.73)	0.0011 (322.75)	0.0077 (305.22)	0.0085 (307.05)	0.0543 (314.00)	0.0121 (315.20)	0.0016 (321.26)
4	0.0376 (280.29)	0.0326 (286.79)	0.0027 (279.49)	0.0572 (286.30)	0.1328 (296.81)	0.0499 (278.80)	0.0757 (279.05)	0.0193 (288.51)	0.0587 (281.35)	0.1335 (293.23)
5	0.0752 (273.77)	0.0575 (282.78)	0.0245 (276.47)	0.0187 (280.11)	0.0028 (281.30)	0.0338 (273.31)	0.0199 (274.76)	0.0681 (280.54)	0.0316 (277.16)	0.1016 (287.80)
6	0.0062 (270.33)	0.0107 (278.30)	0.0283 (269.19)	0.0007 (276.19)	0.0806 (265.20)	0.0736 (266.02)	0.0430 (268.72)	0.0094 (269.89)	0.1115 (271.86)	0.0083 (273.91)
7	0.0374 (253.38)	0.0233 (259.59)	0.2340 (257.54)	0.0136 (255.94)	0.0635 (259.62)	0.0553 (252.28)	0.0478 (250.79)	0.0178 (251.85)	0.0150 (257.11)	0.0379 (260.28)
8	0.0037 (249.31)	0.1918 (252.66)	0.0133 (248.07)	0.3365 (250.17)	0.1807 (249.47)	0.0083 (248.17)	0.2247 (244.97)	0.1585 (249.69)	0.1772 (252.35)	0.0911 (251.07)
9	0.2239 (245.61)	0.0857 (247.39)	0.0152 (246.33)	0.0177 (247.52)	0.0495 (240.75)	0.0678 (241.60)	0.0039 (244.21)	0.1273 (244.66)	0.0366 (249.28)	0.1259 (249.44)
10	0.0041 (229.89)	0.0197 (237.87)	0.0938 (240.26)	0.0066 (237.26)	0.0038 (235.47)	0.1078 (236.61)	0.0048 (236.48)	0.0492 (237.64)	0.0013 (228.75)	0.0699 (233.12)
11	0.0183 (227.71)	0.0349 (231.81)	0.0015 (232.44)	0.0143 (232.66)	0.0127 (232.50)	0.0105 (223.46)	0.0325 (229.90)	0.0252 (225.01)	0.0092 (225.83)	0.0009 (231.02)
12	0.0754 (222.13)	0.1057 (219.96)	0.0615 (208.05)	0.1171 (215.75)	0.0843 (221.89)	0.0545 (216.37)	0.0819 (221.84)	0.1000 (222.48)	0.0481 (222.84)	0.0360 (225.82)
13	0.0855 (205.52)	0.0132 (209.49)	0.0282 (207.33)	0.0136 (210.25)	0.0224 (210.55)	0.0070 (205.92)	0.0729 (206.89)	0.0046 (210.93)	0.0223 (205.44)	0.0707 (209.42)
14	0.0069 (202.96)	0.0270 (208.00)	0.0127 (204.77)	0.0148 (207.81)	0.0445 (207.88)	0.0317 (204.38)	0.0066 (201.30)	0.0161 (207.58)	0.0250 (202.95)	0.0144 (204.64)
15	0.0115 (199.24)	0.0103 (205.11)	0.0494 (200.59)	0.0022 (205.29)	0.0030 (200.06)	0.0051 (198.34)	0.0137 (200.13)	0.1001 (199.47)	0.0299 (200.09)	0.0120 (200.13)
16	0.0192 (198.12)	0.0767 (201.75)	0.0366 (195.56)	0.0025 (201.89)	0.0178 (199.20)	0.0260 (195.68)	0.0091 (199.72)	0.0004 (197.40)	0.0248 (197.62)	0.0003 (196.62)
17	0.0108 (190.54)	0.0089 (194.53)	0.0109 (191.50)	0.1208 (193.23)	0.0050 (198.80)	0.0111 (195.05)	0.0203 (193.44)	0.0305 (190.27)	0.0655 (196.53)	0.0074 (194.37)
18	0.0108 (188.67)	0.0344 (192.40)	0.0507 (189.56)	0.0374 (189.67)	0.0229 (195.81)	0.0149 (192.83)	0.0102 (191.67)	0.0293 (187.83)	0.0154 (194.54)	0.0045 (194.06)
19	0.0058 (187.15)	0.0109 (189.47)	0.0142 (185.00)	0.0074 (187.84)	0.0370 (189.58)	0.0254 (191.82)	0.0287 (188.79)	0.0059 (185.71)	0.0610 (190.07)	0.0027 (192.62)
20	0.0752 (186.16)	0.0133 (186.69)	0.0037 (183.56)	0.0118 (183.88)	0.0412 (188.58)	0.0117 (190.05)	0.0851 (185.60)	0.0021 (183.81)	0.0046 (186.69)	0.0232 (189.61)
21	0.0020 (180.65)	0.0004 (183.53)	0.0229 (182.21)	0.0024 (182.13)	0.0054 (183.92)	0.0503 (185.57)	0.0237 (184.84)	0.0234 (183.30)	0.0360 (184.78)	0.0017 (188.10)
22	0.0435 (177.40)	0.0300 (182.75)	0.0354 (180.15)	0.0697 (180.29)	0.0047 (182.23)	0.0043 (183.47)	0.0305 (178.90)	0.0006 (180.13)	0.0140 (182.43)	0.0017 (185.41)
23	0.0042 (174.74)	0.0456 (179.75)	0.0104 (177.65)	0.0026 (179.83)	0.0022 (181.51)	0.1372 (178.65)	0.0054 (178.35)	0.0834 (177.25)	0.0031 (177.83)	0.0053 (179.19)
24	0.1189 (173.70)	0.0433 (177.87)	0.0207 (176.59)	0.0042 (176.13)	0.0631 (180.46)	0.0044 (177.25)	0.0204 (176.27)	0.1720 (174.09)	0.1060 (173.42)	0.0929 (178.25)
25	0.0009 (172.49)	0.0206 (175.96)	0.0556 (173.18)	0.1285 (174.19)	0.1428 (176.56)	0.0040 (176.58)	0.1043 (172.98)	0.0029 (172.32)	0.0356 (172.56)	0.1578 (175.05)
26	0.0462 (171.41)	0.1791 (174.18)	0.1506 (169.96)	0.0051 (170.22)	0.0026 (173.94)	0.0781 (173.58)	0.0114 (172.43)	0.0650 (171.08)	0.0115 (172.08)	0.0279 (172.81)
27	0.0838 (168.94)	0.0544 (171.37)	0.0227 (169.62)	0.0113 (168.97)	0.0224 (172.63)	0.0783 (172.38)	0.0203 (171.28)	0.0569 (169.93)	0.1703 (170.52)	0.0004 (172.21)
28	0.0910 (166.11)	0.0021 (170.35)	0.0288 (168.69)	0.0231 (168.04)	0.0512 (167.78)	0.0159 (171.95)	0.0016 (169.42)	0.0708 (166.68)	0.0612 (167.10)	0.0151 (170.87)
29	0.1297 (165.70)	0.0088 (168.43)	0.0139 (165.89)	0.0279 (167.41)	0.0461 (166.46)	0.1229 (168.34)	0.0242 (166.39)	0.0069 (166.07)	0.0709 (165.48)	0.0888 (169.89)
30	0.0071 (163.24)	0.0385 (166.51)	0.0418 (165.14)	0.0753 (166.26)	0.0396 (164.88)	0.0580 (164.71)	0.1022 (165.01)	0.0308 (165.44)	0.0430 (165.22)	0.2105 (167.54)

Table 9.S12. (*Continued*)

j	f_j (λ_j, nm)									
	md051#	**md052#**	**md053#**	**md054#**	**md055#**	**md056#**	**md057#**	**md058#**	**md059#**	**md060#**
1	0.0044 (401.04)	0.0099 (409.05)	0.0162 (399.58)	0.0169 (405.80)	0.0049 (398.64)	0.0306 (392.72)	0.0202 (399.99)	0.0103 (404.49)	0.0632 (410.76)	0.0012 (405.86)
2	0.3717 (361.03)	0.3704 (358.47)	0.3706 (354.79)	0.3336 (348.00)	0.3326 (361.49)	0.2914 (352.71)	0.2759 (367.43)	0.3880 (345.98)	0.2763 (360.24)	0.4231 (340.22)
3	0.0028 (322.30)	0.0014 (330.74)	0.0104 (320.01)	0.0040 (330.86)	0.0257 (327.11)	0.0022 (315.70)	0.0056 (323.00)	0.0015 (322.65)	0.0064 (318.30)	0.0091 (330.56)
4	0.0354 (296.09)	0.0620 (290.11)	0.0356 (282.43)	0.0770 (294.83)	0.0344 (293.92)	0.0892 (287.41)	0.0803 (300.64)	0.0148 (279.37)	0.0108 (288.41)	0.0002 (282.03)
5	0.0283 (277.95)	0.0016 (280.73)	0.0423 (278.27)	0.0061 (282.92)	0.0033 (280.28)	0.0083 (278.82)	0.0181 (275.46)	0.0157 (277.94)	0.0373 (281.82)	0.0386 (275.76)
6	0.0072 (277.48)	0.0958 (273.49)	0.0366 (273.83)	0.0906 (268.55)	0.0366 (273.61)	0.0168 (269.81)	0.0371 (275.11)	0.0705 (271.82)	0.0040 (277.79)	0.0671 (266.71)
7	0.0368 (261.92)	0.0033 (260.93)	0.0343 (260.02)	0.0030 (254.46)	0.0109 (254.58)	0.0459 (256.84)	0.1140 (257.88)	0.0776 (251.63)	0.0278 (255.37)	0.0262 (252.34)
8	0.2662 (255.12)	0.2849 (254.76)	0.2147 (253.79)	0.0089 (251.21)	0.0142 (250.50)	0.2919 (248.23)	0.2240 (246.34)	0.0549 (244.24)	0.3758 (250.75)	0.0471 (249.52)
9	0.0340 (245.21)	0.0023 (249.07)	0.0187 (247.17)	0.2677 (247.85)	0.2964 (250.19)	0.0313 (243.07)	0.0056 (242.70)	0.1713 (243.06)	0.0386 (246.79)	0.2258 (245.54)
10	0.0203 (243.04)	0.0029 (239.45)	0.0178 (234.71)	0.0272 (235.33)	0.0240 (237.86)	0.0834 (240.89)	0.0470 (239.49)	0.0188 (239.61)	0.0054 (240.78)	0.0216 (240.67)
11	0.0112 (226.07)	0.0054 (235.47)	0.0435 (233.62)	0.0709 (227.79)	0.0401 (236.63)	0.0138 (234.53)	0.0827 (225.65)	0.0394 (238.27)	0.0047 (235.16)	0.0062 (235.76)
12	0.0875 (222.02)	0.0530 (222.82)	0.0602 (216.62)	0.0033 (223.73)	0.0458 (219.92)	0.0851 (216.96)	0.0096 (223.60)	0.0582 (216.56)	0.0778 (216.25)	0.0561 (213.35)
13	0.0103 (214.85)	0.0130 (207.95)	0.0458 (205.32)	0.0060 (209.63)	0.0076 (214.17)	0.0043 (210.43)	0.0536 (215.93)	0.0431 (202.39)	0.0113 (208.80)	0.0148 (204.35)
14	0.0152 (213.22)	0.0472 (205.43)	0.0124 (202.75)	0.0628 (207.63)	0.0057 (211.94)	0.0331 (208.65)	0.0233 (206.83)	0.0211 (199.33)	0.0045 (207.66)	0.0088 (203.12)
15	0.0028 (202.69)	0.0061 (203.98)	0.0102 (202.16)	0.0086 (200.03)	0.0232 (202.21)	0.0127 (204.74)	0.0061 (200.98)	0.0390 (197.28)	0.0079 (204.53)	0.0235 (202.05)
16	0.0179 (200.82)	0.0325 (200.34)	0.0053 (200.99)	0.0100 (199.46)	0.0193 (196.73)	0.0051 (201.11)	0.0101 (199.86)	0.0034 (196.05)	0.0097 (202.74)	0.0374 (199.12)
17	0.0323 (196.67)	0.0017 (197.70)	0.0902 (198.26)	0.0119 (196.52)	0.0138 (194.90)	0.0226 (196.37)	0.0651 (190.74)	0.0160 (193.91)	0.0538 (196.83)	0.0242 (196.11)
18	0.0040 (194.65)	0.0023 (195.66)	0.0062 (192.11)	0.0036 (191.78)	0.0320 (191.44)	0.0093 (192.77)	0.0026 (189.26)	0.0195 (191.17)	0.0980 (192.35)	0.0311 (190.74)
19	0.1544 (190.39)	0.0540 (191.55)	0.0431 (190.42)	0.0113 (187.54)	0.0382 (186.14)	0.1380 (188.70)	0.0557 (185.94)	0.0302 (188.74)	0.0319 (189.11)	0.0143 (188.18)
20	0.0091 (187.54)	0.1095 (189.24)	0.0060 (187.53)	0.1292 (184.86)	0.0046 (185.60)	0.0012 (186.71)	0.0415 (182.05)	0.1054 (182.94)	0.0177 (187.42)	0.1238 (184.89)
21	0.0056 (182.82)	0.0655 (186.32)	0.0128 (186.34)	0.0060 (181.95)	0.0715 (184.51)	0.0323 (186.33)	0.0088 (180.40)	0.0131 (179.89)	0.0454 (185.23)	0.0239 (183.65)
22	0.0844 (181.42)	0.0023 (183.58)	0.1027 (182.68)	0.0614 (181.16)	0.0719 (183.96)	0.0078 (182.14)	0.0029 (178.85)	0.0182 (179.11)	0.0115 (182.70)	0.0258 (181.94)
23	0.0177 (178.97)	0.0151 (182.71)	0.0326 (180.08)	0.0458 (178.54)	0.0153 (177.48)	0.0073 (180.81)	0.0027 (177.43)	0.0082 (178.47)	0.0338 (180.43)	0.0024 (179.71)
24	0.1312 (174.76)	0.0026 (178.80)	0.0085 (177.77)	0.0200 (176.36)	0.0171 (176.65)	0.0228 (178.95)	0.0951 (175.37)	0.0152 (177.99)	0.0032 (177.68)	0.0088 (177.97)
25	0.0340 (173.59)	0.1333 (176.21)	0.0354 (174.71)	0.0314 (172.68)	0.0020 (174.22)	0.0516 (176.50)	0.0187 (175.33)	0.0148 (175.24)	0.0352 (174.75)	0.0027 (176.47)
26	0.0004 (172.68)	0.0360 (175.32)	0.0703 (174.36)	0.0658 (171.05)	0.0031 (173.02)	0.0962 (172.10)	0.0122 (174.49)	0.0036 (174.25)	0.0426 (173.31)	0.0614 (173.54)
27	0.0039 (172.44)	0.0234 (170.60)	0.0910 (170.69)	0.0030 (170.10)	0.1454 (170.95)	0.0031 (169.06)	0.0054 (171.93)	0.0139 (170.24)	0.0030 (171.96)	0.0353 (173.03)
28	0.0308 (170.43)	0.0255 (169.76)	0.0644 (168.17)	0.0864 (169.43)	0.0270 (170.45)	0.0229 (166.32)	0.1676 (169.00)	0.1316 (168.22)	0.0369 (171.22)	0.0849 (169.03)
29	0.0351 (168.27)	0.0510 (167.47)	0.0399 (166.36)	0.0329 (167.32)	0.0404 (168.69)	0.1276 (165.86)	0.0351 (167.25)	0.0584 (166.86)	0.1079 (169.44)	0.0411 (167.84)
30	0.0271 (167.11)	0.0141 (166.24)	0.0526 (166.19)	0.0044 (164.16)	0.0976 (165.77)	0.0393 (164.61)	0.0367 (165.89)	0.0060 (166.61)	0.0798 (166.46)	0.0206 (166.82)

Table 9.S12. (*Continued*)

j	f_j (λ_j, nm)									
	md061#	**md062#**	**md063#**	**md064#**	**md065#**	**md066#**	**md067#**	**md068#**	**md069#**	**md070#**
1	0.0073 (387.06)	0.0021 (408.96)	0.0011 (406.62)	0.0023 (403.49)	0.0007 (402.38)	0.1118 (373.45)	0.0071 (416.78)	0.0307 (405.19)	0.0016 (420.26)	0.0015 (380.89)
2	0.3688 (355.47)	0.3472 (363.57)	0.3951 (354.20)	0.3687 (352.77)	0.4101 (340.77)	0.1936 (359.81)	0.3264 (370.29)	0.3140 (359.99)	0.3496 (372.28)	0.4418 (332.61)
3	0.0260 (316.37)	0.0006 (325.58)	0.0066 (325.46)	0.0202 (329.35)	0.0279 (330.22)	0.0135 (330.18)	0.0085 (340.01)	0.0073 (333.36)	0.0009 (345.93)	0.0028 (305.24)
4	0.0636 (282.91)	0.0401 (287.39)	0.0037 (282.41)	0.0013 (286.89)	0.0029 (285.70)	0.0857 (296.09)	0.0015 (294.61)	0.0330 (287.99)	0.0004 (302.08)	0.0017 (269.92)
5	0.0093 (277.92)	0.0074 (282.25)	0.0080 (277.98)	0.0322 (276.98)	0.0247 (273.55)	0.0176 (284.76)	0.0624 (279.79)	0.0396 (284.37)	0.0434 (287.45)	0.0382 (265.58)
6	0.0011 (266.03)	0.0208 (279.56)	0.0167 (260.26)	0.0300 (268.25)	0.0316 (270.88)	0.0571 (277.13)	0.0371 (278.24)	0.0876 (277.09)	0.0767 (276.90)	0.0450 (261.56)
7	0.2056 (259.83)	0.0345 (257.48)	0.2141 (252.08)	0.0320 (259.75)	0.0039 (252.24)	0.0832 (271.32)	0.0114 (259.02)	0.0636 (260.39)	0.0003 (266.75)	0.0042 (246.12)
8	0.0715 (250.03)	0.1647 (251.37)	0.0045 (249.99)	0.1142 (256.79)	0.0211 (249.57)	0.0234 (257.79)	0.0590 (255.66)	0.0510 (256.61)	0.0019 (263.19)	0.0021 (241.14)
9	0.0012 (246.10)	0.1270 (248.32)	0.0195 (242.84)	0.0937 (251.32)	0.0423 (247.19)	0.2139 (252.47)	0.2245 (251.38)	0.1904 (253.35)	0.3946 (257.03)	0.3067 (240.23)
10	0.0297 (235.27)	0.0455 (245.36)	0.0845 (240.61)	0.1125 (247.83)	0.3000 (246.17)	0.0433 (247.55)	0.0814 (250.47)	0.0294 (237.24)	0.0062 (250.73)	0.0019 (230.53)
11	0.0062 (234.25)	0.0163 (243.09)	0.0607 (231.81)	0.0127 (243.54)	0.0036 (229.21)	0.0616 (230.37)	0.0376 (243.49)	0.0007 (230.12)	0.0015 (248.77)	0.0069 (228.76)
12	0.0555 (210.57)	0.0793 (216.75)	0.0343 (213.33)	0.0230 (211.43)	0.0901 (212.61)	0.0227 (228.74)	0.0270 (214.97)	0.0647 (220.22)	0.0355 (222.89)	0.0450 (206.23)
13	0.0082 (206.39)	0.0043 (210.48)	0.0616 (200.69)	0.0294 (211.10)	0.0240 (209.48)	0.0059 (217.90)	0.0093 (213.69)	0.0021 (214.55)	0.0012 (219.65)	0.0146 (198.52)
14	0.0050 (204.44)	0.0167 (208.77)	0.0257 (198.02)	0.0165 (206.39)	0.0015 (204.59)	0.0428 (212.99)	0.0604 (211.16)	0.0303 (206.66)	0.0027 (213.49)	0.0016 (196.34)
15	0.0024 (199.33)	0.0058 (204.10)	0.0163 (196.10)	0.0529 (200.73)	0.0251 (200.27)	0.0262 (210.93)	0.0382 (201.86)	0.0400 (203.06)	0.0037 (208.78)	0.0032 (192.23)
16	0.1217 (194.71)	0.0184 (196.93)	0.0224 (192.24)	0.0021 (198.67)	0.0699 (196.62)	0.0093 (206.60)	0.0058 (200.07)	0.0086 (201.75)	0.0096 (205.61)	0.0532 (190.35)
17	0.0078 (191.73)	0.0063 (193.54)	0.0717 (190.29)	0.0329 (196.62)	0.0009 (191.15)	0.0119 (202.29)	0.0035 (198.99)	0.0125 (196.63)	0.0515 (204.92)	0.0062 (187.30)
18	0.0439 (190.32)	0.0863 (192.75)	0.0015 (186.93)	0.0112 (194.82)	0.0255 (190.72)	0.0205 (198.34)	0.0026 (193.75)	0.0059 (190.72)	0.0311 (203.11)	0.0101 (185.57)
19	0.0029 (185.86)	0.0423 (189.45)	0.0108 (184.56)	0.0539 (191.69)	0.0900 (185.55)	0.0257 (195.79)	0.0596 (189.96)	0.1733 (187.63)	0.0188 (197.20)	0.0175 (183.71)
20	0.0231 (182.45)	0.0075 (187.48)	0.0074 (183.65)	0.1392 (188.22)	0.0373 (184.23)	0.0685 (192.14)	0.0029 (187.42)	0.0053 (186.25)	0.0032 (194.18)	0.0895 (181.04)
21	0.0467 (181.12)	0.0687 (186.83)	0.0263 (181.66)	0.0655 (185.90)	0.0085 (182.58)	0.0031 (188.78)	0.1212 (186.07)	0.0156 (184.52)	0.0069 (192.81)	0.0015 (175.78)
22	0.0044 (180.11)	0.0100 (181.69)	0.0721 (179.63)	0.0006 (185.40)	0.0076 (181.16)	0.0093 (187.03)	0.0149 (181.70)	0.0139 (183.21)	0.2429 (189.76)	0.0041 (174.14)
23	0.0016 (179.13)	0.0317 (179.93)	0.0084 (178.16)	0.0213 (181.35)	0.0295 (178.48)	0.0267 (184.29)	0.0392 (180.45)	0.0119 (178.65)	0.0043 (186.04)	0.0150 (173.74)
24	0.0081 (176.65)	0.0013 (178.79)	0.0039 (176.50)	0.0078 (179.90)	0.0050 (175.46)	0.0795 (178.32)	0.0050 (178.85)	0.0243 (177.18)	0.0043 (181.72)	0.0069 (172.91)
25	0.0673 (174.45)	0.2147 (173.29)	0.1033 (172.52)	0.0227 (177.61)	0.0685 (172.04)	0.0372 (177.70)	0.0015 (176.35)	0.0257 (175.87)	0.0566 (180.04)	0.0040 (170.91)
26	0.0023 (172.20)	0.1342 (170.96)	0.0175 (171.08)	0.1437 (174.66)	0.0172 (171.04)	0.0282 (175.61)	0.1573 (174.04)	0.0656 (173.72)	0.0022 (178.41)	0.0057 (168.35)
27	0.2584 (171.62)	0.0200 (170.05)	0.0316 (170.00)	0.0430 (167.75)	0.1109 (169.51)	0.1279 (174.20)	0.0685 (171.47)	0.0848 (171.50)	0.0612 (175.79)	0.3360 (165.93)
28	0.0833 (170.08)	0.0232 (167.30)	0.0439 (167.73)	0.0013 (167.62)	0.0374 (168.73)	0.0285 (171.70)	0.0008 (168.97)	0.0217 (170.11)	0.0598 (171.76)	0.0503 (164.13)
29	0.0101 (165.56)	0.0121 (166.59)	0.0775 (167.22)	0.0783 (166.16)	0.0141 (166.92)	0.0272 (168.96)	0.0186 (166.95)	0.0276 (168.08)	0.0782 (171.29)	0.0454 (161.64)
30	0.0455 (163.93)	0.0445 (165.70)	0.0046 (163.80)	0.0296 (165.17)	0.0078 (165.37)	0.0016 (168.24)	0.0341 (166.66)	0.0304 (165.79)	0.0239 (169.64)	0.0178 (161.48)

Table 9.S12. (*Continued*)

j	$f_j(\lambda_j$, nm)									
	md071#	**md072#**	**md073#**	**md074#**	**md075#**	**md076#**	**md077#**	**md078#**	**md079#**	**md080#**
1	0.0008 (404.11)	0.0110 (405.15)	0.0018 (394.24)	0.0102 (412.25)	0.0054 (386.69)	0.0009 (385.47)	0.0121 (396.69)	0.0006 (387.40)	0.0040 (429.56)	0.0290 (403.61)
2	0.4143 (348.00)	0.3884 (353.01)	0.3495 (366.60)	0.4275 (352.06)	0.3922 (351.62)	0.4219 (344.73)	0.4110 (346.79)	0.4151 (347.94)	0.3298 (376.08)	0.3068 (359.37)
3	0.0011 (324.70)	0.0025 (318.46)	0.0006 (317.18)	0.0011 (325.28)	0.0057 (310.27)	0.0008 (314.38)	0.0034 (318.33)	0.0014 (321.60)	0.0063 (328.92)	0.0122 (320.92)
4	0.0314 (279.01)	0.0064 (280.77)	0.0507 (283.85)	0.0090 (284.34)	0.0490 (280.27)	0.0703 (288.43)	0.0107 (286.81)	0.0225 (287.90)	0.0681 (299.12)	0.1119 (297.41)
5	0.0147 (277.79)	0.0244 (275.13)	0.0057 (279.05)	0.0254 (276.75)	0.0258 (279.04)	0.0061 (274.90)	0.0016 (279.89)	0.0013 (278.99)	0.0013 (279.59)	0.0044 (275.69)
6	0.0592 (269.55)	0.0433 (271.73)	0.0366 (274.35)	0.0712 (272.40)	0.0003 (268.46)	0.0172 (265.54)	0.0676 (270.43)	0.0312 (270.42)	0.0057 (276.65)	0.0400 (273.28)
7	0.0624 (250.88)	0.0086 (253.99)	0.0216 (257.68)	0.0078 (256.37)	0.0049 (251.18)	0.0352 (260.61)	0.0147 (258.46)	0.1464 (258.79)	0.0794 (266.21)	0.0161 (255.04)
8	0.2270 (242.06)	0.3302 (249.66)	0.2573 (252.35)	0.2023 (250.72)	0.2768 (245.94)	0.1732 (252.45)	0.0623 (252.53)	0.1260 (249.81)	0.0063 (251.37)	0.2637 (250.62)
9	0.0171 (241.25)	0.0092 (243.66)	0.0621 (247.20)	0.1119 (246.30)	0.0094 (236.62)	0.0658 (250.32)	0.1922 (247.97)	0.0241 (246.69)	0.0489 (248.59)	0.0132 (242.03)
10	0.0133 (237.11)	0.0185 (240.21)	0.0154 (242.35)	0.0017 (240.54)	0.0225 (234.52)	0.0072 (238.46)	0.0474 (241.03)	0.0009 (244.47)	0.2069 (244.52)	0.0130 (233.01)
11	0.0013 (227.52)	0.0162 (232.57)	0.0063 (238.81)	0.0030 (239.31)	0.0020 (227.45)	0.0060 (233.94)	0.0115 (238.75)	0.0535 (232.82)	0.0267 (237.56)	0.0048 (232.55)
12	0.0573 (213.61)	0.0284 (212.00)	0.0707 (216.35)	0.0342 (212.99)	0.0586 (215.56)	0.0231 (222.01)	0.0058 (214.23)	0.1323 (215.07)	0.1166 (214.38)	0.0643 (221.70)
13	0.0119 (203.60)	0.0372 (209.76)	0.0152 (212.45)	0.0145 (208.71)	0.0110 (203.27)	0.0505 (211.54)	0.0818 (210.47)	0.0034 (213.03)	0.0122 (210.49)	0.0190 (219.07)
14	0.0336 (199.02)	0.0114 (203.89)	0.0556 (203.26)	0.0005 (202.86)	0.0390 (200.20)	0.0053 (204.27)	0.0666 (209.44)	0.0238 (205.38)	0.0157 (207.82)	0.0137 (209.57)
15	0.0111 (196.06)	0.0049 (200.88)	0.0011 (200.93)	0.0272 (200.34)	0.0052 (198.44)	0.0074 (200.96)	0.0743 (203.50)	0.0250 (201.86)	0.0083 (203.51)	0.0059 (201.34)
16	0.0020 (195.77)	0.0194 (196.96)	0.0122 (197.68)	0.0245 (197.85)	0.0018 (195.28)	0.0070 (199.64)	0.0030 (199.46)	0.0083 (201.40)	0.0019 (200.47)	0.0052 (198.32)
17	0.0101 (191.83)	0.0854 (194.22)	0.0137 (193.54)	0.0070 (196.98)	0.0932 (192.68)	0.0085 (196.25)	0.0152 (196.41)	0.0096 (197.37)	0.0112 (195.84)	0.0075 (196.76)
18	0.0281 (189.21)	0.0066 (190.20)	0.0447 (190.89)	0.0077 (193.11)	0.0073 (189.27)	0.0299 (194.71)	0.0667 (193.47)	0.0546 (194.63)	0.1451 (191.90)	0.0418 (191.86)
19	0.0026 (186.63)	0.1153 (186.79)	0.0052 (188.83)	0.1532 (187.66)	0.0092 (186.11)	0.1152 (192.86)	0.0207 (189.31)	0.0062 (188.64)	0.0121 (189.55)	0.0025 (187.98)
20	0.0567 (182.28)	0.0187 (183.74)	0.1468 (185.44)	0.0013 (186.61)	0.0036 (183.46)	0.0045 (187.12)	0.0131 (188.11)	0.0093 (188.41)	0.0219 (188.68)	0.0315 (187.03)
21	0.0036 (180.57)	0.0154 (182.07)	0.0048 (183.48)	0.0470 (184.70)	0.0062 (182.31)	0.0037 (184.83)	0.0047 (185.76)	0.0025 (185.59)	0.0335 (186.69)	0.0111 (183.57)
22	0.0106 (179.02)	0.0003 (181.59)	0.0063 (181.35)	0.0095 (182.98)	0.0094 (180.36)	0.0036 (182.52)	0.0330 (182.76)	0.0073 (183.10)	0.0095 (182.45)	0.0426 (180.29)
23	0.0374 (175.88)	0.0299 (180.25)	0.0224 (179.16)	0.0140 (181.07)	0.4084 (172.16)	0.0148 (181.54)	0.0349 (178.94)	0.0102 (182.13)	0.0061 (180.70)	0.0143 (179.57)
24	0.0191 (172.02)	0.0097 (176.00)	0.0031 (176.03)	0.0032 (177.44)	0.0184 (170.20)	0.0193 (180.30)	0.1517 (176.73)	0.1837 (176.78)	0.0284 (176.99)	0.0079 (175.44)
25	0.0170 (171.24)	0.0009 (175.42)	0.1382 (173.63)	0.0194 (174.03)	0.0231 (168.75)	0.4518 (176.13)	0.0136 (174.84)	0.1312 (174.72)	0.0163 (174.94)	0.0019 (174.71)
26	0.0096 (170.24)	0.0729 (173.10)	0.0549 (173.12)	0.2106 (171.79)	0.0097 (168.69)	0.0570 (175.39)	0.0070 (172.62)	0.1238 (171.93)	0.2445 (172.96)	0.0072 (172.19)
27	0.1906 (167.83)	0.1283 (170.33)	0.0472 (169.94)	0.0096 (170.12)	0.0025 (167.89)	0.0123 (172.69)	0.0537 (170.89)	0.0356 (169.42)	0.0013 (169.67)	0.0566 (171.00)
28	0.0943 (166.77)	0.0097 (168.78)	0.0317 (167.38)	0.0034 (169.35)	0.0068 (166.63)	0.0128 (171.04)	0.0024 (169.59)	0.0461 (167.06)	0.0441 (168.13)	0.1997 (169.03)
29	0.0279 (165.61)	0.0836 (167.92)	0.0011 (165.43)	0.0616 (167.89)	0.1142 (165.10)	0.0046 (168.73)	0.1409 (165.75)	0.0043 (165.93)	0.0156 (167.78)	0.0929 (167.67)
30	0.0090 (163.82)	0.0040 (166.20)	0.0540 (164.90)	0.0096 (167.25)	0.0241 (164.78)	0.0659 (168.48)	0.0162 (165.02)	0.0225 (165.18)	0.1076 (164.09)	0.0381 (165.73)

Table 9.S12. (*Continued*)

j	f_j (λ_j, nm)									
	md081#	**md082#**	**md083#**	**md084#**	**md085#**	**md086#**	**md087#**	**md088#**	**md089#**	**md090#**
1	0.0195 (385.83)	0.0092 (427.28)	0.0089 (395.66)	0.0016 (396.14)	0.0011 (408.42)	0.0224 (376.26)	0.0133 (382.22)	0.0278 (408.24)	0.0181 (401.26)	0.0124 (417.99)
2	0.3091 (352.47)	0.3864 (362.47)	0.4057 (344.43)	0.3765 (353.73)	0.3892 (355.15)	0.3351 (348.20)	0.3679 (347.23)	0.2784 (352.25)	0.3331 (360.25)	0.3611 (359.44)
3	0.0116 (319.34)	0.0146 (327.35)	0.0037 (335.38)	0.0220 (316.52)	0.0031 (316.62)	0.0098 (332.25)	0.0056 (329.66)	0.0565 (333.17)	0.0136 (327.16)	0.0043 (332.24)
4	0.1152 (289.76)	0.0184 (283.26)	0.0405 (290.47)	0.0356 (284.33)	0.0376 (283.31)	0.0051 (286.11)	0.0023 (286.63)	0.0063 (290.47)	0.0699 (302.71)	0.0021 (288.50)
5	0.0366 (276.91)	0.0016 (276.91)	0.0022 (283.19)	0.0033 (279.85)	0.0061 (279.44)	0.0738 (280.83)	0.0455 (279.60)	0.0318 (280.69)	0.0096 (290.40)	0.0304 (280.79)
6	0.0301 (269.52)	0.0472 (273.60)	0.0199 (268.52)	0.0141 (271.76)	0.0240 (271.54)	0.0411 (270.41)	0.0316 (270.84)	0.0427 (271.78)	0.0026 (281.78)	0.0225 (276.59)
7	0.0054 (256.25)	0.0405 (258.80)	0.1051 (261.06)	0.0171 (252.83)	0.0112 (254.06)	0.0154 (266.24)	0.0442 (264.44)	0.0367 (263.85)	0.0482 (264.01)	0.0143 (261.34)
8	0.2350 (254.14)	0.0271 (250.45)	0.0726 (260.19)	0.2418 (248.11)	0.3159 (249.75)	0.1532 (255.39)	0.1198 (254.04)	0.0036 (253.59)	0.1295 (253.52)	0.2048 (256.80)
9	0.0176 (242.19)	0.2661 (249.02)	0.1464 (250.94)	0.0451 (245.11)	0.0310 (243.86)	0.1694 (240.91)	0.0279 (241.16)	0.2075 (245.09)	0.1403 (250.90)	0.0804 (249.83)
10	0.0255 (233.21)	0.0027 (239.93)	0.0171 (249.11)	0.0651 (242.60)	0.0140 (241.47)	0.0420 (236.69)	0.1781 (239.11)	0.1132 (243.60)	0.0288 (246.77)	0.0878 (249.68)
11	0.0022 (228.82)	0.0034 (234.45)	0.0069 (234.81)	0.0161 (230.48)	0.0006 (236.21)	0.0141 (226.92)	0.0315 (227.47)	0.0572 (239.21)	0.0184 (240.30)	0.0044 (238.63)
12	0.0574 (223.74)	0.0095 (214.03)	0.0461 (219.64)	0.0573 (215.25)	0.0525 (214.23)	0.0607 (215.97)	0.0678 (214.20)	0.0091 (215.49)	0.1526 (230.03)	0.0214 (217.98)
13	0.0217 (218.61)	0.0219 (206.67)	0.0402 (212.84)	0.0198 (211.17)	0.0034 (206.51)	0.0038 (211.25)	0.0033 (212.44)	0.0520 (212.61)	0.0129 (216.78)	0.0039 (212.29)
14	0.0391 (210.60)	0.0587 (203.57)	0.0235 (211.11)	0.0071 (208.51)	0.0098 (205.61)	0.0014 (205.35)	0.0020 (206.18)	0.0023 (208.98)	0.0023 (212.35)	0.0040 (209.36)
15	0.0379 (202.24)	0.0016 (198.52)	0.0024 (207.49)	0.0160 (204.77)	0.0322 (202.90)	0.0531 (200.42)	0.0641 (200.58)	0.0292 (203.78)	0.0099 (210.53)	0.0757 (203.72)
16	0.0173 (197.16)	0.1259 (195.19)	0.0633 (202.40)	0.0075 (198.26)	0.0066 (197.40)	0.0429 (197.73)	0.0206 (195.74)	0.0041 (200.38)	0.1588 (203.37)	0.0114 (201.50)
17	0.0329 (194.52)	0.0095 (194.60)	0.0627 (198.45)	0.0512 (191.40)	0.0003 (194.71)	0.0026 (192.95)	0.0038 (192.35)	0.0020 (197.67)	0.0051 (198.29)	0.0031 (197.73)
18	0.0171 (191.68)	0.0050 (190.24)	0.0039 (193.60)	0.0041 (190.12)	0.0870 (191.62)	0.0185 (190.16)	0.0177 (188.78)	0.0007 (192.63)	0.0393 (194.53)	0.0135 (193.59)
19	0.0128 (190.48)	0.0126 (189.32)	0.0673 (192.69)	0.1304 (185.48)	0.0255 (190.47)	0.0078 (188.04)	0.0084 (186.69)	0.0048 (189.63)	0.0133 (190.88)	0.1475 (190.66)
20	0.0166 (186.31)	0.1065 (187.17)	0.0113 (190.44)	0.0019 (183.64)	0.2116 (186.16)	0.0899 (185.87)	0.1585 (183.62)	0.0482 (189.45)	0.0114 (188.84)	0.0007 (188.42)
21	0.0019 (184.52)	0.0134 (185.93)	0.0088 (185.95)	0.0058 (182.58)	0.0397 (182.89)	0.0499 (182.91)	0.0307 (180.45)	0.0783 (187.76)	0.0023 (187.31)	0.1089 (186.61)
22	0.0010 (182.59)	0.0237 (181.70)	0.0087 (182.99)	0.0193 (177.19)	0.0053 (179.16)	0.0062 (181.47)	0.0052 (178.21)	0.0357 (183.67)	0.0084 (184.56)	0.0359 (183.72)
23	0.0121 (177.60)	0.0191 (181.39)	0.0030 (182.28)	0.0149 (176.25)	0.0334 (176.96)	0.0322 (178.59)	0.0018 (177.77)	0.0258 (180.39)	0.0116 (182.40)	0.0126 (180.21)
24	0.1048 (176.47)	0.0177 (177.17)	0.0425 (180.58)	0.0059 (174.75)	0.0005 (175.81)	0.0089 (175.98)	0.0066 (176.70)	0.0348 (179.27)	0.0019 (180.38)	0.0160 (179.43)
25	0.0154 (175.01)	0.0092 (175.62)	0.0697 (179.98)	0.0425 (173.69)	0.0072 (174.14)	0.0275 (173.36)	0.0772 (171.40)	0.0062 (175.69)	0.0638 (176.92)	0.0327 (175.76)
26	0.0801 (174.23)	0.0648 (173.37)	0.0823 (178.36)	0.0091 (170.87)	0.0029 (171.05)	0.1541 (172.56)	0.0381 (171.26)	0.2142 (172.16)	0.1976 (175.59)	0.0112 (175.26)
27	0.0180 (172.64)	0.1893 (172.28)	0.0865 (174.06)	0.0068 (169.72)	0.1857 (170.00)	0.0342 (171.17)	0.0467 (170.32)	0.0092 (170.79)	0.1159 (171.01)	0.1462 (170.71)
28	0.1274 (171.40)	0.0001 (170.52)	0.0699 (171.17)	0.0260 (168.91)	0.0158 (167.62)	0.0093 (170.75)	0.1015 (167.13)	0.0018 (169.86)	0.0242 (167.49)	0.0075 (169.67)
29	0.0621 (170.07)	0.0359 (169.26)	0.0217 (170.48)	0.1073 (165.92)	0.0021 (166.15)	0.0147 (166.68)	0.0554 (165.45)	0.0857 (169.59)	0.0109 (167.39)	0.0273 (167.71)
30	0.0057 (166.93)	0.0394 (169.11)	0.0851 (168.49)	0.0061 (164.33)	0.0396 (166.01)	0.0069 (166.34)	0.0074 (163.16)	0.0342 (166.90)	0.0158 (165.60)	0.0154 (167.21)

Table 9.S12. (*Continued*)

j	$f_j(\lambda_j$, nm)									
	md091#	md092#	md093#	md094#	md095#	md096#	md097#	md098#	md099#	md100#
1	0.0181 (402.41)	0.0042 (393.93)	0.0141 (382.56)	0.0009 (421.74)	0.0007 (429.84)	0.0005 (387.58)	0.0115 (391.16)	0.0002 (393.12)	0.0002 (399.30)	0.0035 (401.16)
2	0.3286 (357.17)	0.3311 (350.68)	0.3570 (344.01)	0.3620 (360.19)	0.4149 (355.84)	0.3686 (349.07)	0.3541 (346.02)	0.3961 (344.98)	0.3873 (347.85)	0.4384 (349.43)
3	0.0048 (321.67)	0.0345 (324.82)	0.0009 (315.45)	0.0022 (326.71)	0.0013 (332.83)	0.0051 (315.52)	0.0035 (316.24)	0.0015 (322.24)	0.0010 (322.49)	0.0134 (327.33)
4	0.0606 (287.82)	0.0800 (290.97)	0.0548 (284.14)	0.0938 (287.37)	0.0008 (286.91)	0.0653 (287.86)	0.0742 (287.28)	0.0373 (284.92)	0.0506 (287.54)	0.0514 (284.59)
5	0.0174 (282.79)	0.0099 (282.44)	0.0036 (275.57)	0.0158 (283.86)	0.0699 (272.15)	0.0062 (274.95)	0.0410 (276.67)	0.0224 (275.89)	0.0234 (283.78)	0.0015 (278.88)
6	0.0236 (275.38)	0.0199 (276.81)	0.0953 (266.89)	0.0290 (273.17)	0.0392 (265.58)	0.0331 (272.03)	0.0162 (273.87)	0.0268 (269.58)	0.0442 (269.73)	0.0618 (274.33)
7	0.0078 (251.16)	0.0580 (262.02)	0.0088 (254.82)	0.0754 (256.57)	0.0320 (251.80)	0.0074 (252.88)	0.0362 (252.21)	0.1483 (258.66)	0.0281 (253.39)	0.0483 (257.30)
8	0.2911 (246.08)	0.2094 (252.71)	0.1016 (250.09)	0.0222 (251.39)	0.2188 (244.67)	0.3141 (246.88)	0.0771 (248.50)	0.0977 (249.66)	0.0007 (246.81)	0.2182 (251.55)
9	0.0530 (243.12)	0.0460 (248.37)	0.1714 (247.69)	0.2093 (245.30)	0.0233 (242.65)	0.0238 (243.24)	0.2091 (243.55)	0.0069 (248.01)	0.1672 (244.79)	0.0010 (245.55)
10	0.0361 (239.03)	0.0178 (242.86)	0.0023 (237.66)	0.0683 (241.14)	0.0699 (242.37)	0.0030 (237.41)	0.0169 (237.27)	0.0660 (242.05)	0.1857 (243.88)	0.0088 (236.54)
11	0.0140 (234.96)	0.0063 (235.87)	0.0094 (232.20)	0.0046 (235.73)	0.0086 (234.28)	0.0032 (231.77)	0.0293 (225.73)	0.0290 (218.58)	0.0041 (233.10)	0.0046 (226.11)
12	0.0719 (216.85)	0.0759 (225.71)	0.0449 (220.64)	0.1036 (215.05)	0.0032 (210.50)	0.0918 (219.94)	0.0661 (221.47)	0.1130 (214.46)	0.0566 (220.03)	0.0666 (217.93)
13	0.0030 (205.90)	0.0020 (213.39)	0.0065 (210.55)	0.0064 (210.37)	0.0300 (203.83)	0.0065 (209.21)	0.0099 (208.23)	0.0048 (205.68)	0.0154 (208.41)	0.0093 (208.87)
14	0.0048 (204.64)	0.0216 (210.60)	0.0246 (204.30)	0.0036 (206.91)	0.0375 (202.01)	0.0109 (204.84)	0.0463 (200.77)	0.0730 (202.89)	0.0014 (207.63)	0.0501 (203.63)
15	0.0068 (203.87)	0.0752 (205.45)	0.0021 (200.43)	0.0021 (202.72)	0.0005 (196.70)	0.0230 (200.83)	0.0025 (198.73)	0.0001 (199.94)	0.0149 (205.34)	0.0346 (201.08)
16	0.0085 (202.27)	0.0457 (204.99)	0.0080 (199.46)	0.0112 (198.68)	0.0060 (191.45)	0.0010 (199.24)	0.0182 (195.82)	0.0046 (197.15)	0.0504 (198.08)	0.0007 (198.44)
17	0.0493 (194.63)	0.0173 (196.98)	0.0054 (194.61)	0.0081 (194.99)	0.0044 (190.97)	0.0017 (196.13)	0.0011 (190.52)	0.0061 (193.80)	0.0209 (193.23)	0.0164 (195.50)
18	0.0367 (191.03)	0.0554 (193.47)	0.0032 (189.59)	0.0848 (191.05)	0.0623 (188.90)	0.0369 (193.46)	0.0039 (187.22)	0.0745 (191.17)	0.0032 (192.32)	0.0082 (190.35)
19	0.0122 (188.46)	0.0033 (190.85)	0.0050 (188.49)	0.0861 (187.69)	0.0036 (187.77)	0.1320 (186.40)	0.0709 (185.98)	0.0014 (186.22)	0.0176 (188.99)	0.0004 (189.27)
20	0.0388 (185.70)	0.0109 (190.35)	0.1225 (184.24)	0.0574 (186.28)	0.0124 (184.47)	0.0175 (185.19)	0.0062 (183.05)	0.0028 (183.03)	0.0514 (184.98)	0.0778 (188.25)
21	0.0166 (183.15)	0.0060 (183.82)	0.0718 (183.60)	0.0060 (183.46)	0.0055 (182.47)	0.0169 (184.07)	0.0100 (182.36)	0.0078 (181.83)	0.1109 (183.19)	0.0066 (182.17)
22	0.0311 (181.16)	0.0020 (182.95)	0.0014 (178.81)	0.0021 (180.41)	0.1305 (182.06)	0.0023 (179.09)	0.0180 (178.92)	0.0031 (180.59)	0.0009 (179.17)	0.0070 (180.97)
23	0.0102 (180.16)	0.0052 (181.11)	0.0228 (177.20)	0.0311 (179.26)	0.0238 (179.16)	0.0044 (176.61)	0.0056 (174.75)	0.0003 (179.78)	0.0160 (178.28)	0.0080 (178.69)
24	0.0483 (178.14)	0.0028 (178.36)	0.0121 (175.64)	0.0051 (177.89)	0.0073 (177.35)	0.0402 (175.90)	0.0367 (171.50)	0.2625 (176.60)	0.0135 (175.20)	0.0570 (177.99)
25	0.0011 (174.60)	0.0643 (177.33)	0.0405 (173.91)	0.0003 (175.12)	0.0125 (171.73)	0.0648 (174.61)	0.0215 (170.92)	0.0163 (174.39)	0.0038 (174.05)	0.0788 (171.97)
26	0.0994 (171.65)	0.1504 (174.87)	0.0543 (172.24)	0.1688 (173.64)	0.0282 (171.11)	0.2127 (170.33)	0.1414 (170.77)	0.0067 (171.06)	0.1388 (170.36)	0.1984 (170.50)
27	0.1288 (169.60)	0.0482 (171.64)	0.1680 (168.98)	0.0211 (166.98)	0.1600 (168.44)	0.0240 (168.05)	0.0584 (166.94)	0.0235 (167.48)	0.0471 (168.43)	0.0406 (169.09)
28	0.0533 (167.33)	0.0225 (171.06)	0.0473 (165.39)	0.0791 (166.83)	0.0841 (167.31)	0.0125 (167.65)	0.1344 (165.25)	0.1341 (166.69)	0.0235 (166.65)	0.0081 (168.30)
29	0.0509 (166.69)	0.0039 (169.54)	0.0168 (164.97)	0.0113 (165.89)	0.0028 (166.72)	0.0912 (166.34)	0.0424 (163.15)	0.0139 (165.28)	0.0071 (164.52)	0.0126 (166.62)
30	0.0571 (165.17)	0.0494 (165.13)	0.0665 (163.95)	0.0388 (164.90)	0.0557 (163.98)	0.0511 (165.21)	0.0043 (162.61)	0.0515 (164.00)	0.0186 (163.45)	0.0171 (165.16)

Part V

Conclusions

Sleeping is giving in
No matter what the time is

— Arcade Fire, *Rebellion (Lies)*

In the last decades, TD-DFT calculations have become the standard method for the theoretical determination of chiroptical properties on small-to-medium sized molecules, due to the reasonable balance between chemical accuracy and computational efficiency;[28] the application of these methods to larger systems is a very promising perspective for future studies on pharmaceutically relevant systems. However, some issues are still limiting a straightforward applicability of TD-DFT methods: for instance, the large number of conformations at equilibrium for large and flexible molecules greatly increases the computational requirements, and the shortcomings in the proper description of weak interactions like dispersion forces and solvation effects have a huge impact on the accuracy and reliability of calculations.[111] The application of improved theoretical methods, such as the resolution of identity (RI) approximation and the semi-classical corrections to the interaction potential accounting for dispersion forces,[224] can benefit the feasibility and reliability of TD-DFT calculations on larger and more flexible systems. On the other hand, implicit continuum solvation models such as PCM[114] and molecular dynamics (MD) simulations can be employed in combination with TD-DFT for a better description of the electronic structure and conformational space of chiral solutes in solvated systems, consequently improving the accuracy of calculated chiroptical properties.

The combination of theoretical chiroptical spectroscopies with experimental techniques is a very versatile approach, allowing the stereochemical characterisation of several classes of molecules and drugs. TD-DFT calculations can be employed together with ECD spectroscopy and enantioselective HPLC to separate and identify the enantiomeric forms of chiral drugs: for example, the AC of a fluorinated arylpropionic acid derivative, belonging to a new class of potential non-steroidal anti-inflammatory drugs, was determined by means of this multidisciplinary approach.[7] The extremely high correlation between experimental and calculated ECD spectra allowed a straightforward AC assignment to the two enantiomeric fractions obtained by enantioselective HPLC.

The same approach was employed for the stereochemical characterisation of difenoconazole, a chiral triazole fungicide used in agriculture and bearing two chiral centres.[8] The four stereoisomers, which display stereoselective biological activities and environmental toxicology, were isolated by enantioselective HPLC and analysed by spectroscopic techniques (1D- and 2D-NMR, ECD). TD-DFT calculations were subsequently carried out to determine the theoretical ECD spectra of the two enantiomeric pairs and assess the AC of each stereoisomer. This study showed the benefits arising from the employment of multiple experimental techniques to improve the accuracy of the characterisation: the large conformational

flexibility of difenoconazole leads to weak ECD spectra which TD-DFT calculations were unable to distinguish unambiguously; the determination of the relative configuration by NMR allowed to simplify the AC assignment.

Chiroptical properties arise from the dissymmetric disposition of atoms around chromophores: different conformations of the same molecule of known AC may display dramatically different chiroptical properties, and the macroscopic properties are simply a weighted average of all the contributions due to the different conformers, according to their equilibrium populations. As a consequence, a proper description of the thermodynamic equilibrium between conformations is crucial for an accurate prediction of chiroptical properties by TD-DFT, particularly for flexible molecules. The diastereomers of the β_2-adrenergic agonist fenoterol, for example, display a complex conformational space, due to the presence of a 5-atom alkylic linker joining two aromatic chromophores. A thorough DFT conformational analysis and TD-DFT calculations allowed to recognise the main contributions of the two stereocenters to the observed chiroptical properties: a different equilibrium between extended and folded conformations of the alkylic linker was observed for the diastereomers of fenoterol, and their AC was confirmed.[11]

The effect of small conformational changes was clearly observed for some (3*R*)-3-hydroxy-4-aryl-β-lactam derivatives, used as chiral building blocks for asymmetric synthesis in the development of new potential drugs.[10] The correlation between AC and chiroptical properties of β-lactam rings is nicely predicted by a series of semi-empirical sector rules (SR), which were successfully employed for the accurate AC assessment of several derivatives, but failed for a thienyl derivative. TD-DFT calculations allowed a correct AC determination for all derivatives and showed that the β-lactam SR heavily rely on the structural and geometric features of the β-lactam ring and on the nature of substituents: when the conformation of the amide bond is slightly perturbed or a heterocyclic substituent is introduced, the SR may fail in predicting the correct AC.

Solvation effects are among the most difficult effects to be described in theoretical chiroptical spectroscopy. Solvation may exert its influence on chiroptical properties at several levels, including electrostatic perturbations to the electronic transitions and conformational perturbations due to weak intermolecular interactions. In some cases, the macroscopic chiroptical properties of a sample are not arising directly from the analyte but are due to chiral imprint phenomena on the first solvation shells.[115] TD-DFT calculations are then very likely to fail in predicting the correct properties if solvation is not accurately described.

The fungal metabolite austdiol is the building block of a series of newly discovered natural products from *Mycoleptodiscus indicus*, named mycoleptones A–C; the stereochemistry of mycoleptone A was fully characterised by a combination of ECD and NMR spectroscopies, TD-DFT calculations and X-ray crystallography.[9] Austdiol, however, clearly shows the importance of a proper description of solvation effects for a correct stereochemical characterisation: when solvation is only treated implicitly in QM calculations with a continuum solvation model, the wrong AC is predicted from the calculated $[\alpha]_D$ values. When solvation is treated explicitly through *ab initio* MD simulations of the solvation dynamics of austdiol in methanol, the description of the chiral environment around the carbonyl chromophores is dramatically improved, and TD-DFT calculations are able to reproduce the experimental chiroptical properties with high accuracy. The improvement is mainly due to a small solvation-induced conformational change involving the hydroxyl group in α-position to the ketone moiety of austdiol, confirming the extreme sensitivity of chiroptical properties to small perturbations to the molecular geometry.

The combination of experimental chiroptical spectroscopies with state-of-the-art QM calculations proved to be a very efficient way to predict the AC of a wide range of bioactive molecules, confirming the recent trend in stereochemical analysis which recognises this multidisciplinary approach as the standard method for the characterisation of chiral systems. In several situations, the stereochemical characterisation of a chiral molecule of unknown AC can be achieved with relative ease by performing a preliminary conformational analysis on all the stereoisomers by DFT and calculating the theoretical chiroptical properties on the optimised conformations by TD-DFT; conformationally-averaged theoretical spectra are then compared with the experimental spectra of the system under investigation. When this method is applied, however, great care must be taken in describing the molecular system in the most accurate fashion: indeed, chiroptical properties can be extremely sensitive to very small perturbations to the electronic structure and geometry of the system. The intrinsic approximations of DFT functionals and errors in the description of the thermodynamic equilibrium between conformers in solution may therefore lead to completely wrong AC predictions. The constant improvement of theoretical models and methods, both in terms of reliability and computational requirements, is a very promising path towards chemical accuracy, which will also benefit stereochemical and pharmaceutical analysis in the investigation of non-trivial effects on chiroptical properties in solvated systems and in the characterisation of the relationship between the AC and the biological activity of complex chiral drugs.

Part VI

Appendix

Everything counts
In large amounts

— Depeche Mode, *Everything Counts*

Chapter A

Data processing

This chapter is dedicated to the description of the mathematical and computational tools used to process the results from QM calculations. The first section reviews the mathematical and statistical treatment of results which allows to derive the theoretical spectra of molecules and the evaluation of geometric parameters from the structure of conformers. The second section reports the implementation of the mathematical tools in a set of UNIX shell scripts, which were developed and used to standardise and speed up the data processing.

A.1 Generation of theoretical spectra

Normal and Cauchy distributions

The experimental absorption bands can be derived from the theoretical values of oscillator and rotational strengths by approximation to a statistical distribution; the shape of a band is thus approximated to a distribution function related to the intensity of a transition. The most used distribution functions are the Gaussian function, employed to approximate the electronic transitions to a normal distribution, and the Lorentzian function, employed to approximate the vibrational transitions to a Cauchy distribution. The general equations and the integral for both the normal and Cauchy distributions will be reviewed with the purpose of showing the mathematical tools needed for the elaboration of theoretical spectra.[262]

The general equation of a Gaussian function is given by:

$$f(x) = a\,\mathrm{e}^{-\left(\frac{|x-b|}{c}\right)^2}\,, \tag{A.1}$$

while the general equation of a Lorentzian function is given by:

$$\begin{aligned} f(x) &= \frac{1}{\pi\gamma\left(1+\left(\frac{|x-b|}{\gamma}\right)^2\right)} \\ &= \frac{1}{\pi}\left(\frac{\gamma}{|x-b|^2+\gamma^2}\right)\,. \end{aligned} \tag{A.2}$$

In the equations above, a, b, $c > 0$ and $\gamma > 0$ are real constants. a is the maximum value of $f(x)$, b is the median of the distribution. c and γ are parameters related to the statistical dispersion of the distribution. Another form for the Lorentzian function, where a is explicitly considered, is given by:

$$\begin{aligned} f(x) &= \frac{a}{1+\left(\frac{|x-b|}{\gamma}\right)^2} \\ &= a\left(\frac{\gamma^2}{|x-b|^2+\gamma^2}\right)\,. \end{aligned} \tag{A.3}$$

The integration of the Gaussian function makes use of the following relation:

$$\int_{-\infty}^{\infty} \mathrm{e}^{-x^2}\,\mathrm{d}x = \sqrt{\pi}\,; \tag{A.4}$$

the integral of equation A.1 becomes:

$$\int_{-\infty}^{\infty} a\,\mathrm{e}^{-\left(\frac{|x-b|}{c}\right)^2} = ac\sqrt{\pi}\,. \tag{A.5}$$

The integration of the Lorentzian function makes use of the following antiderivative:

$$\int \frac{1}{x^2+\alpha^2}\,\mathrm{d}x = \frac{1}{\alpha}\arctan\frac{x}{\alpha} + C\,, \tag{A.6}$$

where C is the constant of integration. The improper integral can be determined:

$$\begin{aligned}\int_{-\infty}^{\infty} \frac{1}{x^2+\alpha^2}\,\mathrm{d}x &= \lim_{a\to-\infty}\left[\frac{1}{\alpha}\arctan\frac{x}{\alpha}\right]_a^0 + \lim_{b\to\infty}\left[\frac{1}{\alpha}\arctan\frac{x}{\alpha}\right]_0^b \\ &= \frac{1}{\alpha}\left[0-\left(-\frac{\pi}{2}\right)\right]+\frac{1}{\alpha}\left[\frac{\pi}{2}-0\right] \\ &= \frac{\pi}{\alpha}\,; \end{aligned} \tag{A.7}$$

subsequently, the integral of equation A.3 becomes:

$$\begin{aligned}\int_{-\infty}^{\infty} a\left(\frac{\gamma^2}{|x-b|^2+\gamma^2}\right)\mathrm{d}x &= a\gamma^2\int_{-\infty}^{\infty}\frac{1}{|x-b|^2+\gamma^2}\,\mathrm{d}x \\ &= a\gamma\pi\,. \end{aligned} \tag{A.8}$$

Electronic absorption spectra

Electronic spectra are usually approximated to a normal distribution: equation A.1 is used to describe ε as a function of wavenumber σ[100] after replacing a with the maximum value of molar absorption coefficient of an absorption band (ε_j), b with the corresponding wavenumber (σ_j) and c with $\Delta\sigma$, which is the parameter that determines the width of the Gaussian curve and is used to describe the broadening of experimental absorption bands. Accordingly, the absorption band associated to the transition to an excited state $j \neq 0$ is given by:

$$\varepsilon_j(\sigma) = \varepsilon_j\,\mathrm{e}^{-\left(\frac{|\sigma-\sigma_j|}{\Delta\sigma}\right)^2}\,, \tag{A.9}$$

where $\Delta\sigma$ is defined as the half-bandwidth of the band when $\Delta\varepsilon = \Delta\varepsilon_{\max}/\,\mathrm{e}$; this parameter is set to an arbitrary value in order to match the breadth of experimental bands.

The integrated intensity of the band is then calculated using equation A.5:

$$\int \varepsilon_j(\sigma)\,\mathrm{d}\sigma = \int \varepsilon_j\,\mathrm{e}^{-\left(\frac{|\sigma-\sigma_j|}{\Delta\sigma}\right)^2}\,\mathrm{d}\sigma = \varepsilon_j\Delta\sigma\sqrt{\pi}\,. \tag{A.10}$$

Equation 2.17 is used to obtain an expression of $\varepsilon_{\max}$ as a function of the oscillator strength, f_j, which is then substituted in equation A.9 to obtain the

Gaussian functions describing ε as a function of σ and f_j for each transition:

$$\begin{aligned} f_j &= 4.31899 \cdot 10^{-9} \int \varepsilon_j(\sigma)\ \mathrm{d}\sigma \\ &= 4.31899 \cdot 10^{-9}\, \varepsilon_j \Delta\sigma \sqrt{\pi}\ ; \end{aligned} \tag{A.11}$$

$$\varepsilon_j = \frac{1}{\Delta\sigma} \cdot \frac{f_j}{7.65521 \cdot 10^{-9}}; \tag{A.12}$$

$$\varepsilon_j(\sigma) = \frac{1}{\Delta\sigma} \cdot \frac{f_j}{7.65521 \cdot 10^{-9}}\, \mathrm{e}^{-\left(\frac{|\sigma-\sigma_j|}{\Delta\sigma}\right)^2}. \tag{A.13}$$

The procedure to obtain the Gaussian functions for the theoretical determination of ECD bands is almost identical; the differential molar absorption coefficient, $\Delta\varepsilon$, takes the place of ε and the rotational strength, R_j, takes the place of f_j:[113]

$$\begin{aligned} R_j &= 2.29648 \cdot 10^{-39} \int \frac{\Delta\varepsilon_j(\sigma)}{\sigma}\ \mathrm{d}\sigma \\ &= 2.29648 \cdot 10^{-39} \Delta\varepsilon_j \frac{\Delta\sigma}{\sigma_j} \sqrt{\pi}\ ; \end{aligned} \tag{A.14}$$

$$\Delta\varepsilon_j = \frac{\sigma_j}{\Delta\sigma} \cdot \frac{R_j}{4.07040 \cdot 10^{-39}}; \tag{A.15}$$

$$\Delta\varepsilon_j(\sigma) = \frac{\sigma_j}{\Delta\sigma} \cdot \frac{R_j}{4.07040 \cdot 10^{-39}}\, \mathrm{e}^{-\left(\frac{|\sigma-\sigma_j|}{\Delta\sigma}\right)^2}. \tag{A.16}$$

In electronic spectroscopy, however, the energy of incident light is frequently reported in terms of wavelength, λ in nm, instead of wavenumber, σ in cm^{-1}, while $\Delta\sigma$ is expressed in electronvolt (eV). The following conversions are useful for a straightforward comparison of computed and experimental bands:

$$\sigma = \frac{10^7}{\lambda} = 8.06554 \cdot 10^3\, E_{\mathrm{eV}}\ ; \tag{A.17}$$

$$\begin{aligned} \varepsilon_j(\lambda) &= \frac{1}{8.06554 \cdot 10^3\, \Delta\sigma_E} \cdot \frac{f_j}{7.65521 \cdot 10^{-9}}\, \mathrm{e}^{-\left(\frac{|10^7/\lambda - 10^7/\lambda_j|}{8.06554 \cdot 10^3\, \Delta\sigma_E}\right)^2} \\ &= 1.61961 \cdot 10^4\, \frac{f_j}{\Delta\sigma_E}\, \mathrm{e}^{-\left(\frac{|10^7/\lambda - 10^7/\lambda_j|}{8.06554 \cdot 10^3\, \Delta\sigma_E}\right)^2}\ ; \end{aligned} \tag{A.18}$$

$$\Delta\varepsilon_j(\lambda) = \frac{10^7/\lambda_j}{8.06554\cdot 10^3\,\Delta\sigma_E}\cdot\frac{R_j}{4.07040\cdot 10^{-39}}\,\mathrm{e}^{-\left(\frac{|10^7/\lambda-10^7/\lambda_j|}{8.06554\cdot 10^3\,\Delta\sigma_E}\right)^2}$$
$$= 3.04660\cdot 10^{41}\,\frac{R_j}{\lambda_j\,\Delta\sigma_E}\,\mathrm{e}^{-\left(\frac{|10^7/\lambda-10^7/\lambda_j|}{8.06554\cdot 10^3\,\Delta\sigma_E}\right)^2}\ . \tag{A.19}$$

Vibrational absorption spectra

Vibrational spectra are usually approximated to a Cauchy distribution: following the same framework used for electronic spectra, equations A.3 and A.8 are used to describe ε (for IR spectra) and $\Delta\varepsilon$ (for VCD spectra) as a function of σ and the integrated intensity of the band for each transition. The following equations are therefore derived:

$$\varepsilon_j(\sigma) = \frac{1}{\Gamma}\,\frac{f_j}{4.31899\cdot 10^{-9}\,\pi}\cdot\left(\frac{\Gamma^2}{|\sigma-\sigma_j|^2+\Gamma^2}\right)$$
$$= 7.37000\cdot 10^7\,f_j\frac{\Gamma}{|\sigma-\sigma_j|^2+\Gamma^2}\ ; \tag{A.20}$$

$$\Delta\varepsilon_j(\sigma) = \frac{\sigma_j}{\Gamma}\,\frac{R_j}{2.29648\cdot 10^{-39}\,\pi}\cdot\left(\frac{\Gamma^2}{|\sigma-\sigma_j|^2+\Gamma^2}\right)$$
$$= 1.38607\cdot 10^{38}\,\sigma_j\,R_j\frac{\Gamma}{|\sigma-\sigma_j|^2+\Gamma^2}\ . \tag{A.21}$$

where Γ is the half-bandwidth of the peak when $\varepsilon = \varepsilon_j/2$, expressed in eV.

SOS expression and conformational averaging

Once the functions for each absorption band are determined, the full spectra of each conformer a may be derived using a sum-over-states (SOS) expression:

$$\varepsilon(\lambda)_a = \sum_{j\neq 0}\varepsilon_j(\lambda)\ ; \tag{A.22}$$

$$\Delta\varepsilon(\lambda)_a = \sum_{j\neq 0}\Delta\varepsilon_j(\lambda)\ . \tag{A.23}$$

The last step in the determination of the theoretical spectra for a molecule is conformational averaging. The contribution of each conformer a to the overall spectrum of the molecule is dictated by its population at equilibrium, i.e. its

molar fraction χ_a, which can be determined by Boltzmann statistics from the calculated energies of conformers:

$$\chi_a = \frac{e^{-\Delta E_a / RT}}{\sum_{a=1}^{X} e^{-\Delta E_a / RT}} , \tag{A.24}$$

where ΔE_a is the relative energy of conformer a compared to the lowest-energy conformer, R is the gas constant, T is the absolute temperature in K and the sum extends over all X conformers.

The physical units of ΔE_a depend upon the units of R: hence, if $R = 1.9872041 \cdot 10^{-3}$ kcal K^{-1} mol^{-1}, then ΔE_a must be expressed in kcal mol^{-1}. Since the energy values are calculated for a single molecule and are expressed in hartrees, [a] the energy of a conformer in kcal mol^{-1} can be derived according to the following conversion:[12]

$$\begin{aligned} 1 \text{ Ha} &= \frac{N_A \cdot (4.35974434 \cdot 10^{-18} \text{ J Ha}^{-1})}{4184 \text{ J kcal}^{-1}} \text{ Ha} \\ &= 627.509474 \text{ kcal mol}^{-1} . \end{aligned} \tag{A.25}$$

The overall absorption spectra of the molecule are finally determined as the sum of the theoretical spectra of conformers weighted by their molar fraction:

$$\varepsilon(\lambda) = \sum_{a=1}^{X} \chi_a \varepsilon(\lambda)_a \ ; \tag{A.26}$$

$$\Delta\varepsilon(\lambda) = \sum_{a=1}^{X} \chi_a \Delta\varepsilon(\lambda)_a \ . \tag{A.27}$$

Optical rotatory dispersion

Equation 2.35 provided a tool to determine the specific rotatory power of a chiral molecule at a specific frequency when all the rotational strengths of its transition are known: in other words, equation 2.35 is already a SOS expression. On this basis, the optical rotatory dispersion (ORD) spectrum of each conformer a can be derived by using an appropriate Lorentzian line shape function for dispersion, $L_j(\nu)$: this function must be in a Kronig-Kramers (KK) relationship with the Lorentzian line shape function for absorption, whose general form is shown in

[a] The hartree (Ha) is the atomic unit for energy. 1 Ha = $4.35974434 \cdot 10^{-18}$ J.

equation A.3. $L_j(\nu)$ is given by:

$$L_j(\nu) = \frac{1}{\nu}\left(\frac{\nu_j - \nu}{(\nu_j - \nu)^2 + \Gamma^2} - \frac{\nu_j + \nu}{(\nu_j + \nu)^2 + \Gamma^2}\right) \; ; \tag{A.28}$$

in this equation Γ is a damping factor, whose meaning is analogous to the half-bandwidth of absorption bands; accordingly, equation 2.35 becomes:

$$\begin{aligned}[\alpha](\nu)_a &= 4800\frac{\pi N_A \nu^2}{hcM}\sum_{j\neq 0}\left[L_j(\nu)R_j\right] \\ &= 4800\frac{\pi N_A \nu}{hcM}\sum_{j\neq 0}\left[\left(\frac{\nu_j - \nu}{(\nu_j - \nu)^2 + \Gamma^2} - \frac{\nu_j + \nu}{(\nu_j + \nu)^2 + \Gamma^2}\right)R_j\right] \; .\end{aligned} \tag{A.29}$$

For $\Gamma \to 0$, equation A.29 reverts to equation 2.35, since:

$$\lim_{\Gamma\to 0} f_j(\nu) = \frac{2}{\nu_j^2 - \nu^2} \; . \tag{A.30}$$

The conversion of equation A.29 to the wavelength domain yields the ORD spectrum of conformer a:

$$\begin{aligned}[\alpha](\lambda)_a = &\frac{4.57481\cdot 10^3}{M}\frac{1}{\lambda}\cdot\sum_{j\neq 0}\left[\left(\frac{\frac{\lambda-\lambda_j}{\lambda\lambda_j}}{\left(\frac{\lambda-\lambda_j}{\lambda\lambda_j}\right)^2 + (8.06554\cdot 10^{-4}\,\Gamma)^2} - \right.\right. \\ &\left.\left. - \frac{\frac{\lambda+\lambda_j}{\lambda\lambda_j}}{\left(\frac{\lambda+\lambda_j}{\lambda\lambda_j}\right)^2 + (8.06554\cdot 10^{-4}\,\Gamma)^2}\right)R_j\right] \; ,\end{aligned} \tag{A.31}$$

where Γ is in eV; usually, Γ is set to the same value as $\Delta\sigma$, hence the conversion allows to use the same parameter for both dispersion and absorption spectra.

The theoretical ORD spectrum of the whole molecule is then derived by conformational averaging based on the Boltzmann population of conformers:

$$[\alpha](\lambda) = \sum_{a=1}^{X}\chi_a\,[\alpha](\lambda)_a \; . \tag{A.32}$$

A.2 Conformational analysis

The analysis of the conformational space of a molecule is concerned with the investigation of the preferred three-dimensional arrangements of atoms at equilibrium: the resulting geometries are called conformers. In order to describe the geometry of conformers, a set of geometric parameters, defined by the position of atoms in the molecule, must be evaluated. Usually, these parameters describe the distance between two atoms (e.g., bond lengths), the plane angle defined by three atoms (e.g., bond angles) or the dihedral angle defined by four atoms (sometimes called torsion angles). When atom positions are defined in a three-dimensional Cartesian coordinate system, such parameters can be calculated using simple vector algebra.

Atom distances

If the position of atom A is defined by Cartesian coordinates x_A, y_A and z_A, then a position vector $\mathbf{r}_A$ can be defined as the vector connecting the origin of the coordinate system to the actual position of the atom:

$$\mathbf{r}_A = x_A\mathbf{i} + y_A\mathbf{j} + z_A\mathbf{k} \,, \tag{A.33}$$

where $\mathbf{i}$, $\mathbf{j}$ and $\mathbf{k}$ are the unit versors of the coordinate system along the x-, y- and z-directions, respectively. The length of the position vector is then determined by:

$$\|\mathbf{r}_A\| = \sqrt{x_A^2 + y_A^2 + z_A^2} \,. \tag{A.34}$$

Similarly, the distance between two atoms A and B can be defined by a distance vector $\mathbf{d}_{AB}$ connecting the two atoms and equal to the difference between the two position vectors $\mathbf{r}_B$ and $\mathbf{r}_A$:

$$\begin{aligned} \mathbf{d}_{AB} &= \mathbf{r}_B - \mathbf{r}_A \\ &= (x_B - x_A)\mathbf{i} + (y_B - y_A)\mathbf{j} + (z_B - z_A)\mathbf{k} \\ &= x_{AB}\mathbf{i} + y_{AB}\mathbf{j} + z_{AB}\mathbf{k} \,, \end{aligned} \tag{A.35}$$

where $x_{AB} = x_B - x_A$, $y_{AB} = y_B - y_A$ and $z_{AB} = z_B - z_A$ are the coordinates of the position vector corresponding to $\mathbf{d}_{AB}$, [b] whose length is then determined

[b] Each vector has a corresponding position vector, starting from the origin and having the same length and direction, which is obtained by translation of the vector to the origin.

similarly to equation A.34:

$$d_{AB} = \|\mathbf{d}_{AB}\| = \sqrt{x_{AB}^2 + y_{AB}^2 + z_{AB}^2} \,. \tag{A.36}$$

Plane angles

Following the same framework, a plane angle defined by three atoms A, B and C can be described as the angle α between the two distance vectors $\mathbf{d}_{AB}$ and $\mathbf{d}_{BC}$. A mathematical expression of α is then provided by the dot product of $\mathbf{d}_{AB}$ and $\mathbf{d}_{BC}$, defined as:

$$\begin{aligned} \mathbf{d}_{AB} \cdot \mathbf{d}_{BC} &= d_{AB}\, d_{BC} \cos\alpha \\ &= x_{AB}x_{BC} + y_{AB}y_{BC} + z_{AB}z_{BC} \,, \end{aligned} \tag{A.37}$$

where $0 \leq \alpha \leq \pi$. Knowing the position coordinates of A, B and C, α can therefore be calculated using the following expression:

$$\begin{aligned} \alpha &= \arccos \frac{\mathbf{d}_{AB} \cdot \mathbf{d}_{BC}}{d_{AB}\, d_{BC}} \\ &= \arccos \frac{x_{AB}x_{BC} + y_{AB}y_{BC} + z_{AB}z_{BC}}{\sqrt{x_{AB}^2 + y_{AB}^2 + z_{AB}^2}\,\sqrt{x_{BC}^2 + y_{BC}^2 + z_{BC}^2}} \,. \end{aligned} \tag{A.38}$$

Dihedral angles

In geometry, a dihedral angle is the angle between two planes. Consequently, a dihedral angle defined by four atoms A, B, C and D can be described as the angle θ between the two half-planes ABC and BCD; according to this definition, the atoms B and C lie on the line of intersection of the two planes, while the atoms A and D define the direction of propagation of the two half-planes originating from the line of intersection.

Geometrically, the dihedral angle between two planes is equal to the angle between the normal vectors to their surface. A mathematical expression of the normal vector $\mathbf{p}_{ABC}$ to a plane, given three points A, B and C lying on that plane, is given by the cross product of the distance vectors $\mathbf{d}_{AB}$ and $\mathbf{d}_{BC}$, defined as:

$$\begin{aligned} \mathbf{p}_{ABC} &= \mathbf{d}_{AB} \times \mathbf{d}_{BC} \\ &= (y_{AB}z_{BC} - z_{AB}y_{BC})\mathbf{i} + (z_{AB}x_{BC} - x_{AB}z_{BC})\mathbf{j} + (x_{AB}y_{BC} - y_{AB}x_{BC})\mathbf{k} \\ &= x_{ABC}\mathbf{i} + y_{ABC}\mathbf{j} + z_{ABC}\mathbf{k} \,, \end{aligned} \tag{A.39}$$

where the short-hand notations $x_{ABC} = y_{AB}z_{BC} - z_{AB}y_{BC}$, $y_{ABC} = z_{AB}x_{BC} - x_{AB}z_{BC}$ and $z_{ABC} = x_{AB}y_{BC} - y_{AB}x_{BC}$ denote the coordinates of the position vector corresponding to the normal vector $\mathbf{p}_{ABC}$.

The dihedral angle θ can therefore be determined as the dot product of the two normal vectors to planes ABC and BCD:

$$\begin{aligned}(\mathbf{d}_{AB} \times \mathbf{d}_{BC}) \cdot (\mathbf{d}_{BC} \times \mathbf{d}_{CD}) &= p_{ABC}\, p_{BCD} \cos\theta \\ &= x_{ABC}x_{BCD} + y_{ABC}y_{BCD} + z_{ABC}z_{BCD}\ , \end{aligned} \tag{A.40}$$

where $-\pi < \alpha \leq \pi$.

The direction of the normal vectors $\mathbf{p}_{ABC}$ and $\mathbf{p}_{BCD}$ depend upon the direction of the distance vectors $\mathbf{d}_{AB}$, $\mathbf{d}_{BC}$ and $\mathbf{d}_{CD}$, i.e. the order of A, B, C and D rules the orientation of the normal vectors and, consequently, determines the sign of θ.

The periodicity of the inverse cosine function needed to calculate θ from equation A.40, however, does not allow the straightforward determination of the sign of θ. For this purpose, an auxiliary dot product can be defined:

$$\begin{aligned}(\mathbf{d}_{AB} \times \mathbf{d}_{BC}) \cdot \mathbf{d}_{CD} &= p_{ABC}\, d_{CD} \cos\theta' \\ &= x_{ABC}x_{CD} + y_{ABC}y_{CD} + z_{ABC}z_{CD}\ , \end{aligned} \tag{A.41}$$

where $\theta' = \theta + \dfrac{\pi}{2}$, since the distance vector $\mathbf{d}_{CD}$ is orthogonal to the cross product vector $\mathbf{p}_{BCD}$; consequently, $\cos\theta' = \sin\theta$.

It follows that θ and the auxiliary dot product have the same sign in the range $(-\pi, \pi)$; the solutions to equation A.40 can then be written as:

$$\theta = \mathrm{pv}\ \arccos\frac{\mathbf{p}_{ABC} \cdot \mathbf{p}_{BCD}}{p_{ABC}\, p_{BCD}} \qquad \text{for } \mathbf{p}_{ABC} \cdot \mathbf{d}_{CD} \geq 0\ ; \tag{A.42}$$

$$\theta = -\mathrm{pv}\ \arccos\frac{\mathbf{p}_{ABC} \cdot \mathbf{p}_{BCD}}{p_{ABC}\, p_{BCD}} \qquad \text{for } \mathbf{p}_{ABC} \cdot \mathbf{d}_{CD} < 0\ , \tag{A.43}$$

where pv denotes the principal value of the inverse cosine function, which is defined in the range $[0, \pi]$.

A.3 Shell scripting

The mathematical tools reviewed in the previous section were implemented in a set of UNIX shell scripts, with the aim of developing reliable routines to process the structural and spectroscopic data from the output of MM and QM calculations. Three UNIX scripts were developed:

a. INPUTGEN processes the output files from MM calculations performed with Spartan'02, DFT geometry optimisation calculations performed with Gaussian 09 and XYZ coordinate files, in order to generate the input files needed for further calculations (geometry optimisations, frequency, VCD, OR and ECD). Moreover, INPUTGEN processes energy data, generates reports on the thermodynamic equilibrium between conformers according to Boltzmann statistics (equation A.24, defines energy thresholds and checks for imaginary frequencies.

b. OUTECD processes the output files from ECD calculations performed with Gaussian 09, in order to retrieve the calculated transition energies, oscillator strengths and rotational strengths and generate the corresponding theoretical ECD, UV and ORD spectra through SOS expressions (equations A.22, A.23 and A.31). OUTECD is also able to perform conformational averaging (equations A.26, A.27 and A.32) when thermodynamic data are available from INPUTGEN.

c. CONFANAL performs a conformational analysis on the input files of Gaussian 09, in order to retrieve the relevant atom distances, plane angles and dihedral angles of conformers (equations A.36, A.38, A.42 and A.43).

The scripts employ standard UNIX utilities to perform their tasks (`ls`, `mv`, `rm`, `wc`, `for` loops, `if` statements, `cat`, `echo`, `gawk`, `grep`, `sed`, `nl`, `sort`, `tail`, `seq`, `paste`, `expr`, `csplit`); INPUTGEN also requires UNIX filesystem permissions for the execution of `chmod`, while OUTECD requires an external package, `gnuplot`, to generate theoretical spectra.

The file names of input and output files for QM calculations have been standardised, allowing to identify them unambiguously. The scripts conform to this standard and automatically generate appropriate file names according to user-defined variables, but require processed files to comply to this standard. The file names contain the following information:

a. a molecule tag identifying the structure and the level of theory employed;

b. a conformer ID tag;

c. a solvation tag identifying the implicit solvation model employed;

d. a type tag identifying the calculation (optimisation, frequency, VCD, OR or ECD).

Each script is commented to explain the tasks performed during the routines.

INPUTGEN

(*Last updated: 10 March 2014*)

```
#!/bin/sh
#
# USER GUIDE
# ----------
#
# INPUTGEN is an interactive shell script which generates the input files (*.com) for DFT calculations
# of theoretical chiroptical properties by Gaussian09.
#
# Four types of calculations (jobs) are supported:
# 1) geometry optimisation followed by frequency calculations (opt-freq)
# 2) geometry optimisation followed by VCD calculations (opt-vcd)
# 3) OR calculations (optrot)
# 4) ECD calculations (ecd)
#
# For geometry optimisations, the source files can be Spartan'02 binary files (*.Conformers1.spartan),
# Spartan'02 archive files (*.sparchive), or *.xyz coordinates.
# Coordinates are automatically converted from atomic units (bohr) to angstroms.
# For chiroptical properties calculations, the source files are the Gaussian output files from
# geometry optimisation (*.log).
#
# INPUTGEN processes the energy data from MM conformational searches and QM geometry optimisations.
# Energies for each conformer are processed and listed in text tables (*_energies-*.txt).
# Input files are only generated for those conformers having relative energies below a certain threshold.
# For MM conformers, this threshold is default to 5 kcal/mol.
# For QM energies, Boltzmann distributions and conformer populations at 298.15 K and 1 bar are calculated.
# The QM energy threshold is user-defined and can be based upon electronic (SCF) or free energies.
# INPUTGEN automatically discards the generation of input files for structures with imaginary frequencies.
#
# Additional output files with energies and Boltzmann populations are created for the generation of
# theoretical ECD spectra by Gnuplot.
# These additional files are used together with the processed ECD data obtained with the script OUTECD.
#
# The *.com files are named following this scheme:
# (molecule tag)-(conformer ID)-(solvation tag)-(job tag).com
#
# In this way, every file has a unique name and it becomes easy to understand the type of calclation
# from the name of the file.
# IMPORTANT: The generation of OR and ECD *.com files requires the *.log files from geometry optimisations
# to follow this naming scheme.
#
# INPUTGEN asks the user to declare the options needed for the generation of input files and stores the
      information
# in a text file (input_$job).
# If an input_$job file is present in the directory, the script retrieves all the options without user
      intervention.
#
# ------------------------------------------------
# FLAGS:
# -----
# Two types of flags are defined to setup the input generation. These must be declared in the following order:
#
#  1) Definition of the job type for which *.com files must be generated (NECESSARY). Four options are
      available:
#     f : geometry optimisation followed by frequency calculations (opt-freq)
#     v : geometry optimisation followed by VCD calculations (opt-vcd)
#     o : OR calculations (optrot)
#     e : ECD calculations (ecd)
#     The appropriate keywords will be added to the Route section of the *.com file, and the tag will be used
#     to name the *.com files.
```

```
#
#  2) Type of energy threshold (NECESSARY for OR and ECD calculations, DO NOT USE with geometry optimisations).
#     Two options are available:
#     s : electronic (SCF) energies
#     g : free (G) energies
#     INPUTGEN will show 5 different thresholds, with the number of conformers and the sum of conformer
      populations
#     within those thresholds.
#     Any positive value of relative energy (in kcal/mol) can be defined as threshold.

echo ""
echo "############################################################"
echo "##                                                        ##"
echo "##                      INPUTGEN v2.0                     ##"
echo "##   Input generator for QM calculations in Gaussian09    ##"
echo "##                                                        ##"
echo "############################################################"
echo "* * * * * * *  Daniele Tedesco - 06 Feb 2013  * * * * * * *"
echo "------------------------------------------------------------"

jobflag=$1

if [ -z $jobflag ]
 then
  echo ""
  echo "WARNING! No job type declared!"
  echo "Please use the appropriate flags (f/v/o/e)."
  echo "Exiting."
  echo ""
  exit 0
fi

if [ $jobflag = f ]
 then
  job=opt-freq
 elif [ $jobflag = v ]
 then
  job=opt-vcd
 elif [ $jobflag = o ]
 then
  job=optrot
 elif [ $jobflag = e ]
 then
  job=ecd
 else
  echo ""
  echo "WARNING! Invalid job type declared!"
  echo "Please use the appropriate flags (f/v/o/e)."
  echo "Exiting."
  echo ""
  exit 0
fi

if [ $job = ecd -o $job = optrot ]
 then
  hold=$2

  if [ -z $hold ]
   then
    echo ""
    echo "Choose the type of energy threshold to be used for data processing"
    echo -n "(s for electronic energies or g for free energies): "
    read hold
   elif [ $hold != s ] && [ $hold != g ]
   then
    echo ""
    echo "Choose the type of energy threshold to be used for data processing"
    echo -n "(s for electronic energies or g for free energies): "
    read hold
  fi

  if [ $hold = s ]
   then
    echo ""
    echo "Conformational averaging based on SCF energies."
    echo ""
   elif [ $hold = g ]
```

```
   then
    echo ""
    echo "Conformational averaging based on G energies."
    echo ""
  fi

fi

# INPUTGEN looks for the input_$job file.
# If found, it retrieves the options automatically and returns the options to stdout.
if [ -f input_$job ]
 then

  # REQUIRED OPTIONS:
  # ----------------
  # A user-defined tag for the set of calculations, which may define the molecule and the level of theory used.
  # This tag will be used to name and distinguish the files for different sets of calculations.
  moltag=`awk 'NR==2' input_$job`
  echo "Calculation tag: $moltag"

  # A full-length description of the molecule, which will be used in the Title section of the *.com file.
  molfull=`awk 'NR==4' input_$job`
  echo "Molecule full name: $molfull"

  # A tag for implicit solvation models.
  # The standard model for Gaussian calculations is IEFPCM.
  # Some predefined tags are used to declare the solvent used for IEFPCM:
  # gas = no IEFPCM, gas phase calculations
  # meoh = methanol
  # iproh = 2-propanol
  # chcl3 = chloroform
  # The extended keyword will be added to the Route section of the *.com file
  # and the tag will be added to the name of the *.com file.
  soltag=`awk 'NR==6' input_$job`

  if [ $soltag = gas ]
   then
    solfun=gas
   elif [ $soltag = meoh ]
   then
    solfun=methanol
   elif [ $soltag = iproh ]
   then
    solfun=2-propanol
   elif [ $soltag = chcl3 ]
   then
    solfun=chloroform
   elif [ $soltag = dmso ]
   then
    solfun=dimethylsulfoxide
   else
    echo -n "   Specify solvation call function: "
    read solfun
    echo ""
  fi

  echo "Environment: $soltag -- $solfun"

  # The memory and CPU requirements for the calculation,
  # which will be added to the Link 0 section of the *.com file.
  memreq=`awk 'NR==8' input_$job`
  echo "Memory requirements (e.g. 72GB): $memreq"

  cpureq=`awk 'NR==10' input_$job`
  echo "CPU requirements: $cpureq"

  # The Gaussian09 call function for the DFT functional to be used in the calculation
  # (refer to the Gaussian09 manual for a list of available functionals).
  dftfun=`awk 'NR==12' input_$job`
  echo "Functional call function: $dftfun"

  # The Gaussian09 call function for the basis set to be used in the calculation
  # (refer to the Gaussian09 manual for a list of available basis sets).
  # User-defined basis sets can be requested by the keyword "gen".
  basisset=`awk 'NR==14' input_$job`
  echo "Basis set call function: $basisset"
```

```
# If a user-defined basis set is required, the file where the specifications of the basis set are stored
# must be declared.
# The basis set file must be in the same directory as INPUTGEN and will be added at the end of the *.com file
    .
bsspec=`awk 'NR==16' input_$job`
echo "Basis set specs: $bsspec"

# A full-length description of the level of theory used in the calculation, which will be added in the
# Title section of the *.com file.
theory=`awk 'NR==18' input_$job`
echo "Functional/Basis set description: $theory"

# JOB-DEPENDENT OPTIONS:
# ----------------------
if [ $job = ecd ]
 then

  # The population of excited states for ECD calculations.
  pecd=`awk 'NR==20' input_$job`
  if [ $pecd != n ]
   then
    pop=$pecd
   else
    pop=none
  fi
  echo "Population of excited states: $pecd -- $pop"

  # The number of excited states to be computed for ECD calculations.
  excst=`awk 'NR==22' input_$job`
  echo "Number of excited states: $excst"

 elif [ $job = optrot ]
 then

  # The population of excited states for OR calculations.
  pord=`awk 'NR==20' input_$job`
  if [ $pord != m ]
   then
    pop=$pord
   else
    pop=minimal
  fi
  echo "Population of excited states: $pord -- $pop"

  # The wavelength at which the specific rotatory power is calculated.
  owl=`awk 'NR==22' input_$job`
  if [ $owl != d ]
   then
    orwl=$owl
   else
    orwl=589.3nm
  fi
  echo "Wavelength of interest: $owl -- $orwl"

 else

  # Turn on the density fitting (resolution of identity) approximation.
  # This feature is only available for pure, non-hybrid DFT functionals on Gaussian09.
  denfit=`awk 'NR==20' input_$job`
  if [ $denfit = y ]
   then
    echo "Density fitting: yes"
   else
    echo "Density fitting: no"
  fi
fi

# If input_$job is not available, INPUTGEN switches to user intervention and stores the options in input_$job.
else

 echo -n "Calculation tag: "
 read moltag
 echo "# moltag = " > input_$job
 echo "$moltag" >> input_$job

 echo -n "Molecule full name: "
 read molfull
```

```
285   echo "# molfull = " >> input_$job
      echo "$molfull" >> input_$job

      echo -n "Environment tag: "
      read soltag
290   if [ $soltag = gas ]
       then
        solfun=gas
       elif [ $soltag = meoh ]
       then
295     solfun=methanol
       elif [ $soltag = iproh ]
       then
        solfun=2-propanol
       elif [ $soltag = chcl3 ]
300    then
        solfun=chloroform
       elif [ $soltag = dmso ]
       then
        solfun=dimethylsulfoxide
305    else
        echo -n "   Specify solvation call function: "
        read solfun
        echo ""
      fi
310   echo "# soltag = " >> input_$job
      echo "$soltag" >> input_$job
      echo "    $solfun"

      echo -n "Memory requirements (e.g. 72GB): "
315   read memreq
      echo "# memreq = " >> input_$job
      echo "$memreq" >> input_$job

      echo -n "CPU requirements: "
320   read cpureq
      echo "# cpureq = " >> input_$job
      echo "$cpureq" >> input_$job

      echo -n "Functional call function: "
325   read dftfun
      echo "# dftfun = " >> input_$job
      echo "$dftfun" >> input_$job

      echo -n "Basis set call function: "
330   read basisset
      echo "# basisset = " >> input_$job
      echo "$basisset" >> input_$job

      if [ $basisset = gen ]
335    then
        echo -n "Basis set specs: "
        read bsspec
      fi
      echo "# bsspec = " >> input_$job
340   echo "$bsspec" >> input_$job

      echo -n "Functional/Basis set description: "
      read theory
      echo "# theory = " >> input_$job
345   echo "$theory" >> input_$job

      if [ $job = ecd ]
       then
        echo -n "Population of excited states (n=none): "
350     read pecd
        echo "# pecd = " >> input_$job
        echo "$pecd" >> input_$job
        if [ $pecd != n ]
         then
355       pop=$pecd
         else
          pop=none
        fi
        echo "    $pop"
360
        echo -n "Number of excited states: "
```

```
      read excst
      echo "# excst = " >> input_$job
      echo "$excst" >> input_$job

    elif [ $job = optrot ]
    then
      echo -n "Population of excited states (m=minimal): "
      read pord
      echo "# pord = " >> input_$job
      echo "$pord" >> input_$job
      if [ $pord != m ]
       then
        pop=$pord
       else
        pop=minimal
      fi
      echo "    $pop"

      echo -n "Wavelength of interest (d=589.3nm): "
      read owl
      echo "# owl = " >> input_$job
      echo "$owl" >> input_$job
      if [ $owl != d ]
       then
        orwl=$owl
       else
        orwl=589.3nm
      fi
      echo "    $orwl"

    else
      echo -n "Use density fitting (available only for pure, non-hybrid DFT functionals)? (y/n) "
      read denfit
      echo "# denfit = " >> input_$job
      echo "$denfit" >> input_$job
   fi

fi
echo ""
echo -n "Specify charge and multiplicity of the molecule in Gaussian format: "
read charmulti
echo ""

# INPUT FILES GENERATION:
# -----------------------
# GEOMETRY OPTIMISATION:

if [ $job = opt-freq -o $job = opt-vcd ]
 then
  echo "Input files for geometry optimisations are being processed ..."
  echo ""

  # Check for the existence of a Spartan'02 binary file
  spartan=`ls *.spartan | wc -l`

  if [ $spartan = 1 ]
   then
    echo "Generating xyz files from Spartan'02 MM conformational search file..."
    echo ""

    # Retrieve the name of the binary file
    inpfile=`ls *.spartan | sed "s/.Conformers1.spartan//"`

    # Retrieve the number of atoms of the molecule
    natoms=`grep -a "MECH" $inpfile.Conformers1.spartan | awk 'END{print $1}'`

    # Set up the conversion file from binary to text
    echo "start" > $inpfile-all.txt
    echo "--" >> $inpfile-all.txt

    # Retrieve all the energies and coordinates of the MM conformers from the binary file
    grep -a "GEOMETRY2" -B 1 -A $natoms $inpfile.Conformers1.spartan >> $inpfile-all.txt

    # Split the coordinate text file in numbered text files, one for each MM conformer
    csplit -ks -f mol -n 3 $inpfile-all.txt /--/ {*}
    rm mol000 $inpfile-all.txt
    tstruct=`ls mol* | wc -l`
```

```
    for n in `seq -f 'mol%03g' 1 $tstruct`
    do
      mv $n $n.tmp
      # Retrieve energies for each MM conformer
      awk -v NAME=$n '(NR==2){printf "%s\t%s\n",NAME,$1}' $n.tmp >> mm_energies1.txt
    done

    # Clean up coordinate files
    sed -i -e "1,3d" mol*.tmp
    sed -i -e "s/
//g" mol*.tmp

    # Calculate relative energies and order conformers upon increasing energies
    mmmin=`awk 'min=="" || $2 < min {min=$2} END{print min}' mm_energies1.txt`
    awk -v MIN=$mmmin '{printf "%.9f\t%s\t%.9f\n",$2-MIN,$1,$2}' mm_energies1.txt > mm_energies2.txt
    sort -n mm_energies2.txt | awk '{printf "%s\t%.9f\t%.9f\n",$2,$3,$1}' > mm_energies1.txt
    rm mm_energies2.txt

    # Select MM conformers within a threshold of 5 kcal/mol and remove duplicate conformations
    echo -n "Energy threshold (kcal/mol): "
    read mmthresh
    awk -v MMTHR=$mmthresh '
        ($3 < MMTHR){printf "%s\t%s\n",$0,p;p=$3}
        ' mm_energies1.txt | awk '
                                {printf "%s\t%.9f\n",$1,$3-$4}
                                ' | awk '
                                        (NR==1){print $1}; ($2 > 0.00000005){print $1}
                                        ' > renametmp.txt
    rename=`cat renametmp.txt | wc -l`

    # Set up energy table for MM conformers
    echo "Energy values for the MM conformational search on $moltag" > ${moltag}_energies-mm.txt
    echo -e "MM Conf.\t\$E\$ (kcal mol\$^{-1}\$)\t\$\\Delta E\$ (kcal mol\$^{1}\$)\tQM ID tag" >> ${moltag}
          _energies-mm.txt
    awk -v MMTHR=$mmthresh '
        ($3 < MMTHR){printf "%s\t%s\n",$0,p;p=$3}
        ' mm_energies1.txt | awk '
                                {printf "%s\t%s\t%s\t%.9f\n",$1,$2,$3,$3-$4}
                                ' | awk '
                                        BEGIN{FS="\t"};
                                        (NR==1){printf "%s\t%.4f\t%.4f\n",$1,$2,$3};
                                        ($4 > 0.00000005){printf "%s\t%.4f\t%.4f\n",$1,$2,$3}
                                        ' >> mm_energies3.txt

    # Rename selected MM conformers to the new QM ID tag
    for m in `seq -f '%02g' 1 $rename`
    do
      awk -v REN=$m '
          (NR==REN){print "mv "$1".tmp "REN".bohr"}
          ' renametmp.txt >> renametmp.sh
      awk -v REN=$m '
          BEGIN{FS="\t"};
          (NR==REN){print $0,"c"REN}
          ' mm_energies3.txt >> ${moltag}_energies-mm.txt
    done
    chmod +x renametmp.sh
    ./renametmp.sh
    rm renametmp.* *.tmp mm_energies3.txt

    # Create list of conformers
    ls *.bohr | sed "s/.bohr//" > conflist.tmp

    # Convert coordinates from atomic units (bohr) to angstrom
    for m in `seq -f '%02g' 1 $rename`
    do
      awk '
          {printf "%3s\t%.6f\t%.6f\t%.6f\n",
                  $1,$2*0.52917721092,$3*0.52917721092,$4*0.52917721092}
          ' $m.bohr > $m.tmp

      # Create *.xyz files
      awk -v ATOM=$natoms -v FILE=$inpfile -v STRU=$m '
          BEGIN{printf "%s\n%s, conf. %s\n",ATOM,FILE,STRU};
          {printf "%3s%15s%15s%15s\n",$1,$2,$3,$4}
          ' $m.tmp > $m.xyz
      rm $m.tmp $m.bohr
```

```
    done

  # If the binary file is not found, check for the existence of Spartan'02 archive files
  elif [ $spartan = 0 ]
  then
   sparch=`ls *.sparchive | wc -l`
   if [ $sparch != 0 ]
    then

     # Clean up archive files
     sed -i -e "s/
//g" *.sparchive

     # Create list of conformers
     ls *.sparchive | sed "s/.sparchive//" > conflist.tmp

     # Convert coordinates from bohr to angstrom
     for m in `seq 1 $sparch`
     do
       confnum=`awk -v NUM=$m '(NR==NUM){print $1}' conflist.tmp`
       natoms=`grep 'MECH' $confnum.sparchive | awk 'END{print $1}'`
       tail -n $natoms $confnum.sparchive >> $confnum.bohr
       awk '
           {printf "%3s\t%.6f\t%.6f\t%.6f\n",
                   $1,$2*0.52917721092,$3*0.52917721092,$4*0.52917721092}
           ' $confnum.bohr > $confnum.tmp

       # Create *.xyz files
       awk -v ATOM=$natoms -v FILE=$inpfile -v STRU=$m '
           BEGIN{printf "%s\n%s, conf. %s\n",ATOM,FILE,STRU};
           {printf "%3s%15s%15s%15s\n",$1,$2,$3,$4}
           ' $confnum.tmp > $confnum.xyz
       rm $confnum.sparchive $confnum.bohr $confnum.tmp
     done

    # If Spartan'02 files are not found, retrieve conformer list from *.xyz files
    else
     ls *.xyz | sed "s/.xyz//" > conflist.tmp
   fi
  fi

  # Retrieve list of conformers and create *.com files for each of them
  nmax=`cat conflist.tmp | wc -l`

  for h in `seq 1 $nmax`
  do
    num=`awk -v NUM=$h '(NR==NUM){print $1}' conflist.tmp`
    outfile=$moltag-c$num-$soltag-${job}01

    # Retrieve number of atoms from *.xyz file
    atoms=`awk '(NR==1){print $1}' $num.xyz`

    # Create Link = section of *.com file
    echo "%rwf=.chk/$outfile.rwf" > $outfile.com
    echo "%NoSave" >> $outfile.com
    echo "%chk=.chk/$outfile.chk" >> $outfile.com
    echo "%mem=$memreq" >> $outfile.com
    echo "%nprocshared=$cpureq" >> $outfile.com

    # Create Route section of *.com file
    if [ $solfun = gas ]
     then
      echo "# $dftfun/$basisset opt freq" >> $outfile.com
     else
      echo "# $dftfun/$basisset opt freq scrf=(iefpcm,solvent=$solfun)" >> $outfile.com
    fi
    echo "" >> $outfile.com

    # Create Title section of *.com file
    echo "$molfull, conf. $num (MMFF) - $job, $solfun, $theory" >> $outfile.com
    echo "" >> $outfile.com

    # Create Molecule specification section of *.com file from xyz coordinates
    echo "$charmulti" >> $outfile.com
    tail -n $atoms $num.xyz >> $outfile.com

    # Retrieve user-defined basis set if necessary
```

```
    if [ $basisset = gen ]
     then
      cat ~/bin/$bsspec.gbs >> $outfile.com
     else
      echo "" >> $outfile.com
      echo "" >> $outfile.com
      echo "" >> $outfile.com
      echo "" >> $outfile.com
      echo "" >> $outfile.com
      echo "" >> $outfile.com
    fi

    # Set VCD calculations
    if [ $job = opt-vcd ]
     then
      sed -i -e "s/opt freq/opt freq=vcd/g" $outfile.com
    fi

    # Set density fitting
    if [ $denfit = y ]
     then
      sed -i -e "s/opt freq/denfit opt freq/g" $outfile.com
    fi
    echo "Input file for conformer $num ready."
  done

 # -----------------------
 # CHIROPTICAL PROPERTIES:
 else

  # Process energy data
  echo "Calculating energies and Boltzmann populations ..."
  echo ""

  # Set up energy tables
  touch ${moltag}_scf-$soltag.txt
  touch ${moltag}_g-$soltag.txt
  echo "Energy values and Boltzmann populations for QM calculations on $moltag (Solvation: $solfun)" > ${moltag
       }_energ.txt
  echo "Conf." >> ${moltag}_energ.txt

  # Retrieve list of conformers from available *.log files
  ls $moltag-*.log | sed "s/$moltag-c//" | awk '
                                           BEGIN{ FS = "-"};
                                           {print $1}
                                           ' > conflist.tmp
  nmax=`cat conflist.tmp | wc -l`

  # Read data from the *.log file for each conformer in the list
  for h in `seq 1 $nmax`
  do
    num=`awk -v NUM=$h '(NR==NUM){print $1}' conflist.tmp`
    logfile=$moltag-c$num-$soltag-opt-*.log
    outfile=$moltag-c$num-$soltag-${job}01
    imagfreq=`grep "Frequencies" $logfile | awk '(NR==1){print $3}'`
    imagcheck=`echo $imagfreq | awk 'BEGIN{FS="."}; {print $1}'`

    # If the molecule has an imaginary frequency, skip the conformer
    if [ $imagcheck -lt 0 ]
     then
      echo "$logfile $imagfreq" >> imagfreq-$moltag-$soltag.txt
      echo "WARNING! Found imaginary frequency for conformer $num ($imagfreq). Skipping file."
     else

      # Create a new list of conformers without imaginary frequencies
      echo $num >> conflist2.tmp
      echo $num >> ${moltag}_energ.txt

      # Retrieve SCF energies for the optimised structures from *.log files
      grep "SCF Done" $logfile | awk -v NUM=${num} '
                                 END{print "E"NUM"="$5}
                                 ' >> ${moltag}_scf-$soltag.txt

      # Retrieve free energies from *.log files
      grep "Free Energies" $logfile | awk -v NUM=${num} '
                                      {print "G"NUM"="$NF}
                                      ' >> ${moltag}_g-$soltag.txt
```

```
  fi
done

# Set new list of conformers as default
nmax=`cat conflist2.tmp | wc -l`

# Find the minimum energies
scfmin=`awk 'BEGIN {FS = "="}; $2 < min {min=$2} END{print min}' ${moltag}_scf-$soltag.txt`
gmin=`awk 'BEGIN {FS = "="}; $2 < min {min=$2} END{print min}' ${moltag}_g-$soltag.txt`

# Calculate relative energies
awk -v MIN=${scfmin} '
    BEGIN {FS = "="};
    {printf "%.7f\t%.7f\n",$2,$2-MIN}
    ' ${moltag}_scf-$soltag.txt >> ${moltag}_scftab1-$soltag.txt
awk -v MIN=${gmin} '
    BEGIN {FS = "="};
    {printf "%.7f\t%.7f\n",$2,$2-MIN}
    ' ${moltag}_g-$soltag.txt >> ${moltag}_gtab1-$soltag.txt

# Print minumum energies
awk 'BEGIN {FS = "="}; $2 < min {min=$2;} END{print "Emin="min}
    ' ${moltag}_scf-$soltag.txt >> ${moltag}_scf-$soltag.txt
awk 'BEGIN {FS = "="}; $2 < min {min=$2;} END{print "Gmin="min}
    ' ${moltag}_g-$soltag.txt >> ${moltag}_g-$soltag.txt

# Print Boltzmann factors
awk '{printf "%.7f\t%.7f\t%.7f\n",$1,$2,exp(-1059.11471*$2)}
    ' ${moltag}_scftab1-$soltag.txt >> ${moltag}_scftab2-$soltag.txt
awk '{printf "%.7f\t%.7f\t%.7f\n",$1,$2,exp(-1059.11471*$2)}
    ' ${moltag}_gtab1-$soltag.txt >> ${moltag}_gtab2-$soltag.txt

# Print headers for tables
echo "" >> ${moltag}_scftab3-$soltag.txt
echo "" >> ${moltag}_gtab3-$soltag.txt
echo -e "\$E\$ (Ha)\t\$\\Delta E\$ (kcal mol\$^{1}\$)\t\$\\ chi\$ (%)" >> ${moltag}_scftab3-$soltag.txt
echo -e "\$G\$ (Ha)\t\$\\Delta G\$ (kcal mol\$^{1}\$)\t\$\\ chi\$ (%)" >> ${moltag}_gtab3-$soltag.txt

# Calculate partition functions
scfsum=`awk '{sum += $3} END{print sum}' ${moltag}_scftab2-$soltag.txt`
gsum=`awk '{sum += $3} END{print sum}' ${moltag}_gtab2-$soltag.txt`

# Print relative energies in kcal/mol and Boltzmann populations of conformers at 298 K and 1 bar
awk -v SUM=${scfsum} '
    {printf "%.8f\t%.3f\t%.2f\n",
            $1,$2*627.509474,$3*100/SUM}
    ' ${moltag}_scftab2-$soltag.txt >> ${moltag}_scftab3-$soltag.txt
awk -v SUM=${gsum} '
    {printf "%.6f\t%.3f\t%.2f\n",
            $1,$2*627.509474,$3*100/SUM}
    ' ${moltag}_gtab2-$soltag.txt >> ${moltag}_gtab3-$soltag.txt

# Create energy tables in text format
paste ${moltag}_energ.txt ${moltag}_scftab3-$soltag.txt ${moltag}_gtab3-$soltag.txt > ${moltag}_energies-
      $soltag.txt

# Delete temporary files
rm ${moltag}_scftab*.txt ${moltag}_gtab*.txt ${moltag}_energ.txt

# Create Gnuplot functions for the processing of theoretical ECD spectra:
# Boltzmann factors
for h in `seq $nmax`
do
  num=`awk -v NUM=$h '(NR==NUM){print $1}' conflist2.tmp`
  echo "P$num=exp(-1.05911471e3*(E$num-(Emin)))" >> ${moltag}_scf-$soltag.txt
  echo "P$num=exp(-1.05911471e3*(G$num-(Gmin)))" >> ${moltag}_g-$soltag.txt
done

# Partition functions
echo -n "Z=" >> ${moltag}_scf-$soltag.txt
echo -n "Z=" >> ${moltag}_g-$soltag.txt
for h in `seq 1 $nmax`
do
  num=`awk -v NUM=$h '(NR==NUM){print $1}' conflist2.tmp`
  echo -n "+P$num" >> ${moltag}_scf-$soltag.txt
  echo -n "+P$num" >> ${moltag}_g-$soltag.txt
```

```
done
echo "" >> ${moltag}_scf-$soltag.txt
echo "" >> ${moltag}_g-$soltag.txt

# Boltzmann populations
for h in `seq 1 $nmax`
do
  num=`awk -v NUM=$h '(NR==NUM){print $1}' conflist2.tmp`
  echo "q$num=P$num/Z" >> ${moltag}_scf-$soltag.txt
  echo "q$num=P$num/Z" >> ${moltag}_g-$soltag.txt
done

# Clean up Gnuplot functions
sed -i -e "s/=+/=/g" ${moltag}_scf-$soltag.txt
sed -i -e "s/=+/=/g" ${moltag}_g-$soltag.txt
sed -i -e "s/ //g" ${moltag}_scf-$soltag.txt
sed -i -e "s/ //g" ${moltag}_g-$soltag.txt
sed -i -e "s/=/ = /g" ${moltag}_scf-$soltag.txt
sed -i -e "s/=/ = /g" ${moltag}_g-$soltag.txt
echo "Done."
echo ""

# Show energies on screen
cat ${moltag}_energies-$soltag.txt
echo ""

# Define free energy threshold for *.com file generation
if [ $hold = g ]
 then
  echo "FREE ENERGY THRESHOLDS:"
  tail -n +3 ${moltag}_energies-$soltag.txt | awk '($6<1){print $0}
     ' | awk '{SUM += $7} END{print NR" conformers within 1.0 kcal/mol (population: "SUM"%)"}'
  tail -n +3 ${moltag}_energies-$soltag.txt | awk '($6<1.5){print $0}
     ' | awk '{SUM += $7} END{print NR" conformers within 1.5 kcal/mol (population: "SUM"%)"}'
  tail -n +3 ${moltag}_energies-$soltag.txt | awk '($6<2){print $0}
     ' | awk '{SUM += $7} END{print NR" conformers within 2.0 kcal/mol (population: "SUM"%)"}'
  tail -n +3 ${moltag}_energies-$soltag.txt | awk '($6<2.5){print $0}
     ' | awk '{SUM += $7} END{print NR" conformers within 2.5 kcal/mol (population: "SUM"%)"}'
  tail -n +3 ${moltag}_energies-$soltag.txt | awk '($6<3){print $0}
     ' | awk '{SUM += $7} END{print NR" conformers within 3.0 kcal/mol (population: "SUM"%)"}'
  echo ""

  # Set threshold value
  echo -n "Define energy threshold (in kcal/mol): "
  read thres
  echo ""

  # Create new list of conformers within energy threshold
  tail -n +3 ${moltag}_energies-$soltag.txt | sed "s/c//" | awk -v HOL=$thres '
                                                          ($6<HOL){print $1}
                                                          ' > conflist3.tmp
  # Set new list of conformers as default
  nmax=`cat conflist3.tmp | wc -l`
  echo "$nmax input files will be generated."

 # Define electronic energy threshold for *.com file generation
 elif [ $hold = s ]
 then
  echo "ELECTRONIC ENERGY THRESHOLDS:"
  tail -n +3 ${moltag}_energies-$soltag.txt | awk '($3<1){print $0}
     ' | awk '{SUM += $4} END{print NR" conformers within 1.0 kcal/mol (population: "SUM"%)"}'
  tail -n +3 ${moltag}_energies-$soltag.txt | awk '($3<1.5){print $0}
     ' | awk '{SUM += $4} END{print NR" conformers within 1.5 kcal/mol (population: "SUM"%)"}'
  tail -n +3 ${moltag}_energies-$soltag.txt | awk '($3<2){print $0}
     ' | awk '{SUM += $4} END{print NR" conformers within 2.0 kcal/mol (population: "SUM"%)"}'
  tail -n +3 ${moltag}_energies-$soltag.txt | awk '($3<2.5){print $0}
     ' | awk '{SUM += $4} END{print NR" conformers within 2.5 kcal/mol (population: "SUM"%)"}'
  tail -n +3 ${moltag}_energies-$soltag.txt | awk '($3<3){print $0}
     ' | awk '{SUM += $4} END{print NR" conformers within 3.0 kcal/mol (population: "SUM"%)"}'
  echo ""

  # Set threshold value
  echo -n "Define energy threshold (in kcal/mol): "
  read thres
  echo ""

  # Create new list of conformers within energy threshold
```

```
  tail -n +3 ${moltag}_energies-$soltag.txt | sed "s/c//" | awk -v HOL=$thres '
                                                          ($3<HOL){print $1}
                                                          ' > conflist3.tmp
  # Set new list of conformers as default
  nmax=`cat conflist3.tmp | wc -l`
  echo "$nmax input files will be generated."
fi
echo ""

# Create *.com file for each conformer in the list
if [ $job = ecd ]
 then
  echo "Input files for ECD calculations are being processed ..."
 elif [ $job = optrot ]
 then
  echo "Input files for OR calculations are being processed ..."
fi
echo ""

for h in `seq $nmax`
do
  num=`awk -v NUM=$h '(NR==NUM){print $1}' conflist3.tmp`
  logfile=$moltag-c$num-$soltag-opt-*.log
  outfile=$moltag-c$num-$soltag-${job}01
  imagfreq=`grep "Frequencies" $logfile | awk '(NR==1){print $3}'`

  # Retrieve number of atoms from *.log file
  atoms=`grep "NAtoms=" $logfile | awk 'END{print $2}'`

  # Line offset for retrieving optimised coordinates from *.log files
  matom=`expr $atoms + 4`

  # Create Link 0 section of *.com files
  echo "%rwf=.chk/$outfile.rwf" > $outfile.com
  echo "%NoSave" >> $outfile.com
  echo "%chk=.chk/$outfile.chk" >> $outfile.com
  echo "%mem=$memreq" >> $outfile.com
  echo "%nprocshared=$cpureq" >> $outfile.com

  # Create Route section of *.com files for ECD calculations
  if [ $job = ecd -a $solfun = gas ]
   then
    echo "# $dftfun/$basisset td=(nstates=$excst) pop=$pop" >> $outfile.com
   elif [ $job = ecd -a $solfun != gas ]
   then
    echo "# $dftfun/$basisset td=(nstates=$excst) pop=$pop scrf=(iefpcm,solvent=$solfun)" >> $outfile.com
  fi

  # Create Route section of *.com files for OR calculations
  if [ $job = optrot -a $solfun = gas ]
   then
    echo "# $dftfun/$basisset polar=optrot cphf=rdfreq pop=$pop" >> $outfile.com
   elif [ $job = optrot -a $solfun != gas ]
   then
    echo "# $dftfun/$basisset polar=optrot cphf=rdfreq pop=$pop scrf=(iefpcm,solvent=$solfun)" >> $outfile.
         com
  fi
  echo "" >> $outfile.com

  # Create Title section of *.com files
  echo "$molfull, conf. $num (MMFF) - $job, $solfun, $theory" >> $outfile.com
  echo "" >> $outfile.com

  # Create Molecule specification of *.com files from *.log files
  echo "$charmulti" >> $outfile.com
  grep "Standard or" -A $matom $logfile | tail -n $atoms | awk '{printf "%3s%20s%12s%12s\n", $2,$4,$5,$6}
                                                          ' >> $outfile.com

  # Define wavelength for OR calculations
  if [ $job = optrot ]
   then
    echo "" >> $outfile.com
    echo "$orwl" >> $outfile.com
  fi

  # Retrieve user-defined basis set if necessary
  if [ $basisset = gen ]
```

```
      then
       cat ~/bin/$bsspec.gbs >> $outfile.com
      else
       echo "" >> $outfile.com
       echo "" >> $outfile.com
       echo "" >> $outfile.com
       echo "" >> $outfile.com
       echo "" >> $outfile.com
       echo "" >> $outfile.com
      fi
      echo "Input file for conformer $num ready."
    done
fi

# Delete temporary files and exit execution
rm *.tmp
echo ""
echo "$nmax input files generated."
echo ""
exit 0
```

OUTECD

(*Last updated: 10 March 2014*)

```
#!/bin/sh
echo "#################################################################"
echo "##                                                             ##"
echo "##                          OUTECD v3.0                        ##"
echo "##  Output generator for TD-DFT calculations in Gaussian 09    ##"
echo "##                                                             ##"
echo "#################################################################"
echo "* * * * * * * * *  Daniele Tedesco - 01 Mar 2014  * * * * * * * * *"
echo "-----------------------------------------------------------------"
echo ""

# OPTIONS:
#
# Two options are available:
# 1) half-bandwidth for Gaussian curves
# 2) generation of ORD curves (o)
# 0.2 is default for option 1
# False (n) is default for option 2
# When required, the half-bandwidth MUST be set as the first option
dsigma=$1
option1=$2

if [ -z $option1 ]
 then
  option1=n
fi

if [ -z $dsigma ]
 then
  dsigma="0.2"
 elif [ $dsigma = o ]
 then
  dsigma="0.2"
  option1=o
fi

echo "Gaussian half-bandwidth: $dsigma eV."
echo ""

if [ $option1 = o ]
 then
  echo "ORD spectra generation: ON"
  echo ""
  echo -n "Molecular weight (g mol^-1): "
  read molweight
  echo ""
 else
```

```
  molweight=n
  echo "ORD spectra generation: OFF"
  echo ""
fi

# Tags and options are automatically retrieved from the names and contents of files
# Retrieve solvation tag
soltag=`ls *ecd*.log | awk 'BEGIN{FS="-"}; END{print $(NF-1)}'`
if [ $soltag = gas ]
 then
  solfun=gas
 elif [ $soltag = meoh ]
 then
  solfun=methanol
 elif [ $soltag = iproh ]
 then
  solfun=2-propanol
 elif [ $soltag = chcl3 ]
 then
  solfun=chloroform
 elif [ $soltag = dmso ]
 then
  solfun=dimethylsulfoxide
 else
  echo -n "   Specify solvation call function: "
  read solfun
  echo ""
fi

# Retrieve molecule tag
moltag='ls *ecd*.log | awk 'END{print $0}' | sed s/$soltag-ecd...log// | sed s/-c..-//'
outfile=$moltag-$soltag

# Generate list of conformers
ls *ecd*.log | awk 'BEGIN{FS="-"}; {print $(NF-2)}' | sed "s/c//" > conflist.tmp

# Retrieve number of conformers
nmax=`cat conflist.tmp | wc -l`

# Retrieve number of excited states
excst=`grep -o -h "nstates=..." *ecd*.log | sed "s/nstates=//" | awk 'BEGIN{FS=")"}; END{print $1}'`

# Set up of tables of properties
echo -n "Rotational strengths (velocity) for the lowest-energy $excst excited states of $moltag " > $outfile-
      rvtab.txt
echo "(Solvation: $solfun)" >> $outfile-rvtab.txt
echo "Exc.St." >> $outfile-rvtab.txt

echo -n "Rotational strengths (length) for the lowest-energy $excst excited states of $moltag " > $outfile-
      rltab.txt
echo "(Solvation: $solfun)" >> $outfile-rltab.txt
echo "Exc.St." >> $outfile-rltab.txt

echo -n "Oscillator strengths for the lowest-energy $excst excited states of $moltag " > $outfile-ftab.txt
echo "(Solvation: $solfun)" >> $outfile-ftab.txt
echo "Exc.St." >> $outfile-ftab.txt

for xst in `seq -f '%03g' $excst`
do
  echo "$xst" >> $outfile-rvtab.txt
  echo "$xst" >> $outfile-rltab.txt
  echo "$xst" >> $outfile-ftab.txt
done

# DATA PROCESSING:
# ----------------
for h in `seq $nmax`
do
  # Retrieve conformer ID from list
  out=`awk -v NUM=$h '(NR==NUM){print $1}' conflist.tmp`
  echo "Processing output files for conformation $out..."

  # Retrieve file name of the appropriate *.log file
  filename=`ls $moltag-c$out-$soltag-ecd*.log`

  # Determine version of Gaussian09 (only version A.02 and C.01 are supported)
  g09version=`grep "Gaussian 09, Rev" $filename | awk 'END{print $4}'`
```

```
# Retrieve rotational strengths in velocity form from *.log file (different layouts in different versions of
    Gaussian09)
if [ $g09version = A.02, ]
 then
  grep "Total R(velocity) tensor for State=" -B 1 $filename | awk 'length($0)>50 {print $5}' > c$out-RV
  cp c$out-RV c$out-RVtab1
  nl -n rz -w 3 -s = c$out-RV > c$out-RVnew
  awk -v OUT=${out} '{printf "R%s%s\n",OUT,$0}' c$out-RVnew > c$out-RV
 else
  grep "R(velocity)" -A $excst $filename > c$out-RVnew
  tail -n $excst c$out-RVnew | awk '{print $5}' > c$out-RV
  cp c$out-RV c$out-RVtab1
  nl -n rz -w 3 -s = c$out-RV > c$out-RVnew
  awk -v OUT=${out} '{printf "R%s%s\n",OUT,$0}' c$out-RVnew > c$out-RV
fi

# Retrieve rotational strengths in length form (version-independent)
grep "R(length)" -A $excst $filename > c$out-RLnew
tail -n $excst c$out-RLnew | awk '{print $5}' > c$out-RL
cp c$out-RL c$out-RLtab1
nl -n rz -w 3 -s = c$out-RL > c$out-RLnew
awk -v OUT=${out} '{printf "R%s%s\n", OUT,$0}' c$out-RLnew > c$out-RL

# Retrieve excitation wavelengths and oscillator strengths
grep "Excited State" $filename | awk '{print $7}' > c$out-exc
grep "Excited State" $filename | awk '{print $9}' > c$out-f
sed -i -e "s/f=//g" c$out-f
cp c$out-exc c$out-exctab1
nl -n rz -w 3 -s = c$out-exc > c$out-excnew
awk -v OUT=${out} '{printf "a%s%s\n", OUT,$0}' c$out-excnew > c$out-exc
cp c$out-f c$out-ftab1
nl -n rz -w 3 -s = c$out-f > c$out-fnew
awk -v OUT=${out} '{printf "F%s%s\n", OUT,$0}' c$out-fnew > c$out-f

# Build up lists of parameters for Gnuplot and tables of properties
outcfile=$outfile-c$out
paste c$out-exctab1 c$out-RVtab1 > $outcfile-rvplot.txt
paste c$out-exctab1 c$out-RLtab1 > $outcfile-rlplot.txt
paste c$out-exctab1 c$out-ftab1 > $outcfile-fplot.txt
echo "" > c$out-RVtab2
echo "" > c$out-RLtab2
echo "" > c$out-ftab2

echo "$out" >> c$out-RVtab2
echo "$out" >> c$out-RLtab2
echo "$out" >> c$out-ftab2

awk '{print $2" ("$1")"}' $outcfile-rvplot.txt >> c$out-RVtab2
awk '{print $2" ("$1")"}' $outcfile-rlplot.txt >> c$out-RLtab2
awk '{print $2" ("$1")"}' $outcfile-fplot.txt >> c$out-ftab2

paste $outfile-rvtab.txt c$out-RVtab2 > RVtab3
paste $outfile-rltab.txt c$out-RLtab2 > RLtab3
paste $outfile-ftab.txt c$out-ftab2 > ftab3
rm *tab.txt c*tab1 c*tab2

mv RVtab3 $outfile-rvtab.txt
mv RLtab3 $outfile-rltab.txt
mv ftab3 $outfile-ftab.txt

cat c$out-exc c$out-RV > $outcfile-rv.txt
cat c$out-exc c$out-RL > $outcfile-rl.txt
cat c$out-exc c$out-f > $outcfile-f.txt
rm c$out-exc c*new c$out-f c$out-RV c$out-RL

# Build Gnuplot script for confomers (ECD)
echo "# PARAMETERS" > $outcfile-ecd.gpl
echo "set samples 1751" >> $outcfile-ecd.gpl
echo "set xrange [150:500]" >> $outcfile-ecd.gpl
echo "set yrange [-100:100]" >> $outcfile-ecd.gpl
echo "set xzeroaxis lt -1" >> $outcfile-ecd.gpl
echo "set nokey" >> $outcfile-ecd.gpl
echo "b = $dsigma" >> $outcfile-ecd.gpl
echo "# LOAD VELOCITY R VALUES" >> $outcfile-ecd.gpl
echo "load '$outcfile-rv.txt'" >> $outcfile-ecd.gpl
echo "# GAUSSIAN CURVES FOR EACH EXCITED STATE" >> $outcfile-ecd.gpl
```

```
  for xst in `seq -f "%03g" $excst`
  do
    echo "f$out$xst(x) = 3.04660e1*(R$out$xst/(a$out$xst*b))*exp(-(abs((1e7/x)-(1e7/a$out$xst))/(8.06554e3*b))
          **2)" >> $outcfile-ecd.gpl
  done
  echo "# SUM-OVER-STATES EXPRESSION" >> $outcfile-ecd.gpl
  echo -n "F$out(x) = f${out}001(x)" >> $outcfile-ecd.gpl
  for mxst in `seq -f "%03g" 2 $excst`
  do
    echo -n " + f$out$mxst(x)" >> $outcfile-ecd.gpl
  done
  echo "" >> $outcfile-ecd.gpl
  echo "# PLOT DATA IN TABLES" >> $outcfile-ecd.gpl
  echo "set table '$outcfile-rv_${dsigma}eV.dat'" >> $outcfile-ecd.gpl
  echo "plot F$out(x)" >> $outcfile-ecd.gpl
  echo "unset table" >> $outcfile-ecd.gpl
  echo "# LOAD LENGTH R VALUES" >> $outcfile-ecd.gpl
  echo "load '$outcfile-rl.txt'" >> $outcfile-ecd.gpl
  echo "# PLOT DATA IN TABLES" >> $outcfile-ecd.gpl
  echo "set table '$outcfile-rl_${dsigma}eV.dat'" >> $outcfile-ecd.gpl
  echo "plot F$out(x)" >> $outcfile-ecd.gpl
  echo "unset table" >> $outcfile-ecd.gpl

  # Build Gnuplot script for confomers (ORD)
  if [ $molweight != n ]
   then
    echo "# PARAMETERS" > $outcfile-ord.gpl
    echo "set samples 5501" >> $outcfile-ord.gpl
    echo "set xrange [150:700]" >> $outcfile-ord.gpl
    echo "set yrange [-10000:10000]" >> $outcfile-ord.gpl
    echo "set xzeroaxis lt -1" >> $outcfile-ord.gpl
    echo "set nokey" >> $outcfile-ord.gpl
    echo "b = $dsigma" >> $outcfile-ord.gpl
    echo "MW = $molweight" >> $outcfile-ord.gpl
    echo "# LOAD VELOCITY R VALUES" >> $outcfile-ord.gpl
    echo "load '$outcfile-rv.txt'" >> $outcfile-ord.gpl
    echo "# GAUSSIAN CURVES FOR EACH EXCITED STATE" >> $outcfile-ord.gpl
    for xst in `seq -f "%03g" $excst`
    do
      echo -n "f$out$xst(x) = 4.57158e3*R$out$xst/(x*MW)*((((x-a$out$xst)/(x*a$out$xst))/" >> $outcfile-ord.gpl
      echo -n "(((x-a$out$xst)/(x*a$out$xst))**2+(8.06554e-4*b)**2))-(((x+a$out$xst)/" >> $outcfile-ord.gpl
      echo "(x*a$out$xst))/(((x+a$out$xst)/(x*a$out$xst))**2+(8.06554e-4*b)**2)))" >> $outcfile-ord.gpl
    done
    echo "# SUM-OVER-STATES EXPRESSION" >> $outcfile-ord.gpl
    echo -n "F$out(x) = f${out}001(x)" >> $outcfile-ord.gpl
    for mxst in `seq -f "%03g" 2 $excst`
    do
      echo -n " + f$out$mxst(x)" >> $outcfile-ord.gpl
    done
    echo "" >> $outcfile-ord.gpl
    echo "# PLOT DATA IN TABLES" >> $outcfile-ord.gpl
    echo "set table '$outcfile-orv_${dsigma}eV.dat'" >> $outcfile-ord.gpl
    echo "plot F$out(x)" >> $outcfile-ord.gpl
    echo "unset table" >> $outcfile-ord.gpl
    echo "# LOAD LENGTH R VALUES" >> $outcfile-ord.gpl
    echo "load '$outcfile-rl.txt'" >> $outcfile-ord.gpl
    echo "# PLOT DATA IN TABLES" >> $outcfile-ord.gpl
    echo "set table '$outcfile-orl_${dsigma}eV.dat'" >> $outcfile-ord.gpl
    echo "plot F$out(x)" >> $outcfile-ord.gpl
    echo "unset table" >> $outcfile-ord.gpl
  fi

# Build Gnuplot script for confomers (UV)
  echo "# PARAMETERS" > $outcfile-uv.gpl
  echo "set samples 1751" >> $outcfile-uv.gpl
  echo "set xrange [150:500]" >> $outcfile-uv.gpl
  echo "set yrange [-100:100]" >> $outcfile-uv.gpl
  echo "set xzeroaxis lt -1" >> $outcfile-uv.gpl
  echo "set nokey" >> $outcfile-uv.gpl
  echo "b = $dsigma" >> $outcfile-uv.gpl
  echo "# LOAD F VALUES" >> $outcfile-uv.gpl
  echo "load '$outcfile-f.txt'" >> $outcfile-uv.gpl
  echo "# GAUSSIAN CURVES FOR EACH EXCITED STATE" >> $outcfile-uv.gpl
  for xst in `seq -f "%03g" $excst`
  do
    echo "u$out$xst(x) = 1.61961e4*(F$out$xst/b)*exp(-(abs((1e7/x)-(1e7/a$out$xst))/(8.06554e3*b))**2)" >>
          $outcfile-uv.gpl
```

```
  done
  echo "# SUM-OVER-STATES EXPRESSION" >> $outcfile-uv.gpl
  echo -n "U$out(x) = u${out}001(x)" >> $outcfile-uv.gpl
  for mxst in `seq -f "%03g" 2 $excst`
  do
    echo -n " + u$out$mxst(x)" >> $outcfile-uv.gpl
  done
  echo "" >> $outcfile-uv.gpl
  echo "# PLOT DATA IN TABLES" >> $outcfile-uv.gpl
  echo "set table '$outcfile-f_${dsigma}eV.dat'" >> $outcfile-uv.gpl
  echo "plot U$out(x)" >> $outcfile-uv.gpl
  echo "unset table" >> $outcfile-uv.gpl
done

# Create Gnuplot script for molecule (ECD)
echo ""
echo "Creating input file for ECD spectra processing..."
echo "# LOAD SCF ENERGIES" > $outfile-ecd.gpl
echo "load '${moltag}_scf-$soltag.txt'" >> $outfile-ecd.gpl
echo "# PROCESS CONFORMERS AND LOAD LENGTH R VALUES" >> $outfile-ecd.gpl
for h in `seq $nmax`
do
  num=`awk -v NUM=$h '(NR==NUM){print $1}' conflist.tmp`
  echo "load '$outfile-c$num-ecd.gpl'" >> $outfile-ecd.gpl
done
echo "# PARAMETERS" >> $outfile-ecd.gpl
echo "set samples 1751" >> $outfile-ecd.gpl
echo "set xrange [150:500]" >> $outfile-ecd.gpl
echo "set yrange [-100:100]" >> $outfile-ecd.gpl
echo "set xzeroaxis lt -1" >> $outfile-ecd.gpl
echo "set nokey" >> $outfile-ecd.gpl
echo "b = $dsigma" >> $outfile-ecd.gpl
echo "# CONFORMATIONAL AVERAGING" >> $outfile-ecd.gpl
num=`awk '(NR==1){print $1}' conflist.tmp`
echo -n "Q(x) = q${num}*F$num(x)" >> $outfile-ecd.gpl
for n in `seq 2 $nmax`
do
  num=`awk -v NUM=$n '(NR==NUM){print $1}' conflist.tmp`
  echo -n " + q${num}*F$num(x)" >> $outfile-ecd.gpl
done
echo "" >> $outfile-ecd.gpl
echo "# PLOT DATA IN TABLES" >> $outfile-ecd.gpl
echo "set table '$outfile-rl_${dsigma}eV_scf.dat'" >> $outfile-ecd.gpl
echo "plot Q(x)" >> $outfile-ecd.gpl
echo "unset table" >> $outfile-ecd.gpl
echo "# LOAD VELOCITY R VALUES" >> $outfile-ecd.gpl
for h in `seq $nmax`
do
  num=`awk -v NUM=$h '(NR==NUM){print $1}' conflist.tmp`
  echo "load '$outfile-c$num-rv.txt'" >> $outfile-ecd.gpl
done
echo "# PLOT DATA IN TABLES" >> $outfile-ecd.gpl
echo "set table '$outfile-rv_${dsigma}eV_scf.dat'" >> $outfile-ecd.gpl
echo "plot Q(x)" >> $outfile-ecd.gpl
echo "unset table" >> $outfile-ecd.gpl
echo "# LOAD FREE ENERGIES" >> $outfile-ecd.gpl
echo "load '${moltag}_g-$soltag.txt'" >> $outfile-ecd.gpl
echo "# PROCESS CONFORMERS AND LOAD LENGTH R VALUES" >> $outfile-ecd.gpl
for h in `seq $nmax`
do
  num=`awk -v NUM=$h '(NR==NUM){print $1}' conflist.tmp`
  echo "load '$outfile-c$num-ecd.gpl'" >> $outfile-ecd.gpl
done
echo "# PARAMETERS" >> $outfile-ecd.gpl
echo "set samples 1751" >> $outfile-ecd.gpl
echo "set xrange [150:500]" >> $outfile-ecd.gpl
echo "set yrange [-100:100]" >> $outfile-ecd.gpl
echo "set xzeroaxis lt -1" >> $outfile-ecd.gpl
echo "set nokey" >> $outfile-ecd.gpl
echo "b = $dsigma" >> $outfile-ecd.gpl
echo "# CONFORMATIONAL AVERAGING" >> $outfile-ecd.gpl
num=`awk '(NR==1){print $1}' conflist.tmp`
echo -n "Q(x) = q${num}*F$num(x)" >> $outfile-ecd.gpl
for h in `seq 2 $nmax`
do
  num=`awk -v NUM=$h '(NR==NUM){print $1}' conflist.tmp`
  echo -n " + q${num}*F$num(x)" >> $outfile-ecd.gpl
```

```
done
echo "" >> $outfile-ecd.gpl
echo "# PLOT DATA IN TABLES" >> $outfile-ecd.gpl
echo "set table '$outfile-rl_${dsigma}eV_g.dat'" >> $outfile-ecd.gpl
echo "plot Q(x)" >> $outfile-ecd.gpl
echo "unset table" >> $outfile-ecd.gpl
echo "# LOAD VELOCITY R VALUES" >> $outfile-ecd.gpl
for h in `seq $nmax`
do
  num=`awk -v NUM=$h '(NR==NUM){print $1}' conflist.tmp`
  echo "load '$outfile-c$num-rv.txt'" >> $outfile-ecd.gpl
done
echo "# PLOT DATA IN TABLES" >> $outfile-ecd.gpl
echo "set table '$outfile-rv_${dsigma}eV_g.dat'" >> $outfile-ecd.gpl
echo "plot Q(x)" >> $outfile-ecd.gpl
echo "unset table" >> $outfile-ecd.gpl

# Create Gnuplot script for molecule (ORD)
if [ $molweight != n ]
 then
  echo ""
  echo "Creating input file for ORD spectra processing..."
  echo "# LOAD SCF ENERGIES" > $outfile-ord.gpl
  echo "load '${moltag}_scf-$soltag.txt'" >> $outfile-ord.gpl
  echo "# PROCESS CONFORMERS AND LOAD LENGTH R VALUES" >> $outfile-ord.gpl
  for h in `seq $nmax`
  do
    num=`awk -v NUM=$h '(NR==NUM){print $1}' conflist.tmp`
    echo "load '$outfile-c$num-ord.gpl'" >> $outfile-ord.gpl
  done
  echo "# PARAMETERS" >> $outfile-ord.gpl
  echo "set samples 6001" >> $outfile-ord.gpl
  echo "set xrange [100:700]" >> $outfile-ord.gpl
  echo "set yrange [-100000:100000]" >> $outfile-ord.gpl
  echo "set xzeroaxis lt -1" >> $outfile-ord.gpl
  echo "set nokey" >> $outfile-ord.gpl
  echo "b = $dsigma" >> $outfile-ord.gpl
  echo "MW = $molweight" >> $outfile-ord.gpl
  echo "# CONFORMATIONAL AVERAGING" >> $outfile-ord.gpl
  num=`awk '(NR==1){print $1}' conflist.tmp`
  echo -n "Q(x) = q${num}*F$num(x)" >> $outfile-ord.gpl
  for n in `seq 2 $nmax`
  do
    num=`awk -v NUM=$n '(NR==NUM){print $1}' conflist.tmp`
    echo -n " + q${num}*F$num(x)" >> $outfile-ord.gpl
  done
  echo "" >> $outfile-ord.gpl
  echo "# PLOT DATA IN TABLES" >> $outfile-ord.gpl
  echo "set table '$outfile-orl_${dsigma}eV_scf.dat'" >> $outfile-ord.gpl
  echo "plot Q(x)" >> $outfile-ord.gpl
  echo "unset table" >> $outfile-ord.gpl
  echo "# LOAD VELOCITY R VALUES" >> $outfile-ord.gpl
  for h in `seq $nmax`
  do
    num=`awk -v NUM=$h '(NR==NUM){print $1}' conflist.tmp`
    echo "load '$outfile-c$num-rv.txt'" >> $outfile-ord.gpl
  done
  echo "# PLOT DATA IN TABLES" >> $outfile-ord.gpl
  echo "set table '$outfile-orv_${dsigma}eV_scf.dat'" >> $outfile-ord.gpl
  echo "plot Q(x)" >> $outfile-ord.gpl
  echo "unset table" >> $outfile-ord.gpl
  echo "# LOAD FREE ENERGIES" >> $outfile-ord.gpl
  echo "load '${moltag}_g-$soltag.txt'" >> $outfile-ord.gpl
  echo "# PROCESS CONFORMERS AND LOAD LENGTH R VALUES" >> $outfile-ord.gpl
  for h in `seq $nmax`
  do
    num=`awk -v NUM=$h '(NR==NUM){print $1}' conflist.tmp`
    echo "load '$outfile-c$num-ord.gpl'" >> $outfile-ord.gpl
  done
  echo "# PARAMETERS" >> $outfile-ord.gpl
  echo "set samples 6001" >> $outfile-ord.gpl
  echo "set xrange [100:700]" >> $outfile-ord.gpl
  echo "set yrange [-100000:100000]" >> $outfile-ord.gpl
  echo "set xzeroaxis lt -1" >> $outfile-ord.gpl
  echo "set nokey" >> $outfile-ord.gpl
  echo "b = $dsigma" >> $outfile-ord.gpl
  echo "MW = $molweight" >> $outfile-ord.gpl
```

```
  echo "# CONFORMATIONAL AVERAGING" >> $outfile-ord.gpl
  num=`awk '(NR==1){print $1}' conflist.tmp`
  echo -n "Q(x) = q${num}*F$num(x)" >> $outfile-ord.gpl
  for h in `seq 2 $nmax`
  do
    num=`awk -v NUM=$h '(NR==NUM){print $1}' conflist.tmp`
    echo -n " + q${num}*F$num(x)" >> $outfile-ord.gpl
  done
  echo "" >> $outfile-ord.gpl
  echo "# PLOT DATA IN TABLES" >> $outfile-ord.gpl
  echo "set table '$outfile-orl_${dsigma}eV_g.dat'" >> $outfile-ord.gpl
  echo "plot Q(x)" >> $outfile-ord.gpl
  echo "unset table" >> $outfile-ord.gpl
  echo "# LOAD VELOCITY R VALUES" >> $outfile-ord.gpl
  for h in `seq $nmax`
  do
    num=`awk -v NUM=$h '(NR==NUM){print $1}' conflist.tmp`
    echo "load '$outfile-c$num-rv.txt'" >> $outfile-ord.gpl
  done
  echo "# PLOT DATA IN TABLES" >> $outfile-ord.gpl
  echo "set table '$outfile-orv_${dsigma}eV_g.dat'" >> $outfile-ord.gpl
  echo "plot Q(x)" >> $outfile-ord.gpl
  echo "unset table" >> $outfile-ord.gpl
fi

# Create Gnuplot script for molecule (UV)
echo ""
echo "Creating input file for UV spectra processing..."
echo "# LOAD SCF ENERGIES" > $outfile-uv.gpl
echo "load '${moltag}_scf-$soltag.txt'" >> $outfile-uv.gpl
echo "# PROCESS CONFORMERS AND LOAD F VALUES" >> $outfile-uv.gpl
for h in `seq $nmax`
do
  num=`awk -v NUM=$h '(NR==NUM){print $1}' conflist.tmp`
  echo "load '$outfile-c$num-uv.gpl'" >> $outfile-uv.gpl
done
echo "# PARAMETERS" >> $outfile-uv.gpl
echo "set samples 1751" >> $outfile-uv.gpl
echo "set xrange [150:500]" >> $outfile-uv.gpl
echo "set yrange [-100:100]" >> $outfile-uv.gpl
echo "set xzeroaxis lt -1" >> $outfile-uv.gpl
echo "set nokey" >> $outfile-uv.gpl
echo "b = $dsigma" >> $outfile-uv.gpl
echo "# CONFORMATIONAL AVERAGING" >> $outfile-uv.gpl
num=`awk '(NR==1){print $1}' conflist.tmp`
echo -n "Q(x) = q${num}*U$num(x)" >> $outfile-uv.gpl
for n in `seq 2 $nmax`
do
  num=`awk -v NUM=$n '(NR==NUM){print $1}' conflist.tmp`
  echo -n " + q${num}*U$num(x)" >> $outfile-uv.gpl
done
echo "" >> $outfile-uv.gpl
echo "# PLOT DATA IN TABLES" >> $outfile-uv.gpl
echo "set table '$outfile-f_${dsigma}eV_scf.dat'" >> $outfile-uv.gpl
echo "plot Q(x)" >> $outfile-uv.gpl
echo "unset table" >> $outfile-uv.gpl
echo "# LOAD FREE ENERGIES" >> $outfile-uv.gpl
echo "load '${moltag}_g-$soltag.txt'" >> $outfile-uv.gpl
echo "# PROCESS CONFORMERS AND LOAD F VALUES" >> $outfile-uv.gpl
for h in `seq $nmax`
do
  num=`awk -v NUM=$h '(NR==NUM){print $1}' conflist.tmp`
  echo "load '$outfile-c$num-uv.gpl'" >> $outfile-uv.gpl
done
echo "# PARAMETERS" >> $outfile-uv.gpl
echo "set samples 1751" >> $outfile-uv.gpl
echo "set xrange [150:500]" >> $outfile-uv.gpl
echo "set yrange [-100:100]" >> $outfile-uv.gpl
echo "set xzeroaxis lt -1" >> $outfile-uv.gpl
echo "set nokey" >> $outfile-uv.gpl
echo "b = $dsigma" >> $outfile-uv.gpl
echo "# CONFORMATIONAL AVERAGING" >> $outfile-uv.gpl
num=`awk '(NR==1){print $1}' conflist.tmp`
echo -n "Q(x) = q${num}*U$num(x)" >> $outfile-uv.gpl
for h in `seq 2 $nmax`
do
  num=`awk -v NUM=$h '(NR==NUM){print $1}' conflist.tmp`
```

```
  echo -n " + q${num}*U$num(x)" >> $outfile-uv.gpl
done
echo "" >> $outfile-uv.gpl
echo "# PLOT DATA IN TABLES" >> $outfile-uv.gpl
echo "set table '$outfile-f_${dsigma}eV_g.dat'" >> $outfile-uv.gpl
echo "plot Q(x)" >> $outfile-uv.gpl
echo "unset table" >> $outfile-uv.gpl

# Clean up temporary files
rm *.tmp

# This last part enables automatic execution of the Gnuplot scripts
# (requires a working Gnuplot installation)
echo ""
echo "Plotting data..."
gnuplot $outfile-ecd.gpl
gnuplot $outfile-uv.gpl
if [ $molweight != n ]
then
  gnuplot $outfile-ord.gpl
fi
echo ""
echo "Cleaning data..."
sed -i -e "1,4d" *.dat
sed -i -e "s/i//g" *.dat
sed -i -e "s/o//g" *.dat
echo ""
echo "Done."
echo ""
exit 0
```

CONFANAL

(*Last updated: 10 March 2014*)

```
#!/bin/sh
echo "################################################################"
echo "##                                                            ##"
echo "##                      CONFANAL v2.0                         ##"
echo "## Conformational analysis for QM geometries in Gaussian09 ##"
echo "##                                                            ##"
echo "################################################################"
echo "* * * * * * * * Daniele Tedesco - 01 Mar 2014 * * * * * * * * *"
echo "----------------------------------------------------------------"
echo ""

# OPTIONS
# One flag is available:
# 1) job type (f/v/o/e; required)
jobflag=$1

if [ -z $jobflag ]
 then
  echo ""
  echo "WARNING! No job type declared!"
  echo "Please use the appropriate flags (f/v/o/e)."
  echo "Exiting."
  echo ""
  exit 0
fi

if [ $jobflag = f ]
 then
  job=opt-freq
 elif [ $jobflag = v ]
 then
  job=opt-vcd
 elif [ $jobflag = o ]
 then
  job=optrot
 elif [ $jobflag = e ]
 then
```

```
  job=ecd
 else
  echo ""
  echo "WARNING! Invalid job type declared!"
  echo "Please use the appropriate flags (f/v/o/e)."
  echo "Exiting."
  echo ""
  exit 0
fi

echo -n "Specify charge and multiplicity of the molecule in Gaussian format: "
read charmulti
echo ""

# Tags and options are automatically retrieved from the names and contents of files
# Retrieve solvation tag
soltag=`ls *.com | sed s@$job...com@@ | awk 'BEGIN{FS="-"}; END{print $(NF-1)}'`

if [ $soltag = gas ]
 then
  solfun=gas
 elif [ $soltag = meoh ]
 then
  solfun=methanol
 elif [ $soltag = iproh ]
 then
  solfun=2-propanol
 elif [ $soltag = chcl3 ]
 then
  solfun=chloroform
 elif [ $soltag = dmso ]
 then
  solfun=dimethylsulfoxide
 else
  echo -n "   Specify solvation call function: "
  read solfun
  echo ""
fi

# Retrieve molecule tag
moltag=`ls *.com | awk 'END{print $0}' | sed s@$soltag-$job...com@@ | sed s@-c..-@@`

# Generate list of conformers
ls *.com | sed s@-$soltag-$job...com@@ | sed s@$moltag-c@@ > conflist.tmp

# Create output file
if [ $job = opt-freq -o $job = opt-vcd ]
 then
  outfile=geom_${moltag}_mm.txt
  echo "Conformational analysis on MM conformers of $moltag" > $outfile
 else
  outfile=geom_${moltag}_$soltag.txt
  echo "Conformational analysis on optimised conformers of $moltag (Solvation: $solfun)" > $outfile
fi

echo "Conf." >> $outfile

# Retrieve number of conformers
nmax=`cat conflist.tmp | wc -l`

# Print conformer IDs in the output file
for cnum in `seq $nmax`
do
 num=`awk -v LIN=$cnum 'NR==LIN' conflist.tmp`
 echo "$num" >> $outfile
done

# Retrieve geometric parameters listed in the input file
if [ -f input_confanal ]
 then
  iter=`cat input_confanal | wc -l`

  # Retrieve parameter type (length, angle, dihedral) for each parameter
  for x in `seq $iter`
  do
   partype=`awk -v LIN=$x '(NR==LIN){print $1}' input_confanal`
```

```
# ------------
# BOND LENGTHS
if [ $partype = L ]
 then
  # Retrieve atom indices
  at1=`awk -v LIN=$x '(NR==LIN){print $2}' input_confanal`
  at2=`awk -v LIN=$x '(NR==LIN){print $3}' input_confanal`
  echo "Processing distance ($at1,$at2) ..."

  # Retrieve atom coordinates for every conformer
  for cnum in `seq $nmax`
  do
   # Retrieve conformer ID
   num=`awk -v LIN=$cnum '(NR==LIN){print "c"$1}' conflist.tmp`
   addhead=`awk '/'"$charmulti"'/ {print NR}' $moltag-$num-$soltag-${job}01.com`
   # Retrieve atoms: A B
   om1=`expr $at1 + $addhead`
   om2=`expr $at2 + $addhead`
   # Print atom coordinates:
   # xA yA zA
   # xB yB zB
   awk -v ATOM1=${om1} -v ATOM2=${om2} '
       (NR==ATOM1){printf "%.9f\t%.9f\t%.9f\t",
                          $2,$3,$4};
       (NR==ATOM2){printf "%.9f\t%.9f\t%.9f\n",
                          $2,$3,$4}
       ' $moltag-$num-$soltag-${job}01.com >> coords.txt
  done

  # Create results file
  echo "" > dst_$x.txt
  echo "L($at1,$at2)" >> dst_$x.txt

  # Calculate distance for every conformer
  # Bond length formula:
  # d_AB = sqrt( xAB^2 + yAB^2 + zAB^2 )
  # xAB = xB-xA
  # yAB = yB-yA
  # zAB = zB-zA
  for num in `seq $nmax`
  do
   awk -v CONF=${num} '
       (NR==CONF){printf "%.3f\n",
                         sqrt(($4-$1)**2+($5-$2)**2+($6-$3)**2)}
       ' coords.txt >> dst_$x.txt
  done

  # Clean up coordinates file
  rm coords.txt
  # Paste results file in output file
  paste $outfile dst_$x.txt > dst_top.txt
  # Clean up results file
  rm dst_$x.txt
  mv dst_top.txt $outfile
  echo "Done."
  echo ""
fi

# ------------
# BOND ANGLES
if [ $partype = A ]
 then
  # Retrieve atom indices
  at1=`awk -v LIN=$x '(NR==LIN){print $2}' input_confanal`
  at2=`awk -v LIN=$x '(NR==LIN){print $3}' input_confanal`
  at3=`awk -v LIN=$x '(NR==LIN){print $4}' input_confanal`
  echo "Processing angle ($at1,$at2,$at3)..."

  # Retrieve atom coordinates for every conformer
  for cnum in `seq $nmax`
  do
   # Retrieve conformer ID
   num=`awk -v LIN=$cnum '(NR==LIN){print "c"$1}' conflist.tmp`
   addhead=`awk '/'"$charmulti"'/ {print NR}' $moltag-$num-$soltag-${job}01.com`
   # Retrieve atoms: A B C
   om1=`expr $at1 + $addhead`
   om2=`expr $at2 + $addhead`
```

```
        om3=`expr $at3 + $addhead`
        # Print atom coordinates:
        # xA yA zA
        # xB yB zB
        # xC yC zC
        awk -v ATOM1=${om1} -v ATOM2=${om2} -v ATOM3=${om3} '
            (NR==ATOM1){printf "%.9f\t%.9f\t%.9f\t",
                              $2,$3,$4};
            (NR==ATOM2){printf "%.9f\t%.9f\t%.9f\t",
                              $2,$3,$4};
            (NR==ATOM3){printf "%.9f\t%.9f\t%.9f\n",
                              $2,$3,$4}
            ' $moltag-$num-$soltag-${job}01.com >> coords.txt
    done

    # Create bond vectors <AB> and <BC> for every conformer
    for num in `seq $nmax`
    do
     # Print vector coordinates:
     # xAB yAB zAB
     # xBC yBC zBC
     awk -v CONF=${num} '
         (NR==CONF){printf "%.9f\t%.9f\n",
                           $4-$1,$5-$2,$6-$3,
                           $7-$4,$8-$5,$9-$6}
         ' coords.txt >> vectors.txt
    done

    # Calculate dot product and length of bond vectors for every conformer
    # Dot product formula:
    # <AB> dot <BC> = xAB*xBC + yAB*yBC + zAB*zBC
    for num in `seq $nmax`
    do
     awk -v CONF=${num} '
         (NR==CONF){printf "%.9f\t%.9f\t%.9f\n",
                           $1*$4+$2*$5+$3*$6,
                           sqrt($1**2+$2**2+$3**2),
                           sqrt($4**2+$5**2+$6**2)}
         ' vectors.txt >> scalars.txt
    done

    # Create results file
    echo "" > an_$x.txt
    echo "A($at1,$at2,$at3)" >> an_$x.txt

    # Calculate angle for every conformer
    # Bond angle formula in degrees:
    # alpha_ABC = arccos((<AB> dot <BC>)/(d_AB*d_BC))
    # arccos(x) = atan2(sqrt(1-x^2),x) / (pi/180)
    # pi = atan2(0,-1)
    for num in `seq $nmax`
    do
     awk -v CONF=${num} '
         function acos(x) { return atan2(sqrt(1-x**2),x)/(atan2(0,-1)/180) }
         (NR==CONF){printf "%.3f\n",
                           acos($1/($2*$3))}
         ' scalars.txt >> an_$x.txt
    done

    # Clean up coordinates file and vector files
    rm coords.txt vectors.txt scalars.txt
    # Paste results file in output file
    paste $outfile an_$x.txt > an_top.txt
    # Clean up results file
    rm an_$x.txt
    mv an_top.txt $outfile
    echo "Done."
    echo ""
fi

# ---------------
# DIHEDRAL ANGLES
if [ $partype = D ]
 then
    # Retrieve atom indices
    at1=`awk -v LIN=$x '(NR==LIN){print $2}' input_confanal`
    at2=`awk -v LIN=$x '(NR==LIN){print $3}' input_confanal`
```

```
        at3=`awk -v LIN=$x '(NR==LIN){print $4}' input_confanal`
        at4=`awk -v LIN=$x '(NR==LIN){print $5}' input_confanal`
        echo "Processing dihedral ($at1,$at2,$at3,$at4) ..."

        # Retrieve atom coordinates for every conformer
        for cnum in `seq $nmax`
        do
         # Retrieve conformer ID
         num=`awk -v LIN=$cnum '(NR==LIN){print "c"$1}' conflist.tmp`
         addhead=`awk '/'"$charmulti"'/ {print NR}' $moltag-$num-$soltag-${job}01.com`
         # Retrieve atoms: A B C D
         om1=`expr $at1 + $addhead`
         om2=`expr $at2 + $addhead`
         om3=`expr $at3 + $addhead`
         om4=`expr $at4 + $addhead`
         # Print atom coordinates:
         # xA yA zA
         # xB yB zB
         # xC yC zC
         # xD yD zD
         awk -v ATOM1=${om1} -v ATOM2=${om2} -v ATOM3=${om3} -v ATOM4=${om4} '
             (NR==ATOM1){printf "%.9f\t%.9f\t%.9f\t",
                               $2,$3,$4};
             (NR==ATOM2){printf "%.9f\t%.9f\t%.9f\t",
                               $2,$3,$4};
             (NR==ATOM3){printf "%.9f\t%.9f\t%.9f\t",
                               $2,$3,$4};
             (NR==ATOM4){printf "%.9f\t%.9f\t%.9f\n",
                               $2,$3,$4}
             ' $moltag-$num-$soltag-${job}01.com >> coords.txt
        done

        # Create vectors <AB>, <BC>, <CD>, <AC>, <BD> and <AD> for every conformer
        for num in `seq $nmax`
        do
         # Print vector coordinates:
         # xAB yAB zAB
         # xBC yBC zBC
         # xCD yCD zCD
         # xAC yAC zAC
         # xBD yBD zBD
         # xAD yAD zAD
         awk -v CONF=${num} '
             (NR==CONF){printf "%.9f\t%.9f\t%.9f\t",$4-$1,$5-$2,$6-$3;
                        printf "%.9f\t%.9f\t%.9f\t",$7-$4,$8-$5,$9-$6;
                        printf "%.9f\t%.9f\t%.9f\t",$10-$7,$11-$8,$12-$9;
                        printf "%.9f\t%.9f\t%.9f\t",$7-$1,$8-$2,$9-$3;
                        printf "%.9f\t%.9f\t%.9f\t",$10-$4,$11-$5,$12-$6;
                        printf "%.9f\t%.9f\t%.9f\n",$10-$1,$11-$2,$12-$3}
             ' coords.txt >> vectors.txt
        done

        # Calculate cross product vectors for every conformer
        # Cross product formula:
        # <AB>x<BC> = (yAB*zBC-zAB*yBC)<x> + (zAB*xBC-xAB*zBC)<y> + (xAB*yBC-yAB*xBC)<z>
        # <BC>x<CD> = (yBC*zCD-zBC*yCD)<x> + (zBC*xCD-xBC*zCD)<y> + (xBC*yCD-yBC*xCD)<z>
        # <x>, <y>, <z> are unit vectors
        for num in `seq $nmax`
        do
         # Print cross vector coordinates: xABC, yABC, zABC, xBCD, yBCD, zBCD
         awk -v CONF=${num} '
             (NR==CONF){printf "%.9f\t%.9f\t%.9f\t%.9f\t%.9f\t%.9f\n",
                               $2*$6-$3*$5,$3*$4-$1*$6,$1*$5-$2*$4,
                               $5*$9-$6*$8,$6*$7-$4*$9,$4*$8-$5*$7}
             ' vectors.txt >> cross.txt
        done

        # Calculate dot product and length of cross vectors for every conformer
        # (<AB>x<BC>) dot (<BC>x<CD>) = xABC*xBCD + yABC*yBCD + zABC*zBCD
        # Cross vector lengths: d_ABC, d_BCD
        for num in `seq $nmax`
        do
         awk -v CONF=${num} '
             (NR==CONF){printf "%.9f\t%.9f\t%.9f\t",
                               $1*$4+$2*$5+$3*$6,
                               sqrt($1**2+$2**2+$3**2),
                               sqrt($4**2+$5**2+$6**2)}
```

```
345             ' cross.txt >> full.txt
        # Calculate auxiliary dot product:
        # (<AB>x<BC>) dot <CD> =  (yAB*zBC - zAB*yBC)*xCD +
        #                         + (zAB*xBC - xAB*zBC)*yCD +
        #                         + (xAB*yBC - yAB*xBC)*zCD
350     # This dot product bears the same sign as the dihedral angle theta_ABCD
        awk -v CONF=${num} '
            (NR==CONF){printf "%.7f\n",
                       ($2*$6-$3*$5)*$7+($3*$4-$1*$6)*$8+($1*$5-$2*$4)*$9}
            ' vectors.txt >> full.txt
355     done

        # Print results file
        echo "" > dh_$x.txt
        echo "D($at1,$at2,$at3,$at4)" >> dh_$x.txt
360
        # Calculate dihedral for every conformer
        # Dihedral angle formula in degrees:
        # theta_ABCD = arccos( ((<AB>x<BC>) dot (<BC>x<CD>))/(d_ABC*d_BCD) )
        # arccos(x) = atan2(sqrt(1-x^2),x) / (pi/180)
365     # pi = atan2(0,-1)
        # The sign of theta is ruled by the sign of the auxiliary dot product
        for num in `seq $nmax`
        do
         awk -v CONF=${num} '
370         function acos(x) { return atan2(sqrt(1-x**2),x)/(atan2(0,-1)/180) }
            (NR==CONF){if ( $4 < 0 ) printf "%.3f\n",-acos($1/($2*$3));
                     else printf "%.3f\n",acos($1/($2*$3))}
            ' full.txt >> dh_$x.txt
        done
375
        # Clean up intermediate files
        rm coords.txt cross.txt full.txt vectors.txt
        # Paste results file in output file
        paste $outfile dh_$x.txt > dh_top.txt
380     # Clean up results file
        rm dh_$x.txt
        mv dh_top.txt $outfile
        echo "Done."
        echo ""
385    fi
      done

      # Clean up list of conformers
      rm conflist.tmp
390   cat $outfile
      echo ""
      exit 0

     # Exit if input file does not exist.
395  else
      rm conflist.tmp $outfile
      echo "No input file input_confanal. Exiting."
      echo ""
      exit 0
400 fi
```

Publications

(*Last updated: 10 March 2014*)

1. Carlo Bertucci, Marco Pistolozzi, Daniele Tedesco, Riccardo Zanasi, Renzo Ruzziconi, Anna Maria Di Pietra (**2012**). Stereochemical characterization of fluorinated 2-(phenanthren-1-yl)propionic acids by enantioselective high performance liquid chromatography analysis and electronic circular dichroism detection. *Journal of Chromatography A 1232*, 128–133.
DOI: 10.1016/j.chroma.2011.10.090; IF 2011: 4.531.

2. Daniele Tedesco, Riccardo Zanasi, Andrea Guerrini, Carlo Bertucci (**2012**). Conformational flexibility and absolute stereochemistry of (3*R*)-3-hydroxy-4-aryl-β-lactams investigated by chiroptical properties and TD-DFT calculations. *Chirality 24*, 741–750.
DOI: 10.1002/chir.22043; IF 2011: 2.350.

3. Carlo Bertucci, Daniele Tedesco (**2012**). Advantages of electronic circular dichroism detection for the stereochemical analysis and characterization of drugs and natural products by liquid chromatography. *Journal of Chromatography A 1269*, 69–81.
DOI: 10.1016/j.chroma.2012.09.046; IF 2011: 4.531.

4. Fengshou Dong, Jing Li, Bezhan Chankvetadze, Yongpu Cheng, Jun Xu, Xingang Liu, Yuanbo Li, Xiu Chen, Carlo Bertucci, Daniele Tedesco, Riccardo Zanasi, Yongquan Zheng (**2013**). Chiral triazole fungicide difenoconazole: Absolute stereochemistry, stereoselective bioactivity, aquatic toxicity, and environmental behavior in vegetables and soil. *Environmental Science and Technology 47*, 3386–3394.
DOI: 10.1021/es304982m; IF 2012: 5.257.

5. Daniele Tedesco, Anna Maria Di Pietra, Francesca Rossi, Marco Garagnani, Elia Del Borrello, Carlo Bertucci, Vincenza Andrisano (**2013**). Determination of dextromethorphan and levomethorphan in seized heroin samples by enantioselective HPLC and electronic CD. *Journal of Pharmaceutical and Biomedical Analysis 81–82*, 76–79.
DOI: 10.1016/j.jpba.2013.03.024; IF 2012: 2.947.

6. Daniele Tedesco, Riccardo Zanasi, Irving W. Wainer, Carlo Bertucci (**2014**). Stereochemical and conformational study on fenoterol by ECD spectroscopy and TD-DFT calculations. *Journal of Pharmaceutical and Biomedical Analysis 91*, 92–96.
DOI: 10.1016/j.jpba.2013.12.018; IF 2012: 2.947.

7. Willian J. Andrioli, Raphael Conti, Magali J. Araújo, Riccardo Zanasi, Bruno C. Cavalcanti, Viviane Manfrim, Juliano S. Toledo, Daniele Tedesco, Manoel O. de Moraes, Cláudia Pessoa, Angela K. Cruz, Carlo Bertucci, José Sabino, Dhammika N.P. Nanayakkara, Mônica. T. Pupo, Jairo K. Bastos (**2013**). Mycoleptones A–C and polyketides from the endophyte *Mycoleptodiscus indicus*. *Journal of Natural Products 77*, 70-78.
DOI: 10.1021/np4006822; IF 2012: 3.285.

Bibliography

[1] Ariëns, E., Soudíjn, W., Timmermans, P., Eds. *Stereochemistry and Biological Activity of Drugs*; Blackwell: London, 1983.

[2] Testa, B. *Chirality* **1989**, *1*, 7–9.

[3] Wainer, I., Ed. *Drug stereochemistry: analytical methods and pharmacology*, 2nd ed.; Marcel Dekker: New York, 1993.

[4] Aboul-Enein, H., Wainer, I., Eds. *Chemical Analysis, vol. 142: The impact of stereochemistry on drug development and use*; Wiley & Sons: New York, 1997.

[5] Polavarapu, P. L. *Chem. Rec.* **2007**, *7*, 125–136.

[6] Bertucci, C.; Tedesco, D. *J. Chromatogr. A* **2012**, *1269*, 69–81.

[7] Bertucci, C.; Pistolozzi, M.; Tedesco, D.; Zanasi, R.; Ruzziconi, R.; Di Pietra, A. M. *J. Chromatogr. A* **2012**, *1232*, 128–133.

[8] Dong, F.; Li, J.; Chankvetadze, B.; Cheng, Y.; Xu, J.; Liu, X.; Li, Y.; Chen, X.; Bertucci, C.; Tedesco, D.; Zanasi, R.; Zheng, Y. *Environ. Sci. Technol.* **2013**, *47*, 3386–3394.

[9] Andrioli, W. J.; Conti, R.; Araújo, M. J.; Zanasi, R.; Cavalcanti, B. C.; Manfrim, V.; Toledo, J. S.; Tedesco, D.; de Moraes, M. O.; Pessoa, C.; Cruz, A. K.; Bertucci, C.; Sabino, J.; Nanayakkara, D. N. P.; Pupo, M. T.; Bastos, J. K. *J. Nat. Prod.* **2014**, *77*, 70–78.

[10] Tedesco, D.; Zanasi, R.; Guerrini, A.; Bertucci, C. *Chirality* **2012**, *24*, 741–750.

[11] Tedesco, D.; Zanasi, R.; Wainer, I. W.; Bertucci, C. *J. Pharm. Biomed. Anal.* **2014**, *91*, 92–96.

[12] Mohr, P. J.; Taylor, B. N.; Newell, D. B. *Rev. Mod. Phys.* **2012**, *84*, 1527–1605.

[13] Mulliken, R. S. *J. Chem. Phys.* **1939**, *7*, 14–20.

[14] Jaffé, H. H.; Orchin, M. *Theory and applications of ultraviolet spectroscopy*; Wiley & Sons: New York, 1966.

[15] Born, M.; Oppenheimer, R. *Ann. Phys.* **1927**, *84*, 457–484.

[16] Einstein, A. *Phys. Z.* **1917**, *18*, 121–128.

[17] Hilborn, R. C. *Am. J. Phys.* **1982**, *50*, 982–986.

[18] Sathyanarayana, D. N. *Electronic absorption spectroscopy and related techniques*; Universities Press: Hyderabad, 2001; pp 209–237.

[19] Eliel, E. L.; Wilen, S. H. *Stereochemistry of organic compounds*; Wiley & Sons: New York, 1994.

[20] Condon, E. U. *Rev. Mod. Phys.* **1937**, *9*, 432–457.

[21] Mason, S. F. *Q. Rev. Chem. Soc.* **1963**, *17*, 20–66.

[22] Schellman, J. A. *Chem. Rev.* **1975**, *75*, 323–331.

[23] Mason, S. F. *Molecular optical activity and the chiral discriminations*, 1st ed.; Cambridge University Press: Cambridge, 1982.

[24] Nakanishi, K., Berova, N., Woody, R. W., Eds. *Circular Dichroism: Principles and Applications*, 1st ed.; VCH Publishers: New York, 1994.

[25] Berova, N., Nakanishi, K., Woody, R. W., Eds. *Circular dichroism: principles and applications*, 2nd ed.; Wiley-VCH: New York, 2000.

[26] Barron, L. D. *Molecular light scattering and optical activity*; Cambridge University Press: Cambridge, 2004.

[27] Pecul, M.; Ruud, K. In *Advances in Quantum Chemistry, vol. 50 - Response Theory and Molecular Properties (A Tribute to Jan Linderberg and Poul Jørgensen)*; Jensen, H. J. Å., Ed.; Academic Press: London, 2005; pp 185–212.

[28] Autschbach, J. *Chirality* **2009**, *21*, E116–E152.

[29] Autschbach, J.; Nitsch-Velasquez, L.; Rudolph, M. In *Topics in Current Chemistry, vol. 298: Electronic and Magnetic Properties of Chiral Molecules and Supramolecular Architectures*; Naaman, R., Beratan, D. N., Waldeck, D., Eds.; Springer: Berlin/Heidelberg, 2011; pp 1–98.

[30] Berova, N., Polavarapu, P. L., Nakanishi, K., Woody, R. W., Eds. *Comprehensive chiroptical spectroscopy, vol. 1-2*; Wiley & Sons: Hoboken, 2012.

[31] Rosenfeld, L. *Z. Phys.* **1929**, *52*, 161–174.

[32] Fasman, G., Ed. *Circular dichroism and the conformational analysis of biomolecules*, 1st ed.; Plenum Press: New York, 1996.

[33] Gottarelli, G.; Lena, S.; Masiero, S.; Pieraccini, S.; Spada, G. P. *Chirality* **2008**, *20*, 471–485.

[34] Kelly, S. M.; Jess, T. J.; Price, N. C. *Biochim. Biophys. Acta* **2005**, *1751*, 119–139.

[35] Whitmore, L.; Wallace, B. A. *Biopolymers* **2008**, *89*, 392–400.

[36] Bertucci, C.; Pistolozzi, M.; De Simone, A. *Curr. Pharm. Biotechnol.* **2011**, *12*, 1508–1516.

[37] Kypr, J.; Kejnovská, I.; Renčiuk, D.; Vorlíčková, M. *Nucleic Acids Res.* **2009**, *37*, 1713–1725.

[38] Zsila, F.; Bikadi, Z.; Fitos, I.; Simonyi, M. *Curr. Drug Discov. Technol.* **2004**, *1*, 133–53.

[39] Bertucci, C.; Pistolozzi, M.; De Simone, A. *Anal. Bioanal. Chem.* **2010**, *398*, 155–166.

[40] Greenfield, N. J. *Methods Mol. Biol.* **2004**, *261*, 55–78.

[41] Salvadori, P.; Bertucci, C.; Rosini, C. *Chirality* **1991**, *3*, 376–385.

[42] Krenn, W.; Verdino, P.; Uray, G.; Faber, K.; Kappe, C. O. *Chirality* **1999**, *11*, 659–662.

[43] Cirilli, R.; Ferretti, R.; La Regina, G.; Morelli, G.; Pierini, M.; Piscitelli, F.; Silvestri, R. *Talanta* **2010**, *82*, 1306–1312.

[44] Platt, J. R. *J. Chem. Phys.* **1949**, *17*, 484–495.

[45] Mislow, K.; Glass, M. A. W.; O'Brien, R. E.; Rutkin, P.; Steinberg, D. H.; Weiss, J.; Djerassi, C. *J. Am. Chem. Soc.* **1962**, *84*, 1455–1478.

[46] Mislow, K.; Bunnenberg, E.; Records, R.; Wellman, K.; Djerassi, C. *J. Am. Chem. Soc.* **1963**, *85*, 1342–1349.

[47] Gawroński, J. K. In *Houben-Weyl Methods of Organic Chemistry, vol. E21a: Stereoselective Synthesis*; Helmchen, G., Hoffmann, R., Mulzer, J., Schaumann, E., Eds.; Thieme: Stuttgart, 1995; pp 499–533.

[48] Gawroński, J. K.; Grycz, P.; Kwit, M.; Rychlewska, U. *Chemistry* **2002**, *8*, 4210–4215.

[49] Smith, H. E. *Chem. Rev.* **1998**, *98*, 1709–1740.

[50] Moscowitz, A.; Charney, E.; Weiss, U.; Ziffer, H. *J. Am. Chem. Soc.* **1961**, *83*, 4661–4663.

[51] Gawroński, J. K.; Walborsky, H. M. In *Circular dichroism: principles and applications*, 1st ed.; Nakanishi, K., Berova, N., Woody, R. W., Eds.; VCH Publishers: New York, 1994; pp 301–334.

[52] Salvadori, P.; Rosini, C.; Bertucci, C. In *Chemical Analysis, vol. 142: The impact of stereochemistry on drug development and use*; Aboul-Enein, H., Wainer, I., Eds.; Wiley & Sons: New York, 1997; pp 493–519.

[53] Charney, E. *The molecular basis of optical activity: optical rotatory dispersion and circular dichroism*; Wiley & Sons: New York, 1979.

[54] Kurtán, T.; Pescitelli, G.; Salvadori, P.; Kenéz, A.; Antus, S.; Szilágyi, L.; Illyés, T.-Z.; Szabó, I. *Chirality* **2008**, *20*, 379–385.

[55] Burgstahler, A. W.; Barkhurst, R. C. *J. Am. Chem. Soc.* **1970**, *92*, 7601–7603.

[56] Djerassi, C. *Optical rotatory dispersion: applications to organic chemistry*; McGraw-Hill: New York, 1960.

[57] Moffitt, W.; Woodward, R. B.; Moscowitz, A.; Klyne, W.; Djerassi, C. *J. Am. Chem. Soc.* **1961**, *83*, 4013–4018.

[58] Lightner, D.; Gurst, J. *Organic Conformational Analysis and Stereochemistry from Circular Dichroism Spectroscopy*; Wiley-VCH: New York, 2000.

[59] Lightner, D. A. In *Circular dichroism: principles and applications*, 2nd ed.; Berova, N., Nakanishi, K., Woody, R. W., Eds.; Wiley-VCH: New York, 2000; pp 261–303.

[60] Rehling, H.; Jensen, H. *Tetrahed. Lett.* **1972**, *13*, 2793–2796.

[61] Ong, E. C.; Cusachs, L. C.; Oscar E. Weigang, J. *J. Chem. Phys.* **1977**, *67*, 3289–3297.

[62] Polonski, T.; Milewska, M. J. *Croat. Chim. Acta* **1989**, *62*, 129–134.

[63] Galle, D.; Tolksdorf, M.; Braun, M. *Tetrahed. Lett.* **1995**, *36*, 4217–4220.

[64] Barbaro, G.; Battaglia, A.; Guerrini, A.; Bertucci, C. *Tetrahed. Asym.* **1998**, *9*, 3401–3409.

[65] Boyd, D. B.; Riehl, J. P.; Richardson, F. S. *Tetrahedron* **1979**, *35*, 1499–1508.

[66] Łysek, R.; Borsuk, K.; Chmielewski, M.; Kałuza, Z.; Urbańczyk-Lipkowska, Z.; Klimek, A.; Frelek, J. *J. Org. Chem.* **2002**, *67*, 1472–1479.

[67] McCann, J.; Rauk, A.; Shustov, G. V.; Wieser, H.; Yang, D. *Appl. Spectr.* **1996**, *50*, 630–641.

[68] Frelek, J.; Kowalska, P.; Masnyk, M.; Kazimierski, A.; Korda, A.; Woźnica, M.; Chmielewski, M.; Furche, F. *Chem. Eur. J.* **2007**, *13*, 6732–6744.

[69] Gedanken, A. In *The chemistry of functional groups, Supplement E2, part 1: The chemistry of hydroxyl, ether and peroxide groups*; Patai, S., Ed.; Wiley & Sons: New York, 1993; pp 87–102.

[70] Michals, D. R.; Smith, H. E. *Chirality* **1993**, *5*, 20–23.

[71] Beigi, F.; Bertucci, C.; Zhu, W.; Chakir, K.; Wainer, I. W.; Xiao, R.-P.; Abernethy, D. R. *Chirality* **2006**, *18*, 822–827.

[72] Raabe, G.; Fleischhauer, J.; Woody, R. W. In *Comprehensive chiroptical spectroscopy, vol. 1*; Berova, N., Polavarapu, P. L., Nakanishi, K., Woody, R. W., Eds.; Wiley & Sons: Hoboken, 2012; Vol. 1; pp 543–591.

[73] Berova, N.; Nakanishi, K. In *Circular dichroism: principles and applications*, 2nd ed.; Berova, N., Nakanishi, K., Woody, R. W., Eds.; Wiley-VCH: New York, 2000; pp 337–382.

[74] Kasha, M.; Rawls, H. R.; Ashraf El-Bayoumi, M. *Pure Appl. Chem.* **1965**, *11*, 371–392.

[75] Mason, S. F. *Proc. Chem. Soc.* **1962**, *1962*, 362–363.

[76] Mason, S. F.; Vane, G. W. *J. Chem. Soc. B* **1966**, *1966*, 370–374.

[77] Harada, N.; Nakanishi, K. *Acc. Chem. Res.* **1972**, *5*, 257–263.

[78] Harada, N.; Nakanishi, K. *Circular dichroic spectroscopy: exciton coupling in organic stereochemistry*; University Science Books: Mill Valley, 1983.

[79] Bellucci, G.; Berti, G.; Chiappe, C.; Lippi, A.; Marioni, F. *J. Med. Chem.* **1987**, *30*, 768–773.

[80] Pini, D.; Petri, A.; Rosini, C.; Salvadori, P.; Giorgi, R.; Di Bugno, C.; Turbanti, L.; Marchetti, F. *Tetrahedron* **1994**, *50*, 205–216.

[81] Parish, C. A.; Dong, J.-G.; Bornmann, W. G.; Chang, J.; Nakanishi, K.; Berova, N. *Tetrahedron* **1998**, *54*, 15739–15758.

[82] Sunazuka, T.; Shirahata, T.; Yoshida, K.; Yamamoto, D.; Harigaya, Y.; Nagai, T.; Kiyohara, H.; Yamada, H.; Kuwajima, I.; Ōmura, S. *Tetrahed. Lett.* **2002**, *43*, 1265–1268.

[83] Molinski, T. F.; Brzezinski, L. J.; Leahy, J. W. *Tetrahed. Asym.* **2002**, *13*, 1013–1016.

[84] DeVoe, H. *J. Chem. Phys.* **1964**, *41*, 393–400.

[85] DeVoe, H. *J. Chem. Phys.* **1965**, *43*, 3199–3208.

[86] Rosini, C.; Zandomeneghi, M.; Salvadori, R. *Tetrahed. Asym.* **1993**, *4*, 545–554.

[87] Salvadori, P.; Bertucci, C.; Rosini, C.; Zandomeneghi, M.; Gallo, G. G.; Martinelli, E.; Ferrari, P. *J. Am. Chem. Soc.* **1981**, *103*, 5553–5557.

[88] Rosini, C.; Bertucci, C.; Salvadori, P.; Zandomeneghi, M. *J. Am. Chem. Soc.* **1985**, *107*, 17–19.

[89] Di Bari, L.; Mannucci, S.; Pescitelli, G.; Salvadori, P. *Chirality* **2002**, *14*, 611–617.

[90] Superchi, S.; Giorgio, E.; Rosini, C. *Chirality* **2004**, *16*, 422–451.

[91] Bode, K. A.; Applequist, J. *J. Am. Chem. Soc.* **1998**, *120*, 10938–10946.

[92] Jensen, F. *Introduction to computational chemistry*; Wiley and Sons: Chichester, 1999.

[93] Hansen, A. E.; Bouman, T. D. In *Advances in Chemical Physics, vol. 44*; Prigogine, I., Rice, S. A., Eds.; Wiley & Sons: New York, 1980; pp 545–644.

[94] Bouman, T. D.; Hansen, A. E. *Croat. Chim. Acta* **1989**, *62*, 227–243.

[95] Hansen, A. E.; Bak, K. *Enantiomer* **1999**, *4*, 455–476.

[96] Koslowski, A.; Sreerama, N.; Woody, R. W. In *Circular dichroism: principles and applications*, 2nd ed.; Berova, N., Nakanishi, K., Woody, R. W., Eds.; Wiley-VCH: New York, 2000; pp 55–96.

[97] Sandström, J. *Chirality* **2000**, *12*, 162–171.

[98] Bringmann, G.; Tasler, S.; Endress, H.; Kraus, J.; Messer, K.; Wohlfarth, M.; Lobin, W. *J. Am. Chem. Soc.* **2001**, *123*, 2703–2711.

[99] Fugmann, B.; Arnold, S.; Steglich, W.; Fleischhauer, J.; Repges, C.; Koslowski, A.; Raabe, G. *Eur. J. Org. Chem.* **2001**, *2001*, 3097–3104.

[100] Harada, N. In *Circular dichroism: principles and applications*, 2nd ed.; Berova, N., Nakanishi, K., Woody, R., Eds.; Wiley-VCH: New York, 2000; pp 431–457.

[101] Charney, E. *Tetrahedron* **1965**, *21*, 3127–3139.

[102] Lynden-Bell, R. M.; Saunders, V. P. *J. Chem. Soc. A* **1967**, *1967*, 2061–2066.

[103] Hug, W.; Wagnière, G. *Theor. Chim. Acta* **1970**, *18*, 57–66.

[104] Brown, A.; Kemp, C. M.; Mason, S. F. *J. Chem. Soc. A* **1971**, *1971*, 751–755.

[105] Snatzke, G. *Angew. Chem. Int. Ed. Engl.* **1979**, *18*, 363–377.

[106] Snatzke, G.; Wynberg, H.; Feringa, B.; Marsman, B. G.; Greydanus, B.; Pluim, H. *J. Org. Chem.* **1980**, *45*, 4094–4096.

[107] Robin, M. B.; Basch, H.; Kuebler, N. A.; Kaplan, B. E.; Meinwald, J. *J. Chem. Phys.* **1968**, *48*, 5037–5047.

[108] Bendazzoli, G. L.; Gottarelli, G.; Palmieri, P. *J. Am. Chem. Soc.* **1974**, *96*, 11–16.

[109] Crawford, T. D. In *Comprehensive chiroptical spectroscopy, vol. 1*; Berova, N., Polavarapu, P. L., Nakanishi, K., Woody, R. W., Eds.; Wiley & Sons: Hoboken, 2012; Vol. 1; pp 675–697.

[110] Autschbach, J. In *Comprehensive chiroptical spectroscopy, vol. 1*; Berova, N., Polavarapu, P. L., Nakanishi, K., Woody, R. W., Eds.; Wiley & Sons: Hoboken, 2012; Vol. 1; pp 593–642.

[111] Goerigk, L.; Kruse, H.; Grimme, S. In *Comprehensive Chiroptical Spectroscopy, vol. 1*; Berova, N., Polavarapu, P. L., Nakanishi, K., Woody, R. W., Eds.; Wiley & Sons: Hoboken, 2012; Vol. 1; pp 643–673.

[112] Polavarapu, P. L. *Chirality* **2012**, *24*, 909–920.

[113] Stephens, P. J.; Harada, N. *Chirality* **2010**, *22*, 229–233.

[114] Tomasi, J.; Mennucci, B.; Cammi, R. *Chem. Rev.* **2005**, *105*, 2999–3094.

[115] Mennucci, B.; Cappelli, C.; Cammi, R.; Tomasi, J. *Chirality* **2011**, *23*, 717–729.

[116] Schlosser, M. *Tetrahedron* **1978**, *34*, 3–17.

[117] Filler, R., Kobayashi, Y., Eds. *Biomedicinal aspects of fluorine chemistry*; Elsevier Biomedical Press: Amsterdam, 1982.

[118] Welch, J.; Eswarakrishnan, S. *Fluorine in Bioorganic Chemistry*; Wiley Interscience Publication; John Wiley & Sons: New York, 1991.

[119] Schlosser, M.; Michel, D. *Tetrahedron* **1996**, *52*, 99–108.

[120] Schlosser, M. *Angew. Chem. Int. Ed. Engl.* **1998**, *37*, 1496–1513.

[121] Schlosser, M. In *Enantiocontrolled Synthesis of Fluoroorganic Compounds: Stereochemical Challenges and Biomedicinal Targets*; Soloshonok, V. A., Ed.; Wiley: Chichester, 1999; Chapter 21, pp 613–659.

[122] Hamman, S. *J. Fluorine Chem.* **1993**, *60*, 225–232.

[123] Eirín, A.; Fernández, F.; Gómez, G.; López, C.; Santos, A.; Calleja, J. M.; Cano, E. *Arch. Pharm. (Weinheim)* **1989**, *322*, 281–284.

[124] Ricci, G.; Ruzziconi, R. *J. Org. Chem.* **2005**, *70*, 611–623.

[125] Halgren, T. A. *J. Comp. Chem.* **1999**, *20*, 720–729.

[126] Spartan'02. 2002; Wavefunction, Inc., Irvine, CA, USA.

[127] Hohenberg, P.; Kohn, W. *Phys. Rev.* **1964**, *136*, B864–B871.

[128] Kohn, W.; Sham, L. J. *Phys. Rev.* **1965**, *140*, A1133–A1138.

[129] Frisch, M. J.; Trucks, G. W.; Schlegel, H. B.; Scuseria, G. E.; Robb, M. A.; Cheeseman, J. R.; Scalmani, G.; Barone, V.; Mennucci, B.; Petersson, G. A.; Nakatsuji, H.; Caricato, M.; Li, X.; Hratchian, H. P.; Izmaylov, A. F.; Bloino, J.; Zheng, G.; Sonnenberg, J. L.; Hada, M.; Ehara, M.; Toyota, K.; Fukuda, R.; Hasegawa, J.; Ishida, M.; Nakajima, T.; Honda, Y.; Kitao, O.; Nakai, H.; Vreven, T.; Jr, J. A. M.; Peralta, J. E.; Ogliaro, F.; Bearpark, M.; Heyd, J. J.; Brothers, E.; Kudin, K. N.; Staroverov, V. N.; Kobayashi, R.; Normand, J.; Raghavachari, K.; Rendell, A.; Burant, J. C.; Iyengar, S. S.; Tomasi, J.; Cossi, M.; Rega, N.; Millam, J. M.; Klene, M.; Knox, J. E.; Cross, J. B.; Bakken, V.; Adamo, C.; Jaramillo, J.; Gomperts, R.; Stratmann, R. E.; Yazyev, O.; Austin, A. J.; Cammi, R.; Pomelli, C.; Ochterski, J. W.; Martin, R. L.; Morokuma, K.; Zakrzewski, V. G.; Voth, G. A.; Salvador, P.; Dannenberg, J. J.; Dapprich, S.; Daniels, A. D.; Farkas, O.; Foresman, J. B.; Ortiz, J. V.; Cioslowski, J.; Fox, D. J. Gaussian 09, Revision A.02. 2009; Gaussian, Inc., Wallingford, CT, USA.

[130] Becke, A. D. *J. Chem. Phys.* **1993**, *98*, 5648–5652.

[131] Lee, C.; Yang, W.; Parr, R. G. *Phys. Rev. B* **1988**, *37*, 785–789.

[132] Vosko, S. H.; Wilk, L.; Nusair, M. *Can. J. Phys.* **1980**, *58*, 1200–1211.

[133] Stephens, P. J.; Devlin, F. J.; Chabalowski, C. F.; Frisch, M. J. *J. Phys. Chem.* **1994**, *98*, 11623–11627.

[134] Huzinaga, S. *J. Chem. Phys.* **1965**, *42*, 1293–1302.

[135] Dunning, T. H. *J. Chem. Phys.* **1971**, *55*, 716–723.

[136] Tomasi, J.; Mennucci, B.; Cancès, E. *J. Mol. Struct. THEOCHEM* **1999**, *464*, 211–226.

[137] Bauernschmitt, R.; Ahlrichs, R. *Chem. Phys. Lett.* **1996**, *256*, 454–464.

[138] Taylor, J. R. *Introduction to error analysis: the study of uncertainties in physical measurements*, 2nd ed.; University Science Books: Sausalito, 1997.

[139] Vawdrey, L.; Grice, K.; Westerhuis, D. *Australas. Plant Pathol.* **2008**, *37*, 552–558.

[140] Horsfield, A.; Wicks, T.; Davies, K.; Wilson, D.; Paton, S. *Australas. Plant Pathol.* **2010**, *39*, 368–375.

[141] European Food Safety Authority, *EFSA Journal* **2011**, *9*, 1967.

[142] Sanderson, J.; Boerma, J.; Lansbergen, G. W.; van den Berg, M. *Toxicol. Appl. Pharmacol.* **2002**, *182*, 44–54.

[143] Sanderson, J. T. *Toxicol. Sci.* **2006**, *94*, 3–21.

[144] Konwick, B. J.; Fisk, A. T.; Garrison, A. W.; Avants, J. K.; Black, M. C. *Environ. Toxicol. Chem.* **2005**, *24*, 2350–2355.

[145] Liu, W.; Ye, J.; Jin, M. *J. Agric. Food Chem.* **2009**, *57*, 2087–2095.

[146] Zhang, Q.; Zhao, M.; Qian, H.; Lu, T.; Zhang, Q.; Liu, W. *Environ. Sci. Technol.* **2012**, *46*, 8405–8412.

[147] Buser, H.-R.; Müller, M. D.; Poiger, T.; Balmer, M. E. *Environ. Sci. Technol.* **2002**, *36*, 221–226.

[148] Wong, C. S.; Lau, F.; Clark, M.; Mabury, S. A.; Muir, D. C. G. *Environ. Sci. Technol.* **2002**, *36*, 1257–1262.

[149] Wong, C. *Anal. Bioanal. Chem.* **2006**, *386*, 544–558.

[150] Konwick, B. J.; Garrison, A. W.; Black, M. C.; Avants, J. K.; Fisk, A. T. *Environ. Sci. Technol.* **2006**, *40*, 2930–2936.

[151] Garrison, A. W.; Avants, J. K.; Jones, W. J. *Environ. Sci. Technol.* **2011**, *45*, 2186–2193.

[152] Xu, M.; Zhang, G.; Wang, M.-C.; Qi, Z.-C. *Chin. J. Magn. Reson.* **2010**, *27*, 642–649.

[153] Becke, A. D. *J. Chem. Phys.* **1997**, *107*, 8554–8560.

[154] Grimme, S. *J. Comp. Chem.* **2006**, *27*, 1787–1799.

[155] Perdew, J. P.; Burke, K.; Ernzerhof, M. *Phys. Rev. Lett.* **1996**, *77*, 3865–3868.

[156] Perdew, J. P.; Burke, K.; Ernzerhof, M. *Phys. Rev. Lett.* **1997**, *78*, 1396–1396.

[157] Adamo, C.; Barone, V. *J. Chem. Phys.* **1999**, *110*, 6158–6170.

[158] Frisch, M. J.; Trucks, G. W.; Schlegel, H. B.; Scuseria, G. E.; Robb, M. A.; Cheeseman, J. R.; Scalmani, G.; Barone, V.; Mennucci, B.; Petersson, G. A.; Nakatsuji, H.; Caricato, M.; Li, X.; Hratchian, H. P.; Izmaylov, A. F.; Bloino, J.; Zheng, G.; Sonnenberg, J. L.; Hada, M.; Ehara, M.; Toyota, K.; Fukuda, R.; Hasegawa, J.; Ishida, M.; Nakajima, T.; Honda, Y.; Kitao, O.; Nakai, H.; Vreven, T.; J. A. Montgomery, J.; Peralta, J. E.; Ogliaro, F.; Bearpark, M.; Heyd, J. J.; Brothers, E.; Kudin, K. N.; Staroverov, V. N.; Keith, T.; Kobayashi, R.; Normand, J.; Raghavachari, K.; Rendell, A.; Burant, J. C.; Iyengar, S. S.; Tomasi, J.; Cossi, M.; Rega, N.; Millam, J. M.; Klene, M.; Knox, J. E.; Cross, J. B.; Bakken, V.; Adamo, C.; Jaramillo, J.; Gomperts, R.; Stratmann, R. E.; Yazyev, O.; Austin, A. J.; Cammi, R.; Pomelli, C.; Ochterski, J. W.; Martin, R. L.; Morokuma, K.; Zakrzewski, V. G.; Voth, G. A.; Salvador, P.; Dannenberg, J. J.; Dapprich, S.; Daniels, A. D.; Farkas, O.; Foresman, J. B.; Ortiz, J. V.; Cioslowski, J.; Fox, D. J. Gaussian 09, Revision C.01. 2010; Gaussian, Inc., Wallingford, CT, USA.

[159] McLean, A. D.; Chandler, G. S. *J. Chem. Phys.* **1980**, *72*, 5639–5648.

[160] Huzinaga, S. *Approximate atomic functions. II*; 1971.

[161] Parthiban, S.; Lee, T. J.; Guha, S.; Francisco, J. S. *J. Am. Chem. Soc.* **2003**, *125*, 10446–10458.

[162] Petrini, O. In *Microbial Ecology of Leaves*; Andrews, J. H., Hirano, S. S., Eds.; Brock/Springer Series in Contemporary Bioscience; Springer: New York, 1991; pp 179–197.

[163] Gunatilaka, A. A. L. *J. Nat. Prod.* **2006**, *69*, 509–526.

[164] Borges, W. d. S.; Borges, K. B.; Bonato, P. S.; Said, S.; Pupo, M. T. *Curr. Org. Chem.* **2009**, *13*, 1137–1163.

[165] Bunyapaiboonsri, T.; Yoiprommarat, S.; Srikitikulchai, P.; Srichomthong, K.; Lumyong, S. *J. Nat. Prod.* **2010**, *73*, 55–59.

[166] Shearer, J. F. *J. Aquat. Plant Manag.* **2002**, *40*, 76–78.

[167] Padhye, A. A.; Davis, M. S.; Reddick, A.; Bell, M. F.; Gearhart, E. D.; Von Moll, L. *J. Clin. Microbiol.* **1995**, *33*, 2796–7.

[168] Garrison, A.; Procop, G.; Vincek, V.; Moon, J.; Morris, M.; Doblecki-Lewis, S.; Cleary, T.; Brust, D.; Rosa-Cunha, I. *Transpl. Infect. Dis.* **2008**, *10*, 218–220.

[169] Steyn, P. S. *Tetrahedron* **1973**, *29*, 107–120.

[170] Vleggaar, R.; Steyn, P. S.; Nagel, D. W. *J. Chem. Soc., Perkin Trans. 1* **1974**, *1974*, 45–49.

[171] Feng, Y.; Blunt, J. W.; Cole, A. L. J.; Munro, M. H. G. *J. Nat. Prod.* **2002**, *65*, 1681–1682.

[172] Fox, C. H.; Huneck, S. *Phytochemistry* **1969**, *8*, 1301–1304.

[173] Joshi, B. S.; Ravindranath, K. R. *J. Chem. Soc., Perkin Trans. 1* **1977**, *1977*, 433–436.

[174] Li, G.-Y.; Li, B.-G.; Yang, T.; Liu, G.-Y.; Zhang, G.-L. *Helv. Chim. Acta* **2008**, *91*, 124–129.

[175] Osmanova, N.; Schultze, W.; Ayoub, N. *Phytochem. Rev.* **2010**, *9*, 315–342.

[176] Gao, J.-M.; Yang, S.-X.; Qin, J.-C. *Chem. Rev.* **2013**, *113*, 4755–4811.

[177] Arai, N.; Shiomi, K.; Tomoda, H.; Tabata, N.; Yang, D.; Masuma, R.; Kawakubo, T.; Omura, S. *J. Antibiot. (Tokyo)* **1995**, *48*, 696–702.

[178] Colombo, L.; Gennari, C.; Ricca, G. S.; Scolastico, C.; Aragozzini, F. *J. Chem. Soc., Chem. Commun.* **1981**, *1981*, 575–576.

[179] Park, J.-H.; Choi, G. J.; Jang, K. S.; Lim, H. K.; Kim, H. T.; Cho, K. Y.; Kim, J.-C. *FEMS Microbiol. Lett.* **2005**, *252*, 309–313.

[180] Du, L.; Li, D.; Zhang, G.; Zhu, T.; Ai, J.; Gu, Q. *Tetrahedron* **2010**, *66*, 9286–9290.

[181] Shao, C.-L.; Wang, C.-Y.; Wei, M.-Y.; Gu, Y.-C.; She, Z.-G.; Qian, P.-Y.; Lin, Y.-C. *Bioorg. Med. Chem. Lett.* **2011**, *21*, 690–693.

[182] Wu, X. Y.; Liu, X. H.; Lin, Y. C.; Luo, J. H.; She, Z. G.; Houjin, L.; Chan, W. L.; Antus, S.; Kurtan, T.; Elsässer, B.; Krohn, K. *Eur. J. Org. Chem.* **2005**, *2005*, 4061–4064.

[183] Krishnan, R.; Binkley, J. S.; Seeger, R.; Pople, J. A. *J. Chem. Phys.* **1980**, *72*, 650–654.

[184] Clark, T.; Chandrasekhar, J.; Spitznagel, G. W.; Schleyer, P. V. R. *J. Comp. Chem.* **1983**, *4*, 294–301.

[185] Frisch, M. J.; Pople, J. A.; Binkley, J. S. *J. Chem. Phys.* **1984**, *80*, 3265–3269.

[186] Lukacs, G., Ohno, M., Eds. *Recent progress in the chemical synthesis of antibiotics*; Springer-Verlag: Berlin, 1990.

[187] Morin, R. B., Gorman, M., Eds. *Chemistry and biology of β-lactam antibiotics, vol. 1-3*; Academic Press: New York, 1982.

[188] Sammes, P. G., Ed. *Topics in antibiotic chemistry, vol. 3*; Ellis Horwood Ltd.: New York, 1980.

[189] O'Sullivan, J.; Abraham, E. P. In *Antibiotics, vol. IV, Biosynthesis*; Corcoran, J. W., Ed.; Springer-Verlag: Berlin, 1982; pp 101–122.

[190] Bentley, P. M., Southgate, R., Eds. *Recent advances in the chemistry of β-lactam antibiotics*; The Royal Society of Chemistry: London, 1989.

[191] Christensen, B. G. In *β-Lactam antibiotics*; Salton, M. R. J., Shockman, G. D., Eds.; Academic Press: New York, 1981; pp 101–122.

[192] Burnett, D. A.; Caplen, M. A.; Davis, H. R.; Burrier, R. E.; Clader, J. W. *J. Med. Chem.* **1994**, *37*, 1733–1736.

[193] Braun, M.; Galle, D. *Synthesis* **1996**, *1996*, 819–820.

[194] Chen, L.-Y.; Zaks, A.; Chackalamannil, S.; Dugar, S. *J. Org. Chem.* **1996**, *61*, 8341–8343.

[195] Adlington, R. M.; Baldwin, J. E.; Becker, G. W.; Chen, B.; Cheng, L.; Cooper, S. L.; Hermann, R. B.; Howe, T. J.; McCoull, W.; McNulty, A. M.; Neubauer, B. L.; Pritchard, G. J. *J. Med. Chem.* **2001**, *44*, 1491–1508.

[196] Ojima, I. In *The organic chemistry of β-lactam antibiotics*; Georg, G. I., Ed.; VCH: New York, 1992; pp 197–255.

[197] Ojima, I.; Habus, I.; Zhao, M.; Zucco, M.; Park, Y. H.; Sun, C. M.; Brigaud, T. *Tetrahedron* **1992**, *48*, 6985–7012.

[198] Ojima, I. *Acc. Chem. Res.* **1995**, *28*, 383–389.

[199] Ojima, I.; Delaloge, F. *Chem. Soc. Rev.* **1997**, *26*, 377–386.

[200] Palomo, C.; Aizpurua, J. M.; Ganboa, I.; Oiarbide, M. *Synlett* **2001**, *2001*, 1813–1826.

[201] Barbaro, G.; Battaglia, A.; Guerrini, A.; Bertucci, C. *Tetrahed. Asym.* **1997**, *8*, 2527–2531.

[202] Barbaro, G.; Battaglia, A.; Guerrini, A.; Bertucci, C. *J. Org. Chem.* **1999**, *64*, 4643–4651.

[203] Barbaro, G.; Battaglia, A.; Di Giuseppe, F.; Giorgianni, P.; Guerrini, A.; Bertucci, C.; Geremia, S. *Tetrahed. Asym.* **1999**, *10*, 2765–2773.

[204] Battaglia, A.; Guerrini, A.; Bertucci, C. *J. Org. Chem.* **2004**, *69*, 9055–9062.

[205] Seebach, D.; Sting, A. R.; Hoffmann, M. *Angew. Chem. Int. Ed. Engl.* **1996**, *35*, 2708–2748.

[206] Huang, X.; Rickman, B. H.; Borhan, B.; Berova, N.; Nakanishi, K. *J. Am. Chem. Soc.* **1998**, *120*, 6185–6186.

[207] Petrovic, A. G.; Chen, Y.; Pescitelli, G.; Berova, N.; Proni, G. *Chirality* **2010**, *22*, 129–139.

[208] Chen, Y.; Petrovic, A. G.; Roje, M.; Pescitelli, G.; Kayser, M. M.; Yang, Y.; Berova, N.; Proni, G. *Chirality* **2010**, *22*, 140–152.

[209] Humphrey, W.; Dalke, A.; Schulten, K. *J. Mol. Graphics* **1996**, *14*, 33–38.

[210] Ditchfield, R.; Hehre, W. J.; Pople, J. A. *J. Chem. Phys.* **1971**, *54*, 724–728.

[211] Hehre, W. J.; Ditchfield, R.; Pople, J. A. *J. Chem. Phys.* **1972**, *56*, 2257–2261.

[212] Hariharan, P. C.; Pople, J. A. *Theor. Chem. Acc.* **1973**, *28*, 213–222.

[213] Gordon, M. S. *Chem. Phys. Lett.* **1980**, *76*, 163–168.

[214] Pescitelli, G.; Di Bari, L.; Berova, N. *Chem. Soc. Rev.* **2011**, *40*, 4603–4625.

[215] Jóźwiak, K.; Płazińska, A.; Toll, L.; Jimenez, L.; Woo, A. Y.-H.; Xiao, R.-P.; Wainer, I. W. *Chirality* **2011**, *23*, E1–E6.

[216] Jóźwiak, K.; Khalid, C.; Tanga, M. J.; Berzetei-Gurske, I.; Jimenez, L.; Kozocas, J. A.; Woo, A.; Zhu, W.; Xiao, R.-P.; Abernethy, D. R.; Wainer, I. W. *J. Med. Chem.* **2007**, *50*, 2903–2915.

[217] Jóźwiak, K.; Woo, A. Y.-H.; Tanga, M. J.; Toll, L.; Jimenez, L.; Kozocas, J. A.; Płazińska, A.; Xiao, R.-P.; Wainer, I. W. *Bioorg. Med. Chem.* **2010**, *18*, 728–736.

[218] Talan, M. I.; Ahmet, I.; Xiao, R. P.; Lakatta, E. G. *J. Mol. Cell. Cardiol.* **2011**, *51*, 529–533.

[219] Toll, L.; Jimenez, L.; Waleh, N.; Jóźwiak, K.; Woo, A. Y. H.; Xiao, R. P.; Bernier, M.; Wainer, I. W. *J. Pharmacol. Exp. Ther.* **2011**, *336*, 524–532.

[220] Paul, R. K.; Ramamoorthy, A.; Scheers, J.; Wersto, R. P.; Toll, L.; Jimenez, L.; Bernier, M.; Wainer, I. W. *J. Pharmacol. Exp. Ther.* **2012**, *343*, 157–166.

[221] Brewster, J. H.; Buta, J. G. *J. Am. Chem. Soc.* **1966**, *88*, 2233–2240.

[222] Smith, H. E.; Fontana, L. P. *J. Org. Chem.* **1991**, *56*, 432–435.

[223] Schäfer, A.; Huber, C.; Ahlrichs, R. *J. Chem. Phys.* **1994**, *100*, 5829–5835.

[224] Grimme, S. *WIREs Comput. Mol. Sci.* **2011**, *1*, 211–228.

[225] Dunlap, B. *J. Chem. Phys.* **1983**, *78*, 3140–3142.

[226] Dunlap, B. I. *J. Mol. Struct. THEOCHEM* **2000**, *529*, 37–40.

[227] Lo Presti, L.; Soave, R.; Destro, R. *Acta Cryst. C* **2003**, *59*, o199–o201.

[228] Lo Presti, L.; Soave, R.; Destro, R. *J. Phys. Chem. B* **2006**, *110*, 6405–6414.

[229] Horeau, A. *Tetrahed. Lett.* **1961**, *2*, 506–512.

[230] Engel, D. W.; Kruger, G. J. *Acta Crystallogr. B* **1976**, *32*, 2545–2548.

[231] IUPAC Commission on food chemistry, eds. Pohland, A. E.; Schuller, P. L.; Steyn, P. S.; Van Egmond, H. P. *Pure Appl. Chem.* **1982**, *54*, 2219–2284.

[232] Pecul, M. In *Comprehensive chiroptical spectroscopy, vol. 1*; Berova, N., Polavarapu, P. L., Nakanishi, K., Woody, R. W., Eds.; Wiley & Sons: Hoboken, 2012; Vol. 1; pp 729–745.

[233] Mukhopadhyay, P.; Zuber, G.; Wipf, P.; Beratan, D. *Angew. Chem. Int. Ed. Engl.* **2007**, *46*, 6450–6452.

[234] Neugebauer, J. *Angew. Chem. Int. Ed. Engl.* **2007**, *46*, 7738–7740.

[235] Frenkel, D.; Smit, B. *Understanding molecular simulation: from algorithms to applications*, 2nd ed.; Academic Press: London, 2002.

[236] Car, R.; Parrinello, M. *Phys. Rev. Lett.* **1985**, *55*, 2471–2474.

[237] Marx, D.; Hutter, J. In *Modern methods and algorithms of quantum chemistry*; Grotendorst, J., Ed.; John von Neumann Institute for Computing: Julich, 2000; Vol. 1; pp 301–449.

[238] Bussi, G.; Donadio, D.; Parrinello, M. *J. Chem. Phys.* **2007**, *126*, 014101.

[239] Jorgensen, W. L.; Maxwell, D. S.; Tirado-Rives, J. *J. Am. Chem. Soc.* **1996**, *118*, 11225–11236.

[240] Essmann, U.; Perera, L.; Berkowitz, M. L.; Darden, T.; Lee, H.; Pedersen, L. G. *J. Chem. Phys.* **1995**, *103*, 8577–8593.

[241] Caleman, C.; van Maaren, P. J.; Hong, M.; Hub, J. S.; Costa, L. T.; van der Spoel, D. *J. Chem. Theory Comput.* **2012**, *8*, 61–74.

[242] Bayly, C. I.; Cieplak, P.; Cornell, W.; Kollman, P. A. *J. Phys. Chem.* **1993**, *97*, 10269–10280.

[243] Slater, J. C. *Phys. Rev.* **1951**, *81*, 385–390.

[244] Nosé, S. *Mol. Phys.* **1984**, *52*, 255–268.

[245] Hoover, W. G. *Phys. Rev. A* **1985**, *31*, 1695–1697.

[246] Martyna, G. J.; Klein, M. L.; Tuckerman, M. *J. Chem. Phys.* **1992**, *97*, 2635–2643.

[247] Parrinello, M.; Rahman, A. *J. Appl. Phys.* **1981**, *52*, 7182–7190.

[248] Nosé, S.; Klein, M. *Mol. Phys.* **1983**, *50*, 1055–1076.

[249] VandeVondele, J.; Krack, M.; Mohamed, F.; Parrinello, M.; Chassaing, T.; Hutter, J. *Comput. Phys. Commun.* **2005**, *167*, 103–128.

[250] Becke, A. D. *Phys. Rev. A* **1988**, *38*, 3098–3100.

[251] Grimme, S.; Antony, J.; Ehrlich, S.; Krieg, H. *J. Chem. Phys.* **2010**, *132*, 154104.

[252] Goedecker, S.; Teter, M.; Hutter, J. *Phys. Rev. B* **1996**, *54*, 1703–1710.

[253] Hartwigsen, C.; Goedecker, S.; Hutter, J. *Phys. Rev. B* **1998**, *58*, 3641–3662.

[254] Krack, M. *Theor. Chem. Acc.* **2005**, *114*, 145–152.

[255] VandeVondele, J.; Hutter, J. *J. Chem. Phys.* **2007**, *127*, 114105.

[256] Hutter, J. *WIREs Comput. Mol. Sci.* **2012**, *2*, 604–612.

[257] CP2K developers group, CP2K version 2.3 (Development Version). 2012; http://www.cp2k.org/.

[258] van der Spoel, D.; Lindahl, E.; Hess, B.; Groenhof, G.; Mark, A. E.; Berendsen, H. J. C. *J. Comp. Chem.* **2005**, *26*, 1701–1718.

[259] Hess, B.; Kutzner, C.; van der Spoel, D.; Lindahl, E. *J. Chem. Theory Comput.* **2008**, *4*, 435–447.

[260] Brehm, M.; Kirchner, B. *J. Chem. Inf. Model.* **2011**, *51*, 2007–2023.

[261] Williams, T.; Kelley, C. Gnuplot 4.6: an interactive plotting program. http://gnuplot.sourceforge.net/, 2013.

[262] Steiner, E. *The chemistry maths book*, 2nd ed.; Oxford University Press: Oxford, 2008.

I miss me
I miss everything I'll never be

— Smashing Pumpkins, *Rocket*

Dottorando: Daniele Tedesco

Tutor: Prof. Carlo Bertucci

Dottorato di Ricerca: Chimica (ciclo XXVI)
Curriculum: Scienze farmaceutiche
Indirizzo: Chimico farmaceutico/analitico-farmaceutico

Titolo tesi: Chiroptical properties of bioactive molecules: sensitivity to conformation and solvation

Durante i tre anni di Dottorato in Chimica l'attività di ricerca del dott. Daniele Tedesco, laureato in Chimica e Tecnologia Farmaceutiche (CTF) presso l'Università di Bologna nel 2009 con una tesi sulle proprietà chirottiche di sistemi liposomiali svolta presso il King's College London (Regno Unito), si è rivolta allo studio sperimentale e teorico delle proprietà chirottiche. In particolare, l'attenzione del dottorando si è concentrata sull'utilizzo della spettroscopia di dicroismo circolare elettronico (ECD) in combinazione con metodi computazionali di calcolo quantomeccanico (QM) nell'ambito della teoria del funzionale densità tempo-dipendente (TD-DFT) per la caratterizzazione stereochimica di molecole chirali di potenziale interesse farmaceutico. I progetti svolti durante il triennio hanno portato alla caratterizzazione stereochimica di vari composti, sia naturali (metaboliti fungini polichetidici) che di sintesi (derivati fluoroarilpropionici e beta-lattamici, difenoconazolo, fenoterolo), e hanno permesso di evidenziare l'estrema sensibilità delle proprietà chirottiche ai cambiamenti strutturali indotti dalla solvatazione, dalla flessibilità conformazionale e dalle interazioni sovramolecolari dei farmaci con le macromolecole biologiche.

Il dottorando è stato attivamente coinvolto in un progetto di ricerca PRIN 2008 finanziato dal MIUR (2008LYSEBR_005) e in due progetti ISCRA di classe C finanziati dal CINECA (IsC08_SCCFPM e IsC10_CSSECP). Nell'ambito del dottorato ha ottenuto un contributo nell'ambito del progetto Marco Polo 2012 per un periodo di ricerca all'estero di 6 mesi presso l'Università di Lipsia (Germania), ospite del gruppo di ricerca della Prof. Dr. Barbara Kirchner, per studiare gli effetti della solvatazione sulle proprietà chirottiche del metabolita fungino austdiol mediante simulazioni di dinamica molecolare *ab initio* (AIMD). L'attività svolta si è finora concretizzata in 7 pubblicazioni su riviste internazionali (*J. Chromatogr. A*, *J. Pharm. Biomed. Anal.*, *Chirality*, *Environ. Sci. Technol.*, *J. Nat. Prod*) e 10 presentazioni in congressi nazionali e internazionali, di cui 3 comunicazioni orali (NPCF5 2011, SSPA 2013, PBA 2013). Il dottorando ha inoltre tenuto 2 seminari su invito presso il Nuovo Centro Ricerche della Chiesi Farmaceutici (Parma, 2012) e presso il Mulliken Center for Theoretical Chemistry (Università di Bonn, Germania, 2013).

Nell'ambito del suo progetto di ricerca, il dottorando ha sviluppato una solida conoscenza delle tecniche spettroscopiche in luce polarizzata e dei metodi computazionali di calcolo QM per la determinazione della configurazione assoluta e per studi conformazionali di farmaci isolati o interagenti con proteine bersaglio; ha dimostrato ottime capacità di organizzazione del proprio lavoro ed ampia autonomia, riuscendo a sviluppare soluzioni originali ai problemi. Oltre alle doti scientifiche, il dottorando ha dimostrato un'elevata attitudine al lavoro di gruppo ed al trasferimento delle conoscenze, risultando correlatore di due tesi sperimentali di laurea in CTF, e ha infine svolto attività didattica, ottenendo 3 contratti di tutorato per i laboratori didattici di analisi farmaceutica del corso di studi in CTF.